

# Advanced Carbon Materials from Biomass: an Overview

GreenCarbon European Training Network

Edited by Joan J. Manyà  
May 2019





# Advanced Carbon Materials from Biomass: an Overview

Edited by Joan J. Manyà  
May 2019



This project has received funding from the European Union's Horizon 2020 Research and Innovation Programme under grant agreement No 721992

Copyright © GreenCarbon Project and Consortium  
<http://greencarbon-etn.eu>

This work is licensed under a Creative Commons Attribution-NonCommercial 4.0 International License  
(<https://creativecommons.org/licenses/by-nc/4.0>)  
A free online version is available from zenodo.org  
DOI: 10.5281/zenodo.3233733



## Preface

This book aims at providing a state-of-the-art review about the production, refining and application of biomass-derived carbon materials. The energy crisis, environmental pollution and global warming are serious problems that are of great concern throughout the world. Around 40% of world's current energy consumption is dedicated to the production of materials and chemicals, which are mostly derived from fossil fuels. These materials need to be simple to synthesise, as cost effective as possible and ideally based on renewable resources. Carbon materials are ideal candidates for performing many of these functions. In the past decade, the nanostructured forms of crystalline carbon (fullerenes, carbon nanotubes and graphene) have received the most attention due to remarkable and unusual physicochemical properties. However, the main disadvantage of using these crystalline nanocarbons for energy and environmental related applications is their high production costs. Alternatively, carbon materials derived from renewable resources (e.g., lignocellulosic biomass) could play a very powerful role in this direction in the near future.

The main objective of the **GreenCarbon European Training Network** (MSCA-ITN-ETN-721991) is to develop new scientific knowledge, technology, and commercial products and processes for biomass-derived carbons. This will be accomplished through outstanding research and training programmes for fourteen early-stage researchers (ESRs). As part of the training programme, all the ESRs have co-authored at least one chapter of the present book. The respective chapters served as pieces of literature summing up the aims and science of the network. Furthermore, this collaborative training activity has provided the ESRs with additional insights into many aspects of the process of writing/editing.

Regarding the organisation and contents of the book, its chapters can be divided into four parts: (1) production of pristine pyrochars from dry biomass feedstocks; (2) production of pristine hydrochars from wet biowastes (including lignin); (3) refining of pristine pyrochars and hydrochars for advanced applications in the fields of adsorption, catalysis and electrochemical conversion; and (4) carbon stability and sequential uses of biochars (i.e., biomass-derived carbon applied to soil). The detailed contents for each part are summarised below.

Chapters 1–4 focus on the production of biomass-derived chars through slow pyrolysis. In chapter 1, the effects of pyrolysis operating conditions on the physicochemical properties of the resulting char are discussed. In chapters 2 and 3, the technologies currently available for the continuous production of char are reviewed. For its part, chapter 4 provides an overview of modelling approaches applied in the thermochemical conversion of biomass.

Since the development of value-added lignin-based materials will be crucial to the economic success of wood-to-chemicals biorefineries, chapter 5 deals with the production and characterisation of lignin-containing streams produced within a lignocellulosic biorefinery framework. These lignin-containing wastes can be converted into value-added activated carbons via sequential hydrothermal carbonisation and activation. Both processes are widely described in chapter 6.

Chapters 7–10 focus on the functionalisation and nanostructuring of pyrochars and hydrochars to be used in adsorption, heterogeneous catalysis, electrocatalysis and direct-carbon fuel cells. In chapter 7, the combination of hydrothermal carbonisation and salt templating is presented as an interesting pathway to produce engineered porous carbons for adsorption of CO<sub>2</sub> and SO<sub>2</sub> in gas phase. The potential of biochar-derived activated carbons as catalysts or catalyst supports is reviewed in chapter 8. In chapter 9, an overview of the most recent advances in the use of hydrochars in catalysis and electrocatalysis is provided. Finally, chapter 10 deals with the use of biomass-derived carbons as fuels in direct-carbon fuel cells.

The most common biochar stability test methods, which are aimed at predicting the long term behaviour of biochar after its addition to soil, are explained and compared in chapter 11. Finally, chapter 12 contains a description of potential synergies in sequential biochar systems. In this sense, recycling of used biochars could maximise the value achieved across the chain. Examples of applications relevant to these systems are also briefly discussed.



## Acknowledgements

I would like to express my deep appreciation to the many people who contributed to this book. First of all, a big thank you to all the Early-Stage Researchers involved within the GreenCarbon European Training Network for their enthusiastic participation: Gianluca Greco (ch. 1), Filipe Rego (ch. 2), Jorge López-Ordovás (ch. 3), Przemyslaw Maziarka (ch. 4), Qusay Ibrahim (ch. 5), Pablo Arauzo (ch. 6), Sabina Nicolae and Xia Wang (ch. 7), Christian Di Stasi (ch. 8), Pierpaolo Modugno and Anthony Szego (ch. 9), Maciej Olszewski (ch. 10), Dilani Chathurika (ch. 11), and Christian Wurzer (ch. 12).

I'm also grateful for the ongoing support of supervisors from the different nodes within GreenCarbon: Jiawei Wang, Yang Yang, Katie Chong and Tony Bridgwater from Aston University; Frederik Ronsse from Ghent University; Moritz Leschinsky from the Fraunhofer Centre for Chemical-Biotechnological Process; Andrea Kruse from University of Hohenheim; Magdalena Titirici from Queen Mary University of London; Niklas Hedin from Stockholm University; and Saran Sohi and Ondrej Masek from the University of Edinburgh.

Thanks also to Belén González for her help throughout the editing process and Pompeyo Planchart for his volunteer contribution to the cover and formatting.



Joan J. Manyà, PhD

Associate Professor of Chemical Engineering, Universidad de Zaragoza

Coordinator of the GreenCarbon ETN



## Table of contents

<b>Chapter 1</b> .....	<b>9</b>
Operating conditions affecting char yield and its potential stability during slow pyrolysis of biomass: a review.	
<b>Chapter 2</b> .....	<b>21</b>
Pyrolysis of biomass and wastes in a continuous screw reactor for char production.	
<b>Chapter 3</b> .....	<b>33</b>
Industrial technologies for slow pyrolysis.	
<b>Chapter 4</b> .....	<b>45</b>
Matter of modelling in thermochemical conversion processes of biomass.	
<b>Chapter 5</b> .....	<b>57</b>
Production and characterisation of lignin and lignin-containing streams obtained through a two-stage fractionation process of lignocellulosic biomass.	
<b>Chapter 6</b> .....	<b>71</b>
Review of the conversion from hydrochar to activated carbon.	
<b>Chapter 7</b> .....	<b>83</b>
Refined biocarbons for gas adsorption and separation.	
<b>Chapter 8</b> .....	<b>101</b>
Biochar as sustainable platform for pyrolysis vapours upgrading.	
<b>Chapter 9</b> .....	<b>111</b>
Hydrothermal carbonisation and its role in catalysis.	
<b>Chapter 10</b> .....	<b>125</b>
Bio-based carbon materials for a direct-carbon fuel cell.	
<b>Chapter 11</b> .....	<b>135</b>
An overview of the methods used in the assessment of biochar carbon stability.	
<b>Chapter 12</b> .....	<b>147</b>
Synergies in sequential biochar systems.	



# Operating conditions affecting char yield and its potential stability during slow pyrolysis of biomass: a review

Gianluca Greco, Belén González, Joan J. Manyà

*Aragón Institute of Engineering Research (I3A), University of Zaragoza, crta. Cuarte s/n, Huesca E-22071, Spain*

## Abstract

The energy crisis, environmental pollution, global warming and the food productivity are serious problems, which have recently generated a growing interest in developing new technologies focused on reducing the greenhouse gas emissions and increasing the carbon sinks. A promising solution for such issues is char, a form of charred organic matter, which is possible to apply to soil in a deliberate manner as a means of potentially improving soil productivity and carbon sequestration. For this purpose, a common route to produce char with high yield from biomass is slow pyrolysis. Given the high number of variables affecting the process and the wide range of available biomass sources, a large variability in the yield and properties of the produced char should be expected. Therefore, one of the main challenges nowadays is to optimise the process conditions of the pyrolysis process for a given biomass feedstock with the aim to obtain a char with the desired properties to be used for a given application. This chapter aims to provide a review on the available alternatives to produce char and the main effects of the process parameters on the char yield and its potential stability.

## 1. Introduction

### 1.1. The global problem of CO<sub>2</sub> emissions

The fossil fuel resources of our planet, estimated between 4000 and 6000 Gt of carbon<sup>1</sup> are the product of biological and geologic processes that occurred over hundreds of millions of years ago and still continue nowadays. The carbon sequestered in these resources was originally a constituent of the atmosphere of a younger Earth. Around 360 million years ago, such atmosphere possessed about 1500 parts per million (ppm) CO<sub>2</sub>.<sup>1</sup> Since the dawn of the industrial age (year 1750 ca), about 5% of these resources was combusted and an estimated amount of 280 Gt-C released back into the atmosphere in the form of CO<sub>2</sub>. In the same period, a further 150 Gt-C was released to the atmosphere from soil carbon pools as a result of changes in land use. The atmospheric, terrestrial and oceanic carbon cycles dispersed the most part of these anthropogenic emissions (i.e., by locking the CO<sub>2</sub> away by dissolution in the oceans and in long-lived carbon pools in soils<sup>1</sup>). Since the industrial age, the CO<sub>2</sub> concentration in the atmosphere has increased from 280 ppm to 368 ppm in 2000. This increase in CO<sub>2</sub> concentration in air influences the balance of incoming and outgoing energy in the Earth-atmosphere system. This is why CO<sub>2</sub> is considered the most significant anthropogenic GreenHouse Gas (GHG).<sup>1,2</sup> Two of the first researchers on the influence of CO<sub>2</sub> on global warming were Tyndall (1859)<sup>3</sup> and Arrhenius (1896). Through their experiments, they determined that the fossil fuels produce a substantial amount of carbon dioxide and observed that their combustion would cause an increase in the average global surface temperatures.<sup>4</sup> The most part of CO<sub>2</sub> emissions is due to the energy production<sup>5</sup>, followed by industry. Around 40% of global anthropogenic CO<sub>2</sub> emissions comes from industrial processes. For example, 60% of the CO<sub>2</sub> produced during cement manufacture comes from the required calcination of limestone<sup>6</sup>, producing CaO and CO<sub>2</sub> from CaCO<sub>3</sub>. Another example is that iron and steel manufacture requires CO to reduce Fe<sub>2</sub>O<sub>3</sub> ore, forming CO<sub>2</sub> and Fe. The release of CO<sub>2</sub> is inevitable without a radical redesign of such processes and many others like them.<sup>7</sup>

The Intergovernmental Panel on Climate Change (IPCC) published the Fourth Assessment Report (AR4) in 2007, which concluded that the average global surface temperature increased by  $0.74 \pm 0.18$  °C over the 20<sup>th</sup> century, and that “most of the observed increase in global average temperatures since the mid-20<sup>th</sup> century was very likely (>90% probability) due to the observed increase in anthropogenic GHG concentrations”.<sup>1</sup> Anthropogenic change also reduced the effectiveness of certain climate feedback mechanisms: changes in land use and land-management practices have reduced the ability of soils to build soil carbon inventory in response to higher atmospheric CO<sub>2</sub> concentration, while the ocean acidification has reduced their capacity to take up additional CO<sub>2</sub> from the atmosphere.<sup>1</sup> In the absence of CO<sub>2</sub> mitigation, the resulting emissions will lead to further increase in atmospheric CO<sub>2</sub> concentration, causing an enhancing warming and inducing many changes in the global climate. Even if the CO<sub>2</sub> concentration is stabilised before 2100, the warming and other climate effects are expected to continue for centuries, due to the long-time scales associated with climate processes. The climate predictions suggest warming over a multicentury time scale in the range from 2 to 9 °C.<sup>1</sup> Hence, it is necessary to urgently find a solution to reduce the CO<sub>2</sub> emissions and, consequently, to mitigate the long-term climate change.

### 1.2. Ameliorating physical and chemical properties of soils

An intensification of agricultural production on a global scale is required in order to ensure the food supply for an increasing world population. Glaser et al.<sup>8</sup> conducted a study on the improvement of the physical and chemical properties of soils in the tropics. They stated that such worldwide need caused a reduction of fallow periods in shifting cultivation in the humid tropics, leading to irreversible soil degradation and to the destruction of remaining natural forests due to cultivation of new areas after slash-and-burn.<sup>9</sup> In many tropical environments, soils lack nutrient contents, meaning that the sustainable agriculture is constrained in such areas. The low nutrient contents typically accelerate the mineralisation of soil organic matter (SOM).<sup>10,11</sup> Consequently, the cation exchange

capacity (CEC) of the soils, which is often low due to their clay mineralogy, decreases further. In these circumstances, the efficiency of applied mineral fertilisers becomes lower.<sup>12,13</sup> In addition, many farmers cannot afford the costs of regular applications of inorganic fertilisers.<sup>8</sup>

The most common route to improve cultivations in the tropics is to employ slash-and-burn techniques. When the biomass burns, the nutrients are rapidly released into the soil. However, they have positive effects on soil fertility only for a short period.<sup>14–16</sup> Furthermore, the biomass burning releases certain amounts of the greenhouse gases CH<sub>4</sub> and N<sub>2</sub>O, enhancing the level of global warming.<sup>17</sup>

Organic matters such as manures, mulches and composts have frequently been applied to increase soil fertility.<sup>8</sup> However, organic matter is usually mineralised very rapidly under tropical conditions<sup>10</sup> and only a small portion of the applied organic matter will be stabilised in the soil in the long term, and it will then be released to the atmosphere as CO<sub>2</sub>.<sup>18</sup>

An alternative pathway for the soil amendment is to employ more stable compounds, such as carbonised materials. This class of materials comprises a wide range of materials, from charred material (e.g., char) to graphite and soot particles.<sup>19</sup> Several investigations<sup>20,21</sup> have been carried out on this topic, showing that carbonised materials produced from the incomplete combustion of organic material (i.e., black C, pyrogenic C, char) are responsible for maintaining high levels of SOM and available nutrients in anthropogenic soils of the Amazonia. These soils are called Terra Preta and they are characterised by a large amount of black C, indicating a high and prolonged input of carbonised organic matter, probably due to the char production in hearts, whereas only low amounts of char are added to soils as a consequence of forest fires and slash-and-burn techniques.<sup>17,18</sup>

## 2. Biomass and char

### 2.1. The potential of biomass resources

Among renewable energy resources, biomass is one of the most plentiful and well-utilised sources in the world.<sup>22</sup> Biomass is defined as the plant material derived from the reaction between CO<sub>2</sub> in the air, water and sunlight by photosynthesis process which produces carbohydrates, the building blocks of biomass.<sup>23</sup> In particular, the term *lignocellulosic biomass* refers to non-edible dry plant matter, which is an abundant and low-cost source of renewable energy.<sup>24</sup> Biomass resources include woody, herbaceous and aquatic plants as well as animal manures and processing residues.<sup>25</sup> The structure of lignocellulosic biomass is typically composed of three main building blocks: cellulose, hemicelluloses and lignin. Cellulose (see Fig. 1a) is the most abundant organic polymer<sup>24</sup>, present in the cell wall of the plant cells. It is a natural polymer of repeating D-glucose unit, a six-carbon ring. Cellulose shows unique properties of mechanical strength and chemical stability, due to its crystalline structure, originated from the three hydroxyl groups in the six-carbon ring which can react among themselves, forming intra- and intermolecular hydrogen bonds. Hemicelluloses (see Fig. 1b), which surrounds the cellulose fibres, represent the link between cellulose and

lignin<sup>24</sup>. Unlike cellulose, hemicelluloses are heterogeneous groups of branched polysaccharides. The structural elements are monomers such as glucose, galactose, mannose, and xylose. Their structures are amorphous, with low physical strength. Lignin (see Fig. 1c) is mainly present in the outer layer of the fibres and is responsible for the structural rigidity and holding the fibres of polysaccharides together. It plays a binding role between hemicelluloses and cellulose. Lignin is an aromatic, three-dimensional and cross-linked phenol polymer consisting of a random assortment “hydroxyl-” and “methoxy-” substituted phenylpropane units, whose monomers can be categorised as syringyl, p-hydroxyphenyl and guaiacyl units.<sup>26,27</sup> The lignin’s structure varies with the type of biomass; for instance, the hardwood lignin has a high methoxyl content, due to the presence of both guaiacyl and syringyl units, whereas the softwood lignin is only composed of guaiacyl units.<sup>28</sup> Extractives and inorganic components are also present in smaller quantities in the biomass. Extractives such as alkaloids, essential oils, fats, gums, and proteins act as intermediates in metabolism, as energy reserves, and as plant defences against microbial and insect attack.<sup>27</sup> The inorganic fraction mainly consists of compounds of potassium, calcium, silicon, sodium, chlorines and phosphorus.<sup>24</sup> Their fraction in the biomass ranges from less than 2% to as much as 15%.<sup>24</sup>

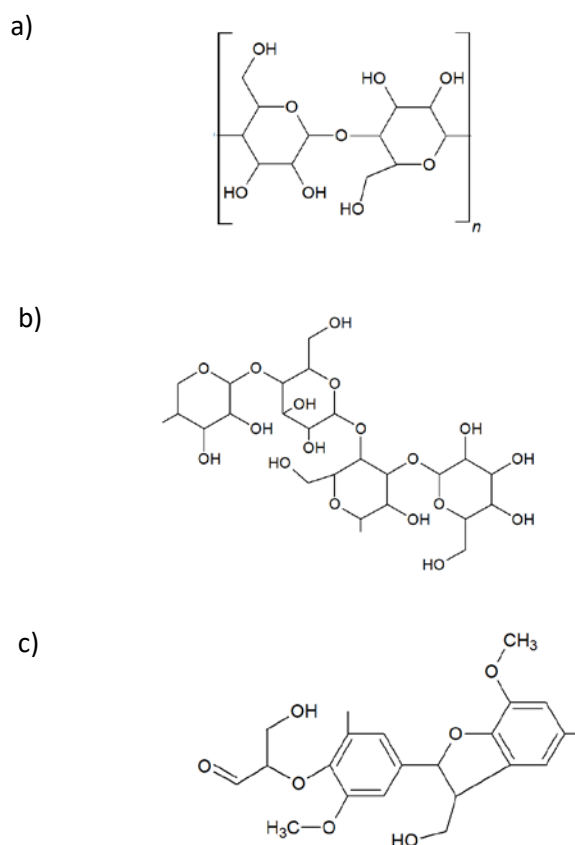


**Figure 1.** Chemical structures of a) cellulose, b) a fraction of hemicellulose, and c) a fraction of lignin.

## 2.2. The biochar concept

Concerns about climate change and food productivity have recently generated interest in biochar<sup>29</sup>, a form of charred organic matter, which is applied to soil in a deliberate manner as a means of potentially improving soil productivity and carbon sequestration.<sup>30</sup> The idea of adding char into soil to obtain a fertility improvement was inspired by the ancient agricultural practices which led to the creation of terra preta soils<sup>31</sup>. A relevant number of studies are focused on the benefits of using char in terms of mitigating global warming and as a solution to manage soil health and productivity.<sup>8,32–35</sup> However, these studies were often geographically limited and constrained by limited experimental data, due to the complexity of the research tasks<sup>29</sup>.

The term *char* refers to a carbon-rich, fine-grained, porous substance, produced by thermal decomposition of biomass under oxygen-limited conditions and at relatively low temperatures (i.e., below 700 °C).<sup>30,31</sup> The definition stated by the International Biochar Initiative (IBI) clarifies the need for purposeful application of this material to soil for both agricultural and environmental gains.<sup>31</sup> Nevertheless, the commercial exploitation of char as a soil amendment is still in its infancy<sup>31</sup>, since the relationship between its properties and its applicability into soil is still unclear<sup>29</sup>. For this reason, a synergic collaboration between different fields of research is needed: production and characterization of char on one side, and investigation of the char behaviour in the agricultural soils on the other side, measuring both environmental and agronomical benefits<sup>29</sup>. Differently from char, charcoal is used as a fuel for heat, as an adsorbent material or as a reducing agent in metallurgical processes.<sup>30</sup>

One of the most interesting properties of char is its porous structure, which is believed to be responsible for improved water retention and increased soil surface area.<sup>31</sup> Furthermore, an increase in the nutrient use efficiency has been observed when the char was added to the soil. This is due to the nutrients contained in the char as well as the extent of physicochemical processes, which allow a better utilisation of soil-inherent or fertiliser-derived nutrients. In addition, a key property of char is its biological and chemical stability<sup>36,37</sup>, allowing it to act as a carbon sink.<sup>31</sup> Therefore, the conversion of biomass to long-term stable soil carbon species can result in a long-term carbon sink, as the biomass removes atmospheric carbon dioxide through photosynthesis<sup>38</sup>, leading to a net removal of carbon from the atmosphere.

According to the above-explained considerations, three complementary goals can be achieved by using char applications for environmental management:

- Soil improvement, from both pollution and productivity point of view.
- Energy production, if energy is captured during the char production process.
- Waste valorisation, if waste biomass is used for this purpose.

Beyond its usefulness as soil amendment and as a mean for the carbon sequestration, char can be used in a wide range of applications<sup>39,40</sup>:

- Energy industry to produce electricity.
- Chemical industry for production of carbon disulphide, sodium cyanide and carbide.
- Smelting and sintering of iron ores or purification of nonferrous metals. Most valued reductant in metallurgical industry.
- Water and gas purification, solvent recovery and wastewater treatment.
- Medical industry for poisons adsorbent
- Skincare, as part of a scrubber or toothpaste

Depending on the final use of the char, different properties are desirable. Therefore, different processes are needed to obtain such wide variety of chars. For example, the desired property in energy production is a high heating value<sup>41</sup>, whereas a high surface area and a good compressive strength are desired properties in the field of catalytic activation<sup>42</sup> and metallurgical industry<sup>39</sup>, respectively.

## 3. Char production

### 3.1. Pyrolysis

In recent years, converting biomass into energy has been based mainly on biochemical and thermochemical processes.

Among all the thermochemical processes, pyrolysis is considered one of the most promising pathways, since its conditions could be optimised to produce any of the three products, pyrolytic oils with a high energy density, the char with key properties for soil amendment or the gas to produce energy<sup>43</sup>. Pyrolysis is the term given to the thermal decomposition of organic matter within an environment with a limited oxygen content. The heating of biomass in an inert atmosphere results in the production of permanent gases (e.g., CO<sub>2</sub>, CO, CH<sub>4</sub> and H<sub>2</sub> and light hydrocarbons), and an organic volatile fraction from the cellulose, hemicelluloses and lignin polymers. These vapours can be condensed, giving an organic liquid known as bio-oil. The bio-oil composition mainly depends on the lignocellulosic composition of the biomass.<sup>44</sup> The non-condensable gases leave the reaction system and can be employed to provide heat for self-sustain the pyrolysis process. The remaining solid carbon-rich product is named char.

Yang et al.<sup>45</sup> investigated the pyrolysis behaviour of cellulose, hemicelluloses and lignin using thermogravimetric analysis (TGA). They pointed out that the decomposition of hemicelluloses occurs at 220–315 °C, whereas the cellulose decomposes at 315–400 °C. Differently from the cellulose and hemicelluloses, the decomposition of lignin occurs in a wider range of temperature: from 160 to 900 °C. Furthermore, the highest solid residue derives from the pyrolysis of lignin.

The operating conditions of the pyrolysis process, such as highest (or peak) temperature, heating rate, residence time, pressure, etc. markedly affect the nature and yields of products.<sup>46</sup> Thus, the process conditions can be adjusted as a function of the desired product. It is well known that high temperatures and long residence times of the vapour phase enhance the secondary reactions, leading to a higher production of non-condensable gases, whereas high

temperature and shorter residence times favour the formation of condensable products. On the other hand, solid products are usually favoured at low temperatures.<sup>47</sup> Hence, the pyrolysis processes can be categorised in two main types (slow and fast) depending on the operating conditions employed.

### 3.1.1. Slow pyrolysis

Slow pyrolysis is one of the most promising ways to obtain an elevated char yield. It is carried out at temperatures of 250–400 °C<sup>39,40</sup>, despite there are wider ranges in the literature (300–700 °C<sup>48</sup>) and slow heating rates (usually lower than 10 °C min<sup>-1</sup>), for long solid and vapour residence times<sup>48</sup> (from minutes up to hours and even days). Long residence times of vapours within the reactor allow intermediate volatiles to continue to react among them, producing further char and gas<sup>27</sup>. Therefore, slow pyrolysis is aimed to produce large amounts of char, although significant quantities of bio-oil and gas are produced<sup>49</sup>. Slow pyrolysis has been used for thousands of years for char production and sometimes it is called conventional pyrolysis, although the technology used at the beginning was based on kilns<sup>39,50</sup> and there are current technologies with a higher level of development<sup>50,51</sup>.

Slow pyrolysis is sometimes confused with torrefaction, which is normally performed at lower temperatures in order to partly decompose the feedstock.<sup>50</sup> Torrefaction leads to a partial degradation of the hemicellulose for densification purposes.<sup>52</sup> This process is typically performed at a temperature comprised between 200 °C and 350 °C<sup>39,48,52,53</sup>, and it is characterised by a higher solid yield (around 80%) than that of slow pyrolysis (30%–35%).<sup>48,53</sup>

### 3.1.2. Fast pyrolysis

Fast pyrolysis uses high heating rates (above 200 °C min<sup>-1</sup>) and short vapour residence time (around 2 s) at temperatures of 500–550 °C.<sup>29</sup> These operating conditions particularly promote the formation of liquid products (bio-oil) at the expense of char.<sup>54</sup> Generally, fast pyrolysis processes produce 60%–75% (wt.) of bio-oil, 15%–25% of solid char, and 10%–20% of non-condensable gases, depending on the feedstock used.

From a chemical point of view, the char obtained at high heating rates shows a higher oxygen content<sup>55</sup> and a lower calorific value<sup>56</sup>, compared to the char produced through slow pyrolysis. This could be due to the shorter residence time of the vapour fraction, which inhibits the extent of secondary charring reactions. However, the char obtained through fast pyrolysis can possess a larger specific surface area for two reasons: first, the relatively small size of the feedstock usually required for such process<sup>29</sup>, and second, the faster devolatilisation, which can lead to more fragmented particles<sup>57</sup> and a certain development of large micropores and mesopores at the expense of narrow micropores (which are dominant in slow pyrolysis-derived chars).

## 3.2. Flash carbonisation

Flash carbonization is a novel technology developed at the University of Hawaii.<sup>29</sup> The process allows the biomass to convert into char in a more efficient way than conventional slow pyrolysis.<sup>58–60</sup> The experimental apparatus consists of a pressurised vessel, which contains a canister with a fixed bed of a given biomass. Air is used to pressurise the vessel to an initial

pressure of 1–2 MPa, and a flash fire is ignited at the bottom of the packed bed. Air is delivered to the top of the packed bed after a short time and the biomass is converted into char. The reaction lasts less than 30 min and the temperature profile is affected by several factors, such as the type of biomass, the total amount of air delivered, the heating time and the moisture content of the feedstock<sup>60</sup>. Regarding the process yields, Antal et al.<sup>60</sup> carried out a study on the flash carbonisation behaviour of some woods and agricultural byproducts. They realized a char yield ranging between 29.5% and 40%, fixed carbon yields from 27.7% to 30.9%, and energy conversion efficiencies of biomass into char of 55.1%–66.3%.

The flash carbonisation process seems to be a promising alternative route to produce char, since the reaction times are very short compared to those of the slow pyrolysis process (in batch operating mode), and even because it would be possible to retain a larger amount of fixed carbon from the feedstock.<sup>60</sup>

## 3.3. Hydropyrolysis

Hydropyrolysis is an alternative pyrolysis process, which is performed in a reductive hydrogen environment instead of an inert one. In hydropyrolysis, the reducing H<sub>2</sub> gas generates hydrogen radicals, which react with the volatiles released from the biomass, leading to the production of H<sub>2</sub>O, CO and CO<sub>2</sub>, and hydrocarbons.<sup>65</sup> Furthermore, many of the reactive volatiles released by the process are capped by the hydrogen radicals, avoiding to undergo polymerisation.<sup>66,67</sup> This leads to the formation of hydrocarbons with higher selectivity, if compared to that of the fast catalytic pyrolysis.<sup>68,69</sup> One of the advantages of hydropyrolysis is that the process is globally exothermic. However, this process requires the supply of H<sub>2</sub> and an operating pressure of 3.0 MPa. Further studies are needed to assess the viability of this technology from both technical and economic points of view.

## 4. Influence of process parameters on the char yield and its stability during slow pyrolysis

Given the high number of variables affecting the process (e.g., pressure, peak temperature, heating rate, gas residence time) and the wide range of available biomass sources, a large variability in the char properties should be expected.<sup>29</sup> In other words, the carbon sequestration potential of produced char can largely be dependent on process operating conditions for a given feedstock. Therefore, one of the main challenges nowadays is to optimise the process conditions of pyrolysis for a given biomass feedstock<sup>70,71</sup> with the aim of obtaining an appropriate yield of char with high stability, an essential requirement for its use to capture CO<sub>2</sub> and as soil amendment. In addition, analysing the effects of pyrolysis process conditions on additional physicochemical properties of char (e.g., porosity, functional groups in surface, conductivity, etc.) is also needed to explore further uses of char in, for instance, adsorption, catalysis and electrochemical applications.

#### 4.1. Effect of peak temperature

Peak temperature is generally defined as the highest temperature reached during the pyrolysis process.<sup>40</sup> In contrast to the effect of pressure and the pyrolysis environment, a large number of studies are available in literature concerning the influence of peak temperature on the char yield and its potential stability. As a general trend, the char yield decreases when the peak temperature increases<sup>56,72–75</sup>, whereas the fixed-carbon content in the final char gradually rises with an increasing temperature<sup>40,76–79</sup>. Furthermore, an increase in peak temperature generally leads to an increment of the aromatic C fraction<sup>78,80,81</sup> and a decrease in both H:C and O:C atomic ratios<sup>77,82,83</sup>, suggesting that the chemical recalcitrance of char (i.e. its ability to resist abiotic and biotic degradation) is improved.

McBeath et al.<sup>84</sup> performed several hydrolysis runs producing char from common feedstocks, at ten temperatures between 300 and 900 °C, in order to assess their influence on carbon stability. Higher temperatures resulted in lower char yields for each feedstock. The initial decline in char yield, which was visible in the range 300–450 °C depending on the feedstock type was mainly due to the thermal decomposition of cellulose and hemicelluloses. In addition, differences in ash content among the feedstocks led to changes in the char yield at the same temperature, probably due to ash-char interactions. When pyrolysis temperature increased from 300 to 600 °C, the char yield decreased to approximately half of the value obtained at 300 °C. Then, the temperature effect above 600 °C (and up to 900 °C) on the char yield was slighter than that observed at lower temperatures. On the other hand, potential char stability was promoted by the increase in temperature. The fraction of stable polycyclic aromatic carbon to total organic carbon (SPAC/TOC) was used as an index for the char stability. More in detail, the SPAC/TOC ratio just increased up to 20% at temperatures lower than 450 °C, whereas an increase greater than 80% was observed for temperatures above 700 °C. Furthermore, the most part of the feedstocks showed a sigmoidal-like progression for the SPAC/TOC, with a minimal formation of SPAC structures in the range 300–400 °C, followed by a rapid increase in SPAC/TOC up to 700 °C, and then a plateau above 700 °C. Hence, a trade-off, in terms of temperature, between the char yield and the char potential stability was found, whose optimum was generally observed between 500 and 700 °C. Manyà et al.<sup>85</sup> confirmed such findings, examining the combined effect of pressure and peak temperature on the potential stability of the char produced from two-phase olive mill waste through slow pyrolysis in a laboratory-scale fixed-bed reactor. In this case, the fraction of aromatic C, the fixed-carbon yield and the atomic H:C and O:C ratios were used as rough indicators of the char stability. They observed a statistical consistency of such parameters (i.e., no contradictory findings were found), confirming their usefulness as indicators for the potential stability of char. They agreed with the previous results found in literature, stating that the temperature negatively affected the char yield, whereas had a favourable effect on the fixed-carbon yield, improving the long-term C sequestration potential of char. The authors established the best operating conditions (in terms of maximising the char potential stability as well as obtaining an acceptable char yield) at 1.1 MPa and

600 °C. Furthermore, the fraction of aromatic C markedly increased with the peak temperature, leading to an increase in pH. This could be due to a decrease in the acid functional groups, resulting in a decline in the cation exchange capacity of char in the soil. In other words, the operating conditions leading to a maximisation of the potential carbon stability can also result in a char with lower capacity for soil improvement purposes.

#### 4.2. Effect of absolute pressure

The pressure effect on the pyrolysis behaviour of any feedstock has not been properly demonstrated yet, as many studies reported in literature are inconsistent with each other. Most of these studies have revealed an increase in the char and gas yields, and a decrease of the liquid yield, when both the pressure and the residence time of the vapour phase were increased.<sup>76,86–90</sup> For instance, Antal et al.<sup>87</sup> carried out experiments using a lab-scale process unit development (PDU) to identify the effects of operating pressure on char yields from macadamia nut shells. They stated that only 0.4 MPa were sufficient to get a yield of 40.5% wt. (see Table 1). A further increase in pressure (i.e., 3.30 MPa) raised the char yield to 51% wt. However, part of this increase was attributed to the higher volatile matter content with higher pressures. Hence, the pressure effect on the char yield was less strong than it appeared. Then, the pressure influence on the char yield was slighter when the pressure value was above 1.0 MPa. In addition, they highlighted a heat transfer improvement within the reactor at higher pressures, leading to the production of a more uniform char and to a reduction of the required heating time. According to this, Qian et al.<sup>90</sup> reported, for the pyrolysis of rice husk, an increase in the yields of char, water, and gas from 0.1 MPa to 1.0 MPa at a constant linear velocity of the gas flow (i.e., constant gas residence time) at the expense of the yield of organic condensable products (bio-oil). This was explained by an enhancement of polycondensation, dehydration and cracking of the volatiles to form more char, water, and gas; respectively. However, the effect of pressure became negligible when the pressure was raised from 1.0 MPa to 5.0 MPa. The same study<sup>90</sup> was then conducted with the same values of pressure, but keeping constant the volume flow rate (i.e., the higher the pressure, the higher the gas residence time). The yields of char and gas obtained under atmospheric pressure were similar to the previous ones, whereas the yield of bio-oil raised to 36.2% wt. and the water yield decreased to 14% wt. This suggests that the vapour residence time plays an important role under atmospheric pressure in promoting the dehydration of volatiles. The yield's trends for char, gas, bio-oil, and water as a function of pressure were similar to those observed at constant linear velocity of gas flow.

On the other hand, Manyà et al.<sup>85</sup> observed a significant decrease in char yield when the pressure was increased, keeping constant the gas residence time within the reactor. Such effect could be attributed to the enhancement of the kinetics of the steam gasification reaction with the pressure (and catalysed by the alkaline metals inherently present in the biomass source). Furthermore, the effect of pressure, combined with the temperature effect, resulted positive on the long-term C sequestration potential of char (i.e., higher fixed-

carbon content and lower H:C and O:C atomic ratios). Similarly, Azuara et al.<sup>91</sup> observed a very slight decrease in char yield (from 32% to 30% wt.) when the pressure increased from 0.1 MPa to 1.1 MPa, during pyrolysis of vine shoots in a lab-scale fixed bed reactor. This was attributed to the above-mentioned promotion of the steam gasification reaction, as well as a dilution effect of pyrolysis volatiles (caused by an increase in the mass flow rate of carrier gas to keep constant its residence time within the reactor). This dilution effect results in a decrease in the partial pressure of volatiles, which can lead to a lower extent of secondary charring reactions. In addition, the fixed-carbon yield was practically unaffected by pressure, suggesting that other process parameters, such as peak temperature, could mainly explain the fixed-carbon content in the produced char. In conclusion, the pressure could affect the potential stability of char and, to a lesser extent, the char yield. The magnitude of its influence will depend on the nature of the feedstock (since a higher content in alkaline metals will further promote gasification) as well as the selected operating conditions in terms of vapour residence time, reactor configuration, and partial pressure of volatiles.

**Table 1.** Effect of pressure on air-dry macadamia nut shell char yield using a lab-scale reactor (source: Antal et al.<sup>87</sup>).

Pressure (MPa)	Char Yield (% wt. dry basis)	Volatile matter in char (% wt. dry basis)
0.40	40.5	20.6
0.70	40.2	17.7
1.00	44.4	25.3
1.10	50.8	28.8
3.30	51.0	29.3

#### 4.3. Effect of pyrolysis environment

Another important parameter affecting the pyrolysis behaviour of biomass is the pyrolysis atmosphere.<sup>91</sup> It could be interesting to study in terms of energy efficiency, since the flue gas generated by combustion of pyrolysis gas can be used as pyrolysis gas environment. This approach can lead to important cost savings<sup>70</sup>, resulting in an improvement in the char production process in terms of economic feasibility, environmental impact, and thermal efficiency. Nevertheless, further investigations are needed to assess the effects of modifying the inert environment (i.e., from pure N<sub>2</sub> to a flue gas containing CO<sub>2</sub>) on the pyrolysis products distribution as well as on the char properties. So far, only few studies have been focused on the effect of pyrolysis environment. Biswas et al.<sup>92</sup> investigated the pyrolysis behaviour of rice straw under carbon dioxide at temperatures ranging from 300 to 450 °C using a fixed-bed reactor. They pointed out a marginally improvement of char and bio-oil yields in the presence of CO<sub>2</sub> instead of N<sub>2</sub>, whereas the gas yield was slightly reduced, as shown in Table 2. The authors stated that the high partial pressure of CO<sub>2</sub> could explain the observed higher yields in condensable organic compounds. Moreover, CO<sub>2</sub> could also promote some repolymerisation reactions, resulting in a higher char yield. Table 3 reports the carbon, hydrogen, and oxygen contents of

the produced chars obtained in study by Biswas et al.<sup>92</sup>. By increasing the temperature, the carbon content became higher more markedly under the CO<sub>2</sub> atmosphere (from 44.90% to 50.95%) than under the N<sub>2</sub> atmosphere (from 42.24%w. to 45.33%w.). The corresponding decreases in hydrogen and oxygen contents were attributed to a higher degree of carbonisation, which is mainly explained by an increased temperature. In contrast to the results reported by Biswas et al.<sup>92</sup>, Azuara et al.<sup>91</sup> did not observe any influence of the pyrolysis environment on the yield of vine shoots-derived char. The effect of the atmosphere was only evident for the gas distributions obtained after the pyrolysis runs. In particular, the main effect was a marked decrease in the CO<sub>2</sub> production, accompanied by a proportional increase in the CO production, due to the high CO<sub>2</sub> partial pressure, which can be related to a promotion of the reverse Boudouard reaction. Furthermore, the extent of the reverse Boudouard reaction enhanced the conversion of carbon, leading to a certain porosity development. Regarding the potential stability of the produced chars, the use of CO<sub>2</sub> instead of N<sub>2</sub> as pyrolysis atmosphere led to similar values of fixed-carbon contents and slightly lower H:C and O:C atomic ratios.

Lee et al.<sup>93</sup> investigated the pyrolysis behaviour of red pepper stalk under a CO<sub>2</sub> environment. The thermal degradation under CO<sub>2</sub> occurred faster than under N<sub>2</sub>, suggesting that CO<sub>2</sub> expedited the thermal degradation of amorphous substances such as lignin. Further effects related to the CO<sub>2</sub> presence were higher degrees of carbonisation, and a clearly enhancement of the thermal cracking of condensable volatiles, resulting in a favourable condition of the syngas generation. As a consequence, the CO<sub>2</sub> presence greatly reduced the liquid formation, since condensable volatiles were used as reaction substrates for the syngas production. The higher degree of carbonisation was confirmed by the analysis of the char composition. In particular, the char produced under CO<sub>2</sub> contained higher aromaticity matter and less aliphatic matter than those of the char produced under N<sub>2</sub>. Since the aromatic carbon is more stable than aliphatic carbon under conditions of biotic and abiotic oxidation, the char produced under CO<sub>2</sub> could result more recalcitrant than that produced under N<sub>2</sub>.

**Table 2.** Product yields of pyrolysis runs conducted between 300 and 450 °C (source: Biswas et al.<sup>92</sup>).

Pyrolysis peak temperature (°C)	Char yield, wt. %		Gas yield, wt. %		Bio-oil yield, wt. %	
	N <sub>2</sub>	CO <sub>2</sub>	N <sub>2</sub>	CO <sub>2</sub>	N <sub>2</sub>	CO <sub>2</sub>
300	39.2	47.0	31.6	21.6	29.2	31.4
350	35.6	42.0	23.9	33.8	30.6	34.1
400	34.2	38.0	27.5	34.8	31.0	34.5
450	33.2	37.0	28.9	37.0	29.8	34.1

**Table 3.** Ultimate analysis of chars produced between 300 and 450 °C (source: Biswas et al.<sup>92</sup>).

Pyrolysis peak temperature (°C)	C, wt.%		H, wt.%		O, wt.%	
	N <sub>2</sub>	CO <sub>2</sub>	N <sub>2</sub>	CO <sub>2</sub>	N <sub>2</sub>	CO <sub>2</sub>
300	42.2	44.4	3.00	4.38	54.0	50.3
350	43.2	43.4	2.46	3.92	53.6	51.9
400	44.0	45.3	2.22	3.53	53.0	50.38
450	45.3	50.9	1.46	3.45	52.5	44.8

#### 4.4. Other effects

Peak temperature, pressure, and pyrolysis atmosphere can be considered as the process variables that mainly affect the char yield and its potential stability. However, there are further factors to mention which could have remarkable effects on the final char properties. Firstly, it should be noted that char yield is influenced by the feedstock composition (i.e., lignin, cellulose, hemicelluloses, extractives and inorganic matter). More in detail, chars produced from feedstocks with high lignin contents generally show higher yields.<sup>40,94</sup> Furthermore, pyrolysis of extractive-rich woods (e.g., chestnut) seemed to lead to higher char production than that obtained from pyrolysis of wood species with lower content of extractives.<sup>95</sup> The moisture content could also affect the char yield, since previous studies<sup>73,87,96,97</sup> indicated that high moisture contents (i.e., ranging from 42% wt. to 62% wt.) can improve the char yield at elevated pressures.

In addition, and as mentioned above, the inorganic fraction present in the feedstock can play a non-negligible role in the pyrolysis process. The presence of alkali and alkaline earth metals (AAEMs) is always associated with low temperatures required for pyrolysis, higher yields of char and gas, and lower yields of condensable products<sup>98,99</sup>. In this sense, Wang et al.<sup>100</sup> reported an increase in the yields of char and gas produced from pine wood through slow pyrolysis by adding K<sub>2</sub>CO<sub>3</sub>. On the other hand, in another work<sup>101</sup>, it was observed that CaO had a catalytic effect on the cracking of volatiles, promoting the decarboxylation of organic acids and leading to the formation of light hydrocarbons. In addition, CaO is a good low-cost sorbent for CO<sub>2</sub>. Manyà et al.<sup>102</sup> conducted a study on the effects of pressure combined with the addition of a rejected material from municipal waste composting on the pyrolysis behaviour of two-phase olive mill waste. Unexpectedly, they observed that the addition of such AAEMs-rich material led to a decrease in the char yield at any pressure. This finding could be related to a higher catalytic role of AAEMs during the primary devolatilisation as well as heterogeneous secondary reactions (e.g., steam gasification). In other words, the secondary charring reactions were not sufficiently promoted by AAEMs. Another factor to consider is the particle size. It is well known in literature<sup>103–105</sup> that an increase in particle size leads to more pronounced gradients of temperature within the particles, with the core temperature lower than that of the particle surface, resulting in higher char yield and lower bio-oil and gas yields. In addition, as the particle size is greater, the diffusion rate of volatiles within the char decreases, leading to a further char

formation by means of secondary reactions.<sup>72,106,107</sup> The possibility of using large biomass particles can also lead to important cost savings: (1) by avoiding the need of severe milling processes (with a high energy consumption), and (2) by improving the self-sustaining nature of the pyrolysis process, since the secondary reactions are exothermic.<sup>87,108</sup>

## 5. Conclusions

From the present review, the following conclusions can be drawn:

- Slow pyrolysis seems to be one of the most suitable pathways to produce char with appropriate yields and high potential carbon sequestration potentials. However, further research is needed to establish the best operating conditions to efficiently produce char for soil amendment and other advanced applications. For this reason, nowadays the process optimisation of slow pyrolysis is a deal of great concern.
- An increase in peak temperature results in lower char yields. However, increasing the peak temperature leads to higher potential stabilities for the char. Hence, in terms of temperature, a reasonable trade-off between char yield and its stability needs to be investigated. According to the current state of knowledge, temperatures between 500 and 600 °C are believed to be the most reliable choice to achieve a good compromise between char yield and potential stability.
- Among the wide range of process parameters that could affect the pyrolysis process, pressure is one of the most interesting one. It is believed that its effect may be positive on char's potential stability. However, the most part of the results reported in the literature are discordant, especially in the mass yield of produced char. Hence, further investigations are needed in order to clarify the true effect of pressure.
- Since the char yield and its stability are apparently slightly affected or even unaffected by the pyrolysis environment, using CO<sub>2</sub> (or a CO<sub>2</sub>-containing flue gas) instead of an expensive inert gas (e.g., N<sub>2</sub>) would be interesting in terms of energy efficiency and economic viability. Nevertheless, further research is needed in order to assess the effects of a higher CO<sub>2</sub> partial pressure on the products' distribution (especially for the gas composition) as well as the surface and textural properties of the resulting char. Using CO<sub>2</sub> at different partial pressures and peak temperatures could be an interesting route to produce chars with an engineered porosity and surface chemistry.

- Other factors related to the biomass feedstock, such as its composition (in terms of hemicellulose, cellulose, lignin, and extractives), moisture content, inorganic fraction's constituents, and particle size could also affect both the yield and final properties of char.
- In light of the current lack of knowledge about the relationship between the char properties and its applicability into soil, great collaborative efforts between different fields of research are required. In this sense, the GreenCarbon's Early-Stage Researcher #1 (G. Greco) is contributing throughout the investigation of the most appropriate slow pyrolysis conditions (with a particular focus on the pressure effect and the pyrolysis environment) in order to improve the char properties for its employment as a carbon sequestration agent.

### Acknowledgements

"This project has received funding from the European Union's Horizon 2020 research and innovation programme under the Marie Skłodowska-Curie grant agreement No 721991".

### References

- (1) Rackley, S. A. *Carbon Capture and Storage*; Joe Hayton: Chennai, 2010.
- (2) IPCC. Summary for Policymakers: Emissions Scenarios. A Special Report of Working Group III of the Intergovernmental Panel on Climate Change. *Group 2000*, 20.
- (3) Tyndall, J. Note on the Transmission of Radiant Heat through Gaseous Bodies. 1859, pp 37–39.
- (4) Arrhenius, S. In the Air upon the Temperature of the Ground. *Philos. Mag. J. Sci.* **1896**, *41*, 237–279.
- (5) SMMT. Total CO<sub>2</sub> emissions from cars in use <https://www.smmt.co.uk/reports/co2-report/> (accessed May 19, 2015).
- (6) Dean, C. C.; Dugwell, D.; Fennell, P. S. Investigation into Potential Synergy between Power Generation, Cement Manufacture and CO<sub>2</sub> Abatement Using the Calcium Looping Cycle. *Energy Environ. Sci.* **2011**, *4* (6), 2050.
- (7) Fennell, P. *Calcium and Chemical Looping Technology for Power Generation and Carbon Dioxide (CO<sub>2</sub>) Capture*; Elsevier, 2015.
- (8) Glaser, B.; Lehmann, J.; Zech, W. Ameliorating Physical and Chemical Properties of Highly Weathered Soils in the Tropics with Charcoal - a Review. *Biol. Fertil. Soils* **2002**, *35*, 219–230.
- (9) Vosti, S. A.; Carpentier, C. L.; Witcover, J.; Valentin, J. F. Intensified Small-Scale Livestock Systems in the Western Brazilian Amazon. In *Agricultural technologies and tropical deforestation*; 2001; pp 113–133.
- (10) Tiessen, H.; Cuevas, E.; Chacon, P. The Role of Soil Organic Matter in Sustaining Soil Fertility. *Nature* **1994**, *371*, 783–785.
- (11) Zech, W.; Senesi, N.; Guggenberger, G.; Kaiser, K.; Lehmann, J.; Miano, T. M.; Miltner, A.; Schroth, G. Factors Controlling Humification and Mineralization of Soil Organic Matter in the Tropics. *Geoderma* **1997**, *79*, 117–161.
- (12) Melgar, R. J.; Smyth, T. J.; Sanchez, P. A.; Cravo, M. S. Fertilizer Nitrogen Movement in a Central Amazon Oxisol and Entisol Cropped to Corn. *Fertil. Res.* **1992**, *31*, 241–252.
- (13) Cahn, M. D.; Bouldin, D. R.; Cravo, M. S.; Bowen, W. T. Cation and Nitrate Leaching in an Oxisol of the Brazilian Amazon. *Agron. J.* **1993**, *85*, 334–340.
- (14) Cochrane, T. T.; Sanchez, P. A. Land Resources, Soil Properties and Their Management in the Amazon Region: A State of Knowledge Report. In *International Conference on Amazon Land Use and Agricultural Research*; 1980.
- (15) Kauffman, J. B.; Cummings, D. L.; Ward, D. E.; Babbitt, R. Fire in the Brazilian Amazon: 1. Biomass, Nutrient Pools, and Losses in Slashed Primary Forests. *Oecologia* **1995**, *104*, 397–408.
- (16) Kleinman, P. J. A.; Pimentel, D.; Bryant, R. B. The Ecological Sustainability of Slash-and-Burn Agriculture. *Agric. Ecosyst. Environ.* **1995**, *52*, 235–249.
- (17) Fearnside, P. M.; Graca, P. M. L.; Filho, N. L.; Rodrigues, F. J. A.; Robinson, J. M. Tropical Forest Burning in Brazilian Amazonia: Measurement of Biomass Loading, Burning Efficiency and Charcoal Formation at Altamira, Pará. *For. Ecol. Manage.* **1999**, *123*, 65–79.
- (18) Fearnside, P. M. Global Warming and Tropical Land-Use Change: Greenhouse Gas Emissions from Biomass Burning, Decomposition and Soils in Forest Conversion, Shifting Cultivation and Secondary Vegetation. *Clim. Change* **2000**, *46*, 115–158.
- (19) Schmidt, M. W. I.; Noak, A. G. Black Carbon in Soils and Sediments: Analysis, Distribution, Implications, and Current Challenges. *Global Biogeochem. Cycles* **2000**, *14*, 777–793.
- (20) Glaser, B.; Balashov, E.; Haumaier, L.; Guggenberger, G.; Zech, W. Black Carbon in Density Fractions of Anthropogenic Soils of the Brazilian Amazon Region. *Org. Geochem.* **2000**, *31*, 669–678.
- (21) Glaser, B.; Haumaier, L.; Guggenberger, G.; Zech, W. The Terra Preta Phenomenon - a Model for Sustainable Agriculture in the Humid Tropics. *Sci. Nat.* **2001**, *88*, 37–41.
- (22) Demirbaş, A. H.; Demirbaş, A. S.; Demirbaş, A. Liquid Fuels from Agricultural Residues via Conventional Pyrolysis. *Energy Sources* **2010**, *26*, 821–827.
- (23) Aysu, T.; Küçük, M. M. Biomass Pyrolysis in a Fixed-Bed Reactor: Effects of Pyrolysis Parameters on Product Yields and Characterization of Products. *Energy* **2014**, *64*, 1002–1025.

- (24) Dhyani, V.; Bhaskar, T. A Comprehensive Review on the Pyrolysis of Lignocellulosic Biomass. *Renew. Energy* **2017**.
- (25) McKendry, P. Energy Production from Biomass (Part 1): Overview of Biomass. *Bioresour. Technol.* **2002**, *83*, 37–46.
- (26) Carrier, M.; Loppinet-serani, A.; Aymonier, C. Thermogravimetric Analysis as a New Method to Determine the Lignocellulosic Composition of Biomass. *Biomass and Bioenergy* **2011**, *35*, 298–307.
- (27) Mohan, D.; Pittman, C. U.; Steele, P. H. Pyrolysis of Wood/Biomass for Bio-Oil: A Critical Review. *Energy & Fuels* **2006**, *20*, 848–889.
- (28) Liu, Q.; Wang, S.; Zheng, Y.; Luo, Z.; Cen, K. Mechanism Study of Wood Lignin Pyrolysis by Using TG-FTIR Analysis. *J. Anal. Appl. Pyrolysis* **2008**, *82*, 170–177.
- (29) Manyà, J. J. Pyrolysis for Biochar Purposes: A Review to Establish Current Knowledge Gaps and Research Needs. *Environ. Sci. Technol.* **2012**, *46*, 7939–7954.
- (30) Lehmann, J.; Joseph, S. Biochar for Environmental Management: An Introduction. In *Biochar for Environmental Management*; Eartschan, 2009; pp 1–10.
- (31) Sohi, S.; Lopez-Capel, S.; Krull, E.; Bol, R. *Biochar, Climate Change and Soil: A Review to Guide Future Research*; 2009.
- (32) Lehmann, J. A Handful of Carbon. *Nature* **2007**, *447*, 143–144.
- (33) Laird, A. D. The Charcoal Vision: A Win-Win-Win Scenario for Simultaneously Producing Bioenergy, Permanently Sequestering Carbon, While Improving Soil and Water Quality. *Agron. J.* **2008**, *100*, 178–181.
- (34) Fowles, M. Black Carbon Sequestration as an Alternative to Bioenergy. *Biomass and Bioenergy* **2007**, *31*, 426–432.
- (35) Gaunt, J. L.; Lehmann, J. Energy Balance and Emissions Associated with Biochar Sequestration and Pyrolysis Bioenergy Production. *Environ. Sci. Technol.* **2008**, *42*, 4152–4158.
- (36) Swift, R. S. Sequestration of Carbon by Soil. *Soil Sci.* **2001**, *166*, 858–871.
- (37) Nguyen, B. T.; Lehmann, J.; Kinyangi, J.; Smernik, R. J.; Riha, S.; Engelhard, M. H. Long-Term Black Carbon Dynamics in Cultivated Soil. *Biogeochemistry* **2009**, *92*, 163–176.
- (38) McHenry, M. P. Agricultural Bio-Char Production, Renewable Energy Generation and Farm Carbon Sequestration in Western Australia: Certainty, Uncertainty and Risk. *Agric. Ecosyst. Environ.* **2009**, *129*, 1–7.
- (39) Basu, P. *Biomass Gasification, Pyrolysis and Torrefaction*; Elsevier Applied Science: Burlington, 2013.
- (40) Antal, M. J.; Gronli, M. The Art, Science, and Technology of Charcoal Production. *Ind. Eng. Chem. Res.* **2003**, *42*, 1619–1640.
- (41) Industrial Charcoal Production, TCP/CRO/3101 (A) Development of a Sustainable Charcoal Industry. In *Food and Agriculture Organization of the United Nations (FAO)*; Zagreb, Croatia, 2008.
- (42) Hao, W.; Björkman, E.; Lilliestråle, M.; Hedin, N. Activated Carbons Prepared from Hydrothermally Carbonized Waste Biomass Used as Adsorbents for CO<sub>2</sub>. *Applied Energy*. 2013, pp 526–532.
- (43) Demiral, I.; Şensöz, S. Fixed-Bed Pyrolysis of Hazelnut (*Corylus Avellana* L.) Bagasse: Influence of Pyrolysis Parameters on Product Yields. *Energy Sources* **2006**, *28*, 1149–1158.
- (44) Mythili, R.; Venkatachalam, P.; Subramanian, P.; Uma, D. Characterization of Bioresidues for Bio-Oil Production through Pyrolysis. *Bioresour. Technol.* **2013**, *138*, 71–78.
- (45) Yang, H.; Yan, R.; Chen, H.; Lee, D. H.; Zheng, C. Characteristics of Hemicellulose, Cellulose and Lignin Pyrolysis. *Fuel* **2007**, *86*, 1781–1788.
- (46) Varma, A. K.; Mondal, P. Pyrolysis of Sugarcane Bagasse in Semi Batch Reactor: Effects of Process Parameters on Product Yields and Characterization of Products. *Ind. Crops Prod.* **2017**, *95*, 704–717.
- (47) Bridgwater, A. V. Review of Fast Pyrolysis of Biomass and Product Upgrading. *Biomass and Bioenergy* **2012**, *38*, 68–94.
- (48) Sadaka, S.; Negi, S. Improvements of Biomass Physical and Thermochemical Characteristics via Torrefaction Process. *Environ. Prog. Sustain. Energy* **2009**, *28*, 427–434.
- (49) Yang, Y.; Brammer, J. G.; Ouadi, M.; Samanya, J.; Hornung, A.; Xu, H. M.; Li, Y. Characterisation of Waste Derived Intermediate Pyrolysis Oils for Use as Diesel Engine Fuels. *Fuel* **2013**, *103*, 247–257.
- (50) López-Ordovás, J. *Industrial-Scale Waste Pyrolysis in a Novel Pyrolysis Reactor*; 2018.
- (51) Garcia-Nunez, J. A.; Pelaez-Samaniego, M. R.; Garcia-Perez, M. E.; Fonts, I.; Abrego, J.; Westerhof, R. J. M.; Garcia-Perez, M. Historical Developments of Pyrolysis Reactors: A Review. *Energy & Fuels* **2017**, *31*, 5751–5775.
- (52) Kolokolova, O.; Levi, T.; Pang, S. Torrefaction and Pyrolysis of Biomass Waste in Continuous Reactors. In *Proceedings of the 13th International Conference on Environmental Science and Technology*; 2013.
- (53) Arias, B.; Pevida, C.; Feroso, J.; Plaza, M. G.; Rubiera, F.; Pis, J. J. Influence of Torrefaction on the Grindability and Reactivity of Woody Biomass. *Fuel Process. Technol.* **2008**, *89*, 169–175.
- (54) Zhang, L.; Chunbao, X.; Champagne, P. Overview of Recent Advances in Thermo-Chemical Conversion of Biomass. *Energy Convers. Manag.* **2010**, *51*, 969–982.
- (55) Yanik, J.; Kornmayer, C.; Saglam, M.; Yüksel, M. Fast Pyrolysis of Agricultural Wastes: Characterization of Pyrolysis Products. *Fuel Process. Technol.* **2007**, *88*, 942–947.

- (56) Duman, G.; Okutucu, C.; Ucar, S.; Stahl, R.; Yanik, J. The Slow and Fast Pyrolysis of Cherry Seed. *Bioresour. Technol.* **2011**, *102*, 1869–1878.
- (57) Scala, F.; Chirone, R.; Salatino, P. Combustion and Attrition of Biomass Chars in a Fluidized Bed. *Energy & Fuels* **2006**, *20*, 91–102.
- (58) Nunoura, T.; Wade, S. R.; Bourke, J.; Antal, M. J. Studies of the Flash Carbonization Process. 1. Propagation of the Flaming Pyrolysis Reaction and Performance of a Catalytic Afterburner. *Ind. Eng. Chem. Res.* **2006**, *45*, 585–599.
- (59) Wade, S. R.; Nunoura, T.; Antal, M. J. Studies of the Flash Carbonization Process. 2. Violent Ignition Behavior of Pressurized Packed Beds of Biomass: A Factorial Study. *Ind. Eng. Chem. Res.* **2006**, *45*, 3512–3519.
- (60) Antal, M. J.; Mochidzuki, K.; Paredes, L. S. Flash Carbonization of Biomass. *Ind. Eng. Chem. Res.* **2003**, *42*, 3690–3699.
- (61) Pan, Y. G.; Velo, E.; Roca, F. X.; Manyà, J. J.; Puigjaner, L. Fluidized-Bed Co-Gasification of Residual Biomass. *Fuel* **2000**, *79*, 1317–1326.
- (62) Rezaian, J.; Cheremisinoff, N. P. *Gasification Technologies - A Primer for Engineers and Scientists*; CRC Press: Boca Raton, 2005.
- (63) Brewer, C. E.; Schmidt-Rohr, K.; Satrio, J. A.; Brown, R. C. Characterization of Biochar from Fast Pyrolysis and Gasification Systems. *Environ. Prog. Sustain. Energy* **2009**, *28*, 386–396.
- (64) Fernandes, M. B.; Brooks, P. Characterization of Carbonaceous Combustion Residues: II. Nonpolar Organic Compounds. *Chemosphere* **2003**, *53*, 447–458.
- (65) Resende, F. L. P. Recent Advances on Fast Hydrolysis of Biomass. *Catal. Today* **2016**, *269*, 148–155.
- (66) Thangalazhy-Gopakumar, S.; Adhikari, S.; Gupta, R. B. Catalytic Pyrolysis of Biomass over H+ZSM-5 under Hydrogen Pressure. *Energy Fuels* **2012**, *26*, 5300–5306.
- (67) Melligan, F.; Hayes, M. H. B.; Kwapinski, W.; Leahy, J. J. A Study of Hydrogen Pressure during Hydrolysis of Miscanthus x Giganteus and Online Catalytic Vapour Upgrading with Ni on ZSM-5. *J. Anal. Appl. Pyrolysis* **2013**, *103*, 369–377.
- (68) Krishna, B. B.; Biswas, B.; Ohri, P.; Kumar, J.; Singh, R.; Bhaskar, T. Pyrolysis of Cedrus Deodara Saw Mill Shavings in Hydrogen and Nitrogen Atmosphere for the Production of Bio-Oil. *Renew. Energy* **2016**, *98*, 238–244.
- (69) Singh, R.; Krishna, B. B.; Mishra, G.; Kumar, J.; Bhaskar, T. Strategies for Selection of Thermo-Chemical Processes for the Valorisation of Biomass. *Renew. Energy* **2016**, *98*, 226–237.
- (70) Mašek, O.; Brownsort, P.; Cross, A.; Sohi, S. Influence of Production Conditions on the Yield and Environmental Stability of Biochar. *Fuel* **2013**, *103*, 151–155.
- (71) Ronsse, F.; van Hecke, S.; Dickinson, D.; Prins, W. Production and Characterization of Slow Pyrolysis Biochar: Influence of Feedstock Type and Pyrolysis Conditions. *GCB Bioenergy* **2013**, *5*, 104–115.
- (72) Di Blasi, C.; Signorelli, G.; Di Russo, C.; Rea, G. Product Distribution from Pyrolysis of Wood and Agricultural Residues. *Ind. Eng. Chem. Res.* **1999**, *38*, 2216–2224.
- (73) Demirbaş, A. Effects of Temperature and Particle Size on Bio-Char Yield from Pyrolysis of Agricultural Residues. *J. Anal. Appl. Pyrolysis* **2004**, *72*, 243–248.
- (74) Abdullah, H.; Wu, H. Biochar as a Fuel: 1. Properties and Grindability of Biochars Produced from the Pyrolysis of Mallee Wood under Slow-Heating Conditions. *Energy Fuels* **2009**, *23*, 4174–4181.
- (75) Méndez, A.; Terradillos, M.; Gascó, G. Physicochemical and Agronomic Properties of Biochar from Sewage Sludge Pyrolysed at Different Temperatures. *J. Anal. Appl. Pyrolysis* **2013**, *102*, 124–130.
- (76) Antal, M. J., J.; Allen, S. G.; Dai, X.; Shimizu, B.; Tam, M. S.; Gronli, M. Attainment of the Theoretical Yield of Carbon from Biomass. *Ind. Eng. Chem. Res.* **2000**, *39*, 4024–4031.
- (77) Enders, A.; Hanley, K.; Whitman, A.; Joseph, S.; Lehmann, J. Characterization of Biochars to Evaluate Recalcitrance and Agronomic Performance. *Bioresour. Technol.* **2012**, *114*, 644–653.
- (78) Zhao, L.; Cao, X.; Mašek, O.; Zimmerman, A. Heterogeneity of Biochar Properties as a Function of Feedstock Sources and Production Temperatures. *J. Hazard. Mater.* **2013**, *256–257*, 1–9.
- (79) Manyà, J. J.; Roca, F. X.; Perales, J. F. J. TGA Study Examining the Effect of Pressure and Peak Temperature on Biochar Yield during Pyrolysis of Two-Phase Olive Mill Waste. *Anal. Appl. Pyrolysis* **2013**, *103*, 86–95.
- (80) McBeath, A. V.; Smernik, R. J.; Schneider, M. P. W.; Schmidt, M. W. I.; Plant, E. L. Determination of the Aromaticity and the Degree of Aromatic Condensation of a Thermosequence of Wood Charcoal Using NMR. *Org. Geochem.* **2011**, *42*, 1194–1202.
- (81) Wu, W.; Yang, M.; Feng, Q.; McGrouther, K.; Wang, H.; Lu, H.; Chen, Y. Chemical Characterization of Rice Straw-Derived Biochar for Soil Amendment. *Biomass and Bioenergy* **2012**, *47*, 268–276.
- (82) Sun, H.; Hockaday, W. C.; Masiello, C. A.; Zygourakis, K. Multiple Controls on the Chemical and Physical Structure of Biochars. *Ind. Eng. Chem. Res.* **2012**, *51*, 3587–3597.
- (83) Ghani, W. A. W. A. K.; Mohd, A.; da Silva, G.; Bachmann, R. T.; Taufiq-Yap, Y. H.; Rashid, U.; Al-Muhtaseb, A. H. Biochar Production from Waste Rubber-Wood-Sawdust and Its Potential Use in C Sequestration: Chemical and Physical Characterization. *Ind. Crops Prod.* **2013**, *44*, 18–24.
- (84) McBeath, A. V.; Wurster, C. M.; Bird, M. I. Influence of Feedstock Properties and Pyrolysis Conditions on Biochar Carbon Stability as Determined by Hydrogen Pyrolysis. *Biomass Bioenergy* **2015**, *73* (155–173).

- (85) Manyà, J. J.; Laguarda, S.; Ortigosa, M. A.; Manso, J. A. Biochar from Slow Pyrolysis of Two-Phase Olive Mill Waste: Effect of Pressure and Peak Temperature on Its Potential Stability. *Energy Fuels* **2014**, *28*, 3271–3280.
- (86) Rousset, P.; Figueiredo, C.; De Souza, M.; Quirino, W. Pressure Effect on the Quality of Eucalyptus Wood Charcoal for the Steel Industry: A Statistical Analysis Approach. *Fuel Process. Technol.* **2011**, *92*, 1890–1897.
- (87) Antal, M. J., Jr.; Croiset, E.; Dai, X.; DeAlmeida, C.; Mok, W. S.; Norberg, N.; Richard, J. R.; Al Majthoub, M. High-Yield Biomass Charcoal. *Energy Fuels* **1996**, *10*, 652–658.
- (88) Noumi, E. S.; Blin, J.; Valette, J.; Rousset, P. Combined Effect of Pyrolysis Pressure and Temperature on the Yield and CO<sub>2</sub> Gasification Reactivity of Acacia Wood in Macro-TG. *Energy Fuels* **2015**, *29*, 7301–7308.
- (89) Recari, J.; Berruoco, C.; Abellò, S.; Montané, D.; Farriol, X. Effect of Temperature and Pressure on Characteristics and Reactivity of Biomass-Derived Chars. *Bioresour. Technol.* **2014**, *170*, 204–210.
- (90) Qian, Y.; Zhang, J.; Wang, J. Pressurized Pyrolysis of Rice Husk in an Inert Gas Sweeping Fixed-Bed Reactor with a Focus on Bio-Oil Deoxygenation. *Bioresour. Technol.* **2014**, *174*, 95–102.
- (91) Azuara, M.; Sáiz, E.; Manso, J. A.; García-Ramos, F. J.; Manyà, J. J. Study on the Effects of Using a Carbon Dioxide Atmosphere on the Properties of Vine Shoots-Derived Biochar. *J. Anal. Appl. Pyrolysis* **2017**, *124*, 719–725.
- (92) Biswas, B.; Singh, R.; Kumar, J.; Singh, R.; Gupta, P.; Krishna, B. B.; Bhaskar, T. Pyrolysis Behavior of Rice Straw under Carbon Dioxide for Production of Bio-Oil. *Renew. Energy* **2018**, *129*, 678–685.
- (93) Lee, J.; Yang, X.; Cho, S. H.; Kim, J. K.; Lee, S. S.; Tsang, D. C. W.; Ok, Y. S.; Kwon, E. E. Pyrolysis Process of Agricultural Waste Using CO<sub>2</sub> for Waste Management, Energy Recovery, and Biochar Fabrication. *Appl. Energy* **2017**, *185*, 214–222.
- (94) Mok, W. S.; Antal, M. J.; Szabo, P.; Varhegyi, G.; Zelei, B. Formation of Charcoal from Biomass in a Sealed Reactor. *Ind. Eng. Chem. Res.* **1992**, *31*, 1162–1166.
- (95) Di Blasi, C.; Branca, C.; Santoro, A.; Hernandez, E. G. Pyrolytic Behavior and Products of Some Wood Varieties. *Combust. Flame* **2001**, *124*, 165–177.
- (96) Dai, X.; Antal, M. J. Synthesis of a High-Yield Activated Carbon by Air Gasification of Macadamia Nut Shell Charcoal. *Ind. Eng. Chem. Res.* **1999**, *38*, 3386–3395.
- (97) Varhegyi, G.; Szabo, P.; Mok, W. S.; Antal, M. J. Kinetics of the Thermal Decomposition of Cellulose in Sealed Vessels at Elevated Pressures. Effects of the Presence of Water on the Reaction Mechanism. *J. Anal. Appl. Pyrolysis* **1993**, *26*, 159–174.
- (98) Raveendran, K.; Ganesh, A.; Khilar, K. C. Influence of Mineral Matter on Biomass Pyrolysis Characteristics. *Fuel* **1995**, *74*, 1812–1822.
- (99) Di Blasi, C.; Galgano, A.; Branca, C. Effects of Potassium Hydroxide Impregnation on Wood Pyrolysis. *Energy & Fuels* **2009**, *23*, 1045–1054.
- (100) Wang, Z.; Wang, F.; Cao, J.; Wang, J. Pyrolysis of Pine Wood in a Slowly Heating Fixed-Bed Reactor: Potassium Carbonate versus Calcium Hydroxide as a Catalyst. *Fuel Process. Technol.* **2010**, *91*, 942–950.
- (101) Wang, D.; Xiao, R.; Zhang, H.; He, G. Comparison of Catalytic Pyrolysis of Biomass with MCM-41 and CaO Catalysts by Using TGA–FTIR Analysis. *J. Anal. Appl. Pyrolysis* **2010**, *89*, 171–177.
- (102) Manyà, J. J.; Alvira, D.; Azuara, M.; Bernin, D.; Hedin, N. Effects of Pressure and the Addition of a Rejected Material from Municipal Waste Composting on the Pyrolysis of Two-Phase Olive Mill Waste. *Energy & Fuels* **2016**, *30*, 8055–8064.
- (103) Şensöz, S.; Kaynar, I. Bio-Oil Production from Soybean (Glycine Max L.): Fuel Properties of Bio-Oil. *Ind. Crops Prod.* **2006**, *23*, 99–105.
- (104) Şensöz, S.; Angin, D.; Yorgun, S. Influence of Particle Size on the Pyrolysis of Rapeseed (Brassica Napus L.): Fuel Properties of Bio-Oil. *Biomass Bioenergy* **2000**, *19*, 271–279.
- (105) Encinar, J. M.; Gonzalez, J. F. Fixed-Bed Pyrolysis of Cynara Carduncules L., Product Yields and Compositions. *Fuel Process. Technol.* **2000**, *68*, 209–222.
- (106) Manyà, J. J.; Ruiz, J.; Arauzo, J. Some Peculiarities of Conventional Pyrolysis of Several Agricultural Residues in a Packed Bed Reactor. *Ind. Eng. Chem. Res.* **2007**, *46*, 9061–9070.
- (107) Varhegyi, G.; Szabo, P.; Till, F.; Zelei, B.; Antal, M. J.; Dai, X. TG, TG-MS, and FTIR Characterization of High-Yield Biomass Charcoals. *Energy Fuels* **1998**, *12*, 969–974.
- (108) Stenseng, M.; Jensen, A.; Dam-Johansen, K. Investigation of Biomass Pyrolysis by Thermogravimetric Analysis and Differential Scanning Calorimetry. *J. Anal. Appl. Pyrolysis* **2001**, *58*, 765–780.



## Pyrolysis of biomass and wastes in a continuous screw reactor for char production

Filipe Rego, Jiawei Wang, Yang Yang, Anthony V. Bridgwater

*European Bioenergy Research Institute (EBRI), School of Engineering and Applied Science, Aston University, Birmingham, B4 7ET, UK*

### Abstract

This chapter addresses the pyrolysis of biomass and wastes, with a focus on processes with the objective of continuous production of the solid product, char. The different types of pyrolysis processes are described, along with a characterisation of the products. Some of the properties and applications of the char product are described, focusing on the potential uses in soil and for adsorption, along with a brief description of the process of activation. The recent research on the use of screw reactors for the pyrolysis of biomass and wastes is reviewed, and the potential, advantages and disadvantages of this type of reactor are also discussed. Some screw reactor systems, such as the lab-scale and the pilot-scale Pyroformer systems at Aston University, are described.

### 1. Introduction

Nowadays it is clear that there are several problems related to the way energy and resources are produced and handled. The generation of energy and products from fossil fuels is releasing greenhouse gases and other pollutants to the environment, leading to increasing ocean acidity, climate change, and risks to fauna and flora worldwide. It is also known that resources are being consumed at an unsustainable pace, and, furthermore, there is an urgent need to reduce the growing amount of waste that is produced all over the world. Therefore, there is a necessity for investment in “clean” technologies, besides solar, wind and others, which can produce the energy and products we use daily, utilising renewable or sustainable resources such as biomass or wastes.

Pyrolysis is an example of the technologies that can be used for these purposes, and it has been known and used for centuries, for the production of charcoal, for example. Recently, there has been an increase in pyrolysis-related research, with the aim at producing biofuels and other valuable products, and some commercial applications with this objective are in place. Solid, liquid and gas products are obtained from the pyrolysis process, with different yields and quality depending on factors such as feedstock and process conditions. Although all of the pyrolysis products are useful, the solid product is particularly interesting due to the broad spectrum of applications: energy production, soil applications, removal of contaminants from water and gas streams, among many other uses.

### 2. Pyrolysis of biomass and wastes

#### 2.1. Characteristics of biomass and wastes

Biomass and wastes are two interconnected groups of resources, with various subtypes. Biomass can be categorised into woody, herbaceous, algal, and waste-based biomass. Woody biomass covers woody products and the residues derived from wood and forestry industries (branches, leaves, bark, sawdust, etc.). Crops and plant species such as wheat, corn, switchgrass,

sugarcane, and many others, compose the herbaceous biomass. The biofuels produced from these crops are the so-called first generation biofuels, but there is a concern that producing these crops leads to competition with food production, and other negative effects, such as over-occupation of land.<sup>1,2</sup> The wastes from the processing of these herbaceous crops (straw, husk, stover, etc.) can also be used, producing the second generation biofuels.<sup>1</sup> The so-called third generation biofuels are produced from algal biomass (micro and macroalgae).<sup>3</sup> The wastes from activities such as farming, food production and consumption, the paper industry, water treatment plants and other activities (e.g., pruning and food residues, sewage sludge), are also considered as biomass.

Biomass and wastes are resources available all over the world, and can be converted by biochemical and thermochemical processes into valuable biofuels or chemicals, promoting the sustainability of resources. What is obtained from the processing of biomass and wastes depends on the composition of the feedstock and the process route and conditions.

As mentioned and described in Chapter 1, biomass is a widely available resource, consisting of a collection of lignocellulosic compounds and other minor components (extractives, inorganics, and proteins).

Non-biological wastes can be made up of many different materials, including plastics, textiles, paper, wood and other lignocellulosic materials. The distribution of these materials in waste has wide variation according to: the origin and collection method, how the wastes were processed, etc. These wastes are inherently heterogeneous materials in comparison with biomass.

Wastes from the consumption of plastics, textiles, and other materials from household, commercial and industrial origin are generated worldwide in large quantities. The wastes that are not separated, recycled and reused (the main strategy that should be used), can be used for energy production, avoiding the process of landfilling. In some cases, they are processed in dedicated facilities to produce Refuse-Derived Fuel (RDF), using a series of steps, including shredding, screening, separation of inerts and metals.<sup>4</sup> RDF, usually pelletised, is used in some coal power plants

and also in the cement industry for energy production. Pyrolysis is another option to obtain energy (and other products) from RDF.

A very important constituent of biomass and wastes is the inorganic matter. The inorganic material exists in the form of carbonates, sulphates, oxalates, oxides, and others<sup>5</sup>, and many different inorganic elements can be present, usually consisting of Ca, K, Mg, Na, P, Cl, Si and S, and also Fe, Mn, Al, and others.<sup>6</sup> In biomass, many of the inorganic elements are essential for the growth of plants, especially the nutrients Ca, K and Mg<sup>7</sup>, and also N and P (main constituents of fertilisers, along with K).<sup>8</sup> The compounds with the elements Na, K, Ca, and Mg, are the so-called alkali and alkaline earth minerals (AAEM), due to being formed with elements from the first and second groups of the periodic table, and they have an important effect in the pyrolysis process. It should also be noted that high temperatures can cause chemical reactions between inorganic compounds, forming other compounds (such as silicates, sulphates, phosphates, etc.), which can cause slagging, fouling and corrosion problems in equipment such as boilers, heat exchangers, and piping.<sup>9</sup>

Wastes such as sewage sludge can have a significant amount of inorganic materials and even of heavy metals, compared to lignocellulosic biomass, and this will affect the products and yields during the thermal processing.

Another important constituent of both biomass and wastes is moisture, which affects storage, transport, handling, and processes such as drying and conversion. A relatively high moisture content can render a thermochemical process economically unfavourable due to the energy needed for drying.

When processing biomass or wastes via pyrolysis, each group of components have different behaviours in the thermochemical process. The composition of biomass and wastes relates to their physicochemical properties, and their knowledge is fundamental for the design and implementation of logistics, pre-treatment, and conversion processes.<sup>10</sup>

## 2.2. The pyrolysis process

As already introduced in Chapter 1, pyrolysis is a thermochemical process in which a material is exposed to heat in an oxygen-limited atmosphere, and produces gaseous, liquid and solid products.<sup>11</sup> Combustion and gasification are other thermochemical processes, in which either an excess of oxygen or an amount below the stoichiometrically necessary for complete combustion is applied, respectively.<sup>11</sup> This higher proportion of oxygen in the process atmosphere leads to mainly obtaining gas products and solids (ash in the case of combustion), while pyrolysis obtains gas, solid, and liquid products, which is advantageous due to the value and possible applications of those products. Further differences are in terms of temperature, which in combustion and gasification needs to be higher than 700 °C, while in pyrolysis it can be as low as 400 °C.<sup>2</sup> The lower temperatures provide a lower heat requirement and energy consumption. Also, the risk of

slagging and fouling by inorganic species due to exposure to high temperatures can be reduced.

Pyrolysis can be applied to several types of materials, such as plastics and its derivatives, waste tires, coal, and biomasses.

In pyrolysis, the volatile matter of the material is broken down and produces vapours, which can then be partially condensed, forming the liquid and non-condensable gas products. The solid left behind is the solid product from pyrolysis, called char. An overall scheme of the pyrolysis process is represented in Figure 1.

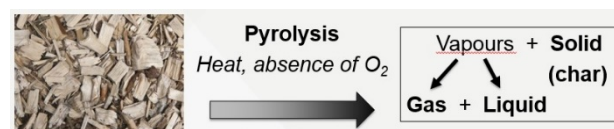
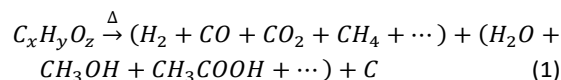


Figure 1. The process of pyrolysis.

The gas product is mainly composed of CO, CO<sub>2</sub>, CH<sub>4</sub>, H<sub>2</sub> and light hydrocarbons, and it can be used for heat and power generation in a gas turbine or engine.<sup>12</sup> The liquid product consists of, besides water, organic compounds such as sugars and their derivatives, acids, aldehydes, and others<sup>11</sup>, in an aqueous and an organic fraction<sup>13</sup>, which can be in a single phase or in two phases. The organic fraction can be upgraded into a biofuel and used for heat and power production.<sup>12</sup> In some cases, individual compounds can be extracted from the liquid, with applications for example in food flavouring and adhesives.<sup>14</sup> The solid product from pyrolysis, referred to as char, is a black and brittle material, with a high proportion of carbon and fixed carbon.<sup>15</sup> The pyrolysis products are sometimes used to provide the energy necessary for the process (e.g., heating the reactor and/or drying the feedstock<sup>11</sup>).

In the pyrolysis process, the feedstock undergoes a complex series of chemical reactions, with different activation energies and kinetics<sup>16</sup>. An overall reaction (over-simplified, not balanced) for the pyrolysis of biomass (represented by C<sub>x</sub>H<sub>y</sub>O<sub>z</sub>) is presented in Eq. 1<sup>17</sup>.



In Eq. 1, the first part of the product side corresponds to the gaseous products, the second part comprises the liquid product, and the third part (C, carbon) represents the solid product, char. The inorganic components of the feedstock (ash) mainly remain in the solid product.<sup>18</sup> In terms of water, it is present in the liquid product, originating from the feedstock moisture, and some water is produced by dehydration and other reactions (water of reaction).<sup>18, 19</sup> More details about the mechanism of degradation in pyrolysis can be found in Chapter 4 of this book.

The pyrolysis process can be influenced by a great variety of variables: the feedstock properties, the temperature and pressure, the residence times (of solids and vapours), the heat transfer method, and the atmosphere. Different combinations of these variables determine the product distributions and qualities.

Heat transfer is a feature with great influence on the pyrolysis process, governing the selection of the reactor type, the heating methods, the use of heat carriers, forms of the feedstock, etc. This has led to the classification of pyrolysis according to how fast the heat transfer occurs, which is in turn related to other parameters. Table 1 summarises different pyrolysis types and a relative comparison of typical process conditions, although there are other types (e.g., flash pyrolysis). In Table 1, *HR* stands for heating rate, *T* stands for temperature, *SRT* for solid residence time, and *VRT* for vapour residence time.

Fast pyrolysis allows to obtain a higher liquid yield, of up to 75 wt. % from wood (dry basis).<sup>12</sup> In the fast pyrolysis process, heat transfer must occur very rapidly and efficiently inside the reactor and within the feedstock particles. For this purpose, the feedstocks are processed with a small particle size, in the order of millimetres or lower.<sup>12</sup> The feedstock is also required to be dried, typically to a maximum water content of 10 wt. %, so as to reduce the process heat required and minimise water content in the liquid product.<sup>14</sup> To provide a faster heat transfer, heat carriers may also be employed in the reactor, for example, in the form of fine heated sand particles, heated steel shot, etc.<sup>12</sup>

The most used reactors for fast pyrolysis are of the fluidised bed type (bubbling and circulating), and other reactor types are the rotating cone, the ablative system, etc.<sup>20</sup> The solid residence time and of the vapours should be minimised, so as to prevent secondary reactions and to extract the maximum possible amount of condensable volatiles from the system and thus a higher liquid yield.<sup>12</sup> For this purpose, relatively high flow rates of inert carrier gas are usually used.

The liquid product from fast pyrolysis (also referred to as bio-oil) is typically dark brown and free flowing, with a distinctive smoky odour.<sup>14</sup> Its high heating value (HHV) is usually between 16 and 19 MJ kg<sup>-1</sup>, with typically 25 wt. % of water content.<sup>14</sup> Water content depends on production and collection methods, and its maximum value in the liquid product is indicated to reach 50 wt. %.<sup>12</sup> The heating value is about 40 % of diesel by weight, while it increases to about 60 % by volume, due to a relatively high density<sup>19</sup> of about 1.2 kg L<sup>-1</sup>. It has a substantial amount of organic acids, which results in an acidic pH which can be as low as 2, making it corrosive to construction materials such as carbon steel and aluminium.<sup>19</sup> The ASTM specification<sup>21</sup> for pyrolysis liquid for use in industrial burners states that the ash content should be below 0.25 wt. %, and the solid content below 2.5 wt. %. It has a relatively poor stability, due to continuous secondary reactions and to its high oxygen content (about 35-40 wt. %, similar to the original biomass)<sup>12</sup>. Due to this instability, its properties can change with time (i.e., aging); for example, viscosity is increased. Phase separation usually occurs with high water contents or due to long term storage, developing an upper aqueous and acidic phase, and a lower organic phase that is very viscous.<sup>19</sup>

**Table 1.** A comparison between pyrolysis types according to their typical process conditions.<sup>2, 12, 22</sup>

	HR	T	SRT	VRT
Slow pyrolysis	Low (under 1 °C s <sup>-1</sup> )	Approx. 400 °C	Long or very long (minutes to days)	Long (over seconds)
Intermediate pyrolysis	Medium	Approx. 500 °C	Long (minutes)	Medium (some seconds)
Fast pyrolysis	Very high (over 10 °C s <sup>-1</sup> )	Approx. 500 °C	Short (a few seconds or less)	Very short (under seconds)

Slow and intermediate pyrolysis, comparing with fast pyrolysis, have a more balanced production of all three pyrolysis products. Typical yields from these pyrolysis types (with wood as feedstock) are presented in Table 2. For char production, the employed temperatures and heating rates are relatively low, and solid residence times are in the order of minutes or higher<sup>15, 23</sup>, which is the case of slow and intermediate pyrolysis. In these processes, a higher contact time between the solid and the produced vapours contributes to a higher char yield through secondary chemical reactions<sup>14, 15</sup>. The use of larger particle sizes (e.g. chips, pellets) also contributes to char production<sup>15</sup>. Using larger feedstock particles is advantageous: it avoids mechanical operations of pre-treatment such as grinding, sieving, etc., increasing the overall process efficiency and reducing the carbon footprint, and adds flexibility to the pyrolysis process. Further advantages of the lower temperatures in slow and intermediate pyrolysis is a lower energy requirement, and a reduced risk of formation of inorganic species that can lead to slagging, fouling and corrosion, as well as reducing tar formation.<sup>24</sup>

The catalytic effect of alkali and alkaline earth metals (AAEM) on secondary reactions is undesired in fast pyrolysis, since it can lower liquid product yields. Therefore there has been significant research on reducing or minimising the AAEM content, usually by washing with water or an acid or alkaline solution<sup>25, 26</sup>. This pre-treatment could however adversely affect the biomass structure (i.e., hydrolysing the hemicellulose and cellulose), which will reduce liquid product yields.<sup>12</sup> For slow and intermediate pyrolysis, however, where the liquid product is not the main focus, the catalytic effect of AAEM species is tolerated and therefore there is higher flexibility in terms of ash content in the feedstocks. Furthermore, the process of removing these species is time and resource consuming, leading to higher costs.

**Table 2.** Typical product yields (dry wood basis) from different pyrolysis types.<sup>14</sup>

	Liquid yield (wt. %)	Gas yield (wt. %)	Solid yield (wt. %)
Slow pyrolysis	30	35	35
Intermediate pyrolysis	50	25	25
Fast pyrolysis	75	13	12

An inert carrier gas is usually used in pyrolysis, to maintain an oxygen-free atmosphere, and, in the case of fast pyrolysis, to minimise contact time between the solid and product vapours. On the other hand, if liquid production is not the main focus, the carrier gas may be absent during operation. Using carrier gas also leads to dilution of the produced gas<sup>27</sup>, which reduces its calorific value. Employing different flow rates of carrier gas and different gases can also affect the product distribution and quality.

### 3. Char properties, applications, and their relation with the process parameters

#### 3.1. General properties and applications of char

Char, as already mentioned, is the solid product from pyrolysis, mainly composed of carbon, and also hydrogen and oxygen, and inorganic elements. It is black in colour, dry, and brittle<sup>15</sup>. An example of a char produced from biomass pyrolysis is shown in Figure 2. Char is more stable than biomass, due to the loss of moisture and volatiles, and it can have a calorific value of about 30 MJ kg<sup>-1</sup>.<sup>15</sup>



**Figure 2.** Char produced from pyrolysis (600 °C, 3 min SRT) of wheat straw pellets in the lab scale screw reactor at Aston University.

Char has been historically used as a fuel for domestic heating and cooking, as well as in metallurgy for smelting (as the reducing agent)<sup>15</sup>. Besides these, char has been employed in soil conditioning and amendment (i.e., biochar), as an additive in cattle feed, as an activated carbon precursor, and there has been research for its use as a catalyst support, for electrochemical applications (e.g. for electrodes), and others<sup>43–45</sup>. Char is also a porous material, which can develop a microporous structure with potential for adsorption applications.<sup>28</sup>

Char for domestic heating (e.g. for cooking) typically has 20-30 wt. % (up to 40 wt. %) of volatile matter, whereas for metallurgical applications it should have a lower value

(<15 wt. %)<sup>15</sup>. Metallurgical applications require a reducing agent (carbon) with high purity.

For pyrolysis focused on the production of char, the most important measure of efficiency of the process is the fixed carbon yield<sup>15, 18, 29</sup>, given by Eq. 2, by multiplying the fixed carbon content in char (wt. %, dry ash-free basis) by the char yield (wt. %, dry ash-free feedstock basis). This measure is more advantageous than char yield or others, since it takes into account both the yield and quality of the solid product.<sup>30</sup>

$$y_{FC} = FC_{char}y_{char} \quad (2)$$

The fixed carbon yield is related to material stability, and so it is relevant for the solid product applications. For example, in combustion, it affects thermal stability, heat release, efficiency, etc., and in soil applications, it affects characteristics such as stability, recalcitrance, and carbon sequestration potential. It has been reported that the fixed carbon yield increases with pyrolysis temperature, up to a certain point, limited by the ash content and nature of the feedstock<sup>15</sup>. With an increase in pyrolysis temperature, more stable chemical structures are formed, making the solid more resistant to thermal and biological degradation.<sup>22</sup>

#### 3.2. Use of char for soil applications

Char can be a sustainable option for soils that have been adversely affected by factors such as intensive agricultural management practises and climate change.

Applying char from biomass pyrolysis in soils has been used to improve soil fertility and increase crop yields. Char can lead to a higher nutrient availability and retention, improvements in soil structure (e.g. density, porosity, stability), and water-holding capacity<sup>31</sup>. Char is usually found favourable for soils when it has certain qualities, including: high carbon content, high proportion of aromatic carbon (for stability), high chemical and biological stability, low density, high porosity and surface area, and high cation exchange capacity (CEC, proportional to availability of nutrients)<sup>32</sup>. Advantages of applying char in agriculture include carbon sequestration, interception of contaminants and improvement of plant growth.<sup>33</sup>

Char quality for soil applications can be improved by changing the pyrolysis parameters, but they can also have contradictory effects: higher temperatures (600-700 °C) lead to higher proportions of aromatic carbon and lower contents of H and O functional groups, at the same time lowering the CEC; on the other hand, relatively lower pyrolysis temperatures lead to a higher proportion of C-O and C-H functional groups, and thus a higher CEC<sup>32</sup>, but stability in terms of fixed-carbon is lower.

Chars can be used to increase the pH of acidic soils, since they are usually alkaline materials<sup>33</sup>. However, this is dependent on the ability of the char to retain its pH value (buffer capacity). Electrical conductivity, related to the ability of plants to extract water from the soil can also be relevant for soil applications<sup>33</sup>. The surface area, which is reported to increase with pyrolysis temperature<sup>30</sup>, is also related to exchange and sorption capacity<sup>33</sup>.

The addition of char to soils has also been found to avoid greenhouse gas emissions ( $\text{CH}_4$ ,  $\text{N}_2\text{O}$ ), possibly through better aeration and stability of the soils<sup>34</sup>. Furthermore, due to its adsorption capability, chars can help prevent leaching of compounds such as nitrates, phosphates, and other ionic solutes.<sup>31, 34</sup>

Recycling of nutrients (e.g., K, Mg, Ca, Na, and P) to the soil can be done if char is applied on them, with benefits for the soil and crops<sup>35</sup>. Regardless, the ash composition of the chars must be assessed in order to check for harmful heavy metals, which can pollute soil and water and be harmful to life.

Precautions should also be taken about the particle size of char for soil applications: it should not be very small (i.e., powder form), since it could be scattered in the air and cause health hazards. It should also be noted that the choice of a char for soil applications depends not only on the quality of the char, but also on the properties and needs of the soil.

### 3.3. Activated carbon

Although there have been examples of research using char for adsorption<sup>36, 37</sup>, the porosity and surface area of chars are relatively low (in the order of  $10^0$  to  $10^2$   $\text{m}^2$   $\text{g}^{-1}$ )<sup>38</sup>, compared with activated carbon (up to  $3000$   $\text{m}^2$   $\text{g}^{-1}$ )<sup>39</sup>. Producing activated carbon from char is an increasingly popular application, due to its usefulness for removal of pollutants, in both gaseous and aqueous streams<sup>40</sup>. Activated carbon had a market of about 1.6 Mton in 2015, and it grows regularly<sup>41</sup>. There has been an increasing interest in this application due to stricter environmental requirements in some countries such as the US, and promising results from research.<sup>40</sup>

Examples of specific applications of activated carbon in gas streams are in gas masks, in inhabited spaces such as offices, and in the purification of exhaust gases in industrial facilities. Activated carbon can also be used as an adsorption medium in the biogas production industry to separate unwanted gases such as  $\text{CO}_2$  and  $\text{H}_2\text{S}$  from the methane<sup>42</sup>. In terms of liquid streams, activated carbon has been used to remove components such as heavy metals, organic molecules (for example tetracycline, phenol), dyes, and others, in wastewater, pools and aquariums.

Activated carbon works with the process of adsorption, in which the target substance to be adsorbed gets concentrated in the interface between the adsorbent (activated carbon) and the bulk fluid with the substance<sup>43</sup>. This process is different than the process of absorption, in which chemical bonds are formed. Instead, intermolecular forces of attraction and repulsion are involved.

Adsorption is a capability of char that can be enhanced by activation. In the activation process, the physical structure of the char is altered: the porosity and surface area are greatly increased, with the disadvantage of consumption of some part of the material. With an increase in surface area, more molecules can be adsorbed on the surface. The process can be performed on the char from pyrolysis (2-step), or directly on the material before pyrolysis (1-step). Furthermore, activation is generally classified in physical or

chemical activation, although both types involve chemical reactions.

The activation conditions greatly affect the activated carbon properties (e.g., the temperature and time of activation, activating agent and proportion used, etc.<sup>39, 40</sup>). The starting material is also a very important factor.

Activated carbon usually originates from materials characterised by a high carbon content and hardness: coconut shell, coal, peat, etc.<sup>44</sup>. Activation is a process with a high production cost<sup>39</sup>, due to energy and resource needs. Because of this, interest is growing on the possibility of using other biomasses such as agricultural wastes in order to reduce costs and to benefit the environment<sup>39</sup>.

Chemical activation is done by mixing a concentrated solution of a chemical agent with the precursor (coal, biomass, or char if it is a 2-step activation), e.g. impregnating the precursor. The most commonly used chemical agents are  $\text{ZnCl}_2$ ,  $\text{H}_3\text{PO}_4$  and  $\text{KOH}$ <sup>45</sup>. The mechanism of chemical activation varies according to the activation agent, but the following principles are common<sup>45</sup>: chemical bonds in the precursor structure start to break during mixing, and ions from the activation agent bind to the surface and occupy voids, defining the porosity created in the subsequent activation. During activation, the chemical agent avoids formation of tars in the pores, and the pores become available post-activation, after washing the material to remove the activation agent. In this way, the porosity and specific surface area increase. However, at high activating agent doses or activation times, small pores can collapse and cause an adverse effect of a decrease in surface area. The peak temperatures to which the material is exposed in chemical activation are in general lower (as low as  $400$  °C) than in physical activation<sup>39</sup>.

In physical activation, the carbonaceous material undergoes partial oxidation to increase porosity and surface area, at temperatures usually above  $700$  °C<sup>44</sup>. The oxidant used is usually steam,  $\text{CO}_2$  or oxygen/air. The process occurs in two stages: firstly, tar is oxidised and clogged pores are opened; and secondly, part of the carbon structure is also oxidised. The second stage, besides creating new pores, or interconnections between pores, can also change the chemical functionalities of the surface. These functionalities include phenolic and carboxylic groups, created on the aromatic surfaces of the material. Since the physical activation normally occurs in two steps (carbonisation and then activation), there is a higher energy consumption and more equipment may be needed, compared with an activation process in one step (carbonisation and activation at the same time). Furthermore, if the char is cooled down between the two steps, it may adsorb some volatiles and tars from the surrounding atmosphere, which will reduce quality (plugging of pores for example). However, chemical activation also has disadvantages (e.g., the requirement of a washing step to remove the chemical agent, thus incurring in further costs and resource usage).

David and Kopac<sup>46</sup> studied the activation of chars from a mixture of rapeseed oil cake and walnut shell in pellet form. Pyrolysis was performed in a vertical fixed bed reactor, at temperatures between 400 and 750 °C, with 5 °C min<sup>-1</sup> heating rate and 60 min hold time at peak temperature. Activation was then performed with CO<sub>2</sub> atmosphere, with the same temperatures of 400 to 750 °C. It was found that the surface area and porosity of the activated carbons depended mainly on activation temperature and activation time. The surface areas (N<sub>2</sub>, BET method) obtained at 600 °C were between 300 and 500 m<sup>2</sup> g<sup>-1</sup> (0.5 to 3.5 h activation time), and 400 and 500 °C yielded small N<sub>2</sub> adsorption. A surface area up to around 1000 m<sup>2</sup> g<sup>-1</sup> was obtained at 750 °C and 3 h of activation time.

Using different atmospheres can have advantages such as increasing the concentration of combustible gases and thus its energy content (15 to 20 MJ m<sup>-3</sup> with steam)<sup>44</sup>. Furthermore, some studies have shown that using a CO<sub>2</sub> atmosphere in pyrolysis decreases the tar content in the solid, improving its quality<sup>47</sup>.

By injecting CO<sub>2</sub> and transforming it in the pyrolysis process, the release of this harmful greenhouse gas into the atmosphere can be reduced. There is much interest nowadays in methods for carbon capture and storage (CCS) and for utilising this gas in other processes, for which activated carbon production is a possibility. Using different carrier gases such as CO<sub>2</sub> in the pyrolysis process can also bring economic advantages, due to avoiding the use of nitrogen as carrier gas.

As a conclusion, to make the best use of char, the effect of different feedstocks and pyrolysis conditions must be better understood. Standardising char characteristics and analyses is very important, and there have been some examples, by the International Biochar Initiative (IBI)<sup>48</sup>, and by the European Biochar Foundation<sup>49</sup>, for char produced for soil applications (commonly referred to as biochar, if produced from biomass with certain characteristics).

Besides the environmental advantages of all applications of char from biomass, it can be a source of income, increasing the feasibility of the pyrolysis process and of the bioeconomy.

#### 4. Pyrolysis with screw reactors

Slow pyrolysis can be performed in many different types of systems. Early on, wood logs (or other biomass materials with a large particle size) were processed in batch systems: earth-made kilns, retorts, wagons, and other systems<sup>50</sup>. Continuous operation was then developed, along with using a smaller particle size (e.g., chips, pellets and crushed residues). Continuous mode systems improve the economics of the process, since less time is spent switching batches. Examples of continuous pyrolysis systems are rotary drums, paddle reactors, moving bed reactors, and screw (also called Auger) reactors<sup>50</sup>. The way of transporting the feed along the reactor changes between systems: by using rotation and inclination, in the case of rotary drums; using paddles or other similar tools; or using

a screw, in the case of Auger reactors. Further description of different reactors used for slow pyrolysis (in industrial scale) is done in Chapter 3.

A screw reactor is heated externally generally using a furnace, and in some cases heat carriers are employed to promote heat transfer inside the reactor (e.g., hot sand, steel particles or metal/ceramic spheres<sup>12</sup>). After being transported to the other end of the reactor, the solid product (char) and the heat carriers (if existent) exit the reactor by gravity into a container. The heat carriers are recycled into the reactor with an appropriate separation and transport system. The vapours that exit the reactor pass through a condensing system, where the condensable fraction forms the liquid product. An example representation of an Auger reactor is shown in Figure 3.

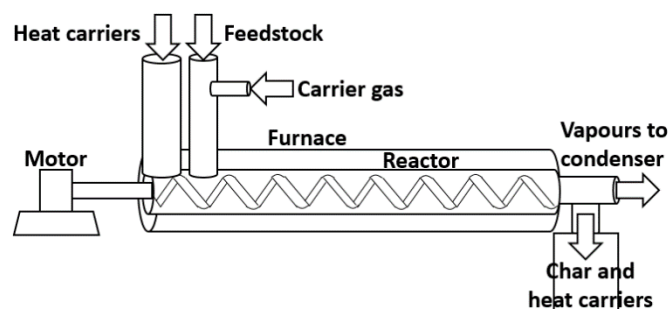


**Figure 3.** Generic scheme representing a typical Auger reactor.

Industrial use of Augers started in the beginning of the 20<sup>th</sup> century, in applications such as conveying, drying, and pyrolysis, firstly of coal. The first known reference<sup>51</sup> of biomass pyrolysis in a screw reactor was in 1969.

Comparing with other reactors, Auger reactors have some advantages. Besides continuous processing, the handling and operation are relatively simple<sup>52</sup>, and the design is compact, allowing for it to be more easily transported<sup>53</sup>. A study demonstrated the feasibility of using modular and transportable Auger reactors for pyrolysis of biomass, which allows for the production of energy in decentralised and/or remote areas<sup>54</sup>, and consequently reduces the costs if biomass is available on site.

Another study used an Auger reactor for continuous pyrolysis of forestry waste and demonstrated that the design was robust and that scaling-up was possible, supported by the fact that the feedstock did not require a significant particle size reduction (i.e., to powder), which makes the process more economic<sup>53</sup>. Auger reactors are in general more flexible to different feedstock types, shapes and sizes, and more adequate for heterogeneous materials<sup>12</sup>, and also the use of carrier gas is optional<sup>52</sup>. The ability to control the solid residence time by changing screw speed is also an advantage.

Some limitations of screw reactors are mechanical issues due to the moving parts, bearings and sealing exposed to high temperatures inside the reactor<sup>27</sup>, and the risk of blockage in the system, due to the accumulation of biomass and/or products inside the inlet, reactor tube or the outlet. Heat transfer also limits scale-up due to the design of the reactor<sup>27</sup>. Heating the screw and reactor tube

with larger dimensions becomes more difficult and energy-demanding.

There is significant research on pyrolysis in Auger reactors (although not as much as with for example fixed and fluidised beds), with important examples in universities in the US (e.g. Mississippi State, Iowa State), at the Karlsruhe Institute of Technology (KIT, Germany), at Ghent University (Belgium), and at the European Bioenergy Research Institute (Aston University, UK).

At Aston University there is a lab-scale ( $300 \text{ g h}^{-1}$ ) single screw Auger reactor. The reactor is a stainless steel cylindrical pipe with 83.5 cm length and internal diameter of about 2.5 cm, with a furnace covering about 40 cm of the pipe. The screw is driven by an electrical motor with controllable speed. The biomass is fed through a vertical inlet pipe, with a valve that can minimise air entrance, and with an input for nitrogen gas. In the system, temperature is monitored with thermocouples in four locations: inside the reactor tube (middle section), around the wall of the pipe, in the vapour exit (similar to the freeboard in a fluidised bed), and in the start of the condensing system. The solid transported along the reactor is collected in a pot, while the vapours go through the cooling system. The cooling/condensing system is comprised by a water-cooler (around  $5 \text{ }^\circ\text{C}$ ), two ice fingers with dry-ice, and a cotton filter for trapping aerosols. The produced gas can be analysed online using a micro-GC after passing through a gas flowmeter. The liquid products are collected in flasks for posterior analysis. The lab-scale screw reactor system at EBRI is represented in Figure 4.<sup>55</sup>

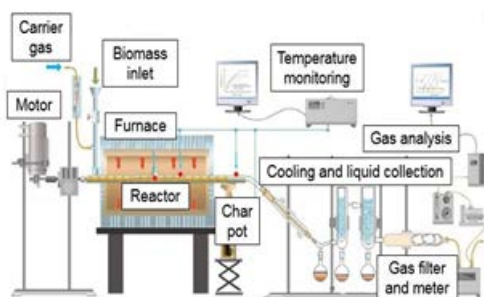


**Figure 4.** Lab-scale Auger reactor available at EBRI (Aston University).

Examples of pilot or demonstration scale Auger reactors that operate in slow or intermediate pyrolysis conditions are the Haloclean system, the Pyroformer, and the Thermo-Catalytic Reformer (TCR).

The Haloclean system was created in 2002 by the Italian company Sea Marconi and the German Forschungszentrum Karlsruhe<sup>56, 57</sup>. After being used for processing waste electronic and electrical equipment into fuels and noble metals<sup>58</sup>, it was found to be a suitable technology for biomass pyrolysis<sup>59</sup>. The system was claimed to produce less tars, a liquid and gas product with lower solids content, and lower acidity in the products, compared with a fast pyrolysis system<sup>59</sup>. A lab-scale system of  $3 \text{ kg h}^{-1}$  was developed, along with a pilot-scale  $100 \text{ kg h}^{-1}$  system<sup>56, 60</sup>. During operation, heat carriers (metal spheres) were employed, which are then separated

from the char, and recycled back to the system with a screw conveyor<sup>60</sup>. Multiple feedstocks were tested in the reactor to produce pyrolysis liquid, for example, coconut and rape residues, wheat straw, olive stones, and rice husk, with particle sizes up to 5 cm.<sup>56</sup>

The Pyroformer, patented in 2009, is a pilot-scale system installed and operated at Aston University<sup>61</sup>. This reactor, represented in Figure 5<sup>62</sup>, has a very important feature: it has two co-axial screws, instead of one screw as usual.

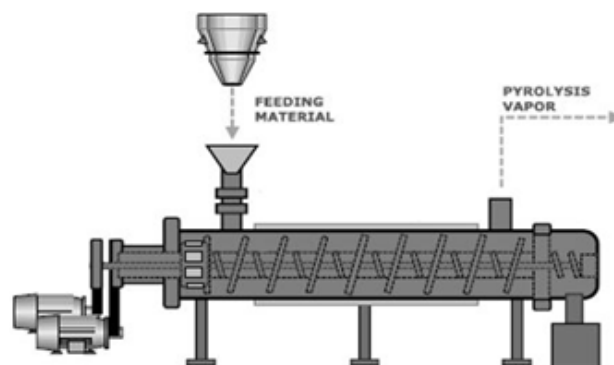


**Figure 5.** Representation of the Pyroformer system (adapted<sup>62</sup>).

These two screws can be moved independently and driven forwards and backwards, and there are slots through which material can pass from one screw to another. This feature allows to recycle char internally and to mix fresh feedstock with the recycled char, which acts both as a heat carrier and as a catalyst for char-producing secondary reactions<sup>24</sup>. The pilot-scale system has a processing capacity of up to  $20 \text{ kg h}^{-1}$ , and there is also a  $100 \text{ kg h}^{-1}$  demonstration system built at Aston University.

In the Pyroformer, the vapours produced leave the reactor and pass through two hot gas filter candles to remove solid particles. After that, the clean vapour passes through a shell and tube heat exchanger where it is condensed and the liquid is collected<sup>63</sup>. The non-condensable gases pass through an electrostatic precipitator (ESP) to remove aerosols, while the char product is collected at the bottom of the reactor in a char pot<sup>64</sup>. Generally, product yields from biomass are: 40-60 wt% of liquid, 15-25 wt% of char, and 20-30 wt% of gas<sup>62</sup>.

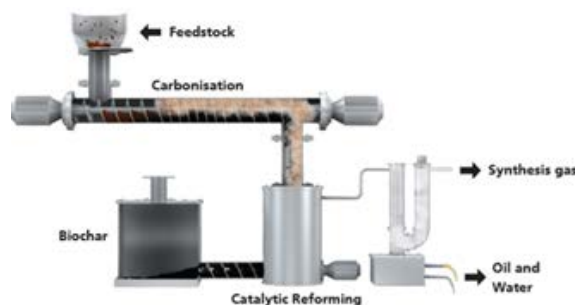


**Figure 6.** Representation of the TCR system.

More recently, the Thermo-Catalytic Reformer (TCR) system was developed in Germany by the Fraunhofer UMSICHT Institute. There are units installed in Germany ( $2 \text{ kg h}^{-1}$ ,  $30 \text{ kg h}^{-1}$ , and a  $300 \text{ kg h}^{-1}$ ), and in Tyseley Energy Park in Birmingham ( $30 \text{ kg h}^{-1}$ ).

The TCR system has a pyrolysis screw reactor combined with a post-reforming reactor. The feed is transported through the first reactor and the products from pyrolysis are directed into the secondary reactor. The char acts as a catalyst to upgrade the quality of the product vapours, before they pass through a condensation system and are separated into the liquid and gaseous products<sup>65</sup>. The pyrolysis reactor works at temperatures usually between 400 and 500 °C, while the reforming reactor operates between 500 and 750 °C. The system is said to be flexible to various feedstocks and with relatively high ash and moisture contents, producing products with improved quality<sup>66</sup>. A representation of the TCR is presented in Figure 6.<sup>67</sup>

There are some examples of commercial units, and, for example, the Canadian company ABRI-Tech develops 1 ton per day screw reactor units<sup>50</sup>. The German company Pyreg has also developed commercial screw reactors for pyrolysis, with units in Germany and Switzerland.<sup>68</sup>

In the literature, a limited number of studies focuses on char production from biomass in Auger reactors. It was also found that research mainly analyses the effect of a limited number of parameters, focusing in most cases on the peak temperature and the feedstock type, and in some cases on the solid residence time and the feedstock flow rate.

Since research with screw reactors mainly focused on liquid production (considered fast pyrolysis), most use a very small particle size (millimetres or lower), heat carriers, and carrier gas, to prevent extended contact between the volatiles and the solid that favours secondary reactions and thus char and gas production. The solid residence time used, however, is higher than in typical fast pyrolysis, and vapour residence times range from 5 to 30 s depending on design and size<sup>12</sup>. Screw reactors could therefore be a useful reactor to produce char in significant quantities. Char yields from Auger reactors with woody biomass are reported<sup>50</sup> to be between 17 and 30 wt. %.

In terms of feedstock, research mainly focused on woody biomass (mostly pine wood), and there are a few accounts of herbaceous biomasses being used: wheat straw (pellets)<sup>56</sup>, barley straw (pellets)<sup>64</sup>, rice husk and corn stalk<sup>55</sup>, switchgrass<sup>69</sup>, rice husk and bran<sup>56</sup>, and rapeseed<sup>56</sup>. Examples of wastes studied in Auger reactors are MSW<sup>70</sup>,<sup>71</sup>, digestate from anaerobic digestion<sup>66, 72, 73</sup>, tyres<sup>74</sup>, and wastes from the wastewater treatment industry (sewage sludge)<sup>75, 76</sup>, the paper industry (de-inking sludge)<sup>62, 77</sup>, and the brewing industry<sup>24</sup>. Some of these wastes were processed in pellet form: de-inking sludge and sewage sludge<sup>62, 77</sup>, paper sludge<sup>72</sup>, and digestate from anaerobic digestion.<sup>66, 72</sup>

A literature survey based on 21 articles found that over half (about 57%) were focusing on the liquid product production, and that mainly temperature, feedstock type and solid residence time were the process variables. A graphic representation of the proportion of articles (excluding the ones focusing on liquid production) that studied temperature, feedstock type, solid residence time, and feedstock flow rate is shown in Figure 7. Limited or no research was found on other parameters, for example, on

the particle size and form (e.g. pellet or powder form), and on the atmosphere inside the reactor.

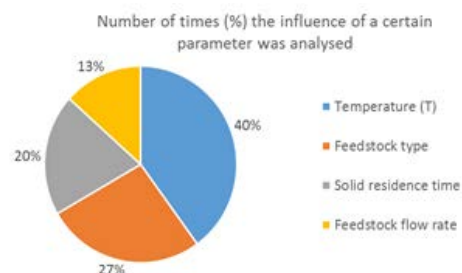


**Figure 7.** Proportion of articles that study different parameters of the pyrolysis of biomass and wastes in auger reactors, excluding the research that focuses on liquid production.

## Conclusions

Slow pyrolysis has been performed for a long time, at first (and still in many cases) with traditional and simple systems, which are not the most efficient or safe for the environment. More recent systems, such as the Auger (screw) reactor, have been developed for pyrolysis with advantages over other systems, e.g. continuous operation, simplicity of operation, flexibility for different particle sizes, among others. Char production can be enhanced by using optimised parameters such as temperature and solid residence time, taking into account char quality as well. The production of char and its derivatives has received increasing attention in terms of research, and many promising and valuable applications have been found, for example in soil treatment, adsorption, catalysis and for electrochemical applications.

The various and useful applications of char make it a worthwhile product and more research must be done in order to improve the understanding of the relation between its properties and production methods, and the feedstocks. As an example, activated carbon from char made from biomass or wastes brings economic and environmental benefits that can, among other things, increase the sustainability of resources.

The aim of the research of the GreenCarbon's Early-Stage Researcher #2 (F. Rego) is to study the pyrolysis of biomass and wastes in a continuous screw reactor, with a focus on the production of char. Objectives include assessing the influence of process parameters such as temperature and solid residence time on the product yields and properties, as well as the possible applications of the produced char. The production of a solid product suitable for use as an adsorbent of contaminants from aqueous solutions is also an objective.

## Acknowledgements

This project has received funding from the European Union's Horizon 2020 research and innovation programme under the Marie Skłodowska-Curie grant agreement No 721991.

## References

- (1) Hayes, D. J. M. Second-Generation Biofuels: Why They Are Taking so Long. *WIREs Energy Env.* **2013**, 2 (June), 304–334.
- (2) Tripathi, M.; Sahu, J. N.; Ganesan, P. Effect of Process Parameters on Production of Biochar from Biomass Waste through Pyrolysis: A Review. *Renew. Sustain. Energy Rev.* **2016**, 55, 467–481.
- (3) Alam, F.; Mobin, S.; Chowdhury, H. Third Generation Biofuel from Algae. In *6th BSME International Conference on Thermal Engineering (ICTE 2014)*; Elsevier B.V., 2015; Vol. 105, pp 763–768.
- (4) Ragland, K.; Bryden, K. *Combustion Engineering*, 2nd Ed.; Ragland, K., Bryden, K., Eds.; CRC Press, 2011.
- (5) Hon, D.; Shiraishi, N. *Wood and Cellulosic Chemistry*; Marcel Dekker, Inc.: New York, 1991.
- (6) Van Loo, S.; Koppejan, J. Chapter 8 - Biomass Ash Characteristics and Behaviour in Combustion Systems. In *The Handbook of Biomass Combustion and Co-firing*; Van Loo, S., Koppejan, J., Eds.; Earthscan, 2008.
- (7) Rowell, R. M.; Pettersen, R.; Han, J. S.; Rowell, J. S.; Tshabalala, M. A. Chapter 3 - Cell Wall Chemistry. In *Handbook of wood chemistry and wood composites*; Rowell, R. M., Ed.; CRC Press, 2005.
- (8) Maguire, R.; Mark, A.; Flowers, W. *Fertilizer Types and Calculating Application Rates*; 2009.
- (9) Holubcik, M.; Jandacka, J.; Malcho, M. Ash Melting Temperature Prediction from Chemical Composition of Biomass Ash. *Holist. Approach to Environ.* **2015**, 5, 119–125.
- (10) Cai, J.; He, Y.; Yu, X.; Banks, S. W.; Yang, Y.; Zhang, X.; Yu, Y.; Liu, R.; Bridgwater, A. V. Review of Physicochemical Properties and Analytical Characterization of Lignocellulosic Biomass. *Renew. Sustain. Energy Rev.* **2017**, 76 (March), 309–322.
- (11) Basu, P. *Biomass Gasification and Pyrolysis: Practical Design and Theory*; Elsevier Inc., 2010.
- (12) Bridgwater, A. V. Review of Fast Pyrolysis of Biomass and Product Upgrading. *Biomass and Bioenergy* **2012**, 38, 68–94.
- (13) Hossain, A. K.; Davies, P. A. Pyrolysis Liquids and Gases as Alternative Fuels in Internal Combustion Engines - A Review. *Renew. Sustain. Energy Rev.* **2013**, 21, 165–189.
- (14) Bridgwater, A. V. Renewable Fuels and Chemicals by Thermal Processing of Biomass. *Chem. Eng. J.* **2003**, 91 (2–3), 87–102.
- (15) Antal, M. J.; Grønli, M. The Art, Science, and Technology of Charcoal Production †. *Ind. Eng. Chem. Res.* **2003**, 42 (8), 1619–1640.
- (16) Radlein, D.; Quignard, A. A Short Historical Review of Fast Pyrolysis of Biomass. *Oil Gas Sci. Technol.* **2013**, 68 (4), 765–783.
- (17) Overend, R.; Milne, T.; Mudge, L. *Fundamentals of Thermochemical Conversion of Biomass*; Overend, R., Milne, T., Mudge, L., Eds.; Elsevier, 1985.
- (18) Di Blasi, C. Modeling Chemical and Physical Processes of Wood and Biomass Pyrolysis. *Prog. Energy Combust. Sci.* **2008**, 34 (1), 47–90.
- (19) Oasmaa, A.; Czernik, S. Fuel Oil Quality of Biomass Pyrolysis Oils - State of the Art for the End Users. *Energy Fuels* **1999**, 13 (4), 914–921.
- (20) Bridgwater, A. V. The Production of Biofuels and Renewable Chemicals by Fast Pyrolysis of Biomass. *Int. J. Glob. Energy Issues* **2007**, 27 (2), 160–203.
- (21) ASTM International. *ASTM D7544-09, Standard Specification for Pyrolysis Liquid Biofuel*; West Conshohocken, PA, 2009.
- (22) Demirbaş, A.; Arin, G. An Overview of Biomass Pyrolysis. *Energy Sources* **2002**, 24 (5), 471–482.
- (23) Demirbas, A. Biomass Resource Facilities and Biomass Conversion Processing for Fuels and Chemicals. *Energy Convers. Manag.* **2001**, 42, 1357–1378.
- (24) Mahmood, A. S. N.; Brammer, J. G.; Hornung, A.; Steele, A.; Poulston, S. The Intermediate Pyrolysis and Catalytic Steam Reforming of Brewers Spent Grain. *J. Anal. Appl. Pyrolysis* **2013**, 103, 328–342.
- (25) Banks, S. W.; Nowakowski, D. J.; Bridgwater, A. V. Impact of Potassium and Phosphorus in Biomass on the Properties of Fast Pyrolysis Bio-Oil. *Energy Fuels* **2016**, 30 (10), 8009–8018.
- (26) Eom, I. Y.; Kim, K. H.; Kim, J. Y.; Lee, S. M.; Yeo, H. M.; Choi, I. G.; Choi, J. W. Characterization of Primary Thermal Degradation Features of Lignocellulosic Biomass after Removal of Inorganic Metals by Diverse Solvents. *Bioresour. Technol.* **2011**, 102 (3), 3437–3444.
- (27) Bahng, M. K.; Mukarakate, C.; Robichaud, D. J.; Nimlos, M. R. Current Technologies for Analysis of Biomass Thermochemical Processing: A Review. *Anal. Chim. Acta* **2009**, 651 (2), 117–138.
- (28) Khalil, L. B. Porosity Characteristics of Chars Derived from Different Lignocellulosic Materials. *Adsorpt. Sci. Technol.* **1999**, 17 (9), 729–739.
- (29) Antal, M. J.; Allen, S. G.; Dai, X.; Shimizu, B.; Tam, M. S.; Grønli, M. Attainment of the Theoretical Yield of Carbon from Biomass. *Ind. Eng. Chem. Res.* **2000**, 39 (11), 4024–4031.
- (30) Manyà, J. J. Pyrolysis for Biochar Purposes: A Review to Establish Current Knowledge Gaps and Research Needs. *Environ. Sci. Technol.* **2012**, 46 (15), 7939–7954.
- (31) Tian, X.; Li, C.; Zhang, M.; Wan, Y.; Xie, Z.; Chen, B.; Li, W. Biochar Derived from Corn Straw Affected Availability and Distribution of Soil Nutrients and Cotton Yield. *PLoS One* **2018**, 13 (1), 1–19.
- (32) Li, Y.; Hu, S.; Chen, J.; Müller, K.; Li, Y.; Fu, W. Effects of Biochar Application in Forest Ecosystems on Soil Properties and Greenhouse Gas Emissions: A Review. *Springer* **2018**, 546–563.
- (33) Allaire, S.; Lange, S.; Auclair, I.; Quinche, M.; Greffard, L. *Analyses of Biochar Properties*; Quebec, 2015.
- (34) Lehmann, J.; Gaunt, J.; Rondon, M. Bio-Char Sequestration in Terrestrial Ecosystems - A Review. *Mitig. Adapt. Strateg. Glob. Chang.* **2006**, 11 (2), 403–427.
- (35) Lehmann, J.; Joseph, S. Biochar for Environmental Management: An Introduction. *Biochar Environ. Manag. - Sci. Technol.* **2009**, 1, 1–12.

- (36) Nartey, O. D.; Zhao, B. Biochar Preparation, Characterization, and Adsorptive Capacity and Its Effect on Bioavailability of Contaminants: An Overview. *Adv. Mater. Sci. Eng.* **2014**, 2014.
- (37) Wang, Y.; Liu, R. Comparison of Characteristics of Twenty-One Types of Biochar and Their Ability to Remove Multi-Heavy Metals and Methylene Blue in Solution. *Fuel Process. Technol.* **2017**, 160, 55–63.
- (38) Budai, A.; Wang, L.; Gronli, M.; Strand, L. T.; Antal, M. J.; Abiven, S.; Dieguez-Alonso, A.; Anca-Couce, A.; Rasse, D. P. Surface Properties and Chemical Composition of Corn cob and Miscanthus Biochars: Effects of Production Temperature and Method. *J. Agric. Food Chem.* **2014**, 62 (17), 3791–3799.
- (39) Dias, J. M.; Alvim-ferraz, M. C. M.; Almeida, M. F.; Sa, M. Waste Materials for Activated Carbon Preparation and Its Use in Aqueous-Phase Treatment : A Review. **2007**, 85, 833–846.
- (40) Schröder, E.; Thomauske, K.; Oechsler, B.; Herberger, S.; Baur, S.; Hornung, A. Chapter 18 - Activated Carbon from Waste Biomass. In *Progress in Biomass and Bioenergy Production*; Shaukat, S., Ed.; InTech, 2011.
- (41) Grand View Research Inc. *Activated Carbon Market Analysis and Segment Forecasts To 2024*; San Francisco, 2016.
- (42) Esteves, I. A. A. C.; Lopes, M. S. S.; Nunes, P. M. C.; Mota, J. P. B. Adsorption of Natural Gas and Biogas Components on Activated Carbon. *Sep. Purif. Technol.* **2008**, 62 (2), 281–296.
- (43) Rouquerol, F.; Rouquerol, J.; Sing, K. *Adsorption by Powders and Porous Solids - Principles, Methodology and Apps*; Academic Press, 1999.
- (44) Prauchner, M. J.; Rodríguez-Reinoso, F. Chemical versus Physical Activation of Coconut Shell: A Comparative Study. *Microporous Mesoporous Mater.* **2012**, 152, 163–171.
- (45) Hagemann, N.; Spokas, K.; Schmidt, H. P.; Kägi, R.; Böhler, M. A.; Bucheli, T. D. Activated Carbon, Biochar and Charcoal: Linkages and Synergies across Pyrogenic Carbon's ABCs. *Water (Switzerland)* **2018**, 10 (2), 1–19.
- (46) David, E.; Kopac, J. Activated Carbons Derived from Residual Biomass Pyrolysis and Their CO<sub>2</sub>adsorption Capacity. *J. Anal. Appl. Pyrolysis* **2014**, 110 (1), 322–332.
- (47) Dutta, T.; Kwon, E.; Bhattacharya, S. S.; Jeon, B. H.; Deep, A.; Uchimiya, M.; Kim, K. H. Polycyclic Aromatic Hydrocarbons and Volatile Organic Compounds in Biochar and Biochar-Amended Soil: A Review. *GCB Bioenergy* **2017**, 9 (6), 990–1004.
- (48) IBI, I. B. I. *Standardized Product Definition and Product Testing Guidelines for Biochar That Is Used in Soil*; 2015.
- (49) European Biochar Foundation (EBC). *European Biochar Certificate - Guidelines for a Sustainable Production of Biochar*; Arbaz, Switzerland, 2012.
- (50) Garcia-Nunez, J. A.; Pelaez-Samaniego, M. R.; Garcia-Perez, M. E.; Fonts, I.; Abrego, J.; Westerhof, R. J. M.; Garcia-Perez, M. Historical Developments of Pyrolysis Reactors: A Review. *Energy and Fuels* **2017**, 31 (6), 5751–5775.
- (51) Lakshmanan, C.; Gal-Or, B.; Hoelscher, H. Production Of Levoglucosan By Pyrolysis Of Carbohydrates. *I&EC Prod. Res. Dev.* **1969**, 8 (3), 261–267.
- (52) Thangalazhy-Gopakumar, S.; Adhikari, S.; Ravindran, H.; Gupta, R. B.; Fasina, O.; Tu, M.; Fernando, S. D. Physiochemical Properties of Bio-Oil Produced at Various Temperatures from Pine Wood Using an Auger Reactor. *Bioresour. Technol.* **2010**, 101 (21), 8389–8395.
- (53) Puy, N.; Murillo, R.; Navarro, M. V.; López, J. M.; Rieradevall, J.; Fowler, G.; Aranguren, I.; García, T.; Bartolí, J.; Mastral, A. M. Valorisation of Forestry Waste by Pyrolysis in an Auger Reactor. *Waste Manag.* **2011**, 31 (6), 1339–1349.
- (54) Badger, P. C.; Fransham, P. Use of Mobile Fast Pyrolysis Plants to Densify Biomass and Reduce Biomass Handling Costs - A Preliminary Assessment. *Biomass Bioenergy* **2006**, 30 (4), 321–325.
- (55) Yu, Y.; Yang, Y.; Cheng, Z.; Blanco, P. H.; Liu, R.; Bridgwater, A. V.; Cai, J. Pyrolysis of Rice Husk and Corn Stalk in Auger Reactor. 1. Characterization of Char and Gas at Various Temperatures. *Energy Fuels* **2016**, 30 (12), 10568–10574.
- (56) Roggero, C. M.; Tumiatti, V.; Scova, A.; De Leo, C.; Binello, A.; Cravotto, G. Characterization of Oils from Haloclean Pyrolysis of Biomasses. *Energy Sources, Part A Recover. Util. Environ. Eff.* **2011**, 33 (5), 467–476.
- (57) Hornung, A.; Bockhorn, H.; Appenzeller, K.; Roggero, C. M.; Tumiatti, W. Patent EP 1 217 318 A1 - Plant for the Thermal Treatment of Material and Operation Process Thereof. EP 1 217 318 A1, 2002.
- (58) Hornung, A.; Koch, W.; Seifert, H. Haloclean and PYDRA - a Dual Staged Pyrolysis Plant for the Recycling Waste Electronic and Electrical Equipment (WEEE). In *Metals and Energy Recovery: Internat.Symp.in Northern Sweden*; Skelleftea, 2003; p 7.
- (59) Sea Marconi. *Haloclean BioEnergy - Pyrolysis Liquid for Power Generation*; PyNe IEA Bioenergy, 2007.
- (60) Hornung, A.; Apfelbacher, A.; Koch, W.; Linek, K.; Sagi, S.; Schoner, J.; Stohr, J.; Seifert, H. Thermo-Chemical Conversion of Straw – Haloclean , an Optimised Low Temperature Pyrolysis. In *14th European Biomass Conference*; Paris, 2005; p 5.
- (61) Hornung, A.; Apfelbacher, A. EP2300560B1 - Thermal Treatment of Biomass. EP2300560B1, 2009.
- (62) Yang, Y.; Brammer, J. G.; Ouali, M.; Samanya, J.; Hornung, A.; Xu, H. M.; Li, Y. Characterisation of Waste Derived Intermediate Pyrolysis Oils for Use as Diesel Engine Fuels. *Fuel* **2013**, 103, 247–257.
- (63) Hornung, A.; Apfelbacher, A.; Sagi, S. Intermediate Pyrolysis: A Sustainable Biomass-to-Energy Concept-Biothermal Valorisation of Biomass (BtVB) Process. *J. Sci. Ind. Res. (India)*. **2011**, 70 (8), 664–667.

- (64) Yang, Y.; Brammer, J. G.; Mahmood, A. S. N.; Hornung, A. Intermediate Pyrolysis of Biomass Energy Pellets for Producing Sustainable Liquid, Gaseous and Solid Fuels. *Bioresour. Technol.* **2014**, *169*, 794–799.
- (65) Jäger, N.; Conti, R.; Neumann, J.; Apfelbacher, A.; Daschner, R.; Binder, S.; Hornung, A. Thermo-Catalytic Reforming of Woody Biomass. *Energy Fuels* **2016**, *30* (10), 7923–7929.
- (66) Neumann, J.; Meyer, J.; Ouadi, M.; Apfelbacher, A.; Binder, S.; Hornung, A. The Conversion of Anaerobic Digestion Waste into Biofuels via a Novel Thermo-Catalytic Reforming Process. *Waste Manage.* **2016**, *47*, 141–148.
- (67) Fraunhofer UMSICHT. *The Biobattery Thermo Catalytic Reforming TCR*®; 2016.
- (68) Hammond, J.; Rödger, J. *Biochar - Climate Saving Soils - Newsletter 1*; 2012; Vol. 1.
- (69) Dalluge, D. L.; Daugaard, T.; Johnston, P.; Kuzhiyil, N.; Wright, M. M.; Brown, R. C. Continuous Production of Sugars from Pyrolysis of Acid-Infused Lignocellulosic Biomass. *Green Chem.* **2014**, *16*, 4144–4155.
- (70) Ouadi, M.; Jaeger, N.; Greenhalf, C.; Santos, J.; Conti, R.; Hornung, A. Thermo-Catalytic Reforming of Municipal Solid Waste. *Waste Manag.* **2017**, *68*, 198–206.
- (71) Yang, Y.; Heaven, S.; Venetsaneas, N.; Banks, C. J.; Bridgwater, A. V. Slow Pyrolysis of Organic Fraction of Municipal Solid Waste (OFMSW): Characterisation of Products and Screening of the Aqueous Liquid Product for Anaerobic Digestion. *Appl. Energy* **2018**, *213* (November 2017), 158–168.
- (72) Conti, R.; Jäger, N.; Neumann, J.; Apfelbacher, A.; Daschner, R.; Hornung, A. Thermocatalytic Reforming of Biomass Waste Streams. *Energy Technol.* **2017**, *5* (1), 104–110.
- (73) Neumann, J.; Binder, S.; Apfelbacher, A.; Gasson, J. R.; Ramírez García, P.; Hornung, A. Production and Characterization of a New Quality Pyrolysis Oil, Char and Syngas from Digestate - Introducing the Thermo-Catalytic Reforming Process. *J. Anal. Appl. Pyrolysis* **2015**, *113*, 137–142.
- (74) Martínez, J. D.; Murillo, R.; García, T.; Veses, A. Demonstration of the Waste Tire Pyrolysis Process on Pilot Scale in a Continuous Auger Reactor. *J. Hazard. Mater.* **2013**, *261*, 637–645.
- (75) Yang, Y. Energy Production from Biomass and Waste Derived Intermediate Pyrolysis, Aston University, 2014.
- (76) Tomasi Morgano, M.; Leibold, H.; Richter, F.; Stapf, D.; Seifert, H. Screw Pyrolysis Technology for Sewage Sludge Treatment. *Waste Manage.* **2017**.
- (77) Ouadi, M.; Brammer, J. G.; Yang, Y.; Hornung, A.; Kay, M. The Intermediate Pyrolysis of de-Inking Sludge to Produce a Sustainable Liquid Fuel. *J. Anal. Appl. Pyrolysis* **2013**, *102*, 24–32.



## Industrial technologies for slow pyrolysis

Jorge López-Ordovás, Katie Chong, Anthony V. Bridgwater, Yang Yang

European Bioenergy Research Institute (EBRI), School of Engineering and Applied Science, Aston University, Birmingham, B4 7ET, UK

### Abstract

This chapter classifies and analyses the technologies available in industry for slow pyrolysis. Depending on the mode of operation, these technologies are classified into batch, semi-continuous and continuous processes; each of them with different characteristics, advantages and disadvantages. Different criteria to help with the choice of a reactor are briefly introduced with all the gathered information presented. Furthermore, the introduction of the reactor in the system is briefly explained, and different options for pre- and post-treatment of the materials are described. In addition to the reactor design, Techno-Economic Assessment (TEA) is explained with all associated costs and economic evaluation methods. The chapter concludes with an explanation of the challenges in the design of this type of reactor, addressing different possibilities for the upcoming research.

### 1. Introduction

Research carried out in academia is very important for both scientific and industrial development. However, most of the studies completed within academia never reach industrial stakeholders for a variety of reasons, and only when the research is shared does it have an impact on society.

One of the challenges to overcome in pyrolysis is the method or technology used to produce char. Despite being made since ancient times and the continuous improvements on the existing technologies, there is no preferred method to produce char. The existing reactors can be classified into different types. Some articles<sup>1-2</sup> divide the industrial processes based on the heating method whilst others make the classification based on the process operation mode<sup>3-6</sup>: batch, semi-continuous and continuous processes. This classification is more intuitive and makes the differences between the technologies much clearer. Regardless of the technology used or the operation mode in the reactor, the feedstock always undergoes the same processes represented in Figure 1.



Figure 1. Main process steps.

One of the characteristics mentioned in pyrolysis is the absence of oxygen. The oxygen-free environment begins at the feeding step where all the air is removed from the raw material. The feedstock has a moisture content, which might need an independent pre-treatment step to reduce it to the required value or this can be done in the reactor if it is not too high. Once the drying phase is complete, pyrolysis begins and starts to degrade the feedstock to the products mentioned. These products need cooling, to avoid auto ignition, to stop any reactions occurring or to condense the vapours to obtain the liquid product. After the process, the products are collected to use them for a range of applications. There might be other pre- or post-treatment steps, but drying and cooling are always required in pyrolysis processes.<sup>5</sup>

### 2. Batch Processes

The batch processes are the most straightforward technology to produce char and have been used for many years. They typically consist of concrete rectangular kilns that are loaded with the feedstock and the temperature is raised to the pyrolysis temperature through internal heating, adding some oxygen for the partial combustion of the feedstock. They require significant time for operation (25-30 days residence time, including cooling down period) with low char yields (5–20 wt. %) (See Figure 2). These processes operate without heat recovery, and a significant fraction of the feedstock is burnt off, but they can cope with a range of feedstocks and are very cheap to construct<sup>2, 6</sup>. The feedstock does not move within the reactor, and, the product only can be collected once it is cooled.<sup>4</sup>

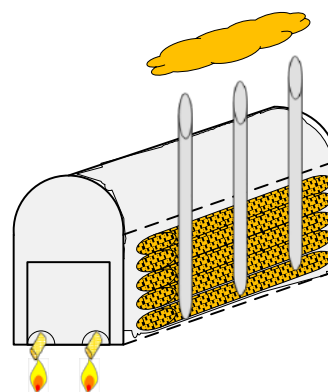


Figure 2. Missouri kiln.

The use of kilns to produce char is still widespread as they are relatively cheap and simple to operate, which makes them attractive despite the low char yield. It is a good option for developing countries like Ghana due to their low investment cost<sup>6</sup>, and it is still used in some industrialised countries like the United States<sup>5</sup>. Kilns are chiefly used in the Brazilian state of Minas Gerais, for instance, particularly by a company called Biocarbon Ind. Com. Ltd<sup>4</sup>. The company Horner Charcoal Company in Taneyville,

Missouri, uses a set of Missouri kilns to produce char<sup>5</sup> (see Figure 2).

### 3. Semi-continuous processes

The semi-continuous processes have a continuous operation, but the feeding of the feedstock and the discharge of the products occur in batches. This characteristic allows the systems to recover part of the energy used in the product. For instance, the gas produced, comprising of the condensable and non-condensable fractions, is usually burnt in a combustion chamber to provide energy for the process, both in the drying and the pyrolysis part.<sup>4, 6</sup>

#### 3.1. Waggon retort

Waggon retort technology consists of a 45 meter-long tunnel divided into three chambers: drying, carbonisation and cooling, separated by doors. The wall of the tunnel is made of perforated steel, which enables the removal of vapours from carbonisation to burn them in an external furnace and recirculate them to the drying and the carbonisation chamber. Two-thirds of the gases from the combustion chamber enter the carbonisation chamber and the one-third left goes to the drying chamber. The cycle of each wagon varies from 25 to 35 h. The process is commercialised by Impianti Trattamento Biomassa with plants in Milazzo and Mortera (Italy), Belišće (Hungary) and Alterna Biocarbon in Prince George (Canada). The average production of this technology is 6000 tons of char each year. A typical waggon retort arrangement is shown in Figure 3. A significant disadvantage of this system is the high operating cost compared to similar technologies such as the Carbo Twin Retort.<sup>2, 4-5</sup>

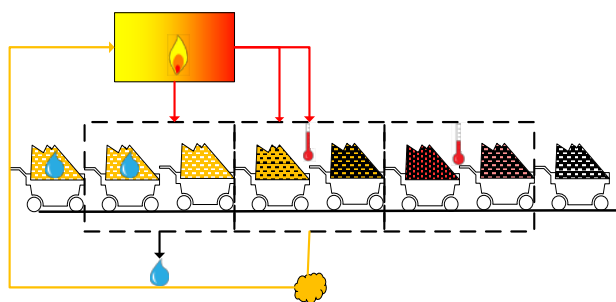


Figure 3. Waggon retort system.

#### 3.2. Shelf reactor

This technology consists of a horizontal retort fed with shelves which enter through two sliding doors. In one of the sections, biomass is dried and then carbonised. Eventually, the shelves go to a cooling chamber. The main characteristic is the need for manual loading of feedstock and discharge of the product and low costs in comparison with more developed technologies.<sup>3-4</sup>

#### 3.3. Carbon twin retort

The system contains two retorts with the same capacity (usually 4.5 m<sup>3</sup>). One of the vessels is loaded with the feedstock and heated using an external source of energy

such as gas or fuel oil. In the meantime, the second vessel is charged with the raw material. The first vessel will undergo carbonisation reactions, and it will release the pyrolytic vapours that will be burnt in an external chamber to provide energy to heat up the second retort, as shown in Figure 4. Once the carbonisation finishes in the first vessel, the reactor will be replaced with a new one with fresh feedstock, leaving the first one to cool down covered with a lid. The time required per vessel for the whole process is 8–12 h and the char yield obtained is 30–32 wt. %<sup>2</sup>. Although it is called twin retort more than two units can be used, for example, 12 vessels would need three workers per shift working on a 24-h basis, and the whole system can produce between 6000 and 7000 tons of char per year. There are some operating plants using this technology in Carbon France (France), Green Coal Estonia (Estonia) and Carbo Group (The Netherlands) and USA.<sup>2, 5</sup>

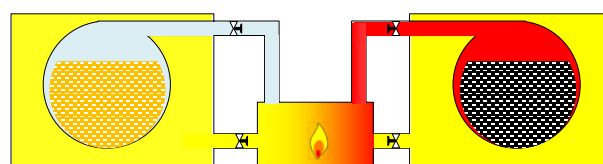


Figure 4. Carbon twin system.

### 4. Continuous processes

Continuous operation and feeding characterise continuous processes. The capital cost is higher, there is a need for external sources of energy, and the systems are not usually portable. However, the yields of the char are higher, and some product characteristics such as surface area and high heating value are, overall, higher. Some by-products like acetic acid can be recovered and the heat required can be partially produced by one or more of the products.<sup>2, 5</sup>

There are different ways to classify the continuous processes further: they can be ranked by heating method or by the feeding method. Some of the technologies are fed in batches of different sizes such as the Lurgi or Reichert reactor, whereas other technologies like rotary kilns or screw reactors use continuous feeding; however, the classification used in this chapter is based on the particle size. Reactors such as Lurgi, Reichert or Lambiotte can deal with big particles like logs, other reactors like the Paddle Pyrolysis Kiln or Herreshoff Multiple-Hearth Furnace usually process smaller particles. There is a comparison of all characteristics of the most common reactor types at the end of this chapter in Table 1.

With a focus on particle size, the reactors designed to work with big particles cannot handle small particles because they would pack tightly and would hinder circulation of gaseous products. The particles would not act as heat carriers, decreasing the heat transfer within the reactor. In contrast, the reactors working with small particles will produce char in a powdery form which is not so easy to handle, and it will need some post-treatment to be sold in the form of char briquettes or pellets.<sup>4</sup>

#### 4.1. Lambiotte

There used to be two types of pyrolysis processes called Lambiotte, SIFIC or CISR, whose main difference was the treatment of pyrolysis vapours. The SIFIC variant took the vapours through some treatment to obtain components to be burnt afterwards. A portion of the gases are re-injected into the retort, and the other part is cooled and used at the bottom of the reactor to cool the char. There is a scheme for this reactor in Figure 5. The limitation of the system is the moisture content of the feed which should be below 25 wt. %.

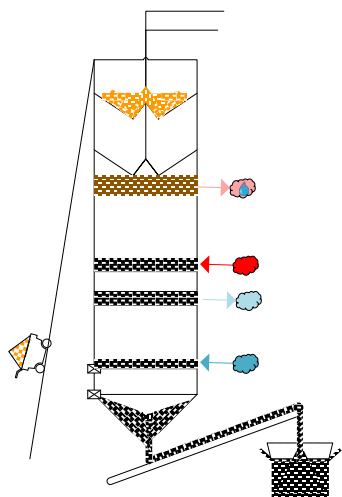


Figure 5. Lambiotte reactor.

The process consists of a vertical retort divided into different hearths, fed from the top into a lock-hopper which prevents gases from escaping and air from entering. The biomass moves slowly down the reactor with a counter-current flow of inert hot gas which dries the wood and increases the temperature. The cycle takes 11 hours since the feedstock enters until it is removed at the bottom as char<sup>2,5</sup>. The feedstock is fed from the upper part, and it goes to a chamber where it is dried with the rising gases coming from the carbonisation zone, which is the hearth below. After the carbonisation hearth, the char goes to other chambers where colder gas is used to cool down the product before it is stored.

The Lambiotte process has several advantages: the quality and yield of char are high, the vapours produced can be used for cogeneration, and there is a high level of automation. On the other hand, it requires the biomass to be pre-dried, so if the feedstock has a high moisture content, some auxiliary fuel for heating would be needed. Also, some corrosion can take place due to the acetic acid produced. The largest plant using this technology was located in Prémery (France)<sup>5</sup> and produced 25000 tons of char per year, but was closed in 2001 due to economic problems. Some units are still operating in Europe and Russia.<sup>3-4</sup>

#### 4.2. Reichert

This retort consists of a conical top and brick-lined bottom fed by a conveyor from the top (see Figure 6). After feeding, a valve is closed, and another valve is opened to let hot gases into the reactor, and the carbonisation starts at the top and moves slowly to the bottom before the char is moved to the cooling bunker. The vapours pass through a cooler and scrubber, and the condensable and non-condensable fraction are separated. The non-condensable fraction is separated, heated to the pyrolysis temperature (450–550 °C) and recirculated to the reactor.<sup>2</sup>

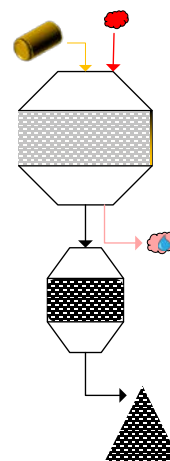


Figure 6. Reichert system.

The capacity of the system is  $7 \cdot 10^4$  tons of beech wood per year, and the annual production is 24000 tons of char, so the yield is around 34 wt. %. It is a system used by Degussa (also known as Chemviron Carbon) and ProFagus, located in Bodenfelde (Germany).<sup>1-2</sup>

#### 4.3. Lurgi

This reactor operates using a similar concept to Lambiotte. It is divided into an upper pyrolysis zone and a lower cooling zone. The particular characteristic of the system is the recirculating gas stream (See Figure 7). The gas recirculation comes from the combustion of the pyrolygneous vapours with air in a combustion chamber. The fraction reinjected in the pyrolysis zone (around one-third of the gases of the combustion chamber) passes through a conditioning step to reach the desired temperature (550–700 °C). Before being reinjected in the cooling zone, the gas is pre-cooled in a scrubber by exchange with water and is injected in the bottom of the reactor.<sup>2</sup>

There is a large plant, part of the Silicon Metal Complex (SIMCOA) in Bunbury, Western Australia, which is producing 27000 tons of char per year in two Lurgi retorts.<sup>2</sup>

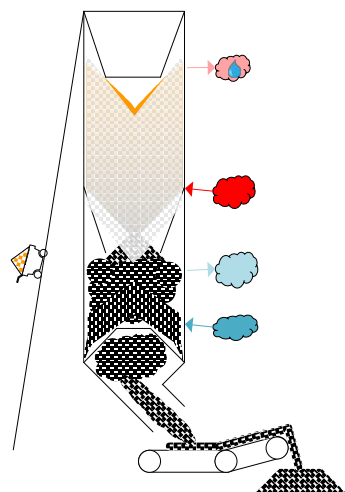


Figure 7. Lurgi reactor.

#### 4.4. Badger-Stafford process

The Badger-Stafford process is an old technology which has a char yield of 20 wt. %, 4.5 wt. % of acetic acid and 10 wt. % tar. Due to the low char yield, it was shut down and, among other disadvantages, it had to be dismantled every two weeks to burn the tar inside the reactor<sup>5, 7-8</sup>. The reactor consists of a wall composed of firebrick, diatomaceous earth and insulating brick. A number of barrel valves regulate the flow of wood particles entering and char removal at the top and the bottom of the reactor. The reactor uses the heat of the exothermic carbonisation to heat the descending column of wood up to 515 °C, which was the set temperature for pyrolysis —although the heat transfer was not very effective and near the wall, the temperature could be as low as 225 °C.<sup>7</sup>

#### 4.5. Herreshoff multiple-hearth furnace

This system includes a vertical kiln made of a refractory-lined steel shell with several plates or circular hearths (4–10 hearths). A shaft rotates at a slow speed (1–2rpm) moving radial toothed-arms located in each furnace. These arms have ploughs attached to move the biomass across each hearth. The biomass falls to the next hearth from the centre or the side, and the system is designed to make the biomass move through the hearths (see Figure 8). Before going to the next hearth, the biomass is agitated and makes contact with hot gases supplied by combustion air blowers from burners or ports. The temperature for the process is within a range of 500–600 °C.<sup>3-4, 9-10</sup>

The system was patented by R.D. Pike in 1921 and was proposed for large capacity units with one ton of char per hour and four tons of biomass capacity per hour. It was widely used in the 1980s with the construction of 16 furnaces in the United States. Although it can efficiently and flexibly use fine-grained materials, the char made needs to be briquetted to be commercialised, and the capital cost is high. NESA commercialised a large pyrolysis unit for waste treatment, and BIG Char from Black Is Green Pty Ltd commercialised a mobile reactor that produces char briquettes.<sup>3-4</sup>

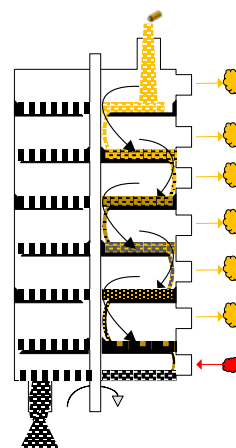


Figure 8. Herreshoff multiple-hearth furnace.

#### 4.6. Moving agitated bed

The process consists of a horizontal surface that is heated by molten salts such as potassium nitrate, sodium nitrate or sodium nitrite. The biomass is transported to the surface with a conveyor (as shown in Figure 9). Pyrovac used this technology as part of the vacuum pyrolysis unit, and some yields for bio-oil were over 50 wt. %. Presently, NewEarth is commercialising a moving bed system. The advantage of this process is the size of the equipment, which is comparable to the height of the fixed bed in a laboratory scale (few cms.). However, in a pilot plant with a capacity of 3 ton h<sup>-1</sup> constructed in Saguanay (Quebec, Canada), some problems with the condensation towers were found.<sup>3-4</sup>

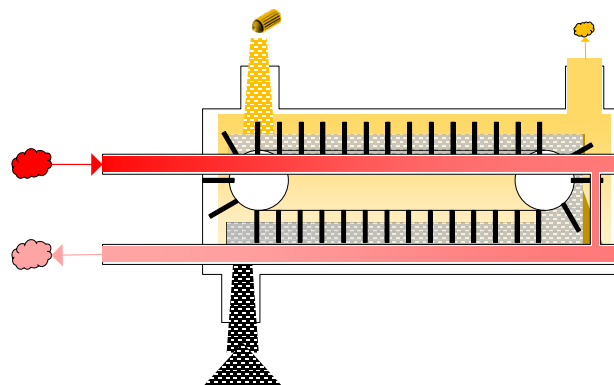


Figure 9. Moving agitated bed.

#### 4.7. Paddle pyrolysis kiln

The Paddle Pyrolysis Kiln consists of a horizontal vessel with an internal mechanism that moves and mixes the biomass (see Figure 10). Overall, the mechanism used to move the biomass is a group of paddles which increases the heat transfer and mixes the biomass. It is used by BEST Energies and is part of the design of Choren.<sup>3-4</sup>

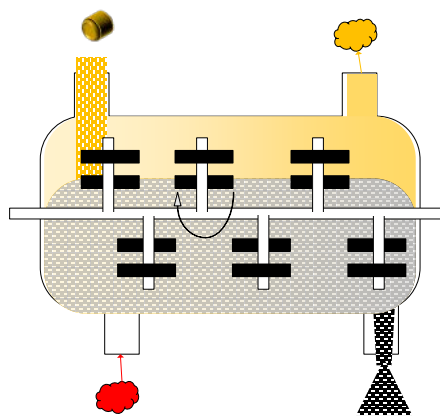


Figure 10. Paddle pyrolysis kiln.

#### 4.8. Screw reactor

This type of pyrolysis reactor is also called an auger reactor and consists of a screw inside a horizontal tubular reactor (see Figure 11). As explained in Chapter 2, it can be a single screw or a twin-screw design. In general, the rotation of the screw moves the biomass along the axis while it is heated and pyrolysed<sup>6</sup>. Due to this characteristic, some screw reactors are designed to produce bio-oil and char, and others are used to produce char and heat.<sup>3-4</sup>

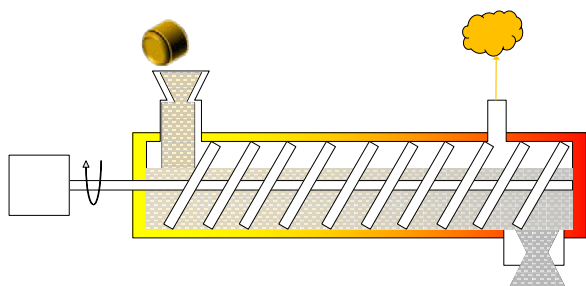


Figure 11. Screw (Auger) reactor.

Char yields are 17–30 wt. % and the bio-oil 48–62 wt. %, although the amount of water is higher (30–55 wt. %) compared to the oil obtained from fast pyrolysis. It is one of the most common systems used for pyrolysis, and some companies such as ABRI-Tech have commercialised several 1 one-per-day capacity units<sup>4</sup>. Renewable Oil International, Biogreen, Advanced Bio-refinery and Forschungszentrum Karlsruhe (FZK) focus their designs on producing bio-oil and char, whereas International Tech Corporation, eGenesis and Agri-tech design the screw reactors to produce char and heat. It is very popular due to the simplicity of construction and operation, and the capacity to handle a wide variety of feedstock with high char yields. However, there are some issues regarding the heat transfer within the system, which could limit the capacity to process biomass<sup>4</sup>, and it is challenging to scale-up the experimental units to the industrial scale<sup>11</sup>. The description of the different heating methods and the systems where an auger reactor is used have been previously described in Chapter 2.

#### 4.9. Rotary kiln

The rotary kiln is a rotating cylindrical shell heated externally. The angle of the drum and the rotation speed control the residence time of the particle within the system, which takes several minutes to go through the reactor (see Figure 12). The residence time is short if it is compared to the traditional batch carbonisation (which takes a day to pyrolyse the biomass)<sup>3, 6, 12</sup>. To improve the heat transfer, there is a sequence of radial steel fins supported on an insulated mantle<sup>4</sup>. Rotary kilns can be described as heat exchangers where energy from the gas phase is transferred to the bed material and, along with this transfer, several thermal processes such as drying, heating and chemical reactions occur at a broad range of temperatures<sup>12</sup>. The rotation speed, and the radius of the drum will determine the mixing inside the reactor, which should be considered for the possible design of a process where a rotary kiln is involved.<sup>13</sup>

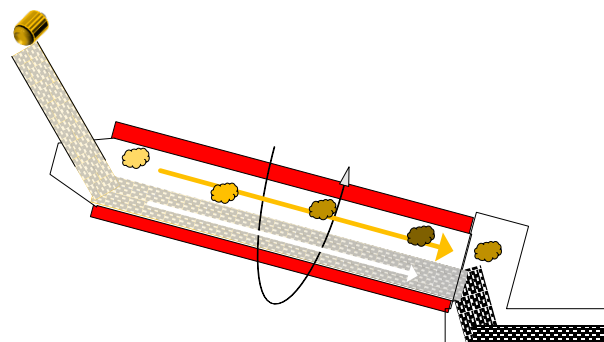


Figure 12. Rotary kiln reactor.

Garcia-Nunez et al.<sup>3</sup> highlight the good balance between yields of oil (37–62 wt. %) and the char obtained (19–38 wt. %). It is a technology widely used for tires, sewage sludge, MSW and plastics. There is a plant in Burgau-Unterknöringen that produces 2.2 MW and another one with a capacity of  $10^5$  tons per year at VEW Energie AG Westfalen in Hamm-Uentrop, both in Germany. Garcia-Nunez et al. point out that the systems that already exist could be adapted to work with biomass. Although the yields of char and bio-oil are typically lower than fluidised bed reactors, Amaron Ltd. got close to that technology through multiple high-intensity burners to optimise heat transfer, an auger arrangement in the feed section and a char outlet below the end of rotating section.<sup>3-4</sup>

## 5. Industrial application

### 5.1. Reactor choice

From the section above, it can be seen that there is a wide range of technologies available to use in waste pyrolysis process. Each technology has advantages and disadvantages. The auger reactor has got very critical issues with the scale-up, especially with the heat transfer to the middle of the particle, and it has got a risk of plugging if it is overfeed; the rotary kiln is challenging to seal; the agitated moving bed has some condensation problems; Lambiotte plant was not profitable; Reichert

technology only works with biomass, and it has not been tested with waste. An optimised design is needed which can be safe to operate and will meet the needs of industry in terms of capacities and feedstocks.

Table 1 makes a comparison of the different characteristics of the reactors. From this table, some criteria can be established to make the best choice, depending on the weight of each parameter on the final decision. Some of the criteria could be whether it needs size reduction, moisture limit, portability, heat transfer methods and its efficiency or the maximum capacity designed.

This data must be interpreted with caution because the interests can be different depending on the stakeholder. We can only look at the char yield, but it should be considered the final use of each technology, which will depend on the process. Moreover, the developing countries will place more importance or weight on the CAPEX and the OPEX than the developed countries where the primary interest can be the production capacity or the yield.<sup>6</sup>

## 5.2. Block diagram

The reactor is the heart aspect of the pyrolysis process. However, it is essential to design the pre-treatment steps for the feedstock to ensure its properties at the entrance of the reactor as well as the treatment post reactor to add the maximum value to the products. Different possibilities for these pre- and post-treatment steps are represented in Figure 13 for the feedstocks studied within the GreenCarbon project. The feedstock and targeted products profoundly influence the pre-treatment and cleaning steps. The economics of each stage has also got a strong influence on its selection. For example, the washing is an excellent step to remove the stones and partially the ash content; however, it means that the feedstock will have to be dried after it, and the energy demand of the system including that step may be too high to be economically feasible.

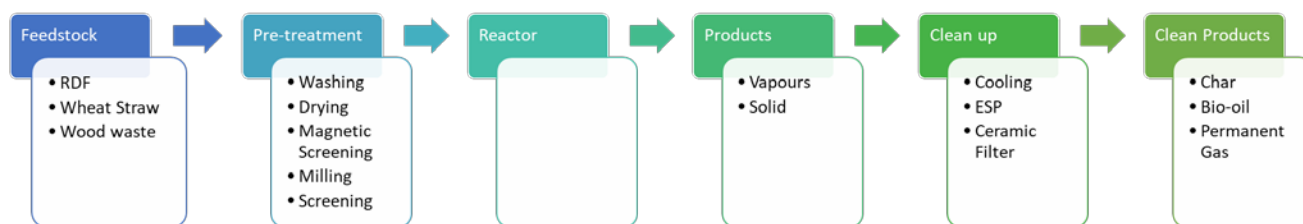


Figure 2. Block diagram.

The feedstock usually needs treatment before being stored and reaching the reactor. It can contain some impurities that will affect the final product such as ash, glass, metals, stones and moisture content. The ash content will mainly remain in the solid and, consequently, the char, increasing the burnout temperature<sup>14</sup> and the burners can be severely damaged if the ash content is high enough. Furthermore, the resulting heating value is lower with high ash content within the feedstock<sup>15</sup>. The only industrial method to reduce the ash content<sup>1</sup> is washing, although it should be studied more closely to examine the feasibility of the step due to its high energy demand. Besides the

partial removal of the ash, it also removes the stones and some extractives from the feedstock. The extractives are mainly organic substances like alkaloids, essential oils and fats<sup>16</sup>. There are other methods at laboratory scale to remove the ash content such as a mixer, vibratory sieve shaker and hammer mill treatment<sup>15</sup>, but they have not been tested at industrial scale.

The reactor is the central part of the system which transforms the feedstock into the products and determines the product distribution from the conditions. The reactor needs energy to increase the temperature of the biomass and start the degradation of the biomass. There are several types of reactors to be used as described previously.

Pyrolysis reactors are very sensitive to water content from an energy point of view, because this increases the energy demand and, consequently, the operating cost. For that reason, a drying step is needed to control the moisture content at the entrance of the reactor. Depending on the feedstock, it may also contain some metal contamination, especially if the feedstock has its origin from municipal waste. The metal screening step will remove the metals, which can then be recycled. With pyrolysis, the heat transfer is a fundamental issue, and it is clear that the heat transfer will take less time if the particle is smaller. Therefore, there should be a milling step followed by screening to specify the particle size which enters the reactor in order to ensure adequate heat transfer.

Once the feedstock is processed, there are different treatments for the products, always focused on the final use. Before storing the char, it needs post-treatment. First, the char requires cooling and, it has to go through a briquetting process before being stored<sup>17</sup>. The vapours obtained from the reactor contain the condensable and the non-condensable fraction and leave the reactor at a very high temperature (400-700°C). Due to the high temperature, a cooling system is needed to condense the bio-oil and separate it from the permanent gas. There are

many different options for this heat exchanger such as a tube and shell, spray tower or a quench column. Once cooled the vapour from the cooling step can still contain some particles of solids and aerosols. The aerosols can be removed from the gas with an electrostatic precipitator (ESP). The solid particles can be retained in a ceramic filter at the end of the process.

Biomass, char, bio-oil and gas have to be stored or disposed of, unless the plant is located next to an end user or any of the products is used as a fuel for the process itself. The treated biomass can be stored in bins protected from moisture until it is required for its processing<sup>18</sup>. The bio-oil

should be stored in tanks<sup>19</sup>; the char is stored in sealed vessels or containers to prevent moisture or oxygen ingress<sup>20</sup> and in a covered area, avoiding the wind and rain. Ash can be sprayed with a small amount of water or mixed with clay slurry to avoid spontaneous combustion<sup>18</sup>. Part of the char could be used in the system for heat generation. The storage of the gas produced is not practical at industrial scale; the most common practice is its disposal to the atmosphere or to flare it at an industrial scale.

### 5.3. Techno-Economic Assessment (TEA)

The reactor has a significant effect on the performance of the whole plant. Therefore it is essential that the entire plant is considered from a chemical engineering point of view. In industry, the techno-economics of the entire system has to be considered to understand the feasibility of such a plant<sup>21</sup>. The TEA of the whole system calculates and evaluates the costs associated with the complete plant, allows the comparison between different scenarios and compares different configurations of the process<sup>22</sup>. The TEA brings together mass and energy balances and the flow of information to work out how much the construction and operation of the plant can cost. The benefit of TEA is that it provides a relatively quick and low-risk method to study the process without building a physical plant. It identifies the viability of the system and the process design can be improved when the critical areas for optimisation are determined.<sup>23</sup>

#### 5.3.1. Costs and Income

The costs are estimated to calculate the profitability of the plant. A classification of the costs is shown in Figure 14. The three central values, capital cost, operating cost and income, in Fig. 14 are estimated based on the mass balance. The value of the plant at the end of its working life, called scrap value should also be taken into account. In general, only 5-10% of the cost is recovered in this value because just the building and some standard items keep their value over the plant lifetime<sup>23</sup>.

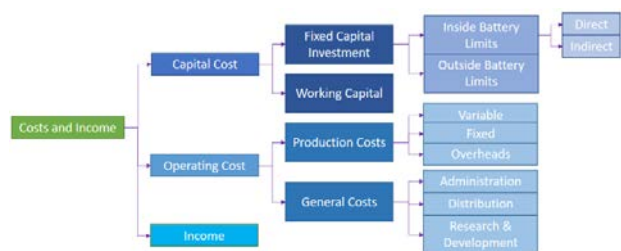


Figure 14. Costs and income.

**Capital Cost.** This term includes all of the capital expenditure to buy the necessary equipment, its installation and the cost to start up the plant. There are two types of Capital Cost: the Fixed Capital Investment and Working Capital. The Fixed Capital Investment is the cost of the design, the construction and the installation of the plant, including the engineering costs and contingency charges. The whole infrastructure of the plant with services such as security, offices and canteen are included in a term called Outside Battery Limits (OSBL). The other word of the

Fixed Capital Investment is Inside Battery Limits (ISBL), whose direct costs cover the expenses associated with the material and installation of the plant and the indirect costs have some possible expenses related to the construction, such as the insurance and fees of the equipment and field expenses.

The Working Capital is the other contributor to the Capital Cost and involves all costs after the construction until the first income is generated. The costs included in this part are the start-up of the plant and the materials, the salaries of the workers, the money for possible emergencies and to maintain the plant in operation. It also used to pay the bills and sustain operation before the product is sold and income is generated.<sup>23-25</sup>

**Operating Costs.** When the plant is in operation, the costs associated with it are called Operating Costs. Similar to the Capital Costs, the Operating Costs are divided into Production Costs and General Costs. The production costs are directly related to the production process, unlike the General Costs which don't alter with the production rate but are related to the sales, research and administration.<sup>24</sup> The Production Costs are divided into Variable Costs, Fixed Costs and Overheads. The Variable Costs are strongly influenced by the plant design, the feedstock and the location of the plant. Besides the raw material and labour, packaging and shipping are also included here. These values are not so closely related to production rate, because they can be heavily influenced by market conditions. To calculate the labour costs, the number of shift staff must be estimated. For this work, this estimate is based on the hypothesis of 4.58 operators per shift position in a four-shift-rotation if the shifts are 12-hours-long, and it takes into account holidays and 40 working hours per week<sup>26</sup>. The Fixed Costs within Production Costs takes into account the maintenance needed, the depreciation, insurance, interest and rates and taxes. The depreciation is crucial because it indicates the value that the equipment loses during a period of time<sup>26</sup>. The Overheads keep the plant operating but are not related to the primary activity of the plant, services such as security or the canteen for the workers<sup>23</sup>.

The General Costs are the Administration where accounting, human resources and IT are included. The Distribution and Marketing involve the sales and advertising; Research and Development invest money in finding improved methods for the product and the corresponding tests<sup>24</sup>.

**Income.** It is the earnings for the sale of the product or products of the plant. It is calculated as a function of the sales price and the market size. However, the forecast is sometimes difficult to calculate. The demand for a product is not constant along the time. Moreover, there can be a time-lag between the plant construction, the operation and the income. The technology also changes, and better equipment can come up to the market. Furthermore, there are factors like changes in the policies which are difficult to control<sup>23</sup>. Depending on what is included in the income, it can be called net income, from which all costs and taxes

are already deducted, or Gross Income, which is the money earned from the sales.<sup>24</sup>

### 5.3.2. Economic evaluation

The profitability is a relationship between the investment needed for a project and the income obtained from it. The profitability is related to the flow of money although it can also be measured with an interest ratio, a rate or time, which can sometimes be a better way to compare different projects<sup>23</sup>. Regarding the investment, it is important to highlight that, the higher the risk taken, the higher the reward level that may be obtained but there is the potential that it could all be lost. There are many methods to compare profitability, among them are the minimum acceptable rate of return, payback time, return on investment, net present value and discounted cash flow rate of return.<sup>23</sup>

**The minimum acceptable rate of return** (see Eq. 1). The value obtained is the division of the expected net profit by the total capital investment and, depending on the value obtained, the level of risk is determined. A value of 4–8 is classified as a safe investment, but values of 32–48 are very risky, and the investment may not be recovered.<sup>23</sup>

$$\text{Rate of return} = \frac{\text{net profit}}{\text{total capital investment}} \quad (1)$$

**Payback time.** The method calculates the time necessary to recover the initial investment, indicating how long the investment is at risk. It is a useful measure to know when the investment is recovered. It is the simplest method to compare profitability. Also, it is straightforward to understand and gives a quick method to estimate the profitability. On the other hand, it does not include the factors that impact the profitability such as the interest or the plant lifetime. Overall, it is not recommended for high investments.<sup>23</sup>

**Return on Investment (ROI)** (see Eq. 2). It is a very common criterion used to compare different options. It calculates the percentage of return on that money invested previously on the project. It is the relationship of the cumulative net cash flow, the plant life and its initial investment. It is essential to clarify what parameters are used for its calculation. The advantage is that it gives a good idea about the profitability of the project and makes it easier to compare projects between them. It is also a very common criterion used in the projects. The disadvantage is that it does not include the time value of money, so it assumes money does not change its value over the time of the project, it does not consider the cash flow on each time and capital investment interest<sup>23</sup>. It includes the original investment but does not include interest.

$$\text{ROI (\%)} = \frac{\text{cumulative net cash flow}}{\text{plant life} \times \text{initial investment}} \times 100 \quad (2)$$

**Net Present Value (NPV)** (see Eq. 3). This method calculates the cash flow for each year applying a constant interest rate for the following years. It gives a measure of the difference of investing the money in the bank with the

interest rate or investing it in the project. This method takes into account the time value of money.<sup>23, 27–28</sup>

$$\text{NPV} = \sum_0^n \frac{(\text{Net Cash Flow})_n}{(1+r)^n} \quad (3)$$

**Discounted Cash Flow Rate of Return** (see Eq. 4). This method establishes the Net Present Value as 0, and the interest rate calculated is the actual rate of return of the project, and it can also be called Internal Rate of Return (IRR). Based on these values, the profitability of the projects can be compared between them. Also, if the value  $i$  is compared with the coefficient  $r$  from NPV, the profitability of the project is being compared to the one in the bank, which would be a low-risk option for the money from the project and would be a general idea about the risk taken.<sup>23, 27–28</sup>

$$\sum_0^n \frac{(\text{Cash Flow})_n}{(1+i)^n} = 0 \quad (4)$$

### 5.4. Role of the industrial partner BPP

Biomass Power Projects (BPP) is a firm created 20 years ago, which engaged in several European and UK projects in emerging low carbon technologies. The company designs manufacture and install waste-to-energy systems for a range of different waste streams. GreenCarbon's Early-Stage Researcher #3 (J. López-Ordovás) is closely working with BPP to get the in-depth industrial insight for the project. Due to the lack of industrially based information in the literature, the interaction and collaboration between the researcher and the company are significant to get the best design in each situation.

Additionally, the company can use the results and learn from the project to aid future construction of an industrial scale reactor with an average throughput of 3 ton h<sup>-1</sup>. This would be very beneficial to validate the results obtained during the PhD project and generate a valuable impact on the GreenCarbon network.

### 5.5. Challenges in the design of a slow pyrolysis reactor

The information available for the design of a slow pyrolysis reactor at industrial scale is very limited compared to laboratory tests. The model can be divided into three different parts: the behaviour of the bed of solids, the heat transfer, and the kinetics of the process. Besides this, a challenge for the research is the validation of the model, which represents an important step to demonstrate that the assumptions did work correctly and the results are as close as possible to the real behaviour of the system.<sup>29</sup>

#### 5.5.1. Behaviour of the bed of solids

The real behaviour of the bed of solids involves many different aspects in the rotary kiln. There are six different motions in the transverse plane, which depend on the radius of the reactor and the rotational speed; they are ordered from high to low rotational rates<sup>12</sup>:

**Centrifuging:** it occurs at very high speed. The material rotates with the drum wall; it would involve very high energy consumption and a poor mixture of the solids.

*Catacting*: it has lower velocities than centrifuging, but they are still high. The solids rise over its level and drop, provoking a perturbation of the system causing instability. It also mixes the biomass axially, which would make the system more difficult to control.

*Cascading*: this motion is very similar to cataracting with lower rotational speed and smaller drops on the surface of solid.

*Rolling*: this rolling motion causes an excellent axial mixing due to the rolling of the bed of solid on its surface and the wall on the bed. It is a steady motion with reasonable uniformity in the properties within each axial profile.

*Slumping*: cyclical variation of the angle of repose and material at the shear edge becomes unstable.

*Slipping*: this motion occurs at the lowest rotational rates. Due to the low speed, the material slides on the wall, and there is not proper movement within the bed of solids which could remain as a solid piece of material.

Besides the behaviour within the bed of solids, the macroscopic behaviour is also essential in the design of the reactor. The height of the bed of solids is likely to be increasing or decreasing along the reactor. This variation of height is another issue to take into account the design of the reactor because it will influence some critical parameters, such as the heat transfer contact area. According to Boateng<sup>12</sup>, the behaviour of solids has been studied through granular flow model in rock falls, snow avalanches or mudflows but the application in rotary kiln has not been defined. However, there is a model made by Saeman<sup>30</sup> which describes the movement of the bed of solids inside the kiln and is able to estimate the height of the bed.<sup>31</sup>

### 5.5.2. Heat transfer

Heat transfer is a critical step in pyrolysis because all the particles have to reach the process temperature to react. In addition, the only source of heat for the reactor is external, although the solid might also be heated by the gas inside. The particle size can vary the product yields by 10 wt. % for each product when the size varies from 0.3 to 1.5 mm, although this effect is negligible for higher sizes<sup>32</sup>. This study shows how important the heat transfer is because the yields differ significantly with the particle size. All the heat transfer mechanisms are present in the reactor (conduction, convection and radiation). Conduction is intuitive; there are interactions between energy carriers within a material. The energy is transferred from the more energetic carrier to the less energetic ones, transferring the energy from hot to cold. This conduction can occur within the same material or different ones. Convection is a particular type of conduction which is treated separately; the heat transfer occurs in a moving medium. This change makes the heat transfer equation a bit different because, besides the conduction, there is an enthalpy carried by the macro-scale flow. This enthalpy includes the effect of the pressure and the volume related to the medium moving.<sup>33</sup> The radiation is produced by the agitation of the atoms, which release energy in the form of electromagnetic waves and is absorbed by other atoms in a less agitated state. The

parameters for the equations for the heat transfer of the freeboard and the bed of solids are different.<sup>12</sup>

### 5.5.3. Kinetics

Kinetics are a challenging part to evaluate in pyrolysis. It is known that there are many different reactions within pyrolysis with their own parameters and orders. Trying to achieve a comprehensive set of reactions, Peters et al.<sup>29</sup> defined 149 individual reactions previously set up by Ranzi et al.<sup>34</sup> in a pyrolysis reactor without being too simple. However, there is a lack of the secondary cracking reactions in this model, and the whole set of reactions would be composed of thousands of still unknown reactions with different parameters. The critical information for the design of the reactor is the product distribution based on the feedstock and the conditions, the properties should be studied once the reaction has been carried out.<sup>29</sup>

## 6. Conclusions

Pyrolysis has been done for centuries for char making purposes; however, none of the technologies used until now is apparently the best choice. Each of them has different advantages and disadvantages. Despite being the char the main product, the significant amounts of bio-oil and gas produced have to be taken to account in the process and the post-treatment.

With this wide range of technologies available, it is essential to define the criteria for the reactor choice and establish a classification based on some characteristics such as feeding capacity, yields or heating methods, among others. Weighting should be associated with each feature for a better evaluation of the alternatives. One example of this type of classification was done by Duku et al.<sup>6</sup> In our case, however, the criteria will be different because it is more focused on the efficiency of the process rather than the investment needed for the technology.

In addition to the reactor selection, the process parameters such as temperature, residence time of solids and liquids, and heating rate will influence the quality of all products, and the influence will vary from each technology. Moreover, the reactor is a vital part of the plant, but the pre-treatment and the post-treatment processes are required to get the maximum value from the feedstock.

Once the reactor is defined, the role of the Early Stage Researcher #3 will be its design, which is still very challenging due to the lack of technical information for it. The methodology is divided into four interconnected parts after selecting the reactor: the behaviour of the solids in the reactor, the heat transfer, the kinetics of pyrolysis and the mechanical specifications. None of these parts is fully defined in the literature for the design of a pyrolysis reactor, and this project gathers all the information available in the literature to design an industrial pyrolysis reactor.

Table 1. Comparison of the reactor technologies available for slow pyrolysis.

Criteria	Reichert Process	Lurgi	Lambiotte Process	Waggon Retort	Twin Retort	Shelf Reactor	Herreshoff Multiple-Hearth Furnace	Rotary Drums	Auger Reactor	Moving Agitated Bed	Paddle Pyrolysis Kiln
<b>1. Technical Aspects</b>											
<b>1.1. Reactor Size</b>											
1.1.1. Dimensions	Large	Large	Large	Small-Large	Small	Small	Large	Small	Small	Medium/Large	Small
1.1.2. Position	Vertical	Vertical	Vertical	Horizontal	Horizontal/Vertical	Horizontal/Vertical	Vertical	Horizontal	Horizontal	Horizontal/vertical	Horizontal
1.1.3. Reactor Volume [m <sup>3</sup> ]	100		600	12	5-16.5	na					
1.1.4. Size [m]	Height: 8.5 Diameter: 5	Height: 27 Diameter: 3	Height: 16.3-18.4 Diameter: 3-4.3	Length: 8-9 Diameter: 2.5	0.3x0.3x0.1					Height: few cm	
1.1.5. Capacity [t/h]	8.7	3.4-6.2	0.4-2.5	2.1	1.1		1-12.5	1.2-12	<2.1	3.0-3.5	
1.1.6. Production [t/h]	3	1.6-1.7	0.25-3	0.75	0.3-0.9		1.9-2.75	0.36-3.6	<0.36		
<b>1.2. Process conditions</b>											
1.2.1. Raw material	Beech wood		Oak wood		Softwood/ Hardwood						
1.2.2. Material Shape	Cordwood	Coorwood	Coorwood	Cordwood	Cordwood/chips	Chips	Chips/ Fine particles	Chips/ Fine particles	Chips/ Fine particles	Chips/ Fine particles	Chips
1.2.3. Particle Size	Length 30-35 cm. Thickness 10-15 cm.		35 cm length 10 cm thickness	1-1.2 m length 0.08-0.12 m Diameter							
1.2.4. Temperature [°C]	450-550	550-700	547-560		580			500			
1.2.5. Pressure	Atmospheric	Atmospheric	Atmospheric	Atmospheric	Atmospheric	Atmospheric	Atmospheric	Atmospheric	Atmospheric	Atmospheric	Atmospheric
1.2.6. Pretreatment needed	None Max. Moisture 25%	30% maximum	30% maximum	Drying 25% moisture maximum	None	Pre-dried	Drying in chips/fine particles	Ground into chips	None	Pre-dried	None
1.2.7. Feeding method	Batches	Batches	Batches	5-7 m <sup>3</sup> batches	5-16.5 m <sup>3</sup> batches	Shelves	Continuous	Continuous	Continuous	Continuous	Continuous
1.2.8. Process Control	Direct measurement	Direct measurement of temperature	Direct measurement of temperature	Direct measurement of temperature	Direct measurement of temperature	Direct measurement of temperature	Direct measurement of temperature	Direct measurement of temperature	Direct measurement of temperature	Direct measurement of temperature	Direct measurement of temperature
1.2.9. Cycle Time [h]	16-20		11	25-35	22-36						
1.2.10. Targeted product	Biochar	Biochar and bio-oil	Biochar and bio-oil	Biochar and bio-oil	Biochar, bio-oil and gases	Biochar and bio-oil	Biochar	Biochar/heat	Biochar/bio-oil/gases	Biochar/ bio-oil	Biochar
1.2.11. Average Gas yield [wt.%]				20-30					18-35		
1.2.12. Average Bio-oil yield [wt.%]				30-50				37-62	48-62	>50	
1.2.13. Average Char yield [wt.%]	33-38	30-40%	30-35	30-38	22-33		25-30	19-38	17-30		
Criteria	Reichert Process	Lurgi	Lambiotte Process	Waggon Retort	Twin Retort	Shelf Reactor	Herreshoff Multiple-Hearth Furnace	Rotary Drums	Auger Reactor	Moving Agitated Bed	Paddle Pyrolysis Kiln
<b>1.3. Heat transfer</b>											
1.3.1. Heating method	Direct contact with hot gases	Contact with heat gases	Contact with heat gases	Indirect heat	Indirect Heat through the walls	Indirect heat	Contact with hot gases Combustion of pyrolysis gases and/or auxiliary gases	Contact with hot gases Combustion of auxiliary fuels and direct or indirect contact of combustion gases	Direct contact with hot gases/ Use of a hot heat carrier/ indirect heating	Indirect heating (sometime molten salts)	Indirect heating
1.3.2. Charge ignition method	N/A	Hot gases generated in an external oven	Hot gases generated in an external oven	Heating with an external volatiles combustion chamber	External heat and volatiles combustion	Direct measurement	Volatile external combustion chamber to produce hot gases	External heating and volatile combustion	Heating with an external combustion chamber	External oven	External heater
1.3.3. Heat transfer rate achieved	Slow Pyrolysis	Slow pyrolysis	Slow pyrolysis	Slow Pyrolysis	Slow Pyrolysis	Slow or Fast Pyrolysis	Typically slow pyrolysis (could be used for fast pyrolysis)	Slow or potentially fast pyrolysis	Slow or fast pyrolysis	Fast/slow	Slow pyrolysis
<b>2. Economics and Construction</b>											
<b>2.1. Construction</b>											
2.1.1. Materials	Metal	Metal	Metal	Steel High Temperature Steel	Steel/iron/brick	Metal	Metal/ Steel Vessel and piping components	Steel	Metal	Metal	Metal
2.1.2. Portability	Stationary	Stationary	Stationary	Stationary	Stationary	Stationary	Stationary	Stationary	Stationary or portable	Stationary	Stationary
2.1.3. Loading and discharge methods	Mechanical	Mechanical	Mechanical	Waggon use	Manual	Manual/ mechanical	Mechanical	Mechanical	Mechanical	Mechanical	Mechanical
<b>2.2. Economics</b>											
2.2.1. CAPEX [pound/annual char ton]		1.15	60-62.5		120-175				68.5		
2.2.2. OPEX [pound/ char ton]		280	315		332						
<b>3. Others</b>											
3.1. Companies with the technology		Bunbury (Australia) Biochar Engineering (Colorado)	Lambiotte & Cie (France and Belgium) Units in Europe and Balt Carbon Ltd. (supplier for Russia) Biochar Solutions Inc. (USA)	Impianti Trattamento Biomasse (Italy) Alterna Biocarbon (Canada)	Carbo Group (Estonia, Ghana and China) JCKB International		BIG Char (Black is Green Pty LTD) (Australia) NESA	Siemens, Mitsui Babcock, Ethos energy, Graveson Energy Management, Metso, Umwelttechnik GmbH & Co, ML Entosorgungs and Energianlagen GmbH, Noell-KRC, Amaron Energy, Pyreg	Renewable Oil International, Biogreen, Advanced Bio-refinery, Forschungszentrum Karlsruhe (FZK), International Tech Corporation, eGenesis, Agri-tech	Pyrovac International (Canada) NewEarth	Choren, BEST

### Acknowledgements

This project has received funding from the European Union's Horizon 2020 research and innovation programme under the Marie Skłodowska-Curie grant agreement No 721991.

### References

- (1) Antal, M. J.; Grønli, M., The Art, Science, and Technology of Charcoal Production. *Ind. Eng. Chem. Res.* **2003**, *42* (8), 1619–1640.
- (2) Grønli, M.; Antal, M. J.; Schenkel, Y.; Crehay, R. *The Science and Technology of Charcoal Production*; 9781872691923; PyNe Subject Group: 2005.
- (3) Garcia-Nunez, J. A.; Pelaez-Samaniego, M. R.; Garcia-Perez, M. E.; Fonts, I.; Abrego, J.; Westerhof, R. J. M.; Garcia-Perez, M., Historical Developments of Pyrolysis Reactors: A Review. *Energy Fuels* **2017**, *31* (6), 5751–5775.
- (4) Garcia-Perez, M.; Lewis, T.; Kruger, C. E. *Methods for Producing Biochar and Advanced Biofuels in Washington State Part 1: Literature Review of Pyrolysis Reactors*; 11-07-017; Washington State University: Pullman, WA, July 2011, 2011; p 137 pp.
- (5) *Industrial charcoal production, TCP/CRO/3101 (A) development of a sustainable charcoal industry*; Food and Agriculture Organization of the United Nations (FAO): Zagreb, Croatia, June 2008.
- (6) Duku, M. H.; Gu, S.; Hagan, E. B., Biochar production potential in Ghana—A review. *Renew. Sustain. Energy Rev.* **2011**, *15* (8), 3539–3551.
- (7) Nelson, W. G., Waste-wood Utilization by the Badger-Stafford Process1 the ford Wood-Distillation Plant at Iron Mountain. *Ind. Eng. Chem.* **1930**, *22* (4), 312–315.
- (8) Emrich, W., *Handbook of Charcoal Making: the Traditional and Industrial Methods*. 1985.
- (9) *Industrial Charcoal Making*. Food and Agriculture Organization of the United Nations (FAO): Rome Bernan Press(PA), 1985.
- (10) Perry, R. H.; Green, D. W., *Perry's chemical engineers' handbook*. New York : McGraw-Hill, ©2008. 8th ed. / prepared by a staff of specialists under the editorial direction of editor-in-chief, Don W. Green, late editor, Robert H. Perry: 2008.
- (11) Brassard, P.; Godbout, S.; Raghavan, V., Pyrolysis in auger reactors for biochar and bio-oil production: A review. *Biosystems Eng.* **2017**, *161*, 80–92.
- (12) Boateng, A. A., *Rotary kilns: transport phenomena and transport processes*. Amsterdam ; Boston : Elsevier/Butterworth-Heinemann: 2008.
- (13) Fantozzi, F.; Colantoni, S.; Bartocci, P.; Desideri, U., *Rotary Kiln Slow Pyrolysis for Syngas and Char Production From Biomass and Waste—Part I: Working Envelope of the Reactor*. 2007; Vol. 129, p 901-907.
- (14) Mayer, Z. A.; Apfelbacher, A.; Hornung, A., A comparative study on the pyrolysis of metal- and ash-enriched wood and the combustion properties of the gained char. *J. Anal. Appl. Pyrolysis* **2012**, *96*, 196–202.
- (15) Pradhan, U. Physical treatments for reducing biomass ash and effect of ash content on pyrolysis products. Auburn University, Auburn, Alabama, 2015.
- (16) Dhyani, V.; Bhaskar, T., A comprehensive review on the pyrolysis of lignocellulosic biomass. *Renew. Energy* **2018**, *129*, 695–716.
- (17) OY, C., CARBOFEX OY- Sustainable Industrial Production of Biochar. In *WASTE TO VALUABLES*, OY, C., Ed. CARBOFEX OY: Hiedranranta, Tampere, Finland, 2017.
- (18) Lynch, J.; Stephen, J. *Guidelines for the Development and Testing of Pyrolysis Plants to Produce Biochar*; International Biochar Initiative, 2010; p 32.
- (19) Rogers, J. G. A techno-economic assessment of the use of fast pyrolysis bio-oil from UK energy crops in the production of electricity and combined heat and power. Aston University, 2009.
- (20) Major, J. *Guidelines on Practical Aspects of Biochar Application to Field Soil in Various Soil Management Systems*; International Biochar Initiative: 9 November 2010, 2010; p 23.
- (21) Chong, K. J. A methodology for the generation and evaluation of biorefinery process chains, in order to identify the most promising biorefineries for the EU. Doctoral Thesis, Aston University, Birmingham, 2011.
- (22) Olszewski, M.; Kempegowda, R. S.; Skreiberg, Ø.; Wang, L.; Løvås, T., Techno-Economics of Biocarbon Production Processes under Norwegian Conditions. *Energy Fuels* **2017**, *31* (12), 14338–14356.
- (23) Chong, K., CE3001: Process economics and loss prevention course. Aston University, 2017.
- (24) Peters, M. S.; Timmerhaus, K., *Plant design and economics for chemical engineers*. 4th ed ed.; McGraw-Hill: New York, 1991.
- (25) P. Towler, G.; Sinnott, R. K., *Chemical Engineering Design: Principles, Practice and Economics of Plant and Process Design*. 2013.
- (26) Garrett, D. E., *Chemical engineering economics*. Van Nostrand Reinhold: New York, 1989.
- (27) Olivares-Olivares, P., Module 04: Finance and Economic Project Management. In *Master in Project Management*, Kühnel Business School: Zaragoza, Spain, 2017.
- (28) Perez-Perez, M., Quality Management and Production Organization. In *Chemical Engineering Degree*, Zaragoza, Ed. University of Zaragoza: Zaragoza, 2013.
- (29) Peters, J. F.; Banks, S. W.; Bridgwater, A. V.; Dufour, J., A kinetic reaction model for biomass pyrolysis processes in Aspen Plus. *Appl. Energy* **2017**, *188*, 595–603.
- (30) Saeman, W. C., Passage of Solid through Rotary Kiln. *Chem. Eng. Progress* **1951**, *47* (10), 508–514.
- (31) Babler, M. U.; Phounglamcheik, A.; Amovic, M.; Ljunggren, R.; Engvall, K., Modelling and pilot plant runs of slow biomass pyrolysis in a rotary kiln. *Appl. Energy* **2017**, *207*, 123–133.
- (32) Shen, J.; Wang, X.-S.; Garcia-Perez, M.; Mourant, D.; Rhodes, M. J.; Li, C.-Z., Effects of particle size on the fast pyrolysis of oil mallee woody biomass. *Fuel* **2009**, *88* (10), 1810–1817.
- (33) Nellis, G.; Klein, S. A., *Heat transfer*. New York : Cambridge University Press, 2012.
- (34) Ranzi, E.; Cuoci, A.; Faravelli, T.; Frassoldati, A.; Migliavacca, G.; Pierucci, S.; Sommariva, S., Chemical Kinetics of Biomass Pyrolysis. *Energy Fuels* **2008**, *22* (6), 4292–4300.



## Matter of modelling in thermochemical conversion processes of biomass

Przemyslaw Maziarka, Frederik Ronsse

*Department of Green Chemistry and Technology, Ghent University, Coupure links 653, 9000 Gent, Belgium*

### Abstract

Modeling is a complex task combining elements of knowledge in the field of computer science, mathematics and natural sciences (fluid dynamics, mass and heat transfer, chemistry). In order to correctly model the process of biomass thermal degradation, in-depth knowledge of multi-scale unit processes is necessary. The biomass processing model can be divided into three main subparts depending on the scale of unit processes: molecular, single particle model and reactor model. Molecular models describe the chemical changes in biomass structural compounds. The model of the single particle corresponds to the description of the biomass structure and its influence on the thermophysical behavior and the subsequent reactions of the compounds released during biomass decomposition. The largest subpart and at the same time the most difficult to describe is the reactor model, which describes the behavior of a vast number of particles, the flow of the reactor gases as well as the interaction between them and the reactor. This chapter contains a basic explanation about what the model is and how it works from a practical point of view. In addition, an extended description of each subpart is presented.

### 1. Introduction

Biomass was the primary source of energy and materials until the Industrial Revolution<sup>1</sup>. With the increase of availability and usage of the cheaper and more abundant fossil resources, biomass, a crucial resource so far, was put aside. Since the negative influence of greenhouse gases (GHG) on the climate became to be a recognised phenomenon (mainly related to CO<sub>2</sub>), strong actions against its emissions started to take place. Additionally, society self-awareness about the depletion of fossil resources and the ecological capacity of the environment regarding pollution gave strong and positive feedback on the research and development of more sustainable technologies. Reduction of GHG and pollution has taken place by the partial replacement of energy from fossil fuels by more sustainable and eco-friendly energy sources like, e.g., sunlight or water movements. There is also a steady trend of replacing the fossil origin carbonaceous materials with materials of biomass origin. In the case of the production of materials, there is no other natural resource, like in case of energy, so its production is only possible through biomass processing. The replacement has two main advantages. Firstly, it lowers the environmental impact of materials during its production, usage, and utilisation through its significantly lower or in some case even neutral GHG emissions<sup>2-3</sup>. The second main advantage is the sustainability regarding the resource renewal and variety of feedstock type.<sup>4-5</sup>

One of the most important processes of the primary biomass conversion into carbonaceous materials is pyrolysis. It can be defined as the thermal conversion of biomass in an atmosphere with reduced oxygen content to prevent its burnout. The "idea" of the process is not a new concept and has been known since ancient times<sup>6</sup>. As one can presume, older technologies are based on very basic solutions, like kilns or burning pits, which are simple in operation, but its efficiency and process control are relatively poor. Not without significance is the fact that in the past the knowledge about the conversion process itself was not broad and did not allow for significant

improvements of technologies. In the last four decades, due to social pressure and though research initiatives, the knowledge gaps started to be filled and new, more efficient solutions start to appear. Unfortunately, despite the pressure on fossils replacement, the alternative materials produced with novel technologies are in many cases not sufficiently engineered or their price is uncompetitive on the current market. For this purpose, new and more sophisticated methods of research as well as new technological ideas are being developed to meet both economic and engineering ends of the problem.

### 2. Biomass conversion - modelers approach

#### 2.1. Simulation and its uncertainties

Substantial improvement in the last 30 years of the computer science brought ease and spread the access to a robust tool —the numerical modeling. Simulations conducted on numerical models allow to significantly improve the pace of research and development in the biomass processing field.

Some commonly used words need to be defined and clarified before the explanation of the computational modeling. A model is the mathematically described (by algorithms and equations) representation of system existing in real life, and a simulation is an action of performing a test on a model. The term numerical means that the mathematical model is translated into a numerical language (through informatics) to conduct computation on a numerical tool, more straightforward, and on the computer<sup>7</sup>. Models can be various, depending on the field where they are used, but in natural sciences and engineering, the most commonly used ones are the numerical models.

It needs to be kept in mind that models are only a representation of the real system, and in most cases, they assume simplifications and approximations. Moreover, the model background is often based on experimental data, which could be burdened with an error. Therefore, simulation results in most cases show discrepancies from "true" results, caused by unknown deviations of the model

elements, which are known as uncertainties. To be able to diminish the deviation of the result from reality, uncertainties need to be found, quantify and clarified. The sources of uncertainty can be divided into<sup>8</sup>:

- *Parameter uncertainty*. The parameters used in the model, which cannot be experimentally measured (too hard or too expensive) and had to be assumed in the model.
- *Model inadequacy*. Lack of full knowledge about the theory behind the modeled system or influence of the simplifying assumptions.
- *Residual variability*. Simulation output differs from the experimentally obtained output through random fluctuations of parameters in a real situation (low repeatability of the real system).
- *Parametric variability*. The modeled system is not sufficiently described/measured, and input values have to be assumed.
- *Observation error (experimental uncertainty)*. The deviation in values due to the variability of experimental measurements.
- *Interpolation uncertainty*. Assumption of the tendency of the parameter in the range of experimental results between measured data points.
- *Code uncertainty (numerical uncertainty)*. The strongest related with numerical procedures, caused by the lack of possibility of exactly solving the problem (technical boundaries) and use of the approximation while solving (e.g., a partial approximation of the partial differential equation by a finite element solution method).

A clear indication of the individual share of each uncertainty on the total is not simple, but a proper clarification of each improves the model's accuracy. In the modeling, researchers are advised to keep a critical and very careful approach.

A simplified scheme of simulation study with the linkage between the experiments, theory, and model is shown on Figure 1. As it can be seen, the simulation has to be validated to have certainty about its usefulness. Models based on experimental data are reliable only in a specified range of experimental value and, only for this range, results are valid. Therefore, it is always better to set the foundation of the model on the fully established theories, which in general have a broader range.

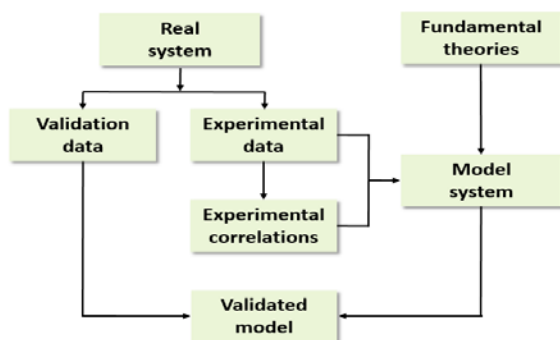


Figure 1. Simplified scheme of simulation study.<sup>9</sup>

## 2.2. Simulation and profit

Simulations on the properly constructed model result in valuable information about the system behavior, which often cannot be obtained through measurement. Such knowledge can give a significant boost for innovative solutions in development and help to identify the critical points of the system (bottlenecks). In general, using the modeling in studies of technology development brings four main advantages:<sup>7</sup>

- To allow to conduct Proof of Concept analysis at the very beginning of the project (low sunk cost in case of failure).
- To allow to perform numerous tests with a low unit cost.
- To increase the knowledge about dependencies in a real system.
- To accumulate the obtained datasets and simplify their treatment and sharing (Big Data processing).

All of the mentioned advantages can have crucial meaning for the economic feasibility of new technological solutions development. As it is shown in Figure 2, the application of the simulation can reduce the overall cost of new solution implementation and decrease the risk of the project's unprofitability, which in the development of new technologies is a strong benefit.

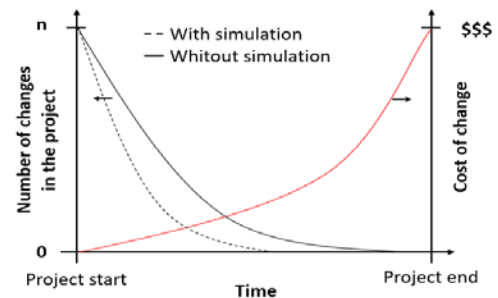


Figure 2. Changes of the new idea implementation costs, through the project time.<sup>7</sup>

Models are more flexible than real processes, so changes in modeled systems and its influence can be quickly verified. It allows for solving technical problems in the early stage, which is the most costly option. Modeling can also expand the knowledge about the investigated process. If the model is detailed and mimics the real system adequately, there is a possibility to investigate and validate new correlation and theories through large and detailed databases of the process history.

## 3. Idea behind the CFD-DEM method

### 3.1. Computational Fluid Dynamics

As defined, Computational Fluid Dynamics (CFD) is the analysis of systems involving fluid flow, heat transfer and associated phenomena (e.g., chemical reactions) by using computer-based simulation<sup>10</sup>. In general, it can be stated that CFD is the integration of the fields of natural sciences (physics and chemistry), mathematics and computer science<sup>11</sup>, as it is shown on Figure 3.

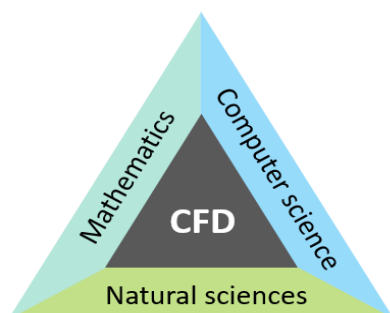


**Figure 3.** Scientific fields included in the CFD.<sup>11</sup>

According to the fluid dynamics principles covered in CFD, the flow of matter (fluid) is treated as a continuum (Eulerian approach). In the Eulerian approach of fluid dynamics descriptions, the points in the entire geometry do not change their position with the fluid motion<sup>12-13</sup>. Therefore, the Eulerian approach allows only for the description of parameters changes at a certain point of the investigated geometry as the change of the parameter field. Such an approach also indicates no distinction for specific molecules/particles, so their time-based investigation is not possible. The model behavior is based on governing equations—the mathematically described physical behavior in the form of differential equations (e.g., Navier-Stokes equations). To solve mathematical equations, computer scientists developed high-level computer programming languages, which convert them into computer programs or software packages possible to understand by a computing machine. CFD, for its computation, uses the dimensional geometrical domains, which are the backbone for the mathematical construction of the model. Prior to performing a simulation, the specified geometry (domain) needs to be subdivided into a finite number of smaller, non-overlapping subdomains called cells. The process of domain division into the subdomains is called meshing and results in a grid of cells overlying the whole domain geometry, as shown in Figure 4.

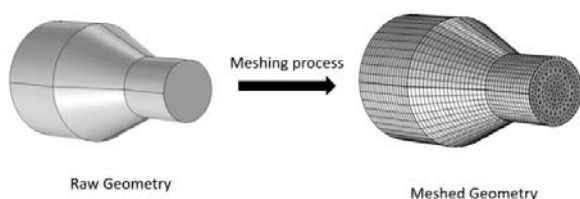


**Figure 4.** Visualization of meshing based on finite volume method (from COMSOL Multiphysics 5.3).

The cell can be defined as representative of an element or a volume, depending on the division method (finite element or finite volume). In most commercially available CFD software, geometry division method is already implemented in the code. Each cell consists of a node, which hold all the information about a certain point of the geometry. Information stored in the node changes according to the applied physics and chemistry (governing

equations). The accuracy and precision of the result from a CFD model are based on a number of cells contained in the grid (mesh coarsens). The increase in the number of cells will result in an improvement of model accuracy, but only until the point when the addition of new cells does influence the result, so until the point when the result becomes grid independent. The most coarse grid, in which further mesh densification does not lead to improvement of the solution, is called independent grid<sup>10</sup>. Conducting simulations on an independent grid has a major advantage: smallest numerical error with simultaneous less possible coarse mesh (lowest computational burden).

A detailed explanation of the procedure for a CFD solution is robust and very complex, and goes beyond the purpose of this chapter; therefore, it will be omitted. Nevertheless, a brief introduction to the matter is provided. A simplified scheme of CFD data treatment and computing procedure is shown in Figure 5. The framework procedure for the CFD code consists of three main elements solution:<sup>11</sup>

- **Pre-processor.** It is a part of the code responsible for implementation of investigated geometry, and its consecutive meshing. Mesh obtained in the pre-processor is the foundation for the future implementation of governing equations and shapes the process of simulation.
- **Solver.** It is responsible for the performance simulation. It contains and processes all information regarding the applied physics and chemistry located in the nodes of the grid. Through implemented solution methods, it simulates the changes of the parameters in nodes according to the applied governing equations and boundaries parameters.
- **Post-processor.** It is responsible for the visualization of the results (data sets) obtained in simulations. Most post-processors allow for quick creation of 1D plots and presentation of parameters of interest on the applied geometry (2D and 3D plots). As well as for the solver, foundations of the visualisation are the mesh. Therefore, the results can be as detailed as an applied mesh.

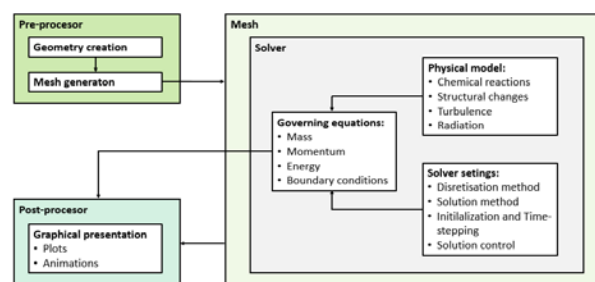


**Figure 5.** CFD code solution scheme.<sup>11</sup>

### 3.2. Lagrangian method

The method that allows for the distinction of individual particle behavior in the system is called the Discrete Element Method (DEM). The single particle movement in the DEM method is based on the Lagrangian approach, built on Newton's second law of motion<sup>14-15</sup>. In the Lagrangian approach, each particle is modeled with its own

body (subdomain), which moves in applied geometry according to forces affecting the particle. It allows for investigation of the particle's trajectory. The visualization of the difference between Eulerian and Lagrangian approaches is shown in Figure 6. The particles movement independence leads to their different thermal and chemical behavior, due to different position and different residence time in the processing environment. Moreover, the Lagrangian description allows for the implementation of particles mechanical interactions. It opens the possibility for the investigation of the particle-particle and particle-wall interactions.

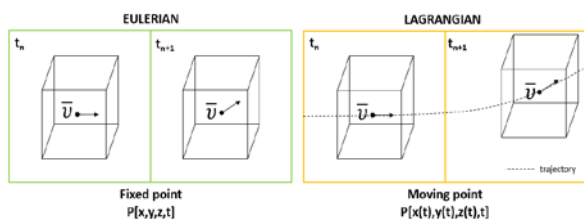


**Figure 6.** Simplified visualization of the difference between Eulerian and Lagrangian approach.

### 3.3. Two phase flow description

For single-phase flow description, the Eulerian description can cover all significant unit processes. Unfortunately, such a method can be insufficient in the case where the flow is two-phased (gas-solid systems). In peculiar cases, when the particles size is significantly small, there is a possibility of simplification. Such approach leads to the assumption that particles suspended in the fluid are “dissolved” in it. Therefore they can be treated as a part of the fluid and behave as such (quasi-continuous models). The assumption leads to a change from the two-phase model to the one-phase model. Models that describe the two-phase model as one-phase are called Eulerian-Eulerian models. It indicates that both gases and solids are described by the Eulerian approach, and during the simulation the distinction of the particles in the flow is not necessary nor possible. This simplification is very convenient in terms of mathematical description because it does not require the implementation of different terms for suspended particles movement, and simultaneously can cope with their physical and chemical behaviour. As it can be expected, applying the simplification to relatively large size particles introduces larger deviation between reality and model. It results in significant model inadequacy and low result accuracy.

A comprehensive and complete description of the behaviour of the two-phase gas-solid system is provided by the Eulerian-Lagrangian approach. The first part of the approaches name is related to the gaseous phase description (fluid with continuum properties). In a model, its properties are stored in grid nodes of applied geometry. The fluid movement does not interfere with the grid arrangement. The second part is related to the solid particles. They are not constricted with the fluid grid, and particles subdomains can move freely through the applied geometry. Nevertheless, the movement of the particles

subdomain along applied geometry causes change in the fluid grid. Therefore, the movement of solids has an influence on fluid behaviour. Combination of the Eulerian and Lagrangian approaches is called CFD-DEM method<sup>14</sup> or XDEM (eXtended DEM)<sup>16</sup>. With the increase in the amount of investigated particles, as well as the complexity of the model of single particle behaviour, the quantity of data that needs to be handled by the solver grows exorbitantly. Therefore, proper implementation of the Eulerian-Lagrangian method into the investigated system, besides the in-depth knowledge on its description and variety of input data, needs a robust numerical software and powerful hardware.

### 3.4. Structure of a comprehensive model

First, it needs to be mentioned that all the schemes described in this section are treated as first-order Arrhenius reactions, with the pre-exponential parameters set as constant or temperature-dependent. Furthermore, to narrow down the description possibilities and limit the data regarding biomass properties, the wood will be treated as the exemplary lignocellulosic biomass type. The building of a comprehensive/multi-scale model for biomass conversion can be divided into parts according to the scale in which the crucial processes take place. It is illustrated in Figure 7. Besides combined implementation, each model part can be studied separately, experimentally or through simulation, leading to expanding the knowledge of certain biomass conversion process phenomena.

Model	Considered size	Covered processes	Need of numerical solvers
 Molecular	Biomass structural polymers	<ul style="list-style-type: none"> <li>Primary bio-polymers degradation</li> <li>Secondary charring</li> <li>Secondary tar cracking</li> <li>Catalytic effects</li> </ul>	NO
 Single Particle	Single particle of porous biomass	<ul style="list-style-type: none"> <li>Reaction kinetics</li> <li>Particle drying</li> <li>Internal flow and heat and mass transport</li> <li>Internal structure change</li> </ul>	YES
 Reactor	Pyrolysis reactor environment	<ul style="list-style-type: none"> <li>Behaviour of single particle</li> <li>Reactor's fluid dynamics</li> <li>Reactor's heat and mass transfer</li> <li>Particle - particle/wall/ gas interactions</li> </ul>	YES

**Figure 7.** The idea of comprehensive biomass conversion model construction, adapted from Anca-Couce.<sup>17</sup>

The smallest considered scale in the comprehensive model is named molecular model. It describes the chemical reactions of organic compounds and catalytic effects of inorganic compounds, which take place during the biomass conversion process. Chemical reactions are not dependent on spatial dimensions. Therefore, implementation of the geometry can be omitted. The amount of data that is in use for this scale allows for simulations without robust numerical solvers.

A model covering sizes larger than molecular is named single-particle model. It describes the behavior of one particle of biomass for which temperature and pressure gradients during the process play a crucial role and cannot be diminished. In respect to the real system, the single-particle model needs to contain a description of the heat and mass transport and fluid dynamics within the particle. The model covers changes in particle size, shape and structure (porosity) as well as bio-polymers chemical reactions and the water evaporation process. The behavior

of gaseous product mixture has a strong influence on the final products yield and composition<sup>17</sup>. Thus, the fluid movement within the particle as well as its chemistry has to be described in a very detailed manner. In the model, gases and liquids are treated as fluids, and biomass as stagnant solids, which is indicated in the model description as separate phase system. Therefore, the Eulerian description is sufficient to cope with such physical behaviour. As mentioned before, the model is strongly dependent on the geometry, so the use of a numerical solver is necessary to perform simulations.

The last subpart of biomass conversion model is the reactor model. It covers the description of every relevant unit process in reactor for biomass thermo-chemical conversion. The behaviour of each biomass particle in most cases should be described separately, according to the single particle model. Besides particle conversion, the model also consists of flow and thermal behaviour of gases, particle movement (collisions with each other and walls) and thermo-physical interactions between gas and solid phase. If a simplification is not applied, the total flow through the reactor is two-phased due to the immersion of the biomass particles in the reactor gas. Therefore, in the reactor model, the Eulerian description for fluids needs to be combined with the Lagrangian description for biomass particles. As it can be anticipated, the quantity of equations and the amount of data needed to be processed in this model is the largest among other sub-parts of a comprehensive model. Besides of the need of a numerical solver to conduct the simulation, its performance in an efficient manner requires appropriately large computational power resources.

## 4. Molecular model

### 4.1. Single component and competitive schemes

Historically, research started with the introduction of the simplest biomass pyrolysis models, due to low technical feasibilities of the detailed investigation. It had only limited ability for outcome prediction. Simple, single component models aim at predicting the yield of the three main products from biomass pyrolysis: char, tar, and gas, without distinguishing their detailed composition. They include one reaction (decomposition of biomass into three products) and therefore, they cover only primary pyrolysis reactions<sup>18</sup>. Further improvements of the single models were made after the discovery of the cracking reaction of condensable vapors (named tars) at temperatures higher than 500 °C. The single component model with implemented consecutive tars reactions is named competitive kinetic scheme. The most often used is the one proposed by Shafizadeh and Chin<sup>19</sup>, which is shown in Figure 8. This model, however, does not consider low temperature (below 500 °C) tar-char interactions, called secondary charring reactions<sup>17</sup>. In most cases, secondary charring reactions in single component models are hindered in the values of the primary kinetic reaction parameters. It leads to major discrepancies in values of

kinetic parameters between biomass pyrolysis investigations. Fluctuations in the kinetic values available in the literature are also caused by application of feedstock with different bio-composition, size, and morphology as well as the application of different research methodologies.

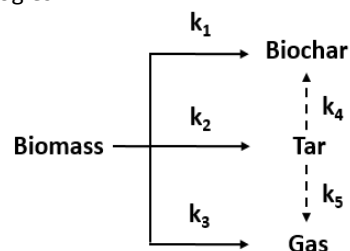


**Figure 8.** Shafizadeh and Chin's competitive biomass pyrolysis scheme including high-temperature tar cracking.<sup>17</sup>

In the literature, extensions/improvements of the Shafizadeh and Chin competitive scheme (e.g., with intermediate components) can be found, but all of them shows only moderate improvement regarding the model accuracy<sup>20-21</sup>. For the more accurate outcome of the model, they needed to undergo significant development in terms of bio-components thermal degradation, together with a detailed description of the degradation of consecutive (secondary) products.

### 4.2. Detailed reaction schemes: Ranzi scheme

A very detailed description was firstly introduced by Ranzi et al.<sup>22</sup>, and it was further improved by him and his co-workers<sup>23-27</sup>. The Ranzi's model combines all findings related to the thermal decomposition of each biomass major component: cellulose, hemicellulose, and lignin<sup>28-30</sup>. It also distinguishes total lignin between 3 artificial types of lignin: LIG-H, LIG-O, and LIG-C, according to their chemical structure. Another innovation of the Ranzi's model is the char description, which distinguishes "pure" char and the volatiles "trapped" within a char metaplastic phase (e.g., G [CO]). Thermally unstable "traps" degrade according to the applied kinetic reaction, releasing captured volatiles. Such a description allows for the introduction of char devolatilisation into the kinetic scheme. Reactions of extractives were introduced in the Ranzi model by Debiagi et al.<sup>31</sup>. The extension assumes reactions of two representative compounds (tannin and triglyceride) and it significantly broadened the range of the biomasses for which the model is valid. Ranzi's model does not cover all possible evolved species, but reduces its amount to 20 representatives, most abundant in non- and condensable vapors. The Ranzi scheme allowed for the derivation of complex reaction schemes, combining separate chemical reactions into the consolidated model, which is summarised in Figure 9. Most up to date kinetic parameters and heat of reaction for Ranzi's scheme, composition of vapors, kinetic parameters, and reaction heat can be found in the work of Ranzi<sup>26-27</sup> and Anca-Couce.<sup>32</sup>

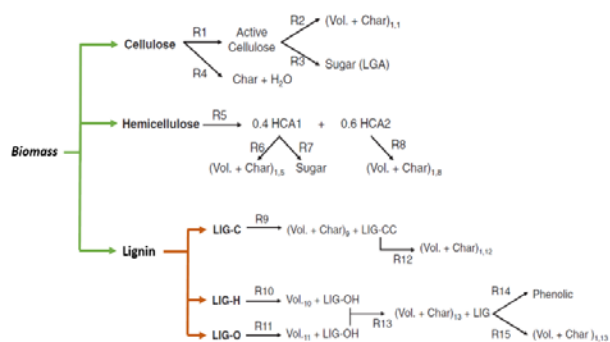


Figure 9. Ranzi's kinetic scheme, adapted from Anca-Couce.<sup>17</sup>

For an implementation of the Ranzi's model, knowledge about the biomass bio-composition is necessary. Investigation of the analytical method in order to obtain the most reliable bio-components composition was made by the NREL research group<sup>33-34</sup>. It resulted in a detailed analytical procedure<sup>35</sup>. Despite the high accuracy and repeatability of the NREL method, it is very time-consuming. Therefore, only a minority of authors conduct/commission the bio-components measurement. To by-pass experimental measurements, Debiagi et al.<sup>31</sup> proposed a correlation between biomass elemental and bio-components composition. Elemental analysis has a much more simple procedure and the equipment needed for its performance is much more available in academia and in industry. For now, the correlation has low accuracy, due to the low amount of input data, but its further improvement will have a beneficial effect on the simplification of obtaining initial parameters.

The Ranzi's model is a milestone in the description of pyrolysis kinetics, but there are a few areas in which improvement or extensions can be made. The kinetic scheme does not cover tar-char reactions at low temperatures, and it does not consider the catalytic influence of the mineral matter (mainly alkali and alkaline-Earth species, AAEM) contained in biomass. Moreover, the pyrolytic mechanics of the phenolic compounds evolution is not considered. Such limitations of the model result in over-estimation of the sugar products and under-estimation of the production of BTXs.<sup>17, 36</sup>

#### 4.3. Detailed reaction schemes: Ranzi and Anca-Couce model

A partial extension of secondary charring reactions to the Ranzi's scheme was introduced by Anca-Couce et al.<sup>32</sup> This adaptation was named as RAC (Ranzi and Anca-Couce) model, which is shown in Figure 10. A full description of the model and its kinetic and thermal parameters can be found in the works by Anca-Couce et al.<sup>36-37</sup>

As can be observed in Figure 10, the RAC model introduces an adjustable parameter "x," which defines the proportion of the alternative route of degradation (secondary reactions, e.g., charring reaction) in the overall degradation process. The adjustable parameter also partially takes into account the influence of inorganics, which have a role in leading the way of the degradation reactions.

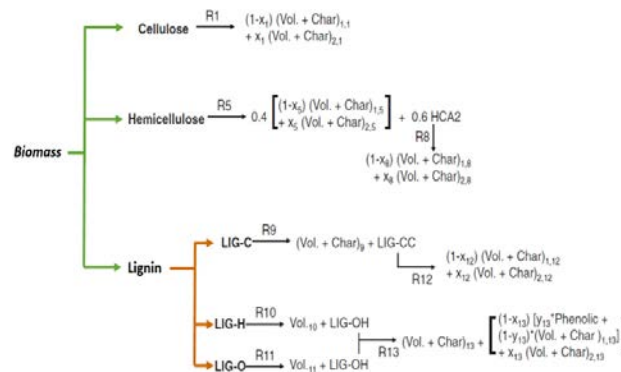


Figure 10. RAC kinetic scheme adapted from Anca-Couce.<sup>17</sup>

The main events that increase the value of the adjustable parameters are<sup>17</sup>:

- A decrease in temperature.
- A decrease in heating rate.
- An increase in volatiles retention time into the particle (larger particle or slower gas flow rates).
- An increase in pressure.
- An increase in the content of inorganics (especially AAEM).

In the theory behind the scheme, the amounts of secondary reactions, indicated by the value of the "x" parameter, differ for each bio-component. Unfortunately, the lack of a quantitative correlation between the conditions of pyrolysis, biomass parameters and amounts of secondary charring reactions causes the need for an iterative fitting of those parameters to the experimental result. A common approach is to set the adjustable parameter as the same for all bio-components *a priori*, based on the available experimental data. From examples of data fitting to experimental results, it can be stated that, for pyrolysis and torrefaction in a fixed bed, values of x can be adjusted in the range of 0.3–0.4; for fluidized bed they should be lower than for fixed bed, due to higher gas movements; and for experiments in micro-TGA, the proper value should be around 0.2, due to significant fragmentation of investigated material<sup>17, 38</sup>. It is worth to mention that the proportion of the secondary charring reactions have a noticeable influence on the heat of the reactions, as it was observed by Rath et al.<sup>39</sup> during the investigation of spruce wood pyrolysis.

The RAC scheme does not cover all areas, in which the Ranzi scheme lacks (e.g., a detailed description of AAEM's influence or insights into polycyclic aromatic compounds formation). Constant work and recent findings on the subject give promise of improvement and further extension of the pyrolysis scheme, which would allow for better understanding of biomass pyrolysis process and predict its outcome with higher accuracy.<sup>40-42</sup>

## 5. Single-particle model

The single-particle model focuses on the influence of the boundary conditions and thermo-physical properties of the particle and other products on the behaviour of a single

biomass particle during the processing. The biomass particle, due to its structure, cannot be treated as an unpermeable solid block, since the description of the porous structure needs to be implemented. In applications outside research, biomass is rarely fed to a pyrolysis process in a dry state. Therefore, for boarding application of the model, besides the description of the pyrolytic behaviour, it needs to cover the drying process and a description of the water movements within the particle.

### 5.1. Definitions of phases in particle structure

A wet biomass feedstock used for the process consists at least of four different phases: liquid water, bounded water, gas mixture and solid. The bounded water is distinguished from liquid water due to its significant difference in behaviour. Each of the mentioned phases needs to be identified and described for further investigation. All of the phases are treated as a continuum, for which conservation laws must be satisfied. A primary but detailed description of each phase was made by Whitaker<sup>43</sup>, for which the boundary surface between each phase has to be differentiated in order to calculate phase fractions. Wood structure has a very complex geometric structure. Therefore, it would be hard to describe the boundary surfaces and keep track on them during the pyrolysis process, and the amount of computation for such sophisticated model would be very burdensome for the solver. The problem of efficient description was further investigated by Perre and co-workers<sup>44-45</sup>, and an elegant description of this issue was presented by Grønli<sup>46</sup>. The improved approach assumes the application of the conservation equations volume averaging over a representative volume, which contains all existing phases. It results in a set of conservation equations for every phase, valid within the applied particle geometry.

For a further description it will be helpful to define the artificial variable  $\varphi$ . Its spatial average defined over the applied geometry is the averaged value of geometry total volume and contains all the phases existing in the particle. The spatial average is defined as:

$$\langle \varphi \rangle = \frac{1}{V} \int_V \varphi dV \quad (1)$$

The average for one of the phases is defined in general as  $\gamma$  and the phase average is defined as:

$$\langle \varphi \rangle^\gamma = \frac{1}{V_\gamma} \int_{V_\gamma} \varphi dV \quad (2)$$

where  $\langle \varphi \rangle^\gamma$  is the averaged value of the quantity in the phase  $\gamma$ , and  $V_\gamma$  is the volume of the phase in the representative volume. The volume fraction occupied by the phase  $\gamma$  is defined as:

$$\varepsilon_\gamma = \frac{V_\gamma}{V} \quad (3)$$

where  $\varepsilon_\gamma$  is the fraction of total volume occupied by the phase  $\gamma$ . The relation of the averaged value quantity between the one located in phase  $\gamma$  and the spatial average can be calculated as follows:

$$\langle \varphi \rangle = \varepsilon_\gamma \langle \varphi \rangle^\gamma \quad (4)$$

In other words, it can be stated that  $\langle \varphi \rangle^\gamma$  is the intrinsic or true value of the quantity, and  $\langle \varphi \rangle$  is the average value of the quantity in the representative volume. For example,  $\langle \rho_S \rangle^S$  will be defined as the true density of the solid from which the porous structure is made of, and  $\langle \rho_S \rangle$  will be defined as the density of the solid contained in a representative volume of the porous structure, so averaged volume density of the solid with porous space (bulk density). The notation with the  $\langle, \rangle$  brackets is based on the fact that the authors believe that it is clearer in reception and of course, is not mandatory.

As it was mentioned, the particle is made at most out of four phases, therefore the representative volume can be treated as the sum of the volume of each phase:

$$V = V_S + V_L + V_B + V_G \quad (5)$$

where the subscripts S, L, B, and G represent a phase of solid, liquid water, bounded water and gas, respectively. The sum of the volume fraction occupied by each phase sums into one, so:

$$\varepsilon_G = 1 - (\varepsilon_S + \varepsilon_L + \varepsilon_B) \quad (6)$$

$$\varepsilon_G = 1 - \left( \frac{\langle \rho_S \rangle}{\langle \rho_S \rangle^S} + \frac{\langle \rho_L \rangle}{\langle \rho_L \rangle^L} + \frac{\langle \rho_B \rangle}{\langle \rho_B \rangle^B} \right) \quad (7)$$

This means that the volume fraction occupied by the gas is possible to obtain knowing the intrinsic and average density of the solid, liquid, and bounded water. A visual representation of the real system in the Whitaker theory is given in Figure 11.

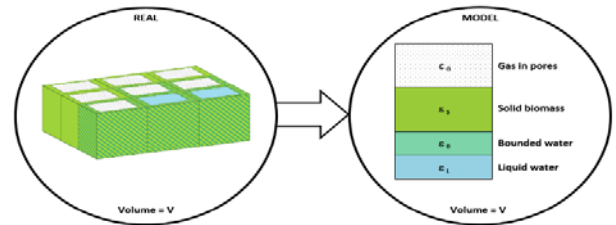


**Figure 11.** Visual representation of the conversion of the real system into the model system according to the Whitaker theory.

### 5.2. Governing equations

In this section, the explanation of the conservation laws is introduced, but no explanation of the theory behind the conservation laws is provided. For the sake of the description clarity and simplicity, the one-component kinetic scheme is used for explanation of principles. The authors will keep to the most general description; therefore, the negative sign will be originated only from the mathematical derivations, not from the values of actual parameters. The equations given in this subsection are valid only within the applied geometry, and they do not describe the interactions of the particle with the environment outside of it. In general, it is worth to keep in mind that all conservation equations are referred to the single representative volume.

### 5.2.1. Mass conservation equations: Solids

At any time of the reaction, the volume of the solid is represented by either biomass or biochar, and hence, it can be stated that:

$$\langle \rho_S \rangle = \langle \rho_{BM} \rangle + \langle \rho_{BC} \rangle \quad (8)$$

where  $\langle \rho_S \rangle$ ,  $\langle \rho_{BM} \rangle$  and  $\langle \rho_{BC} \rangle$  are the volume-averaged density of solid, biomass and biochar; respectively. The mass conservation equation for the biomass can be written as:

$$\frac{\partial}{\partial t} \langle \rho_{BM} \rangle = \dot{\omega}_{BM} \quad (9)$$

where  $\dot{\omega}_{BM}$  is the biomass mass change rate caused by degradation reactions. As it was mentioned, despite the fact that the degradation reaction leads to the reduction of mass, in the equation the negative sign is not used, because the value of the time derivative will be negative. Similarly, the mass conservation equation can be derived for the biochar:

$$\frac{\partial}{\partial t} \langle \rho_{BC} \rangle = \dot{\omega}_{BC} \quad (10)$$

Therefore, in the most general form the mass conservation is defined as:

$$\frac{\partial}{\partial t} \langle \rho_S \rangle = \dot{\omega}_S \quad (11)$$

where  $\dot{\omega}_S$  is the total mass change of the solid obtained from the sum of the reaction of biomass and char.

### 5.2.2. Mass conservation equations: Single component of the gas mixture

The equation for the mass conservation of the  $i$ th component of the gas mixture:

$$\frac{\partial}{\partial t} (\varepsilon_G \langle \rho_i \rangle^G) + \nabla \langle u_i \rho_i \rangle = \dot{\omega}_i \frac{\partial}{\partial t} \langle \rho_S \rangle = \dot{\omega}_S \quad (12)$$

where  $\langle \rho_i \rangle^G$  is the density of the  $i$ th component in the gaseous phase,  $\langle u_i \rho_i \rangle$  the  $i$ th component transport term, and  $\dot{\omega}_i$  the mass change rate caused by formation/degradation reaction of the  $i$ th gas component (e.g., water vapour, gas or tar). Transport of the gas takes place by two phenomena (convection and diffusion) and therefore, the transportation term is defined as:

$$\begin{aligned} \langle u_i \rho_i \rangle &= u_G \langle \rho_i \rangle^G \\ -\langle \rho_G \rangle^G D_{eff} \nabla \left( \frac{\langle \rho_i \rangle^G}{\langle \rho_G \rangle^G} \right) \end{aligned} \quad (13)$$

where  $u_G$  is the superficial gas velocity,  $\langle \rho_G \rangle^G$  the total density of the gas mixture in the gas phase, and  $D_{eff}$  the effective gas diffusion coefficient. Due to the low permeability of the biomass structure, which results in general low superficial velocities of fluids, the Darcy law is valid to obtain the value of superficial gas velocity:

$$\langle u_G \rangle = \frac{K_{G,eff}}{\mu_G} \nabla \langle P_G \rangle^G \quad (14)$$

where  $K_{G,eff}$  is the effective gas permeability,  $\mu_G$  the gas dynamic viscosity, and  $\langle P_G \rangle^G$  the pressure of the gas mixture.

### 5.2.3. Mass conservation equations: Liquid water

The mass conservation equation for liquid water can be written as:

$$\frac{\partial}{\partial t} \langle \rho_L \rangle + \nabla \langle u_L \rho_L \rangle = \dot{\omega}_L \quad (15)$$

where  $\langle \rho_L \rangle$  is the volume-averaged liquid water density,  $\langle u_L \rho_L \rangle$  the transport term, and  $\dot{\omega}_L$  the mass change rate caused by evaporation and/or re-condensation. It is assumed that liquid water migrates through the structure entirely due to the pressure changes (convectively), and therefore its transport term can be expressed as:

$$\langle u_L \rho_L \rangle = u_L \langle \rho_L \rangle \quad (16)$$

where  $u_L$  is the superficial velocity of the liquid water. The Darcy law is also applied to obtain the superficial liquid velocity:

$$\langle u_L \rangle = \frac{K_{L,eff}}{\mu_L} \nabla \langle P_L \rangle^L \quad (17)$$

where  $K_{L,eff}$  is the effective liquid water permeability,  $\mu_L$  the liquid water dynamic viscosity, and  $\langle P_L \rangle^L$  the pressure of liquid water.  $\langle P_L \rangle^L$  is connected with gas pressure and capillary pressure through the following equation ( $P_C$  is the capillary pressure):

$$\langle P_L \rangle^L = \langle P_G \rangle^G + P_C \quad (18)$$

### 5.2.4. Mass conservation equations: Bounded water

The mass conservation equation of bounded water is defined as:

$$\frac{\partial}{\partial t} \langle \rho_B \rangle + \nabla \langle u_B \rho_B \rangle = \dot{\omega}_B \quad (19)$$

where  $\langle \rho_B \rangle$  is the volume-averaged bounded water density,  $\langle u_B \rho_B \rangle$  the bounded water transport term, and  $\dot{\omega}_B$  the mass change rate caused by unbounding. In opposition to liquid water, it is assumed that bounded water migrates entirely by diffusion, and therefore, its transport term is defined as follows:

$$\langle u_B \rho_B \rangle = -\langle \rho_S \rangle D_B \nabla \left( \frac{\langle \rho_B \rangle}{\langle \rho_S \rangle} \right) \quad (20)$$

where  $D_B$  is the bounded water diffusion coefficient.

### 5.2.5. Energy conservation equation

The energy conservation equation is based on the assumption of local thermal equilibrium for gas, liquid, and solid in the particle:

$$\begin{aligned} \frac{\partial T}{\partial t} (\langle \rho_S \rangle C_{p,S} + \langle \rho_L \rangle C_{p,L} + \langle \rho_B \rangle C_{p,B} + \varepsilon_G \langle \rho_G \rangle^G C_{p,G}) \\ + \nabla T \left( \langle u_L \rho_L \rangle C_{p,L} + \langle u_B \rho_B \rangle C_{p,B} + \varepsilon_G \sum_{i=1}^N \langle u_i \rho_i \rangle C_{p,i} \right) = \\ = \nabla (\lambda_{eff} \nabla T) + Q \end{aligned} \quad (21)$$

where  $C_p$  is the specific heat, whereas subscripts  $S$ ,  $L$ ,  $B$  and  $i$  indicate solid, liquid water, bounded water, and  $i$ th component of the gas mixture; respectively.  $\lambda_{eff}$  is the

effective thermal conductivity and  $Q$  is the total heat produced by occurring reactions, which is defined as:

$$Q = \sum_i^N H_i \dot{\omega}_i + H_L \dot{\omega}_L + H_B \dot{\omega}_B + H_S \dot{\omega}_S \quad (22)$$

Where  $H$  is the heat of the reaction. In the most general case, the transport term is treated in conservative form, and the energy conservation equation takes into account the heat transfer through the convective transport and diffusion<sup>46-48</sup>. Some authors apply simplification in defining the transport, omitting the heat transported through diffusion, assuming that the amount of heat exchanged through this phenomenon is negligible<sup>15, 20, 49-50</sup>. With the mentioned assumption, the energy conservation equation takes the following form:

$$\begin{aligned} \frac{\partial T}{\partial t} (<\rho_S> C_{p,S} + <\rho_L> C_{p,L} + <\rho_B> C_{p,B} + \varepsilon_G <\rho_G> C_{p,G}) \\ + \nabla T (u_L <\rho_L> C_{p,L} + u_B <\rho_B> C_{p,B} + u_G \varepsilon_G <\rho_G> C_{p,G}) \\ = \nabla(\lambda_{eff} \nabla T) + Q \end{aligned} \quad (23)$$

### 5.2.6. Reactions

The mass change rate of every reaction in the kinetic scheme is defined as:

$$\dot{\omega}_j = k_j <\rho_j> = k_j \varepsilon_\gamma <\rho_j>^\gamma \quad (24)$$

where  $\dot{\omega}_j$  is the mass change rate of  $j^{th}$  species (e.g., biomass, tar, gas),  $k_j$  is the reaction rate of  $j^{th}$  species,  $<\rho_j>$  is the averaged volume density of the  $j^{th}$  species, and  $<\rho_j>^\gamma$  is the intrinsic density of the  $j^{th}$  species in phase  $\gamma$ . Depending on the applied drying/evaporation model (e.g., equilibrium, heat sink, kinetic), the mass change rate for the liquid water and bounded water will take a form suitable for the chosen model.

## 6. Reactor model and multiscale

The reactor model is the final and, at the same time, the most difficult and time-consuming subpart of the comprehensive modeling of the process of biomass thermal conversion. In this subpart, the division between the reactor gases and processed material phase description have to be considered due to significant physical, chemical and thermal differences.

### 6.1. Gases in reactor

The reactor gas as the fluid is always modeled via the Eulerian approach, which makes it a less challenging part of the reactor modeling, in comparison to particles' description. In terms of the fluid in the reactor, the following has to be described: fluid motion within the reactor geometry, taking into account its moving parts, changes of reactor volume due to particles movement, and heat transport from reactor walls to fluid and from fluid to particles. Moreover, the description of the reactor gas has to cope with the chemical behavior of the species contained in it (e.g., secondary tar cracking).

### 6.2. Identification of the scale on single particle model

As it was mentioned in previous sections, there is a possibility for simplification of the comprehensive model (from two-phase fluid into one) when the single particles are sufficiently small. In order to assess if such approach is valid, the investigation of two non-dimensional numbers is done: thermal Biot number (Bi) and pyrolysis number (Py), which has the Thiele modulus as its inverse<sup>15</sup>. Based on those numbers, the particle can be assigned to one of four thermal regimes: pure kinetic, thermally thin, thermal wave, and thermally thick. Each of the regimes indicates that thermal phenomena (chemical reactions, intra-particle or extra-particle heat exchange) have the strongest influence on the particle thermal behaviour<sup>18, 51-54</sup>. The most complex description of particle behaviour is valid for all regimes, but in case it is not necessary, there is no need to overcomplicate the model.

The simplification is most valid for particles in pure kinetic regime, for which the size, in general, is lower than 1 mm<sup>17</sup>. The particles in the thin thermal regime, due to their structure, do not show thermal or pressure gradient, and thus, the application of the simplification should not introduce a significant error to the model. For particles in the thermal wave regime, application of the simplification is not advised due to the existence of significant gradients during their processing. Nevertheless, there is the possibility of partial simplification of their complex thermo-physical description by the implementation of an unreacted shrinking core model, a volumetric model or a layer model<sup>17, 55</sup>. It is possible because, in the mentioned regime, the conversion of the particle takes place in the thin surface front, and therefore; the assumption that the conversion front thickness converges to 0 is not a large deviation from reality.

The most complex model is needed for particles in the thermally thick regime, which is controlled by both internal heat transfer and chemical reactions, and shows the highest temperature gradients among regimes. There is no stiff boundary from where the thermally thick regime starts, but in the literature, it can be found that a particle is in the mentioned regime for Bi number higher than 40–100 and thermal Thiele modulus (1/Py) number higher than 100–1400, depending on the source.<sup>53, 56</sup>

### 6.3. Particles size and motion

For fixed-bed reactors, the only limitation for the particle size is the reactor dimensions. Therefore, the largest particles can be processed. For fixed beds where the movement of the particles is negligible, and the mixing of solids is not significant, Wurzenberger et al.<sup>57</sup> proposed the application of the Representative Particle Model (RPM). It assumes that the processing parameters for the whole reactor can be treated as homogenous, so all processed particles will have the same behaviour. Hence, the single particle model has to be solved only once for the applied boundary and initial conditions (for one representative particle). Application of the RPM model for fixed-bed modeling reduces the computational time significantly and shows good agreement with experimental results.<sup>16-17</sup>

In general, it can be stated that the cases when the particles are in motion are more challenging. Particles can be forced to move due to changes in pressure (pneumatically), or due to the physical force of a rotary element (mechanically). In the last scenario, the moving element also has an influence on the gas motion in the reactor, which needs to be implemented.

The selection of the reactor technology (factor inducing the movement of particles) puts the boundaries on the size of the particles applied into the model. For fluidised beds, the particle size has to be significantly small to be able to be dragged by the fluidising gas. In general, it can be stated that particle size in fluidised-bed reactors does not exceed 2–3 mm. For small particles in a fluidised-bed reactor, a simplification in the flow description can be applied, which significantly reduces the complexity and simultaneously reduces the computation burden.

For rotary reactors (auger/screw or rotary kiln reactors) particle size is usually larger than in fluidised-bed reactors, but its maximum size is limited to the moving parts dimensions (screw size), mechanical durability of material, and mixing and homogenous distribution of solid material within the reactor. Due to the size of the particles, the application of the flow description simplification is not possible, and thus, the full Eulerian-Lagrangian description of the two-phase flow has to be implemented. Additionally, the movement of the rotary element and its influence on the flow behaviour have to be consistent in the reactor description. Based on all of this, it can be stated that models for rotary reactors are, among the others, the most demanding, both for the model builder and the hardware requirements to conduct simulations.

#### 6.4. Reactor model consolidation

The applied equations and their shape in the reactor model strongly depend on the type of reactor, and therefore, their detailed description will be omitted. An extensive review of this matter can be found in the work by Jurtz et al.<sup>58</sup> and Subramaniam<sup>59</sup>. The model with coupled gas phase (continuous) and solid particles (discrete) can be found in the work of Mahmoudi et al.<sup>16</sup>, who used eXtended Discrete Element Method (XDEM). It is worth to mention the work by Funke et al.<sup>60</sup>, where for the first time the heat transfer between particles in an auger type reactor was calculated, using a combined fundamental heat transfer model and DEM simulation.

#### 6.5. Reactor model and computation power

Complex kinetic models with constricted relations between compounds lead to the improvement of the model predictions accuracy and bring the model closer to the description of reality. The application of detailed models brings the issue of implementation of the vast amount of input data (biomass initial composition and thermo-physical parameters). When the complex molecular sub-model is implemented into the comprehensive larger scale model, it leads to a significant increase in the computation load, which in most cases results in a significant increase in computation time.

The main disadvantage of incorporating a particle model into a reactor model from the practical point of view is the need for a high amount of computational power resources and knowledge on its use in a sufficient manner<sup>17</sup>. Such computation power demand is caused mainly by the large number of particles that have to be considered within the model. Besides the quantity of the particles, also the complexity of the description of their conversion plays a part in the amount of power needed for computation.

It needs to be mentioned that the very complex single particle model and the limited computation power resources result in computation time, which does not allow for relatively rapid adaptation of the investigated model. Currently, the computational power is not the only factor hindering the reactor modeling development, but also the lack of a detailed description of the solid surface interactions, and particle mechanical changes. From a practical point-of-view, insufficiently developed software have problems with mesh adaptation<sup>58</sup> (e.g., in the case of complex rotary reactors, which in many cases represents a barrier in its application in models for biomass processing).

## 7. Conclusion

Numerical modeling is a very robust tool, which allows for low cost research and development of technologies within the thermal processing of biomass field. As indicated in this chapter, for its proper application, knowledge from different areas of science have to be combined in order to obtain reliable and valuable results. In theory, there is no limitation in modeling any processing technology, and applying it to broad processing parameters or different feedstock. From a practical point of view, it must be kept in mind that the selected environment or material imposes strong boundaries on the validity of the applied molecular, single-particle, and reactor models. The complexity and selection of proper models have a significant influence on the accuracy and realism of the investigated case. In general, it can be stated that it is better to apply a description as detailed as available. Nevertheless, the balance between computing power, computation time, and model complexity also have to be taken as main priorities. It is highly recommended to check if the model cannot be simplified due to the fundamental phenomena occurring in the process, without loss of the model accuracy.

## Acknowledgements

“This project has received funding from the European Union’s Horizon 2020 research and innovation programme under the Marie Skłodowska-Curie grant agreement No 721991”.

## References

- (1) EIA, Energy sources have changed throughout the history of the United States [https://www.eia.gov/todayinenergy/detail.php?id=11951].
- (2) Norgate, T.; Haque, N.; Somerville, M.; Jahanshahi, S. Biomass as a Source of Renewable Carbon for Iron and Steelmaking. *ISIJ Int.* **2012**, *52* (8), 1472–1481.
- (3) Lehmann, J.; Joseph, S. Biochar for environmental management: science and technology. Earthscan: London; Sterling, VA, 2009.
- (4) Faaij, A. Large Scale International Bio-Energy Trade. In 12th European Conf. and Technology Exhibition on Biomass for Energy, Industry and Climate Change Protection, Amsterdam, 2002.
- (5) de Wit, M.; Faaij, A. European biomass resource potential and costs. *Biomass Bioenergy* **2010**, *34* (2), 188–202.
- (6) Antal, M. J.; Grønli, M. The Art, Science, and Technology of Charcoal Production. *Ind. Eng. Chem. Res.* **2003**, *42* (8), 1619–1640.
- (7) Dubois, G. Modeling and simulation : challenges and best practices for industry, 2018.
- (8) Kennedy, M. C.; O'Hagan, A. Bayesian calibration of computer models. *J. Royal Statistical Soc. Series B (Statistical Methodology)* **2001**, *63* (3), 425–464.
- (9) Balci O. In Guidelines for successful simulation studies, Winter Simulation Conference Proceedings, 9–12 Dec. 1990; 1990; pp 25–32.
- (10) Versteeg, H. K.; Malalasekera, W. An introduction to computational fluid dynamics: the finite volume method. Pearson Education: Harlow, 2011.
- (11) Tu, J.; Yeoh, G. H.; Liu, C. Computational fluid dynamics: a practical approach, 2018.
- (12) Childress, S. An introduction to theoretical fluid mechanics, 2009.
- (13) Batchelor, G. K. P. An introduction to fluid dynamics. Cambridge University Press: Cambridge, 2013.
- (14) Sakai, M. How Should the Discrete Element Method Be Applied in Industrial Systems? A Review. *KONA Powder Particle J.* **2016**, *33*, 169–178.
- (15) Anca-Couce, A.; Zobel, N. Numerical analysis of a biomass pyrolysis particle model: Solution method optimized for the coupling to reactor models. *Fuel* **2012**, *97*, 80–88.
- (16) Mahmoudi, A. H.; Hoffmann, F.; Peters, B. Detailed numerical modeling of pyrolysis in a heterogeneous packed bed using XDEM. *J. Anal. Appl. Pyrolysis* **2014**, *106*, 9–20.
- (17) Anca-Couce, A. Reaction mechanisms and multi-scale modelling of lignocellulosic biomass pyrolysis. *Prog. Energy Combust. Sci.* **2016**, *53*, 41–79.
- (18) Di Blasi, C. Modeling chemical and physical processes of wood and biomass pyrolysis. *Prog. Energy Combust. Sci.* **2008**, *34* (1), 47–90.
- (19) Shafizadeh, F.; Chin, P. P. S. Thermal Deterioration of Wood. In Wood Technology: Chemical Aspects, American Chemical Society: 1977; Vol. 43, pp 57–81.
- (20) Park, W. C.; Atreya, A.; Baum, H. R. Experimental and theoretical investigation of heat and mass transfer processes during wood pyrolysis. *Combust. Flame* **2010**, *157* (3), 481–494.
- (21) Koufopoulos, C. A.; Lucchesi, A.; Maschio, G. Kinetic modelling of the pyrolysis of biomass and biomass components. *Can. J. Chem. Eng.* **1989**, *67* (1), 75–84.
- (22) Ranzi, E.; Cuoci, A.; Faravelli, T.; Frassoldati, A.; Migliavacca, G.; Pierucci, S.; Sommariva, S. Chemical Kinetics of Biomass Pyrolysis. *Energy Fuels* **2008**, *22* (6), 4292–4300.
- (23) Cuoci, A. F. T.; Frassoldati, A.; Granata, S.; Migliavacca, G.; Ranzi, E. In A general mathematical model of biomass devolatilization. Note 1. Lumped kinetic models of cellulose, hemicellulose and lignin,, Proceedings of the 30th combustion meeting of the Italian Section of the Combustion Institute VI,, 2007; pp 2.1–2.6.
- (24) Cuoci, A. F. T.; Frassoldati, A.; Granata, S.; Migliavacca, G.; Pierucci, S. A general mathematical model of biomass devolatilization. Note 2. Detailed kinetics of volatile species. Proceedings of the 30th combustion meeting of the Italian Section of the Combustion Institute VI, 2007, 3.1–3.6.
- (25) Corbetta, M.; Frassoldati, A.; Bennadji, H.; Smith, K.; Serapiglia, M. J.; Gauthier, G.; Melkior, T.; Ranzi, E.; Fisher, E. M., Pyrolysis of Centimeter-Scale Woody Biomass Particles: Kinetic Modeling and Experimental Validation. *Energy Fuels* **2014**, *28* (6), 3884–3898.
- (26) Ranzi, E.; Debiagi, P. E. A.; Frassoldati, A. Mathematical Modeling of Fast Biomass Pyrolysis and Bio-Oil Formation. Note I: Kinetic Mechanism of Biomass Pyrolysis. *ACS Sustain. Chem. Eng.* **2017**, *5* (4), 2867–2881.
- (27) Ranzi, E.; Debiagi, P. E. A.; Frassoldati, A. Mathematical Modeling of Fast Biomass Pyrolysis and Bio-Oil Formation. Note II: Secondary Gas-Phase Reactions and Bio-Oil Formation. *ACS Sustain. Chem. Eng.* **2017**, *5* (4), 2882–2896.
- (28) Mamleev, V.; Bourbigot, S.; Le Bras, M.; Yvon, J. The facts and hypotheses relating to the phenomenological model of cellulose pyrolysis: Interdependence of the steps. *J. Anal. Appl. Pyrolysis* **2009**, *84* (1), 1–17.
- (29) Piskorz, J.; Radlein, D. S. A. G.; Scott, D. S.; Czernik, S. Pretreatment of wood and cellulose for production of sugars by fast pyrolysis. *J. Anal. Appl. Pyrolysis* **1989**, *16* (2), 127–142.
- (30) Faravelli, T.; Frassoldati, A.; Migliavacca, G.; Ranzi, E. Detailed kinetic modeling of the thermal degradation of lignins. *Biomass Bioenergy* **2010**, *34* (3), 290–301.
- (31) Debiagi, P. E. A.; Pecchi, C.; Gentile, G.; Frassoldati, A.; Cuoci, A.; Faravelli, T.; Ranzi, E. Extractives Extend the Applicability of Multistep Kinetic Scheme of Biomass Pyrolysis. *Energy Fuels* **2015**, *29* (10), 6544–6555.

- (32) Anca-Couce, A.; Sommersacher, P.; Scharler, R. Online experiments and modelling with a detailed reaction scheme of single particle biomass pyrolysis. *J. Anal. Appl. Pyrolysis* **2017**, *127*, 411–425.
- (33) Sluiter, J. B.; Ruiz, R. O.; Scarlata, C. J.; Sluiter, A. D.; Templeton, D. W. Compositional Analysis of Lignocellulosic Feedstocks. 1. Review and Description of Methods. *J. Agric. Food Chem.* **2010**, *58* (16), 9043–9053.
- (34) Templeton, D. W.; Scarlata, C. J.; Sluiter, J. B.; Wolfrum, E. J. Compositional Analysis of Lignocellulosic Feedstocks. 2. Method Uncertainties. *J. Agric. Food Chem.* **2010**, *58* (16), 9054–9062.
- (35) National Renewable Energy Laboratory (NREL). Determination of structural carbohydrates and lignin in biomass: laboratory analytical procedure, 2011.
- (36) Anca-Couce, A.; Mehrabian, R.; Scharler, R.; Obernberger, I. Kinetic scheme of biomass pyrolysis considering secondary charring reactions. *Energy Conversion Manage.* **2014**, *87*, 687–696.
- (37) Anca-Couce, A.; Scharler, R. Modelling heat of reaction in biomass pyrolysis with detailed reaction schemes. *Fuel* **2017**, *206*, 572–579.
- (38) Anca-Couce, A.; Obernberger, I. Application of a detailed biomass pyrolysis kinetic scheme to hardwood and softwood torrefaction. *Fuel* **2016**, *167*, 158–167.
- (39) Rath, J.; Wolfinger, M. G.; Steiner, G.; Krammer, G.; Barontini, F.; Cozzani, V. Heat of wood pyrolysis. *Fuel* **2003**, *82* (1), 81–91.
- (40) Norinaga, K.; Shoji, T.; Kudo, S.; Hayashi, J.-i. Detailed chemical kinetic modelling of vapour-phase cracking of multi-component molecular mixtures derived from the fast pyrolysis of cellulose. *Fuel* **2013**, *103*, 141–150.
- (41) Nowakowska, M.; Herbinet, O.; Dufour, A.; Glaude, P.-A. Detailed kinetic study of anisole pyrolysis and oxidation to understand tar formation during biomass combustion and gasification. *Combust. Flame* **2014**, *161* (6), 1474–1488.
- (42) Trendewicz, A.; Evans, R.; Dutta, A.; Sykes, R.; Carpenter, D.; Braun, R. Evaluating the effect of potassium on cellulose pyrolysis reaction kinetics. *Biomass Bioenergy* **2015**, *74*, 15–25.
- (43) Whitaker, S. Simultaneous Heat, Mass, and Momentum Transfer in Porous Media: A Theory of Drying. In: *Advances in Heat Transfer*, Hartnett, J. P.; Irvine, T. F., Eds. Elsevier: 1977; Vol. 13, pp 119–203.
- (44) Perré, P.; Turner, I. W. A 3-D version of TransPore: a comprehensive heat and mass transfer computational model for simulating the drying of porous media. *Int. J. Heat Mass Transfer* **1999**, *42* (24), 4501–4521.
- (45) Nasrallah, S. B.; Perre, P. Detailed study of a model of heat and mass transfer during convective drying of porous media. *Int. J. Heat Mass Transfer* **1988**, *31* (5), 957–967.
- (46) Grønli, M. G. A theoretical and experimental study of thermal degradation of biomass, 1996.
- (47) Jalili, M.; Anca-Couce, A.; Zobel, N. On the Uncertainty of a Mathematical Model for Drying of a Wood Particle. *Energy Fuels* **2013**, *27* (11), 6705–6717.
- (48) Melaaen, M. C. Numerical Analysis of Heat and Mass Transfer in Drying and Pyrolysis of Porous Media. *Numer. Heat Transfer A* **1996**, *29* (4), 331–355.
- (49) Fatehi, H.; Bai, X. S. A Comprehensive Mathematical Model for Biomass Combustion. *Combust. Sci. Technol.* **2014**, *186* (4–5), 574–593.
- (50) Shi, X. Computational fluid dynamics modelling of biomass slow pyrolysis in screw reactors for the production of biochar and charcoal. Ghent University, 2017.
- (51) Mettler, M. S.; Mushrif, S. H.; Paulsen, A. D.; Javadekar, A. D.; Vlachos, D. G.; Dauenhauer, P. J. Revealing pyrolysis chemistry for biofuels production: Conversion of cellulose to furans and small oxygenates. *Energy Environ. Sci.* **2012**, *5* (1), 5414–5424.
- (52) Paulsen, A. D.; Mettler, M. S.; Dauenhauer, P. J. The Role of Sample Dimension and Temperature in Cellulose Pyrolysis. *Energy Fuels* **2013**, *27* (4), 2126–2134.
- (53) Pyle, D. L.; Zaror, C. A. Heat transfer and kinetics in the low temperature pyrolysis of solids. *Chem. Eng. Sci.* **1984**, *39* (1), 147–158.
- (54) Di Blasi, C. Heat, momentum and mass transport through a shrinking biomass particle exposed to thermal radiation. *Chem. Eng. Sci.* **1996**, *51* (7), 1121–1132.
- (55) Mehrabian, R.; Zahirovic, S.; Scharler, R.; Obernberger, I.; Kleditzsch, S.; Wirtz, S.; Scherer, V.; Lu, H.; Baxter, L. L. A CFD model for thermal conversion of thermally thick biomass particles. *Fuel Process. Technol.* **2012**, *95*, 96–108.
- (56) Villermaux, J.; Antoine, B.; Lede, J.; Soullignac, F. A new model for thermal volatilization of solid particles undergoing fast pyrolysis. *Chem. Eng. Sci.* **1986**, *41* (1), 151–157.
- (57) Wurzenberger, J. C.; Wallner, S.; Raupenstrauch, H.; Khinast, J. G. Thermal conversion of biomass: Comprehensive reactor and particle modeling. *AIChE J.* **2004**, *48* (10), 2398–2411.
- (58) Jurtz, N.; Kraume, M.; Wehinger Gregor, D. Advances in fixed-bed reactor modeling using particle-resolved computational fluid dynamics (CFD). *Rev. Chem. Eng.* **2019**, *35*, 139–190.
- (59) Subramaniam, S. Lagrangian–Eulerian methods for multiphase flows. *Prog. Energy Combust. Sci.* **2013**, *39* (2), 215–245.
- (60) Funke, A.; Grandl, R.; Ernst, M.; Dahmen, N. Modelling and improvement of heat transfer coefficient in auger type reactors for fast pyrolysis application. *Chem. Eng. Process.: Process Intensification* **2018**, *130*, 67–75.

# Production and characterisation of lignin and lignin-containing streams obtained through a two-stage fractionation process of lignocellulosic biomass

Qusay Ibrahim<sup>a,b</sup>, Moritz Leschinsky<sup>b</sup>, Andrea Kruse<sup>a</sup>

<sup>a</sup> Department of Conversion Technologies of Biobased Resources, Institute of Agricultural Engineering, University of Hohenheim, Garbenstrasse 9, 70599 Stuttgart, Germany

<sup>b</sup> Pretreatment and Fractionation of Renewable Feedstocks. Fraunhofer Center for Chemical-Biotechnological Process CBP, Amhaupttor (Tor 12, Bau 1251), 06237 Leuna, Germany

## Abstract

One of the main challenges in lignocellulosic biorefinery framework is to develop and optimise an efficient fractionation process to recover and produce high purity grades of lignin and lignin-rich side streams to be used in further processes and applications. This chapter aims to give a review on the two-stage processes to fractionate lignocellulosic biomass and the effect of their operating conditions on the yield and the specifications of the resulted fractions. The focus is on the main composition of lignocellulosic biomass (lignin, cellulose, and hemicellulose). Furthermore, kraft, sulphite and the organosolv pulping process are discussed, including the advantages of organosolv pulping over the other processes. In addition to that, the enzymatic hydrolysis, as a further step to produce sugars from the cellulose stream as well as hydrolysis lignin as a side-stream, is introduced.

## 1. Introduction

Lignocellulosic biomass is the most bountiful biomass on the earth. Compared to fossil fuels sources, lignocellulosic biomass has the ability to diminish carbon dioxide emissions by 75%–100%, because the carbon dioxide bounded by the lignocellulosic biomass during photosynthesis is the same that that released during the combustion of biofuel produced from it<sup>1</sup>. In addition, lignocellulosic biomass does not compete with food as a source for chemicals and materials, it has low costs and comes in most cases from sustainable sources. Lignocellulosic biomass is mainly comprised of lignin, cellulose and hemicellulose, as well as other minor components like extractives, water, minerals and protein. The percentage of these components differs with the source of lignocellulosic biomass. Table 1 shows the major composition of common sources of biomass.

**Table 1.** Major constituents for different biomass sources.<sup>2</sup>

Biomass source	Cellulose (wt. %)	Hemicellulose (wt. %)	Lignin (wt. %)
Hardwood	40–55	24–40	18–25
Softwood	45–50	25–35	25–35
Nut shells	25–30	25–30	30–40
Corn cobs	45	35	15
Grasses	25–40	35–50	10–30
Paper	85–99	0	0–15
Wheat Straw	30	50	15
Sorted refuse	60	20	20
Leaves	15–20	80–85	0
Newspapers	40–55	25–40	18–30
Swine waste	6	28	NA
Switchgrass	45	31.4	12.0
Miscanthus	35–40	16–20	20–25

Sugar units are the building blocks in cellulose and hemicellulose, and are considered as the main potential source of fermentable sugars after biomass saccharification. The most important monosaccharides are glucose, mannose and xylose. Additionally, lignin is the main potential source for phenolic compounds (e.g., as platform chemicals for chemical industry). The process of sugar production from hemicellulose through hydrolysis is partially easier than that from cellulose. The crystalline structure of cellulose requires harsher treatment and more severe conditions like using acids, the presence of enzymes or high temperature for hydrolysis to monosaccharides (glucose). Typical challenges in lignocellulose fractionation processes are: (i) poor separation of both cellulose and lignin, (ii) the formation of compounds that inhibit ethanol fermentation (formation of furans from sugars, acetic acid from hemicellulose and phenolic compounds from lignin fractions), (iii) the requirement of high amounts of energy and/or chemicals, and (iv) the production of wastes at the end of the process.

### 1.1. Composition of Lignocellulosic biomass

#### 1.1.1. Cellulose

As one of the major components of lignocellulosic biomass, cellulose is composed of glucose monomers that are connected into cellobiose subunits by  $\beta$ -1,4-glycosidic bonds. Cellulose has  $(C_6H_{10}O_5)_n$  as a molecular formula<sup>3</sup>. Figure 1 shows the structure of a single cellulose molecule.

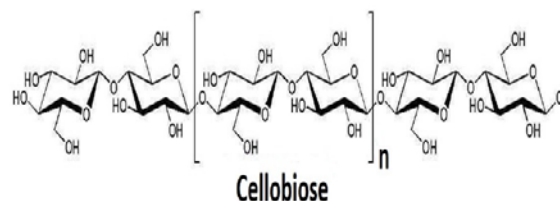


**Figure 1.** Molecular chain structure of cellulose (adapted from <sup>3</sup>).

Cellulose characteristics depend on the degree of polymerization (DP) which is defined as the number of glucose units that form one polymer molecule. Depending on the source of cellulose, the DP ranges can vary from 3000 to 15000 (for instance, it is about 10000 in wood<sup>4</sup>). 1,4-glycosidic bonds force cellulose to form long and robust straight chains that interact with each other through hydrogen bonds to form fibres. Hydroxide groups on both sides of the monomers lead to the formation of hydrogen bonds between the linear glucan chains, which is the reason for the crystalline structure as shown in Figure 2.<sup>5-7</sup>

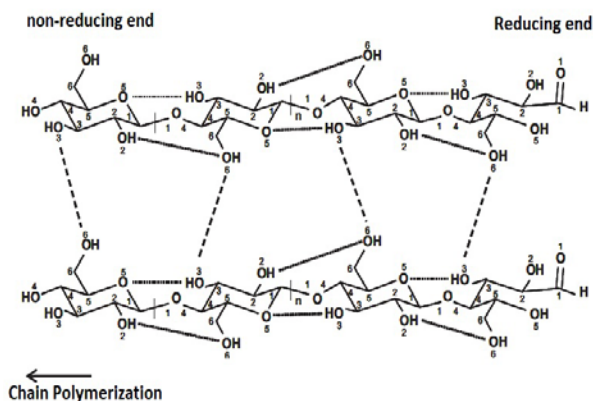


**Figure 2.** Demonstration of the inter- and intra-chain hydrogen bonding pattern in cellulose type I. Dashed lines are inter-chain hydrogen bonding and dotted lines are intra-chain hydrogen bonding (adapted from<sup>7</sup>).

Cellulose is found in one of these two forms: crystalline or non-crystalline structure. It has six different known structures (Cellulose I, II, III<sub>i</sub>, III<sub>ii</sub>, IV<sub>i</sub>, and IV<sub>ii</sub>)<sup>7</sup>. Under normal atmospheric conditions (20 °C, 60% relative humidity), cellulose absorbs water. At normal temperatures, cellulose is insoluble in water, dilute acidic solutions, and alkaline solutions<sup>5,8</sup>. Concentrated acids mainly hydrolyse the cellulose and normally only the low-DP fractions are soluble. In addition, cellulose is only soluble in very specific solvents like aqueous solutions of copper (II) tetra hydroxide (Schweitzer's reagent/Cuoxam). Additionally, cellulose does not melt but decomposes starting from 180 °C.<sup>9</sup>

### 1.1.2. Hemicellulose

The second component of lignocellulosic biomass, hemicellulose, is a branched polysaccharide that consists of pentoses, hexoses and sugar acids such as xylose, glucose and 4-O-methylglucuronic acid, respectively<sup>9</sup>. The extraction method and the species of the plant affect the composition and the structure of these sugars<sup>10</sup>. The main hemicelluloses of softwood are galactoglucomannans and arabinoglucuronoxylan, while in hardwood glucuronoxylan and glucomannan are the dominant species. Hemicelluloses are partly acetylated. Figure 3 shows the principal structure of hemicellulose in hardwood, whereas Figure 4 shows hemicelluloses in softwood. In hardwood, the main component of hemicellulose is xylose. One of the most important features of hardwood xylan is that it lacks crystallinity due to the branched structure and acetyl groups that are connected to the polymeric chain.<sup>4</sup>

The solubility of hemicellulose in aqueous solutions depends on its chemical structure, the DP and the pH of the solution<sup>11</sup>. Normally, hemicellulose has good solubility in alkaline solutions. Moreover, acidity and high temperatures lead to the hydrolysis of hemicellulose.

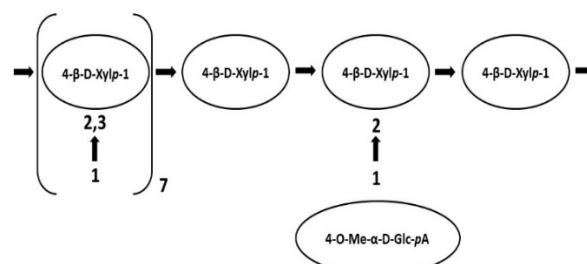


**Figure 3.** Schematic representative of Glucuronoxylan in hardwood (Adapted from<sup>12</sup>).

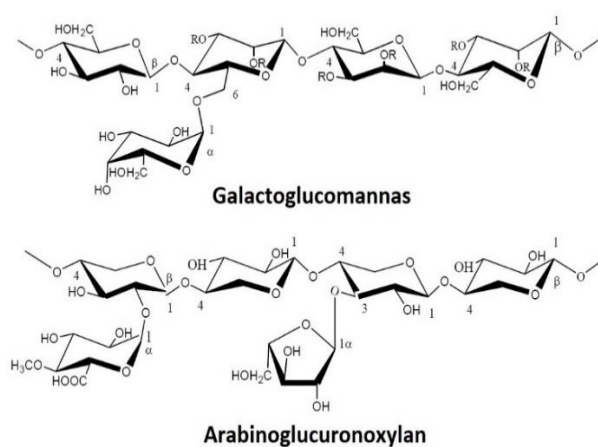


**Figure 4.** Schematic representative of galactoglucomannans and arabinoglucuronoxylan in softwood (adapted from<sup>12</sup>).

### 1.1.3. Lignin

Besides cellulose, lignin is considered as the second most abundant renewable source and the largest source for aromatic compounds on earth. It constitutes up to 10%–25% (wt.) of lignocellulosic feedstock.<sup>9</sup> Valorisation of lignin is considered as a challenge because of its amorphous and heterogeneous structure. Lignin has been applied in surfactants, stabilisers, epoxy resins, superabsorbent hydrogels and in different polymeric applications. Furthermore, lignin is a water-insoluble material, stable in nature and connected to both cellulosic and hemicellulosic layers. Lignin is a three-dimensional, highly cross-linked macromolecule, which consists of three major units of substituted phenols: sinapyl, coniferyl and p-coumaryl alcohols as shown in Figures 5 and 6. Hardwood lignin contains more than 90% of sinapyl alcohol with some coniferyl units. On the other hand, softwood lignin contains mainly coniferyl alcohol units.<sup>14</sup>

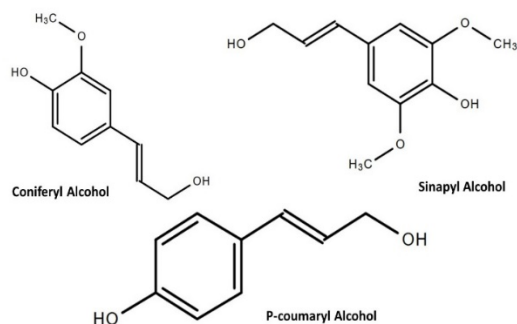


**Figure 5.** Building blocks of the three-dimensional polymer lignin.

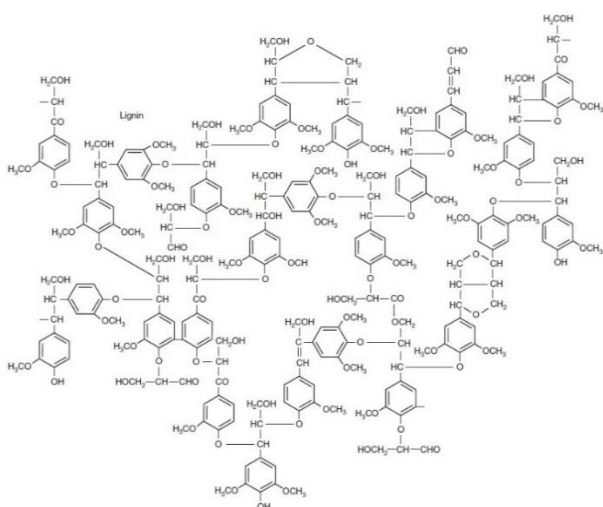


**Figure 6.** Suggested structural model of a section of hardwood lignin.<sup>13</sup>

## 2. Delignification of lignocellulosic biomass

Delignification is the chemical separation of lignin from lignocellulosic biomass. Lignin needs to be separated from lignocellulosic biomass to allow the production of high quality lignin and lignin-rich side streams. Pre-treatment methods have many goals, such as improving the accessibility of lignocellulosic biomass and easing enzymes' work during enzymatic hydrolysis to increase the yield of reducing sugars.<sup>15</sup>

According to Wyman *et al.*, there are many factors to consider for the selection of a pre-treatment method<sup>16</sup>: avoiding the size reduction of biomass, avoiding the formation of degradation products and inhibitory toxic by-products, allowing lignin recovery, decreasing energy demands and using low cost catalyst and/or low cost regeneration process for catalyst recovery.

Many physical and/or chemical pre-treatment methods to change the properties or fractionate lignocellulosic biomass have been suggested, including steam explosion, pre-hydrolysis, auto hydrolysis, enzymatic hydrolysis, kraft pulping, sulphite pulping, organosolv, ammonia, aqueous lime, sodium hydroxide, and wet oxidation<sup>15,17-19</sup>. A sequential combination between two or more processes is possible for fractionation of lignocellulosic biomass like the combination between pre-hydrolysis and organosolv delignification.

Today, Kraft and sulphite pulping are the most common chemical processes used in paper making industry. Kraft pulping is an alkaline process that uses sodium hydroxide and sodium sulphide to delignify lignocellulosic biomass. For its part, sulphite pulping is an acidic process that uses magnesium bisulphide and excess of sulphur dioxide. Furthermore, sodium sulphide is used in Kraft process to break the bonds that connect lignin, cellulose and hemicellulose (enhance ether cleavage) as well as to prevent unwanted condensation reactions. As a result, strong and weak fibres are produced by Kraft and sulphite processes, respectively. Despite the high amounts of lignin extracted from both processes, they have many disadvantages, such as the release of sulphide-containing compounds and other volatile sulphur compounds.<sup>20</sup>

### 2.1. Organosolv delignification

Compared with the sulphite and Kraft processes, organosolv pulping can be understood as an environmentally friendly chemical process for the fractionation of lignocellulosic biomass; in which delignification is achieved using organic solvents (generally ethanol) mixed with water<sup>21-23</sup>. The treatment of lignocellulosic biomass typically occurs at temperatures in the range of 130–200 °C with or without catalyst. Alcohols like ethanol, methanol, butanol, ethylene glycol and glycerine are regularly used as solvents for the delignification of lignocellulosic biomass. Moreover, mineral acids such as HCl, H<sub>2</sub>SO<sub>4</sub> and H<sub>3</sub>PO<sub>4</sub> are used as catalysts to enhance the delignification process<sup>24</sup>. Through the process, the structure of lignin is fragmented into smaller fractions and dissolved from the lignocellulosic biomass. The extract is separated in the form of liquid phase, which is rich in phenolic compounds like dissolved lignin, vanillin, syringaldehyde, phenol and substituted phenols but also contains part of the dissolved and degraded hemicellulose.<sup>22, 23</sup>

There are many reported advantages of the organosolv process, for example, the production of sulphur-free lignin; therefore, it has a significantly lower effect on the environment. It can be conducted at a smaller scale compared with the Kraft process, and resulting by-products might have a significant commercial interest like furfural and lignin. The recovery of the used solvent is relatively easy (it could be used again for another pulping process) and less reagents are used during the process.<sup>25,22,26-28</sup>

### 2.2. Pre-hydrolysis

Pre-hydrolysis is defined as the process in which the lignocellulosic biomass is treated by saturated steam or hot water with or without the addition of small amounts of acids or alkali. Typically, pre-hydrolysis is used as a means to remove the hemicellulose prior to Kraft pulping when dissolving pulp is produced (i.e., the so-called pre-hydrolysis Kraft process, "PHK"). The principle of autohydrolysis or hydrothermolysis is applied in other processes like steam explosion. In this process, most of hemicellulose can be recovered in the liquid phase as xylooligosaccharides and xylose without causing significant dissolution of cellulose and lignin<sup>29</sup>. Lignin and cellulose remain in the solid phase and show enhanced capability to further fractionation<sup>30,31</sup>. Pre-hydrolysis is an effective, simple and selective pre-treatment, which enables the production of soluble hemicellulose oligosaccharides from the liquid phase and allows high recovery of lignin and cellulose in the solid

phase. This is why pre-hydrolysis might be investigated as a first step in biorefinery concepts prior to the delignification process<sup>32,33</sup>. Furthermore, pre-hydrolysis will reduce carbohydrate loss for the subsequent processes<sup>35-37</sup>. On the other hand, applying the organosolv delignification process directly to the lignocellulosic biomass results a liquid stream containing both lignin and hemicellulose that will require further purification and separation for lignin recovery.<sup>34</sup>

### 2.3. Why a sequential pre-hydrolysis and organosolv process is suggested?

In an effort to overcome the drawbacks of concentrated and diluted acids, a two-stage process is proposed. A two-stage concept can enhance the hydrolysis of hemicellulose by diminishing the degradation into furans, which play a role as enzyme and fermentation inhibitor. A pre-hydrolysis step recovers the cellulose in a less recalcitrant form, thereby facilitating its reactivity to enzymes. If conducted under mild conditions, the lignin becomes very reactive towards subsequent delignification. This eases the development of a process with lower energy costs through decreasing the process temperature and lowers equipment costs by decreasing the generated pressure in the subsequent organosolv step.

### 2.4. Overview of two-stage process combination including organosolv delignification

Given the high number of factors affecting the two-stage fractionation process (e.g., temperature, residence time, amount and type of catalyst, and the used solvent and its ratio) as well as the wide range of lignocellulosic biomass sources (e.g., softwood, hardwood and agricultural residues), it is expected to obtain three different fractions (lignin, cellulose and hemicellulose) with different yields and properties. Previous variables and their effects on the two-stage fractionation process were studied extensively. These variables were used to fractionate variety of lignocellulosic biomass and their effects were evaluated according to the yield of lignin, the yield of sugars and the formation of degradation compounds during the process. In addition, analysing the effects of the two-stage fractionation process on the characteristics of the extracted lignin (e.g., the average molecular weight,  $M_w$ ; the number average of molecular weight,  $M_n$ ; the dispersity index,  $M_w/M_n$ ; phenolic-hydroxyl and carboxyl groups contents, thermal properties, and sugar content) is also needed to explore additional applications of lignin. These include its use as a starting material in hydrothermal processes as used in the production of chemicals and polymer industry. Therefore, researchers were conducted several studies in this field and an overview of the conducted studies (grouped into categories according to the studied variable) is given below.

#### 2.4.1. The effect of temperature and residence time

Before the description of the effects "harshness" of the treatment conditions on the fractionation process and the final fractions (lignin, cellulose and hemicellulose), we have to define a term/expression that it used to describe them. In other words, treatment conditions are combined together in one expression called the "reaction ordinate" to determine the hydrolysis extent. The severity factor ( $R_0$ ) was the first reaction ordinate that was developed by Overend *et al.*<sup>38</sup>, where both

temperature and time were combined. It was employed successfully for describing the harshness of treatment conditions of hot water treatment, steam treatment and steam-explosion, and Kraft pulping. Moreover, it was used successfully in organosolv and liquefaction of the polymers that resulted from the treatment process.<sup>39</sup>

Lora *et al.*<sup>40</sup> studied the effect of a two-stage process consisting of autohydrolysis and organosolv delignification on aspen, eucalyptus and fast-growing poplar wood in separated experiments. All feedstocks were autohydrolysed at temperatures between 175 and 225 °C for 13–21 min. Afterwards, the treated wood was delignified separately by extraction with 9:1 dioxane-water or 1% sodium hydroxide solutions at mild conditions (soxhlet extraction, refluxing for 3–4 h). The results showed that the maximum delignification was achieved at higher autohydrolysis temperatures and short times (i.e., 215 °C and 4 min). The main finding was that the solubility of lignin in dioxane-water and NaOH in the second step manifested a clear maximum at certain autohydrolysis conditions. Too severe and long autohydrolysis conditions led to an important decrease in delignification, indicating the occurrence of lignin recondensation.

April *et al.*<sup>41</sup> also tested a two-stage process of pre-hydrolysis and organosolv delignification of southern yellow pine wood. This study was done in order to know the effect of pre-hydrolysis on organosolv delignification by comparing the results obtained through direct organosolv with those obtained from delignification of pre-treated wood. Pine wood was pre-hydrolysed at 180–250 °C for 0–3 h. Afterwards, the treated pine wood was delignified with 1:1 n-butanol: water solution at temperatures of 180–250 °C for 30–180 min. The results obtained from this study showed that the yield of pulp of pre-treated wood after delignification was the same than that obtained for the non-pretreated wood. Moreover, higher hydrolysis rate was obtained at higher temperatures, where the optimum conditions for pre-hydrolysis without significant degradation of hemicellulose were 200 °C and 105 min. The lignin yield from treated pine wood increased with time at a constant temperature (180, 200 or 250 °C).

In another study, Patel *et al.*<sup>42</sup> studied the effect of pre-soaking with 1% H<sub>2</sub>O<sub>2</sub> and the acidic pre-hydrolysis on organosolv delignification of sugarcane bagasse. As a first step prior the pre-hydrolysis, sugarcane bagasse was soaked with 1% H<sub>2</sub>O<sub>2</sub> in order to increase the susceptibility of sugarcane bagasse to enzymatic hydrolysis. After that, the soaked material was pre-hydrolysed in the presence of 0.1% H<sub>2</sub>SO<sub>4</sub> at temperatures of 125–175 °C for 4 h. The treated wood was delignified with 50 wt. % aqueous ethanol at 200 °C for 1–2 h. As a result, about 41 wt. % of the hemicellulose was recovered without any significant degradation of lignin and cellulose, and without the formation of degradation side products like furfural. Moreover, about 90 wt. % of the lignin was recovered and most of the remaining hemicellulose without significant degradation of cellulose.

A similar study was conducted by Thring *et al.*<sup>43</sup>, who used a two-stage process of pre-hydrolysis and organosolv to delignify populus deltoids. In terms of severity factor, populus deltoids were aqueous-steam pre-hydrolysed at a severity factor of 3.8 and the pretreated wood was delignified with ethylene glycol at

a severity factor of 6.2 (temperature range of 110–170 °C). Ethylene glycol was used to prevent the degradation of cellulose during the organosolv process even at high temperatures. As a result, the recovery of hemicellulose was 90 wt. % in the pre-hydrolysis step and the recovery of lignin was 20 wt. % from the original wood. Moreover, about 73 wt. % of the lignin was recovered as acid insoluble lignin.

In another study, Hongzhang *et al.*<sup>44</sup> investigated the fractionation of wheat straw through a two-stage process of steam explosion and organosolv delignification. Steam explosion was done using the optimum conditions determined by Chen *et al.*<sup>84</sup> (pressure: 1.4 MPa, moisture: 34%, and treatment time: 4.5 min). The treated wheat straw was delignified with 20–70 wt. % of aqueous ethanol at 80–180 °C for 5–100 min in the presence of 0.1 wt. % of sodium hydroxide as catalyst (see Figure 7). About 75 wt. % of lignin with high purity was recovered by acid precipitation.

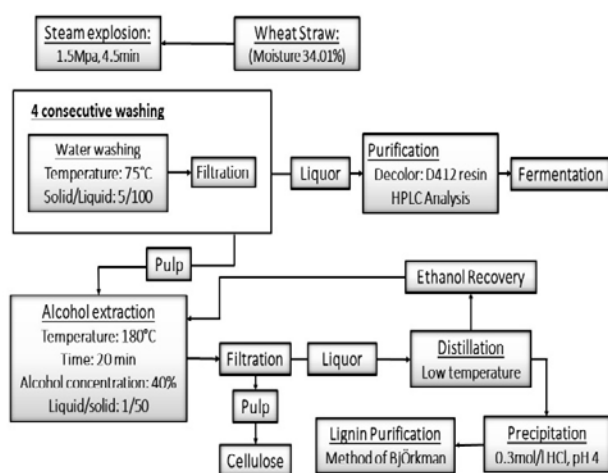


**Figure 7.** Schematic representation of the fractionation process followed by Hangzhang *et al.*<sup>44</sup>

Brosse *et al.*<sup>45</sup> studied the effect of two-stage process of pre-soaking with dilute acid and organosolv delignification of miscanthus giganteus. The feedstock was pre-soaked with 0.9 wt. % of  $H_2SO_4$  at 180 °C for 2 min. The treated miscanthus was delignified using aqueous ethanol at temperatures ranging from 170 to 190 °C for a holding time of 2–80 min, using  $H_2SO_4$  as a catalyst to enhance the delignification process. Better recovery of xylan was achieved with 71 wt. % of lignin being recovered, since the pre-soaking step prior to the delignification step enhanced the digestibility of resulted cellulose for enzymes. In a related study, Brosse *et al.*<sup>46</sup> studied the same process under mild conditions. Thus, miscanthus was pre-soaked using 0.9 wt. %  $H_2SO_4$  at 100 °C overnight. The treated material was then delignified with aqueous ethanol at 170–190 °C for 2–10 min. As compared to the previous study, pre-soaking step at lower severity enhanced the fractionation of miscanthus with good yields and low amounts of degradation compounds (like furans) were produced. Figure 8 shows a schematic representation of the process.

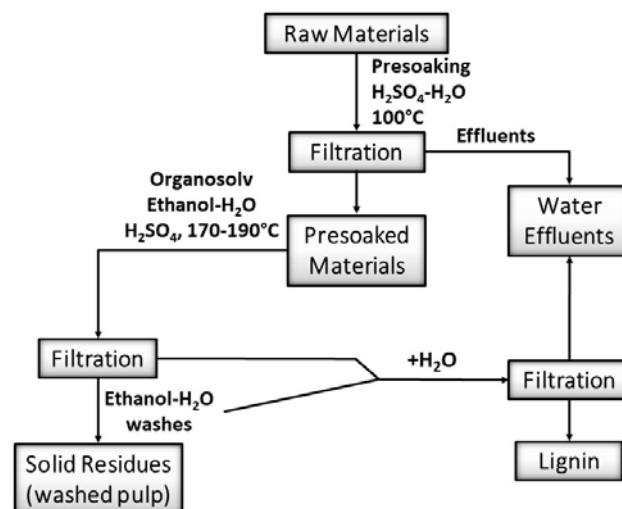


**Figure 8.** Schematic representation of sulphuric acid pre-soaking and ethanol organosolv delignification (Brosse *et al.*<sup>46</sup>).

In order to enhance the efficiency of delignification process, El hage *et al.*<sup>47</sup> studied a two-stage process of catalysed autohydrolysis and organosolv delignification of miscanthus giganteus (see Figure 9). In this process, miscanthus was autohydrolysed at temperatures of 130–150 °C, with/without 2-naphthol (used to prevent lignin recondensation) and severity of 4.1 for 0–43 h. The treated miscanthus was then delignified with 80 wt. % of aqueous ethanol at 170 °C in the presence of 0.5 wt. %  $H_2SO_4$  as catalyst for 60 min. It was found that the higher temperature of autohydrolysis stage had a large effect on the delignification process and the structure of resulting lignin. Further, the used catalyst had a large impact on autohydrolysis, which led to enhanced delignification and better sugar recovery.

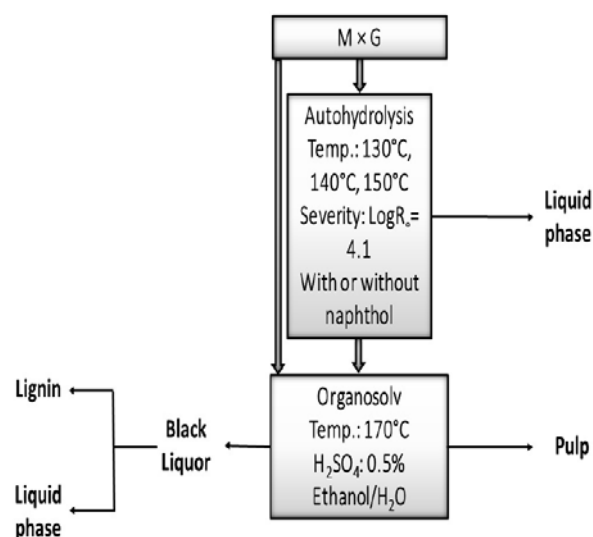


**Figure 9.** Schematic process followed by El hage *et al.*<sup>47</sup>

Ruiz *et al.*<sup>48</sup> applied a two-stage process of autohydrolysis and organosolv delignification to fractionate wheat straw. In the first stage, wheat straw was autohydrolysed at 180 °C for 30 min. The treated wheat straw was delignified with 40 wt. %

aqueous ethanol at different temperatures range from 180 to 200 °C in the presence of 0.1 wt. % sodium hydroxide catalyst for 20–40 min. The conclusion was that both temperature and time played a key role in lignin recovery. The maximum yield of lignin after delignification step was 3.25 g lignin per 100 mL of liquor. Moreover, about 78 wt. % of sugars were recovered as xylooligosaccharides. In a similar way, but using a different lignocellulosic biomass, Romani *et al.*<sup>49</sup> carried out a study of a two-stage process consisting of autohydrolysis and uncatalysed organosolv delignification to fractionate eucalyptus globulus wood as shown in Figure 10. The autohydrolysis stage was performed according to the parameters adopted by Romani *et al.*<sup>85</sup>. Furthermore, organosolv delignification was carried out using 48–72 wt. % of aqueous ethanol at 172–203 °C for a holding time of 1 h. They found that using 60 wt. % of ethanol without using any catalyst at 180–200 °C were the best conditions for the delignification process in terms of yield of lignin. Moreover, sugars from hemicellulose were recovered as mono- and oligosaccharides.

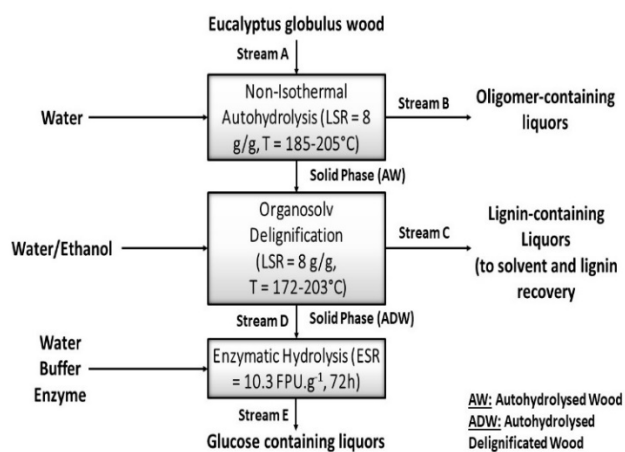


**Figure 10.** Schematic representation of autohydrolysis and ethanol organosolv delignification (Romani *et al.*<sup>49</sup>).

Not only single lignocellulosic biomass was studied but also a mixture of them was investigated. In the study by Liu *et al.*<sup>50</sup>, the fractionation of a mixture of lignocellulosic biomass (which was composed of maple, poplar and birch) using two-stage process of pre-hydrolysis and ethanol extraction was executed. As shown in Figure 11, the pre-hydrolysis stage was carried out using steam at 170 °C for 30 min to separate hemicellulose. Lignin was precipitated by acidifying pre-hydrolysis liquor using polyethylene oxide and poly-aluminium chloride. It was found that the two-stage process of pre-hydrolysis and ethanol extraction led to the recovery of lignin, hemicellulose and pure cellulose from this wood chips mixture.

One of the most attractive features of organosolv process or derived two-stage process is that it can use any lignocellulosic biomass. For instance, Amendola *et al.*<sup>51</sup> used red grape stalks in their study of a two-stage process of autohydrolysis and uncatalysed organosolv delignification. In this study, red grape stalks were autohydrolysed at 180 °C for 30 min. An uncatalysed process of ethanol organosolv was used to recover lignin from autohydrolysis grape stalks at 180 °C for 90 min. Autohydrolysis successfully recovered hemicellulose as free sugars and oligomers. Lignin recovery from pre-hydrolysed grape stalk by

uncatalysed ethanol organosolv was inconsistent on the basis of previous studies.

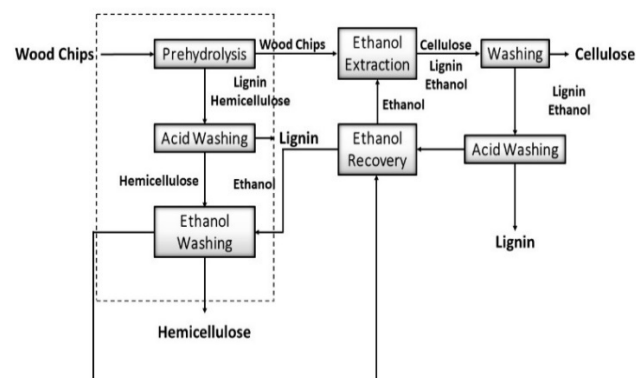


**Figure 11.** Flow diagram representing the process followed by Liu *et al.*<sup>50</sup>

Another two-stage process of acidified pre-hydrolysis and organosolv delignification was carried out by Huijgen *et al.*<sup>52</sup> to fractionate wheat straw. The study was based on two steps: a first one consisting of an acidified pre-hydrolysis to recover sugars from hemicellulose, and a second one consisting of organosolv delignification. Pre-hydrolysis stage was used to prevent degradation of hemicellulose sugar during organosolv delignification process. As shown in Figure 12, wheat straw was pre-hydrolysed by acidified water at temperatures of 160–190 °C for 30 min. Likewise, delignification of treated wheat straw was carried out using 60% aqueous ethanol at temperatures of 190–220°C for 60 min. The pre-hydrolysis stage enhanced the sugar yield and, at the same time, reduced the yield of lignin, probably due to the formation of pseudo lignin and lignin recondensation. In addition, Huijgen *et al.* found that increasing the temperature of organosolv process resulted in improved enzymatic hydrolysis, thus the glucose yield was about 93 wt. %. Furthermore, temperature could partially reduce yield problem by increasing the temperature of organosolv delignification.

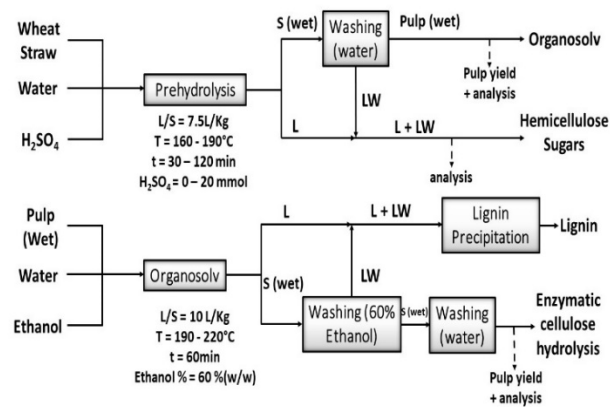


**Figure 12.** Scheme representing pre-hydrolysis and organosolv delignification process (Huijgen *et al.*<sup>52</sup>).

Tunc *et al.*<sup>53</sup> observed the effect of using organic acids like acetic acid and formic acid to catalyse the autohydrolysis process during the organosolv delignification of pre-treated wood chips. A mixture of southern hardwoods chips were pretreated with 10 g L<sup>-1</sup> of formic acid at 160 °C for 90 min. Then, the pretreated wood chips were delignified (without catalyst) with 50 wt. % aqueous ethanol at 160 °C for 90 min. Consequently, the severe acid conditions in autohydrolysis stage increased the selectivity of lignin removal in organosolv stage. Thus, about 9.7 wt. % of lignin was recovered from the original lignin in the wood chips and selective sugar removal was achieved in the autohydrolysis stage without lignin recondensation. Furthermore, Tunc *et al.* found that formic acid was more effective than acetic acid, due to its higher acidity.

Vallejos *et al.*<sup>54</sup> studied the two-stage process of hot water autohydrolysis and organosolv delignification of sugarcane bagasse. The innovative aspect of this study was the use of a relatively low liquid/solid ratio (with minimum consumption of hot water in the autohydrolysis step) to enhance the efficiency of organosolv delignification step. Autohydrolysis was carried out at 170 °C for 60 min using a liquid/solid ratio of 1:6. Organosolv delignification was accomplished using 50 wt. % of aqueous ethanol at different temperatures from 160 to 190 °C during 30–150 min. As a result, sugarcane bagasse was fractionated into three main components (lignin, cellulose and hemicellulose) with lower yield than that achieved using higher liquid/solid ratio. Similarly, in the study by Zhu *et al.*<sup>55</sup>, lignin with good characteristics and chemical reactivity was obtained through a two-stage process of hydrothermal autohydrolysis and organosolv delignification of *Eucommia ulmoides* Oliver. Firstly, the feedstock was hydrothermally auto hydrolysed at 180 °C for 30 min after soaking with water. The second stage (organosolv delignification) was conducted using 50 % of aqueous ethanol for 30 min in the presence of 1% of HCl as catalyst. As a result, 14.5 g of lignin, 9.5 g of xlyooligosaccharides and 41.0 g of cellulose-rich residues were obtained from 100 g of feedstock. The resulting lignin had distinctive characteristics such as high purity, narrow polydispersity, low molecular weight, and high chemical reactivity.

In a different study, Moniz *et al.*<sup>56</sup> conducted experiments of autohydrolysis and mild organosolv to fractionate rice straw into lignin and hemicellulose. At the first stage, rice straw was autohydrolysed at 195–220 °C with severity factors ranging from 3.66 to 4.36. Moniz *et al.* observed that the best temperature for autohydrolysis was 210 °C. For the second stage, treated rice straw was delignified at 30 °C (nearly room temperature) using different ratios of aqueous ethanol ranging from 33.05 to 71.90 wt. % and holding times of 0–24 h. The optimised autohydrolysis at 210 °C enhanced the digestibility of cellulose residues to enzymes, produced liquid phase rich in pentoses (particularly in oligomeric form), and produced a solid phase rich in lignin and glucan. The mild organosolv of treated rice straw allowed the production of low molecular weight lignin in yields lower than those obtained from the regular organosolv delignification process.

Amiri *et al.*<sup>57</sup> carried out a two-stage process of autohydrolysis and organosolv followed by enzymatic hydrolysis to delignify and fractionate pine wood and elm wood. Woods were autohydrolysed separately at 180 °C for 60 min. The treated woods were delignified at 180 °C with 40 wt. % aqueous ethanol for 60 min in the presence of 1% H<sub>2</sub>SO<sub>4</sub>. The two-stage process played various vital roles in the composition of final treated woods. The first stage (autohydrolysis) removed about 53%–61% of hemicellulose, whereas in the second stage (organosolv) the removal was lower than 23 wt. %. About 95 wt. % of the delignification was observed in the second stage (organosolv). About 100–140 g of lignin was produced from each 1 kg of wood.

Gurgel *et al.*<sup>58</sup> carried out a similar process with the assistance of CO<sub>2</sub> (as a catalyst) organosolv step to delignify pre-hydrolysed sugarcane bagasse, which was pre-hydrolysed with liquid hot water at 180 °C for 20 min. The treated bagasse was then delignified with the assistance of high pressure CO<sub>2</sub> and using 50% of aqueous ethanol at different temperatures in the range of 112–168 °C for 24–66 min. As a result, a lower lignin recovery and higher delignification at low temperatures (112–140 °C) was obtained compared with regular organosolv delignification process.

A recent study based on using a two-stage process of autohydrolysis and glycerol organosolv delignification was conducted by Meighan *et al.*<sup>59</sup>. Sugarcane bagasse was autohydrolysed at 176 °C during 49 min. The pretreated material was delignified at temperature of 210 °C for 40 min with 80% of pure glycerol. The study showed a decrease in the delignification rates as well as important changes in the lignin structure, probably due to the increase in the severity of the autohydrolysis step.

More recently, Matsakas *et al.*<sup>60</sup> conducted a study on birch wood chips using a novel hybrid organosolv process, in which the inclusion of a steam explosion pre-treatment led to better results than those reported by Nitsos *et al.*<sup>61</sup>, who utilised an organosolv delignification process at higher temperature. Matsakas *et al.* evaluated the effect of reaction time, amount of sulphuric acid and the percentage of aqueous ethanol on the fractionation process and the resulting product fractions. Wood chips were pre-treated with steam inside a steam explosion reactor and subsequently delignified at 200 °C with different amounts of H<sub>2</sub>SO<sub>4</sub> (0–1% wt. basis) and different aqueous ethanol percentages for various reaction times (15–60 min). As a result, they achieved a delignification yield of 86.2% with high purity lignin and 87 wt. % of cellulose. Moreover, the remaining pulp contained lower amounts of residual lignin, which had a positive effect on the enzymatic hydrolysis (increased cellulose digestibility). Definitely, it seems clear that the organosolv temperature has a significant effect on the delignification as well as on the residual lignin in pulp. However, it should be kept in mind that additional variables, such as the conditions at which the pre-treatment step is conducted, can also play an important role.

### 3. Enzymatic hydrolysis

Regardless of the delignification process used (single-step or multi-step process), cellulose is obtained in the form of cellulosic fibres or pulp. The recalcitrance of cellulose to enzymatic hydrolysis is related to the diversity, heterogeneity and complexity of cellulosic biomass<sup>62</sup>. Due to this complexity and heterogeneity of cellulose substrates, the mechanism of cellulose hydrolysis is not fully understood.

The main objective for most of pre-treatment processes for lignocellulosic biomass is to separate hemicellulose or lignin. The main purpose of any pre-treatment method is to obtain high yields of products through sequential enzymatic hydrolysis at minimum costs. Otherwise, formation of by-products or degradation products from lignin or sugars (like furfural and its derivatives, which inhibit the enzymatic hydrolysis) should be minimised. As mentioned in the literature, the lignin content and its distribution have an impact on the performance of the enzymatic hydrolysis process<sup>63, 64</sup>. High rates of enzymatic hydrolysis conversion of cellulose have been obtained from extensively delignified wood. On the other hand, partial lignin removal has resulted in decreased hydrolysis yields.<sup>65, 66</sup>

Amorphous cellulose is rapidly hydrolysed with the increase in the degree of crystallinity and thus, a typical time of hydrolysis was suggested by Mansfield *et al.*<sup>67</sup>. Furthermore, the conventional time for enzymatic hydrolysis of lignocellulosic biomass is characterised by a fast initial rate of hydrolysis followed by a slower and insufficient hydrolysis rate, as shown in Figure 13.

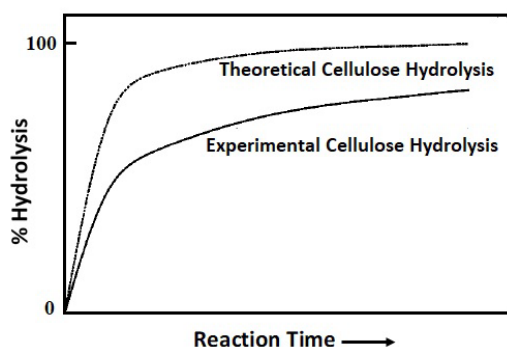


**Figure 13.** Typical time course of the enzymatic hydrolysis of lignocellulosic biomass (adapted from Mansfield *et al.*<sup>67</sup>).

According to Fan *et al.*<sup>68</sup>, the rate of enzymatic hydrolysis of lignocellulosic biomass is strongly affected by structural characteristics of cellulose; for instance: degree of polymerisation, available surface area, crystallinity of cellulose, structural organisation, and the presence of other materials like hemicellulose and lignin. Furthermore, Fan *et al.*<sup>68, 69</sup> suggested that the most important factor affecting the hydrolysis rate is the crystallinity of substrate, while other researchers suggested that the degree of crystallinity has no effect on the hydrolysis rate.<sup>70</sup>

Moreover, the degree of polymerisation (DP) is identified as the number of glycosyl residues per cellulose chain. The effect of DP on the hydrolysis rate is linked to the other characteristics of substrate, like crystallinity. Zhang *et al.*<sup>71</sup> argued that the depolymerisation is mostly a function of the nature of the cellulosic substrate being attacked. Endo-glucanases prefer to

attack less ordered regions of the cellulose chain, which cause a decrease in DP. On the other hand, exo-glucanases attack the ends of cellulose chains, leading to a release of cellobiose as a product with slight effect on the DP. Nevertheless, regardless of the substrate to be hydrolysed, the DP is associated with an increased recalcitrance of crystalline cellulose, as illustrated in Figure 14.

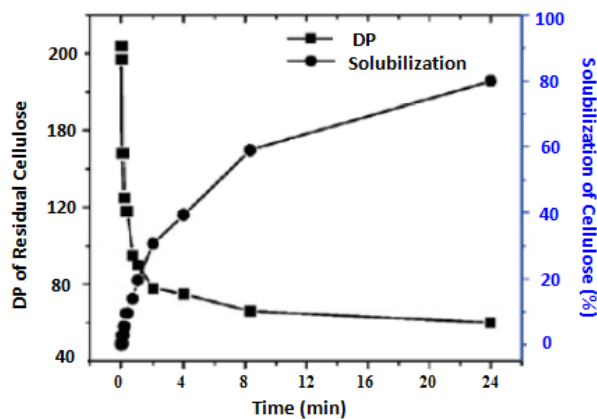


**Figure 14.** The decrease in DP of cellulose with time during enzymatic hydrolysis of phosphoric acid inflated cellulose (PASC) by *Trichoderma reesei* cellulase complex (adapted from <sup>71</sup>).

Another important characteristic that prompts enzymatic hydrolysis is the accessible surface area of the substrate. Usually, accessible surface area is measured using the BET (Bennet–Emmit–Teller) method from N<sub>2</sub> adsorption isotherms at 77 K<sup>72</sup>. As reported in the literature, this method has many defects that include the drying of the substrate, which does not allow measurements in inflated state of substrate. Consequently, specific surface area (SSA) can be overestimated, since the relatively small nitrogen molecules have the ability to access to pores and cavities on the substrate surface that enzymes cannot enter<sup>73</sup>. Therefore, enzyme molecules attached to cellulose surface cover a number of glucose units, as long as the hydrolysis reaction proceeds, only on one  $\beta$ -glucosidic bond (see Figure 15).

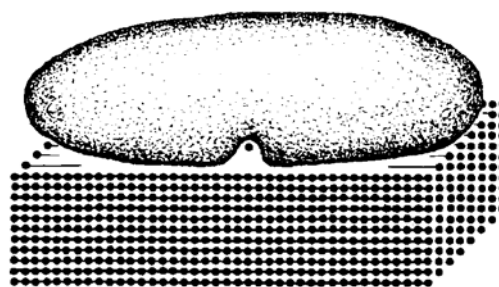


**Figure 15.** Representative drawing of enzyme-catalysed reaction on insoluble substrate.<sup>73</sup>

Both the shape and particle size of any substrate are closely connected to the external surface area. Accordingly, more adsorption positions per mass of substrate could be achieved in case of high surface area to weight of substrate ratio. Therefore, any pre-treatment method of lignocellulosic biomass usually involves reduction in size by cutting the lignocellulosic biomass

substrate, which results in an increased SSA. Additionally, pre-treatment methods include the removal of both lignin and hemicellulose that causes extended changes in the structure and accessibility of cellulose. Moreover, removing lignin and hemicellulose facilitates enzyme attack.<sup>70</sup>

### 3.1. Hydrolysis Lignin

Lignocellulosic biomass is generally pre-treated in order to produce lignin, cellulose fibres and hemicellulose. Moreover, these products are further processed using different methods. For instance, lignin is used for the production of phenolic compounds, vanillin, phenol derivatives, etc.; whereas hemicellulose is used to produce xylose. In addition, cellulose fibres are enzymatically hydrolysed in order to enhance the production of glucose and generate hydrolysis lignin as by-product.

The enzymatic hydrolysis is a heterogeneous reaction; thus, the first step in cellulose hydrolysis is the attachment of the enzyme molecules to the substrate by adsorption. Cellulose is converted to cellobiose by the bounding part of endo-glucanase and exo-glucanase. Otherwise, cellobiose is converted into glucose by the unbound part of  $\beta$ -glycosidase. As a result, the bound part of both endo- and exo-glucanase is responsible for cellobiose formation and the unbounding part of  $\beta$ -glycosidase is responsible for glucose production<sup>74</sup>. After finishing the adsorption step, hydrolysis reaction occurs.

The negative effect of lignin on enzymatic hydrolysis of cellulose substrates has been reported in different ways: 1) lignin inhibits the accessibility of cellulose to the enzyme by acting as a barrier; and 2) lignin absorbs cellulose via hydrophobic, ionic and hydrogen interactions and thus, cellulose becomes less available for enzymatic hydrolysis<sup>75-77</sup>. Moreover, recent studies stated that lignin content, composition of functional groups of lignin and physical distribution could affect the enzymatic hydrolysis.<sup>78, 79</sup>

On the other hand, several studies have been conducted using different types of enzymes. These studies assessed the influence of degradation products from lignin (e.g., furfural and its derivatives) on the inhibition or deactivation of enzyme activity<sup>80, 81</sup>. Nevertheless, Ko *et al* argued that the biomass type and/or the pre-treatment method played a vital role in the characteristics of lignin, which affect enzyme adsorption<sup>82</sup>. For example, lignin extracted from hardwood at higher harshness conditions resulted in a severe inhibition on the hydrolysis of cellulose<sup>83</sup>. Furthermore, a negative effect was also observed on the hydrolysis of cellulose from softwood, which was previously pre-treated at harshness conditions.<sup>80</sup>

## 4 Future work

From analysing the previous studies available on the two-stage fractionation process, the GreenCarbon's Early-Stage Researcher #5 (Q. Ibrahim) plan to develop and optimise a process of two sequential steps including organosolv delignification of beech wood at both lab and pilot scales. The effect of sequential processes for delignification of lignocellulosic biomass on the cellulose digestibility will be evaluated by enzymatic hydrolysis of the remaining solids (pulp).

A general scheme of the proposed approach is shown in Figure 16. Several parameters have to be evaluated and compared on the basis of pulp yield, acid insoluble lignin content, carbohydrate hydrolysis, and lignin yield. Moreover, hemicelluloses will be separated in the process prior to the organosolv delignification as xylan, while lignin will be separated through the organosolv process using a mixture of ethanol and water. Afterwards, solid residues will be further processed through enzymatic hydrolysis to produce hydrolysis lignin and enhance the production of glucose.

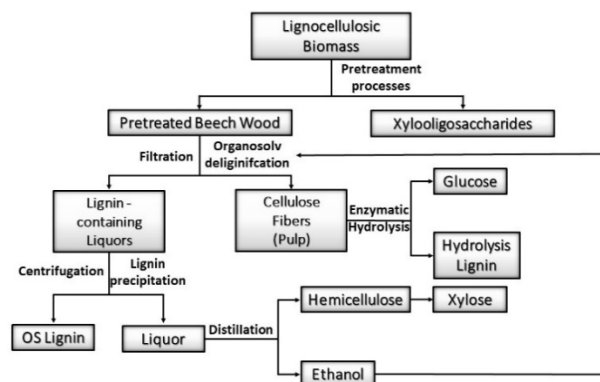


Figure 16. Scheme of the two-stage fractionation process considered in future work.

## 5. Conclusions

A two-stage process is a promising pathway for the delignification and fractionation of lignocellulosic biomass into lignin, cellulose and hemicellulose with feasible yields and distinctive characteristics of final products. However, the following points have to be considered:

- Lignin can be degraded or hydrolysed during the auto-hydrolysis or pre-hydrolysis step and its chemical structure can change, causing the generation of phenolic fractions in the reaction medium.
- It has been reported in previous studies that the auto-hydrolysis or pre-hydrolysis of the lignocellulosic biomass is generally conducted at 170–200 °C (near the glass transition temperature of lignin)<sup>83,89</sup>. Thus, the possibility of lignin recondensation could be relatively high, leading to a lignin in viscous state.
- Lignin droplets will be formed due to the precipitation of high molecular weight lignin fragments on the surface of fibres during the cooling of the reactor.<sup>89</sup>
- Residual lignin in remaining pulp after two-stage fractionation process can reduce the efficiency of the enzymatic hydrolysis process. Lignin can act as a physical barrier and inhibit the access of enzymes to cellulose cell wall.<sup>83</sup>

- The difficulty of lignin removal after pre-hydrolysis or auto-hydrolysis can be explained by a certain lignin repolymerisation, which also leads to the formation of carbonium ions intermediate, thereby, promoting the formation of new carbon-carbon bonds like  $\beta$ - $\beta$ ,  $\beta$ -1 and  $\beta$ -5.<sup>87, 88</sup>
- The resulted fractions could be used for further applications or processes; for example, cellulose fibres for enzymatic hydrolysis, lignin for hydrothermal processes and chemicals production, and sugars for biofuel production.
- Alternative pre-treatment methods (e.g., fungal and enzymatic pre-treatments) prior organosolv delignification could be used to avoid the problems related to the chemical pre-treatment methods.

### Acknowledgements

This project has received funding from the European Union's Horizon 2020 research and innovation programme under the Marie Skłodowska-Curie grant agreement No 721991.

### References

- (1) Fulton, L.; Jowes, T.; Hardy, J. *Biofuels for transport: An International Perspective*; International Energy Agency: Paris, 2004.
- (2) Sun, Y.; Cheng, J. Hydrolysis of lignocellulosic materials for ethanol production: a review. *Bioresour. Technol.* **2002**, *83*, 1–11.
- (3) Zugenmaier, P. Conformation and packing of various crystalline cellulose fibers. *Prog. Polym. Sci.* **2001**, *26*, 1341–1417.
- (4) Otmer, K. *Encyclopedia of chemical technology*; John Wiley & Sons: New Jersey, 2001.
- (5) Faulon, J. L.; Carlson, G. A.; Hatcher, P. G. A three-dimensional model for lignocellulose from gymnospermous wood. *Org. Geochem.* **1994**, *21*, 1169–1179.
- (6) Harmsen, P. F. H.; Huijten, W. J. J.; Lopez, B. L. M.; Bakker, R. R. C. *Literature Review of Physical and Chemical Processes for Lignocellulosic Biomass, Biosynergy project*, 2010.
- (7) Festucci-Buselli, R. A.; Ortoni, W. C.; Joshi, C. P. Structure, organization, and functions of cellulose synthase complexes in higher plants. *Braz. J. Plant Physiol.* **2007**, *19*, 1–13.
- (8) Krassig, H.; Schurz, J.; *Ullmann's Encyclopaedia of Industrial Chemistry*; Wiley-VCH: Weinheim, 2002.
- (9) Timell, T. E. Wood Hemicelluloses: Part I. *Adv. Carbohydrate Chem.* **1964**, *19*, 247–302.
- (10) *ThermoWood Handbook*; International ThermoWood Association: Helsinki, 2003.
- (11) Ban, L.; Chai, X.; Guo, J.; Ban, W.; Lucia, L. A. Chemical Response of Hardwood Oligosaccharides as a Statistical Function of Isolation Protocol. *J. Agric. Food Chem.* **2008**, *56*, 2953–2959.
- (12) Sjostrom, E.; *Wood Chemistry: Fundamental and Applications*; Academic press: Sand Diego, 1993.
- (13) Qiu, W. H.; Chen, H. Z. Structure, Function and Higher Value Application of Lignin. *Cellul. Sci. Technol.* **2006**, *14*, 52–59.
- (14) Brinchi, L.; Cotana, F.; Fortunati, E.; Kenny, J. M. Production of nanocrystalline cellulose from lignocellulosic biomass: technology and applications. *Carbohydr. Polym.* **2013**, *94*, 154–169.
- (15) Alvira, P.; Pejo, T.E.; Ballesteros, M.; Negro, M. J. Pretreatment technologies for an efficient bioethanol production process based on enzymatic hydrolysis: A review. *Bioresour. Technol.* **2010**, *101*, 4851–4861.
- (16) Wyman, C. E. Biomass Ethanol : Technical Progress, Opportunities, and Commercial Challenges. *Ann. Rev. Energy. Environ.* **1999**, *24*, 159–226.
- (17) Carvalheiro, F.; Duarte, L. C.; Girio, F. M. Hemicellulose biorefineries: a review on biomass pretreatments. *J. Sci. Ind. Res.* **2008**, *67*, 849–864.
- (18) Hendriks, A. T. W. M.; Zeeman, G. Pretreatments to enhance the digestibility of lignocellulosic biomass. *Bioresour. Technol.* **2008**, *100*, 10–18.
- (19) Taherzadeh, M. J.; Karimi, K. Advances in lignocellulosic biotechnology: A brief review on lignocellulosic biomass and cellulases. *Bioresour. Technol.* **2008**, *9*, 1621–1651.
- (20) Viikari, L.; Suurnäkki, A.; Grönquist, S.; Raaska, L.; Ragauska, A. *Forest Products: Biotechnology in Pulp and Paper Processing*; Elsevier: Helsinki, 2009.
- (21) Aziz, S.; Sarkanen, K. Organosolv pulping—a review. *Tappi J.* **1989**, *72*, 169–175.
- (22) Young, R. A.; Akhtar, M. *Environmentally Friendly Technology for the Pulp and Paper Industry*; Wiley: NY, 1998.
- (23) Shirkolaei, Y. Z.; Rovshandeh, J. M.; Charani, P. R.; Khajeheian, M. B. Study on cellulose degradation during organosolv delignification of wheat straw and evaluation of pulp properties. *Iran. Polym. J.* **2007**, *16*, 83–96.
- (24) Sun, Y.; Cheng, J. Hydrolysis of lignocellulosic materials for ethanol production: a review. *Bioresour. Technol.* **2002**, *83*, 1–11.
- (25) Garrote, G.; Eugenio, M.E.; Diaz, M. J. Ariza, J.; Lopez, F. Hydrothermal and pulp processing of Eucalyptus. *Bioresour. Technol.* **2003**, *88*, 61–68.
- (26) Gilarranz, M. A.; Oliet, M.; Rodriguez, F.; Tijero, J. Ethanol-Water Pulping: Cooking Variables Optimization. *Can. J. Chem. Eng.* **1998**, *76*, 253–260.
- (27) Jimenez, L.; Garcia, J. C.; Perez, I., Ariza, J.; Lopez, F. Acetone Pulping of Wheat Straw. Influence of the Cooking and Beating Conditions on the Resulting Paper Sheets. *Ind. Eng. Chem. Res.* **2001**, *40*, 6201–6206.
- (28) Gargulak, J.; Lebo, S. *In Lignin: Historical, Biological and materials perspectives*; American Chemical Society: Washington DC, 2000.

- (29) Garrote, G.; Dominoguez, H.; Parajo, J. C. Manufacture of xylose-based fermentation media from corncobs by posthydrolysis of autohydrolysis liquors. *Appl. Biochem. Biotechnol.* **2001**, *95*, 195–207.
- (30) Kim, Y.; Mosier, N.S.; Ladisch, M. R. Enzymatic digestion of liquid hot water pretreated hybrid poplar. *Biotechnol. Prog.* **2009**, *25*, 340–348.
- (31) Laser, M.; Schulamn, D. Allen, S. G.; Lichwa, J.; Antal, J. M.; Lynd, I. R. A comparison of liquid hot water and steam pretreatments of sugar cane bagasse for bioconversion to ethanol. *Bioresour. Technol.* **2002**, *81*, 33–44.
- (32) Carvalheiro, F.; Silva, F. T.; Duarte, L. C.; Girio, F. M. Wheat straw autohydrolysis: process optimization and products characterization. *Appl. Biochem. Biotechnol.* **2009**, *153*, 84–93.
- (33) Moniz, P.; Pereira, H.; Quilho, T.; Carvalheiro, F. Characterisation and hydrothermal processing of corn straw towards the selective fractionation of hemicelluloses. *Ind. Crop. Prod.* **2013**, *50*, 145–153.
- (34) Harmsen, P.; Huijgen, W.; Bermudez, L.; Bakker, R. Literature review of physical and chemical pretreatment processes for lignocellulosic biomass. *Bioenergy project*, Report 1184; 2010.
- (35) Huijgen, W. J. J.; Reith, J.H.; den Uil, H. Pretreatment and Fractionation of Wheat Straw by an Acetone-Based Organosolv Process. *Ind. Eng. Chem. Res.* **2010**, *49*, 10132–10140.
- (36) Bozell, J. J.; Black, S.K.; Myers, M.; Cahill, D.; Miller, W. P.; Park, S. Solvent fractionation of renewable woody feedstocks: organosolv generation of biorefinery process streams for the production of biobased chemicals. *Biomass Bioenergy* **2011**, *35*, 4197–4208.
- (37) Toledano, A.; Serrano, L.; Balu, A. M.; Luque, R.; Pineda, A.; Labidi, J. Fractionation of organosolv lignin from olive tree clippings and its valorization to simple phenolic compounds. *ChemSusChem* **2013**, *6*, 529–536.
- (38) Overend, R. P.; Chornet, E.; Gascoigne, J.A. Fractionation of lignocellulosics by steam-aqueous pretreatments. *Phil. Trans. R. Soc.* **1987**, *321*, 523–536.
- (39) Chornet, E.; Overend, R. P. In: *Steam Explosion Techniques: Fundamentals and Industrial Applications. Proceedings of the International Workshop on Steam Explosion Techniques*. CRC Press, Milan: 1988, p. 21–58.
- (40) Lora, J. H.; Wayman, H. Delignification of hardwoods by autohydrolysis and extraction. *Tappi J.* **1978**, *61*, 47–50.
- (41) April, G. C.; Bharoocha, R.; Sheng, J.; Hansen, S. Prehydrolysis achieves higher organosolv delignification. *Tappi J.* **1982**, *65*, 41–44.
- (42) Patel, D.P.; Varshney, A.K. The effect of presoaking and prehydrolysis on organosolv delignification of bagasse. *Indian J. Technol.* **1989**, *27*, 285–288.
- (43) Thring, R. W.; Chornet, E. Fractionation of woodmeal by prehydrolysis and thermal organosolv. Process strategy, recovery of constituents, and solvent fractionation of lignins co-produced. *Can. J. Chem. Eng.* **1993**, *71*, 116–123.
- (44) Hongzhang, C.; Liying, L. Unpolluted fractionation of wheat straw by steam explosion and ethanol extraction. *Bioresour. Technol.* **2007**, *98*, 666–676.
- (45) Bross, N.; Sannigrahi, P.; Ragauskas, A. Pretreatment of *Miscanthus x giganteus* using the Ethanol Organosolv Process for Ethanol Production. *Ind. Eng. Chem. Res.* **2009**, *48*, 8328–8334.
- (46) Brosse, N.; El Hage, R.; Sannigrahi, P.; Ragauskas, A. Dilute sulphuric acid and Ethanol Organosolv Pretreatment of *Miscanthus x Giganteus*. *Cellulose Chem. Technol.* **2010**, *44*, 71–78.
- (47) El Hage, R.; Chrusciel, L.; Desharnais, L.; Brosse, N. Effect of autohydrolysis of *Miscanthus x giganteus* on lignin structure and organosolv delignification. *Bioresour. Technol.* **2010**, *101*, 9321–9329.
- (48) Ruiz, H. A.; Ruzene, D. S.; Silva, D. P.; da Silva, F. F. M.; Vicente, A. A.; Teixeira, J. A. Development and characterization of an environmentally friendly process sequence (autohydrolysis and organosolv) for wheat straw delignification. *Appl. Biochem. Biotechnol.* **2011**, *164*, 629–641.
- (49) Romani, A.; Garrote, G.; Lopez, F.; Parajo, J.C. Eucalyptus globulus wood fractionation by autohydrolysis and organosolv delignification. *Bioresour. Technol.* **2011**, *102*, 5896–5904.
- (50) Liu, Z.; Fatehi, P.; Jahan, M. S.; Ni, Y. Separation of lignocellulosic materials by combined processes of pre-hydrolysis and ethanol extraction. *Bioresour. Technol.* **2011**, *102*, 1264–1269.
- (51) Amendola, D.; De Faveri, D. M.; Egües, I.; Labidi, J.; Spingo, G. Autohydrolysis and organosolv process for recovery of hemicellulose, phenolic compounds and lignin from grape stalks. *Bioresour. Technol.* **2012**, *107*, 267–274.
- (52) Huijgen, W. J. J.; Smit, A. T.; de Wild, P. J.; den Uil, H. Fractionation of Wheat straw by prehydrolysis, organosolv delignification and enzymatic hydrolysis for production of sugars and lignin. *Bioresour. Technol.* **2012**, *114*, 389–398.
- (53) Tunc, M. S.; Chheda, J.; van der Heide, E.; Morris, J.; Heiningen, A. Two. Stage fractionation of hardwoods. *Bioresour.* **2013**, *8*, 4380–4395.
- (54) Vallejos, M. E.; Zambon, M. D.; Area, M. C.; da Silva-Curvelo, A. A. Low liquid–solid ratio fractionation of sugarcane bagasse by hot water autohydrolysis and organosolv delignification *Ind. Crops. Prod.* **2015**, *65*, 349–353.

- (55) Zhu, M. Q.; Wen, J. L.; Su, Y. Q.; Wie, Q.; Sun, R. C. Effect of structural changes of lignin during autohydrolysis and organosolv pretreatment on *Eucommia ulmoides* Oliver for an effective enzymatic hydrolysis. *Bioresour. Technol.* **2015**, *185*, 378–385.
- (56) Moniz, P.; Lino, J.; Duarte, L. C.; Roserio, L. B.; Boeriu, C. G.; Pereira, H.; Carvalheiro, F. Fractionation of hemicelluloses and lignin from rice straw by combining autohydrolysis and optimised mild organosolv delignification. *Bioresour.* **2015**, *10*, 2626–2641.
- (57) Amiri, H.; Karimi, K. Integration of Autohydrolysis and Organosolv Delignification for Efficient Acetone, Butanol, and Ethanol Production and Lignin Recovery. *Ind. Eng. Chem. Res.* **2016**, *55*, 4836–4845.
- (58) Gurgel, L. V. A.; Pimenta, M. T. B.; da Silva-Curvelo, A. A. Ethanol-water organosolv delignification of liquid hot water (LHW) pretreated sugarcane bagasse enhanced by high-pressure carbon dioxide (HP-CO<sub>2</sub>). *Ind. Crops. Prod.* **2016**, *94*, 942–950.
- (59) Meighan, B. N.; Lima, D. R. S.; Cardoso, W. J.; Baeta, B. E. L.; Adarme, O. F. H.; Santucci, B. S.; Pimenta, M. T. B.; de Aquino, S. F.; Gurgel, L. V. A. Two-stage fractionation of sugarcane bagasse by autohydrolysis and glycerol organosolv delignification in a lignocellulosic biorefinery concept. *Ind. Crops. Prod.* **2017**, *108*, 431–441.
- (60) Matsakas, L.; Nitsos, C.; Raghavendran, V.; Yakimenko, O.; Persson, G.; Olson, E.; Rova, U.; Olsson, L.; Christakopoulos, P. A novel hybrid organosolv: steam explosion method for the efficient fractionation and pretreatment of birch biomass. *Biotechnol. Biofuels* **2018**, *11*, 1–14.
- (61) Matsakas, L.; Nitsos, C.; Raghavendran, V.; Yakimenko, O.; Persson, G.; Olson, E.; Rova, U.; Olsson, L.; Christakopoulos, P. Isolation and Characterization of Organosolv and Alkaline Lignins from Hardwood and Softwood Biomass. *ACS Sustain. Chem. Eng.* **2016**, *4*, 5181–5193.
- (62) Arantes, V.; Gourlay, K.; Saddler, J.N. The enzymatic hydrolysis of pretreated pulp fibers predominantly involves “peeling/erosion” modes of action. *Biotechnol. Biofuels* **2014**, *7*, 1–10.
- (63) Vinzant, T. B.; Ehrman, C. I.; Himmel, M. E. Simultaneous saccharification and fermentation of pretreated hardwoods: effect of native lignin content. *Appl. Biochem. Biotechnol.* **1997**, *62*, 97–102.
- (64) Mooney, C. A.; Mansfield, S. H.; Touhy, M. G.; Saddler, J. N. The effect of initial pore size and lignin content on the enzymatic hydrolysis of softwood. *Bioresour. Technol.* **1998**, *64*, 113–119.
- (65) Gusakov, A. V.; Sinitsyn, A. P. A theoretical analysis of cellulose product inhibition: effect of cellulose binding constant, enzyme/substrate ratio, and  $\beta$ -glucosidase activity on the inhibition pattern. *Biotechnol. Bioeng.* **1992**, *40*, 663–671.
- (66) Ooshima, H.; Burns, D. S.; Converse, A. O. Adsorption of cellulase from *Trichoderma reesei* on cellulose and lignocellulosic residue in wood pretreated by dilute sulfuric acid with explosive decompression. *Biotechnol. Bioeng.* **1990**, *36*, 446–452.
- (67) Mansfield, S. D.; Mooney, C.; Saddler, J. N. Substrate and Enzyme Characteristics that Limit Cellulose Hydrolysis. *Biotechnol. Prog.* **1999**, *15*, 804–916.
- (68) Fan, L. T.; Lee, Y. H.; Beardmore, D. R. The influence of major structural features of cellulose on rate of enzymatic hydrolysis. *Biotechnol. Bioeng.* **1981**, *23*, 419–424.
- (69) Fan, L. T.; Lee, Y. H.; Beardmore, D.R. Mechanism of the enzymatic hydrolysis of cellulose: Effects of major structural features of cellulose on enzymatic hydrolysis. *Biotechnol. Bioeng.* **1980**, *22*, 177–199.
- (70) Grethlein, H. E.; Allen, D. C.; Converse, A. O. A comparative study of the enzymatic hydrolysis of acid pretreated white pine and mixed hardwood. *Biotechnol. Bioeng.* **1984**, *26*, 1498–1505.
- (71) Zhang Y.-H. P.; Lynd, L. R. Toward an aggregated understanding of enzymatic hydrolysis of cellulose: noncomplexed cellulose systems. *Biotechnol. Bioeng.* **2004**, *88*, 797–824.
- (72) Masamune, S.; Smith, J. M. Adsorption rate studies—significance of pore diffusion. *AIChE J.* **1964**, *10*, 246–252.
- (73) Brown, R. F.; Holtzapfel, M. T. A comparison of the Michaelis–Menten and HCH-1 models. *Biotechnol. Bioeng.* **1990**, *36*, 1151–1154.
- (74) Fenila, F.; Shastri, Y. Optimal control of enzymatic hydrolysis of lignocellulosic biomass. *Resour.-Effic. Technol.* **2016**, *2*, S96–S104.
- (75) Zhao, X.; Zhang, J.; Liu, D. Biomass Recalcitrance Part I: The Chemical Compositions and Physical Structures Affecting the Enzymatic Hydrolysis of Lignocellulose. *Biofuels, Bioprod. Biorefin.* **2011**, *6*, 465–482.
- (76) Berlin, A.; Balakshin, M.; Gilkes, N.; Kadla, J.; Maximenko, V.; Kubo, S.; Saddler, J. J. Inhibition of cellulase, xylanase and  $\beta$ -glucosidase activities by softwood lignin preparations. *J. Biotechnol.* **2006**, *125*, 198–209.
- (77) Pan, X. Role of Functional Groups in Lignin Inhibition of Enzymatic Hydrolysis of Cellulose to Glucose. *J. Biobased Mater. Bioenergy* **2008**, *2*, 25–32.
- (78) Nakagame, S.; Chandra, R. P.; Kadla, J. F.; Saddler, J. N. The isolation, characterization and effect of lignin isolated from steam pretreated Douglas-fir on the enzymatic hydrolysis of cellulose. *Bioresour. Technol.* **2011**, *102*, 4507–4517.
- (79) Yuan, T. Q.; Wang, W.; Zhang, L. M.; Xu, F.; Sun, R. C. Reconstitution of cellulose and lignin after [C<sub>2</sub>mim][OAc] pretreatment and its relation to

- enzymatic hydrolysis. *Biotechnol. Bioeng.* **2013**, *110*, 729–736.
- (80) Ximenes, E.; Kim, Y.; Mosier, N.; Dien, B.; Ladlisch, M. Inhibition of cellulases by phenols. *Enzyme Microb. Technol.* **2010**, *46*, 170–176.
- (81) Ximenes, E.; Kim, Y.; Mosier, N.; Dien, B.; Ladlisch, M. Deactivation of cellulases by phenols. *Enzyme Microb. Technol.* **2011**, *48*, 54–60.
- (82) Ko, J. K.; Kim, Y.; Ximenes, E.; Ladlisch, M. Adsorption of enzyme onto lignins of liquid hot water pretreated hardwoods. *Biotechnol. Bioeng.* **2015**, *112*, 447–456.
- (83) Ko, J. K.; Kim, Y.; Ximenes, E.; Ladlisch, M. Effect of liquid hot water pretreatment severity on properties of hardwood lignin and enzymatic hydrolysis of cellulose. *Biotechnol. Bioeng.* **2015**, *112*, 252–262.
- (84) Chen, H. Z.; Chen, J. Z.; Liu, J.; Li, Z. H. Studies on steam explosion of wheat straw I. Effects of the operating conditions for steam explosion of wheat straw and analysis of the process. *J. Cellulose Sci. Technol.* **1999**, *7*, 60–67.
- (85) Romani, A.; Garrote, G.; Alonso, J.L.; Parajo, J. C. Experimental Assessment on the Enzymatic Hydrolysis of Hydrothermally Pretreated Eucalyptus globulus Wood. *Ind. Eng. Chem. Res.* **2010**, *49*, 4653–4663.
- (86) Zhang, Y.; Qin, M.; Xu, W.; Fu, Y.; Wang, Z.; Li, Z.; Willför, S.; Xu, C.; Hou Q. Structural changes of bamboo-derived lignin in an integrated process of autohydrolysis and formic acid inducing rapid delignification. *Ind. Crops. Prod.* **2018**, *115*, 194–201.
- (87) Leschinsky, M.; Zuckerstatter, G.; Weber, H.K.; Patt, R.; Sixta, H. Effect of autohydrolysis of Eucalyptus globulus wood on lignin structure. Part 1: Comparison of different lignin fractions formed during water prehydrolysis. *Holzforschung.* **2008**, *62*, 645–652.
- (88) Leschinsky, M.; Zuckerstatter, G.; Weber, H.K.; Patt, R.; Sixta, H. Effect of autohydrolysis of Eucalyptus globulus wood on lignin structure. Part 2: influence of autohydrolysis intensity. *Holzforschung.* **2008**, *62*, 653–658.
- (89) Zhuang, X.; Yu, Q.; Yuan, Z.; Kong, X.; Qi, W. Effect of hydrothermal pretreatment of sugarcane bagasse on enzymatic digestibility. *J. Chem. Technol. Biotechnol.* **2015**, *90*, 1515–1520.



## Review of the conversion from hydrochar to activated carbon

Pablo J. Arauzo<sup>a</sup>, Maciej P. Olszewski<sup>a</sup>, Michela Lucian<sup>b</sup>, Catalina Rodríguez-Correa<sup>a</sup>, Yvonne Ringelspacher<sup>a</sup>, Andrea Kruse<sup>a</sup>, Luca Fiori<sup>b</sup>

<sup>a</sup> *Department of Conversion Technologies of Biobased Resources, Institute of Agricultural Engineering, University of Hohenheim, Garbenstrasse 9, 70599 Stuttgart, Germany*

<sup>b</sup> *Department of Civil, Environmental and Mechanical Engineering, University of Trento, Via Mesiano 77, 38123 Trento, Italy*

### Abstract

Conversion of agricultural wastes using biogas plants is a possibility for the production of renewable energy. The residues produced after biogas treatment (i.e., digestates) can be used for the production of activated carbon. On the other hand, hydrothermal carbonisation (HTC) is considered a pretreatment for the conversion of initial wet biomass into carbonaceous material called hydrochar. The aim of this chapter is to show the different parameters that influence the conversion from the initial biogas residues to hydrochars as well as the subsequent activation of hydrochars.

### 1. Introduction

Biogas is an important resource for renewable heat, electricity and fuel generation. A large variety of biomass (for instance, agricultural or forestry resources, sewage, wastes, such as municipal solid wastes, industrial and household wastes) can be used as raw materials, giving the possibility of organic waste disposal in biogas plants<sup>1</sup>. Due to benefits of biogas production, the number of installed biogas plants in Europe is increasing. Biogas is produced by anaerobic digestion of biomass, at which an additional residual product, referred to as digestate, is formed.

The large amount of generated digestate must be disposed, or better to find applications, to avoid constraints in the development of biogas production. Until now, digestate is mainly used as fertiliser and soil conditioner. It provides a good source of available nutrients (especially nitrogen and phosphorus) and has positive effects on the biological properties of soil; however, its use in agriculture is restricted, since it needs to fulfil certain quality standards (for instance in hygiene and biodegradability). Additionally, an improper use can lead to ecological problems, such as metal accumulation in soil (in particular Cu and Zn) or soil salinization.<sup>2,3</sup>

Recent studies have reported the generation of highly adsorptive activated carbons by hydrothermal carbonisation (HTC) of lignocellulosic biomass and subsequent activation. These activated carbons can, for instance, be applied in supercapacitors, for selective gas storage or as catalysts<sup>4-9</sup>. Since digestate also contains lignocellulosic compounds, the production of activated carbon provides an alternative utilisation.<sup>10</sup>

During HTC, a raw material (in principle any type of biomass) is heated in presence of liquid water at elevated temperatures (usually 180–250 °C) under autogenous pressure, whereupon a solid carbon-rich material, referred to as hydrochar, is generated. The process conditions of HTC, such as temperature, residence time and starting pH influence the characteristics of both the hydrochar and subsequent activated carbon. The effects of temperature and residence time are well

investigated; however, there is not enough data about the influence of catalysts and starting pH.<sup>11</sup>

It is known that the overall reaction rate of HTC is improved at weakly acidic conditions. During HTC, organic acids, such as levulinic acid, formic acid and acetic acid, are formed, exhibiting autocatalytic effects on the reaction. Acid addition is used to enhance the reaction, while the type of acid used plays an important role<sup>12</sup>. Nevertheless, there is few literature data discussing the role of the type of acid. Reiche et al.<sup>13</sup> proved an oxidising effect of nitric acid during HTC of glucose at low pH ranges (pH ≤ 1.5). Lynam et al.<sup>14</sup> showed that acetic acid addition during HTC of loblolly pine led to a shift in reaction equilibrium, resulting in a lower production of acetic acid. The impact of acid addition depends on the type of feedstock and acid addition does not always show catalytic effects.<sup>15</sup>

### 2. Characterisation of activated carbon (AC)

Due to their high adsorptive capacity, activated carbons are widely used in chemical, food and pharmaceutical industries for purification and separation processes and in catalysis. Typical applications are, for instance: water purification, gas storage or separation<sup>16</sup>. Recently, ACs are also used as electrode materials in supercapacitors<sup>5,17</sup> or Li-S battery cells.<sup>18</sup>

The applicability of an activated carbon depends on its adsorptive characteristics, which are on the one hand attributed to its textural properties and porous structure and on the other hand, to functional groups bonded on the carbon surface. Besides carbon, AC also contains small amounts of oxygen, hydrogen, nitrogen and sulphur, contributing to the adsorptive properties. Therefore, pore structure analysis (such as determination of pore size distribution, surface area and pore volume) and analysis of functional surface groups are important to characterise ACs.

#### 2.1. Adsorption capacity of model substances

To determine the adsorption capacity of AC, the adsorption of model substances, typically methylene blue, iodine and phenol can be tested, giving also an indication of present pore sizes in the AC. Methylene blue and iodine adsorption is usually used to

study mesopores or large micropores; the methylene blue molecule is accessible to pores with diameters larger than 1.5 nm, while the iodine molecule can be adsorbed in pores larger than 1 nm. Phenol can be used for micropore analysis, since it can be adsorbed in pores smaller than 2 nm or even 0.7 nm<sup>19</sup>. Adsorption capacities of activated carbons are additionally influenced by the presence of surface groups<sup>20</sup>.

## 2.2. Pore structure analysis by gas adsorption experiments

More detailed information about pore structure and pore size distribution can be gained by gas adsorption experiments, allowing an assessment of pore sizes from 0.35 to 100 nm<sup>21</sup>. According to IUPAC recommendation<sup>22</sup>, pores are classified by their size:

- (i) Pores with widths exceeding about 50 nm are called macropores.
- (ii) Pores of widths between 2 nm and 50 nm are called mesopores.
- (iii) Pores with widths not exceeding about 2 nm are called micropores.

During adsorption experiments, a known amount of gas is admitted to a confined, calibrated volume containing the sample. Due to adsorption, the pressure in the confined volume falls. As the temperature is held constant during the experiment, the adsorbed gas amount can be determined from the pressure decrease by applying the ideal gas law. The adsorbed gas amount is the difference between the admitted gas amount and the required amount of gas to fill the void space, which has to be determined previously. By varying the amount of admitted gas, an adsorption/desorption isotherm, showing the amount of adsorbed gas at various relative pressures, can be obtained. Isotherm shapes are classified according to IUPAC as shown in Fig. 1.<sup>22</sup>

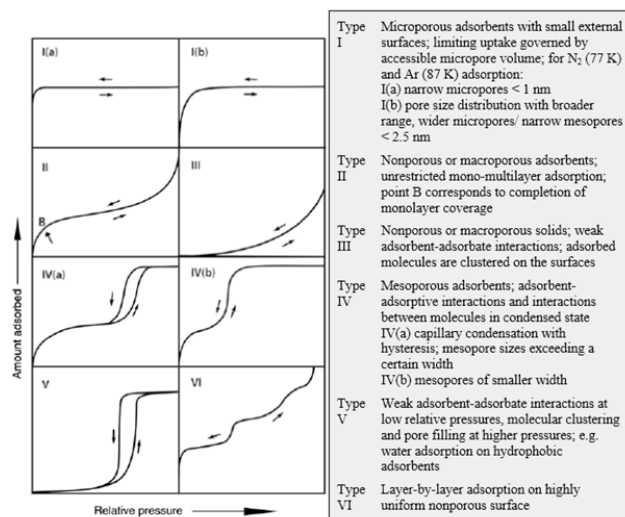


Figure 1. Classification of adsorption isotherms according to IUPAC.<sup>22</sup>

If the amount of adsorbed gas during desorption at a respective pressure deviates from the amount during adsorption, the isotherm shows a hysteresis loop. Hysteresis is associated with capillary condensation resulting in delayed desorption. It occurs

when the pore width exceeds a certain critical width (about 4 nm for N<sub>2</sub> adsorption at 77 K) and pore condensation takes place at a pressure less than the saturation value. Types of hysteresis loops are classified by IUPAC as shown in Fig. 2.

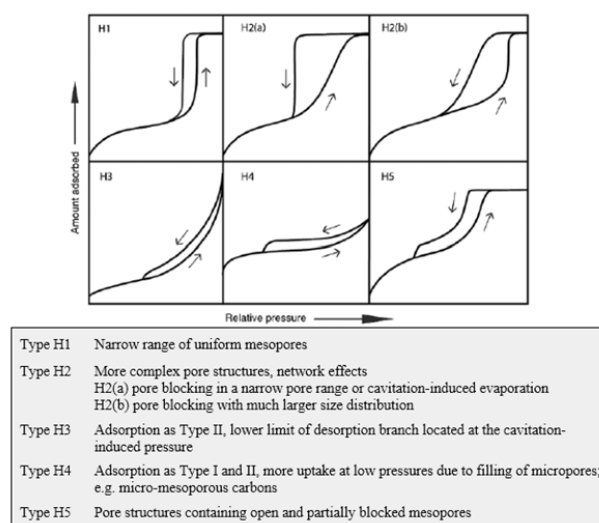


Figure 2. Types of hysteresis loops in adsorption isotherms.<sup>22</sup>

As adsorbate, several gases at different temperatures can be used. Nitrogen at its boiling temperature (77 K at atmospheric pressure) and carbon dioxide at 273.15 K are one of the most commonly used. Since CO<sub>2</sub> at 273.15 K diffuses faster in micropores and CO<sub>2</sub> adsorption starts at higher pressures compared to N<sub>2</sub> at 77 K, the use of CO<sub>2</sub> is advantageous for micropore analysis. CO<sub>2</sub> adsorption experiments are faster and do not require high vacuum systems. However, from CO<sub>2</sub> adsorption isotherms only pore sizes up to 1.5 nm can be determined. Therefore, it is reasonable to combine CO<sub>2</sub> isotherms for micropore analysis with N<sub>2</sub> measurements for mesopore determination.<sup>23</sup>

For the evaluation of gas adsorption experiments, there are several models, allowing estimations of surface areas, pore volumes and pore size distribution. Table 1 lists the most common used methods, as described in the operation manual of a commercial gas adsorption device.<sup>24</sup>

**Table 1.** Evaluation methods for gas adsorption experiments<sup>24</sup>.

Method name	Purpose	Description
Brunauer-Emmett-Teller (BET) method	Specific surface area	Linear plot of BET equation, describing the relation between weights of gas adsorbed and adsorbate constituting a monolayer of surface coverage at a relative pressure $p/p_0$ .
Barrett, Joyner, Halenda (BJH) method	Pore size distribution (mesopores)	Assumes that at $p/p_0 = 1$ all pores are filled with liquid; as the pressure is lowered, adsorbed liquid evaporates and desorbs; according to Kelvin equation, the pressure at which evaporation or condensation occurs depends on pore radius; thus, the corresponding pore volume is calculated for different pore radii.
Langmuir method	Surface area of microporous samples in the absence of meso- and macropores	Limiting case of BET equation in the absence of meso- and macropores.
V-t method (t-method)	Micropores surface area and micropore volume in the presence of mesopores	Calculation of $t$ , the statistical thickness of an adsorbed film at a corresponding relative pressure $p/p_0$ using de Boer, Carbon Black or Halsey equation; plot of adsorbed volume $V$ versus $t$ .
Alpha-s method	Micropores surface area and micropore volume in the presence of mesopores	Empirical analogue to $t$ -method
Dubinin-Radushkevich (DR) method	Micropore volume, pore size distribution of micropores	Fraction of adsorption volume $V$ occupied by liquid adsorbate is expressed as a Gaussian function; it assumes homogeneous pore size distribution; adoption of model parameters.
Dubinin-Astakhov (DA) method	Micropore volume, pore size distribution of micropores	Generalised form of DR method, also for heterogeneous pore size distributions
Horvath-Kawazoe (HK) method	Pore size distribution of micropores	Calculation of pore size distribution of micropores from low relative pressure region, independent of Kelvin equation; it assumes slit-like pores
Saito-Foley (SF) method	Pore size distribution of micropores	Alternative to HK method; it assumes cylindrical pore geometry.
Density Functional Theory (DFT) and Monte Carlo Simulation (MC) methods	Pore size distribution	More realistic description of micropores; numerical solution of Generalized Adsorption Isotherm (GAI) equation

### 2.3. Analysis of functional surface groups

To determine functional surface groups, FTIR spectroscopy is often used<sup>25,26</sup>. A simpler method is the Boehm titration, which determines the surface acidity or basicity of AC. Surface groups such as carboxylic groups, lactones, lactoles and hydroxyl groups of phenolic character have acidic characters and can be neutralised by alkaline titration. Since these groups have different acidic strengths, they can be differentiated by neutralisation with 0.05 M solutions of bases with different strengths. Sodium hydroxide (NaOH) neutralises all acidic groups, sodium carbonate ( $\text{Na}_2\text{CO}_3$ ) neutralises carboxylic and lactonic groups and sodium bicarbonate ( $\text{NaHCO}_3$ ) neutralises only carboxylic groups. Basic groups, which origin is still in discussion, can be neutralised with hydrochloric acid. There are several hypotheses about the origin of the surface basicity, such as  $\pi$  basicity of graphene layers or pyrone-type structures; however, basicity caused by these structures are weaker than proven basicity. Stronger basicity can be obtained from pyrone-type structures, where the carbonyl group and the ring oxygen are distributed on polycyclic aromatic compounds.<sup>27,28</sup>

## 3. The activation process

The activation process leads to an increase in internal surface areas of a carbonaceous precursor. As precursors, for instance coal, pitch, agricultural by-products and polymeric materials are used<sup>29</sup>. There are various patented methods for activation, where it is generally differed between physical and chemical activation. Physical activation includes two steps: carbonisation and activation. During carbonisation, the precursor is pyrolysed in an inert (mostly nitrogen) atmosphere at 600–900 °C. The carbonised precursor is then activated with oxidising gases, such as carbon dioxide or water steam at 600–1200 °C. During chemical activation, the precursor is mixed with a chemical reagent and heated in an inert atmosphere (usually nitrogen) to 450–900 °C<sup>25</sup>. Various reagents, such as  $\text{ZnCl}_2$ ,  $\text{H}_3\text{PO}_4$ ,  $\text{K}_2\text{CO}_3$ ,  $\text{Na}_2\text{CO}_3$ ,  $\text{AlCl}_3$ ,  $\text{KOH}$  or  $\text{NaOH}$  can be used, leading to different chemical reactions with the precursor. Chemical activation has several advantages compared to physical activation: it requires lower temperatures, produces much higher yields and allows to obtain very high surface areas. The microporosity can be well developed and the pore size distribution controlled by the process conditions. However, corrosive reagents have to be used and an additional washing step is required<sup>30</sup>. Chemical activation can be performed as a one-step method, but with an additional pre-carbonisation step higher adsorption capacities, higher surface areas and pore volumes can be obtained.<sup>26</sup>

### 3.1. Process conditions of chemical activation

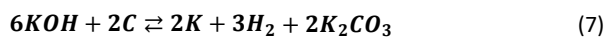
#### 3.1.1. Type of chemical reagent

The type of activation agent plays the major role in the activation process.  $\text{H}_3\text{PO}_4$ ,  $\text{ZnCl}_2$ ,  $\text{NaOH}$  and  $\text{KOH}$  are the most commonly used activation agents. A different type of chemical reagent leads to different chemical mechanisms during activation and therefore to different AC characteristics. Studies comparing different chemical reagents show that  $\text{ZnCl}_2$  and  $\text{H}_3\text{PO}_4$  do not work efficiently at temperatures above 600 °C, and that using alkali hydroxides ( $\text{NaOH}$  or  $\text{KOH}$ ) or their

carbonates much higher pore volumes and surface areas can be obtained<sup>31,32</sup>. Compared to activation with NaOH, KOH activation can lead to a narrower pore size distribution.<sup>33</sup> Since very high surface areas (up to 3000 m<sup>2</sup> g<sup>-1</sup>) and well defined micropore volumes can be obtained, there are various studies about activation with alkali hydroxides (NaOH and KOH) for the production of new carbon materials<sup>5,17,18</sup>, and mechanisms during KOH and NaOH activation are widely discussed. Otowa et al.<sup>34</sup> proved the formation of larger amounts of H<sub>2</sub>, smaller amounts of CO, CO<sub>2</sub>, CH<sub>4</sub> and K<sub>2</sub>CO<sub>3</sub> and observed the formation of metallic potassium during KOH activation. They considered the following reactions to contribute to activation:



Lillo-Ródenas et al.<sup>35</sup> showed that there was a reaction between the alkali metal hydroxide and carbon during KOH activation. They proposed the following reaction during KOH activation:



Three main effects during activation with alkali metal hydroxides contributing to pore formation can be summarised: (i) etching of the carbon framework by redox reactions (3), (6) and (7) with carbon; (ii) formation of H<sub>2</sub>O and CO<sub>2</sub> via reactions (4) and (5), favouring further carbon gasification; and (iii) intercalation of metallic potassium leading to micropore formation after washing.<sup>18,29,36</sup>

### 3.1.2. Reagent to precursor ratio

Several studies showed a positive effect on total pore volume and surface area of high reagent to precursor ratios during activation with H<sub>3</sub>PO<sub>4</sub><sup>37</sup>, KOH<sup>26,33,38,39</sup> or NaOH<sup>33</sup>, regardless of the type of precursor. For KOH activation, a KOH to precursor weight ratio of 4:1 was found as an optimum, resulting to highest pore volumes and surface areas<sup>26</sup>. An increasing reagent to precursor ratio leads to pore widening and therefore, to a change in pore size distribution, indicating that the reagent to precursor ratio can be used to control the porosity of AC.<sup>26,33,38</sup>

### 3.1.3. Mixing method

There are two ways to mix the precursor with the chemical reagent agents: the pure, dry reagent can be mixed with the precursor and directly activated or, alternatively, the precursor can be impregnated by mixing it with the reagent solution and drying the mixture prior to activation. The advantage of the latter method is a better distribution of chemical agents into the solid mass; however, an additional drying step is required. Ahmadpour and Do<sup>31</sup> showed that impregnation prior to activation led to AC with higher BET surfaces and higher micropore volumes compared to AC prepared by physical mixing with the reagent. Teng et al.<sup>37</sup> have investigated the impregnation time and temperature of coal prior to chemical activation with H<sub>3</sub>PO<sub>4</sub>. In a time range from 1 to 3 hours and

temperature range from 50 to 85 °C, they only observed minor effects of impregnation time or temperature on pore volume and BET surface area.

### 3.1.4. Temperature

The effect of temperature depends strongly on the activation agent. In principle, high temperatures promote the activation process and the higher the temperature, the more pores are formed to certain extents; however, if a certain temperature level is exceeded, total surface areas in AC decrease. Therefore, to obtain a maximal surface area, for every activation agent there is an optimal activation temperature, depending also on the type of precursor.

If the temperature is increased to a certain level, pores will grow and combinations of pores are formed, resulting to a decrease in specific surface area and micropore volume, and an increase in mesopore volume. This effect plays an important role during activation with alkaline hydroxides and was observed during KOH activation above 800 °C by Hu and Srinivasan<sup>38</sup> and Hayashi et al.<sup>32</sup>.

During H<sub>3</sub>PO<sub>4</sub> and ZnCl<sub>2</sub> activation, at a certain temperature level, carbon shrinkage occurs leading to decreases in surface areas and pore volumes; this was observed above 500–600 °C by Ahmadpour and Do<sup>31</sup>, Teng et al.<sup>37</sup>, Hayashi et al.<sup>32</sup> and Fierro et al.<sup>40</sup> On the other hand, with increasing temperature, a decrease of functional surface groups was observed.<sup>40</sup>

### 3.1.5. Gas flow rate

Nitrogen is the gas most commonly used in chemical activation. However, there are few studies about the role of nitrogen during chemical activation. Lillo-Ródenas et al.<sup>30</sup> compared chemical activation with NaOH in a nitrogen, carbon dioxide and steam atmosphere and varied also the flow rate. They showed that there was no porosity developed when carbon dioxide was used and that the surface areas of AC produced in a steam atmosphere were lower compared to AC generated in a nitrogen atmosphere. AC produced at a 500 mL min<sup>-1</sup> STP nitrogen flow showed much higher BET surface areas compared to AC made at lower flow rates (100 and 40 mL min<sup>-1</sup>). This indicated that nitrogen flow plays an important role during chemical activation. While carbon dioxide is not suitable for chemical activation, steam could be alternatively used; however, using nitrogen results in higher pore volumes.

### 3.1.6. Carbonisation time

Usual activation times range from 1 to 3 hours. In this range, comparably low effects of activation time were observed. For KOH and H<sub>3</sub>PO<sub>4</sub> activation, there was a slight increase in BET surface area and pore volume with increasing carbonization time<sup>31,37,41</sup>. For ZnCl<sub>2</sub> activation, however, a slightly negative effect on BET surface area and micropore volume was observed by Ahmadpour and Do.<sup>31</sup>

### 3.1.7. Type of precursor and material pre-treatment

As precursors for activation, coal, peat, different types of biomass or biochars are used. Since the type of precursor plays an important role on AC characteristics, mixture of different materials<sup>42</sup> or pre-treatments of the raw materials can be used to tailor AC porosity. For instance, acid pre-

treatment is used to reduce the mineral content of the precursor<sup>31,40</sup>. However, Ahmadpour and Do<sup>31</sup> found only a negligible effect of acid pre-treatment during KOH or ZnCl<sub>2</sub> activation of coal. Fierro et al.<sup>40</sup> showed that minerals had a positive effect on the activation of lignin with H<sub>3</sub>PO<sub>4</sub> and AC from untreated lignin exhibited higher pore volumes and better methylene blue adsorption compared to AC from sulphuric acid pre-treated lignin.

Several authors pyrolysed the raw material prior to activation by heating it in an inert gas atmosphere in a conventional device<sup>39,43</sup> or using microwave ovens.<sup>42,44</sup> Nevertheless, HTC is considered to be a more suitable pre-treatment for activation compared to conventional pyrolysis. Since it uses lower temperatures, hydrochars exhibit a lower degree of aromatisation, a higher oxygen content and are more reactive. Hydrothermal treatment increases the content of oxygenated functional groups (OFG) contributing to adsorptive characteristics of AC<sup>9,11</sup> and increasing the chemical reactivity. Therefore, activation works effectively used hydrochars as precursors.<sup>4,8</sup> Table 2 lists some publications where hydrochars were used as precursors for AC production. As can be seen in this table, first publications were released in 2011 and the amount of studies focusing on HTC activation routes have increased from 2013.

Functionalities and pore structure of AC can be controlled by HTC and activation parameters. The following paragraphs abstract the literature available on HTC and its most important reaction parameters.

**Table 2.** Previous studies available on activation pathways based on hydrochar as precursor.

Feedstock	HTC conditions	Activation conditions	Reference
Glucose	190 °C, 4 h	KOH 4:1, 600 °C, 2 h, N <sub>2</sub>	45
Walnut shell, sunflower stem, olive stone	220 °C, 20 h	CO <sub>2</sub> , 850 °C, 30 min Air, 250 °C, 30 min	8
Hazelnut shell	250 °C, 7.5 h, citric acid addition	KOH 4:1, 600 °C, 2 h, N <sub>2</sub>	9
Glucose, cellulose, rye straw	180–240 °C	KOH 3:1, 750 °C, 2 h, N <sub>2</sub>	4
Spruce, corncob	200 °C, 24 h	KOH 4:1, 700 °C, 1 h	5
Grass cuttings, horse manure, beer waste, bio-sludge	Purchased	CO <sub>2</sub> , 800 °C, 2 h	7
Glucoseamine in the presence of graphene oxide	180 °C, 12 h, pH 11, NaOH	KOH 2:1, 600 °C, 4 h, N <sub>2</sub>	6
Coconut shells	200 °C, 20 min, H <sub>2</sub> O <sub>2</sub> addition	CO <sub>2</sub> , 800 °C, 2h	46
Coconut shell	200–350 °C, 20 min, ZnCl <sub>2</sub> addition	ZnCl <sub>2</sub> , 1:1, 2:1, 3:1, 800 °C, N <sub>2</sub> , CO <sub>2</sub>	47

## 4. Hydrothermal carbonisation

In recent years, HTC has widely been investigated. In contrast to other coalification processes, such as dry pyrolysis, during HTC the raw material must be submerged in water and hence, no pre-drying step is required. This offers the possibility of the use of a new range of feedstock, such as sewage sludge, wet agricultural residues or digestate<sup>48</sup>. Most of the research focuses on the application of hydrochars as an alternative energy carrier or as soil ameliorant. Table 3 shows a summary of the existing literature about HTC and the corresponding aim of study. Even if research about the application of HTC is still in progress, it is not a new technology. It was already used in the beginning of the 20's century by the chemist Friedrich Bergius as a simulation process for natural coalification<sup>49</sup>. In his review from 1928, he describes how he used elevated temperatures (170 to 340 °C) to accelerate coal formation, lasting millions of years in nature. To avoid local overheating, he used water as a heat transfer medium in a pressure resistant container to exclude evaporation. As raw materials, he used cellulose, wood, turf, sugar and grass. Independently of the feedstock, the chars showed an increasing carbon content with increasing applied temperature or residence time. Chars with a similar composition to brown coal could be obtained<sup>49</sup>. Berl and Schmidt<sup>50</sup> showed that water was not only a heat transfer medium, but also an important reaction partner during the carbonisation process.

During the 20<sup>th</sup> century, many publications about pressurised heating of biomass in the presence of water were released. The aim, rather than applications of artificial coal, was to get a deeper understanding about the natural coalification. In 2007, two reviews on HTC were published suggesting the use of hydrothermal treated biomass as an alternative energy carrier to treat the CO<sub>2</sub> problem<sup>51,52</sup>. From then on, the interest in the application of HTC have increased over the years.

### 4.1. Definition of hydrothermal carbonisation

Hydrothermal carbonization (HTC) is an exothermal process increasing the degree of carbonisation of biomass; i.e., it lowers its hydrogen and oxygen content (leading to lower atomic O/C and H/C ratios). In principle, any organic material can be used as feedstock<sup>12</sup>.

HTC is performed in the presence of water at elevated temperatures (typically in a range of 180 to 250 °C) under subcritical conditions. Since the feed must be submerged with liquid water during the whole process, pressure must exceed the saturation pressure of water. According to Funke and Ziegler<sup>12</sup>, the pH should be neutral or weakly acidic, since at alkaline conditions, different reactions occur. However, some authors have also conducted HTC under alkaline conditions.<sup>6</sup>

**Table 3.** Summary of available previous studies on HTC.

Feedstock	HTC process conditions	Aim of study	Reference
Cellulose, wood, turf, sugar, grass	170–340 °C; 1–230 h	Simulation of natural coalification	49
Cellulose	150–350 °C; 6 h	Understanding the degradation of cellulose	50
Wood, lignin, cellulose	150–350 °C; 8–72 h	Comparison of artificial and natural coal	53
Biomass waste, subbituminous coal	120–390 °C; 1 min–6 months	Understanding the effect of conditions on HTC	54
Pine needles, pine cones, oak leaves, orange peels	180–250 °C; 16 h; 12.5%–50% w/v of biomass, citric acid addition	Conversion of biomass to mesoporous carbons as an alternative energy carrier	51
Cellulose	180–200 °C; 3–5 h; 20% dry mass, pH of 1.97–4.93	Application of HTC in a continuous plant	56
Mixture of Jeffrey pine and white fir	215–290 °C; 5–60 min; 12.5% w/w biomass	Assessment of the effect of temperature and time on HTC results	57
General comparative review		Comparison of HTC and dry pyrolysis	48
Loblolly pine	230 °C; 5 min; 20% w/w biomass, acetic acid/lithium chloride addition	Investigation of the effect of acetic acid and lithium chloride addition during HTC	14
Digestate from maize silage	190–270 °C; 2–10 h; citric acid addition, pH of 3, 5, and 7	Investigation of the effect of temperature, time, and pH on HTC results	58
Sugarcane bagasse	180 °C; 5–30 min; 10%–22% w/v biomass, H <sub>2</sub> SO <sub>4</sub> addition	Investigation of the effect of time, acid addition, and solid-liquid ratio on HTC outputs	59
Sewage sludge	200–220 °C; 5–7 h, citric acid addition	Feasibility study of HTC as a drying technology	60
Spent grains (draff)	185–245 °C; 1–6 h; 8.8%–16.8% w/v dry mass	Description of HTC by kinetic models	61
Wheat straw digestate	230 °C; 6 h	Comparison of HTC and dry vapothermal carbonisation	62
Agricultural residues	220 °C, then 180 °C; 4 h; 15% w/w dry matter	HTC of agricultural residues for solid fuel production	63

**Table 3 (continued)**

Sewage sludge	200 °C; 4–12 h, 85.7% w/w moisture	Conversion of sewage sludge to solid fuel	64
Empty Palm Oil Fruit Bunches (EFB)	220 °C; 4 h; 7%–32% w/w water content	HTC of EFB as energy carrier	65
Black liquor lignin	280–365 °C; 2 h; 3% w/v solid load	Study on degradation of lignin	66
Loblolly pine	200–230 °C; 1–5 min; 0.6–2.38 mm particle size	Investigation of HTC parameters: temperature, time, and particle size	67
Glucose	220 °C; 6 h; pH of 0–6, nitric acid and hydrochloric acid addition	Influence of oxidative strength and pH on HTC results	13
Wheat straw	190–245 °C; 150–570 min; citric acid addition (pH of 3, 5, and 7)	Prediction of product mass yields using severity models	68
Digestate	190–245 °C; 140–560 min; citric acid addition (pH of 3, 5, and 7)		15
Kraft lignin	240 °C; 22 h; H <sub>2</sub> SO <sub>4</sub> and FeCl <sub>2</sub> addition	Investigation of structural changes of lignin during HTC	69

#### 4.2. Chemical mechanisms during HTC of lignocellulosic biomass

The complex reaction mechanisms occurring during HTC are not fully understood yet. Hydrolysis, dehydration, decarboxylation, polymerisation and aromatisation are considered as the main mechanisms during HTC, forming a parallel network of different reaction paths.

Generally, hydrochar formation can be summarised as follows: biomass components are hydrolysed to oligomers and monomers, partly soluble in water. Solved fragments degrade further, while highly reactive intermediates, such as 5-hydroxymethylfurfural (HMF), are formed. Polymerisation of solved fragments leads to the generation of larger, water insoluble molecules forming the solid product. Parts of the raw material, which are not degraded to water solvable fragments, are also part of the hydrochar.<sup>12</sup>

Hydrolysis is the cleavage of chemical bonds, such as ether and ester bonds, by addition of water. Hydrolysis of cellulose was already described by Berl and Schmidt<sup>50</sup> during pressure heating of cotton. By cleavage of  $\beta$ -1,4-glycosidic linkages, oligosaccharides and monosaccharides are formed.

Dehydration and decarboxylation are considered as the main reasons for carbonisation of the biomass by lowering the H/C and O/C ratios. Dehydration leads to the formation of water, generally explained by the elimination of hydroxyl groups. During decarboxylation, carboxyl and carbonyl groups are degraded forming carbon dioxide and carbon

monoxide. The elimination of hydroxyl and carboxyl groups leads to unsaturated compounds, which polymerise easily to larger molecules. Polymerisation occurs mainly by condensation under the formation of water.<sup>12</sup>

Under hydrothermal conditions, aromatic structures are formed. Aromatisation is significantly temperature dependent and is enhanced by alkaline conditions. Aromatic structures are stable under hydrothermal conditions and are therefore considered as basic building blocks of hydrochars and as well as of natural coal.<sup>12</sup>

Due to the high thermal stability of aromatic structures, the effect of hydrothermal treatment decreases with the amount of aromatic structures in the biomass<sup>12</sup>. Therefore, HTC at 240–280 °C induces only small structural changes of lignin, which contains a high amount of aromatic structures<sup>66,69</sup>. Structural changes of lignin occur mainly by the cleavage of  $\beta$ -O-4 ether bonds and demethylation under the formation of radicals (see Fig. 3)<sup>69</sup>. Lignin degrades further at higher temperatures in the range from 310 to 365 °C.<sup>66</sup> Mechanisms of hydrochar formation from cellulose are described by Sevilla and Fuertes<sup>55</sup>, as shown in Fig. 4.

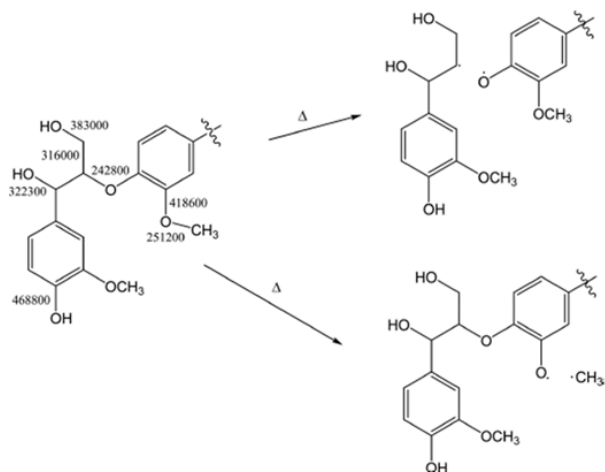


**Figure 3.** Homolysis of the C-O and O-C bonds during heat treatment of lignin.<sup>69</sup>

### 4.3. Effect of process conditions on HTC

#### 4.3.1. Temperature

Temperature is the main influencing factor on HTC. Higher temperatures promote degradation and carbonisation of biomass and usually result in a decrease in solid yield, an increase in liquid and gas yields, and a higher carbon content of the solid product<sup>12,15,58,68</sup>. At temperatures above 260 °C, HTC tends to liquefaction.<sup>69,70</sup>

HTC temperature also affects AC's characteristics, if hydrochars are used as precursors. Due to partial hydrolysis of polysaccharides and lignin, hydrothermal treatment increases the amount of oxygenated functional groups (OFG) to some extent. However, if a certain level is exceeded, OFG are decomposed under formation of gaseous products and the chemical reactivity of the hydrochars is lowered<sup>5,11,47</sup>. Therefore, there is an optimal HTC temperature leading to hydrochars with a maximal OFG content, which depends on residence time, solid to liquid ratio, and biomass

composition<sup>11</sup>. Since lignin exhibits a more stable structure compared to cellulose and hemicelluloses, higher temperatures (or residence times) are required for biomass degradation if the lignin content is high. A higher solid concentration also requires higher temperatures (or residence times) to obtain same effects. For these reasons, the temperature optimum is shifted to higher temperatures, if the lignin content of the biomass or the solid to liquid ratio is increased (see Fig.5a).

Falco et al.<sup>4</sup> performed HTC trials with glucose, cellulose and rye straw prior to KOH activation, varying the HTC temperature from 180 to 280 °C. They observed that the highest BET surface area was obtained for the activated hydrochar obtained at 240 °C. Jain et al.<sup>47</sup> found an optimal HTC temperature of 275 °C for the production of ZnCl<sub>2</sub> activated carbons from coconut shell.

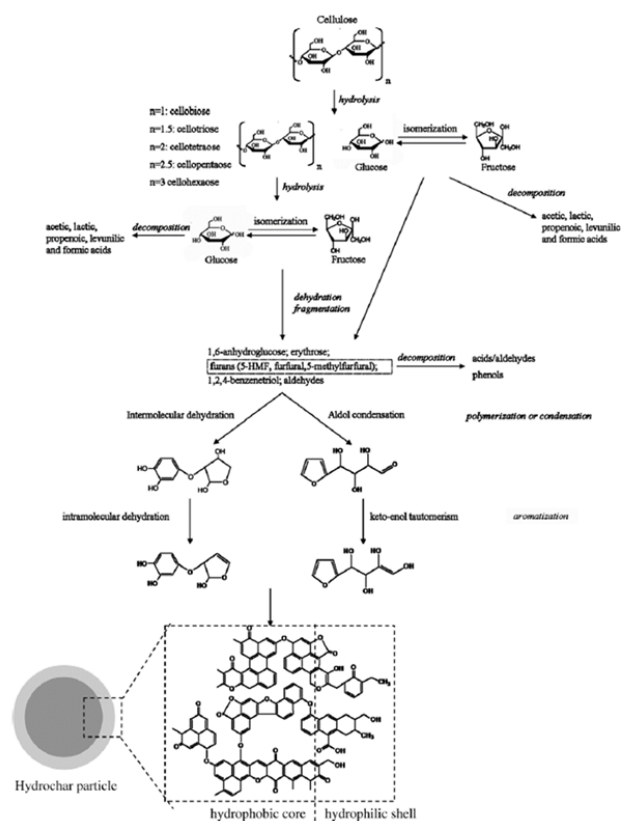


**Figure 4.** Mechanisms of formation of hydrochar particles from cellulose by HTC.<sup>55</sup>

#### 4.3.2. Residence time

Residence time is the second most important influencing factor<sup>12,15,58,68</sup>. Typically, an increase in residence time leads, like a temperature increase, to a decrease in solid yield and to a higher carbon content of the resulting hydrochar. But in some cases, an increase in the solid yield with increasing residence time was observed, probably due to ongoing polymerisation. Residence time should thus be high enough to complete hydrothermal reactions<sup>12</sup>. The effect of residence time on the amount of OFG is similar to that observed for the temperature. At lower residence times, the amount of OFG increases, due to ongoing hydrolysis. However, a further increase in the residence time could

result in an excessive dehydration/carbonisation, leading to the formation of more stable oxygen groups (ether or quinones) or decomposition of OFGs. The time where the amount of OFG is maximal depends on temperature, solid content and lignin concentration (see Fig. 5b)<sup>11</sup>; for instance, a time of 6 h was the most appropriate during HTC of sewage sludge with a moisture content of 86 % at 200 °C.<sup>64</sup>

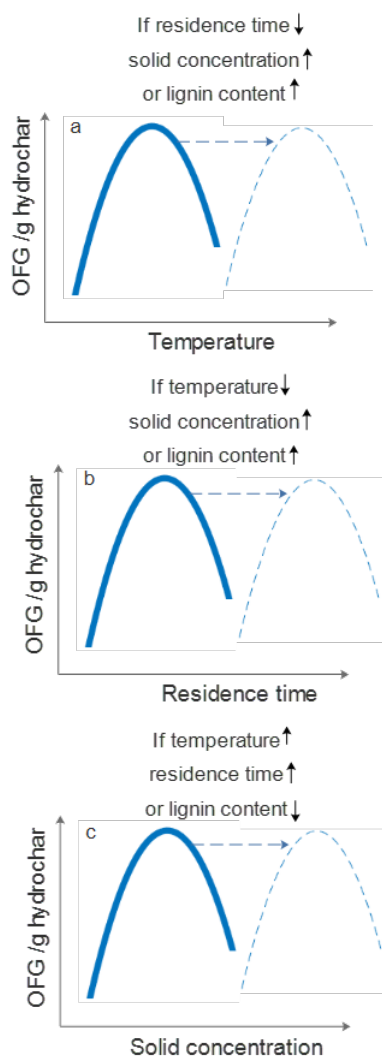


**Figure 5.** Trends of oxygenated functional groups (OFG) with temperature (a), residence time (b) and solid concentration (c).<sup>11</sup>

The effect of temperature and residence time is often described by reaction severity. The model by Ruyter describes the reaction severity  $f$  (as a function of the residence time, in s, and the absolute temperature) as shown in Eq. (8).

$$f = 50 \cdot (t)^{0.2} \cdot \exp\left(-\frac{3500}{T}\right) \quad (8)$$

The higher the reaction severity (i.e., higher temperature and/or residence time) the higher the carbon content and the lower the mass yield, within a certain temperature and time range.

### 4.3.3. Pressure

Pressure is not controlled during HTC and its influence is hardly discussed in literature. The reaction pressure influences the reaction network according to the principles of LeChatelier (i.e., with increasing pressure the reaction equilibrium shifts to solid and liquid phases and to reactants with a lower number of moles). However, the effect of pressure on HTC is low.<sup>12</sup>

### 4.3.4. Solid to liquid ratio

Funke and Ziegler<sup>12</sup> suggested to choose the solid to liquid ratio as high as possible to promote polymerisation. The solid mass must, however, be completely submerged in water during the whole process, since water is important as heat transfer medium, solvent and reactant. Chen et al.<sup>59</sup> showed that a higher solid to liquid ratio during HTC of sugar cane led to higher mass and energy yields. Sevilla and Fuertes<sup>55</sup> observed less condensed products (high O/C and H/C ratios) using higher solid loads, due to a lower extent of hydrolysis of the biomass. According to Jain et al.<sup>11</sup>, similar results can be obtained at higher solid to liquid ratio, if higher temperature or residence times are used or if the lignin content of the biomass is lower (See Fig. 5c).

### 4.3.5. Starting pH and use of catalysts

A weakly acidic environment is necessary for hydrothermal degradation. Acid formation during HTC leads to a pH drop during the reaction and to autocatalysis. Nevertheless, acid addition can enhance the reaction process and increase the degree of carbonisation, while the type of acid plays an important role<sup>12</sup>. Literature data show that acid addition prior to HTC has diverse effects. Mumme et al.<sup>58</sup> investigated the effect of citric acid addition on HTC of digestate from maize silage. Citric acid addition did not show any significant effect on carbon content, but lowered the mass yield of the solid product. Lynam et al.<sup>14</sup> observed a decrease in mass yield and an increase in higher heating value (HHV) when acetic acid was added before HTC of loblolly pine. Acetic acid addition led to a shift of reaction equilibrium, while less acetic acid was formed. Chen et al.<sup>59</sup> found a lower O/C ratio, a decreased solid mass yield and an increase in the energy enhancement factor (EEF) by sulphuric acid addition prior to HTC of sugarcane bagasse. Reiche et al.<sup>13</sup> investigated the effect of nitric acid and hydrochloric acid during HTC of glucose at pH ranges from 0 to 6. They showed that type of acid and acid concentration (starting pH) play an important role. A transition of colour from brown to black and an increase in powder density and particle size of the resulting hydrochars were observed when the pH value was decreased below 3. Above pH 3, hydrochloric acid as well as nitric acid concentration did hardly affect the carbon yield. Below pH 3, a decrease in carbon yield with increasing hydrochloric acid concentration was observed. The carbon yield decreased between pH 3 and 1.5 and increased again at pH 1 when nitric acid was added. The authors proved an oxidising effect of nitric acid at low pH ranges. Wikberg et al.<sup>69</sup> proved a promotion of lignin degradation by sulphuric acid addition. The formed hydrochars showed a higher thermal stability when sulphuric acid was added prior to

HTC. Moreover, Suwelack et al. observed that citric acid addition increased reaction severity of HTC of digestate, but did not have any reasonable impact on the HTC of wheat straw<sup>15,68</sup>. They applied a severity model, which includes temperature, retention time, as well as citric acid addition (see Eq. 9):

$$f = \exp\left(\frac{X - X_{ref}}{\lambda X_{ref}}\right) \cdot \exp\left(\frac{T_p - T_{p,ref}}{\omega}\right) \cdot d_R \quad (9)$$

where  $X$  and  $X_{ref}$  are the initial and reference concentrations, respectively, of citric acid (in mass fraction).  $T_p$  and  $T_{p,ref}$  are the process and reference temperatures, respectively;  $d_R$  corresponds to the retention time, whereas both  $\lambda$  and  $\omega$  are model parameters, which depend on the biomass feedstock. The severity model is suitable to predict gas, liquid and solid yield of HTC and degree of carbonisation of the hydrochar. For every type of feedstock, experiments are necessary to estimate the value of the model parameters  $\lambda$  and  $\omega$ . Besides temperature, time and pH, other parameters are not considered in severity models yet.

Apart from acids, other catalysts can be used to enhance HTC. A decreased mass yield and increased HHV was found after HTC of loblolly pine when lithium chloride was added. The effect was higher when it was added in combination with acetic acid. LiCl reduces the reaction pressure improving safety and lowering costs of the operation<sup>14</sup>. Some authors used iron or zinc salts, such as  $\text{Fe}(\text{NH}_4)_2(\text{SO}_4)_2$ ,  $\text{Fe}_2\text{O}_3$ ,  $\text{FeCl}_2$  or  $\text{ZnCl}_2$  to improve dehydration during HTC. Using  $\text{Fe}_2\text{O}_3$ , BET surface areas of  $400 \text{ m}^2 \text{ g}^{-1}$  for hydrochars from starch could be obtained<sup>11</sup>. Wikberg et al.<sup>69</sup> showed that  $\text{FeCl}_2$  had only slight effects on HTC catalysis of lignin. Higher contents of oxygenated functional groups (OFG) could be obtained when  $\text{ZnCl}_2$ <sup>47</sup> or  $\text{H}_2\text{O}_2$ <sup>46</sup> were used during HTC, which resulted in an efficient activation and higher porosity of the hydrochar-derived ACs.

#### 4.3.6. Particle size of feedstock

A feedstock with a lower particle size exhibits larger surface areas, theoretically enhancing chemical and physical processes. Yan et al.<sup>67</sup> showed that a smaller particle size promoted HTC of loblolly pine, although the effect was relatively low over the particle size range investigated.

#### 4.3.7. Technical aspects

HTC is performed in pressure resistant containers usually equipped with a temperature and pressure sensor, sometimes additionally with a stirring unit<sup>14,57,58,60</sup>. In some cases, oxygen is replaced by an inert gas, such as nitrogen or helium prior to reaction<sup>14,57</sup>. For industrial applications, continuously working HTC plants have already been developed<sup>56</sup>. Technical realisation of HTC can influence reaction mechanisms. For instance, condensation reactions are enhanced by stirring the suspension during HTC.<sup>13</sup>

## 5. Conclusion

Using a digestate for the production of carbonaceous materials appears to be a very interesting option, leading to a higher product (AC) value than current applications such as fertiliser or soil conditioner. ACs can be produced from

hydrochars obtained through HTC, which is a promising conversion technology for the conversion of wet feedstock. High water content of the HTC is taken as an advantage.

The porosity of ACs derived from HTC chars are generally dominated by micropores. Chemical activation seems more promising than physical one. NaOH and KOH are promising chemical agents for achieving high surface areas, up to  $3000 \text{ m}^2 \text{ g}^{-1}$ .

The understanding of the chemical mechanisms during the production of AC and during the HTC is a complex study. The addition of catalysts during the HTC process, which improve the hydrolysis reaction mechanism, and/or the use of chemicals during hydrochar activation result in important changes in the textural properties of the resulting ACs.

## Acknowledgements

"This project has received funding from the European Union's Horizon 2020 research and innovation programme under the Marie Skłodowska-Curie grant agreement No 721991".

## References

- (1) Mao, C.; Feng, Y.; Wang, X.; Ren, G. Review on research achievements of biogas from anaerobic digestion. *Renew. Sustain. Energy Rev.* **2015**, *45*, 540–555.
- (2) Albuquerque, J. A.; La Fuente, C. de; Campoy, M.; Carrasco, L.; Nájera, I.; Baixauli, C.; Caravaca, F.; Roldán, A.; Cegarra, J.; Bernal, M. P. Agricultural use of digestate for horticultural crop production and improvement of soil properties. *European J. Agronomy* **2012**, *43*, 119–128.
- (3) Albuquerque, J. A.; La Fuente, C. de; Ferrer-Costa, A.; Carrasco, L.; Cegarra, J.; Abad, M.; Bernal, M. P. Assessment of the fertiliser potential of digestates from farm and agroindustrial residues. *Biomass Bioenergy* **2012**, *40*, 181–189.
- (4) Falco, C.; Marco-Lozar, J. P.; Salinas-Torres, D.; Morallón, E.; Cazorla-Amorós, D.; Titirici, M. M.; Lozano-Castelló, D. Tailoring the porosity of chemically activated hydrothermal carbons: Influence of the precursor and hydrothermal carbonization temperature. *Carbon* **2013**, *62*, 346–355.
- (5) Falco, C.; Sieben, J. M.; Brun, N.; Sevilla, M.; van der Maelen, T.; Morallón, E.; Cazorla-Amorós, D.; Titirici, M.-M. Hydrothermal carbons from hemicellulose-derived aqueous hydrolysis products as electrode materials for supercapacitors. *ChemSusChem* **2013**, *6*, 374–382.
- (6) Fan, X.; Yu, C.; Yang, J.; Ling, Z.; Qiu, J. Hydrothermal synthesis and activation of graphene-incorporated nitrogen-rich carbon composite for high-performance supercapacitors. *Carbon* **2014**, *70*, 130–141.

- (7) Hao, W.; Björkman, E.; Lilliestråle, M.; Hedin, N. Activated carbons prepared from hydrothermally carbonized waste biomass used as adsorbents for CO<sub>2</sub>. *Appl. Energy* **2013**, *112*, 526–532.
- (8) Román, S.; Valente Nabais, J. M.; Ledesma, B.; González, J. F.; Laginhas, C.; Titirici, M. M. Production of low-cost adsorbents with tunable surface chemistry by conjunction of hydrothermal carbonization and activation processes. *Microporous Mesoporous Mat.* **2013**, *165*, 127–133.
- (9) Unur, E. Functional nanoporous carbons from hydrothermally treated biomass for environmental purification. *Microporous Mesoporous Mat.* **2013**, *168*, 92–101.
- (10) Rodriguez Correa, C.; Bernardo, M.; Ribeiro, R. P.P.L.; Esteves, I. A.A.C.; Kruse, A. Evaluation of hydrothermal carbonization as a preliminary step for the production of functional materials from biogas digestate. *J. Anal. Appl. Pyrolysis* **2017**, *124*, 461–474.
- (11) Jain, A.; Balasubramanian, R.; Srinivasan, M. P. Hydrothermal conversion of biomass waste to activated carbon with high porosity: A review. *Chem. Eng. J.* **2016**, *283*, 789–805.
- (12) Funke, A.; Ziegler, F. Hydrothermal carbonization of biomass: A summary and discussion of chemical mechanisms for process engineering. *Biofuels, Bioprod. Bioref.* **2010**, *4*, 160–177.
- (13) Reiche, S.; Kowalew, N.; Schlögl, R. Influence of synthesis pH and oxidative strength of the catalyzing acid on the morphology and chemical structure of hydrothermal carbon. *Chemphyschem* **2015**, *16*, 579–587.
- (14) Lynam, J. G.; Coronella, C. J.; Yan, W.; Reza, M. T.; Vasquez, V. R. Acetic acid and lithium chloride effects on hydrothermal carbonization of lignocellulosic biomass. *Bioresour. Technol.* **2011**, *102*, 6192–6199.
- (15) Suwelack, K.; Wüst, D.; Zeller, M.; Kruse, A.; Krümpel, J. Hydrothermal carbonization of wheat straw—prediction of product mass yields and degree of carbonization by severity parameter. *Biomass Conv. Bioref.* **2016**, *6*, 347–354.
- (16) May-Britt Hagg; Xuezhong He. *Carbon Molecular Sieve Membranes for Gas Separation, Chapter 15*, 2011.
- (17) Qu, W.-H.; Xu, Y.-Y.; Lu, A.-H.; Zhang, X.-Q.; Li, W.-C. Converting biowaste corncob residue into high value added porous carbon for supercapacitor electrodes. *Bioresour. Technol.* **2015**, *189*, 285–291.
- (18) Wang, J.; Kaskel, S. KOH activation of carbon-based materials for energy storage. *J. Mater. Chem.* **2012**, *22*, 23710–23725.
- (19) Aygün, A.; Yenisoy-Karakaş, S.; Duman, I. Production of granular activated carbon from fruit stones and nutshells and evaluation of their physical, chemical and adsorption properties. *Microporous Mesoporous Mat.* **2003**, *66*, 189–195.
- (20) Pereira, M. F. R.; Soares, S. F.; Órfão, J. J.M.; Figueiredo, J. L. Adsorption of dyes on activated carbons: Influence of surface chemical groups. *Carbon* **2003**, *41*, 811–821.
- (21) Lowell, S. Characterization of porous solids and powders: Surface area, pore size and density. In: *Particle technology series v16*; London; Kluwer Academic: Dordrecht, 2004.
- (22) Thommes, M.; Kaneko, K.; Neimark, A. V.; Olivier, J. P.; Rodriguez-Reinoso, F.; Rouquerol, J.; Sing, K. S.W. Physisorption of gases, with special reference to the evaluation of surface area and pore size distribution (IUPAC Technical Report). *Pure Appl. Chem.* **2015**, *87*, 160.
- (23) Quantachrome Instruments. Powder Tech Note 35: Micropore size analysis of porous carbons using CO<sub>2</sub> adsorption at 273.15 K (0 °C), Boynton Beach, USA. 2010.
- (24) Quantachrome Instruments. autosorb iQ Brochure: Characterization Porous Materials and Powders: Autosorb iQ and ASIqwin. Gas sorption system operation manual Version 2.0, Boynton Beach, USA. 2009–2011.
- (25) Suhas; Carrott, P. J. M.; Ribeiro Carrott, M. M. L. Lignin—from natural adsorbent to activated carbon: A review. *Bioresour. Technol.* **2007**, *98*, 2301–2312.
- (26) Oh, G. H.; Park, C. R. Preparation and characteristics of rice-straw-based porous carbons with high adsorption capacity. *Fuel* **2002**, *81*, 327–336.
- (27) Boehm, H.P. Surface oxides on carbon and their analysis: A critical assessment. *Carbon* **2002**, *40*, 145–149.
- (28) Goertzen, S. L.; Thériault, K. D.; Oickle, A. M.; Tarasuk, A. C.; Andreas, H. A. Standardization of the Boehm titration. Part I. CO<sub>2</sub> expulsion and endpoint determination. *Carbon* **2010**, *48*, 1252–1261.
- (29) Alcañiz-Monge, J.; Illán-Gómez, M. J. Insight into hydroxides-activated coals: Chemical or physical activation? *J. Colloid Interface Sci.* **2008**, *318*, 35–41.
- (30) Lillo-Ródenas, M.A.; Cazorla-Amorós, D.; Linares-Solano, A. Understanding chemical reactions between carbons and NaOH and KOH. *Carbon* **2003**, *41*, 267–275.
- (31) Ahmadpour, A.; Do, D. D. The preparation of active carbons from coal by chemical and physical activation. *Carbon* **1996**, *34*, 471–479.
- (32) Hayashi, J.; Kazehaya, A.; Muroyama, K.; Watkinson, A.P. Preparation of activated carbon from lignin by chemical activation. *Carbon* **2000**, *38*, 1873–1878.
- (33) Maciá-Agulló, J. A.; Moore, B. C.; Cazorla-Amorós, D.; Linares-Solano, A. Activation of coal tar pitch carbon fibres: Physical activation vs. chemical activation. *Carbon* **2004**, *42*, 1367–1370.
- (34) Otowa, T. Activation Mechanism, Surface Properties and Adsorption Characteristics of KOH Activated High Surface Area Carbon. In: *Fundamentals of Adsorption: Proceedings of the Fifth International Conference on Fundamentals of Adsorption*, 1996, p. 709–716.

- (35) Lillo-Ródenas, M. A.; Juan-Juan, J.; Cazorla-Amorós, D.; Linares-Solano, A. About reactions occurring during chemical activation with hydroxides. *Carbon* **2004**, *42*, 1371–1375.
- (36) Stavropoulos, G. G. Precursor materials suitability for super activated carbons production. *Fuel Proces. Technol.* **2005**, *86*, 1165–1173.
- (37) Teng, H.; Yeh, T.-S.; Hsu, L.-Y. Preparation of activated carbon from bituminous coal with phosphoric acid activation. *Carbon* **1998**, *36*, 1387–1395.
- (38) Hu, Z.; Srinivasan, M.P. Preparation of high-surface-area activated carbons from coconut shell. *Microporous Mesoporous Mat.* **1999**, *27*, 11–18.
- (39) Khezami, L.; Chetouani, A.; Taouk, B.; Capart, R. Production and characterisation of activated carbon from wood components in powder: Cellulose, lignin, xylan. *Powder Technol.* **2005**, *157*, 48–56.
- (40) Fierro, V.; Torné-Fernández, V.; Celzard, A.; Montané, D. Influence of the demineralisation on the chemical activation of Kraft lignin with orthophosphoric acid. *J. Hazardous Mat.* **2007**, *149*, 126–133.
- (41) Sudaryanto, Y.; Hartono, S. B.; Irawaty, W.; Hindarso, H.; Ismadji, S. High surface area activated carbon prepared from cassava peel by chemical activation. *Bioresour. Technol.* **2006**, *97*, 734–739.
- (42) Tiryaki, B.; Yagmur, E.; Banford, A.; Aktas, Z. Comparison of activated carbon produced from natural biomass and equivalent chemical compositions. *J. Anal. Appl. Pyrolysis* **2014**, *105*, 276–283.
- (43) Hameed, B. H.; Din, A. T. M.; Ahmad, A. L. Adsorption of methylene blue onto bamboo-based activated carbon: Kinetics and equilibrium studies. *J. Hazardous Mat.* **2007**, *141*, 819–825.
- (44) Yagmur, E.; Ozmak, M.; Aktas, Z. A novel method for production of activated carbon from waste tea by chemical activation with microwave energy. *Fuel* **2008**, *87*, 3278–3285.
- (45) Li, M.; Li, W.; Liu, S. Hydrothermal synthesis, characterization, and KOH activation of carbon spheres from glucose. *Carbohydrate Res.* **2011**, *346*, 999–1004.
- (46) Jain, A.; Balasubramanian, R.; Srinivasan, M. P. Production of high surface area mesoporous activated carbons from waste biomass using hydrogen peroxide-mediated hydrothermal treatment for adsorption applications. *Chem. Eng. J.* **2015**, *273*, 622–629.
- (47) Jain, A.; Balasubramanian, R.; Srinivasan, M. P. Tuning hydrochar properties for enhanced mesopore development in activated carbon by hydrothermal carbonization. *Microporous Mesoporous Mat.* **2015**, *203*, 178–185.
- (48) Libra, J. A.; Ro, K. S.; Kammann, C.; Funke, A.; Berge, N. D.; Neubauer, Y.; Titirici, M.-M.; Fühner, C.; Bens, O.; Kern, J. *et al.* Hydrothermal carbonization of biomass residuals: A comparative review of the chemistry, processes and applications of wet and dry pyrolysis. *Biofuels* **2014**, *2*, 71–106.
- (49) Bergius, F. Beitrge zur Theorie der Kohleentstehung. *Naturwissenschaften* **1928**, *16*, 104.
- (50) Berl, E.; Schmidt, A. Über das Verhalten der Cellulose bei der Druckerhitzung mit Wasser. *Justus Liebig's Ann. Chem.* **1928**, *461*, 192–220.
- (51) Titirici, M. M.; Thomas, A.; Yu, S.-H.; Müller, J.-O.; Antonietti, M. A Direct Synthesis of Mesoporous Carbons with Bicontinuous Pore Morphology from Crude Plant Material by Hydrothermal Carbonization. *Chem. Mater.* **2007**, *19*, 4205–4212.
- (52) Titirici, M.-M.; Thomas, A.; Antonietti, M. Back in the black: Hydrothermal carbonization of plant material as an efficient chemical process to treat the CO<sub>2</sub> problem? *New J. Chem.* **2007**, *31*, 787.
- (53) Tsukashima, H. The Infrared Spectra of Artificial Coal made from Submerged Wood at Uozu, Toyama Prefecture, Japan. *BCSJ* **1966**, *39*, 460–465.
- (54) Ruyter, H. P. Coalification model. *Fuel* **1982**, *61*, 1182–1187.
- (55) Sevilla, M.; Fuertes, A. B. The production of carbon materials by hydrothermal carbonization of cellulose. *Carbon* **2009**, *47*, 2281–2289.
- (56) Buttman, M. Klimafreundliche Kohle durch Hydrothermale Karbonisierung von Biomasse. *Chemie Ingenieur Technik* **2011**, *83*, 1890–1896.
- (57) Hoekman, S. K.; Broch, A.; Robbins, C. Hydrothermal Carbonization (HTC) of Lignocellulosic Biomass. *Energy Fuels* **2011**, *25*, 1802–1810.
- (58) Mumme, J.; Eckervogt, L.; Pielert, J.; Diakité, M.; Rupp, F.; Kern, J. Hydrothermal carbonization of anaerobically digested maize silage. *Bioresour. Technol.* **2011**, *102*, 9255–9260.
- (59) Chen, W.-H.; Ye, S.-C.; Sheen, H.-K. Hydrothermal carbonization of sugarcane bagasse via wet torrefaction in association with microwave heating. *Bioresour. Technol.* **2012**, *118*, 195–203.
- (60) Escala, M.; Zumbühl, T.; Koller, C.; Junge, R.; Krebs, R. Hydrothermal Carbonization as an Energy-Efficient Alternative to Established Drying Technologies for Sewage Sludge: A Feasibility Study on a Laboratory Scale. *Energy Fuels* **2012**, *27*, 454–460.
- (61) Kruse, A.; Badoux, F.; Grandl, R.; Wüst, D. Hydrothermale Karbonisierung: 2. Kinetik der Biertreber-Umwandlung. *Chemie Ingenieur Technik* **2012**, *84*, 509–512.
- (62) Funke, A.; Reeb, F.; Kruse, A. Experimental comparison of hydrothermal and vapothermal carbonization. *Fuel Proces. Technol.* **2013**, *115*, 261–269.
- (63) Oliveira, I.; Blöhse, D.; Ramke, H.-G. Hydrothermal carbonization of agricultural residues. *Bioresour. Technol.* **2013**, *142*, 138–146.

- 
- (64) He, C.; Giannis, A.; Wang, J.-Y. Conversion of sewage sludge to clean solid fuel using hydrothermal carbonization: Hydrochar fuel characteristics and combustion behavior. *Appl. Energy* **2013**, *111*, 257–266.
- (65) Stemann, J.; Erlach, B.; Ziegler, F. Hydrothermal Carbonisation of Empty Palm Oil Fruit Bunches: Laboratory Trials, Plant Simulation, Carbon Avoidance, and Economic Feasibility. *Waste Biomass Valor.* **2013**, *4*, 441–454.
- (66) Hu, J.; Shen, D.; Wu, S.; Zhang, H.; Xiao, R. Effect of temperature on structure evolution in char from hydrothermal degradation of lignin. *J. Anal. Appl. Pyrolysis* **2014**, *106*, 118–124.
- (67) Yan, W.; Hoekman, S. K.; Broch, A.; Coronella, C. J. Effect of hydrothermal carbonization reaction parameters on the properties of hydrochar and pellets. *Environ. Prog. Sustain. Energy* **2014**, *33*, 676–680.
- (68) Suwelack, K. U.; Wüst, D.; Fleischmann, P.; Kruse, A. Prediction of gaseous, liquid and solid mass yields from hydrothermal carbonization of biogas digestate by severity parameter. *Biomass Conv. Bioref.* **2016**, *6*, 151–160.
- (69) Wikberg, H.; Ohra-aho, T.; Pileidis, F.; Titirici, M.-M. Structural and Morphological Changes in Kraft Lignin during Hydrothermal Carbonization. *ACS Sustain. Chem. Eng.* **2015**, *3*, 2737–2745.
- (70) Akhtar, J.; Amin, N. A. S. A review on process conditions for optimum bio-oil yield in hydrothermal liquefaction of biomass. *Renewable and Sustainable Energy Rev.* **2011**, *15*, 1615–1624.
-

## Refined biocarbons for gas adsorption and separation

Sabina A. Nicolae<sup>a</sup>, Xia Wang<sup>b</sup>, Niklas Hedin<sup>b</sup>, Maria-Magdalena Titirici<sup>a</sup>

<sup>a</sup> *School of Engineering and Material Science, Queen Mary University of London, Mile End Road, London E1 4NS, UK*

<sup>b</sup> *Department of Material and Environmental Chemistry, Stockholm University, SE-106 91 Stockholm, Sweden*

### Abstract

Nowadays challenges presented by the growing population and excessive consumption of fossil fuels can be overcome by developments of renewable and green technologies for energy production and storage, air depollution and water treatment. For diminution of gaseous pollutants CO<sub>2</sub>, CH<sub>4</sub>, and H<sub>2</sub>S; adsorption processes are in several cases bringing both economic and environment advantages, over other technologies. Zeolites and porous carbon materials are the most popular adsorbents studied for gas capture. Porous carbon materials are studied and used because of affordability, availability, high hydrophobicity, and reusability. They have been popular in applications since long time. The first recorded case dates back to 3750 BC, when Egyptians and Sumerians used wood char for the reduction of copper, zinc and tin ores in the manufacture of bronze. Later on, around 1550 BC, the Egyptians used such carbon materials for medicinal purposes. Present day applications use porous carbons for environmental remediation, gas storage, catalysis and energy storage.

### 1. Introduction

Climate change is a matter of great concern and primarily related to the increasing concentration of CO<sub>2</sub> in the atmosphere, contributing to the global warming. Studies have shown that an increase in the global average temperature with more than 2 °C, above preindustrial levels, poses severe risks for ecosystems, human health and overall well-being.<sup>1</sup> CO<sub>2</sub> absorbs and emits infrared radiation at its two infrared-active vibrational frequencies and contributes to surface warming in the lower part of the atmosphere and cooling in the upper part. The increased CO<sub>2</sub> concentration does not only influence the global surface temperature, but in turn, the increased global temperature also contributes to increase the very concentrations of CO<sub>2</sub> in the atmosphere. As stated in IPCC's Third Assessment Report,<sup>2</sup> human activities, like deforestation, combustion of fossil fuels, biomass burning, and cement production represent the main cause of global warming, since 1950. Several other gases are also important for the enhanced greenhouse effect.

Another important aspect of a more sustainable world is to counteract air pollution. Civilizations have always been accompanied by a degree of air pollution. It started from prehistoric times when people created the first fires. It has been described that "soot" was found on ceilings of prehistoric caves and related to inadequate ventilation of open fires.<sup>3</sup> Nowadays, major sources of air pollution come from emissions from motor vehicles, power plants, and industries. China, US, Russia, India, Mexico, and Japan are the world leaders when it comes to air pollution,<sup>4</sup> and these emissions are severely reducing the average life spans of numerous humans.

The most frequent contaminants are chlorinated hydrocarbons (CHF), heavy metals, zinc, arsenic, benzene, H<sub>2</sub>S, etc. H<sub>2</sub>S has an unpleasant smell and is toxic, even in small amounts. The human nose can sense H<sub>2</sub>S at very low concentrations (0.4 ppb), and the toxicity threshold is about 10 ppm<sub>v</sub>. Apart from its toxicity, H<sub>2</sub>S is highly corrosive to piping and production facility in both gaseous and solution state; it can provoke acid rain when is oxidized to sulphur oxide (SO<sub>2</sub>), and many industrial processes (hydrogenation, ammonia synthesis, and fuel cells);

it also has a high poisoning effect on noble metal catalysts, even in very small amounts. Unfortunately, H<sub>2</sub>S is largely emitted from chemical processes, like natural gas processing and utilization, hydrodesulphurisation of crude oil, and coal chemistry.<sup>5</sup> Moreover, CO<sub>2</sub> and H<sub>2</sub>S, are the major impurities in natural refinery gases, synthesis gas for ammonia production, synthetic natural gas, and hydrogen manufacturing.<sup>6</sup>

Because of all the damages and inconvenience created by the gas emissions, many technologies have been developed for their capture and removal. The main options for reducing CO<sub>2</sub> emissions are: (i) increasing efficiency to reduce energy consumption; (ii) reducing the quantity of carbons from fuels; (iii) improving the use of nuclear and renewable energy sources; (iv) to strengthen the biological absorption capacity of forest and soils to capture CO<sub>2</sub>; and (v) to involve chemically and physically methods to capture CO<sub>2</sub>.<sup>7</sup>

With respect to the technologies for H<sub>2</sub>S removal, we can point out the following: (i) absorption via conventional absorption process or membrane contactor (for the improvement of absorption performance); (ii) adsorption using porous carbon materials, metal oxides adsorbents; (iii) conversion via *Claus process* (conversion of gaseous H<sub>2</sub>S into elemental sulphur), selective catalytic oxidation, liquid redox sulphur recovery; and (iv) catalytic membrane reactor via H<sub>2</sub>S decomposition into H<sub>2</sub> and S, H<sub>2</sub>S desulfurisation.<sup>8</sup>

Among all the methodologies mentioned above for both CO<sub>2</sub> and H<sub>2</sub>S removal, adsorption is either highly promising (CO<sub>2</sub> capture) or one of the most used (H<sub>2</sub>S capture). The reason for this preference can be related to some advantages such as reversibility and recyclability of the processes. The adsorbents are used usually in the form of spherical pellets, rods, monoliths or powders. Important adsorbents are: (i) oxygen-containing compounds (hydrophilic and polar, including materials such as silica gel and zeolites); (ii) carbon-based compounds (hydrophobic and non-polar), including materials such as activated carbon (AC) and graphite; (iii) amine modified materials; and (iv) polymer based compounds (polar and non-polar functional groups in a porous polymer matrix).<sup>9</sup>

There are clear evidence of a long history of use of AC, but the exact time and date for the first use has not been determined. The Ancient Egyptians mentioned the charcoal in a papyrus

from 1550 BC as a way to adsorb unpleasant odours, and in 400 BC, the Old Hindus and Phoenicians had started using charcoal to clean water, because of its antiseptic properties. The earliest time in which active carbon was mentioned as an adsorptive material was in 1773, when Scheele reported experiments with gases. In 1862, Frederick Lipscombe introduced AC for commercial applications, by using the material to purify potable water, and in 1881 Heinrich Kayser mentioned the ability of charcoal to uptake gases. AC was implemented at industrial scale in the beginning of twentieth century, by *Chemische Werke* and, during the First World War, it was used in gas masks works by American soldiers to protect them from poison gas. Today, the applications of ACs are on the rise and they are being used in numerous applications in medicine, water cleaning, gas cleaning, etc.<sup>10</sup>

## 2. Present technologies for gas capture

### 2.1. Carbon dioxide chemistry

CO<sub>2</sub> is a non-polar, colorless and odorless gas (at low concentration) with a density about 60% higher than that of dry air. It is relatively nontoxic and noncombustible, and C is double bonded to O. The C=O bonds are equivalent and its length is 1.163 Å (0.1163 nm). As mentioned, it has two IR active bands: an antisymmetric stretching mode at 2350 cm<sup>-1</sup> and a degenerate pair of bending modes at 667 cm<sup>-1</sup>.<sup>11</sup> The two equal electric dipoles in CO<sub>2</sub> molecular fall on the same line and are oppositely directed, so the total dipole moment of CO<sub>2</sub> is zero. However, because of the strong and oppositely directed dipole moments, the CO<sub>2</sub> molecule has a strong electric quadrupole moment, which interacts with electrical field gradients on porous materials allowing the gas molecule to adsorb on pore surfaces.<sup>12</sup> Other flue gas components such as N<sub>2</sub>, H<sub>2</sub>, O<sub>2</sub> and methane have either zero (methane) or much smaller quadrupole moments, which then give them less tendencies to adsorption.<sup>13</sup> Table 1 provides some physical properties of CO<sub>2</sub>.<sup>14,15</sup>

**Table 1.** Physical properties of CO<sub>2</sub>

Physical Properties of CO <sub>2</sub>	
Molar mass	44.009 g·mol <sup>-1</sup>
Molecular shape	Linear
Kinetic diameter	0.330 nm
Critical pressure (bar)	73.9
Critical temperature (°C)	31.1
Acidity (pKa)	6.35, 10.33
Specific volume at STP	0.506 m <sup>3</sup> kg <sup>-1</sup>
Gas density at STP	1.976 kg m <sup>-3</sup>
Dynamic viscosity at STP	13.72 μN s m <sup>-2</sup>
Normal boiling point (°C)	-78.5
pH of saturated CO <sub>2</sub> solutions	3.7 at 101 kPa, 3.2 at 2370 kPa

### 2.2. Gas capture and storage techniques

Various technologies for capture and storage of CO<sub>2</sub> and H<sub>2</sub>S have been developed, which can be classified in separation with chemical/physical solvents (absorption), conversion, gas

separation/absorption membranes, and separation through adsorption.

#### 2.2.1. Separation with chemical/physical solvents (absorption)

Absorption is one of the most used techniques for treating high volume gas streams containing both H<sub>2</sub>S and CO<sub>2</sub>, and it involves the usage of many solvents, like primary, secondary or ternary amines, activators, propylene carbonate, sulfolin, etc.<sup>16</sup> However, the related scrubbing processes require high energy input and is accompanied by corrosion and solvent degradation.<sup>16</sup>

For example, H<sub>2</sub>S removal takes place in aqueous solutions of alkanolamines. These are used in columns which can be either packed or plate columns, with working temperatures for the sorption step of 35–50 °C and absolute pressures of 5–205 atm.<sup>16</sup> Regeneration is performed at an elevated temperature. Another option is to use hollow fibre membrane contactors for the scrubbing of acid gas mixtures, which can operate at reduced temperatures, between 25 and 50 °C.<sup>16</sup>

For CO<sub>2</sub> capture, the same scrubbing approach with absorption using, for example monoethanolamine (MEA), is a commonly used process.<sup>17</sup> The efficiency of this removal is based on the acidic properties of CO<sub>2</sub> and the base properties of the amine. As an effect, CO<sub>2</sub> will be absorbed from the flue gas stream and reacted with the amine in the scrubbing liquid. After the absorption, heat is applied to the absorbent liquid to release the CO<sub>2</sub> for storage and simultaneously the solvent is regenerated.<sup>18</sup> Besides the amines, there are other solvents which could be used, including sodium hydroxide (NaOH), sodium hypochlorite (NaClO), sodium or potassium carbonate (Na<sub>2</sub>CO<sub>3</sub> and K<sub>2</sub>CO<sub>3</sub>), which can be used to dissolve H<sub>2</sub>S and CO<sub>2</sub>.<sup>5</sup>

#### 2.2.2. Conversion of H<sub>2</sub>S and CO<sub>2</sub>

Both H<sub>2</sub>S and CO<sub>2</sub> can be converted into other molecules and solids. One of the most significant processes for H<sub>2</sub>S conversion is the Claus process, which was patented in 1883 by the chemist Carl Friedrich Claus. This process consists of recovering elemental sulphur by oxidation of gaseous H<sub>2</sub>S, which is found in raw natural gas, biogas, and by-product gases in refineries and other industrial processes. The process involves thermal oxidation and catalytic reaction. Because of thermodynamic limitations of this process, a few per cent of H<sub>2</sub>S remains in the treated gas stream, which is removed in a second step via selective catalytic oxidation using a fixed bed reactor.<sup>19</sup> Conversion of CO<sub>2</sub> can be performed via numerous approaches and is a very active research field and relates to the concept of CO<sub>2</sub> reduction obtaining formic acid (HCOOH), methanol (CH<sub>3</sub>OH), ethylene (C<sub>2</sub>H<sub>4</sub>), methane (CH<sub>4</sub>) and carbon monoxide.<sup>20</sup>

#### 2.2.3. Gas separation/adsorption membranes

A highly explored set of technologies for the removal of acidic gases relies on separation via polymeric membranes. Many studies have been devoted to new materials and manufacturing pathways for the development of permeable membrane, appropriate for efficient CO<sub>2</sub> and H<sub>2</sub>S separation from natural gas streams.<sup>21</sup> Despite of that focus, the technologies based on

membrane separation have some drawbacks. These drawbacks include the easiness of alteration of the separation efficiency because of different contaminants, concentration polarisation phenomena, when adsorbed gases are accumulated in the boundary layer of the membrane without diffusion and also, the balance between selectivity and permeability.<sup>22</sup>

## 2.2.4. Adsorption

### 2.2.4.1. Mechanism of adsorption

In adsorption, atoms, ions or molecules are concentrated at an interface. *Adsorbate* denotes the adsorbing molecule and *adsorbent* the material containing the interfaces, often a porous solid. When a gas mixture is contacted with an adsorbent with a high internal surface and small pores, the components adsorb at different extent. The adsorption capacity depends on the specific surface of the adsorbent and the gas-solid interactions. We distinguish physical adsorption (physisorption) from chemical adsorption (chemisorption)<sup>23</sup> with respect to the nature of the interactions.<sup>12</sup> The collections of intermolecular physical interactions grouped in the term “van der Waals interactions” are dominant in physisorption. It has a relatively low degree of specificity, taking place, initially in a monolayer and then usually in multilayer, and the process is reversible. Physical adsorption is always exothermic, and the energy involved is larger than the energy of the condensation of the molecules.<sup>23</sup> Chemisorption, on the other hand, implies that covalent bonds form between the molecules and adsorbent, which are usually much stronger than van der Waals interactions.<sup>24</sup> It is sometimes a non-reversible process. For chemisorption to take place, sometimes a significant activation energy is involved.<sup>23</sup>

Both physisorption and chemisorption are described by adsorption isotherms. They describe the pressure dependency of the amount of gas that adsorb or desorb on the adsorbent at a given temperature. Experimental adsorption and desorption isotherms present a variety of shapes and forms. But, the majority of the isotherms resulted from physical adsorption have been classified in six types, according to IUPAC (see Fig. 1).<sup>25</sup>

Type I or Langmuir isotherms describe the adsorption on microporous solids with relatively small external surfaces, for example zeolites or certain porous oxides. In this case, the amount adsorbed approaches a limiting value, governed by the accessible micropore volume. Type I(a) are usually characteristic of the adsorption on microporous materials with mainly narrow micropores (< 1nm) and type I(b) describes the adsorption on materials having wider micropores and possibly small mesopores (< 2.5nm).

Isotherms of type II are usually obtained from the physisorption of most gases on nonporous or macroporous adsorbents. Their shape is related to the multilayer adsorption, the completion of the monolayer is marked by the point B.<sup>25</sup> Type III isotherms are characteristic of nonporous or macroporous solids. The monolayer is not identifiable in this case, and the molecules tend to form clusters around the most favourable adsorption sites because of weak interactions between adsorbent and adsorbate.<sup>25</sup> The mesoporous adsorbents are described by type IV isotherms. The adsorption in mesopores is influenced by both adsorptive interactions and the interactions between the

molecules and condensed state. Type IV(a) appears when capillary condensation is accompanied by hysteresis and the pore width exceeds a certain critical width. Type IV(b) is common for closed conical and cylindrical mesopores,<sup>25</sup> with pore sizes smaller than the dimension being characteristic of the cavitation of the adsorbate in its liquid form. Type V is obtained for hydrophobic microporous and mesoporous adsorbents, and type VI describes a highly uniform nonporous surface.<sup>25</sup> Chemisorption isotherms are usually described by a plateau being formed at lower pressures than the micropore-filling plateau. The adsorption is limited in this case by the number of available sites for chemisorption. The shape of chemisorption isotherms may be similar to that of Langmuir isotherms but the related adsorption mechanisms are different.<sup>23</sup>

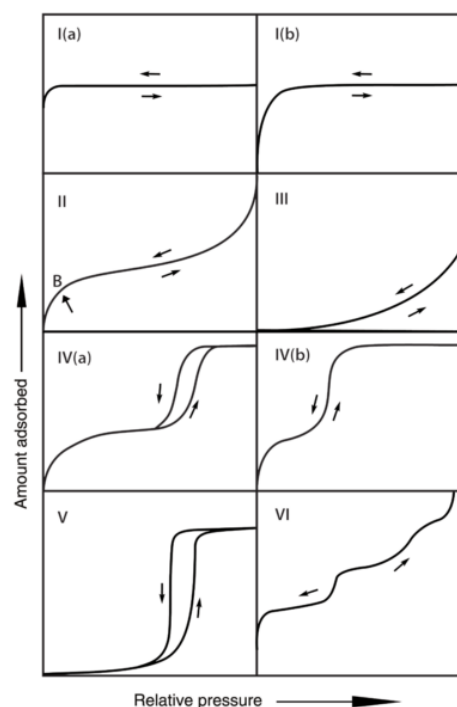


**Figure 1.** Physical adsorption isotherms according to IUPAC (reproduced from<sup>25</sup>).

### 2.2.4.2. Types of adsorbents

The sorbents used for gas separation applications are diverse and include low-temperature (< 200 °C) solid adsorbents (carbon based adsorbents, zeolite based adsorbents, metal organic frameworks, alkali metal carbonate based adsorbents, amine-based solid adsorbents); intermediate-temperature (200–400 °C) solid adsorbents (layered double hydroxides, magnesium oxide) and high-temperature (> 400 °C) solid adsorbents (calcium based adsorbents, alkali ceramic based adsorbents).<sup>26</sup>

#### Non-carbonaceous adsorbents

Zeolites are used in several industrial gas separation processes and many studies have been performed. Most of them have used as adsorbents the materials with high crystallinity and high surface area, like zeolite X, Y, and A. For example, Siriwardane *et al.*<sup>27</sup> studied the CO<sub>2</sub> adsorption capacity for zeolite 13X and 4A at 25 °C and 1 atm of CO<sub>2</sub> partial pressure, concluding that both were performing similar, with highest adsorption

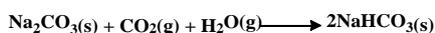
capacities of 3.64 mmol g<sup>-1</sup> for 13X and 3.07 mmol g<sup>-1</sup> for 4A. Zeolites have also been studied for H<sub>2</sub>S adsorption. Ducom et al. reported on the adsorption of H<sub>2</sub>S on zeolite 13X. In that study, 10 g of adsorbent was subjected to 80 ppm<sub>v</sub> of H<sub>2</sub>S and a capacity of 133 mg<sub>H<sub>2</sub>S</sub> g<sup>-1</sup> was observed. Hernandez *et al.*<sup>28</sup> conducted a comparative study of different adsorbents for biogas desulphurisation using Cu and Cr salts-impregnated on AC (RGM-3), zeolite 13X, Sylobead 522 and Sylobead 534 molecular sieve and two metal oxides, commercially known as ST and Sulfcatch ECN. They reported the metal-impregnated carbon as the most efficient adsorbent, followed by zeolite 13X, which performed better than the molecular sieves and the metal oxides. Certain metal organic frameworks are very good adsorbents for the adsorption of CO<sub>2</sub> at low pressures because of a strong interaction.

Metal organic frameworks (MOFs) have been reported as good adsorbents for CO<sub>2</sub><sup>29–31</sup> and desulphurisation.<sup>32,33</sup> For example, Hamon *et al.*<sup>34</sup> studied H<sub>2</sub>S adsorption on several MOFs such as MIL-53 (Al<sup>III</sup>, Cr<sup>III</sup>, Fe<sup>III</sup>), MIL-47 (V<sup>IV</sup>), MIL-100(Cr) and MIL-101(Cr). The first two materials were small-pore, about 11 Å, and the last ones were large pore, of about 25 and 30 Å. The maximum H<sub>2</sub>S uptake was obtained on MIL-101 at 30 °C and 20 bar

(38.4 mmol g<sup>-1</sup>). MIL-53 (Al, Cr), MIL-47 and MIL-100 adsorbed in between 11.8 and 16.7 mmol g<sup>-1</sup>. Yang *et al.*<sup>33</sup> studied the H<sub>2</sub>S adsorption on MIL-68(Al) at room temperature. They reported that the material was completely regenerable for five cycles, retaining about 12 mmol g<sup>-1</sup> of H<sub>2</sub>S at 30 °C and 12 bar.

Kumar *et al.*<sup>35</sup> studied the CO<sub>2</sub> adsorption on Mg-MOF-74. In this way, they reported 165 cm<sup>3</sup> g<sup>-1</sup> CO<sub>2</sub> at RTP on the pristine Mg-MOF-74, followed by a decrease once the material has been exposed to moisture. They observed that one day exposure to humidity reduced the adsorption capacity to 127 cm<sup>3</sup> g<sup>-1</sup> CO<sub>2</sub>; 7 days to about 79 cm<sup>3</sup> g<sup>-1</sup> CO<sub>2</sub> and 14 days to 53 cm<sup>3</sup> g<sup>-1</sup> CO<sub>2</sub>. Cho *et al.*<sup>36</sup> studied the adsorptive properties of Co-MOF-74 for CO<sub>2</sub>. Adsorption and desorption cycles at RTP conditions showed a positive affinity of CO<sub>2</sub> on Co-MOF-74, retaining up to 288 mg g<sup>-1</sup> of CO<sub>2</sub>. The selectivity towards CO<sub>2</sub> over N<sub>2</sub> in Co-MOF-74 was high as well (CO<sub>2</sub>:N<sub>2</sub> = 25:1); the authors concluded that CO<sub>2</sub> was more strongly adsorbed than N<sub>2</sub> because of a stronger quadrupole moment. There are countless studies on CO<sub>2</sub> adsorption on MOFs and to highlight one of them, Nandi *et al.*<sup>37</sup> reported the synthesis of a 2D Cu based ultramicroporous MOF (IISERP-MOF20), which showed moderate CO<sub>2</sub> uptake as well as CO<sub>2</sub>:N<sub>2</sub> selectivity for flue gas composition at room temperature. At 1 bar and 25 °C, IISERP-MOF20 adsorbed 3.5 mmol g<sup>-1</sup> of CO<sub>2</sub>, reaching a saturation capacity of about 9 mmol g<sup>-1</sup> at 1 bar and -78 °C.

Different studies have been performed on alkali metal carbonate-based adsorbents. Liang *et al.* and Chao *et al.*<sup>38,39</sup> studied the mechanism of the CO<sub>2</sub> capture on Na<sub>2</sub>CO<sub>3</sub>. They proposed the follow reactions:



The theoretical adsorption capacities for CO<sub>2</sub>, calculated from the first and second reaction were 9.43 and 5.66 mmol g<sup>-1</sup>, respectively. K<sub>2</sub>O<sub>3</sub>-based adsorbents behave similar to Na<sub>2</sub>CO<sub>3</sub>-based ones. However, these reactions are highly exothermic

and reversible, so the energy management is a problem to take into account in possible applications. Amine based solid adsorbents, like polymers or organic molecules containing NHx groups, showed high potential for CO<sub>2</sub> and H<sub>2</sub>S capture, because of the possibility to bind chemically with acidic molecules.<sup>40</sup>

#### Carbon based adsorbents

ACs are very popular for their adsorption properties. They present several advantages over the other adsorbents, such as: (i) the low price of the raw materials; (ii) the fact that they can be produced from coals (coal, lignite), industrial by-products (scraps of polymeric materials, petroleum) and sustainable resources (wood or biomass sources);<sup>40</sup> and (iii) their relatively high degree of microporosity and high surface areas. Usually, carbonaceous adsorbents are prepared via carbonisation from different carbon sources, like wood, coal, sugars, etc. at high temperatures. To create porosity and increase the specific surface area, activation processes can be employed. Physical activation can be conducted by partial gasification of chars with CO<sub>2</sub>, steam, air, or a mixture of them; at high temperatures (800–1000 °C). Alternatively, chemical activation, which takes place at lower temperatures and is based on the introduction of chemicals (like KOH, NaOH, K<sub>2</sub>CO<sub>3</sub>, and H<sub>3</sub>PO<sub>4</sub>) with the purpose to open the pores and create a well-developed carbons structure.<sup>41</sup> Due to all these possibilities, a lot of research studies were carried out using carbon-based adsorbents with engineered textural properties.

#### *a) CO<sub>2</sub> adsorption on ACs*

The use of ACs and other carbon-based adsorbents is also studied for potential use in CCS.<sup>42</sup> The prospect of CO<sub>2</sub> removal using specifically carbonaceous materials obtained by using through HTC of biomass as a pre-treatment step has been of a great interest for many research groups. For example, Sevilla *et al.*<sup>43</sup> reported the synthesis of highly microporous carbon materials by direct activation of glucose with potassium oxalate at high temperatures (> 800 °C) under N<sub>2</sub> flow. The micropores volume was in between 0.49 and 0.67 cm<sup>3</sup> g<sup>-1</sup> (Dubinin-Radushkevich model), and CO<sub>2</sub> uptake at 25 °C and 1 bar was about 4.5 mmol g<sup>-1</sup>. By adding small amounts of melamine, they tuned the structure more towards mesopores regime, underlined by a decrease in CO<sub>2</sub> adsorption capacities with almost 50%, maximum CO<sub>2</sub> uptake for the melamine containing samples being 2.5 mmol g<sup>-1</sup>, in the same conditions. Sevilla *et al.*<sup>44</sup> reported important adsorption capacities (both for H<sub>2</sub> and CO<sub>2</sub>) using porous carbon materials derived from three different biomass sources (starch, cellulose and sawdust) by means of hydrothermal carbonisation (HTC) and subsequent chemical activation. The high surface areas (2690–3540 m<sup>2</sup> g<sup>-1</sup>) combined with bimodal porosity in the micromesopore range led to high CO<sub>2</sub> adsorption capacities, such as 20–21 mmol g<sup>-1</sup>, at 20 bars and 25 °C. By extending the pressure range, up to 40 bars, the CO<sub>2</sub> uptake was considerably increased to 30–31 mmol g<sup>-1</sup>. Xiao *et al.*<sup>45</sup> reported adsorption capacities for CO<sub>2</sub> of about 4.7 mmol g<sup>-1</sup>, at 0 °C and 1 atm, using nitrogen-doped carbon materials obtained from glucosamine via HTC-soft templating approach. CO<sub>2</sub> adsorption was performed also by Boyjoo *et al.*,<sup>46</sup> who reported an adsorption capacity of about 5.22 mmol g<sup>-1</sup> at RTP conditions, using as adsorbents activated hydrochars produced from CocaCola™-derived wastes. The

value was even higher, at 0 °C and 1 atm, reaching about 6.27 mmol g<sup>-1</sup>. In their study, they prepared three ACs, starting from the same biomass precursor and changing either the mass ratio between the activator and hydrochar or the activation agent: (1) activation with ZnCl<sub>2</sub>, denoted as CMC\_1 and CMC\_2 (at ZnCl<sub>2</sub>/HTC carbon mass ratios of 1 and 3, respectively), and (2) activation with KOH, denoted as CMC\_3 (KOH/HTC carbon = 4). The adsorption capacities at 0 °C and 1 atm were approximately 4.8 mmol g<sup>-1</sup> for ZnCl<sub>2</sub> activated samples and 6.27 mmol g<sup>-1</sup> for KOH activated sample. Bellemare *et al.*<sup>47</sup> reported a high CO<sub>2</sub> uptake by using sucrose-derived carbon materials. The adsorbents had been synthesised by combining ice and hard templating and physical activation (via CO<sub>2</sub>). The obtained carbon materials possessed high surface areas with values ranging from 2560 and 2770 m<sup>2</sup> g<sup>-1</sup>. The micropore surface areas were calculated via the t-plot method from N<sub>2</sub> adsorption data and had values of 260–500 m<sup>2</sup> g<sup>-1</sup>. The samples exhibited a CO<sub>2</sub> uptake of 3.8 mmol g<sup>-1</sup> at 25 °C and 1 bar. Sevilla *et al.*<sup>44</sup> prepared mesoporous and microporous ACs materials containing high concentration of functional groups. The ACs have been prepared by dry chemical activation through carbonisation of biomass, (starch and gelatine), at different ratios (gelatine: starch = 1:1, 2:1, 1:2). After carbonisation, the powders were further chemically activated with KOH, at 1/4 carbon/KOH mass ratio. The materials have been characterised and tested for CO<sub>2</sub> adsorption at 0 °C and 25 °C at 1 bar, using a volumetric method. The highest CO<sub>2</sub> uptake was 7.49 mmol g<sup>-1</sup> at 0 °C and 1 bar, decreasing with approximately 50% at room temperature. Pure gelatine-derived carbon exhibited about 4.25 mmol g<sup>-1</sup> at STP conditions and 3.30 mmol g<sup>-1</sup> at 25 °C (RTP conditions). Starch-derived carbon exhibited the lowest CO<sub>2</sub> uptake among all the samples: 3.02 mmol g<sup>-1</sup> (at STP) and 2.81 mmol g<sup>-1</sup> (at RTP). The improved adsorption capacity for the gelatine-starch samples was tentatively ascribed to N-doping. Moreover, the ACs showed a good CO<sub>2</sub>/N<sub>2</sub> selectivity, up to 98/1 at 0 °C and 1 bar. The power of N-doping to enhance the adsorption capacity of ACs has though been convincingly challenged.<sup>48</sup> In another study, Yaumi *et al.*<sup>49</sup> studied the CO<sub>2</sub> capture using rice husk derived carbon materials. The authors prepared carbon adsorbents starting from rice husk by chemical activation with H<sub>3</sub>PO<sub>4</sub> and melamine, at different mass ratios of acid impregnated rice husk to melamine. The obtained carbons performed well for CO<sub>2</sub> uptake, the adsorption capacities being in between 1.08 and 4.41 mmol g<sup>-1</sup>, at 30 °C and 1 bar. The best performance was achieved for the sample impregnated with phosphoric acid at a mass ratio of 1:2, and subsequently modified with melamine at a ratio of 5:1 (rice husk containing H<sub>3</sub>PO<sub>4</sub> : melamine). An increase in melamine concentration caused a decrease in CO<sub>2</sub> sorption capacity, probably because of a high number of nitrogen species, which could block part of the pores and decrease the accessible surface area. Also, by means of chemical activation, Ello *et al.*<sup>50</sup> prepared activated biocarbons with high surface area and adsorption capacity towards CO<sub>2</sub>. They used *Arundo donax* or giant cane as carbon precursor and KOH as chemical activator. The dried material was crushed and sieved into fine particles and mixed with KOH. To optimise the effect of activation, different KOH/biomass mass ratios were used. Subsequently, the mixtures were calcined at 600 °C, for 2h, under N<sub>2</sub> flow. The surface area and

pore volume were highly influenced by the amount of activating agent. When the amount of KOH was increased, both surface area and pore volume increased up to 1122 m<sup>2</sup> g<sup>-1</sup> and 0.59 cm<sup>3</sup> g<sup>-1</sup>, respectively. By increasing further the amount of activating agent, the textural properties were affected, decreasing up to 849 m<sup>2</sup> g<sup>-1</sup> and 0.5 cm<sup>3</sup> g<sup>-1</sup>, respectively; probably because of the over-oxidation phenomenon of carbon walls with the generated CO<sub>2</sub> and CO gases from the activating agent, and formation of insoluble potassium residues or minerals. The ACs were tested for CO<sub>2</sub> adsorption, and the uptake values followed the same trend as the surface area. First, it increased with the KOH concentration reaching a highest CO<sub>2</sub> uptake of 6.3 mmol g<sup>-1</sup> at 0 °C and 1 bar. Further increases in the KOH concentration caused a decrease in the CO<sub>2</sub> uptake (up to 3.7 mmol g<sup>-1</sup>). The above-mentioned highest adsorption capacity was observed for the 1:2 biomass/KOH mass ratio, which had the highest surface area and micropore volume together with a flat morphology of the carbon particles. The CO<sub>2</sub> uptake at 30 bar and 0 °C was about 15.4 mmol g<sup>-1</sup>. The value obtained at STP (6.3 mmol g<sup>-1</sup>) was similar to that measured for African palm shell-based carbons,<sup>50</sup> and slightly higher than those derived from rice husk (6.2 mmol g<sup>-1</sup>),<sup>51</sup> sawdust (6.1 mmol g<sup>-1</sup>),<sup>52</sup> celtuce leaves (6.0 mmol g<sup>-1</sup>),<sup>53</sup> and wheat flour (5.7 mmol g<sup>-1</sup>).<sup>54</sup>

#### b) H<sub>2</sub>S adsorption on ACs

Considering all the harmful properties of H<sub>2</sub>S, many studies have been focused towards development of new, efficient and sustainable adsorbents for its removal.<sup>55–57</sup> Among the present technologies for desulphurisation<sup>5</sup>, removal of H<sub>2</sub>S with carbon based adsorbents has been recently reported.<sup>58–61</sup> For example, Olalere *et al.*<sup>62</sup> recently studied the H<sub>2</sub>S removal from waste water using coconut shell-based ACs. The carbon-based adsorbents were prepared by pyrolysis combined with chemical activation using KOH. The obtained powders were characterised by a porous structure composed of about 76% C and 19% O, the rest was traces of Al, Si, and K. During the adsorption experiments, the influence of initial concentration of H<sub>2</sub>S was tested. The adsorption was measured under stirring, with a gas flow starting from 100 mg L<sup>-1</sup> up to 500 mg L<sup>-1</sup>. The H<sub>2</sub>S adsorption capacity increased by increasing the initial gas concentration, varying from 2.52 to 13 mmol g<sup>-1</sup>, after 14 h contact time, using 1 g of adsorbent. Shang *et al.*<sup>63</sup> reported the adsorption of H<sub>2</sub>S on biochars derived from agricultural and forestry waste, such as camphor tree, rice hull and bamboo. The obtained adsorption capacities were smaller than those reported by Habeeb *et al.*<sup>62</sup> with values of 0.05–11.2 mmol g<sup>-1</sup>. The maximum adsorption capacity was achieved for the biochar with the higher specific surface area (115 m<sup>2</sup>/g) and the higher carbon content (rice hull, 26% C), which was expected as the number of adsorption sites for H<sub>2</sub>S increases. The experiments were performed at room temperature, using 1 g of adsorbent for each test. Mochizuki *et al.*<sup>64</sup> studied the adsorption behaviour of H<sub>2</sub>S on ACs prepared from petroleum coke by KOH chemical activation. The H<sub>2</sub>S uptake was tested at 30 °C at H<sub>2</sub>S partial pressure 0.2 kPa for different times (5, 15, 24 and 48 h). The H<sub>2</sub>S uptake increased with increasing the weight ratio of KOH-petcoke (the carbon source). The maximum adsorption capacity for H<sub>2</sub>S obtained was about 3 mmol g<sup>-1</sup>. Zhang *et al.*<sup>65</sup> reported on H<sub>2</sub>S removal with ACs prepared from black liquor.

They used a gravimetric method with a spring balance to record the mass at room temperature, 35 °C and 45°C. The gas concentration was varied from 200 to 800 ppm. It was observed that the amount of gas adsorbed decreased as the adsorption temperature was increased, consistent with the exothermal nature of adsorption.

Bagreev and Bandosz *et al.*<sup>8</sup> studied the influence of alkali compound on the carbon surface, such as NaOH and K<sub>2</sub>CO<sub>3</sub>. Their results showed an improvement in the sorption capacity for H<sub>2</sub>S. The highest uptake were observed for a moderate amount of impregnated NaOH as an excess resulted in pore blocking. Castrillon *et al.*<sup>57</sup> also studied the influence of carbon modified with caustic materials and iron oxide (Fe<sub>2</sub>O<sub>3</sub> for CO<sub>2</sub> and H<sub>2</sub>S removal from CH<sub>4</sub> streams). Several studies were dedicated to proving the benefits on sorption capacity for H<sub>2</sub>S when combining physical adsorption with a preceding chemical reaction. Based on the same idea, Fe<sub>2</sub>O<sub>3</sub> was reported as an able inorganic compound for the removal of H<sub>2</sub>S. Since H<sub>2</sub>S is a diprotic acid, it might react with impregnated surfaces, according to the following reactions:

- Impregnation with NaOH<sup>55</sup>  

$$\text{H}_2\text{S} + \text{NaOH} \longrightarrow \text{NaHS} + \text{H}_2\text{O} \quad (1)$$

$$\text{H}_2\text{S} + 2\text{NaOH} \longrightarrow \text{Na}_2\text{S} + 2\text{H}_2\text{O} \quad (1a)$$
- Impregnation with K<sub>2</sub>CO<sub>3</sub><sup>66</sup>  

$$\text{H}_2\text{S} + \text{K}_2\text{CO}_3 \longrightarrow \text{KHS} + \text{KHCO}_3 \quad (2)$$

$$\text{H}_2\text{S} + \text{K}_2\text{CO}_3 \longrightarrow \text{K}_2\text{S} + \text{H}_2\text{CO}_3 \quad (2a)$$
- Impregnation with Fe<sub>2</sub>O<sub>3</sub><sup>61</sup>  

$$\text{Fe}_2\text{O}_3 + \text{H}_2\text{S} \longrightarrow \text{FeS} + \text{Fe}_2\text{O}_3 \quad (3)$$

$$\text{Fe}_2\text{O}_3 + 3\text{H}_2\text{S} \longrightarrow \text{Fe}_2\text{S}_3 + 3\text{H}_2\text{O} \quad (3a)$$

$$2\text{Fe}_2\text{O}_3 + 3\text{O}_2 \longrightarrow 2\text{Fe}_2\text{S}_3 + 6\text{S} \quad (3b)$$

In the study conducted by Castrillon *et al.*<sup>57</sup>, three commercial ACs produced by Donau Carbon GmbH (Germany), with specific surface areas in the range 815–1005 m<sup>2</sup> g<sup>-1</sup>, were tested for their CO<sub>2</sub> and H<sub>2</sub>S uptake capacities. Co-adsorption of H<sub>2</sub>O and H<sub>2</sub>S enhanced the adsorption of H<sub>2</sub>S. Under dry conditions, the adsorption capacity of H<sub>2</sub>S was 8.2 mmol g<sup>-1</sup>, meanwhile under humid conditions, it was almost four times higher (30.9 mmol g<sup>-1</sup>). The CO<sub>2</sub> adsorption capacity was considerably smaller with a value of 1.67 mmol g<sup>-1</sup>.

Sethupathi *et al.*<sup>58</sup> conducted a study involving biochars as potentials adsorbents of CH<sub>4</sub>, CO<sub>2</sub> and H<sub>2</sub>S. They investigated four types of optimised biochars derived from perilla leaf, soybean stover, Korean oak and Japanese oak. When adsorbed together, CO<sub>2</sub> and H<sub>2</sub>S are competing. In order to study in more detail this competition phenomenon, the authors conducted a single-gas study for CO<sub>2</sub>, H<sub>2</sub>S and CH<sub>4</sub>. During the measurement, it was observed that without the CH<sub>4</sub> and CO<sub>2</sub>, all the biochars performed better for H<sub>2</sub>S adsorption compared to the simultaneous adsorption experiments, and a single-gas adsorption measurement for H<sub>2</sub>S revealed about 294 mg g<sup>-1</sup> adsorption capacity, which was significantly higher than that obtained in a similar study (73 mg g<sup>-1</sup>) and also higher than the adsorption capacity obtained during simultaneous tests. It was also observed that all biochars showed higher preference for H<sub>2</sub>S than CO<sub>2</sub>. This was based on that CO<sub>2</sub> adsorbs mainly through physisorption, and the mode of H<sub>2</sub>S adsorption depends on the local pH within the pores.<sup>67</sup>

All of the studies mentioned above seem to support that biomass represents a very good precursor for ACs. Beside of the advantageous of a low cost and sustainable activation processes, the availability and recyclability of carbon are environmentally sound. There are plenty resources of biomass, which can be exploited, such as wood and waste wood, leaves of the plants, agricultural waste, waste paper, garbage, and human waste. Recent articles reported that the globally food waste each year is 1.3 billion tonnes, including about 45% of all fruits and vegetables, 35% of fish and seafood, 30% of cereals, 20% of dairy products and 20% of meat. In UK, 15 million tonnes of food is wasted each year from which 4.2 million tonnes of edible food each year, meaning that a family throws away £700 worth of perfectly good food every year.<sup>68</sup> Biomass can be further processed and used in different applications, as energy storage, electrocatalysis and photocatalysis, heterogeneous catalysis, gas storage and conversion. One of the processes with the smallest ecological foot print is HTC through which the biomass can be further converted to carbon. As a general principle, HTC allows the production of coal in similar way like in nature, but in shorter time in the laboratory.

#### 2.2.4.3. Post-combustion CO<sub>2</sub> capture

In relation to the carbon materials studied for CCS (see above) it is important to reflect on the different approaches to CCS. There are mainly three different configurations of technologies applied to capture CO<sub>2</sub> from flue gas: post-combustion, pre-combustion and oxyfuel combustion.<sup>69</sup> In post-combustion CO<sub>2</sub> capture, the main challenge is to separate CO<sub>2</sub> in a dilute mixture at close to ambient pressure of mainly N<sub>2</sub>.<sup>70</sup> The emitted flue gas is typically at a temperature of 45–180 °C, a pressure close to 1 atm,<sup>71</sup> and has a partial pressure of 0.05–0.15 atm of CO<sub>2</sub>. A low temperature is typical for a modern combustion unit with effective heat integration. Fig. 2 shows a diagram of carbon capture and compression process in a coal-fired power plant.<sup>70</sup>

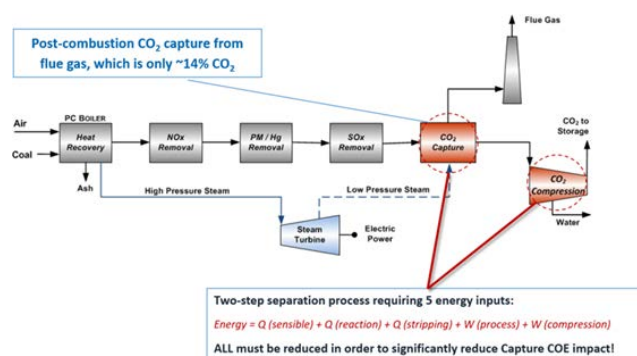


**Figure 2.** Process diagram of carbon capture and compression in a coal-fired power plant.<sup>70</sup>

In adsorption processes, adsorbents are typically granulated and put in two or more interconnected columns. In a case of two columns, the flue gas first is contacted with column 1 where the more interacting CO<sub>2</sub> is adsorbing preferably and a N<sub>2</sub> rich gas is flowing out of the column 1 outlet. When the column 1 capacity is exhausted, the flue gas stream is switched to column 2 where CO<sub>2</sub> continues to adsorb; meanwhile, the CO<sub>2</sub> in

column 1 is recovered/desorbed by either a reduced total pressure (pressure swing or vacuum swing adsorption, PSA, VSA) or by an increased temperature (temperature swing adsorption, TSA). Due to the massive flows of flue gas, it becomes critical that the PSA/VSA/TSA have much shorter cycle times than what is usual in adsorption driven technologies, which puts additional demands on the adsorbent and the structuring of the adsorbent.

Gas separation with adsorption can be either under thermodynamic control or under kinetic control, where the different diffusion rates of the different gases within the micropores can contribute to the selectivity.<sup>72</sup> Almost all commercialised PSA/VSA/TSA processes operate under equilibrium or close to equilibrium processes with notable exceptions including the purification of N<sub>2</sub> from air with carbon molecular sieves. For AC, which is a nonpolar adsorbent, the van der Waals interaction of the dispersion plays a significant role. The size and the polarizability of the adsorbate and the pore size distribution of adsorbent are influential, while the surface chemistry of the adsorbent is less important. According to the International Union of Pure and Applied Chemistry (IUPAC),<sup>72,73</sup> the pore size classification is shown in Tab. 2. So, if the flue gas is not to be compressed it will be the effective uptake capacity of the ACs in the domain of about 0.01–0.1 bar of CO<sub>2</sub> at about

50 °C that will be important in a VSA process.

**Table 2.** The pore size classification in IUPAC

Type	Pore size (nm)
Ultramicro-pores	< 0.7
Supramicro-pores	0.7–2
Micro-pores	< 2
Meso-pores	2–50
Macro-pores	> 50
pH of saturated CO <sub>2</sub> solutions	3.7 at 101 kPa, 3.2 at 2370 kPa

### 3. Carbon materials and HTC

This section describes several synthetic routes used to get a well-defined porosity in hydrothermal carbons. Different methods to create and develop porosity based on the usage of structure-directing agents (organic or inorganic templates) is discussed and explained here. The methods introduced below allow customising the carbon structure via the tools of colloid and polymer science, leading to well-developed morphologies for a broad range of applications.

#### 3.1. Introduction

Porous hydrothermal carbon materials have attracted considerable attention, over the time, because of their wide range of applications. HTC is a methodology developed 100 years ago, but it is one of the most used strategies for the production of carbon materials. This method proceeds at low carbonisation temperatures (180–250 °C), and self-generated pressure; the solvent normally used is water; the particles present spherical shape and small sizes in the domain of

microns; the porosity can be changed by using natural templates or activation procedures; their chemical and physical properties can be easily changed by the combination of the carbon materials with different components, such as inorganic compounds, and they can be further functionalised because of the highly oxygenated surface of the carbons.

#### 3.2. Templating methods

One of the first attempts using templating methods to develop porous carbon materials was carried out by Gilbert *et al.*<sup>74</sup> in 1982. They synthesised porous glassy carbons by impregnation of the silica template with phenol-formaldehyde resin mixture. This methodology reflects the “hard(exo) templating” approach (Fig. 3b), and, in general, is based on the mixture of a carbon precursor (usually phenolic resins) with a hard template. In this way, the carbon precursor infiltrates in the structure of the template and is carbonised within the pores (at high temperatures, > 700 °C). Finally, the template is removed, leaving behind a well-defined structure. Later on, Dai *et al.*<sup>75</sup> developed a new strategy for creating porous carbon materials based on the self-assembly properties of block copolymers and aromatic resins, such as phloroglucinol, or resorcinol/formaldehyde. This method is known as “soft (endo) templating” and is a classical way to produce inorganic porous materials (Fig. 3a). The classical carbonisation techniques, such as pyrolysis, present many drawbacks when compared to HTC. Since HTC takes place in aqueous phase, it can be easily combined with these templating methods. The use of carbohydrates as carbon precursors together with different templates might improve textural properties. In addition, the surface chemistry of the resulting hydrothermal carbons is highly populated oxygenated groups and can be further modified.

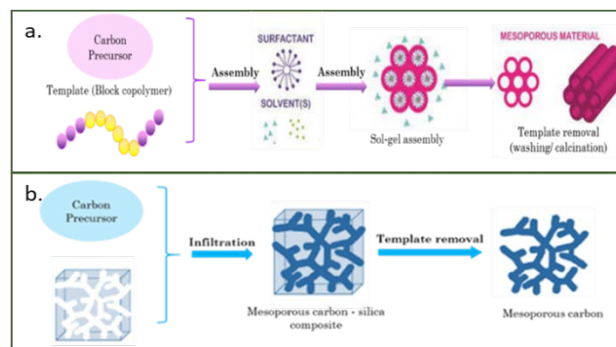


**Figure 3.** Graphical representation of the templating methods: soft templating (a), and hard templating (b).<sup>76</sup>

#### 3.2.1. Soft templated carbons and its interfacing with HTC

Nanostructured HTC-derived materials can be synthesised using polymeric templates of defined size and shape. In soft templating, an amphiphilic molecule such as a surfactant or block-copolymer is self-assembling with the carbon precursor into an organised mesophase, which is stabilised by the thermal treatment. The process is influenced by several parameters, like concentration, temperature, hydrophilic or hydrophobic reaction, pH, etc. The most common polymers used are poly(ethylene oxide)-b-poly(propylene oxide)-b-PEO from the Pluronic family,<sup>77</sup> polystyrene-b-poly(ethylene oxide)

(PS-*b*-PEO)<sup>78</sup> or polystyrene *b*-poly (4-vinylpyridine) (PS-*b*-poly (ethylene oxide)), triblockcopolymers (PEO-*b*-PPO-*b*-P4VP); carbon precursors are small clusters of phenol-formaldehyde, or “resol” or phloroglucinol-formaldehyde resins. The main reason for using resins as carbon precursor is their high number of hydroxyl groups that can form very strong hydrogen bonds with the miscible segment of the block copolymer, which creates micelles, responsible for producing mesoporosity in the resulted carbon. Liang *et al.*<sup>75</sup> prepared highly ordered porous carbon films by using block copolymers (PS-P4VP) and resorcinol. The synthesis was performed sequentially by monomer-blockcopolymer film casting, solvent annealing, polymerisation, and finally carbonisation. The highly ordered carbon film possessed a thickness from several tens of nanometers up to about 1  $\mu\text{m}$  and sizes up to 6  $\text{cm}^2$ . In another study, Tanaka *et al.*<sup>79</sup> prepared mesoporous carbon membranes using soft-templating route. They started from resorcinol, phloroglucinol and formaldehyde together with Pluronic F127 as structuring agent. The reason to use a combination of phloroglucinol-resorcinol-formaldehyde, instead of the standard mixture of resorcinol-formaldehyde, was to improve on the thermal stability and to reduce the weight loss. The resulted membrane was porous (Fig. 4c), having a surface area of  $670 \text{ m}^2 \text{ g}^{-1}$  and a pore volume of  $0.58 \text{ cm}^3 \text{ g}^{-1}$ . The average pore diameter was approximately 4 nm as estimated from BET and TEM measurements (Figs. 4a,b). The stability of the membrane was also studied. The membrane was subjected to a hydrothermal treatment at 90 °C and the structure characteristics and gas permeation of the carbon material remained unchanged.

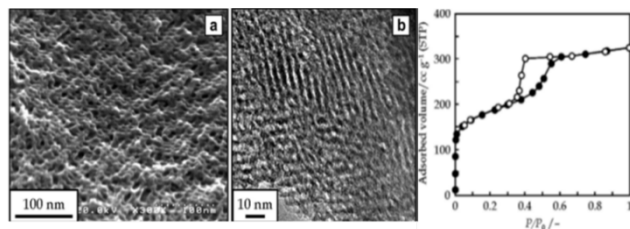


**Figure 4.** (a) Top-view SEM, (b) TEM micrographs and (c)  $\text{N}_2$  adsorption/desorption isotherm of the mesoporous carbon membrane carbonised at 600 °C (reproduced from<sup>79</sup>).

Starting from phloroglucinol-formaldehyde system, Chengdu *et al.*<sup>80</sup> prepared composites of carbon-carbon nanotubes for Li-ion batteries. They used Pluronic F127 as template and the final products were carbonised at 550 °C to preserve a high number of defects. The samples showed porous structure with surface areas between 378 and  $570 \text{ m}^2 \text{ g}^{-1}$ .

Qiao *et al.*<sup>81</sup> reported on the synthesis of mesoporous carbon nanospheres starting from resorcinol and formaldehyde. Fig. 5 shows the spherical morphology of the carbon spheres. The porosity was analysed by  $\text{N}_2$  adsorption-desorption isotherms. The isotherms showed a multimodal distribution of pores, it had an intermediate shape in between type I, characteristic for micropores, and type IV characteristic for mesopores (Fig. 6). The pore sizes from the adsorption analyses were in good agreement with TEM indicating a small pore size of about 3 nm.

The specific surface areas were between  $640$  and  $857 \text{ m}^2 \text{ g}^{-1}$ , and the total pore volumes between  $0.34$  and  $0.45 \text{ cm}^3 \text{ g}^{-1}$ , depending on the high temperature treatment.

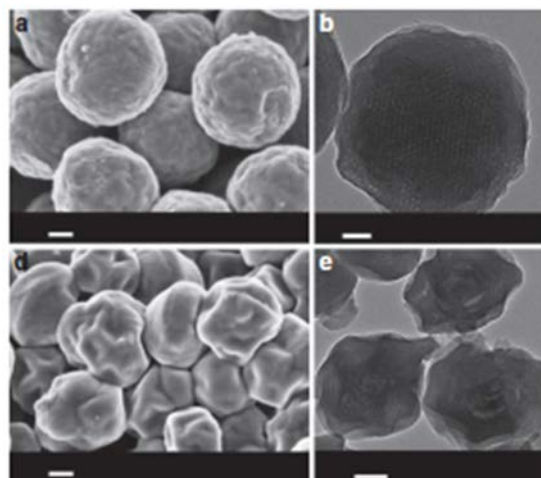


**Figure 5.** (a,d) HRSEM images, scale bar, 100nm; (b,e) TEM images, b – scale bar, 50nm, e – scale bar, 100nm (reproduced from<sup>81</sup>).

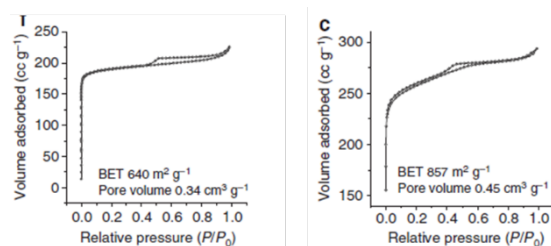


**Figure 6.**  $\text{N}_2$  sorption isotherms for mesoporous carbonaceous nanospheres carbonised at 400 °C (left side) and 600 °C (right side) (reproduced from<sup>81</sup>).

The soft templating method has been shown to be efficient for the development of carbon structures and studies have used different carbon precursors, such as carbohydrates,<sup>82</sup> nitrogen and carbon rich compounds, like melamine,<sup>83</sup> glucosamine,<sup>84</sup> and natural polymers (lignin, chitin, cellulose).<sup>85</sup> The synthesis of ordered porous carbon materials derived from fructose has been reported. Kubo *et al.*<sup>82</sup> used the advantages of HTC together with the soft-templating method. By performing the HTC at 130 °C, they ensured the stability of the polymer and created the necessary conditions for HTC of fructose. In their first attempt, the HTC of fructose was performed with the F127 block copolymer surfactant. The final composite presented ordered porosity with pores diameter around 10 nm and wall thickness of 6 nm, indicating that the self-assembly of the polymer together with fructose was successful. SEM shows the presence of spherical particles derived from fructose (Fig. 7a), and TEM presents the ordered porosity of the carbonaceous material (Figs. 7b-c). The  $\text{N}_2$  sorption isotherms show a non-reversible microporous type I isotherm, with a pore size distribution composed of a sharp peak at 0.9 nm and a shoulder around 2 nm. The material had a surface area of  $257 \text{ m}^2 \text{ g}^{-1}$  and a pore volume of  $0.14 \text{ cm}^3 \text{ g}^{-1}$ .

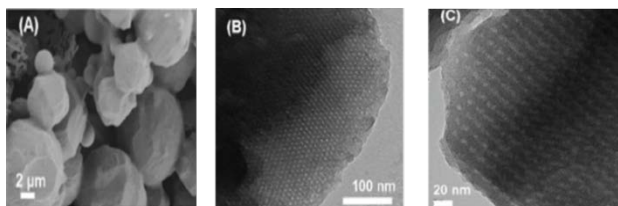


**Figure 7.** (a) SEM, (b) TEM, and (c) HRTEM micrographs of ordered mesoporous carbons derived from fructose. (reproduced from<sup>82</sup>).

Yan *et al.*<sup>83</sup> reported on the synthesis of mesoporous graphitic carbon nitrides, which are potential photo catalysts for the H<sub>2</sub> evolution reaction. Melamine was used as both the carbon precursor and nitrogen source, and Pluronic P123 as soft template for the preparation of graphitic-C<sub>3</sub>N<sub>4</sub>. This solid had a high surface area and extended light absorption towards the maximum of the solar spectrum (800 nm), which is promising for the use of this class of materials for the photocatalytic preparation of H<sub>2</sub> using visible light. The mesopores could also be observed from TEM analysis, as shown in Fig. 8. The graphitic-C<sub>3</sub>N<sub>4</sub> had a plate-like surface morphology with a worm-like porous structure. Without the soft template, only few worm-like pores were observed and it was clear from that study that the template played an important role in controlling both the morphology and pores.

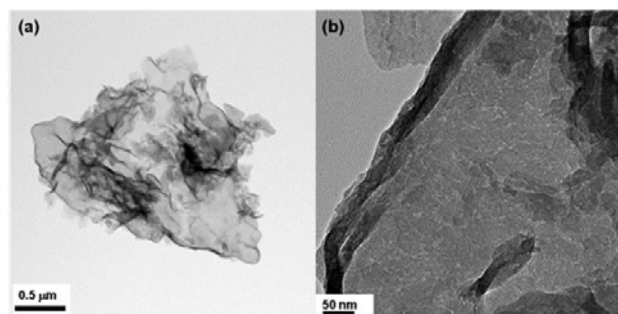


**Figure 8.** TEM images of g-C<sub>3</sub>N<sub>4</sub> prepared with Pluronic P123: (a) low magnification, (b) high magnification. (Reproduced from<sup>83</sup>).

Another study involving the soft-templating method was conducted by Xiao *et al.*<sup>84</sup> HTC coupled with soft templating was used to prepare porous carbon materials using glucosamine as the carbon precursor and the triblock copolymer P123 as a soft template. They considered the influence of pH and amount of template. By moving from neutral to acidic conditions during synthesis, the specific surface area of the final carbon product increased from 550 to 980 m<sup>2</sup> g<sup>-1</sup>. As was expected, an increased amount of template in the synthesis led to that the pore volume of the carbon material increased. The N<sub>2</sub> sorption isotherms revealed that the materials had both micro and mesopores with Type I and IV isotherms characteristics, and H4 hysteresis loops (Fig. 9). Due to these specific textural properties, the carbon materials displayed adsorption capacities of CO<sub>2</sub> between 3.7 and 4.7 mmol g<sup>-1</sup>, at 25 °C and 100 kPa.

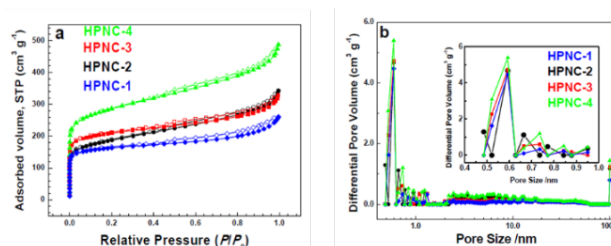


**Figure 9.** Nitrogen sorption isotherms (a) and pore size distribution (b) of the soft templating materials. (reproduced from<sup>86</sup>).

Overall, soft-templating method can be easily used in the synthesis of nanostructured HTC-derived materials. By using block copolymers during HTC treatment, we can tune the shape and size of the materials. Moreover, the template can easily be removed by treating the material at high temperature under inert atmosphere.

### 3.2.2. Hard templated carbons

Carbon materials with ordered porous structures can be prepared from hard-templating processes. Starting from a porous silica mold, a porous carbon negative replica can be produced by first infiltrating the silica with a carbon precursor, followed by subsequent pyrolysis and final dissolution of the silica template.<sup>87–90</sup> For instance, similarly to the production of CMK-type materials pioneered by Jun *et al.*,<sup>91</sup> hexagonally-ordered mesoporous SBA-15 silica has also successfully been used as the sacrificial inorganic template for the preparation of ordered carbonaceous replicas, using furfural as carbon precursor, synthesized under hydrothermal conditions.<sup>92</sup> Significantly, it was found that it is important to match the template surface polarity (e.g., hydroxylated vs. calcined silica) with that of the carbon precursor, so that HTC decomposition products can successfully penetrate the pores of the template. Demir-Cakan *et al.*<sup>100</sup> reported on the synthesis of mesoporous carbon materials with increased and versatile functionality. This replication was achieved by performing the HTC of glucose in the presence of small amounts of water-soluble vinyl monomers.

#### 3.2.2.1. Zeolite-templated microporous carbons

Although carbon mesostructures can be prepared by filling the ordered mesopores of silica scaffolds, and removing the silica afterwards, preparing well-defined ordered microporous (pore diameter < 2 nm) carbon materials has been a long-standing challenge. A variety of inorganic templates (e.g., mesoporous silicas) and various carbon sources (including sucrose, furfuryl alcohol, acrylonitrile, propylene, pyrene, vinyl acetate, and acetonitrile) have been used to prepare porous carbons.<sup>95</sup> However, these have consisted of not only micropores but also a large amount of mesopores. Based on the hard template techniques, carbon replicas from microporous materials such as zeolites have also been synthesised. Typically, carbon can be introduced into the nanochannels of the microporous materials by means of polymer impregnation (e.g., furfuryl alcohol-impregnation at a reduced pressure) followed by carbonisation and/or chemical vapour

deposition (CVD) using small molecules, such as ethylene and acetylene as a carbon source for achieving successful carbonisation within the zeolite pores. After removal of the zeolite, a zeolite-templated carbon (ZTC) can be obtained as a reverse replica of the parent zeolite. Ma. *et. al.* reported on certain carbon replicas prepared from zeolite Y (with a framework type code of FAU<sup>96</sup>) that possessed a periodic ordering structure, an impressively high surface area and large micropore volume. The framework type FAU is three-dimensional and belongs to the 12-ring zeolites, which have the smallest interconnecting pore openings construed of 12 oxygen-linked aluminum or silicon atoms. In this experiment, zeolite channels were first filled with furfuryl alcohol (FA) by impregnation and then additional C was deposited into zeolite channels by a propylene CVD process. The carbon/zeolite Y composite was further heat-treated at 900 °C under a N<sub>2</sub> flow, and the resultant carbon was liberated from the zeolite framework by a reactive treatment with hydrogen fluoride (HF). In other experiments, zeolites with large pore materials (e.g., those with framework type codes of \*BEA, LTL and MOR, which have interconnected pore channels with sizes up to 12-rings) allow more carbon precursor loading. There are different parameters influencing the results of the carbon replication. The disorder or the symmetry of the structure, which is the case for zeolite beta (\*BEA framework type code) and zeolite Y (FAU framework type code), while zeolite L (LTL framework type code) that possesses a one-dimensional channel system could not produce a three-dimensional carbon replica. Moreover, the intersecting pore channel systems of mordenite (MOR structure code) with 12- and 8-rings did not result in a carbon network because of poor carbon infiltration throughout the small 8-ring pore openings. Gaslain *et.al.*<sup>97</sup> used the zeolite EMC-2 (EMT structure code) and achieved a microporous carbon with three well-resolved XRD peaks. Nishihara and Kyotani summarised in a recent article<sup>98</sup> that ZTC with a 3D graphene framework is free from graphene aggregation/stacking, therefore, unlike representative nanocarbons C60, SWCNT, graphene of 0D, 1D, and 2D structures, which inevitably cause unfavourable surface loss, the 3D ZTC with a self-standing open framework can almost fully expose the entire surface. The high geometric surface area of ZTC (3710 m<sup>2</sup> g<sup>-1</sup>) can exceed the value of graphene (2630 m<sup>2</sup>g<sup>-1</sup>), and the experimentally measured highest surface area of ZTC (3730 m<sup>2</sup>g<sup>-1</sup>) is almost the same as the geometric one.

Zeolite-type materials represent an interesting and extreme test for replication strategies, because the dimensions of their channels and cages are quite similar to those of the infiltrated materials that constitute the replica. For instance, Kim *et al*<sup>99</sup> described a new strategy to prepare these materials with unprecedented precision. However, common carbon precursors such as sucrose or furfuryl alcohol are too large to easily diffuse in the 0.5–1.3 nm-sized pores of zeolites. Smaller precursor molecules like ethylene decompose only at high temperatures, resulting in incomplete pore filling and carbon structures being formed outside the zeolite pores, while using the

lanthanum, yttrium or calcium catalysts lowers the decomposition temperature of ethylene by 200 °C. Although the exact catalytic mechanism remains unclear, it results in carbon formation exclusively inside of the zeolite pores in which the catalyst is present. After zeolite removal, a well-defined, ordered and interconnected microporous carbon structure was obtained. The same strategy was applied to several different zeolite structures, with pores down to 0.71 nm. Three-dimensional open zeolite porosity leads to interconnected carbon networks. Interestingly, also well-defined carbon quantum dots with intriguing optical properties can be formed.<sup>100</sup>

In terms of these hard templated carbons, a stoichiometric removal of the zeolite framework is promoted by using HF or NaOH under hydrothermal conditions<sup>101</sup>; however, as HF imposes safety hazards, it limits the options for industrialisation. For the hydrothermal treatment with NaOH, zeolites are sometimes dissolved and recrystallised. For instance, van Tendeloo *et al.*<sup>102</sup> showed that a commercial NH<sub>4</sub><sup>+</sup>-zeolite Y zeolite transformed into five different frameworks types depending on the cations of the base but with NaOH, the zeolite-Y framework largely persisted.

### 3.2.2.2. (Silico)aluminophosphate templated carbons

Aluminophosphate molecular sieves (AIPO<sub>4</sub>s) have attracted considerable interest since they were first synthesised a few decades ago at Union Carbide Laboratories.<sup>103</sup> They are isoelectronic representations of microporous silicates (SiO<sub>2</sub>), with alternating and oxygen-linked aluminum and phosphorous atoms. Their frameworks are mainly covalently bonded. The chemistry of AIPO<sub>4</sub>s and microporous silicates (SiO<sub>2</sub>) are different and AIPO<sub>4</sub>s can be dissolved in aqueous solutions of HCl.<sup>104,105,106</sup> Even though this chemical difference is promising for the use of AIPO<sub>4</sub>s to derive ACs, only a limited amount of work has been performed. AIPO<sub>4</sub>-5 (AFI), with the space group of P6cc<sup>2</sup> or P6/mmc<sup>3</sup> was the first member of the family studied for carbon replication. It is a material with potential application in catalysis, separation technology and nonlinear optics, but it is particularly relevant in model systems as the pore walls are smooth.<sup>103</sup> Tang *et.al*<sup>107</sup> synthesised hexagonal carbon micro and submicro tubes within the channels of an AIPO<sub>4</sub>-5 material; however, its one dimensional pore system makes it less useful for the synthesis of ACs. We expect that the pore systems of suitable AIPO<sub>4</sub> templates should be three or at least two dimensional, have sufficiently large pore window apertures and high thermal stability.<sup>108</sup> A related class of suitable templates is the microporous silicoaluminophosphates (SAPOs). Similar to zeolites (aluminosilicates), SAPOs have a negatively charged framework. Si (formal charge of +4) replaces P (formal charge of +5) in SAPOs.<sup>109</sup> H-SAPOs can be used for acid catalysis,<sup>110</sup> which is relevant for promoting the CVD of carbon precursors.

For the reasons mentioned above, synthesis of ACs derived from a SAPO/AIPO/MAPO whose framework can be removed under mild conditions without using HF would be

meaningful. We initially started the studies from SAPO-37-templated carbon synthesis, because of several reasons. Similar with zeolite Y, SAPO-37 has FAU framework.<sup>96</sup> In addition to having a 3D structure, large pores and pore window apertures, H-SAPO-37 is highly acidic and its -OH groups are thermally stable (up to 1000 °C)<sup>111</sup>. Nevertheless, after removing the organic template, it becomes amorphous in an ambient atmosphere when being exposed to water vapour.<sup>112</sup> The high thermal stability and acidity of H-SAPO-37 are advantageous for infiltration and deposition of carbon precursors at high temperature. On the other hand, its low hydrothermal stability makes it promising for dissolution under mild conditions. Details of the templating of the H-SAPO-37 will be shown in the PhD Thesis of GreenCarbon's ESR 8 (Xia Wang) and the associated publications, and be compared with templating using zeolite Y. The comparison will involve detailed characterization with methods that include TEM/SEM, infrared and Raman spectroscopy, adsorption studies and various digestions studies comparing the ease of removing the SAPO-37 with that of zeolite Y from carbon-zeolite composites. Table 3 provides the list of already synthesised SAPO/AIPO/MAPOs with pore window apertures  $\geq 10$ - rings and at least two dimensional pores systems, as derived from the current zeolite database.<sup>96</sup> These molecular sieves could be used as templates for hydrothermal carbon synthesis. Recently, Braun *et al.*<sup>113</sup> developed a theoretical framework to generate a ZTC model from any given zeolite structure, predicting the structure of known ZTCs, which would be a reference for future SAPO/AIPO/MAPO-templated carbon studies. In this work, HTC technique will be used to fill the carbon precursor into the SAPO/AIPO/MAPO micropores using a modification of the protocol by Demir-Cakan *et al.*<sup>100</sup> followed by CVD of selected precursors.

### 3.2.3. Salt templating

Another approach to generate porosity in the structure of the carbon materials is called "salt templating" (see Fig. 10). This method uses inorganic salts as templates during the synthesis at elevated temperatures. The melting points of the salts are reduced by addition in eutectic compositions and at high temperatures, ion pair or clusters in the carbon structure are formed. Finally, the salts are removed by washing with water, leaving pores behind<sup>114,139</sup>. The advantage of this process is the possibility to improve the ratio of micropores to macropores, obtaining a structure with multimodal pore size distribution. Fechler *et al.*<sup>114</sup> showed that, by changing the components of the eutectic mixture, the porosity of the resulting carbon could be controlled. For example, moving from LiCl/ZnCl<sub>2</sub> to KCl/ZnCl<sub>2</sub>, the porosity varied from microporous structure to mesoporous and then macroporous structure (Fig. 11). The specific surface areas of the carbons ranged from 1100 to 2000 m<sup>2</sup> g<sup>-1</sup> and they had different morphologies. With mixtures with LiCl, the materials exhibited mainly micropores, maybe because in this case, the salts act as molecular templates forming ion pairs or clusters of free minimal energy.

**Table 3.** Structure codes and properties of selected SAPO/AIPO/MAPOs from zeolite database.

Structure code	Name and reference	Dimension	Largest ring	Accessible volume (%)
AFR	SAPO-40 <sup>115</sup>	2	12	19.60
AFS	MAPSO-46 <sup>116</sup> MAPO-46 <sup>117</sup>	3	12	21.06
AFY	CoAPO-50 <sup>116</sup> MgAPO-50 <sup>118</sup> MnAPO-50 <sup>119</sup> ZnAPO-50 <sup>120</sup>	3	12	21.88
BPH	ZnAPO-64 <sup>121</sup> [Co-P-O]-CAN <sup>122</sup> [Zn-P-O]-CAN <sup>123</sup>	3	12	21.65
-CLO	[Mn-Ga-P-O]-CLO <sup>124</sup> [Zn-Ga-P-O]-CLO <sup>124</sup> [Al-P-O]-CLO <sup>125</sup>	3	20	33.76
FAU	SAPO-37 <sup>109</sup> [Co-Al-P-O]-FAU <sup>126</sup> Berylllophosphate X <sup>127</sup> Zincophosphate X <sup>127</sup>	3	12	27.42
LTL	[Al-P-O]-LTL <sup>128</sup>	3	12	15.37
MEI	ECR-40 <sup>129</sup>	3	10	21.11

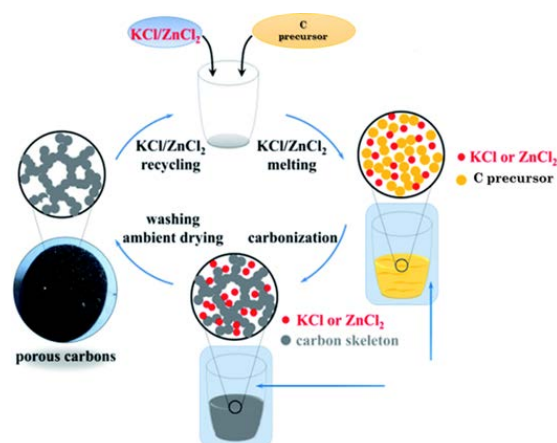


**Figure 10.** Graphical representation of the salt-templating method (reproduced from<sup>130</sup>).

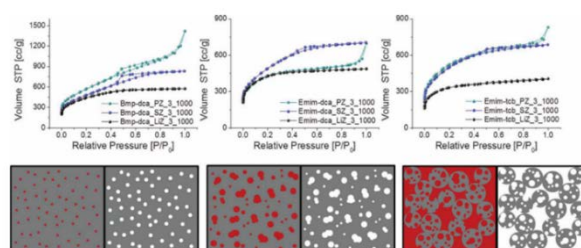


**Figure 11.** N<sub>2</sub> sorption isotherms of carbons templated with LiCl/ZnCl<sub>2</sub>, NaCl/ZnCl<sub>2</sub>, KCl/ZnCl<sub>2</sub> (upper part) and schematic representation of pore formation (lower part). Each left image depicts the carbon (grey)/salt (red) composite and each right image the carbon after washing; reproduced from<sup>114</sup>.

Using NaCl, mesopores were formed, which was ascribed to the lower melting point of NaCl and tentatively to the formation of bigger salt clusters. Finally, when KCl was used as a component of the eutectic mixture (the salt with the lowest melting point), sorption isotherms typical for macropores were obtained.<sup>114</sup> Another attempt using the salt templating approach has been described by Kumar *et al.*<sup>131</sup>, where they used a eutectic mixture of LiCl/ZnCl<sub>2</sub> together with a biomass derived precursor. They studied the influence of the salt concentration and biomass precursor type. Their materials had surface areas from 520–1000 m<sup>2</sup> g<sup>-1</sup>. An increase in the salts concentration seemed to have altered the dimension of the pores in such a way that by using small amount of salts, the final product exhibited multimodal structure with large micropores, approximately 1.3 nm, and mesopores with dimensions of 3–4 nm. By increasing the amount of salt, the samples tended to have lost some micropores, possessing more mesopores or with even more salt only mesopores. This switch could have occurred that by increasing the salt concentration, the clusters that formed at a high temperature tended to increase in size and in turn formed large pores. In that study, the highest specific surface areas were achieved when a mixed precursor consisting of algae and arginine was used. These surface areas were tentatively rationalised by the ability of arginine to carbonise within the pores of carbonised algae. TEM images of the carbon materials derived from different precursors are shown in Fig. 12. They confirm the presence of ribbon-like morphology in the case of samples prepared from arginine and mixture of arginine and algae. The carbon materials derived from pure algae showed neither oriented porosity nor distinctive morphologies. Overall, the salt templating method provides control over textural properties, porosity and surface areas. Because of the possibility to create multimodal pore structures, the final materials are targeted in plenty of applications such as gas storage and conversion, water treatment and catalysis.

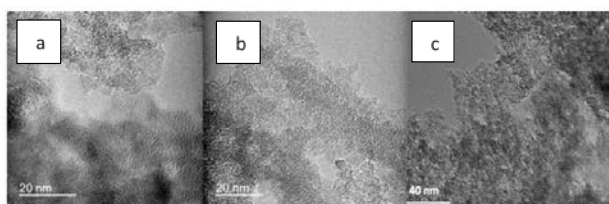


**Figure 12.** TEM micrographs of carbon materials derived from (a) pure algae, (b) algae and arginine mixture, and (c) pure arginine, at molar ratio 1:4, biomass to salts mixture. (reproduced from<sup>131</sup>).

#### 4. Application of Transmission Electron Microscopy for studies of porous material

The lowest point resolution of our eyes is 100–200  $\mu\text{m}$ , and microscopy is a large set of techniques used to study objects that are too small to be examined by the naked eye. For example, the distance between atoms in a solid is generally in the range of 2–3  $\text{\AA}$ . Here we discuss TEM, which was developed because of the limitation of image resolution in light microscopes. After electron microscopes

had been developed, it was realised that there are many other decent reasons for using electrons, most of which are used to some extent in a modern TEM instrument.

##### 4.1. The instrument

Max Knoll and Ernst Ruska invented the first TEM instrument in 1931 at the Technische Hochschule Berlin, which was capable of displaying magnified images of a thin specimen with a magnification of  $10^3$ – $10^6$ . In a TEM instrument, electrons are emitted by the electron source situated at the top of the microscope column and are accelerated towards the specimen with the positive electric potential. Then, the beam of electrons is condensed by the first and second condenser lenses on the way to the specimen. The fast electrons are transmitted through the sample, which are normally prepared to be thin enough so that the electron beam can pass through without losing too much intensity. After interacting with the sample, the electrons are focused by the objective lens to form an image. There is an objective aperture just above the objective lens, which can be used to select either direct or scattered electrons to contribute an image. Below the specimen, series of lenses are used to magnify the images or electron diffraction (ED) patterns, which are very useful for analysing crystalline matter. Fig. 13 shows the schematic diagrams of projecting the image and the ED pattern onto the screen by both image diffraction modes. Modern TEM instruments are able to achieve a very high resolution, and usually consist of a beam column as tall as 2.5 m with a diameter of about 30 cm, while the addition of aberration correctors compensates the spherical aberration.

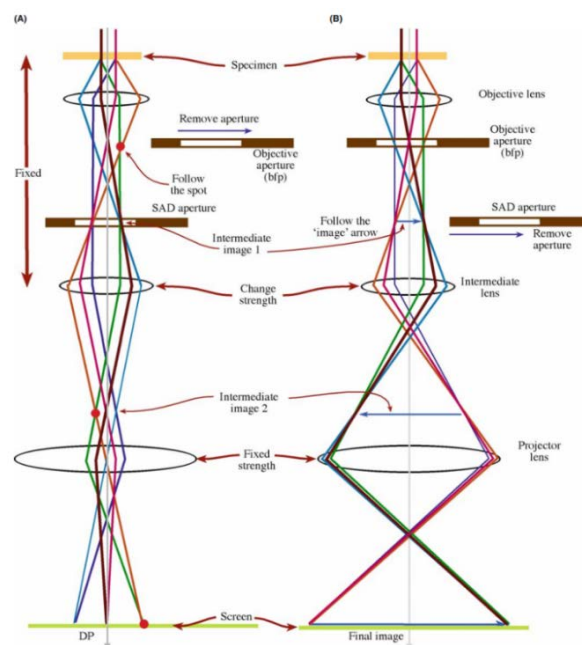


**Figure 13.** Schematic diagram of (A) diffraction mode: projecting the diffraction pattern onto the viewing screen, and (B) image mode: projecting the image onto the screen.<sup>132</sup>

#### 4.2. TEM images

TEM images are magnified images of the electron intensity on the bottom surface of the specimen. The contrast of images arises if the intensity varies significantly from one region to another. There are several types of contrast in TEM imaging: mass-thickness contrast, and diffraction contrast make the most contribution to the images. TEM imaging is extensively applied to both amorphous and crystalline specimens. In crystalline samples, the contrast mostly contributes to the diffraction contrast.

#### 4.3. Electron diffraction (ED)

The elastic electron scattering in a crystalline material is called diffraction. The regularity of the atomic nuclei spacing leads to a redistribution of the angular scattering, which can be displayed on the TEM instrument's screen by weakening the intermediate lens. Then, the intermediate and projector lenses magnify the initially formed small diffraction pattern at the back-focal plane of the objective lens.

The ED patterns can be interpreted with the reciprocal lattice concept. Every crystalline material can be described with two lattices, one is a real lattice, and the other is a reciprocal lattice. The reciprocal lattice is related to the real one via the Fourier transformation. Comparing it with X-ray diffraction, which is the atom plane diffraction of X-rays in a crystal, is helpful to understand the electronic diffraction mechanism. X-ray diffraction can be explained by the Bragg's reflection law:

$$n\lambda = 2d \sin \theta \quad (4)$$

where  $\lambda$  is the X-ray wavelength,  $d$  is the spacing between atomic planes measured in a direction perpendicular to the planes, and  $n$  is an integer that represents the order of reflection. Fig.14 shows an ED pattern of an amorphous carbon material.

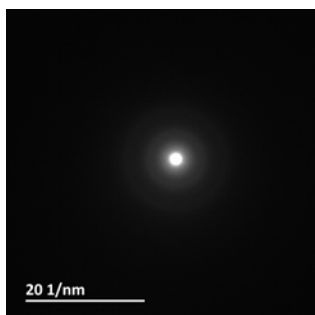


**Figure 14.** Diffraction pattern of an amorphous carbon material.

#### 4.4. X-ray energy-dispersive spectrometry (EDS)

EDS can be used as an elemental composition analysis technique by measuring the number and energy of the X-rays emitted by the sample. The main principle here is that each element has its own atomic structure, allowing a unique set of characteristic X-ray peaks. When a high-energy beam of charged particles such as electrons or protons or a beam of X-rays is focused into the sample, an atom within the sample contains unexcited electrons bound to the nucleus. Then, an electron in an inner shell is

excited by the incident beam, creating an electron hole where the electron was initially. Another electron from an outer, higher-energy shell will fill the hole, and the difference of energy between the higher-energy shell and the lower energy shell may be released, forming a characteristic X-ray, which can be measured by EDS.

#### 4.5. Electron energy-loss spectroscopy (EELS)

When a high-energy electron passes through a thin specimen, either it penetrates it without losing any energy or it may suffer inelastic scattering, losing energy via a variety of processes. EELS can separate these inelastically scattered electrons into a spectrum and be used to analyse the energy distribution of these electrons to form images or DPs from electrons of specific energy, which can be interpreted and quantified. EELS offers more information than mere elemental identification, and it is well suited to detect light elements, which are difficult to analyse with EDS. In amorphous carbon films, C-C bonds with  $sp^2$ - and  $sp^3$ -type hybridisations occur, which can be analysed by studying the K- edge region in an EELS. A common method for quantifying the  $sp^2$  bonding fraction in an amorphous carbon film was described by Berger *et al.*<sup>133</sup>

In addition, there are numerous types of TEMs and they include HRTEMs, STEMs, AEMs, etc., but normally a new 200 or 300 keV TEM can combine aspects of all the above microscope types of TEMs. Fig. 15 shows a picture of a given TEM instrument (JEOL JEM-2100F) with field emission gun (FEG), used for the TEM related work in this chapter. Also, sample preparation is a key factor for successful TEM experimentation. Using or developing a preparation technique that does not change the properties of the samples under study is of great significance.



**Figure 15.** Photograph of the Transmission Electron Microscopy used in this chapter, JEOL JEM-2100F, with field emission gun (FEG), situated at the Arrhenius Laboratory, Stockholm University (Sept. 2018).

## 5. Conclusions

This chapter summarises technologies for gas separation, mainly focused on adsorption process together with some examples of adsorbents used for CO<sub>2</sub> and H<sub>2</sub>S storage. The second part of this section describes the HTC coupled with templating methods, and the main possibilities to improve the textural properties of the final product. Among all the technologies for gas separation, adsorption processes are of great interest because of the variety of adsorbents that can be used, as well as the flexibility of the process conditions to achieve the adsorption capacity as highest as possible. Carbon-based adsorbents are known for their gas separation properties, since the ancient times and nowadays they are among the most used materials for these kinds of applications. HTC is an advantageous method for the synthesis of carbon-based adsorbents. Due to the possibility to combine the HTC with templating techniques, the structure of the final carbons can be easily improved. Besides, their chemical and physical properties can be modified by the combination of carbon with different compounds and thanks to the high number of oxygenated groups from the carbon surface, further functionalisation is achieved. When HTC is combined with soft-templating methods, the possibilities to obtain an ordered porous material increase. This occurs because of direct arrangements of the block copolymer aggregates. By using a hard template, the advantage comes with the possibility to obtain nanostructured materials with different surface functionalities, and easiness in controlling the final structure, but the removal of the template is more challenging than in the case of soft template approach. SAPO-templated carbons have industrial potential for CO<sub>2</sub> separation not only because of its high surface area, well-ordered ultramicropore structure as other hard-templated carbons, but also because of the non-toxic prepapring procedure when it is compared with zeolite-templated carbons. To ensure the presence of a multimodal pore structure, the salt templating technique is promising; a change of the salt composition and concentration makes that the size of the pores can be shifted from micropores to mesopores, or even macropores. Furthermore, the surface area can be easily increased by modification in the salt mixtures concentration. TEM is an important tool to deeply characterise engineered porous carbons.

## Acknowledgements

This project has received funding from the European Union's Horizon 2020 research and innovation programme under the Marie Skłodowska-Curie grant agreement No 721991.

## References

- (1) Annual Report 2010-2011 Academic Year – Universitat Oberta de Catalunya (UOC) <https://www.uoc.edu/memories/memoria1011/english/teaching/departments-schools-chairs/ecs.html> (accessed Jan 31, 2019).
- (2) J.T. Houghton, Y. Ding, D.J. Griggs, M. Noguera, P.J. van der Linden, X. Dai, K. Maskell, C. A. J. *Climate Change 2001: The Scientific Basis*; Cambridge University Press: Cambridge, 2001.
- (3) Spengler, J. D.; Sexton, K. Indoor Air Pollution: A Public Health Perspective. *Science* **1983**, *221* (4605), 9–17.
- (4) Barnett, J. Security and Climate Change. *Glob. Environ. Chang.* **2003**, *13* (1), 7–17.
- (5) Wiheeb, A. D.; Shamsudin, I. K.; Ahmad, M. A.; Murat, M. N.; Kim, J.; Othman, M. R. Present Technologies for Hydrogen Sulfide Removal from Gaseous Mixtures. *Rev. Chem. Eng.* **2013**, *29* (6), 449–470.
- (6) Mandal, B. P.; Bandyopadhyay, S. S. Absorption of Carbon Dioxide into Aqueous Blends of 2-Amino-2-Methyl-1-Propanol and Monoethanolamine. *Chem. Eng. Sci.* **2006**, *61* (16), 5440–5447.
- (7) Plaza, M. G.; Pevida, C.; Arenillas, A.; Rubiera, F.; Pis, J. J. CO<sub>2</sub> capture by Adsorption with Nitrogen Enriched Carbons. *Fuel* **2007**, *86* (14), 2204–2212.
- (8) Bagreev, A.; Bandoz, T. J. A Role of Sodium Hydroxide in the Process of Hydrogen Sulfide Adsorption / Oxidation on Caustic-Impregnated Activated Carbons. *Ind. Eng. Chem. Res.* **2002**, *41* (4), 672–679.
- (9) D'Alessandro, D. M.; Smit, B.; Long, J. R. Carbon Dioxide Capture: Prospects for New Materials. *Angew. Chem. Int. Ed.* **2010**, *49* (35), 6058–6082.
- (10) The history of activated carbon <https://www.jurassiccarbon.com/> (accessed Feb 25, 2019).
- (11) Ngoy, J. M. A CO<sub>2</sub> Capture Technology Using Carbon Nanotubes with Polyaspartamide Surfactant. Ph.D. Thesis, University of the Witwatersrand, Johannesburg. **2016**, 287.
- (12) Wilcox, J. *Carbon Capture*; Springer-Verlag: New York, 2012.
- (13) Liu, Y.; Wilcox, J. Molecular Simulation Studies of CO<sub>2</sub> Adsorption by Carbon Model Compounds for Carbon Capture and Sequestration Applications. *Environ. Sci. Technol.* **2013**, *47* (1), 95–101.
- (14) Carbon Dioxide. *Wikipedia* (accessed Feb 25, 2019).
- (15) Pubchem. Carbon dioxide <https://pubchem.ncbi.nlm.nih.gov/compound/280> (accessed Feb 25, 2019).
- (16) Wiheeb, A. D.; Shamsudin, I. K.; Ahmad, M. A.; Murat, M. N.; Kim, J.; Othman, M. R. Present Technologies for Hydrogen Sulfide Removal from Gaseous Mixtures. *Rev. Chem. Eng.* **2013**, *29* (6).
- (17) Mandal, B.; Bandyopadhyay, S. S. Simultaneous Absorption of CO<sub>2</sub> and H<sub>2</sub>S Into Aqueous Blends of N -Methyldiethanolamine and Diethanolamine. *Environ. Sci. Technol.* **2006**, *40* (19), 6076–6084.
- (18) Yagi, T.; Shibuya, H.; Sasaki, T. Application of Chemical Absorption Process to CO<sub>2</sub> Recovery from Flue-Gas Generated in Power-Plants. *Energy Convers. Manage.* **1992**, *33* (5–8), 349–355.
- (19) McIntyre, G.; Lyddon, L. Claus Sulphur Recovery Options. *Pet. Technol. Quarterly* **1997**, 1–8.
- (20) Zhao, C.; Wang, J. Electrochemical Reduction of CO<sub>2</sub> to Formate in Aqueous Solution Using Electro-Deposited Sn Catalysts. *Chem. Eng. J.* **2016**, *293*, 161–170.

- (21) Hao, J.; Rice, P. A.; Stern, S. A. Upgrading Low-Quality Natural Gas with H<sub>2</sub>S- and CO<sub>2</sub>-Selective Polymer Membranes Part I. Process Design and Economics of Membrane Stages without Recycle Streams. *J. Membr. Sci.* **2002**, *177*, 177-206.
- (22) Ahmad, F.; Keong, L. L.; Shariff, A.; Removal of CO<sub>2</sub> from Natural Gas Using Membrane Process: Design, Fabrication and Parametric Study. In: EMS Summer School, Germany, 2010.
- (23) Rouquerol, F.; Rouquerol, J.; Sing, K. S. W.; Llewellyn, P.; Maurin, G. *Adsorption by Powders and Porous Solids*; 2nd ed.; Academic Press: France, 2014.
- (24) Burwell, R. L. Manual of Symbols and Terminology for Physicochemical Quantities and Units—Appendix II. *Pure Appl. Chem.* **1976**, *46*, 71–90.
- (25) Thommes, M.; Kaneko, K.; Neimark, A. V.; Olivier, J. P.; Rodriguez-Reinoso, F.; Rouquerol, J.; Sing, K. S. W. Physisorption of Gases, with Special Reference to the Evaluation of Surface Area and Pore Size Distribution (IUPAC Technical Report). *Pure Appl. Chem.* **2015**, *87* (9–10), 1051–1069.
- (26) Wang, Q.; Luo, J.; Zhong, Z.; Borgna, A. CO<sub>2</sub> Capture by Solid Adsorbents and Their Applications: Current Status and New Trends. *Energy Environ. Sci.* **2011**, *4* (1), 42–55.
- (27) Siriwardane, R. V.; Shen, M.-S.; Fisher, E. P.; Poston, J. A. Adsorption of CO<sub>2</sub> on Molecular Sieves and Activated Carbon. *Energy Fuels* **2001**, *15* (2), 279–284.
- (28) Hernández, S. P.; Scarpa, F.; Fino, D.; Conti, R. Biogas Purification for MCFC Application. *Int. J. Hydrogen Energy* **2011**, *36* (13), 8112–8118.
- (29) Yu, J.; Xie, L.-H.; Li, J.-R.; Ma, Y.; Seminario, J. M.; Balbuena, P. B. CO<sub>2</sub> Capture and Separations Using MOFs: Computational and Experimental Studies. *Chem. Rev.* **2017**, *117* (14), 9674–9754.
- (30) Britt, D.; Furukawa, H.; Wang, B.; Glover, T. G.; Yaghi, O. M. Highly Efficient Separation of Carbon Dioxide by a Metal-Organic Framework Replete with Open Metal Sites. *Proc. Natl. Acad. Sci. U.S.A.* **2009**, *106* (49), 20637–20640.
- (31) Rosi, N. L.; Kim, J.; Eddaoudi, M.; Chen, B.; O’Keeffe, M.; Yaghi, O. M. Rod Packings and Metal–Organic Frameworks Constructed from Rod-Shaped Secondary Building Units. *J. Am. Chem. Soc.* **2005**, *127* (5), 1504–1518.
- (32) Han, L.; Budge, M.; Alex Greaney, P. Relationship between Thermal Conductivity and Framework Architecture in MOF-5. *Comput. Mater. Sci.* **2014**, *94*, 292–297.
- (33) Yang, Q.; Vaesen, S.; Vishnuvarthan, M.; Ragon, F.; Serre, C.; Vimont, A.; Daturi, M.; De Weireld, G.; Maurin, G. Probing the Adsorption Performance of the Hybrid Porous MIL-68(Al): A Synergic Combination of Experimental and Modelling Tools. *J. Mater. Chem.* **2012**, *22* (20), 10210 - 10220.
- (34) Hamon, L.; Serre, C.; Devic, T.; Loiseau, T.; Millange, F.; Férey, G.; De Weireld, G. Comparative Study of Hydrogen Sulfide Adsorption in the MIL-53(Al, Cr, Fe), MIL-47(V), MIL-100(Cr), and MIL-101(Cr) Metal-Organic Frameworks at Room Temperature. *J. Am. Chem. Soc.* **2009**, *131* (25), 8775–8777.
- (35) Kumar, A.; Madden, D. G.; Lusi, M.; Chen, K.-J.; Daniels, E. A.; Curtin, T.; Perry, J. J.; Zaworotko, M. J. Direct Air Capture of CO<sub>2</sub> by Physisorbent Materials. *Angew. Chem. Int. Ed.* **2015**, *54* (48), 14372–14377.
- (36) Cho, H.-Y.; Yang, D.-A.; Kim, J.; Jeong, S.-Y.; Ahn, W.-S. CO<sub>2</sub> Adsorption and Catalytic Application of Co-MOF-74 Synthesized by Microwave Heating. *Catal. Today* **2012**, *185* (1), 35–40.
- (37) Nandi, S.; Maity, R.; Chakraborty, D.; Ballav, H.; Vaidhyanathan, R. Preferential Adsorption of CO<sub>2</sub> in an Ultramicroporous MOF with Cavities Lined by Basic Groups and Open-Metal Sites. *Inorg. Chem.* **2018**, *57* (9), 5267–5272.
- (38) Liang, Y.; Harrison, D. P.; Gupta, R. P.; Green, D. a.; McMichael, W. J. Carbon Dioxide Capture Using Dry Sodium-Based Sorbents. *Energy Fuels* **2004**, *18* (2), 569–575.
- (39) Zhao, C.; Chen, X.; Zhao, C. Study on CO<sub>2</sub> Capture Using Dry Potassium-Based Sorbents through Orthogonal Test Method. *Int. J. Greenhouse Gas Control* **2010**, *4* (4), 655–658.
- (40) Choi, S.; Drese, J. H.; Jones, C. W. Adsorbent Materials for Carbon Dioxide Capture from Large Anthropogenic Point Sources. *ChemSusChem* **2009**, *2* (9), 796–854.
- (41) Ahmadvpour, A.; Do, D. D. The Preparation of Active Carbons from Coal by Chemical and Physical Activation. *Carbon* **1996**, *34* (4), 471–479.
- (42) Creamer, A. E.; Gao, B. Carbon-Based Adsorbents for Postcombustion CO<sub>2</sub> Capture: A Critical Review. *Environ. Sci. Technol.* **2016**, *50* (14), 7276–7289.
- (43) Sevilla, M.; Al-Jumaily, A. S. M.; Fuertes, A. B.; Mokaya, R. Optimization of the Pore Structure of Biomass-Based Carbons in Relation to Their Use for CO<sub>2</sub> Capture under Low- and High-Pressure Regimes. *ACS Appl. Mater. Interfaces* **2018**, *10* (2), 1623–1633.
- (44) Sevilla, M.; Sangchoom, W.; Balahmar, N.; Fuertes, A. B.; Mokaya, R. Highly Porous Renewable Carbons for Enhanced Storage of Energy-Related Gases (H<sub>2</sub> and CO<sub>2</sub>) at High Pressures. *ACS Sustain. Chem. Eng.* **2016**, *4* (9), 4710–4716.
- (45) Xiao, P.-W.; Guo, D.; Zhao, L.; Han, B.-H. Soft Templating Synthesis of Nitrogen-Doped Porous Hydrothermal Carbons and Their Applications in Carbon Dioxide and Hydrogen Adsorption. *Microporous Mesoporous Mater.* **2016**, *220*, 129–135.
- (46) Boyjoo, Y.; Cheng, Y.; Zhong, H.; Tian, H.; Pan, J.; Pareek, V. K.; Jiang, S. P.; Lamonier, J.-F.; Jaroniec, M.; Liu, J. From Waste Coca Cola® to Activated Carbons with Impressive Capabilities for CO<sub>2</sub> Adsorption and Supercapacitors. *Carbon* **2017**, *116*, 490–499.
- (47) Bellemare, M. F.; Çakir, M.; Peterson, H. H.; Novak, L.; Rudi, J. On the Measurement of Food Waste. *Am. J. Agricultural Economics* **2017**, *99* (5), 1148–1158.
- (48) Sevilla, M.; Parra, J. B.; Fuertes, A. B. Assessment of the Role of Micropore Size and N-Doping in CO<sub>2</sub> Capture by Porous Carbons. *ACS Appl. Mater. Interfaces* **2013**, *5* (13), 6360–6368.
- (49) Yaumi, A. L.; Bakar, M. Z. A.; Hameed, B. H. Melamine-Nitrogenated Mesoporous Activated Carbon Derived from Rice Husk for Carbon Dioxide Adsorption in Fixed-Bed. *Energy* **2018**, *155*, 46–55.

- (50) Ello, A. S.; de Souza, L. K. C.; Trokourey, A.; Jaroniec, M. Development of Microporous Carbons for CO<sub>2</sub> Capture by KOH Activation of African Palm Shells. *J. CO<sub>2</sub> Util.* **2013**, *2*, 35–38.
- (51) Li, D.; Ma, T.; Zhang, R.; Tian, Y.; Qiao, Y. Preparation of Porous Carbons with High Low-Pressure CO<sub>2</sub> Uptake by KOH Activation of Rice Husk Char. *Fuel* **2015**, *139*, 68–70.
- (52) Sevilla, M.; Fuertes, A. B. Sustainable Porous Carbons with a Superior Performance for CO<sub>2</sub> Capture. *Energy Environ. Sci.* **2011**, *4* (5), 1765–1771.
- (53) Wang, R.; Wang, P.; Yan, X.; Lang, J.; Peng, C.; Xue, Q. Promising Porous Carbon Derived from Celuce Leaves with Outstanding Supercapacitance and CO<sub>2</sub> Capture Performance. *ACS Appl. Mater. Interfaces* **2012**, *4* (11), 5800–5806.
- (54) Hong, S.-M.; Jang, E.; Dysart, A. D.; Pol, V. G.; Lee, K. B. CO<sub>2</sub> Capture in the Sustainable Wheat-Derived Activated Microporous Carbon Compartments. *Sci. Reports* **2016**, *6* (1).
- (55) Tsai, J.-H.; Jeng, F.-T.; Chiang, H.-L. Removal of H<sub>2</sub>S from Exhaust Gas by Use of Alkaline Activated Carbon. *Adsorption* **2001**, *7* (4), 357–366.
- (56) Guo, J.; Luo, Y.; Lua, A. C.; Chi, R.; Chen, Y.; Bao, X.; Xiang, S. Adsorption of Hydrogen Sulphide (H<sub>2</sub>S) by Activated Carbons Derived from Oil-Palm Shell. *Carbon* **2007**, *45* (2), 330–336.
- (57) Castrillon, M. C.; Moura, K. O.; Alves, C. A.; Bastos-Neto, M.; Azevedo, D. C. S.; Hofmann, J.; Möllmer, J.; Einicke, W.-D.; Gläser, R. CO<sub>2</sub> and H<sub>2</sub>S Removal from CH<sub>4</sub>-Rich Streams by Adsorption on Activated Carbons Modified with K<sub>2</sub>CO<sub>3</sub>, NaOH, or Fe<sub>2</sub>O<sub>3</sub>. *Energy Fuels* **2016**, *30* (11), 9596–9604.
- (58) Sethupathi, S.; Zhang, M.; Rajapaksha, A.; Lee, S.; Mohamad Nor, N.; Mohamed, A.; Al-Wabel, M.; Lee, S.; Ok, Y. Biochars as Potential Adsorbers of CH<sub>4</sub>, CO<sub>2</sub> and H<sub>2</sub>S. *Sustainability* **2017**, *9* (1), 121–131.
- (59) Bagreev, A.; Bandosz, T. J. Study of Hydrogen Sulfide Adsorption on Activated Carbons Using Inverse Gas Chromatography at Infinite Dilution. *J. Phys. Chem. B* **2000**, *104* (37), 8841–8847.
- (60) Bandosz, T. J.; Bagreev, A.; Adib, F.; Turk, A. Unmodified versus Caustics-Impregnated Carbons for Control of Hydrogen Sulfide Emissions from Sewage Treatment Plants. *Environ. Sci. Technol.* **2000**, *34* (6), 1069–1074.
- (61) Bagreev, A.; Bashkova, S.; Locke, D. C.; Bandosz, T. J. Sewage Sludge-Derived Materials as Efficient Adsorbents for Removal of Hydrogen Sulfide. *Environ. Sci. Technol.* **2001**, *35* (7), 1537–1543.
- (62) Habeeb, O. A.; Ramesh, K.; Ali, G. A. M.; Yunus, R. M.; Thanusha, T. K.; Olalere, O. A. Modeling and Optimization for H<sub>2</sub>S Adsorption from Wastewater Using Coconut Shell Based Activated Carbon. *Aust. J. Basic Applied Sci.* **2016**, *10* (17), 136–147.
- (63) Shang, G.; Li, Q.; Liu, L.; Chen, P.; Huang, X. Adsorption of Hydrogen Sulfide by Biochars Derived from Pyrolysis of Different Agricultural/Forestry Wastes. *J. Air Waste Manage Assoc.* **2016**, *66* (1), 8–16.
- (64) Mochizuki, T.; Kubota, M.; Matsuda, H.; D'Elia Camacho, L. F. Adsorption Behaviors of Ammonia and Hydrogen Sulfide on Activated Carbon Prepared from Petroleum Coke by KOH Chemical Activation. *Fuel Process. Technol.* **2016**, *144*, 164–169.
- (65) Zhang, J. ping; Sun, Y.; Woo, M. W.; Zhang, L.; Xu, K. Z. Preparation of Steam Activated Carbon from Black Liquor by Flue Gas Precipitation and Its Performance in Hydrogen Sulfide Removal: Experimental and Simulation Works. *J. Taiwan Inst. Chem. Eng.* **2016**, *59*, 395–404.
- (66) Przepiorski, J.; Oya, A. K<sub>2</sub>CO<sub>3</sub>-Loaded Deodorizing Activated Carbon Fibre Against H<sub>2</sub>S Gas: Factors Influencing the Deodorizing Efficiency and the Regeneration Method. *J. Mater. Sci. Lett.* **1998**, *17* (8), 679–682.
- (67) Sethupathi, S.; Zhang, M.; Rajapaksha, A. U.; Lee, S. R.; Nor, N. M.; Mohamed, A. R.; Al-Wabel, M.; Lee, S. S.; Ok, Y. S. Biochars as Potential Adsorbers of CH<sub>4</sub>, CO<sub>2</sub> and H<sub>2</sub>S. *Sustainability (Switzerland)* **2017**, *9* (1), 1–10.
- (68) Lyons, K.; Swann, G.; Levett, C. Produced but Never Eaten: A Visual Guide to Food Waste. *The Guardian*. Aug. 12, 2015.
- (69) Global CCS Institute. Data & knowledge. <https://www.globalccsinstitute.com/consultancy/our-services/data-knowledge/> (accessed Feb 18, 2019).
- (70) National Energy Technology Laboratory. Post-combustion CO<sub>2</sub> Capture <https://www.netl.doe.gov/research/coal/carbon-capture/post-combustion> (accessed Aug 30, 2018).
- (71) Zevenhoven, R.; Kilpinen, P. *Control of Pollutants in Flue Gases and Fuel Gases*; Helsinki University of Technology: Espoo, 2001.
- (72) Burwell, R. L. Manual of Symbols and Terminology for Physicochemical Quantities and Units—Appendix II. *Pure and Appl. Chem.* **1976**, *46*, 71–90.
- (73) Zdravkov, B.; Čermák, J.; Šefara, M.; Janků, J. Pore Classification in the Characterization of Porous Materials: A Perspective. *Open Chem.* **2007**, *5* (2), 385–395.
- (74) Gilbert, M. T.; Knox, J. H.; Kaur, B. Porous Glassy Carbon, a New Columns Packing Material for Gas Chromatography and High-Performance Liquid Chromatography. *Chromatographia* **1982**, *16* (1), 138–146.
- (75) Liang, C.; Hong, K.; Guiochon, G. A.; Mays, J. W.; Dai, S. Synthesis of a Large-Scale Highly Ordered Porous Carbon Film by Self-Assembly of Block Copolymers. *Angew. Chem. Int. Ed.* **2004**, *43* (43), 5785–5789.
- (76) Zhang, Y.; Liu, L.; Van der Bruggen, B.; Yang, F. Nanocarbon Based Composite Electrodes and Their Application in Microbial Fuel Cells. *J. Mater. Chem. A* **2017**, *5* (25), 12673–12698.
- (77) Wang, L.; Yang, R. T. Significantly Increased CO<sub>2</sub> Adsorption Performance of Nanostructured Templated Carbon by Tuning Surface Area and Nitrogen Doping. *J. Phys. Chem. C* **2012**, *116* (1), 1099–1106.
- (78) Bagshaw, S. a; Prouzet, E.; Pinnavaia, T. J. Templating of Mesoporous Molecular Sieves by Nonionic Polyethylene Oxide Surfactants. *Science (New York, N.Y.)* **1995**, *269* (5228), 1242–1244.
- (79) Tanaka, S.; Nakatani, N.; Doi, A.; Miyake, Y. Preparation of Ordered Mesoporous Carbon Membranes by a Soft-Templating Method. *Carbon* **2011**, *49* (10), 3184–3189.

- (80) Liang, C.; Dai, S. Synthesis of Mesoporous Carbon Materials via Enhanced Hydrogen-Bonding Interaction. *J. Am. Chem. Soc.* **2006**, *128* (16), 5316–5317.
- (81) Liu, J.; Yang, T.; Wang, D. W.; Lu, G. Q.; Zhao, D.; Qiao, S. Z. A Facile Soft-Template Synthesis of Mesoporous Polymeric and Carbonaceous Nanospheres. *Nat. Commun.* **2013**, *4*, 1–7.
- (82) Kubo, S.; White, R. J.; Yoshizawa, N.; Antonietti, M.; Titirici, M. M. Ordered Carbohydrate-Derived Porous Carbons. *Chem. Mater.* **2011**, *23* (22), 4882–4885.
- (83) Yan, H. Soft-Templating Synthesis of Mesoporous Graphitic Carbon Nitride with Enhanced Photocatalytic H<sub>2</sub> Evolution under Visible Light. *Chem. Commun.* **2012**, *48* (28), 3430–3432.
- (84) Xiao, P. W.; Guo, D.; Zhao, L.; Han, B. H. Soft Templating Synthesis of Nitrogen-Doped Porous Hydrothermal Carbons and Their Applications in Carbon Dioxide and Hydrogen Adsorption. *Microporous Mesoporous Mater.* **2016**, *220*, 129–135.
- (85) Deng, J.; Li, M.; Wang, Y. Biomass-Derived Carbon: Synthesis and Applications in Energy Storage and Conversion. *Green Chem.* **2016**, *18* (18), 4824–4854.
- (86) Xiao, P. W.; Guo, D.; Zhao, L.; Han, B. H. Soft Templating Synthesis of Nitrogen-Doped Porous Hydrothermal Carbons and Their Applications in Carbon Dioxide and Hydrogen Adsorption. *Microporous Mesoporous Mater.* **2016**, *220*, 129–135.
- (87) Li, R.; Shahbazi, A. A Review of Hydrothermal Carbonization of Carbohydrates for Carbon Spheres Preparation. *Trends Renew. Energ.* **2015**, *1* (1), 43–56.
- (88) Titirici, M.-M. *Sustainable Carbon Materials from Hydrothermal Processes*; John Wiley & Sons: London, 2013.
- (89) Yu, L.; Brun, N.; Sakaushi, K.; Eckert, J.; Titirici, M. M. Hydrothermal Nanocasting: Synthesis of Hierarchically Porous Carbon Monoliths and Their Application in Lithium–Sulfur Batteries. *Carbon* **2013**, *61*, 245–253.
- (90) Titirici, M.-M.; Thomas, A.; Antonietti, M. Replication and Coating of Silica Templates by Hydrothermal Carbonization. *Adv. Funct. Mater.* **2007**, *17* (6), 1010–1018.
- (91) Jun, S.; Joo, S. H.; Ryoo, R.; Kruk, M.; Jaroniec, M.; Liu, Z.; Ohsuna, T.; Terasaki, O. Synthesis of New, Nanoporous Carbon with Hexagonally Ordered Mesostructure. *J. Am. Chem. Soc.* **2000**, *122* (43), 10712–10713.
- (92) Titirici, M.-M.; Thomas, A.; Antonietti, M. Aminated Hydrophilic Ordered Mesoporous Carbons. *J. Mater. Chem.* **2007**, *17* (32), 3412–3418.
- (93) Demir-Cakan, R.; Baccile, N.; Antonietti, M.; Titirici, M.-M. Carboxylate-Rich Carbonaceous Materials via One-Step Hydrothermal Carbonization of Glucose in the Presence of Acrylic Acid. *Chem. Mater.* **2009**, *21* (3), 484–490.
- (94) Demir-Cakan, R.; Makowski, P.; Antonietti, M.; Goettmann, F.; Titirici, M.-M. Hydrothermal Synthesis of Imidazole Functionalized Carbon Spheres and Their Application in Catalysis. *Catal. Today* **2010**, *150* (1), 115–118.
- (95) Yang, Z.; Xia, Y.; Sun, X.; Mokaya, R. Preparation and Hydrogen Storage Properties of Zeolite-Templated Carbon Materials Nanocast via Chemical Vapor Deposition: Effect of the Zeolite Template and Nitrogen Doping. *J. Phys. Chem. B* **2006**, *110* (37), 18424–18431.
- (96) Baerlocher Ch.; McCusker, L.B. Database of Zeolite Structures <http://www.iza-structure.org/databases/> (accessed Jul 6, 2018).
- (97) Gaslain, F. O. M.; Parmentier, J.; Valtchev, V. P.; Patarin, J. First Zeolite Carbon Replica with a Well Resolved X-Ray Diffraction Pattern. *Chem. Commun.* **2006**, *0* (9), 991–993.
- (98) Nishihara, H.; Kyotani, T. Zeolite-Templated Carbons-Three-Dimensional Microporous Graphene Frameworks. *Chem. Commun.* **2018**, *54* (45), 5648–5673.
- (99) Kim, K.; Lee, T.; Kwon, Y.; Seo, Y.; Song, J.; Park, J. K.; Lee, H.; Park, J. Y.; Ihee, H.; Cho, S. J.; et al. Lanthanum-Catalysed Synthesis of Microporous 3D Graphene-like Carbons in a Zeolite Template. *Nature* **2016**, *535* (7610), 131–135.
- (100) PE De Jongh, P. E. Miniature Structures Meticulously Replicated in Carbon. *NPG Asia Materials* **2017**, *9* (1), 339–339.
- (101) Inagaki, M.; Kang, F.; Toyoda, M.; Konno, H. *Advanced Materials Science and Engineering of Carbon. Chapter 7 - Template Carbonization: Morphology and Pore Control*. In *Adv. Mater. Sci. Eng. Carbon*, Boston, 2014, 133–163.
- (102) Van Tendeloo, L.; Gobechiya, E.; Breyneart, E.; Martens, J. a; Kirschhock, C. E. a. Alkaline Cations Directing the Transformation of FAU Zeolites into Five Different Framework Types. *Chem. Commun.* **2013**, *49* (100), 11737–11739.
- (103) Wilson, S. T.; Lok, B. M.; Messina, C. A.; Cannan, T. R.; Flanigen, E. M. Aluminophosphate Molecular Sieves: A New Class of Microporous Crystalline Inorganic Solids. *J. Am. Chem. Soc.* **1982**, *104* (4), 1146–1147.
- (104) Davis, M. E. Ordered Porous Materials for Emerging Applications. *Nature* **2002**, *417* (6891), 813–821.
- (105) Winiiecki, A. M.; Suib, S. L. Chemical Stability of Aluminophosphate Molecular Sieves during HCl Treatment. *Langmuir* **1989**, *5*, 333–338.
- (106) Liu, G.; Liu, Y.; Zhang, X.; Yuan, X.; Zhang, M.; Zhang, W.; Jia, M. Characterization and Catalytic Performance of Porous Carbon Prepared Using in Situ-Formed Aluminophosphate Framework as Template. *J. Colloid Interface Sci.* **2010**, *342* (2), 467–473.
- (107) Tang, Z. K.; Wang, N.; Zhang, X. X.; Wang, J. N.; Chan, C. T.; Sheng, P. Novel Properties of 0.4 Nm Single-Walled Carbon Nanotubes Templated in the Channels of AlPO<sub>4</sub>-5 Single Crystals. *New J. Phys.* **2003**, *5*, 146–146.
- (108) Kyotani, T.; Ma, Z.; Tomita, A. Template Synthesis of Novel Porous Carbons Using Various Types of Zeolites. *Carbon* **2003**, *41* (7), 1451–1459.
- (109) Lok, B. M.; Messina, C. A.; Patton, R. L.; Gajek, R. T.; Cannan, T. R.; Flanigen, E. M. Silicoaluminophosphate Molecular Sieves: Another New Class of Microporous Crystalline Inorganic Solids. *J. Am. Chem. Soc.* **1984**, *0* (8), 6092–6093.

- (110) Chen, J.; Wright, P. A.; Thomas, J. M.; Natarajan, S.; Marchese, L.; Bradley, S. M.; Sankar, G.; Catlow, C. R. A.; Gai-Boyes, P. L. SAPO-18 Catalysts and Their Brønsted Acid Sites. *J. Phys. Chem.* **1994**, *98* (40), 10216–10224.
- (111) Dzwigaj, S.; Briend, M.; Shikholeslami, A.; Peltre, M. J.; Barthomeuf, D. The Acidic Properties of SAPO-37 Compared to Faujasites and SAPO-5. *Zeolites* **1990**, *10* (3), 157–162.
- (112) Briend, M.; Shikholeslami, A.; Peltre, M.-J.; Delafosse, D.; Barthomeuf, D. Thermal and Hydrothermal Stability of SAPO-5 and SAPO-37 Molecular Sieves. *J. Chem. Soc., Dalton Trans.* **1989**, *7*, 1361–1362.
- (113) Braun, E.; Lee, Y.; Moosavi, S. M.; Barthel, S.; Mercado, R.; Baburin, I. A.; Proserpio, D. M.; Smit, B. Generating Carbon Schwarzites via Zeolite-Templating. *Proc. Natl. Acad. Sci. U.S.A.* **2018**, *115* (35), 8116–8124.
- (114) Fechler, N.; Fellinger, T. P.; Antonietti, M. “salt Templating”: A Simple and Sustainable Pathway toward Highly Porous Functional Carbons from Ionic Liquids. *Adv. Mater.* **2013**, *25* (1), 75–79.
- (115) Estermann, M. A.; McCusker, L. B.; Baerlocher, C. Ab Initio Structure Determination from Severely Overlapping Powder Diffraction Data. *J. Appl. Crystallogr.* **1992**, *25* (4), 539–543.
- (116) Bennett, J. M.; Marcus, B. K. The Crystal Structures of Several Metal Aluminophosphate Molecular Sieves. In *Studies in Surface Science and Catalysis*; Grobet, P. J., Mortier, W. J., Vansant, E. F., Schulz-Ekloff, G., Eds.; Innovation in Zeolite Materials Science; Elsevier: 1988; Vol. 37, pp 269–279.
- (117) Akolekar, B.; Kaliaguine, S. Synthesis, Characterization, Thermal Stability, Acidity and Catalytic Properties of Large-Pore MAPO-46. *J. Chem. Soc., Faraday Trans.* **1993**, *89*, 4141–4147.
- (118) Akolekar, D. B. Novel, Crystalline, Large-Pore Magnesium Aluminophosphate Molecular Sieve of Type 50: Preparation, Characterization, and Structural Stability. *Zeolites* **1995**, *15* (7), 583–590.
- (119) Novak Tušar, N.; Ristić, A.; Meden, A.; Kaučič, V. Large-Pore Molecular Sieve MnAPO-50: Synthesis, Single-Crystal Structure Analysis and Thermal Stability. *Microporous Mesoporous Mater.* **2000**, *37* (3), 303–311.
- (120) Arcon, I.; Tusar, N. N.; Ristić, A.; Kaucic, V.; Kodre, A.; Helliwell, M. Incorporation of Mn, Co and Zn Cations into Large-Pore Aluminophosphate Molecular Sieves MeAPO-50. *J. Synchrotron Rad.* **2001**, *8*, 590–592.
- (121) Broach, R. W.; Greenlay, N.; Jakubczak, P.; Knight, L. M.; Miller, S. R.; Mowat, J. P. S.; Stanczyk, J.; Lewis, G. J. New ABC-6 Net Molecular Sieves ZnAPO-57 and ZnAPO-59: Framework Charge Density-Induced Transition from Two- to Three-Dimensional Porosity. *Microporous Mesoporous Mater.* **2014**, *189*, 49–63.
- (122) Bieniok, A.; Brendel, U.; Paulus, E. F.; Amthauer, G. Microporous cobalto- and zincophosphates with the framework-type of cancrinite. *Eur. J. Mineral.* **2005**, *17* (6), 813–818.
- (123) Yakubovich, O.; Karimova, O.; Melnikov, O. A new representative of the cancrinite family (Cs,K)0.33[Na0.18Fe0.16(H2O)1.05]{ZnPO4}: Preparation and crystal structure. *Crystallogr. Rep.* **1994**, *39* (4), 630–634.
- (124) Yoshino, M.; Matsuda, M.; Miyake, M. Effect of Transition Metal Doping on Crystallization of Cloverite. *Solid State Ionics.* **2002**, *151* (1), 269–274.
- (125) Wei, Y.; Tian, Z.; Gies, H.; Xu, R.; Ma, H.; Pei, R.; Zhang, W.; Xu, Y.; Wang, L.; Li, K.; et al. Ionothermal Synthesis of an Aluminophosphate Molecular Sieve with 20-Ring Pore Openings. *Angew. Chem. Int. Ed.* **2010**, *49* (31), 5367–5370.
- (126) Feng, P.; Bu, X.; Stucky, G. D. Hydrothermal Syntheses and Structural Characterization of Zeolite Analogue Compounds Based on Cobalt Phosphate. *Nature* **1997**, *388* (6644), 735–741.
- (127) Harrison, W. T. A.; Gier, T. E.; Moran, K. L.; Nicol, J. M.; Eckert, H.; Stucky, G. D. Structures and Properties of New Zeolite X-Type Zincophosphate and Beryllphosphate Molecular Sieves. *Chem. Mater.* **1991**, *3* (1), 27–29.
- (128) Venkatathri, N. Synthesis and Characterization of AlPO<sub>4</sub>-n Molecular Sieves from Hexamethyleneimine Template. *Indian J. Chem.* **2002**, *41A*, 2223–2230.
- (129) Afeworki, M.; Dorset, D. L.; Kennedy, G. J.; Strohmaier, K. G. Synthesis and Structure of ECR-40: An Ordered Sapo Having the MEI Framework. In *Studies in Surface Science and Catalysis*; van Steen, E., Claeys, M., Callanan, L. H., Eds.; Recent Advances in the Science and Technology of Zeolites and Related Materials Part B; Elsevier, 2004; Vol. 154, pp 1274–1281.
- (130) Zhang, Z.; Feng, J.; Jiang, Y.; Feng, J. High-Pressure Salt Templating Strategy toward Intact Isochoric Hierarchically Porous Carbon Monoliths from Ionic Liquids. *RSC Adv.* **2017**, *7* (81), 51096–51103.
- (131) Kumar, K. V.; Gadipelli, S.; Preuss, K.; Porwal, H.; Zhao, T.; Guo, Z. X.; Titirici, M. M. Salt Templating with Pore Padding: Hierarchical Pore Tailoring towards Functionalised Porous Carbons. *ChemSusChem* **2017**, *10* (1), 199–209.
- (132) Williams, D. B.; Carter, C. B. *Transmission Electron Microscopy: A Textbook for Materials Science*, 2nd ed.; Springer: New York, 2008.
- (133) Berger, S. D.; McKenzie, D. R.; Martin, P. J. EELS Analysis of Vacuum Arc-Deposited Diamond-like Films. *Philos. Mag. Lett.* **1988**, *57* (6), 285–290.

## Biochar as sustainable platform for pyrolysis vapours upgrading

Christian Di Stasi, Gianluca Greco, Belén Gonzalez, Joan J. Manyà

Aragón Institute of Engineering Research (I3A), University of Zaragoza, crta. Cuarte s/n, Huesca E-22071, Spain

### Abstract

Thanks to their potential applications in catalysis, adsorption and energy storage, porous carbon materials are considered promising candidates to address environmental issues related to global warming and pollution. The main problem is that their production frequently involves carbon fossil feedstocks and high energy demand synthesis procedures. An interesting alternative pathway to obtain such materials is the slow pyrolysis of biomass with production of a carbon-rich solid product, called "biochar". According to the different final applications, biochar may need a post-production treatment (activation) aimed at improving some properties (i.e., the specific surface area or the surface functional groups). Slow pyrolysis not only produce biochar but also a gas stream and a high oxygenated liquid called "bio-oil". The presence of a liquid phase leads to low yields of gas and solid and, moreover, it can condensate inside the pipelines, causing clogging problems. One of the most interesting application of the biochar is the production of a biochar-based metal catalyst for upgrading of pyrolytic vapours through catalytic steam/dry reforming. The specific aim of this chapter is to give an overview on the different types of activated biochars and on their application in bio-oil upgrading processes.

### 1. Introduction

Carbon materials, such as carbon nanotubes, amorphous carbons and activated carbons, are considered good candidates for adsorption and/or catalytic applications. The main drawback is that their production can involve electrochemical treatment or organic solvents, which make difficult the commercialisation of such materials. Furthermore, they often require carbon fossil precursors, which are not environmentally sustainable options.

An alternative to the above-mentioned route is to produce carbon materials starting from biomass and, through a thermal process, which leads to the carbonisation of the organic matter, producing biochar. The word *biochar* refers to a carbon-rich product when biomass such as wood, manure or leaves is heated in a closed container with little or unavailable air<sup>1</sup>. It represents a suitable way for the long-term storage of carbon matter. The production of biochar can be obtained through different processes such as fast and slow pyrolysis, which were already discussed in Chapter 1, and hydrothermal carbonisation, described in Chapter 6.

### 2. Biochar production

Pyrolysis operating conditions have a key role in the products distribution. Choosing the best combination of peak temperature, heating rate, pressure and inert gas used, it is possible to address the process to the production of more bio-oil, gases, or biochar. In many studies, it is accepted that high temperatures and high heating rates promote the formation of volatile compounds, whereas low temperatures and low heating rates increase the yield of biochar. On the other hand, also the composition of original biomass is responsible for the final distribution of the products. For example, pyrolysis of biomass with a high lignin content offers high yields of biochar.<sup>2</sup>

The whole pyrolysis process involves decomposition reactions of the three main components of the lignocellulosic feedstock: cellulose, hemicelluloses and

lignin. Due to the complexity of the whole reaction system and to the possibility of interactions between the intermediate reaction products, in literature, the degradation pathways of the three components are studied separately. Each reaction is classified depending on when it takes place. Following this criterion, they are labelled as primary or secondary reactions.

Primary reactions involve the degradation and rupture of the bonds within the biomass constituents. Collard and Blin<sup>3,4</sup>, in their review, categorised the primary reactions in three different type: reactions that leads to char formation, depolymerisation and fragmentation.

The char formation is due to the production of benzene molecules and other aromatic compounds with subsequent rearrangement of these molecules in a polycyclic structure, followed by the release of water and permanent gases<sup>5</sup>.

Depolymerisation reactions occur when the bonds between the monomers of the original biopolymer are broken. These reactions lead to a decrease of the polymerisation degree. The obtained products are smaller molecules if compared with the original ones, which are recovered in the pyrolysis liquid. The formation of permanent gases is due to the rupture of covalent bonds within the polymers (i.e. fragmentation reactions). Besides permanent gases, condensable molecules like acids and alcohols are produced too.

When the products of primary reactions are not chemically stable under pyrolysis conditions, they undergo further transformations. The reactions in series of all the above-mentioned are called "secondary reactions". Such reactions mainly involve thermal cracking and other recombination reactions. Cracking essentially consists on the rupture of the bonds within the molecules, obtaining compounds with a lower molar weight. On the other hand, recombination reactions between volatile molecules lead to the formation of higher molecular weight products which are likely to condense above the char structure, resulting in the so-called "secondary char formation".

This section is only aimed to give a brief overview about the main reactions involved in biochar production. More detailed information is available in Chapter 4.

### 3. Biochar Characterisation

A deep characterisation of biochar is an essential step to evaluate its suitability for further applications. The first analysis that is usually performed is the assessment of the amount of moisture, ash, volatile matter and fixed-carbon. These values are obtained by means of a proximate analysis. The measurement can be performed in accordance with the American Society for Testing and Materials (ASTM) standards. However, for a detailed description of the procedures, Cai et al.<sup>6</sup> provided a complete review on this topic.

Proximate analysis is usually used to evaluate, in a preliminary way, the characteristics of the biochar; however, it should be necessary to perform additional characterisations for a given application. For example, when the biochar is produced for catalytic purposes, it is very important to investigate both bulk and surface properties of the solid. For the morphological characterisation of biochar, the most used techniques are the transmission electron microscopy (TEM) and scanning electron microscopy (SEM)<sup>7,8</sup>. Bulk chemical characterisation can be done using Raman spectroscopy, solid-state <sup>13</sup>C and <sup>1</sup>H nuclear magnetic resonance (NMR)<sup>9</sup> and X-ray diffraction (XRD)<sup>10</sup>.

The textural properties (i.e., specific surface area and pore size distribution) can be evaluated from the adsorption isotherm of N<sub>2</sub> at -196 °C, using BET and DFT models. However, nitrogen at cryogenic temperatures cannot access the small micropores. Thus, the volume of narrower micropores (pore size below 0.7 nm) should be estimated from the CO<sub>2</sub> adsorption isotherm at 0 °C<sup>11,12</sup>.

Bulk composition of inorganics is assessed using inductively coupled plasma atomic emission spectroscopy (ICP-AES)<sup>13</sup> or X-ray fluorescence (XRF)<sup>14</sup>.

The elemental analysis for carbon, hydrogen, oxygen, nitrogen and sulphur (CHNS analysis) are usually determined by oxidation methods (combustion analysis)<sup>15</sup>. Pristine biochar can contain different surface functional groups, depending on the production conditions. Such functional groups can interact with the reactants/products of a specific reaction, leading to an increase in the selectivity of the process. In other words, it is possible to produce a high selective catalyst by adding chemical functional groups on the surface of the biochar. The identification and quantification of these groups is obtained using X-ray photoemission spectroscopy (XPS)<sup>16</sup>, Boehm titration<sup>8</sup>, Fourier transform infrared spectroscopy (FTIR)<sup>17</sup>, and temperature-programmed desorption (TPD)<sup>18</sup>. Table 1 summarises all the techniques that can be employed in biochar characterisation.

**Table 1.** Most used techniques for the characterisation of bulk and surface of biochar.

Proximate analysis	
Moisture	ASTM standard E1756-08
Volatile matter	ASTM standard E872-82
Ash content	ASTM standard E1755-01
Fixed carbon	Determined by difference
Structure	
Macro analysis	SEM, TEM
Micro analysis	XRD, Raman, NMR
Surface area	BET (N <sub>2</sub> at 77K and CO <sub>2</sub> at 273 K)
Functional groups	
Surface functional groups	XPS, FTIR, TPD, Boehm titration
Elemental Composition	
Bulk inorganics	ICP-AES, XRF
CHNS-O	Combustion analysis

### 4. Biochar Activation

Generally, raw biochar has only a limited number of functional groups, such as C=O, OH and COOH, and a relatively specific surface area mainly dominated by narrow micropores. These poor properties hinder the direct application of biochar in different fields such as catalysis and adsorption, in which the presence of specific functional groups on the surface and of a hierarchical pore size distribution is mandatory.

Nevertheless, biochar can be easily activated by means of chemical or physical processes aimed at introducing some specific functional groups and increase the solid textural properties. Fig. 1 illustrates the different pathways to produce a biochar-derived activated carbon depending on its final application.

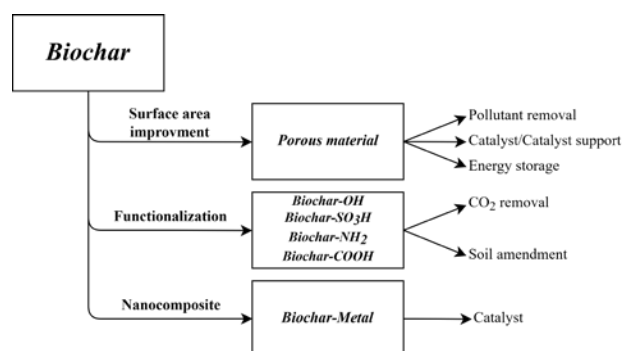


**Figure 1.** Main pathways and applications of raw biochar.

#### 4.1. Development of surface area

As stated before, biochar is a good platform to produce activated carbons via physical or chemical activations. In order to avoid structural and chemical modification during its utilisation, it is extremely important that the activation procedure has to be carried out under temperatures and pressures not lower than those used in the final application of the activated biochar.

#### 4.1.1. Physical activation

Physical activation is the process in which the development of porosity is obtained by a controlled gasification of the solid through an oxidising agent such as CO<sub>2</sub> or steam. In practice, carbon atoms present on the surface are converted into gaseous species, leading to the formation of a porous structure. Generally, the physical activation is performed exposing the biochar to the activating agent under high temperatures (700–900 °C)<sup>19,20</sup>. The main reactions involved in the physical activation process are:



The extent of the gasification process, which is a function of different variables such as soaking time, temperature and activating agent, is evaluated through the “burn-off degree”, which is defined as the relative difference between the initial and the final mass of biochar.

Table 2 reports some results of physical activations reported in literature, which clearly show that, through physical activation, it is possible to produce activated carbons with relatively high specific surface areas.

**Table 2.** Some examples from literature of physically activated biochars (initial and final  $S_{\text{BET}}$  values, in  $\text{m}^2 \text{g}^{-1}$ , correspond to the  $S_{\text{BET}}$  measured for raw and activated biochar, respectively).

Biomass	Agent	Temp. (°C)	Time (min)	Initial $S_{\text{BET}}$	Final $S_{\text{BET}}$	Ref.
Olive stones	CO <sub>2</sub>	800	120	43	1079	20
Almond shell	CO <sub>2</sub>	700	–	21	1090	21
Oak wood	CO <sub>2</sub>	900	120	107	1126	22
Coconut shell	CO <sub>2</sub>	800	60	–	720	23
Peanut hull	CO <sub>2</sub>	900	120	7	1308	19
Palm Shell	H <sub>2</sub> O	500	10	111	571	24
Wood waste	H <sub>2</sub> O/O <sub>2</sub>	900/200	60/30	50	1025	25

Since the reaction rate of water gasification (Reaction 1) is faster than CO<sub>2</sub> gasification (Reaction 2), the activation process with steam is usually faster. Chang and co-workers<sup>26</sup> compared the results of the activation of a corn cob biochar with CO<sub>2</sub> and H<sub>2</sub>O. Their results showed that water activation led to the formation of a microporous structure, whereas with the employment of CO<sub>2</sub> as activating agent, it was possible to produce an activated carbon with a higher fraction of mesopores.

As stated before, the production of an activated carbon involves two different phases: the pyrolysis of biomass, and the partial gasification of the resulting biochar. Azuara et al.<sup>27</sup> studied the application of CO<sub>2</sub> as carrier gas during the pyrolysis of biomass. In this way, it is possible to

produce and activate the biochar at the same time in a single-step process as well as recycling CO<sub>2</sub> from residual flue gases and therefore avoiding the use of expensive inert gases (like N<sub>2</sub>). The biochar obtained from their experiments had a moderate high surface area ( $S_{\text{BET}} = 197 \text{ m}^2 \text{g}^{-1}$ ) and a microporous structure.

#### 4.1.2. Chemical Activation

When the activation of biochar is conducted using a chemical agent, which promotes the gasification of the solid (i.e., chemical activation), two different pathways are possible:

(1) Mixing the raw biomass with an activating agent followed by a heating step (under inert atmosphere) resulting in the production of activated biochar (see Fig. 2a).

(2) The biochar produced via pyrolysis is then mixed with the activating agent and heated again under inert atmosphere (see Fig. 2b).

Furthermore, it is also possible to distinguish between wet and dry mixing, depending on how the activating agent is added (as a solid or as an aqueous solution, respectively). The most used chemical agents are H<sub>3</sub>PO<sub>4</sub>, ZnCl<sub>2</sub>, KOH and NaOH. These agents, besides the benefits on the gasification step, have also dehydrating properties that can influence the pyrolysis vapours during the carbonisation process, increasing the carbon yield<sup>28</sup>. Despite the fact that these chemicals are the most studied, their employment at industrial scale has different drawbacks. Residual ZnCl<sub>2</sub> is not easily separated from the activated biochar, and this leads to pollution and waste disposal problems. H<sub>3</sub>PO<sub>4</sub> can cause an increased eutrophication if the char is finally applied for soil remediation purposes<sup>29</sup>. Furthermore, also the application of hydroxides, such as KOH and NaOH, is problematic because of corrosion issues<sup>30</sup>.

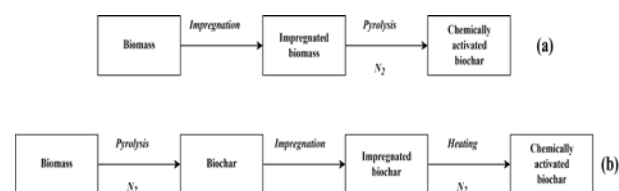


**Figure 2.** The two different ways to chemically activate a biochar (wet mixing): (a) starting from the impregnation of biomass or (b) starting from the raw biochar.

An interesting alternative is using K<sub>2</sub>CO<sub>3</sub>, which is a cheap and non-hazardous compound and already studied in literature<sup>31,32</sup>.

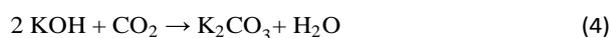
The first phase of the chemical activation process is the impregnation of the biomass/biochar that is usually carried out at 50 °C in order to enhance the diffusion of the agent inside the inner structure of the biochar. The following step is the separation of the impregnated biomass/biochar from the solution and its drying to remove the remaining water. Dehkoda et al.<sup>33</sup> found that the ratio between mesopores and micropores can be modulated by changing the drying atmosphere and duration. If air is used in the drying step, the carbon solid is characterised by the presence of both

micro- and mesopores. Furthermore, using N<sub>2</sub> it is possible to obtain a solid with a narrower pore size distribution in the range of micropores.

Chemical activation mechanism is not yet completely understood<sup>34</sup>. In the case of the activation with KOH, the porosity development can be ascribed to three different phenomena:

- (1) KOH can react with the carbon matrix, releasing CO and H<sub>2</sub>.
- (2) CO<sub>2</sub> and H<sub>2</sub>O resulting from the thermal degradation of biochar can react with KOH producing K<sub>2</sub>CO<sub>3</sub>, which can react with carbon to release more gaseous species.
- (3) The metallic K produced in situ can intercalate in the matrix of the biochar, leading to the formation of larger pores (after the removal of K species through an acidic solution).

These effects are the results of the Reactions 4–7<sup>35</sup>.



The most important parameter in this kind of activation is the amount of chemical agent used for the impregnation, the so-called impregnation ratio, which corresponds to the mass ratio between the chemical and precursor (biochar). The effects of using different impregnation ratios depend on the feedstock and the chemical agent. After the carbonisation step, the resulting activated carbon can still contain part of the activating agent or related compounds, which can clog the pores of the material and/or alter its pH. Thus, a cleaning step is required. For this purpose, a diluted acid solution is commonly used. However, in the case of water-soluble compounds like K<sub>2</sub>CO<sub>3</sub>, a rinse performed with hot water could be enough. The process temperature is a relevant parameter, since depending on the activation agent, it is possible to promote some reactions over others. Hayashi et al.<sup>30</sup> studied the influence of the carbonisation temperature on the pore size distribution of the produced activated carbon using K<sub>2</sub>CO<sub>3</sub>. The results showed that higher temperatures led to an increase in the total and mesopore volumes. Results from several previous studies (using different precursors and activating agents) are given in Table 3.

**Table 3.** Some results reported in literature of biochar chemical activation via wet impregnation (ratio is given in mass basis chemical/precursor;  $S_{\text{BET}}$  in m<sup>2</sup> g<sup>-1</sup>).

Biomass	Agent	Ratio	Temp. (°C)	Time (min)	$S_{\text{BET}}$	Ref.
Palm shell	K <sub>2</sub> CO <sub>3</sub>	1	800	120	1170	<sup>36</sup>
Soybean oil cake	KOH	1	800	60	618	<sup>32</sup>
Soybean oil cake	K <sub>2</sub> CO <sub>3</sub>	1	800	60	1352	<sup>32</sup>
Safflower seed	ZnCl <sub>2</sub>	4	900	60	802	<sup>37</sup>
Peach stones	H <sub>3</sub> PO <sub>4</sub>	0.43	800	60	1393	<sup>38</sup>
Apricot shell	NaOH	2	400	60	2335	<sup>39</sup>
Vine shoots	KOH	2	700	60	1671	<sup>12</sup>

#### 4.2. Biochar functionalisation

Some functional groups containing S, N, and O can be available in the raw biochar. These groups make the biochar suitable for adsorption and catalytic applications<sup>40</sup>. If the aim is to enhance the activity of the biochar, it is possible to add some interesting surface functional groups. For example, groups such as C=O, OH, COOH are important if the final purpose of the biochar is to be used as adsorbent for heavy-metal removal or when it has to be applied in aqueous systems.

The functionalisation can be done through surface oxidation, which is the most used method of carbon surface modification, using reactants such as air, O<sub>2</sub>, H<sub>2</sub>O<sub>2</sub><sup>41</sup> or O<sub>3</sub><sup>42</sup>. Usually, the process is carried out at high temperature (200–350 °C) using a continuous flow of oxidant agent followed by a rinse step with water to remove water-soluble products<sup>43</sup>.

During the production of a biochar-supported catalyst by impregnation, low dispersion of the active phase is usually obtained. This is mainly due to the fact that biochar surface has a hydrophobic behaviour, which hinders the homogeneous distribution of the metal particles. It was demonstrated that the addition of acidic groups on biochar surface leads to an increase in the hydrophilicity, making the surface more accessible to the aqueous solution of the active phase precursor<sup>44</sup> and resulting in a better dispersion of the metal on the biochar.

The introduction of sulphur functionalities is usually done by heating the carbonaceous material in presence of elemental sulphur or hydrogen sulphide<sup>45</sup>. SO<sub>3</sub>H group could be added using a concentrated sulphuric acid and the so-called “solid acid” can find applications in esterification reactions<sup>46,47</sup>, such as the production of biodiesel and hydrolysis of biomass.

The presence of amino groups on the surface of the biochar, on the other hand, can enhance the performance of CO<sub>2</sub> capture in gas-cleaning processes. The methods used to provide these groups to a carbon solid is the

nitration, using  $\text{HNO}_3$ , or a procedure that involves amino-containing reagents<sup>48</sup>.

Finally, halogen groups can also be added to the surface of biochar and the stability of the complex carbon-halogen decreases in the order chlorine > bromine > iodine<sup>43</sup>. The treatment can be carried out employing a halogen vapour or an aqueous solution of halogens. Chlorine, for example, can be incorporated into the surface of a carbon material by contact with a continuous flow of  $\text{Cl}_2$  at high temperature<sup>49</sup>.

### 4.3. Biochar-supported metal catalyst

As stated before, biochar and carbon material are, in general, a good platform to produce catalyst supports. Carbonaceous supports have different advantages over the traditional supports such as alumina and silica. For example, carbon surface is resistant to acid and basic agents and its structure is stable at high temperatures. Furthermore, the combustion of the spent catalyst allows the recovery of the active phase in an easy way<sup>43</sup>.

The active phase can be loaded on the support in two different ways:

- (1) By impregnation of the starting material (i.e., raw biomass) with a solution containing the active phase and subsequent carbonisation step, where the metal ions are reduced to zero oxidation state. In this case, the metal can also promote further char gasification (leading to a more porous product).
- (2) By impregnation of the pristine biochar. In this case, the catalyst must be activated by heating under a reducing atmosphere.

## 5. Pyrolysis Vapours

Bio-oil (also called as pyrolysis liquid) is a dark brown viscous liquid with a high concentration of oxygen-containing compounds, the presence of which is the main difference between a bio-oil and a conventional liquid fuel derived from fossil sources. Depending on its properties, the bio-oil can be used directly as low-grade fuel for diesel engines or gas turbines, transportation fuel or platform for the production of other chemicals. All these applications make the bio-oil feasible to replace the fossil oil in different fields or, at least, to reduce the world dependence on non-renewable resources.

Bio-oil is not the product of thermodynamic equilibrium, since it is produced at a relatively short residence time and is usually recovered through a quick quenching after the exit of the pyrolysis system. Therefore, the chemical composition of the bio-oil tends to change during its storage<sup>50</sup>.

The chemical composition of the biomass feedstock is an important factor, which has influence on the pyrolysis liquid yield. Furthermore, the ash content of the feedstock also affects the yield of bio-oil. In fact, the liquid yield is higher when the used biomass has a low content in ashes<sup>51</sup>. Moreover, also the liquid water-fraction increases when

alkaline compounds are present in the feedstock, leading, in some cases, to the formation of a double-phase bio-oil. Likewise, also pyrolysis temperature is an influent parameter that has to take into account. Higher temperatures result in a higher production of aromatic compounds, which, through condensation reactions, tend to create polyaromatic structures (see Fig. 3<sup>52</sup>).

With regards to the influence of the particles size of the feedstock, it was observed that using large particle sizes results in a decreased bio-oil yield. It is assumed that the “actual heating rate” experienced by biomass, which decreases with increasing particle size, is the major factor contributing to the decrease in the yield of pyrolysis liquid<sup>53</sup>.

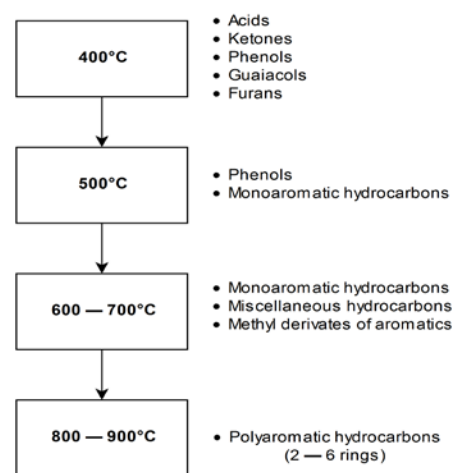


**Figure 3.** Influence of temperature on the distribution of pyrolysis products.

### 5.1. Pyrolysis liquid characterisation

Bio-oil is a multicomponent mixture of hundreds of organic compounds derived from the depolymerisation and fragmentation of the three main “bricks” of biomass: lignin, cellulose and hemicelluloses. Therefore, the composition strictly depends on the nature of the feedstock (in terms of its composition) and, to a lesser extent, of the operating conditions of pyrolysis.

The main compounds present in the mixture are alkanes, aromatic hydrocarbons, phenol derivatives and ketones, esters, ethers, sugars, amines, and alcohols. The collection of the liquid in lab-scale is usually conducted by condensation of the outlet stream from the reactor and the simpler configuration consists of one or more ice-cooled traps. An alternative method is the fractional condensation system, which consists on a series of condensers operating at different temperatures in which, typically, the first bottle is operating at a higher temperature in order to condensate only the heaviest fraction. In this way, it is possible to obtain a more accurate separation of the compounds based on the different boiling points. The condensers can also be filled with a solvent, or a mixture of them, in order to avoid further reactions among the compounds of the liquid. The most used solvents in literature are isopropanol, methanol and dichloromethane.<sup>14,54–56</sup>

Mass spectrometry coupled to gas chromatography (MS/GC) is commonly used to identify and quantify volatile substances present in organic liquids. The main problem of this kind of analysis is that they can only detect about 40 wt. % of conventional pyrolysis oil components because of the low volatility resulting from the high molecular weight of the mixture. Therefore, complementary analysis techniques are necessary<sup>57</sup>. Oasmaa and co-workers have developed a solvent fractionation method, which can be able to characterise all the chemical families present in the mixture<sup>58</sup> (see Fig. 4).

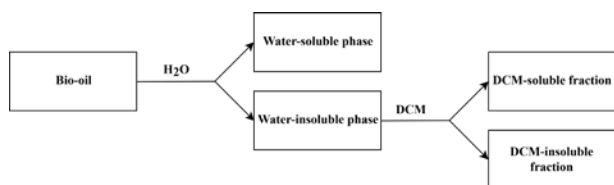


**Figure 4.** Bio-oil characterisation method suggested by Oasmaa et al.<sup>58</sup> (DCM: dichloromethane).

Addition of water aliquots to the bio-oil leads to a phase separation, dividing the liquid into a water-soluble and water-insoluble fraction. The latter undergoes further separation with dichloromethane (DCM) in order to obtain two solutions with different molecular size distribution. The analysis of the different fractions is carried out with different analytical techniques, as mentioned by Oasmaa<sup>56</sup>. The water-insoluble fraction contains mainly lignin-derived compounds, extractives and solids. Meanwhile, in the aqueous phase, it is possible to find sugar-type compounds, acids, aldehydes, ketones, pyrans, and furans. The content of water of the mixture, which is the result of the original moisture of the feedstock as well as dehydration reactions occurring during the pyrolysis, is within the range of 35–85 wt. %. The presence of water has advantages and disadvantages. For example, it reduces the viscosity of the whole liquid, enhancing the fluidity<sup>59</sup> but, on the other hand, water lowers the heating value of the mixture making necessary subsequent separation processes (i.e., more expensive process). Water in bio-oil can be found dissolved in the pyrolytic liquid or can be present as an emulsion. Generally, it cannot be removed by physical separation methods such as centrifugation<sup>60</sup>. The percentage of water is commonly measured using Karl Fischer titration, according to ASTM E 203-96 standard.

## 6. Upgrading of pyrolysis vapours

Slow pyrolysis is mainly aimed at producing biochar; thus, the liquid fraction is considered a problem, since it reduces the yield of the main product and can also condense inside the pipelines or filters, causing clogging and the subsequent breakdown of the entire system. To avoid these problems and upgrade the composition of the pyrolysis gas, it is important to reduce the yield of liquid by choosing the optimal operating conditions and/or remove such fraction via downstream processes (e.g., thermal cracking or catalytic reforming).

These processes can be classified in two categories, depending on where they take place (see Fig. 5). If the upgrading process is performed within the pyrolysis process system, using as reagents the CO<sub>2</sub> and water produced during the overall process, it is called “primary process”. On the other hand, the liquid can be fed in downstream processes where water, CO<sub>2</sub> or both can be supplied externally. In this case, it is called “secondary process”.

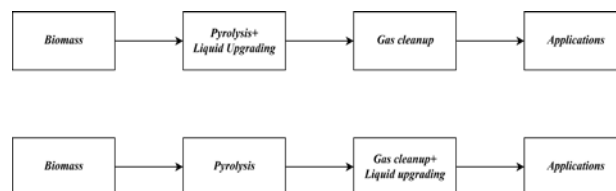
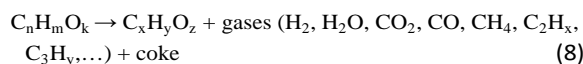


**Figure 5.** Primary and secondary upgrading processes of the pyrolysis liquid.

### 6.1. Cracking

Cracking of bio-oil aims at producing lighter compounds by breaking the bonds of the longer molecules. The main reaction involved in this process is the thermal degradation (Reaction 8).

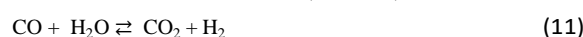
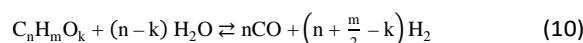
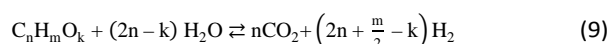


This process is carried out feeding the pyrolysis vapours to a secondary reactor at high temperature (700–1000 °C) without the addition of external reagents. There are two kinds of cracking processes: (1) catalytic cracking, where bio-oil is converted using a metal-based catalyst such as nickel; and (2) thermal cracking by partial oxidation or direct thermal contact.

Both processes have drawbacks: catalytic cracking is more effective and leads to higher conversion, but it is also more expensive because of the catalyst. On the other hand, thermal cracking is cheaper, because no catalyst is required, but, due to the fact that the pyrolytic liquid is a very refractory substance<sup>61</sup>, higher temperatures (up to 1000 °C) are required to achieve an appropriate conversion.

### 6.2. Steam reforming

Among the existing several methods for pyrolytic vapours upgrading, catalytic reforming is considered to be the most promising for large-scale applications, because of its high rate of reaction and high reliability<sup>14</sup>. Reforming process is generally used when the objective is the production of an H<sub>2</sub>-rich syngas. However, besides hydrogen, also other permanent gases such as CO, CO<sub>2</sub> and light hydrocarbons are produced and, depending on the products distribution, the effluent gas can be used as fuel or as a platform for the synthesis of chemicals. The main reactions involved in the steam reforming of oxygenated compounds are:



Reforming is usually carried out using a supported metal catalyst to improve the conversion and the selectivity of the process (catalytic steam reforming).

Besides the steam reforming (Reactions 10 and 11), and water gas shift (Reaction 11), also thermal cracking (Reaction 8) can take place, leading to the formation of coke deposition on the catalyst, which is the main cause of deactivation. It was reported by Czernik et al.<sup>62</sup> that, using a fixed bed reactor operating at 850 °C with a commercial nickel catalyst, it was possible to achieve a yield of hydrogen equal to 80%. Conversely, after 4 hours, the activity of the catalyst decreased markedly as a result of the coke deposition on the catalyst surface, making a regeneration step necessary.

An important parameter of steam reforming is the molar proportion between water and carbon, called steam-to-carbon ratio. The excess of water promotes coke gasification and the subsequent in-situ regeneration of the catalyst, but it also leads to a dilution of the reagents and products.

The catalyst needs to be supported, commonly by alumina monoliths, to enhance its mechanical and textural properties. The support is usually doped with a chemical agent which promotes specific reactions during the process. For example, the acidity of alumina promotes cracking reactions that lead to coke formation with subsequent deactivation of the catalyst. Therefore, the support is doped with basic oxides like CaO, MgO and K<sub>2</sub>O that help to avoid such coke formation. A study carried out by Adrados et al.<sup>63</sup> has shown that, through the doping with CeO<sub>2</sub> of a Ni/Al<sub>2</sub>O<sub>3</sub> catalyst, it is possible to obtain better performances, in terms of produced hydrogen, than that those obtained using a zirconia-doped support.

Another important parameter is the pore size distribution of the catalyst. The pores responsible for the adsorption of the organic compounds are the micropores<sup>64</sup>, but also larger pores are essential for making the micropores accessible to the aromatic molecules.

The employment of specific catalysts in steam reforming process can also allow to work at lower temperatures, maintaining a reasonable level of reactant conversion and product selectivity. In fact, using a commercial nickel catalyst (C11-PR) at 500 °C in a second stage reformer, an increase in the total gas yield of 58% was obtained<sup>65</sup>.

Recent studies suggested that a biochar-based catalyst can represent a valid and sustainable alternative to the commercial products<sup>66–68</sup>. Iron-supported biochar, for example, was successfully used in gas-cleaning applications. At 800 °C, iron-supported biochar was able to convert 100% of toluene in lighter compounds, with 0% of benzene selectivity<sup>69</sup>. Shen et al.<sup>70</sup> studied the application of different metal catalysts supported by a biochar produced from slow pyrolysis of rice husk. They found that a char-supported Ni-Fe catalyst, used in pyrolysis processes, was able to reduce liquid yield by 92.3%.<sup>14</sup>

The metal active phase is not the only factor that influences the activity and the efficiency of the biochar-supported catalyst. Inherent alkali and alkaline earth metallic species, present in the original biomass, can also

modify the performance of the catalyst, as well as the above-mentioned doping compounds. Feng et al.<sup>71</sup> compared the effects of K and Ca on the catalyst performance in steam reforming of a model compounds (naphthalene and toluene), finding that a high concentration of K in the catalyst led to a higher liquid conversion.

Despite the high conversions usually obtained in steam reforming, the outlet syngas still contains a small percentage of unreacted bio-oil or some condensable subproducts. When a high purity syngas is required, the steam reforming process can be coupled in series by an adsorption step in a fixed-bed reactor, using activated carbons as adsorbent material.<sup>72</sup>

As stated at the beginning of this section, the produced syngas can find application in different fields. The most important parameter is the molar ratio H<sub>2</sub>/CO and every process that employs syngas as reactant has an ideal value of this ratio. The production of hydrogen and carbon monoxide is in a first-place influenced by the composition of bio-oil and then by the reforming conditions. A way to modify such ratio is to simultaneously feed CO<sub>2</sub> and steam in order to displace the water gas shift reaction towards the formation of CO.<sup>73</sup>

## 7. Conclusions

Pyrolysis-derived biochar represents a sustainable precursor for advanced carbon materials. Its easy functionalisation makes the biochar to be a versatile material, which can be used in different fields such as catalyst and adsorption. To be employed in such fields, a deep characterisation of the biochar structure and chemical composition is needed. Depending on the production condition and its final application, the biochar could not have the appropriate textural properties or the required functional groups. Thus, an activation step aimed at expanding the biochar porosity and/or at introducing some specific functional group, is mandatory. Besides its direct application, biochar can also be used to create metal composites to be used in catalyst. In fact, carbon surface has some interesting inherent properties, such as the high temperature stability and the acid/base resistance, which made biochar a good platform for the production of catalyst supports.

One of the most interesting application of biochar-based catalysts is their use in bio-oil upgrading processes, in which the condensable phase resulting from pyrolysis is converted, through catalytic cracking and/or steam reforming, to permanent gases such as CO<sub>2</sub>, CO, CH<sub>4</sub>, H<sub>2</sub> and light hydrocarbons. In this way, it is possible to enhance the efficiency of the pyrolysis process, increasing the heating value of the gaseous products. Furthermore, the spent biochar-based catalyst can be regenerated or burnt/gasified to recover more energy.

The specific aim of the GreenCarbon's ESR 10 (Christian Di Stasi) is to produce metallic catalysts supported by chemically and physically activated biochars. The produced catalysts are addressed to be used in bio-oil upgrading

processes with focus on hydrogen production through steam and dry reforming. This study is carried out in close collaboration with the ERS 1 (Gianluca Greco), who will provide the ESR 10 with all the raw biochars needed for further activation and metal dispersion.

### Acknowledgments

This project has received funding from the European Union's Horizon 2020 research and innovation programme under the Marie Skłodowska-Curie grant agreement No 721991.

### References

- (1) Shackley, S.; Carter, S.; Knowles, T.; Middelink, E.; Haefele, S.; Sohi, S.; Cross, A.; Haszeldine, S. Sustainable Gasification–biochar Systems? A Case-Study of Rice-Husk Gasification in Cambodia, Part I: Context, Chemical Properties, Environmental and Health and Safety Issues. *Energy Policy* **2011**, *42*, 49–58.
- (2) Antal, M. J.; Grønli, M. The Art, Science, and Technology of Charcoal Production. *Ind. Eng. Chem. Res.* **2003**, *42* (8), 1619–1640.
- (3) Collard, F. X.; Blin, J. A Review on Pyrolysis of Biomass Constituents: Mechanisms and Composition of the Products Obtained from the Conversion of Cellulose, Hemicelluloses and Lignin. *Renew. Sustain. Energy Rev.* **2014**, *38*, 594–608.
- (4) Van de Velden, M.; Baeyens, J.; Brems, A.; Janssens, B.; Dewil, R. Fundamentals, Kinetics and Endothermicity of the Biomass Pyrolysis Reaction. *Renew. Energy* **2010**, *35* (1), 232–242.
- (5) McGrath, T. E.; Geoffrey Chan, W.; Hajaligol, M. R. Low Temperature Mechanism for the Formation of Polycyclic Aromatic Hydrocarbons from the Pyrolysis of Cellulose. *J. Anal. Appl. Pyrolysis* **2003**, *66* (1), 51–70.
- (6) Cai, J.; He, Y.; Yu, X.; Banks, S. W.; Yang, Y.; Zhang, X.; Yu, Y.; Liu, R.; Bridgwater, A. V. Review of Physicochemical Properties and Analytical Characterization of Lignocellulosic Biomass. *Renew. Sustain. Energy Rev.* **2017**, *76*, 309–322.
- (7) Zhu, J.; Jia, J.; Kwong, F. L.; Ng, D. H. L.; Tjong, S. C. Synthesis of Multiwalled Carbon Nanotubes from Bamboo Charcoal and the Roles of Minerals on Their Growth. *Biomass Bioenergy* **2012**, *36*, 12–19.
- (8) Suliman, W.; Harsh, J. B.; Abu-Lail, N. I.; Fortuna, A. M.; Dallmeyer, I.; Garcia-Perez, M. Influence of Feedstock Source and Pyrolysis Temperature on Biochar Bulk and Surface Properties. *Biomass Bioenergy* **2016**, *84*, 37–48.
- (9) Cao, X.; Pignatello, J. J.; Li, Y.; Latta, C.; Chappell, M. A.; Chen, N.; Miller, L. F.; Mao, J. Characterization of Wood Chars Produced at Different Temperatures Using Advanced Solid-State <sup>13</sup>C NMR Spectroscopic Techniques. *Energy Fuels* **2012**, *26* (9), 5983–5991.
- (10) Ghani, W. A. W. A. K.; Mohd, A.; da Silva, G.; Bachmann, R. T.; Taufiq-Yap, Y. H.; Rashid, U.; Al-Muhtaseb, A. H. Biochar Production from Waste Rubber-Wood-Sawdust and Its Potential Use in C Sequestration: Chemical and Physical Characterization. *Ind. Crops Prod.* **2013**, *44*, 18–24.
- (11) Jagiello, J.; Thommes, M. Comparison of DFT Characterization Methods Based on N<sub>2</sub>, Ar, CO<sub>2</sub>, and H<sub>2</sub> Adsorption Applied to Carbons with Various Pore Size Distributions. *Carbon* **2004**, *42* (7), 1227–1232.
- (12) Manyà, J. J.; González, B.; Azuara, M.; Arner, G. Ultra-Microporous Adsorbents Prepared from Vine Shoots-Derived Biochar with High CO<sub>2</sub> Uptake and CO<sub>2</sub>/N<sub>2</sub> Selectivity. *Chem. Eng. J.* **2018**, *345*, 631–639.
- (13) Mohanty, P.; Nanda, S.; Pant, K. K.; Naik, S.; Kozinski, J. A.; Dalai, A. K. Evaluation of the Physicochemical Development of Biochars Obtained from Pyrolysis of Wheat Straw, Timothy Grass and Pinewood: Effects of Heating Rate. *J. Anal. Appl. Pyrolysis* **2013**, *104*, 485–493.
- (14) Shen, Y.; Zhao, P.; Shao, Q.; Ma, D.; Takahashi, F.; Yoshikawa, K. In-Situ Catalytic Conversion of Tar Using Rice Husk Char-Supported Nickel-Iron Catalysts for Biomass Pyrolysis/Gasification. *Appl. Catal. B Environ.* **2014**, *152–153* (1), 140–151.
- (15) Bahng, M. K.; Mukarakate, C.; Robichaud, D. J.; Nimlos, M. R. Current Technologies for Analysis of Biomass Thermochemical Processing: A Review. *Anal. Chim. Acta* **2009**, *651* (2), 117–138.
- (16) Singh, B.; Fang, Y.; Cowie, B. C. C.; Thomsen, L. NEXAFS and XPS Characterisation of Carbon Functional Groups of Fresh and Aged Biochars. *Org. Geochem.* **2014**, *77*, 1–10.
- (17) Jensen, A.; Dam-Johansen, K.; Wójtowicz, M. A.; Serio, M. A. TG-FTIR Study of the Influence of Potassium Chloride on Wheat Straw Pyrolysis. *Energy Fuels* **1998**, *12* (5), 929–938.
- (18) Lillo-Ródenas, M. A.; Cazorla-Amorós, D.; Linares-Solano, A. Behaviour of Activated Carbons with Different Pore Size Distributions and Surface Oxygen Groups for Benzene and Toluene Adsorption at Low Concentrations. *Carbon* **2005**, *43* (8), 1758–1767.
- (19) Fang, J.; Gao, B.; Zimmerman, A. R.; Ro, K. S.; Chen, J. Physically (CO<sub>2</sub>) Activated Hydrochars from Hickory and Peanut Hull: Preparation, Characterization, and Sorption of Methylene Blue, Lead, Copper, and Cadmium. *RSC Adv.* **2016**, *6*, 24906–24911.
- (20) Plaza, M. G.; Pevida, C.; Arias, B.; Feroso, J.; Casal, M. D.; Martín, C. F.; Rubiera, F.; Pis, J. J. Development of Low-Cost Biomass-Based Adsorbents for Postcombustion CO<sub>2</sub> Capture. *Fuel* **2009**, *88*, 2442–2447.
- (21) Plaza, M. G.; Pevida, C.; Martín, C. F.; Feroso, J.; Pis, J. J.; Rubiera, F. Developing Almond Shell-Derived Activated Carbons as CO<sub>2</sub> Adsorbents. *Sep. Purif. Technol.* **2010**, *71* (1), 102–106.

- (22) Jung, S. H.; Kim, J. S. Production of Biochars by Intermediate Pyrolysis and Activated Carbons from Oak by Three Activation Methods Using CO<sub>2</sub>. *J. Anal. Appl. Pyrolysis* **2014**, *107*, 116–122.
- (23) Laine, J.; Calafat, A. Factors Affecting the Preparation of Activated Carbons from Coconut Shell Catalized by Potassium. *Carbon* **1991**, *29* (7), 949–953.
- (24) Yek, P. N. Y.; Liew, R. K.; Osman, M. S.; Lee, C. L.; Chuah, J. H.; Park, Y.-K.; Lam, S. S. Microwave Steam Activation, an Innovative Pyrolysis Approach to Convert Waste Palm Shell into Highly Microporous Activated Carbon. *J. Environ. Manage.* **2019**, *236*, 245–253.
- (25) Bardestani, R.; Kaliaguine, S. Steam Activation and Mild Air Oxidation of Vacuum Pyrolysis Biochar. *Biomass Bioenergy* **2018**, *108*, 101–112.
- (26) Chang, C. F.; Chang, C. Y.; Tsai, W. T. Effects of Burn-off and Activation Temperature on Preparation of Activated Carbon from Corn Cob Agrowaste by CO<sub>2</sub> and Steam. *J. Colloid Interface Sci.* **2000**, *232* (1), 45–49.
- (27) Azuara, M.; Sáiz, E.; Manso, J. A.; García-Ramos, F. J.; Manyà, J. J. Study on the Effects of Using a Carbon Dioxide Atmosphere on the Properties of Vine Shoots-Derived Biochar. *J. Anal. Appl. Pyrolysis* **2017**, *124*, 719–725.
- (28) Kandiyoti, R.; John I. Lazaridis; Bo Dyrvold; C. Ravindra Weerasinghe. Pyrolysis of a ZnCl<sub>2</sub>-Impregnated Inert Atmosphere. *Fuel* **1984**, *63* (11), 1583–1587.
- (29) Tsai, W. T.; Chang, C. Y.; Wang, S. Y.; Chang, C. F.; Chien, S. F.; Sun, H. F. Preparation of Activated Carbons from Corn Cob Catalyzed by Potassium Salts and Subsequent Gasification with CO<sub>2</sub>. *Bioresour. Technol.* **2001**, *78* (2), 203–208.
- (30) Hayashi, J.; Horikawa, T.; Takeda, I.; Muroyama, K.; Nasir Ani, F. Preparing Activated Carbon from Various Nutshells by Chemical Activation with K<sub>2</sub>CO<sub>3</sub>. *Carbon* **2002**, *40* (13), 2381–2386.
- (31) Di Blasi, C.; Galgano, A.; Branca, C. Influences of the Chemical State of Alkaline Compounds and the Nature of Alkali Metal on Wood Pyrolysis. *Ind. Eng. Chem. Res.* **2009**, *48* (7), 3359–3369.
- (32) Tay, T.; Ucar, S.; Karagöz, S. Preparation and Characterization of Activated Carbon from Waste Biomass. *J. Hazard. Mater.* **2009**, *165* (1–3), 481–485.
- (33) Dehkoda, A. M.; Gyenge, E.; Ellis, N. A Novel Method to Tailor the Porous Structure of KOH-Activated Biochar and Its Application in Capacitive Deionization and Energy Storage. *Biomass Bioenergy* **2016**, *87*, 107–121.
- (34) Lillo-Ródenas, M. A.; Lozano-Castelló, D.; Cazorla-Amorós, D.; Linares-Solano, A. Preparation of Activated Carbons from Spanish Anthracite - II. Activation by NaOH. *Carbon* **2001**, *39* (5), 751–759.
- (35) Wang, J.; Kaskel, S. KOH Activation of Carbon-Based Materials for Energy Storage. *J. Mater. Chem.* **2012**, *22*, 23710–23725.
- (36) Adinata, D.; Wan Daud, W. M. A.; Aroua, M. K. Preparation and Characterization of Activated Carbon from Palm Shell by Chemical Activation with K<sub>2</sub>CO<sub>3</sub>. *Bioresour. Technol.* **2007**, *98* (1), 145–149.
- (37) Angin, D.; Altintig, E.; Köse, T. E. Influence of Process Parameters on the Surface and Chemical Properties of Activated Carbon Obtained from Biochar by Chemical Activation. *Bioresour. Technol.* **2013**, *148*, 542–549.
- (38) Attia, A. A.; Girgis, B. S.; Fathy, N. A. Removal of Methylene Blue by Carbons Derived from Peach Stones by H<sub>3</sub>PO<sub>4</sub> Activation: Batch and Column Studies. *Dyes Pigments* **2008**, *76* (1), 282–289.
- (39) Xu, B.; Chen, Y.; Wei, G.; Cao, G.; Zhang, H.; Yang, Y. Activated Carbon with High Capacitance Prepared by NaOH Activation for Supercapacitors. *Mater. Chem. Phys.* **2010**, *124* (1), 504–509.
- (40) Su, D. S.; Zhang, J.; Frank, B.; Thomas, A.; Wang, X.; Paraknowitsch, J.; Schlögl, R. Metal-Free Heterogeneous Catalysis for Sustainable Chemistry. *ChemSusChem* **2010**, *3* (2), 169–180.
- (41) Xue, Y.; Gao, B.; Yao, Y.; Inyang, M.; Zimmerman, A. R.; Zhang, M.; Ro, K. S. Hydrogen Peroxide Modification Enhances the Ability of Biochar (Hydrochar) Produced from Hydrothermal Carbonization of Peanut Hull to Remove Aqueous Heavy Metals: Batch and Column Tests. *Chem. Eng. J.* **2012**, *200–202*, 673–680.
- (42) Jimenez-Cordero, D.; Heras, F.; Alonso-Morales, N.; Gilarranz, M. A.; Rodriguez, J. J. Ozone as Oxidation Agent in Cyclic Activation of Biochar. *Fuel Process. Technol.* **2015**, *139*, 42–48.
- (43) Serp, P.; Figueiredo, J. L. *Carbon Materials for Catalysis*; John Wiley & Sons, Inc.: Hoboken, NJ, USA, 2008.
- (44) Prado-Burguete, C.; Linares-Solano, A.; Rodriguez-Reinoso, F.; De Lecea, C. S. M. Effect of Carbon Support and Mean Pt Particle Size on Hydrogen Chemisorption by Carbon-Supported Pt Catalysts. *J. Catal.* **1991**, *128* (2), 397–404.
- (45) Feng, W.; Kwon, S.; Borguet, E.; Vidic, R. Adsorption of Hydrogen Sulfide onto Activated Carbon Fibers: Effect of Pore Structure and Surface Chemistry. *Environ. Sci. Technol.* **2005**, *39* (24), 9744–9749.
- (46) Kastner, J. R.; Miller, J.; Geller, D. P.; Locklin, J.; Keith, L. H.; Johnson, T. Catalytic Esterification of Fatty Acids Using Solid Acid Catalysts Generated from Biochar and Activated Carbon. *Catal. Today* **2012**, *190* (1), 122–132.
- (47) Dehkoda, A. M.; Ellis, N. Biochar-Based Catalyst for Simultaneous Reactions of Esterification and Transesterification. *Catal. Today* **2013**, *207*, 86–92.
- (48) Titirici, M. M.; Thomas, A.; Antonietti, M. Aminated Hydrophilic Ordered Mesoporous Carbons. *J. Mater. Chem.* **2007**, *17*, 3412–3418.
- (49) Pérez-Cadenas, A. F.; Maldonado-Hódar, F. J.; Moreno-Castilla, C. On the Nature of Surface Acid Sites of Chlorinated Activated Carbons. *Carbon* **2003**, *41* (3), 473–478.
- (50) Zhang, Q.; Chang, J.; Wang, T.; Xu, Y. Review of Biomass Pyrolysis Oil Properties and Upgrading Research. *Energy Convers. Manage.* **2007**, *48* (1), 87–92.

- (51) Oasmaa, A.; Solantausta, Y.; Arpiainen, V.; Kuoppala, E.; Sipilä, K. Fast Pyrolysis Bio-Oils from Wood and Agricultural Residues. *Energy Fuels* **2010**, *24* (2), 1380–1388.
- (52) Blanco, P. H.; Wu, C.; Onwudili, J. A.; Williams, P. T. Characterization of Tar from the Pyrolysis/Gasification of Refuse Derived Fuel: Influence of Process Parameters and Catalysis. *Energy Fuels* **2012**, *26* (4), 2107–2115.
- (53) Shen, J.; Wang, X.-S.; Garcia-Perez, M.; Mourant, D.; Rhodes, M. J.; Li, C.-Z. Effects of Particle Size on the Fast Pyrolysis of Oil Mallee Woody Biomass. *Fuel* **2009**, *88* (10), 1810–1817.
- (54) Volpe, M.; D'Anna, C.; Messineo, S.; Volpe, R.; Messineo, A. Sustainable Production of Bio-Combustibles from Pyrolysis of Agro-Industrial Wastes. *Sustainability* **2014**, *6* (11), 7866–7882.
- (55) Volpe, M.; Panno, D.; Volpe, R.; Messineo, A. Upgrade of Citrus Waste as a Biofuel via Slow Pyrolysis. *J. Anal. Appl. Pyrolysis* **2015**, *115*, 66–76.
- (56) Oasmaa, A.; Leppämaeki, E.; Koponen, P.; Levander, J.; Tapola, E. Physical characterization of biomass-based pyrolysis liquids. Application of standard fuel oil analyses. Finland: N. p., 1997. Web.
- (57) Scholze, B.; Meier, D. Characterization of the Water-Insoluble Fraction from Pyrolysis Oil (Pyrolytic Lignin). Part I. PY-GC/MS, FTIR, and Functional Groups. *J. Anal. Appl. Pyrolysis* **2001**, *60* (1), 41–54.
- (58) Oasmaa, A.; Kuoppala, E. Fast Pyrolysis of Forestry Residue. 3. Storage Stability of Liquid Fuel. *Energy Fuels* **2003**, *17* (4), 1075–1084.
- (59) Sipilä, K.; Kuoppala, E.; Fagernäs, L.; Oasmaa, A. Characterization of Biomass-Based Flash Pyrolysis Oils. *Biomass Bioenergy* **1998**, *14* (2), 103–113.
- (60) Elliott, D. C. Water, Alkali and Char in Flash Pyrolysis Oils. *Biomass Bioenergy* **1994**, *7* (1–6), 179–185.
- (61) Bridgwater, A. V. The Technical and Economic Feasibility of Biomass Gasification for Power Generation. *Fuel* **1995**, *74* (5), 631–653.
- (62) Czernik, S.; French, R.; Feik, C.; Chornet, E. Hydrogen by Catalytic Steam Reforming of Liquid Byproducts from Biomass Thermoconversion Processes. *Ind. Eng. Chem. Res.* **2002**, *41* (17), 4209–4215.
- (63) Adrados, A.; Lopez-Uriónabarrenechea, A.; Solar, J.; Requies, J.; De Marco, I.; Cambra, J. F. Upgrading of Pyrolysis Vapours from Biomass Carbonization. *J. Anal. Appl. Pyrolysis* **2013**, *103*, 293–299.
- (64) Hosokai, S.; Kumabe, K.; Ohshita, M.; Norinaga, K.; Li, C. Z.; Hayashi, J. Mechanism of Decomposition of Aromatics over Charcoal and Necessary Condition for Maintaining Its Activity. *Fuel* **2008**, *87* (13–14), 2914–2922.
- (65) Hornung, U.; Schneider, D.; Hornung, A.; Tumiatti, V.; Seifert, H. Sequential Pyrolysis and Catalytic Low Temperature Reforming of Wheat Straw. *J. Anal. Appl. Pyrolysis* **2009**, *85* (1–2), 145–150.
- (66) Abu El-Rub, Z.; Bramer, E. A.; Brem, G. Experimental Comparison of Biomass Chars with Other Catalysts for Tar Reduction. *Fuel* **2008**, *87* (10–11), 2243–2252.
- (67) Bhandari, P. N.; Kumar, A.; Bellmer, D. D.; Huhnke, R. L. Synthesis and Evaluation of Biochar-Derived Catalysts for Removal of Toluene (Model Tar) from Biomass-Generated Producer Gas. *Renew. Energy* **2014**, *66*, 346–353.
- (68) Gilbert, P.; Ryu, C.; Sharifi, V.; Swithenbank, J. Tar Reduction in Pyrolysis Vapours from Biomass over a Hot Char Bed. *Bioresour. Technol.* **2009**, *100* (23), 6045–6051.
- (69) Kastner, J. R.; Mani, S.; Juneja, A. Catalytic Decomposition of Tar Using Iron Supported Biochar. *Fuel Process. Technol.* **2015**, *130*, 31–37.
- (70) Hosokai, S.; Norinaga, K.; Kimura, T.; Nakano, M.; Li, C. Z.; Hayashi, J. Reforming of Volatiles from the Biomass Pyrolysis over Charcoal in a Sequence of Coke Deposition and Steam Gasification of Coke. *Energy Fuels* **2011**, *25* (11), 5387–5393.
- (71) Feng, D.; Zhao, Y.; Zhang, Y.; Sun, S.; Meng, S.; Guo, Y.; Huang, Y. Effects of K and Ca on Reforming of Model Tar Compounds with Pyrolysis Biochars under H<sub>2</sub>O or CO<sub>2</sub>. *Chem. Eng. J.* **2016**, *306*, 422–432.
- (72) Phuphuakrat, T.; Namioka, T.; Yoshikawa, K. Tar Removal from Biomass Pyrolysis Gas in Two-Step Function of Decomposition and Adsorption. *Appl. Energy* **2010**, *87* (7), 2203–2211.
- (73) Choudhary, V. R.; Rajput, A. M. Simultaneous Carbon Dioxide and Steam Reforming of Methane to Syngas over NiO-CaO Catalyst. *Ind. Eng. Chem. Res.* **1996**, *35* (11), 3934–3939.

## Hydrothermal carbonisation and its role in catalysis

Pierpaolo Modugno<sup>a</sup>, Anthony E. Szego<sup>b</sup>, Maria-Magdalena Titirici<sup>a</sup>, Niklas Hedin<sup>b</sup>

<sup>a</sup> *School of Engineering and Material Science, Queen Mary University of London, Mile End Road, London E1 4NS, UK*

<sup>b</sup> *Department of Material and Environmental Chemistry, Stockholm University, SE-106 91 Stockholm, Sweden*

### Abstract

This chapter provides an overview of the most recent advances in the mechanistic study of hydrothermal carbonisation (HTC) and the strategies to improve the conversion by using carbon-based catalysts. HTC, although not a recent discovery, has lately been receiving increasingly attention by both academic and industrial sectors due to the possibility to exploit this process to perform a simple, green and inexpensive conversion of bio-derived waste material into valuable chemicals and advanced materials and, as such, this chapter will also look into the use of hydrochars formed in HTC and their application in catalysis, more specifically heterogeneous catalysis with a mention on electrocatalysis. The versatility and tuneability of these solids give rise to the great range of applicability in different fields. A detailed overview of the HTC process is presented and the main uses of hydrochars in catalysis is then shown, highlighting their use as solid acid catalysts, as pristine solid catalysts, as sacrificial agents in synthesis, since their removal through combustion is easy, and the niche application of these solids in electrocatalysis for future research perspective.

### 1. Introduction

The term hydrothermal carbonisation (HTC) is referred to as a process in which an aqueous solution or dispersion of carbon containing compounds, typically lignocellulosic biomass or saccharides, are heated under water at subcritical temperatures, at moderate to high pressures. HTC was first studied about a century ago<sup>1,2</sup> as a way to mimic natural conversion process of biomass into fossil fuel. However, in the last decades<sup>3–9</sup>, it has become object of intense research because it potentially allows the conversion of ubiquitous and inexpensive cellulose – derived from agricultural waste– into: (a) other chemicals, like furfural, 5-hydroxymethylfurfural (5-HMF), levulinic acid (LA), formic acid, acetic acid and lactic acid; some of which being recognised as platform chemicals for the transition to a greener chemistry<sup>10</sup>; and (b) carbonaceous materials (i.e., hydrochar). Through a sequence of dehydration, polymerisation, and aromatisation reactions, this previously mentioned hydrochar is formed, mostly composed of condensed furan rings bridged by aliphatic regions with terminal hydroxyl and carbonyl functional groups. Upon the “polymerisation” of 5-HMF or furfural, nucleation takes place followed by growth of the particles upon further incorporation of 5-HMF-derived monomers, which leads to the formation of spherically shaped particles.

One of the main disadvantages of hydrochars is that they present limited porosity and surface area. For certain applications, a nanoscale porosity is highly desirable. There are many well established technologies to produce porous carbons among which the most common ones are chemical activation<sup>11</sup> and templating methodologies.<sup>12</sup>

Nonetheless, there are advantages to using this method. HTC has been considered as energy- and atom-economical process because only one-third of the combustion energy is released via dehydration; pre-drying process is unnecessary due to the aqueous reaction media and the carbon efficiency is close to one after suitable operational

conditions<sup>13</sup>. Coupled with these advantages is the ability to tune or manipulate the surface of the resulting hydrochar during the HTC process such as increasing acidity (using different acids in a one-pot synthesis).<sup>14</sup> The most common way hydrochars might be used in catalysis is as support for metal or metal oxide active sites. However, since the surface of hydrochar involves many oxygen functionalities such as furanic, phenolic, or carboxylic oxygen atoms, catalytic activity can also be achieved through surface functionalities alone. Modification of the conditions during the synthesis or post-treatment of the material can allow the addition of metallic or metal oxide particles on the structure. Another useful function of hydrochars is that they can be eliminated through combustion in air. Taking all these properties into account, this book chapter analyses the use of hydrochars in heterogeneous catalysis in three groups: sulfonated (solid acid catalysts) and pristine hydrochars, as support, and as a sacrificial agent. Another important subject of analysis is the process through which these materials are obtained: HTC. The use of hydrochars in electrocatalysis is also mentioned, as there is a growing interest in the use of these solids in such processes.

### 2. Hydrothermal carbonisation: mechanism

A deep and thorough understanding of the mechanisms of carbonisation of cellulosic biomass is the key to control the process and, therefore, make it scalable for industrial conversion of biowaste. Although the complex network of transformations and decomposition of cellulosic materials under hydrothermal conditions is still not fully understood and subject of debate, it can be summarised in a few basic steps: (i) hydrolysis of long cellulose and hemicellulose chains into their constituting monomers (mainly glucose and other C6 and C5 sugars); (ii) dehydration of C6 sugars to 5-HMF and C5 sugars to furfural; (iii) decomposition to lower molecular weight compounds or, alternatively,

condensation and aromatization reaction, to produce hydrochar (see Fig. 1).

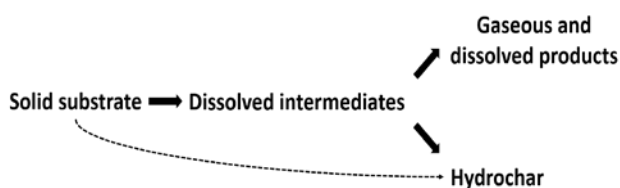


Figure 1. General hydrothermal reaction scheme.

Many studies in the last twenty years have contributed to put together this general scheme, by focusing on different aspects of the whole process. Since the dawn of the “rediscover” of HTC, it is known that the decomposition of glucose under neutral hydrothermal treatment produces fructose, dihydroxyacetone, glyceraldehyde, erythrose, glycolaldehyde, pyruvaldehyde, 1,6-anhydroglucose, 5-HMF, acetic acid, formic acid and hydrothermal carbon<sup>15</sup>. In 2007, Asghari and Yoshida<sup>16</sup> reported the results from a study on the reactivity of fructose under hydrothermal conditions in presence of HCl as an acid catalyst. This study proved the dehydration path of fructose under hydrothermal conditions to 5-HMF, which can easily undergo hydration reaction, with loss of a C atom in form of formic acid (FA) and subsequent ring opening to form LA. While the latter two do not undergo any further reactions, fructose and 5-HMF can also form soluble polymers through distinct paths. 2-furaldehyde (2FA), originated only from fructose, was also detected. Finally, the study proved that pressure had a minor impact on products yield, compared to other reaction parameters such as temperature, initial pH and composition of feedstocks.

Recently, Buendia-Kandia et al.<sup>17</sup> have provided a quite exhaustive scheme of the dehydration, decomposition and condensation pathways that take place during HTC (see Fig. 2). The scheme has been elaborated by studying the decomposition of microcrystalline cellulose in hydrothermal conditions, testing three temperatures (180, 220, and 260 °C), sampling the liquid phase every 20 min on an overall reaction time of 120 min. Their results confirmed the pathway proposed by Matsumura<sup>18</sup>: long chains of cellulose are firstly hydrolysed to smaller oligomers or monomers of glucose. Glucose can undergo isomerisation to fructose via Lobry de Bruyn–Alberda–van Ekenstein transformation or epimerisation to mannose. Dehydration reaction of fructose produces 5-HMF, which is readily decomposed to levulinic and formic acid; glucose oligomers can undergo dehydration before complete hydrolysis, producing cellobiosan and subsequently levoglucosan. Retro-aldol condensation of glucose produces erythrose and glycolaldehyde from which lactic and acetic acid are derived. Decarbonylation and decarboxylation reactions account for the production of CO and CO<sub>2</sub>. Finally, due to limited access of water molecules on the inner cellulose fibres, pyrolysis of cellulose can occur, leading to direct formation of hydrochar.

It is worth noting how water can serve as both acid and basic catalyst, in sub-critical condition, as pointed out by

Jin et al.<sup>19</sup>, who studied the production of lactic acid during hydrothermal treatment of cellulose and glucose. In fact, although lactic acid is traditionally known to be a product of alkaline degradation of sugars, it has been detected in large amounts even in neutral condition. Its production has been explained by the benzylic acid rearrangement of pyruvaldehyde, which in turn is a product of a retro-aldol condensation of fructose. This rearrangement proved that water under sub-critical condition can act as a Brønsted acid catalyst when catalysing isomerisation of glucose to fructose and also as an effective Brønsted base catalyst in catalysing rearrangement of pyruvaldehyde to lactic acid.

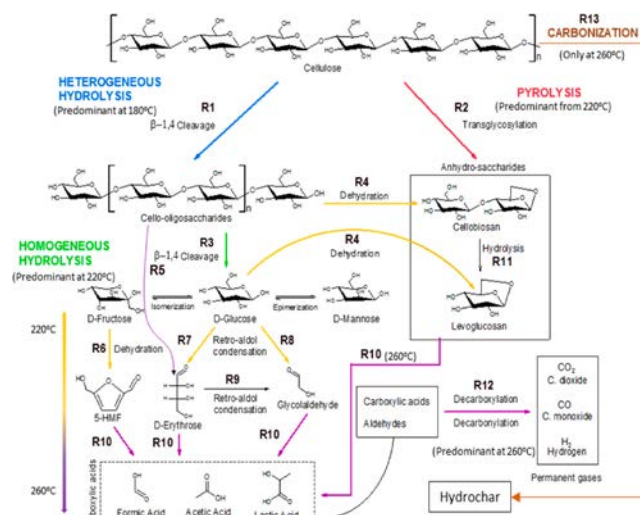


Figure 2. Scheme of reaction pathways of cellulose decomposition as proposed by Buendia-Kandia<sup>17</sup>.

More recently, some studies have emphasised some discrepancies between experimental observations and the common belief of formic acid and levulinic being present in equal concentration<sup>20</sup>. Yang et al.<sup>21</sup> have explained this excess of FA by a sequence of reactions that entail a retro-aldol pathway; furthermore, they have demonstrated, using computational methods (in particular Density functional theory, DFT, calculations) the possibility of two alternative dehydration pathways of glucose and fructose: the former produces 5-HMF and dominates at low temperatures and low rates of conversion; the latter does not involve 5-HMF and proceeds through retro-aldol reaction and secondary furfuryl alcohol chemistry, contributing to the FA excess. Latest studies, nonetheless, tend to assume that dehydration of glucose to 5-HMF mainly happen via an isomerisation step to fructose, which is also a rate limiting step.<sup>22</sup>

## 2.1 Organic compounds in the liquid phase

A large variety of chemical compounds can be found in the liquid phase after a hydrothermal decomposition of cellulosic biomass. Among them, 5-HMF is a very promising, highly functionalised, bio-based chemical building block, produced from the dehydration of hexoses, which can play a key role not only as intermediate for the production of the biofuel dimethylfuran (DMF), but also for other biomass-derived intermediates, such as 2,5-furan-

dicarboxylic acid<sup>23</sup>, 2,5-dimethylfuran<sup>24,25</sup>, adipic acid and LA<sup>26</sup>. 5-HMF is synthesized mainly by the dehydration of monosaccharides such as fructose<sup>27</sup> and glucose<sup>28,29</sup>, through the loss of three water molecules. Disaccharides or polysaccharides, such as sucrose<sup>22</sup> or cellulose<sup>30,31</sup>, can be used as starting materials, but hydrolysis is necessary for depolymerisation. Sucrose hydrolysis is more efficiently catalysed by a base; however, dehydration of the monomers is catalysed by acids. This difference introduces a problem, namely that the formation of 5-HMF by dehydration is a very complex process because of the possibility of side-reactions. Moreover, with respect to the dehydration reaction which leads to the formation of 5-HMF, glucose (an aldose) reactivity is lower than that of fructose (a ketose). Since the ultimate aim is to convert cellulosic biomass into 5-HMF, hydrolysis of the cellulose polymer to give glucose must be followed by a further step of isomerisation to fructose in order to enhance the final yield. Finally, it is important not only to optimise the synthesis of this compound, but also to develop an efficient isolation method. 5-HMF is not easy to extract from an aqueous phase, since the distribution coefficient between the organic and the aqueous phase is not favourable<sup>32</sup>. LA, also named 4-oxopentanoic acid, is derived from 5-HMF which, under hydrothermal conditions, is rehydrated to form LA along with formic acid. LA is considered as one of the most promising platform chemicals derived from lignocellulosic biomass for the synthesis of fuels and chemicals<sup>10,33</sup>. It is regarded as a platform chemical that finds applications for several purposes, such as source of monomers for the synthesis of polymer resins as well as components in flavouring and fragrance industries<sup>34</sup>, textile dyes, additives, extenders for fuels, antimicrobial agents, herbicides and plasticisers<sup>35,36</sup>. Many of the processes for the highly selective production and separation of LA are still early in their development stage. Thus, finding an economically viable process for converting more complex biomass feedstock to fuels and to chemical precursors for industrial production would be attractive to reduce the release of atmospheric CO<sub>2</sub>, without compromising food supply.

## 2.2 Hydrochar: morphology and chemistry

Synthesis of carbonaceous spheres via HTC of sugars was first reported in 2001, in a study by Wang et al.<sup>3</sup> In this study, it was noted that the diameter of these particles grew proportionally with both dwell time and initial concentration of the precursor. The spherical appearance of these carbon particles was attributed to the separation of early sugar dehydration products from the aqueous solution and subsequent formation of an emulsion, from which first nuclei originates.

Better insights on the chemical structure of these carbon spheres were later provided by Baccile et al.<sup>37</sup>, who used different solid-state <sup>13</sup>C NMR techniques to characterise the carbon product of HTC of glucose. Their results indicated that the core of the carbonaceous scaffold consists on condensed furan rings linked either via the  $\alpha$ -carbon or via sp<sup>2</sup>- or sp<sup>3</sup>- type carbon<sup>37</sup>. This structure

suggests that 5-HMF and furfural are the main building blocks of hydrochar. More recent investigations by van Zandvoort et al.<sup>38</sup> has provided further details about the chemical structure of hydrochar (see Fig. 3). In fact, a better characterisation of the linkages between furanic units has been achieved by means of 1D and 2D solid-state NMR spectra of <sup>13</sup>C-labeled humins. The most abundant are C <sub>$\alpha$</sub> -C<sub>aliphatic</sub> and C <sub>$\alpha$</sub> -C <sub>$\alpha$</sub>  linkages, whereas other ones such as C <sub>$\beta$</sub> -C <sub>$\beta$</sub>  and C <sub>$\beta$</sub> -C<sub>aliphatic</sub> cross-links appear to have smaller contribution to the overall structure. This difference shows that furan rings are mostly linked to each other by short aliphatic chains; LA is also included in the structure through covalent bonds. A chemical structure (see Fig. 2) has been proposed.

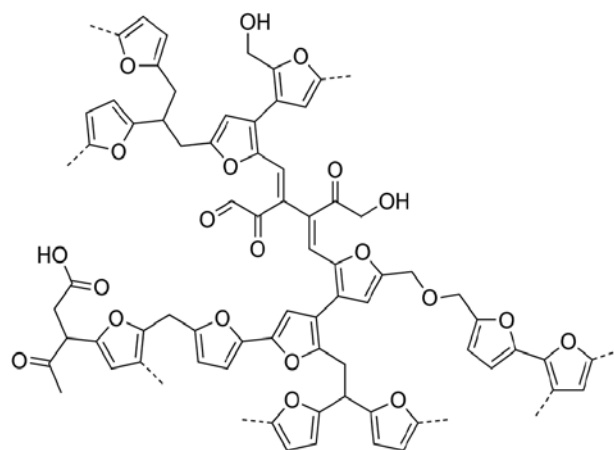


**Figure 3.** Chemical structure of humins proposed by van Zandvoort<sup>24</sup>.

DFT calculations have also proved to be helpful in supplying more information about the chemical structure of hydrochar. A study by Brown et al.<sup>39</sup> proposed two possible structures: (1) a structure consisting of arene domains comprised of 6-8 rings connected via aliphatic chains; (2) a furan/arene structure consisting primarily of single furans and 2 or 3 ring arenes. These two structures have been inferred by simulating Raman spectra of model constituents of hydrochar by means of DFT and subsequently fitting the experimental Raman hydrochar spectrum with a 12-peak fit. Following NMR and IR analysis, however, suggested that the latter model is more consistent with the experimental observations.

Formation and growth mechanism of carbonaceous spheres (such as those in Fig. 4) is still object of debate. Based on their observations regarding the dissolution behaviour of cellulose under hydrothermal conditions, Sevilla and Fuertes<sup>9</sup> proposed a nucleation pathway to explain the formation of the typical carbonaceous spheres. This pathway encompasses six steps: (1) hydrolysis of cellulose chains; (2) dehydration and fragmentation into soluble products of the monomers that come from the hydrolysis of cellulose; (3) polymerisation or condensation of the soluble products; (4) aromatisation of the polymers thus formed; (5) appearance of a short burst of nucleation; (6) growth of the nuclei formed by diffusion and linkage of species from the solution to the surface of the nuclei.

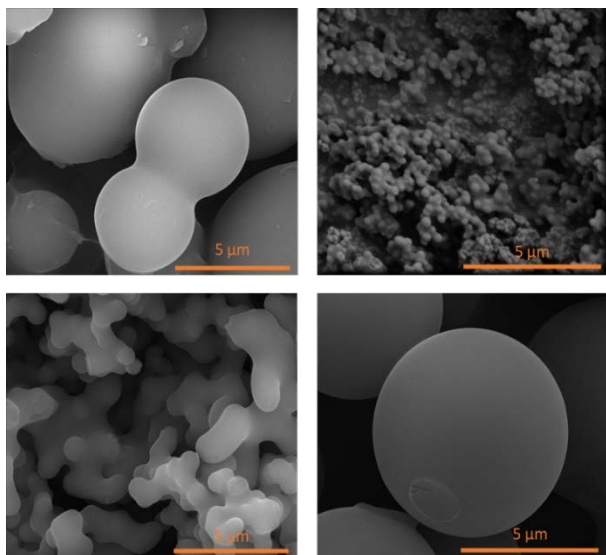


**Figure 4.** SEM image of carbonaceous spheres obtained by hydrothermal carbonization of sugars.

5-HMF obviously plays a major part in the carbon spheres formation, as highlighted by their chemical structure of linked furan rings. Acid catalysed degradation of 5-HMF has been studied by Tsilomelekis et al.<sup>40</sup> by means of ATR-FTIR spectroscopy, Scanning Electron Microscopy (SEM) and Dynamic Light Scattering (DLS) to understand the growth mechanism of 5-HMF derived humins. The proposed mechanism involves an initial nucleophilic attack of

a 5-HMF carbonyl group to the  $\alpha$ - or  $\beta$ -position of the furanic ring, along with aldolic condensation and etherification. This condensation leads to the formation of small, soluble oligomers that grow heavier until they form small solid nuclei through phase separation. Further growth is the result of both smaller particles aggregation and continuous 5-HMF Addition. It is unclear if aggregation of constituting small particles is based on chemical reactions or physical interaction. Cheng et al.<sup>41</sup> have noted that humins, which are related to hydrochars, can be partially dissolved by multistage dissolution in organic solvent to oligomers that have mass numbers ranging from 200 to 600 Da, as detected by LC-MS. This observation may, in fact, suggest that humins are actually aggregates of oligomeric species rather than macromolecules. How that relates to hydrochars is still not fully resolved.

Formic acid and LA are abundant in the reaction medium during HTC, where formation and growth of hydrochar based spherical particles take place. It is reasonable to think that these acids might play a role in the process. In fact, it has been shown that formic acid, due to its rather high  $pK_a$ , significantly increases the rate of conversion of C6 sugar to 5-HMF in an autocatalytic fashion, therefore speeding up the growth of the spherical particles of hydrochar. LA, on the other hand, has a lower  $pK_a$  and therefore does not have a strong Brønsted catalytic effect, but it does effect the growth of the spherical particles taking part in the process as building units and slowing the growth by reducing the surface density of hydroxyl groups of carbonaceous spheres.<sup>42</sup>

### 2.3 Carbon dots

The name “carbon dots” encompasses different carbon-based nanomaterials whose properties resembles those of well-known metal-based quantum dots. Since their fortuitous discover in 2004 by Xu et al.<sup>43</sup>, this new class of material has been object of intense study and research because of their promising and sometimes outstanding properties. Carbon dots are fluorescent and have tuneable emission wavelengths, like traditional metal quantum dots, but, unlike their inorganic cognate, they show better aqueous solubility, photo-stability, ease to be functionalised, low toxicity and, therefore, good biocompatibility. They also have a much lower cost compared to the heavy metal based quantum dots, as they can be synthesised using biomass waste as raw carbon source.

Carbon dots can be divided in two sub-groups, based on their morphology: graphene quantum dots (GQDs) and carbon quantum dots (CQDs). Graphene quantum dots are small, single- or multi-layered graphene discs with diameters ranging from 3 to 20 nm and carboxylic functionalities on the edges<sup>44</sup>. It can be argued that this kind of nanoparticles, commonly referred to as graphene quantum dots, are in fact graphene oxide quantum dots, due to the high amount of oxygen-containing groups on their surface and edges. In fact, true oxygen-free graphene quantum dots have been produced by Fei et al.<sup>45</sup> through solvent exfoliation of graphite nanoparticles.

Carbon quantum dots are quasi-spherical carbon nanoparticles, with diameters around or below 10 nm<sup>46</sup>; they can have an amorphous or nanocrystalline structure with  $sp^2$  carbon clusters<sup>47</sup> with high amount of oxygen atoms and carboxylic groups on their surface<sup>48</sup>. First chemical route to synthesis of CQDs was developed by Pan et al. in 2010, through hydrothermal treatment of graphene sheets.<sup>49</sup>

The approaches to the synthesis of carbon dots are two: “top-down” and “bottom-up”. Bottom-up approach relies on small molecular precursors as seeds for the carbon dots to grow, whereas top-down method consists in the breaking down of macromolecules derived from larger carbon structures, biomass included, into small carbon dots. Given the purpose of this chapter, only examples of top-down approaches via HTC are relevant and therefore will be mentioned. A vast variety of biomass has been used as carbon source to successfully synthesize CDs in one-pot reactions: papaya powder<sup>50</sup>, coconut water<sup>51</sup>, peach gum<sup>52</sup>, *prunus avium*<sup>53</sup>, salep flour<sup>54</sup>, unripe *prunus mume*<sup>55</sup> and grape skin<sup>56</sup> just to name a few. CQDs can be doped with different elements, in order to enhance their properties through the addition of dopants (boron<sup>57</sup>, nitrogen<sup>52,53,57</sup>) or carefully choosing biomass which naturally contains heteroatoms (N- and S-doped CQDs from garlic<sup>58,59</sup>). These materials have proven to be effective as probes for the detection of metal ions<sup>52,53,57,58</sup> (due to the quenching effect of these species on the fluorescence of the CDs) and other chemicals<sup>54,56,59</sup>, as catalyst<sup>54</sup> or for imaging of cells<sup>55</sup>.

HTC for the synthesis of carbon dots is a sustainable, low cost and relatively easy strategy to turn biomass waste into a valuable material. However, this hydrothermal route produces high amounts of by-products, mostly hydrothermal carbon. Although hydrothermal carbon is itself a valuable, versatile and promising material, as it will be mentioned later on, the whole process of HTC still needs a deeper, insightful comprehension of its mechanisms, in order to selectively drive the reaction towards the desired products (soluble chemicals, hydrothermal carbon or nanoparticles).

#### 2.4 Carbon catalysts for hydrothermal conversion of biomass

Nowadays, industrial processes for the production of 5-HMF and LA from cellulosic biomass rely on mineral acids as homogeneous catalysts of fructose dehydration<sup>60,61</sup>. Despite satisfactory yields of conversion and selectivity achieved, the use of mineral acids as homogeneous catalysts poses some challenges, namely uneasy acid recovery and high maintenance costs due to pipe corrosion. These difficulties could easily be overcome by means of heterogeneous catalysis. A large variety of heterogeneous acid catalysts have been developed to perform catalytic conversion of biomass or biomass-derived sugars, such as mixed metal oxides<sup>62</sup>, phosphates<sup>63</sup>, zeolites<sup>64,65</sup> to name a few.

Carbonaceous materials can also serve as a starting material for the synthesis of solid acid catalysts. Shen et al.<sup>66</sup> have prepared a bi-functional carbon based acid hetero-catalyst through hard-templating using sucralose as carbon source. Due to the use of this synthetic chlorinated sugar, the resulting carbon material possessed  $-Cl$  groups able to bind cellulose and  $-SO_3H$  to catalyse depolymerisation and dehydration. With this catalyst, LA was formed from untreated cellulose in pure water with yields as high as 51.5%. Ball-milling pretreatment of cellulose improved the performance of the solid acid catalyst. However, a downside of this preparation resides in the use of a synthetic sugar, not readily available from natural sources, which requires previous treatment and possibly higher costs. Recently, Zhang et al.<sup>67</sup> developed a macro-/mesoporous carbonaceous catalyst with hybrid Brønsted-Lewis acid sites (sulfonic groups and  $Zr^{IV}$  respectively). This catalyst was tested for the thermal conversion of fructose and glucose in a water/DMSO biphasic solvent and cellulose in a 1-butyl-3-methylimidazolium chloride ([BMIM]-Cl) ionic liquid. Conversion and 5-HMF yield was high, with a remarkable 5-HMF yield (43.1%) and selectivity (57.7%) from cellulose. Although this synthetic route allows excellent control of porosity and very fine surface functionalisation, it requires non-renewable precursors and transition metals and it involves several preparation steps. Metal organic frameworks (MOFs) can also serve as starting material for the synthesis of carbonaceous catalysts, as reported by Jin et al.<sup>68</sup>, who fabricated a MOF starting from zinc nitrate hexahydrate and terephthalic acid. The MOF was subsequently carbonised and treated with concentrated sulphuric acid to

add sulfonic groups to the carbon structure. The MOF-derived sulfonated carbon was macro/mesoporous and active towards the dehydration of fructose to 5-HMF in isopropanol/DMSO with a yield of 89.6% in the optimal conditions. An interesting alternative consists on the use of carbonaceous materials derived from biomass waste. In fact, effective carbon-based catalysts can be prepared from a variety of bio-derived carbon sources. Moreover, their preparation usually requires a reduced number of steps. Hu et al.<sup>69</sup> have reported the preparation of magnetic lignin-derived carbon catalyst from enzymatic hydrolysis lignin (EHL), a residue of enzymatic hydrolysis of lignocellulosic biomass to separate cellulose from lignin. EHL was impregnated with an aqueous solution of  $FeCl_3$  10  $mmol \cdot L^{-1}$ , then dried and carbonised at 400 °C and finally treated with  $H_2SO_4$  for sulfonation.  $Fe^{III}$  salts are found to be reduced to  $Fe_3O_4$  during carbonisation. The catalysts demonstrated high performance in fructose conversion in DMSO and 5-HMF yield, good recyclability and excellent recovery due to its magnetic properties.

Amongst the biomass-derived carbonaceous materials, humins are promising starting material for the synthesis of solid catalysts. Hydrochars, which are usually regarded to as by-products of the hydrothermal conversion of biomass, are rich in oxygen functionalities on their surface such as hydroxyl, carbonyl and carboxylic groups<sup>9</sup> which provide acid sites for catalytic purposes or further functionalisation. Moreover, hydrochars porosity can be enhanced by activation<sup>70</sup>. All these features make hydrochars promising for the development of carbon-based heterogeneous catalysts, as it will be further discussed in this chapter.

### 3. Hydrochar applied for heterogeneous catalysis

After establishing the fundamentals of the HTC process, this next section will deal with the use of these formed hydrochars as heterogeneous catalysts. Carbon-based materials have long been used in heterogeneous catalysis reactions because of their desired properties for catalyst support and carbon-based materials act as direct catalysts in many industrial applications<sup>71</sup>. This kind of materials are especially suitable for catalysis because of their resistance to acid/base media, porosity and surface chemistry control as well as for environmental aspects.

Along with the use of hydrochars as-produced, a lot of research has been applied to devise various modification approaches to further expand its activation capacities<sup>72</sup>. Given that hydrochars can be a highly porous and carbon-rich, they are promising alternatives to replace conventional solid carbon-based catalysts with some known demerits (e.g., high costs and environmentally unfriendliness).

Since catalytic activity is highly dependent on accessibility to catalytic active sites dispersed throughout the internal pores, the morphology and porosity of hydrochars without activation exhibit very poor catalytic properties. To overcome these issues, many studies have been directed

to modifying the morphology and porosity of hydrochars via various treatments<sup>73</sup>.

Hydrochars and related compounds have been used in catalysis in many ways. On their own they can be used as catalysts, mainly as solid acid catalysts. This functionality is secured by introducing strong Brønsted acidity, mainly by sulfonated groups on the surface of the hydrochar particles.

Another widely spread use of hydrochar particles is as catalyst support. The tuneability of their surface polarity and area facilitate the anchoring of metal nanoparticles, which can then be used in different reactions.

A last and least studied use for these hydrochars is the use of them as templates. Since hydrochar can be eliminated by combustion in air at temperatures that are not too drastic, they can be used as structural directing agents.

### 3.1 Sulfonated hydrochar catalysts

Addition of sulfonated groups to HTC synthesised carbon materials give rise to introduction of sulfonic acid groups leading to the formation of a solid acid catalyst that can be used in catalytic reactions such as those tested by Roldán *et al.*<sup>74</sup> (see Fig. 5). These catalysts can be recovered through simple filtration methods and are generally made by treatment of porous carbon in concentrated sulphuric acid at high temperatures. Roldán *et al.* prepared catalysts in this way and tested them in esterification reactions of palmitic acid with methanol, observing in the end a change in the deactivation of the catalyst depending on the activation temperature employed for each catalyst. When temperatures lower than 500 °C were used, the deactivation of the catalyst was attributed to formation of surface sulfonate esters on the surface of the carbon particles, and while for those treated at higher temperature it is thought that accumulation of reactants and products in the pores of the particles is the main cause of deactivation.

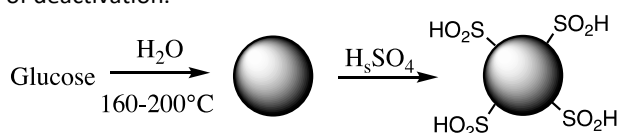


**Figure 5.** Schematic view of sulfonation of porous carbon.

Similar catalysts have been used for the esterification of glycerol<sup>75</sup> and oleic acid<sup>76</sup>. In this case, the glucose used as carbon source was treated for 19 h at 195 °C, leading to the formation of a carbonaceous material, which contained 67.9% carbon and 27.5% oxygen. It was observed that after sulfonation (150 °C, 15 h), the carbon content decreased to 55.8% and oxygen content increased to 40.5%. From this change in values and taking into account the amount of sulphur added, one conclusion is that additional oxygen other than that of the sulfonated groups was added during the treatment with sulphuric acid. This inclusion of O may have happened by water addition to double bonds, hydrolysis of furan groups, or other functionalities. The sulfonated catalyst was tested in the esterification of glycerol with acetic, butyric, and caprylic acid and the catalytic performance compared to the one of commercial

sulfonated resins<sup>75</sup>. Turnover numbers of glycerol and the acetic acid were in the same range for both the commercial and the hydrochar solid catalysts. To reuse the catalysts, these were first treated with acid to cleave the esterified sulfonic groups, which could have formed regenerating the acidity of the surface of the catalyst.

Pileidis *et al.*<sup>77</sup> also prepared hydrochars (HTC conditions 230 °C, 24 h), turned them into solid catalysts, and studied them for the esterification of LA. In this case, not only glucose was used. Cellulose and rice straw were used as carbon sources as well. These sources led to hydrochars with 80, 76, and 70% carbon (for glucose, cellulose and rice straw, respectively) and were then sulfonated (80 °C, 4 h) introducing 5%–6% sulphur. Esterification was carried out at 60 °C and after 3 h almost full conversion was achieved using the glucose-derived catalyst and a 97% selectivity toward the ester. The second best in performance was the catalyst prepared from rice straw with 92% of both conversion and selectivity. With carbonised and sulfonated cellulose, 89% conversion and selectivity were observed.

It is worthy to note that it has been reported that sulfonation at high temperature (150 °C) induces changes in the structure of hydrochar. This change is due to decreasing the abundance of furanic groups and increasing the presence of benzenic rings<sup>78</sup>.

Sulfonated hydrochar has been used for the production of biomass-derived platform molecules, such as monosaccharides or 5-HMF by hydrolysis and dehydration reactions. In this way, glucose or sucrose were transformed into hydrochar at 180 °C for 10–15 h and sulfonated with concentrated sulphuric acid at 200 °C for 15 h.<sup>79</sup>

Alternative methods of sulfonation have been proposed, such as direct HTC with sulfonic precursors (mainly hydroxyethylsulfonic acid)<sup>80</sup>. The catalysts prepared using this method presented very high stability and reusability, enabling future applications.

### 3.2 Pristine hydrochar as catalysts

Sulfonation is a simple method to introduce strong acidic sites into hydrochar. However, the pristine surface also possesses catalytic properties because of the high density of hydroxyl and carboxylic groups. This property has been demonstrated in the application of such catalysts for the 5-HMF production from fructose in ionic liquid<sup>81</sup>. Hydrochar was produced from glucose at 180 °C and 10 h and used after oven-drying without any further treatment. The results showed that fructose was converted into 5-HMF with a maximum yield of 80% after 120 min of reaction time. The stability of these catalysts was not properly evaluated, hence, clarification would be needed; however, this study showed that even sulphur-free surfaces of hydrochars presented catalytic activity in reactions such as the dehydration of fructose.

Hydrochar also permits alkaline functionalisation of surfaces and their use in catalysis<sup>82</sup>. Hence, spherical particles of hydrochar were synthesised from glucose at 160 °C maintaining the temperature for 12 h. Thereafter, acidic functionalities such as carboxylic and hydroxyl

groups were neutralised with sodium hydroxide at room temperature. The sodium-hydroxide-treated hydrochar was active for the base-catalysed aldol condensation<sup>82</sup>. Benzaldehyde was reacted with acetaldehyde to form cinnamaldehyde. High selectivity (94%) was achieved at 34% conversion based on benzaldehyde consumption. At this conversion value, the cinnamaldehyde also started to react with acetaldehyde to produce the higher weight homolog. In comparison with sodium hydroxide solutions, the modified hydrochar is less active but more selective and can be used in three catalytic runs with the same activity.

In summary, it can be said that hydrochar possesses a promising potential as a metal-free catalyst for industrial application. Introduction of strong Brønsted acid sites is straightforward by sulfonation, for example, by treatment with sulphuric acid. However, oxygen functionalities of pristine hydrochar can also be used for catalytic transformation.

### 3.3 Hydrochar as catalyst support

Active carbons are classical supports for numerous catalysts found in commercial processes. This widespread use is due to their high stability and surface area. In general, activated carbons possess a high surface area of 1000–1500 m<sup>2</sup>g<sup>-1</sup>, and they can be made nonpolar and hydrophobic if they have a low oxygen content. In contrast, hydrochar has a very polar surface and a much lower surface area. By reduction of oxygen content and increasing that of carbon, the properties of hydrochars can become closer to those of nonpolar activated carbon<sup>74</sup>. By tuning these parameters (surface area and polarity) the deposition of metal precursors can be enhanced. Hydrochars with or without further modification have been employed as carbon support for metals<sup>83–86</sup>. The process is, in most cases, the same. A hydrochar is synthesised and then activated (thermally or chemically) to support the metal precursor, which is then reduced by addition of a reducing agent (NaBH<sub>4</sub> for example). In some cases, the reduction step can be avoided when using pristine carbon surfaces<sup>87,88</sup>, as C is a common reduction agent. Glucose-derived and modified hydrochars support and stabilise the metal nanoparticles (NPs) and keep them active for prolonged time under reaction conditions. Palladium NPs supported onto hydrochar were employed for the Suzuki–Miyaura coupling<sup>83</sup>. The catalyst demonstrated high catalytic activity for the reaction of many aryl halides and boronic acids. It could be recycled for up to five times through simple centrifugation. In liquid-state reactions, leaching of the supported metal is usually a problem but the properties of hydrochar favours the redeposition of leached particles during cool-down of the reaction.

More elaborated supports can be designed by combining HTC with a porous polymer as template. Such was done by Cheng *et al.*<sup>89</sup> where, in this case, a polymer was introduced during the HTC process serving as a template, which was then treated at 700 °C in a reducing atmosphere. This thermal treatment increased the BET

surface area significantly. This adsorbent was then loaded with gold NPs and tested for the hydrogenation of 4-nitrophenol to 4-aminophenol with sodium borohydride, resulting in high catalytic activity.

As mentioned before, hydrochars can be treated under basic condition neutralising any acid surface functionality. This neutralisation can be interesting when using them as supports such as when loading palladium NPs and using them in oxidation reactions<sup>82</sup>. The absence of acid sites lowers the number of side reactions that can occur augmenting selectivity, and the high dispersion of the metal allows high activities to be achieved. This high dispersion is aided by this basic pre-treatment of the material as evidenced when smaller palladium NPs were observed for those samples treated with higher concentration of basic solution (2.7 nm versus 7.5 nm).

The hydrothermal process can also be performed together with metal oxide particles<sup>90–92</sup>. Hence, using magnetic metal oxide cores, a magnetically active material can be obtained. In this way, active catalysts for the Suzuki–Miyaura cross-coupling reaction have been prepared with palladium and platinum NPs as active sites<sup>90</sup>. In this work, Fe<sub>3</sub>O<sub>4</sub> particles (magnetite) were introduced during the carbonisation of glucose at 180 °C for 4 h. After this, palladium or platinum NPs were deposited on the carbon shell and the whole material protected by a further layer of approx. 35 nm thickness of mesoporous silica. The silica was added to prevent sintering of the metal NPs while its porosity allowed the organic molecules tested to pass through it. The magnetite particles had a uniform diameter of approx. 180 nm composed of nanocrystals of approx. 8 nm sizes. The carbon shell thickness was measured to be approx. 15 nm. The size of the supported palladium and platinum particles was determined by HRTEM and mean diameters of 14 and 25 nm were obtained, respectively. The hydrophilic surface of the hydrochar facilitated dispersion of the particles in water during the mesoporous silica synthesis and allowed a regular coverage of the particles. At all stages of the synthesis, the particles showed high superparamagnetic properties, which facilitated the retrieval of the catalyst. High conversions were shown by the catalysts (77%–99%) depending on the nature of the reactants.

It can be seen from this overview that carbonaceous materials synthesised through the HTC process have a very wide application as catalysts support thanks to their physical and chemical properties.

### 3.4 Hydrochar as sacrificial component

The defined structure and geometry of the spherical particles of hydrochar can be used as a template, since it can be easily removed with a thermal treatment in air at about 500 °C.<sup>93–95</sup> With this in mind, very effective catalysts for the low-temperature oxidation of CO were produced<sup>93</sup>. In his work, Zhao *et al.* produced gold NPs by bringing in contact the gold precursor and glucose in water. Glucose has two main roles in this synthesis, it acts as reducing agent and it is also a carbon source for generating the hydrochar. Once the gold NPs were formed, the cerium

precursor was added and the mixture heated to 180 °C for different periods of time (1, 6, 10, and 20 h). Afterward, the solid was collected and calcined at different temperatures in the range of 300–600 °C for 6 h, eliminating all hydrochar (see Fig. 6). TEM images (of the calcined samples) showed gold NPs of an average size of 11 nm after 1 h hydrothermal treatment and the whole diameter of the core-shell structure was about 40 nm. When the hydrothermal treatment was prolonged to 10 h, gold NPs grew to 16 nm and the shells to 100 nm. The best catalytic performance in carbon monoxide oxidation was that shown by the catalyst that was prepared by hydrothermal treatment for 10 h and was subsequently calcined at 600 °C. This catalyst allowed the reduction of the reaction temperature from 300 to 155 °C for full conversion and it was also tested on stream for 70 h without any deactivation being evident.

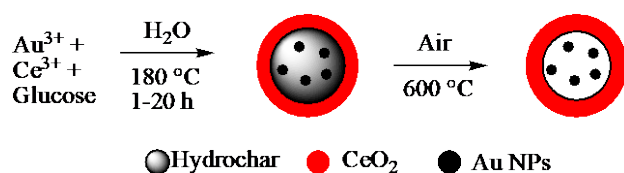


**Figure 6.** Schematic representation of the synthesis of core-shell distribution of gold particles and cerium oxide.

Similarly, cobalt NPs protected within hollow mesoporous silica spheres were synthesized<sup>94</sup>. Starting from spherical particles of hydrochar with diameters of 100–150 nm and synthesised from glucose at 180 °C for 4.5 h. After impregnation with cobalt nitrate providing NPs of approx. 4 nm and the synthesis of a mesoporous silica shell (thickness approx. 20 nm) with cetyltrimethylammonium bromide-based structures as soft template, all organic material was removed by calcination at 430 °C. This synthesis procedure provided a catalyst with interesting performance in the epoxidation of alkenes. When the cobalt/silica hollow spheres were employed in the epoxidation of styrene with oxygen, a 94% selectivity toward the epoxide was achieved at almost complete conversion.

#### 4. Hydrochars in electrocatalysis

Electrocatalysis plays a crucial role in many energy storage and conversion technologies such as the oxygen reduction reaction (ORR) at the cathode of metal-air batteries or fuel cells, the oxygen evolution reaction (OER) and hydrogen evolution reaction (HER) at either electrode of water electrolyzers, and CO<sub>2</sub> reduction in liquid fuel conversion devices. The problem of these electrocatalytic reactions is that they generally display slow kinetics and as such requires the development of a catalyst that can improve and give future perspective to these technologies<sup>96</sup>.

An important reaction in sustainable energy systems is the oxygen reduction reaction (ORR). Out of the metal-free ORR electrocatalysts tested, significant research has been focused on nitrogen-doped carbon materials<sup>97–101</sup>. Inside the graphitic matrix of carbon materials, polarised C-N bonds (whose polarisation strength depends on the type of

nitrogen contained) modifies the energies of adjacent carbon atoms, generating active sites for the ORR reaction. At the same time, the delocalisation of donated electrons within the  $\pi$ -system translates into an increase in the n-type conductivity of the material<sup>102</sup>. Examples of these nitrogen-doped carbon materials have been synthesised using natural halloysite as a template and urea as the nitrogen source<sup>98</sup>; a flaky morphology was obtained with glucose as a carbon source, whereas using furfural resulted in rod-like structures. The metal-free electrocatalysts were tested for ORR in alkaline aqueous electrolytes, and the rod-like catalyst demonstrated a better performance than the flaky material. Due to both of them containing a similar amount of N and graphitisation degrees, the high performance of the rod-like catalysts was attributed to the high surface area and large pore volume (which provided more active sites), the great complexity in pore size distribution, and the rod-like morphology, which facilitated electron transport. Compared to a commercial Pt/C (20 wt. %) catalyst, the carbon catalysts demonstrated a higher retention in diffusion limiting current density (after 3000 cycles) and enhanced methanol tolerances. When tested as cathodes in a single cell fuel cell of the H<sub>2</sub>/O<sub>2</sub> anion exchange membrane kind, the rod-like catalyst delivered a peak power density as high as 703 mW cm<sup>-2</sup> (vs 1100 mW cm<sup>-2</sup> with the commercial Pt/C cathode catalyst). Time and resources have also been invested in researching doping with different heteroatoms such as B and S<sup>99,103,104</sup>. In one study of carbogels derived from glucose and ovalbumin, the synergistic effect of boron and nitrogen was thought to augment the electron transfer numbers and lower hydrogen peroxide yields when compared to those observed in purely N-doped systems, whereas the presence of S decreased the surface area and nitrogen content resulting in diminished ORR performance<sup>99</sup>. In contrast, sulphur doping of 5.5 wt. % in SiO<sub>2</sub>-templated mesoporous ordered carbons was found to enhance the electrocatalytic activity in the ORR in alkaline solution, likely because the mesoporous structure was retained from the templating method.<sup>103</sup>

Heteroatom-doped systems are not only used for ORR, they have also been tested for the HER. 2D crystalline carbons were obtained from hydrochars of glucose, fructose or cellulose with guanine, which played an important role in producing the 2D-morphology of the resultant carbon materials<sup>105</sup>. The porous N-doped carbons were not only found to be highly active towards ORR, but also showed efficiency for HER with a very low overpotential of 0.35 V to achieve 10 mA cm<sup>-2</sup> in alkaline medium.

In the other half of the water splitting reaction, suitable catalysts are also required for the ORR; in the past, the development of fuel cells has been held back by the slow kinetics of the OER. Non-noble metal alternatives for OER are often based on transition metal oxides, while carbon-based materials have generally been underexplored because of their relatively poor performance. However, one approach used activated carbon cloth by creating oxygen-containing functional groups on its surface using

peroxovanadium complexes, which results in a higher specific surface area and faster electron transfer rate, when compared to a pristine carbon cloth<sup>106</sup>. The overpotential (310 mV) at 10 mA cm<sup>-2</sup> of the activated carbon cloth is much lower than the pristine material and comparable to that of RuO<sub>2</sub>/C (280 mV), making the carbon cloth a competitive non-metal catalyst for OER. The growth of transition metals on a carbon fabric can also improve electrocatalytic performance. In one study, highly porous and granular Ni-Co nanowires were grown hydrothermally on a carbon fibre woven fabric and then coated with a conductive shell by glucose carbonisation<sup>107</sup>. The structure of the nanowires greatly increased the catalytic surface area delivering an overpotential of 302 mV at a current density of 10 mA cm<sup>-2</sup>. The conductive carbon layer not only enabled facile electron transport throughout the entire electrode, but also prevented fragmentation of the nanowires during reaction, resulting in greater structural integrity and more reliable performance.

Lastly, HTC has been used to prepare a 3D hierarchical structure of mesoporous SnO<sub>2</sub> nano-sheets supported on flexible carbon cloth, which could efficiently and selectively electrochemically reduce CO<sub>2</sub> to formate in aqueous conditions<sup>108</sup>. The electrode exhibited a partial current density of 45 mA cm<sup>-2</sup> at a moderate overpotential (0.88 V) with high Faradaic efficiency (87%), even larger than most gas diffusion electrodes. The performance was attributed to the presence of SnO<sub>2</sub> particles, which showed high selectivity in the reduction of CO<sub>2</sub>. The highly porous structure provided a large surface area increasing the contact surface between electrode and electrolyte and facilitating mass and charge transfer, and the robust structure maintained the high stability of the electrocatalyst during long-term operation.

In summary, hydrochars and related compounds have a wide range of applicability, going beyond heterogeneous catalysis and going into the niche field of electrocatalysis.

## 5. Conclusions

In this chapter, the HTC process has been explained and we can conclude that it has established itself as a very promising strategy to emancipate from fossil fuel by usage of bio-based waste. This conceptually simple process allows to obtain valuable platform chemicals (5-HMF, LA), hydrochar and carbon dots. Although many advances have been achieved in the last two decades in the comprehension of the mechanisms of this HTC process, many efforts are still needed to shed light on the complex networks of reaction and interaction pathways that lead to the formation of the aforementioned products. Moreover, there is still a strong need for an optimisation of the process through development of catalysts, which can drive selectively the reaction towards the desired product, avoiding loss of material and synthesis of by-products. Carbon-based catalyst can potentially fulfil this requirement because of their great versatility, the abundance of functionalities on their surface and the easy tuneability of their physical properties such as porosity.

Another important aspect shown here is the use of these hydrochars in heterogeneous catalytic applications. Pristine hydrochar surfaces that do not require addition of any extra species contain a wide variety of oxygen functionalities that can be exploited for catalytic purposes. Further than this, modification of the surface through thermal treatment reduces the oxygen content and shifts hydrophilicity of the materials as well as increases the surface area.

We can find similarities between hydrochar and silica with the exception that hydrochar can be easily combusted. Making use of these similarities, various complex structured materials can be prepared.

Although many of the works cited in this chapter used glucose as a carbon source due to it being more scientifically reproducible, the outlook of all experiments is the use of real raw biomass as this carbon source.

In conclusion, from the information recapped, it seems proven that HTC is a valuable asset both in refinement of bio-waste as well as in synthesis of catalysts. The preparation of hydrochar, and its chemical reactivity, allows the incorporation of heteroatoms other than O. This flexibility has been exploited in material synthesis, but for catalysis, further research is needed. Many impulses from HTC for catalysis can be expected in the future that might also lead to industrial applications following a sustainable alternative to already established processes.

## Acknowledgements

This project has received funding from the European Union's Horizon 2020 research and innovation programme under the Marie Skłodowska-Curie grant agreement No 721991.

## References

- (1) Marinovic, A.; Pileidis, F. D.; Titirici, M.-M. CHAPTER 5. Hydrothermal Carbonisation (HTC): History, State-of-the-Art and Chemistry. In *Porous Carbon Materials from Sustainable Precursors*; The Royal Society of Chemistry, 2015; pp 129–155.
- (2) Funke, A.; Ziegler, F. Hydrothermal Carbonization of Biomass: A Summary and Discussion of Chemical Mechanisms for Process Engineering. *Biofuels, Bioprod. Biorefining* **2010**, *4* (2), 160–177.
- (3) Wang, Q.; Li, H.; Chen, L.; Huang, X.; Qing, W.; Hong, L.; Lique, C.; Xuejie, H. Monodispersed Hard Carbon Spherules with Uniform Nanopores. *Carbon* **2001**, *39*, 2211–2214.
- (4) Falco, C.; Baccile, N.; Titirici, M. M. Morphological and Structural Differences between Glucose, Cellulose and Lignocellulosic Biomass Derived Hydrothermal Carbons. *Green Chem.* **2011**, *13* (11), 3273–3281.
- (5) Falco, C.; Perez Caballero, F.; Babonneau, F.; Gervais, C.; Laurent, G.; Titirici, M. M.; Baccile, N. Hydrothermal Carbon from Biomass: Structural Differences between Hydrothermal and Pyrolyzed Carbons via <sup>13</sup>C Solid State NMR. *Langmuir* **2011**, *27* (23), 14460–14471.

- (6) Camillo, F.; Manuel, S. J.; Nicolas, B.; Marta, S.; Torbjorn, van der M.; Emilia, M.; Diego, C.; Maria-Magdalena, T. Hydrothermal Carbons from Hemicellulose-Derived Aqueous Hydrolysis Products as Electrode Materials for Supercapacitors. *ChemSusChem* **2013**, *6* (2), 374–382.
- (7) Arne, T.; Markus, A.; Titirici, M.-M.; Thomas, A.; Antonietti, M. Back in the Black: Hydrothermal Carbonization of Plant Material as an Efficient Chemical Process to Treat the CO<sub>2</sub> Problem? *New J. Chem.* **2007**, *31* (6), 787–789.
- (8) Titirici, M. M.; Thomas, A.; Antonietti, M. Aminated Hydrophilic Ordered Mesoporous Carbons. *J. Mater. Chem.* **2007**, *17* (32), 3412–3418.
- (9) Fuertes, A. B.; Sevilla, M. The Production of Carbon Materials by Hydrothermal Carbonization of Cellulose. *Carbon* **2009**, *47* (9), 2281–2289.
- (10) Werpy, T.; Petersen, G. *Top Value Added Chemicals from Biomass*, Vol. I. National Renewable Energy Laboratory (NREL), report DOE/GO-102004-1992, 2004.
- (11) Yahya, M. A.; Al-Qodah, Z.; Ngah, C. W. Z. Agricultural Bio-Waste Materials as Potential Sustainable Precursors Used for Activated Carbon Production: A Review. *Renew. Sustain. Energy Rev.* **2015**, *46*, 218–235.
- (12) Lu, A. H.; Schüth, F. Nanocasting: A Versatile Strategy for Creating Nanostructured Porous Materials. *Adv. Mater.* **2006**, *18* (14), 1793–1805.
- (13) Kubo, S.; Demir-Cakan, R.; Zhao, L.; White, R. J.; Titirici, M. M. Porous Carbohydrate-Based Materials via Hard Templating. *ChemSusChem* **2010**, *3* (2), 188–194.
- (14) Demir-Cakan, R.; Baccile, N.; Antonietti, M.; Titirici, M.-M. Carboxylate-Rich Carbonaceous Materials via One-Step Hydrothermal Carbonization of Glucose in the Presence of Acrylic Acid. *Chem. Mater.* **2009**, *21* (3), 484–490.
- (15) Kabyemela, B. M.; Adschiri, T.; Malaluan, R. M.; Arai, K. Glucose and Fructose Decomposition in Subcritical and Supercritical Water: Detailed Reaction Pathway, Mechanisms, and Kinetics. *Ind. Eng. Chem. Res.* **1999**, *38* (8), 2888–2895.
- (16) Asghari, F. S.; Yoshida, H. Kinetics of the Decomposition of Fructose Catalyzed by Hydrochloric Acid in Subcritical Water: Formation of 5-Hydroxymethylfurfural, Levulinic, and Formic Acids. *Ind. Eng. Chem. Res.* **2007**, *46* (23), 7703–7710.
- (17) Buendia-Kandia, F.; Mauviel, G.; Guedon, E.; Rondags, E.; Petitjean, D.; Dufour, A. Decomposition of Cellulose in Hot-Compressed Water: Detailed Analysis of the Products and Effect of Operating Conditions. *Energy Fuels* **2018**, *32* (4), 4127–4138.
- (18) Matsumura, Y.; Sasaki, M.; Okuda, K.; Takami, S.; Ohara, S.; Umetsu, M.; Adschiri, T. Supercritical Water Treatment of Biomass for Energy and Material Recovery. *Combust. Sci. Technol.* **2007**, *178*, 509–536.
- (19) Jin, F.; Zhou, Z.; Enomoto, H.; Moriya, T.; Higashijima, H. Conversion Mechanism of Cellulosic Biomass to Lactic Acid in Subcritical Water and Acid–Base Catalytic Effect of Subcritical Water. *Chem. Lett.* **2004**, *33* (2), 126–127.
- (20) Flannelly, T.; Lopes, M.; Kupiainen, L.; Dooley, S.; Leahy, J. J. RSC Advances Levulinic Acids from the Hydrolysis of Biomass Derived Hexose Carbohydrates. *RSC Adv.* **2016**, *6* (7), 5797–5804.
- (21) Yang, L.; Tsilomelekis, G.; Caratzoulas, S.; Vlachos, D. G. Cover Picture: Mechanism of Brønsted Acid-Catalyzed Glucose Dehydration (ChemSusChem 8/2015). *ChemSusChem* **2015**, *8*, 1289–1289.
- (22) Steinbach, D.; Kruse, A.; Sauer, J.; Vetter, P. Sucrose Is a Promising Feedstock for the Synthesis of the Platform Chemical Hydroxymethylfurfural. *Energies* **2018**, *11* (3), 645.
- (23) Pacheco, J. J.; Davis, M. E. Synthesis of Terephthalic Acid via Diels-Alder Reactions with Ethylene and Oxidized Variants of 5-Hydroxymethylfurfural. *Proc. Natl. Acad. Sci.* **2014**, *111* (23), 8363–8367.
- (24) Liu, Z. Y.; Dumesic, J. A.; Barrett, C. J.; Román-Leshkov, Y. Production of Dimethylfuran for Liquid Fuels from Biomass-Derived Carbohydrates. *Nature* **2007**, *447* (7147), 982–985.
- (25) Jae, J.; Zheng, W.; Lobo, R. F.; Vlachos, D. G. Production of Dimethylfuran from Hydroxymethylfurfural through Catalytic Transfer Hydrogenation with Ruthenium Supported on Carbon. *ChemSusChem* **2013**, *6* (7), 1158–1162.
- (26) González Maldonado, G. M.; Assary, R. S.; Dumesic, J.; Curtiss, L. A. Experimental and Theoretical Studies of the Acid-Catalyzed Conversion of Furfuryl Alcohol to Levulinic Acid in Aqueous Solution. *Energy Environ. Sci.* **2012**, *5* (5), 6981–6989.
- (27) Asghari, F. S.; Yoshida, H. Acid-Catalyzed Production of 5-Hydroxymethyl Furfural from D-Fructose in Subcritical Water. *Ind. Eng. Chem. Res.* **2006**, *45* (7), 2163–2173.
- (28) Haibo Zhao; Johnathan E. Holladay; Heather Brown; Z. Conrad Zhang. Metal Chlorides in Ionic Liquid Solvents Convert Sugars to 5-Hydroxymethylfurfural. *Science* **2007**, *316* (15), 1597–1600.
- (29) Alipour, S. High Yield 5-(Hydroxymethyl)Furfural Production from Biomass Sugars under Facile Reaction Conditions: A Hybrid Enzyme- and Chemo-Catalytic Technology. *Green Chem.* **2016**, *18* (18), 4990–4998.
- (30) Li, C.; Zhang, Z.; Zhao, Z. K. Direct Conversion of Glucose and Cellulose to 5-Hydroxymethylfurfural in Ionic Liquid under Microwave Irradiation. *Tetrahedron Lett.* **2009**, *50* (38), 5403–5405.
- (31) Eminov, S.; Filippousi, P.; Brandt, A.; Wilton-Ely, J.; Hallett, J. Direct Catalytic Conversion of Cellulose to 5-Hydroxymethylfurfural Using Ionic Liquids. *Inorganics* **2016**, *4* (4), 32.
- (32) Kuster, B. F. M. 5-Hydroxymethylfurfural (HMF). A Review Focussing on Its Manufacture. *Starch-starke* **1990**, *42* (8), 314–321.

- (33) Bozell, J. J.; Petersen, G. R. Technology Development for the Production of Biobased Products from Biorefinery Carbohydrates - The US Department of Energy's "Top 10" Revisited. *Green Chem.* **2010**, *12* (4), 539–554.
- (34) Ghorpade, V.; Hanna, M. Industrial Applications for Levulinic Acid. In *Cereals*; Springer US: Boston, MA, **2013**; pp 49–55.
- (35) Fang, Q.; Hanna, M. A. Experimental Studies for Levulinic Acid Production from Whole Kernel Grain Sorghum. *Bioresour. Technol.* **2002**, *81* (3), 187–192.
- (36) Suganuma, S.; Nakajima, K.; Kitano, M.; Yamaguchi, D.; Kato, H.; Hayashi, S.; Hara, M. Hydrolysis of Cellulose by Amorphous Carbon Bearing SO<sub>3</sub>H, COOH, and OH Groups. *J. Am. Chem. Soc.* **2008**, *130* (38), 12787–12793.
- (37) Baccile, N.; Laurent, G.; Babonneau, F.; Fayon, F.; Titirici, M. M.; Antonietti, M. Structural Characterization of Hydrothermal Carbon Spheres by Advanced Solid-State MAS <sup>13</sup>C NMR Investigations. *J. Phys. Chem. C* **2009**, *113* (22), 9644–9654.
- (38) Van Zandvoort, I.; Koers, E. J.; Weingarth, M.; Buijninx, P. C. A.; Baldus, M.; Weckhuysen, B. M. Structural Characterization of <sup>13</sup>C-Enriched Humins and Alkali-Treated <sup>13</sup>C Humins by 2D Solid-State NMR. *Green Chem.* **2015**, *17* (8), 4383–4392.
- (39) Brown, A. B.; McKeogh, B. J.; Tompsett, G. A.; Lewis, R.; Deskins, N. A.; Timko, M. T. Structural Analysis of Hydrothermal Char and Its Models by Density Functional Theory Simulation of Vibrational Spectroscopy. *Carbon* **2017**, *125*, 614–629.
- (40) Tsilomelekis, G.; Orella, M. J.; Lin, Z.; Cheng, Z.; Zheng, W.; Nikolakis, V.; Vlachos, D. G. Molecular Structure, Morphology and Growth Mechanisms and Rates of 5-Hydroxymethyl Furfural (HMF) Derived Humins. *Green Chem.* **2016**, *18* (7), 1983–1993.
- (41) Cheng, Z.; Everhart, J. L.; Tsilomelekis, G.; Nikolakis, V.; Saha, B.; Vlachos, D. G. Structural Analysis of Humins Formed in the Brønsted Acid Catalyzed Dehydration of Fructose. *Green Chem.* **2018**, *20* (5), 997–1006.
- (42) Qi, Y.; Song, B.; Qi, Y. The Roles of Formic Acid and Levulinic Acid on the Formation and Growth of Carbonaceous Spheres by Hydrothermal Carbonization. *RSC Adv.* **2016**, *6* (104), 102428–102435.
- (43) Xu, X.; Ray, R.; Gu, Y.; Ploehn, H. J.; Gearheart, L.; Raker, K.; Scrivens, W. A. Electrophoretic Analysis and Purification of Fluorescent Single-Walled Carbon Nanotube Fragments. *J. Am. Chem. Soc.* **2004**, *126* (40), 12736–12737.
- (44) Shen, J.; Zhu, Y.; Yang, X.; Li, C. Graphene Quantum Dots: Emergent Nanolights for Bioimaging, Sensors, Catalysis and Photovoltaic Devices. *Chem. Commun.* **2012**, *48* (31), 3686–3699.
- (45) Liu, F.; Jang, M. H.; Ha, H. D.; Kim, J. H.; Cho, Y. H.; Seo, T. S. Facile Synthetic Method for Pristine Graphene Quantum Dots and Graphene Oxide Quantum Dots: Origin of Blue and Green Luminescence. *Adv. Mater.* **2013**, *25* (27), 3657–3662.
- (46) Zheng, X. T.; Ananthanarayanan, A.; Luo, K. Q.; Chen, P. Glowing Graphene Quantum Dots and Carbon Dots: Properties, Syntheses, and Biological Applications. *Small* **2015**, *11* (14), 1620–1636.
- (47) Ray, S. C.; Saha, A.; Jana, N. R.; Sarkar, R. Fluorescent Carbon Nanoparticles: Synthesis, Characterization, and Bioimaging Application. *J. Phys. Chem. C* **2009**, *113* (43), 18546–18551.
- (48) Baker, S. N.; Baker, G. A. Luminescent Carbon Nanodots: Emergent Nanolights. *Angew. Chemie - Int. Ed.* **2010**, *49* (38), 6726–6744.
- (49) Pan, D.; Zhang, J.; Li, Z.; Wu, M. Hydrothermal Route for Cutting Graphene Sheets into Blue-Luminescent Graphene Quantum Dots. *Adv. Mater.* **2010**, *22* (6), 734–738.
- (50) Wang, N.; Wang, Y.; Guo, T.; Yang, T.; Chen, M.; Wang, J. Green Preparation of Carbon Dots with Papaya as Carbon Source for Effective Fluorescent Sensing of Iron (III) and Escherichia Coli. *Biosens. Bioelectron.* **2016**, *85*, 68–75.
- (51) Purbia, R.; Paria, S. Green Synthesis of Single-Crystalline Akaganeite Nanorods for Peroxidase Mimic Colorimetric Sensing of Ultralow-Level Vitamin B1 and Sulfide Ions. *ACS Appl. Nano Mater.* **2018**, *1* (3), 1236–1246.
- (52) Liao, J.; Cheng, Z.; Zhou, L. Nitrogen-Doping Enhanced Fluorescent Carbon Dots: Green Synthesis and Their Applications for Bioimaging and Label-Free Detection of Au<sup>3+</sup> Ions. *ACS Sustain. Chem. Eng.* **2016**, *4* (6), 3053–3061.
- (53) Edison, T. N. J. I.; Atchudan, R.; Shim, J. J.; Kalimuthu, S.; Ahn, B. C.; Lee, Y. R. Turn-off Fluorescence Sensor for the Detection of Ferric Ion in Water Using Green Synthesized N-Doped Carbon Dots and Its Bio-Imaging. *J. Photochem. Photobiol. B Biol.* **2016**, *158*, 235–242.
- (54) Jahanbakhshi, M.; Habibi, B. A Novel and Facile Synthesis of Carbon Quantum Dots via Salep Hydrothermal Treatment as the Silver Nanoparticles Support: Application to Electroanalytical Determination of H<sub>2</sub>O<sub>2</sub> in Fetal Bovine Serum. *Biosens. Bioelectron.* **2016**, *81*, 143–150.
- (55) Atchudan, R.; Edison, T. N. J. I.; Sethuraman, M. G.; Lee, Y. R. Efficient Synthesis of Highly Fluorescent Nitrogen-Doped Carbon Dots for Cell Imaging Using Unripe Fruit Extract of Prunus Mume. *Appl. Surf. Sci.* **2016**, *384*, 432–441.
- (56) Li, J.; Zhang, L.; Li, P.; Zhang, Y.; Dong, C. One Step Hydrothermal Synthesis of Carbon Nanodots to Realize the Fluorescence Detection of Picric Acid in Real Samples. *Sensors Actuators, B Chem.* **2018**, *258*, 580–588.
- (57) Wang, F.; Hao, Q.; Zhang, Y.; Xu, Y.; Lei, W. Fluorescence Quenchometric Method for Determination of Ferric Ion Using Boron-Doped Carbon Dots. *Microchim. Acta* **2016**, *183* (1), 273–279.

- (58) Chen, Y.; Wu, Y.; Weng, B.; Wang, B.; Li, C. Facile Synthesis of Nitrogen and Sulfur Co-Doped Carbon Dots and Application for Fe(III) Ions Detection and Cell Imaging. *Sensors Actuators, B Chem.* **2016**, *223*, 689–696.
- (59) Guo, Y.; Yang, L.; Li, W.; Wang, X.; Shang, Y.; Li, B. Carbon Dots Doped with Nitrogen and Sulfur and Loaded with Copper(II) as a “Turn-on” Fluorescent Probe for Cystein, Glutathione and Homocysteine. *Microchim. Acta* **2016**, *183* (4), 1409–1416.
- (60) Krawielitzki, S.; Kläusli, T. M. Modified Hydrothermal Carbonization Process for Producing Biobased 5-HMF Platform Chemical. *Ind. Biotechnol.* **2015**, *11* (1), 6–8.
- (61) Hayes, D. J.; Fitzpatrick, S.; Hayes, M. H. B.; Ross, J. R. H. The Biofine Process – Production of Levulinic Acid, Furfural, and Formic Acid from Lignocellulosic Feedstocks, in Biorefineries-Industrial Processes and Products: Status Quo and Future Directions. *Biorefineries - Ind. Process. Prod.* **2006**, *1* (1), 139–164.
- (62) Wang, P.; Yu, H.; Zhan, S.; Wang, S. Catalytic Hydrolysis of Lignocellulosic Biomass into 5-Hydroxymethylfurfural in Ionic Liquid. *Bioresour. Technol.* **2011**, *102* (5), 4179–4183.
- (63) Asghari, F. S.; Yoshida, H. Dehydration of Fructose to 5-Hydroxymethylfurfural in Sub-Critical Water over Heterogeneous Zirconium Phosphate Catalysts. *Carbohydr. Res.* **2006**, *341* (14), 2379–2387.
- (64) Nandiwale, K. Y.; Galande, N. D.; Thakur, P.; Sawant, S. D.; Zambre, V. P.; Bokade, V. V. One-Pot Synthesis of 5-Hydroxymethylfurfural by Cellulose Hydrolysis over Highly Active Bimodal Micro/Mesoporous H-ZSM-5 Catalyst. *ACS Sustain. Chem. Eng.* **2014**, *2* (7), 1928–1932.
- (65) Ramli, N. A. S.; Amin, N. A. S. Kinetic Study of Glucose Conversion to Levulinic Acid over Fe/HY Zeolite Catalyst. *Chem. Eng. J.* **2016**, *283*, 150–159.
- (66) Shen, F.; Smith, R. L.; Li, L.; Yan, L.; Qi, X. Eco-Friendly Method for Efficient Conversion of Cellulose into Levulinic Acid in Pure Water with Cellulase-Mimetic Solid Acid Catalyst. *ACS Sustain. Chem. Eng.* **2017**, *5* (3), 2421–2427.
- (67) Zhang, T.; Li, W.; Xu, Z.; Liu, Q.; Ma, Q.; Jameel, H.; Chang, H. min; Ma, L. Catalytic Conversion of Xylose and Corn Stalk into Furfural over Carbon Solid Acid Catalyst in  $\gamma$ -Valerolactone. *Bioresour. Technol.* **2016**, *209*, 108–114.
- (68) Jin, P.; Zhang, Y.; Chen, Y.; Pan, J.; Dai, X.; Liu, M.; Yan, Y.; Li, C. Facile Synthesis of Hierarchical Porous Catalysts for Enhanced Conversion of Fructose to 5-Hydroxymethylfurfural. *J. Taiwan Institute Chem. Eng.* **2017**, *75*, 59–69.
- (69) Hu, L.; Tang, X.; Wu, Z.; Lin, L.; Xu, J.; Xu, N.; Dai, B. Magnetic Lignin-Derived Carbonaceous Catalyst for the Dehydration of Fructose into 5-Hydroxymethylfurfural in Dimethylsulfoxide. *Chem. Eng. J.* **2015**, *263*, 299–308.
- (70) Sevilla, M.; Fuertes, A. B. Sustainable Porous Carbons with a Superior Performance for CO<sub>2</sub>capture. *Energy Environ. Sci.* **2011**, *4* (5), 1765–1771.
- (71) Rodríguez-Reinoso, F. The Role of Carbon Materials in Heterogeneous Catalysis. *Carbon* **1998**, *36* (3), 159–175.
- (72) Qian, K.; Kumar, A.; Zhang, H.; Bellmer, D.; Huhnke, R. Recent Advances in Utilization of Biochar. *Renew. Sustain. Energy Rev.* **2015**, *42*, 1055–1064.
- (73) He, X.; Zhang, Y.; Zhu, C.; Huang, H.; Hu, H.; Liu, Y.; Kang, Z. Mesoporous Carbon Nanoparticles: A Super Catalyst Support for Fuel Cells. *New J. Chem.* **2015**, *39* (11), 8667–8672.
- (74) Roldán, L.; Pires, E.; Fraile, J. M.; García-Bordejé, E. Impact of Sulfonated Hydrothermal Carbon Texture and Surface Chemistry on Its Catalytic Performance in Esterification Reaction. *Catal. Today* **2015**, *249*, 153–160.
- (75) De La Calle, C.; Fraile, J. M.; García-Bordejé, E.; Pires, E.; Roldán, L. Biobased Catalyst in Biorefinery Processes: Sulphonated Hydrothermal Carbon for Glycerol Esterification. *Catal. Sci. Technol.* **2015**, *5* (5), 2897–2903.
- (76) Laohapornchaiphon, J.; Smith, C. B.; Smith, S. M. One-Step Preparation of Carbon-Based Solid Acid Catalyst from Water Hyacinth Leaves for Esterification of Oleic Acid and Dehydration of Xylose. *Chem. Asian J.* **2017**, *12* (24), 3178–3186.
- (77) Pileidis, F. D.; Tabassum, M.; Coutts, S.; Ttitirici, M. M.; Titirici, M.-M. Esterification of Levulinic Acid into Ethyl Levulinate Catalysed by Sulfonated Hydrothermal Carbons. *Chinese J. Catal.* **2014**, *35* (6), 929–936.
- (78) Fraile, J. M.; García-Bordejé, E.; Pires, E.; Roldán, L. New Insights into the Strength and Accessibility of Acid Sites of Sulfonated Hydrothermal Carbon. *Carbon* **2014**, *77*, 1157–1167.
- (79) Liu, M.; Jia, S.; Gong, Y.; Song, C.; Guo, X. Effective Hydrolysis of Cellulose into Glucose over Sulfonated Sugar-Derived Carbon in an Ionic Liquid. *Ind. Eng. Chem. Res.* **2013**, *52* (24), 8167–8173.
- (80) Nata, I. F.; Putra, M. D.; Irawan, C.; Lee, C.-K. Catalytic Performance of Sulfonated Carbon-Based Solid Acid Catalyst on Esterification of Waste Cooking Oil for Biodiesel Production. *J. Environ. Chem. Eng.* **2017**, *5* (3), 2171–2175.
- (81) Qi, X.; Liu, N.; Lian, Y. Carbonaceous Microspheres Prepared by Hydrothermal Carbonization of Glucose for Direct Use in Catalytic Dehydration of Fructose. *RSC Adv.* **2015**, *5* (23), 17526–17531.
- (82) Yan, Y.; Dai, Y.; Wang, S.; Jia, X.; Yu, H.; Yang, Y. Catalytic Applications of Alkali-Functionalized Carbon Nanospheres and Their Supported Pd Nanoparticles. *Appl. Catal. B Environ.* **2016**, *184*, 104–118.
- (83) Dong, W.; Cheng, S.; Feng, C.; Shang, N.; Gao, S.; Wang, C.; Wang, Z. Carbon Nanospheres with Well-Controlled Nano-Morphologies as Support for Palladium-Catalyzed Suzuki Coupling Reaction. *Appl. Organomet. Chem.* **2017**, *31* (10), e3741.

- (84) Eiad-Ua, A.; Jomhataikool, B.; Gunpum, W.; Viriya-Empikul, N.; Faungnawakij, K. Synthesis of Copper/Carbon Support Catalyst from Cattail Flower by Calcination with Hydrothermal Carbonization. *Mater. Today Proc.* **2017**, *4* (5), 6153–6158.
- (85) Liu, J.; Wickramaratne, N. P.; Qiao, S. Z.; Jaroniec, M. Molecular-Based Design and Emerging Applications of Nanoporous Carbon Spheres. *Nat. Mater.* **2015**, *14* (8), 763–774.
- (86) Gai, C.; Zhang, F.; Yang, T.; Liu, Z.; Jiao, W.; Peng, N.; Liu, T.; Lang, Q.; Xia, Y. Hydrochar Supported Bimetallic Ni–Fe Nanocatalysts with Tailored Composition, Size and Shape for Improved Biomass Steam Reforming Performance. *Green Chem.* **2018**, *20* (12), 2788–2800.
- (87) Lu, Y. M.; Zhu, H. Z.; Li, W. G.; Hu, B.; Yu, S. H. Size-Controllable Palladium Nanoparticles Immobilized on Carbon Nanospheres for Nitroaromatic Hydrogenation. *J. Mater. Chem. A* **2013**, *1* (11), 3783–3788.
- (88) Dubey, S. P.; Dwivedi, A. D.; Kim, I.-C. C.; Sillanpaa, M.; Kwon, Y.-N. N.; Lee, C. Synthesis of Graphene-Carbon Sphere Hybrid Aerogel with Silver Nanoparticles and Its Catalytic and Adsorption Applications. *Chem. Eng. J.* **2014**, *244*, 160–167.
- (89) Cheng, J.; Wang, Y.; Teng, C.; Shang, Y.; Ren, L.; Jiang, B. Preparation and Characterization of Monodisperse, Micrometer-Sized, Hierarchically Porous Carbon Spheres as Catalyst Support. *Chem. Eng. J.* **2013**, *242*, 285–293.
- (90) Sun, Z.; Yang, J.; Wang, J.; Li, W.; Kaliaguine, S.; Hou, X.; Deng, Y.; Zhao, D. A Versatile Designed Synthesis of Magnetically Separable Nano-Catalysts with Well-Defined Core-Shell Nanostructures. *J. Mater. Chem. A* **2014**, *2* (17), 6071–6074.
- (91) Yu, J.; Yan, L.; Tu, G.; Xu, C.; Ye, X.; Zhong, Y.; Zhu, W.; Xiao, Q. Magnetically Responsive Core-Shell Pd/Fe<sub>3</sub>O<sub>4</sub>@C Composite Catalysts for the Hydrogenation of Cinnamaldehyde. *Catal. Letters* **2014**, *144* (12), 2065–2070.
- (92) Zhang, F.; Hu, H.; Zhong, H.; Yan, N.; Chen, Q. Preparation of  $\gamma$ -Fe<sub>2</sub>O<sub>3</sub>@C@MoO<sub>3</sub> Core/Shell Nanocomposites as Magnetically Recyclable Catalysts for Efficient and Selective Epoxidation of Olefins. *Dalt. Trans.* **2014**, *43* (16), 6041–6049.
- (93) He, B.; Zhao, Q.; Zeng, Z.; Wang, X.; Han, S. Effect of Hydrothermal Reaction Time and Calcination Temperature on Properties of Au@CeO<sub>2</sub>core-Shell Catalyst for CO Oxidation at Low Temperature. *J. Mater. Sci.* **2015**, *50* (19), 6339–6348.
- (94) Shi, Z. Q.; Jiao, L. X.; Sun, J.; Chen, Z. B.; Chen, Y. Z.; Zhu, X. H.; Zhou, J. H.; Zhou, X. C.; Li, X. Z.; Li, R. Cobalt Nanoparticles in Hollow Mesoporous Spheres as a Highly Efficient and Rapid Magnetically Separable Catalyst for Selective Epoxidation of Styrene with Molecular Oxygen. *RSC Adv.* **2014**, *4* (1), 47–53.
- (95) Sun, Y.; Zhang, L.; Wang, Y.; Chen, P.; Xin, S.; Jiu, H.; Liu, J. Hollow and Hollow Core/Shell CeO<sub>2</sub>/SiO<sub>2</sub>@CeO<sub>2</sub> Spheres: Synthesis, Structure Evolution and Catalytic Properties. *J. Alloys Compd.* **2014**, *586*, 441–447.
- (96) Tang, C.; Titirici, M.-M.; Zhang, Q.; Cheng, T.; Maria-Magdalena, T.; Qiang, Z. A Review of Nanocarbons in Energy Electrocatalysis: Multifunctional Substrates and Highly Active Sites. *J. Energy Chem.* **2017**, *26* (6), 1077–1093.
- (97) Alatalo, S.-M. M.; Qiu, K.; Preuss, K.; Marinovic, A.; Sevilla, M.; Sillanpää, M.; Guo, X.; Titirici, M.-M. M. Soy Protein Directed Hydrothermal Synthesis of Porous Carbon Aerogels for Electrocatalytic Oxygen Reduction. *Carbon* **2016**, *96*, 622–630.
- (98) Lu, Y.; Wang, L.; Preuß, K.; Qiao, M.; Titirici, M.-M. M.; Varcoe, J.; Cai, Q. Halloysite-Derived Nitrogen Doped Carbon Electrocatalysts for Anion Exchange Membrane Fuel Cells. *J. Power Sources* **2017**, *372*, 82–90.
- (99) Preuss, K.; Tănase, L. C.; Teodorescu, C. M.; Abrahams, I.; Titirici, M. M.; Tănase, L. C.; Teodorescu, C. M.; Abrahams, I.; Titirici, M. M. Sustainable Metal-Free Carbogels as Oxygen Reduction Electrocatalysts. *J. Mater. Chem. A* **2017**, *5* (31), 16336–16343.
- (100) Huijun, Y.; Lu, S.; Tong, B.; Run, S.; N., W. G. I.; Yufei, Z.; Chao, Z.; Li-Zhu, W.; Chen-Ho, T.; Tierui, Z. Nitrogen-Doped Porous Carbon Nanosheets Templated from g-C<sub>3</sub>N<sub>4</sub> as Metal-Free Electrocatalysts for Efficient Oxygen Reduction Reaction. *Adv. Mater.* **2016**, *28* (25), 5080–5086.
- (101) Qiao, M.; Tang, C.; He, G.; Qiu, K.; Binions, R.; Parkin, I. P.; Zhang, Q.; Guo, Z.; Titirici, M. M. Graphene/Nitrogen-Doped Porous Carbon Sandwiches for the Metal-Free Oxygen Reduction Reaction: Conductivity: Versus Active Sites. *J. Mater. Chem. A* **2016**, *4* (32), 12658–12666.
- (102) Terrones, M.; Ajayan, P. M.; Banhart, F.; Blase, X.; Carroll, D. L.; Charlier, J. C.; Czerw, R.; Foley, B.; Grobert, N.; Kamalakaran, R.; et al. N-Doping and Coalescence of Carbon Nanotubes: Synthesis and Electronic Properties. *Appl. Phys. A Mater. Sci. Process.* **2002**, *74* (3), 355–361.
- (103) Wang, L.; Jia, W.; Liu, X.; Li, J.; Titirici, M. M. Sulphur-Doped Ordered Mesoporous Carbon with Enhanced Electrocatalytic Activity for the Oxygen Reduction Reaction. *J. Energy Chem.* **2016**, *25* (4), 566–570.
- (104) Wan, W.; Wang, Q.; Zhang, L.; Liang, H. W.; Chen, P.; Yu, S. H. N-, P- and Fe-Tridoped Nanoporous Carbon Derived from Plant Biomass: An Excellent Oxygen Reduction Electrocatalyst for Zinc-Air Batteries. *J. Mater. Chem. A* **2016**, *4* (22), 8602–8609.
- (105) Liu, Y.; Huang, B.; Lin, X.; Xie, Z. Biomass-Derived Hierarchical Porous Carbons: Boosting the Energy Density of Supercapacitors via an Ionothermal Approach. *J. Mater. Chem. A* **2017**, *5* (25), 13009–13018.
- (106) Huang, D.; Li, S.; Zhang, X.; Luo, Y.; Xiao, J.; Chen, H. A Novel Method to Significantly Boost the Electrocatalytic Activity of Carbon Cloth for Oxygen Evolution Reaction. *Carbon* **2018**, *129*, 468–475.

- 
- (107) Bae, S.; Kim, H.; Lee, Y.; Xu, X.; Park, J.-S.; Zheng, Y.; Balakrishnan, J.; Lei, T.; Ri Kim, H.; Song, Y. II; et al. Roll-to-Roll Production of 30-Inch Graphene Films for Transparent Electrodes. *Nat. Nanotechnol.* **2010**, *5* (8), 574–578.
- (108) Zhang, J.; MacFarlane, D. R.; Li, F.; Chen, L.; Knowles, G. P.; MacFarlane, D. R.; Zhang, J.; Fengwang, L.; Lu, C.; P., K. G.; et al. Hierarchical Mesoporous SnO<sub>2</sub> Nanosheets on Carbon Cloth: A Robust and Flexible Electrocatalyst for CO<sub>2</sub> Reduction with High Efficiency and Selectivity. *Angew. Chemie - Int. Ed.* **2016**, *56* (2), 505–509.

## Bio-based carbon materials for a direct-carbon fuel cell

Maciej P. Olszewski, Pablo J. Arauzo, Joscha Zimmermann, Dennis Jung, Viola Hoffmann, Andrea Kruse

*Department of Conversion Technologies of Biobased Resources, Institute of Agricultural Engineering, University of Hohenheim, Garbenstrasse 9, 70599 Stuttgart, Germany*

### Abstract

Due to the rapid and constantly developing society, there is an increase in the demand for electricity. Most of the electricity generated in the world is produced by burning fossil fuels (mostly coal, natural gas, and oil). Also, all type of transportation including land, maritime and air are powered by engines using processed crude oil. This leads to the depletion of fossil fuel reserves and increasing the price of fuels. Moreover, combustion releases enormous amounts of CO<sub>2</sub>, particulate matter and other pollutants into the atmosphere, which leads to the environmental pollution as well as global warming. To reduce the consumption of fossil fuels and related emissions, biomass can be used in specific applications. Bio-based carbon materials can be used as electrodes in supercapacitors as well as in batteries. Furthermore, bio-based carbons can be used as fuel for high-efficiency electricity production in electrochemical reaction occurring in a direct-carbon fuel cell, which represents a promising technology for electricity generation. In this review, the theoretical background and principles of operation of different types of direct-carbon fuel cells are presented. Besides, the required properties of carbon materials used as a fuel are listed.

### 1. Introduction

The depletion and increasing price of fossil fuels, as well as the climate change and the need to decrease CO<sub>2</sub> emission, are currently a major interest on a global scale. However, rapid economic growth and increasing population on the Earth results in high demand for modern electronic devices. It requires continuous improvement of energy storage systems including faster charging, longer lifetime, higher conversion efficiency and maintaining the lowest possible price. This focused the researchers' attention on enhancing the use of biomass for more efficient production of electricity (direct-carbon fuel cell) and carbon materials. According to recently published research, bio-based carbon materials achieve similar or even better properties than fossil equivalent. These materials are used as electrode material in energy storage devices, including supercapacitors, lithium-ion batteries (LIBs), sodium ion batteries (SIBs), and as a fuel in direct-carbon fuel cells (DCFCs)<sup>1–3</sup>. Biomass can be converted into carbon-rich material using several conversion technologies; herein, hydrothermal carbonisation process are described as well as direct carbon fuel cells.

### 2. Hydrothermal carbonisation

The fundamental process of hydrothermal carbonisation (HTC) has been known for a century. In 1913, the process was firstly reported when Friedrich Bergius was investigating the production of a synthetic coal by subjecting a material to heating water and pressure<sup>4</sup>. Bergius compared the hydrothermal carbonisation with the natural coalification process that takes place during millions of years, which he accomplished in a much more rapid reaction. However, the idea to hydrothermally convert biomass is relatively young<sup>5</sup> and according to Titirici et al<sup>6</sup>, the somewhat forgotten “synthetic coalification” has a new renaissance of interest since the turn of the twenty-first century.

#### 2.1. Hydrothermal process

HTC is a thermochemical process, converting biomass in a coal-like product. The feedstock is a favourable wet biomass<sup>7</sup>, in principle any lignocellulosic material, as well as pure lignin<sup>8,9</sup>. The process temperatures are in general relatively low, around 150–350 °C<sup>10–16</sup>. The selected temperature is primary depending on the type of starting material and the favoured product. Because the process runs in a closed system, a high autogenous pressure is generated. Furthermore, the temperature is determining the pressure by the vapour pressure curve and is limited by the critical point in the phase diagram of water. Increasing the temperature and crossing this, these limits will lead to a higher liquid and gas fraction of the product (i.e., liquefaction and gasification).

The hydrothermal conversion of biomass into a carbon material occurs in water, which acts as a catalyst by facilitating the hydrolysis of organic polymers. In general, the process of HTC involves several mechanisms, including hydrolysis, dehydration, polymerisation, aromatisation, and decarboxylation. The three essential mechanisms for the production of hydrochar are hydrolysis, dehydration, and polymerisation. Aromatisation and decarboxylation usually occur at higher operating temperatures and extended reaction times.

The HTC-process starts with the hydrolysis of the carbohydrates in the biomass structure. During this step, the polymer chains of cellulose and hemicellulose are split up into monomers (e.g., glucose from cellulose). Hydrolysis of hemicellulose produces acetic acid, D-xylose, D-mannose, D-galactose and D-glucose. It is deduced that lignin dissolved slowly, and exposed fragments of non-dissolved lignin in water are decomposed into phenolics<sup>17</sup>. Hydrolysis of hemicellulose begins approx. at 180 °C, while cellulose and lignin hydrolysis occur above 200 °C<sup>8,18</sup>. A complete hydrolysis of cellulose and lignin will not occur, rather two reaction pathways will lead to the solid char. One through a (1) solid-solid conversion and (2) aqueous phase degradation<sup>7,19</sup>. It is assumed that in reaction pathway (1), the cellulose-bound in the lignin structure is

unable to hydrolyse and thus maintains structural elements of the precursor biomass<sup>20</sup>. The product is called 'primary char'. Final knowledge about the molecular structure is still missing and researchers are debating about it. Previous statements assumed that the structure is polyaromatic<sup>21,22</sup>, but Brown et al.<sup>23</sup> suggested a polymer of furans and arene with carbonyl-substituted compounds. In reaction pathway (2), the liquid state reacts further by polymerisation namely. The solid product ends up as a fraction of the HTC-char and is called 'secondary char', a polymerised hydrochar.

During dehydration, single sugars in the liquid phase are converted into furfurals, namely 5-Hydroxymethylfurfural (hereafter 'HMF') and organic acids, namely levulinic and formic acid<sup>8,24</sup>. This intramolecular step significantly carbonises the biomass since the hydrogen-to-carbon ratio (H/C) and the oxygen-to-carbon ratio (O/C) is reduced by seceding H<sub>2</sub>O. Dehydration with the preceding hydrolysis is shown within the example of cellulose in Fig. 1.

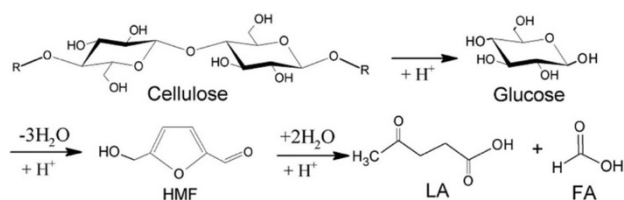


**Figure 1.** Mechanism of acid-catalysed cellulose hydrolysis to glucose and conversion to hydroxymethylfurfural (HMF), and levulinic acid (LA), and formic acid (FA) (adapted from <sup>79</sup>).

## 2.2. Process parameters and their influence

The final structure and composition of the product is mainly determined by the feedstock<sup>6,8</sup>. But by controlling the temperature, residence time, solid load and pH-value, the characteristics of the hydrochar can be influenced.

The temperature is an important process parameter by determining the fate of degradation reactions and reaction rate according to the thermodynamic equilibrium. Ionic reactions occur at lower temperatures, since an acidic environment improves the hydrolysis. At higher temperatures, homolytic cleavage dominates, due to a reduction of the acidic dissociation constant ( $K_a$ -value)<sup>25</sup>. Elevating the temperature can also lead to the formation of a wider range of products and higher gas yield<sup>26</sup>. Additionally, a higher temperature extends the dehydration and increases the degree of condensation of the hydrochar. Sevilla et al.<sup>18</sup> reported that especially the O/C and H/C ratios are decreasing during the hydrothermal process at 230–250 °C. However, Kang et al.<sup>17</sup> reported a small decrease in the yield of hydrochar based on cellulose with an increasing temperature of 225–265 °C.

A longer residence time increases the carbonisation of the resulting char while reducing the mass yield. In terms of energy yield, a longer residence time is positive, since dehydration and subsequent condensation polymerisation processes in the liquid state enhance the production of the secondary char. Since operation temperature and residence time interact and affect the product, both

cannot be analysed separately. Another influencing parameter is the concentration of precursor. According to Jung et al.<sup>27</sup>, the reaction order of the hydrochar formation is higher than one and hence, a lower precursor concentration or additional water results in more carbon in the liquid phase.

As previously referenced, protons enhance the hydrolysis and have a catalytic effect on the production of HMF<sup>28</sup>. However, a lowered pH-value can also increase the production of levulinic acid, which is also dependent on the present acid<sup>29</sup>. Reza et al.<sup>30</sup> refer to that hemicellulose and cellulose are less reactive within a basic environment, contrarily to lignin's enhanced reactivity.

## 2.3. Hydrochar

The resulting hydrochar is a coal-like product with a quite similar higher heating value (hereafter 'HHV'). During the process, the HHV is increased by ca. 40% of the starting biomass precursor, by rising the carbon content<sup>6</sup>. Furthermore, carbonic organic compounds are lost to the solvent and a minor amount is gasified (up to 5%)<sup>31</sup>. Compared to biochars produced via pyrolysis, the carbonisation of hydrochar is lower, as well the crosslinking and polymerisation and thus the thermal stability is. This also implies a higher O/C and H/C ratio and hence a richer surface chemistry with high content of OFG (oxygenated functional group). These OFGs make them an interesting feedstock to produce activated carbon<sup>32</sup>.

Depending on the precursor biomass and treatment method, a hydrochar with special characteristics can be created<sup>9</sup>. Nanospheres, nanocables, nanofibers, submicrocables, submicrotubes, carbon gels and porous structures are reported by Titirici et al.<sup>6</sup> and Hu et al.<sup>33</sup>, which are expected to be advanced carbon materials for applications in supercapacitors, membranes or in the production of fuels, fertilisers or energy storage systems. An interesting application of hydrochar is its use in a direct-carbon fuel cell to generate electricity with very high efficiency.

## 3. Direct carbon fuel cell background

The first direct-carbon fuel cell (DCFC) was built by William W. Jacques and patented in 1896<sup>34</sup>. However, his results were not reproducible until the seventies. For a long time, his concept was suspected to generate electricity by a thermoelectric effect (conversion of temperature into electric voltage) not by an electrochemical reaction. In the 1970s, the US Stanford Research Institute finally showed that such a system was feasible<sup>2</sup>. Since the nineties, the fuel cell technology has been significantly developed.

The DCFC technology has the potential to utilise an abundant and relatively easily accessible primary energy sources as fuel. Various carbon materials can be utilised, such as fossil bituminous coal or lignite, charred and untreated biomass or even waste products like plastic<sup>2</sup>. Furthermore, the carbon fuel is easy to handle and compared to hydrogen, which is often used in fuel cells, easy to store. The substantial advantage of a fuel cell is the

direct electrochemical conversion of chemical energy into electricity. This conversion is highly efficient, since intermediary processes are eliminated. For example, the direct conversion of carbon into carbon dioxide has a theoretical thermodynamic efficiency of 100%; from thermal conversion, less than the half is typical obtained<sup>35</sup>. The practical efficiency is stated with 80%<sup>36,37</sup>, which is much higher than that of a coal-fired power plant with 30%–40% (without cogeneration).<sup>35,38</sup>

The fuel cells exhaust, in principle, zero harmful emissions to the environment. A hydrogen fuel cell produces water as a reaction product and a DCFC almost pure CO<sub>2</sub>, which can be easily separated and used in a further process. By utilising biomass, this gives the opportunity to sequester CO<sub>2</sub> from the atmosphere.

Despite the stated advantages, the fuel cell cannot be seen as the ‘Holy Grail’ for the prospective energy supply by means of fuels, since it comes also with many disadvantages, especially those related to the conversion of carbon. The following section summarises the fundamentals in electrochemistry and thermodynamics, showing advantages and disadvantages, as well as different concepts and the state of the art.

### 3.1. Fundamentals in electrochemistry and thermodynamics

A fuel cell operating on carbon fuel is named carbon fuel cells and is related to the concept of a galvanic cell. An idealized DCFC system is schematically shown in Fig. 2. It consists of an electrolyte and two electrodes, namely cathode and anode. The electrolyte can mobilise ions, but at the same time, it is electronically insulating (not transferring electrons).<sup>35</sup>

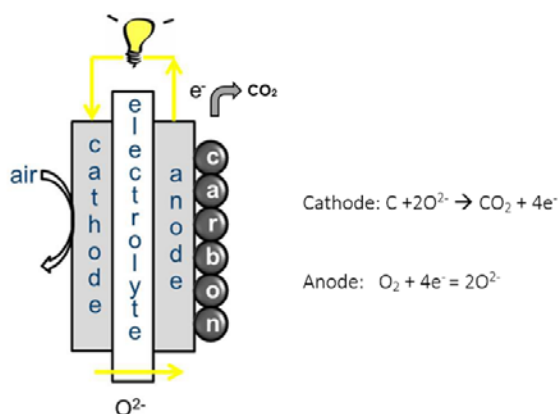
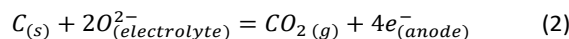
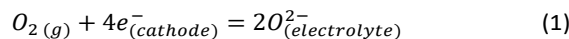


Fig. 2. Illustration of an idealized direct-carbon fuel cell (adapted from<sup>39</sup>).

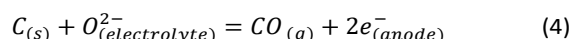
The type of electrolyte is classifying the DCFCs into hydroxide, molten carbonate, and solid oxide types. The oxygen (O<sub>2</sub>) is reduced with four electrons at the cathode and then transported through the electrolyte. The anode consisting of the fuel in form of solid carbon is oxidised to carbon dioxide by releasing four electrons. Accordingly, the desired cathode and anode reactions for a DCFC are:



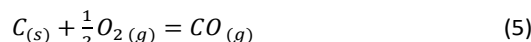
Combination of Eq. (1) and Eq. (2) gives the overall reaction, running in a DCFC:



The desired anode reaction is referred in Eq. (2) as a full oxidation, but in most cases, a partial oxidation of carbon occurs by releasing only two electrons and carbon monoxide.<sup>38</sup>



This gives an undesired overall reaction:



In a galvanic cell, the chemical energy is converted directly into electrical energy. The proportion of maximum electrical energy is referred to as a change in Gibbs free energy of reaction. The change of Gibbs free energy of the electrochemical reaction gives the maximum of electrical work obtained in a fuel cell<sup>40</sup>. Therefore, Eq. (6) is applied.

$$W = \Delta_r G = -nF\Delta E_0 \quad (6)$$

In Eq. (6),  $W$  is the electrical work,  $\Delta_r G$  is the change in Gibbs free energy,  $n$  the number electrons transferred in the reaction,  $F$  the Faraday constant, and  $\Delta E_0$  is the equilibrium potential of the cell, which is defined by Eq. (7).

$$\Delta E_0 = E_0 \text{ Cathode} - E_0 \text{ Anode} \quad (7)$$

At standard conditions (pressure of 10<sup>5</sup> Pa)<sup>41</sup>, the temperature dependency is introduced to indicate the operation temperature of the fuel cell. Accordingly, the value of the thermodynamic equilibrium potential can be calculated from Eq. (8).

$$\Delta E_0^*(T) = -\frac{\Delta_r G(T)}{nF} \quad (8)$$

This theoretical value makes it possible to compare different fuels at different operation temperatures. The electrochemical conversion offers inherently higher thermodynamic efficiency than incineration into electrical energy. The theoretical efficiency of a common incineration power plant is defined by Eq. (9)<sup>38,42</sup>, in which  $T_1$  and  $T_2$  are the lowest and highest temperatures of the process, respectively.

$$\eta_{th \text{ Carnot}} = 1 - \frac{T_1}{T_2} \quad (9)$$

By contrast, the electrochemical oxidation of carbon inside a DCFC runs isothermal and isobaric. Additionally, the reactants and product streams are separated by the electrolyte and physical states. Further entropic losses due to mixing are eliminated. The theoretical efficiency is defined by the thermodynamic state functions shown in Eq. (10).<sup>38,40</sup>

$$\eta_{th \text{ DCFC}} = \frac{\Delta_r G}{\Delta_r H} = 1 - \frac{T\Delta_r S}{\Delta_r H} \quad (10)$$

The common approach to calculate the cell efficiency would add further efficiency factors for cell polarisation losses, current (or Coulombic) efficiency at the electrodes and the efficiency of fuel utilisation. Since DCFC runs on a solid fuel, Brentan et al.<sup>43</sup> proposed the following equation:

$$\eta_{cell} = \frac{E \int idA}{\dot{m}_{char} HHV_{char}} \quad (11)$$

where the term in the numerator represents the total power of the cell (in W), whereas  $m_{char}$  is the mass consumption rate (in  $\text{kg s}^{-1}$ ) and  $HHV_{char}$  the higher heating value of the char (in  $\text{J kg}^{-1}$ ).

### 3.2. Efficiency and equilibrium cell potential

In the case of the full oxidation shown in Eq. (3), the thermodynamic data is given in Table 1. The reaction is exergonic and exothermic since the Change in Gibbs free energy and enthalpy is negative. The change in entropy is for the case of full oxidation positive, but nearly zero since the amount of substance in the gas phase is unchanging. One mole of  $\text{O}_2$  reacts to one mole of  $\text{CO}_2$ . This is also the compensatory advantage in contrast to other fuel cell system<sup>44</sup>. Additionally, the disarray of the system increases, as  $\text{CO}_2$  has a higher degree of freedom compared to  $\text{O}_2$ . Consequently, the theoretical cell conversion efficiency ( $\eta_{th}$ ) is practically independent of temperature. Most importantly, the small value for the entropy change results in yielding a conversion efficiency of 100% over the whole temperature spectrum. This provides a major advantage for electrochemical conversion of carbon over chemical processes at favoured temperatures, although it is usually difficult to achieve direct conversion.

**Table 1.** Total and partial oxidation of carbon. Thermodynamic data at Temperatures of 300, 600, 900 and 1200 K (calculated with data from Ref.<sup>45</sup>).

Full oxidation	$\text{C}_{(s)} + \text{O}_{2(g)} \rightarrow \text{CO}_{2(g)}$			
T [K]	300	600	900	1200
$\Delta_r G$ [kJ mol <sup>-1</sup> ]	-394.37	-395.14	-395.68	-396.01
$\Delta_r H$ [kJ mol <sup>-1</sup> ]	-393.51	-393.80	-394.41	-395.04
$\Delta_r S$ [J K <sup>-1</sup> mol <sup>-1</sup> ]	2.88	2.22	1.41	0.80

In Fig. 3, the temperature dependency of different fuel cell systems is shown on their theoretical efficiency, calculated using literature data<sup>45</sup> and Eq. (10). It is shown that the efficiency level of a hydrogen or carbon monoxide cell is decreasing with an increasing temperature. However, in DCFC systems the oxidation reactions of carbon are in competition with the Boudouard reaction, as released  $\text{CO}_2$  reacts with the solid carbon fuel to CO. This reaction is endothermic and lowers the fuel utilisation.

The previous paragraph introduced the equilibrium cell potential and its temperature dependency, according to Eq. (8). However, for the case of full carbon oxidation, the potential behaves similar to the efficiency and can be seen as constant. Fig. 4 shows the temperature dependency of various oxidation reactions. It can be noticed that the equilibrium cell potential of oxidation of  $\text{H}_2$  and CO are decreasing with an increasing temperature. Nonetheless, it must be considered that the curve of the oxidation of CO and the partial oxidation of C is mirrored. The result of adding these two reactions again gives the full oxidation.

However, at increasing temperature, the formation of CO is preferred over  $\text{CO}_2$ . This phenomenon is related again to the Boudouard equilibrium and is discussed below.

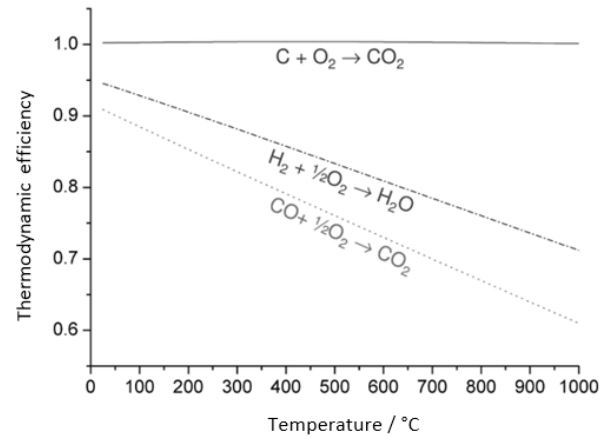


**Figure 3.** Temperature dependence of the thermodynamic efficiency for different fuel cell systems.

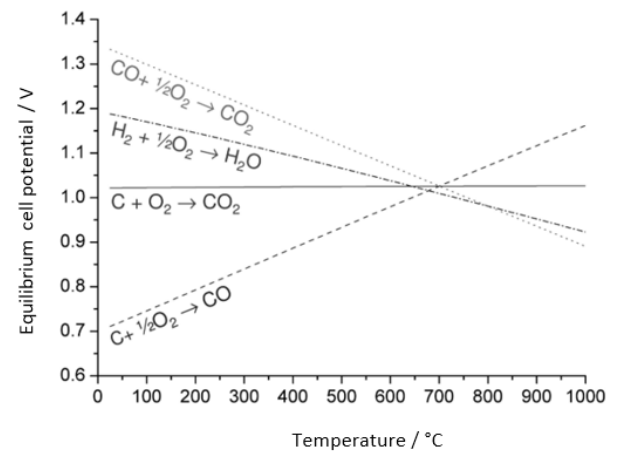


**Figure 4.** Temperature dependence of the equilibrium potential for different fuel cell systems.

### 3.3. Efficiency and equilibrium cell potential

Another way to define the ideal performance of a fuel cell is the Nernst potential, represented again as a cell voltage. The Nernst equation describes the relationship between the ideal standard potential  $\Delta E_0^*(T)$  at standard temperature and pressure for the fuel cell reaction and the ideal equilibrium potential  $\Delta E_0(T)$  at changing temperatures and pressures of reactants and products. Once the ideal potential at standard conditions is known, Eq. (12) can be used to determine the ideal potential at changing temperatures and pressures.

$$\Delta E_0(T) = \Delta E_0^*(T) - \frac{RT}{nF} \ln Q \quad (12)$$

To calculate the reaction quotient ( $Q$ ) of the thermodynamic activity of each half-cell, Eq. (13) is applied.

$$Q = \frac{[P_1]^{u_{p1}} [P_2]^{u_{p2}}}{[R_1]^{u_{r1}} [R_2]^{u_{r2}}} \quad (13)$$

where  $[P_i]$  is the concentration (dissolved form) or pressure (gaseous form) of product,  $[R_i]$  the concentration (dissolved form) or pressure (gaseous form) of reactant,

whereas  $u_{pi}$  and  $u_{ri}$  correspond to the stoichiometric coefficients of products and reactants, respectively. A further and deeper explanation and derivation of the Nernst equation is referend in a previous study.<sup>41</sup>

### 3.4. Boudouard equilibrium

In addition to the electrochemical reactions given in Eq. (2) and Eq. (4), CO and CO<sub>2</sub> react in contact with carbon in a redox reaction according to a chemical equilibrium, the so-called Boudouard equilibrium.<sup>2</sup>



The equilibrium constant of this reaction ( $K_B$ ) is defined by Eq. (15), which can be calculated, as the partial pressures of the respective gasses are known or with the operation temperature and the relative Gibbs free energy.

$$K_B = \frac{p_{CO}^2}{p_{CO_2}} = \exp\left(\frac{\Delta_r G(T)}{RT}\right) \quad (15)$$

The thermodynamic equilibrium of the reaction is strongly dependent on the operating temperature as well as the applied pressure in the system. The corresponding values provided in Table 2 are calculated at 1 atm. As expected, the formation of CO<sub>2</sub> is thermodynamically favoured at low temperatures. In contrast, elevated temperatures favour the formation of CO. The resulting carbon monoxide can be further electrochemically oxidised to CO<sub>2</sub> in a second step, but isn't efficient as the direct conversion of solid carbon<sup>38</sup>, as it yields only two electrons.

**Table 2.** Temperature dependency of Boudouard constant ( $K_B$ ) and the respective equilibrium partial pressures for CO and CO<sub>2</sub> at 1 atm. (calculated from Thermochemical Data<sup>45</sup>).

$T$ [K]	800	1000	1200
$K_B$	0.01	1.76	53.75
$p_{CO}$	0.09	0.71	0.98
$p_{CO_2}$	0.91	0.29	0.02

The CO oxidation is described by Eq. (16). Such chemical losses due to the Boudouard consumption highly decrease the carbon conversion efficiency. This concludes a reduction of the operating temperatures in the DCFC, to avoid this phenomenon shown in Fig. 5, without decreasing the kinetics of ongoing reactions.

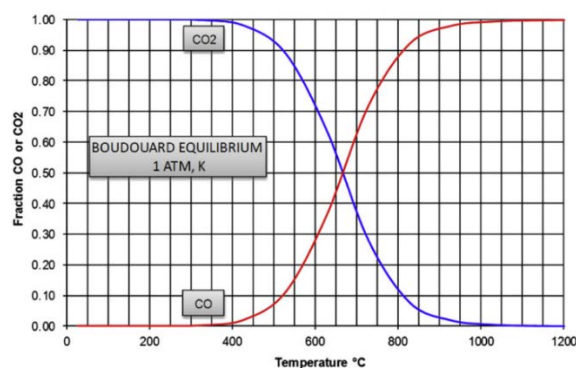
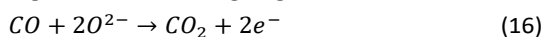


**Figure 5.** Boudouard equilibrium at 1 atm (adapted from<sup>80</sup>).

## 4. DCFC concepts and reaction mechanism

State of the art, different DCFC concepts with three possible types of electrolyte have been developed. Namely a liquid hydroxide molten electrolyte or alkaline fuel cell (hereafter AFC)<sup>46,47</sup>, a liquid molten carbonate electrolyte fuel cell (MCFC)<sup>48,49</sup> and a solid oxide ceramic electrolyte (SOFC)<sup>50,51</sup>. All concepts have their advantages and disadvantages, further explained in this section. To overcome specific disadvantages, recently, hybrid technologies have also been developed, representing a combination of different concepts. For example, a solid oxide system with a molten carbonate<sup>52</sup> or a molten hydroxide with a molten carbonate.<sup>53</sup>

### 4.1. Hydroxide fuel cell

This type of DCFC uses a molten hydroxide as the electrolyte. The electrolyte, mainly KOH or NaOH, is contained within a metallic container, which also acts as the cathode. The anode is made with carbon and is dipped into the electrolyte.

The advantages of using hydroxide as electrolyte come with a high ionic conductivity<sup>54</sup>, especially when mixed with water<sup>55</sup> and a high reactivity on the carbon fuel<sup>56</sup>. Additionally, hydroxides have a relatively low melting point and thus the operating temperatures of the fuel cells are 400–650 °C<sup>46</sup>. Since temperatures below 700 °C favour the oxidation of carbon to CO<sub>2</sub> rather than CO, according to the Boudouard equilibrium, the fuel utilisation is higher, which result in a higher system efficiency. Despite the advantages, the fundamental problem of a hydroxide electrolyte is the formation of carbonate, already experienced by Jacques<sup>34</sup>. Further technical challenges are the high corrosion rates of metals used in the cell and fuel pre-treatment. Since volatile hydrocarbons and mineral ash reduce the performance of the electrolyte<sup>57</sup>, they must be removed. Because of referenced issues, this fuel cell concept will not be discussed any further in this work.

### 4.2. Molten carbonate fuel cell

Replacing the hydroxide melt by a carbonate melt as an electrolyte distinguish or minimise the previously mentioned problems. So far, the most frequently used concept of a DCFC is based on molten carbonate fuel cell (MCFC). The carbon is distributed and surrounded in the

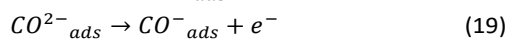
liquid electrolyte, which consists of a eutectic carbonate mixture, typically  $\text{Li}_2\text{CO}_3$ ,  $\text{K}_2\text{CO}_3$  and/or  $\text{Na}_2\text{CO}_3$ .

The advantages of carbonates are unlike hydroxides, a good long-term stability of the electrolyte in  $\text{CO}_2$ <sup>58,59</sup>. Additionally, carbonates show a high ionic conductivity and have sufficient contact area between the carbon and the electrolyte<sup>60,61</sup>. Furthermore, the operating temperatures are in a wide range and usually defined by the composition of the electrolyte; typically between 500 and 900 °C<sup>48,49,62</sup>. In the system, carbonate ions ( $\text{CO}_3^{2-}$ ) are involved in the electrochemical oxidation of carbon. Therefore, oxygen and carbon dioxide are needed on the cathode side. A recycle of 2/3 of generated  $\text{CO}_2$  is required<sup>38</sup>. The lifetime is the main issue for a MCFC, since the cathode suffers degradation due to carbonate attacks.

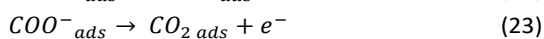
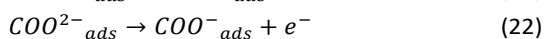
A reaction mechanism for the oxidation of carbon in a molten carbonate was suggested by Cherepy et al.<sup>60</sup>. At a temperature of 700 °C, the molten carbonate electrolyte shows a strong dissociation, leading to the formation of oxygen ions.



The electrochemical oxidation of carbon is then divided into seven further steps. Firstly, the oxygen ions yielded in Eq. (17) are adsorbed on the carbon atoms of the fuel. Therefore, two separate adsorptions take place. The first adsorption of an oxygen ion is described by Eq. (18), followed with two fast electronic discharges, given in Eq. (19) and (20). The process is summarised in Fig. 6a. The resulting functional group decomposes very slowly to form free CO; thus, a second mechanism step can take place.



In the second step, another oxygen ion is adsorbed, as shown in Eq. (21). This adsorption is considered to be the rate-determining step for the whole carbon oxidation, since it is kinetically hindered and requires a considerable overpotential. Analogous to the previous step, a rapid discharge takes place and two electrons are yielded, as described by Eq. (22) and (23).



Finally, the carbon dioxide desorbs from the surface. This reaction involves the two adsorbed  $\text{O}^{2-}$  ions and the active carbon on the surface, as described in Eq. (24) and shown in Fig. 6b.

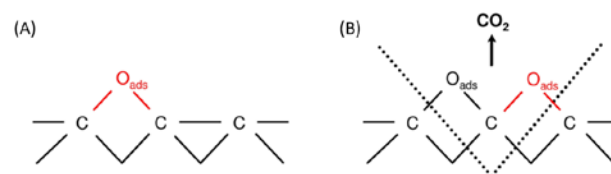


**Figure 6.** Mechanism of electrochemical oxidation of carbon in a molten carbonate: (a), first adsorption of  $\text{O}^{2-}$  ion; (b), second adsorption of  $\text{O}^{2-}$  ion and  $\text{CO}_2$  formation.

### 4.3. Solid oxide fuel cell

The concept of a Solid Oxide Fuel Cell (SOFC) reduces or even removes previous issues. Especially corrosion and material stability, coming with hydroxide and carbonate melts, are eliminated. Additionally, kinetic and transport limitations due to low viscosity of the melt shortened. The conventional electrolyte is a ceramic material made from yttrium stabilised zirconia (YSZ), providing a good ion conductivity and stable structure at low to high-temperature conditions, in general in the range of 700–1000 °C.<sup>35</sup>

The requirements for an anode material in an SOFC include a high electronic conductive material with a catalytic activity to accelerate the kinetics of electrochemical oxidation of carbon. The common anodes are nickel and platinum, since they are extensively studied and have excellent catalytic activities. Also, carbides and vanadium found to be good catalysts. The anodic half reactions occur at the triple phase boundary (TPB), where fuel, electron-conducting material (anode) and ion-conducting material (electrolyte) meet. The simplified interactions on the reactive surface (no liquid phase) avoid phenomena like bubbling and flooding, which can lower again the conversion efficiency<sup>38</sup>. On the other hand, this solid/solid interface provides a poor contact between the fuel anode surfaces, which hinder the electrons to flow<sup>63</sup>. To promote electrochemical oxidation and electron flow and surface contact, molten metals are used. Ju et al.<sup>64</sup> developed a Ni-YSZ anode supported with Sn to build a favourable bridge between the solid carbon and anode. Additionally, carbon particles in the liquid metal phase are gasified to CO via a 2-electron transfer. The CO can then further be utilised in the DCFC as a gaseous fuel.

It is assumed that the electrochemical oxidation in an SOFC is proceeding similar to the carbonate mechanism<sup>2</sup>. Unlike an MCFC, the  $\text{O}^{2-}$  ions are delivered directly from the electrolyte through bulk transfer.  $\text{Y}^{3+}$  ions replace  $\text{Zr}^{4+}$  on the cationic sub-lattice, thus generating oxygen vacancies<sup>65</sup> and providing ion conductivity at elevated temperatures, while electrical conductivity is prevented. This can be described by the so-called Kröger-Vink notation. The reaction is described in Eq. (25), the oxygen adsorbed by the crystal lattice of a particle is indicated as  $\text{O}_o^x$ , whereas the vacancies for an oxygen ion are designed as  $\text{V}_o^{\bullet\bullet}$ .



This mechanism was proposed by Li et al.<sup>66</sup> The first adsorption of an  $\text{O}^{2-}$  ion followed by the discharging in two steps is the same as stated in Eqs. (18), (19) and (20).

Subsequently, carbon monoxide is desorbed from the carbon surface, as shown in Fig. 7a and Eq. (26).



The mechanism can react further by adsorbing again an  $O^{2-}$  ion (see Fig. 7b), which leads to the formation of  $CO_2$ , as described in Eqs. (21), (22), (23) and (24).

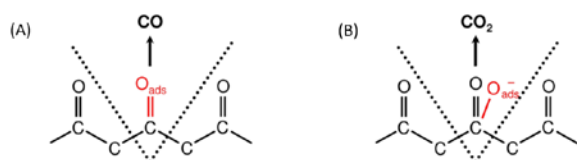


**Figure 7.** Mechanism of electrochemical oxidation of carbon on the electrolyte surface: (a), first  $O^{2-}$  ion adsorption and CO formation; (b), second  $O^{2-}$  ion adsorption and  $CO_2$  formation.

#### 4.4. Hybrid technology

The concept of a hybrid DCFC merges the electrolyte of a SOFC and MCFC, which result in a binary electrolyte. Due to the solid oxide electrolyte, the cathode can be separated from the anode compartment. Additionally, the molten carbonate is utilised in the anode compartment.

This concept brings some advantages. Firstly, recirculation of  $CO_2$ , which is necessary for an MCFC, is not needed anymore. Secondly, the cathode material is not exposed to the carbonate, which normally performs corrosive. Thus, several oxygen reducing materials that are already developed for SOFCs are accessible. Thirdly, the contact between fuel and electrolyte is improved, since carbonate is a slurry. This result in an enhanced oxidation, especially at lower temperatures<sup>67</sup>. Nabaie et al<sup>68</sup> presented two kinds of possible reaction schemes, which are illustrated in Fig. 8.

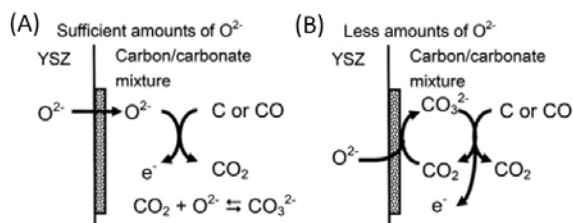


**Figure 8.** Possible reaction schemes of the direct oxidation of solid carbon with (a) sufficient supply of  $O^{2-}$ , (b) less amount of  $O^{2-}$  (adapted from<sup>68</sup>).

In general, a supply of  $O^{2-}$  ions is needed, which will be dissolved in the carbonate slurry up to a certain concentration (0.5 mol. % at 400–700 °C<sup>69</sup>). This supply is provided by the solid oxide electrolyte. Mechanism (a) describes a sufficient supply of  $O^{2-}$  into the carbonate, which works as an oxidiser of carbon to  $CO_2$  or even convert  $CO_2$  into  $CO_3^{2-}$ , keeping the concentration low and thus the effect of the Boudouard reaction. Mechanism (b) describes a reduced supply of  $O^{2-}$ , which would result in a decomposition of the carbonate. Consequently,  $CO_3^{2-}$  needs to be regenerated.

#### 4.5. Fuel properties

The basic principle of a DCFC is the utilisation of carbon as fuel. Therefore, various materials are available, ranging from biomass waste residues<sup>70</sup>, biochars<sup>71</sup>, lignite and bituminous coal and highly carbonised, pure materials like carbon blacks. Since the different sources influence the fuels chemical and physical properties, improving or impairing further utilisation, this chapter gives an overview.

According to Kinoshita et al.<sup>72</sup>, a crucial parameter for the reactivity in the oxidation of a carbon material is the structure and its surface, depending on the dimensions of the specific surface area and crystallinity. Amorphous carbon materials show a higher reactivity, since the number of defects (e.g., edges and steps) on the surface act as an active layer. A bigger surface provides more active sites, leading to a higher current density in the DCFC.<sup>51</sup>

Another important parameter is the conductivity, since the carbon material performs as fuel and anode in the same moment. Thus, resulting electrons need to be transferred. The intrinsic conductivity in carbon particles strongly depends again on the surface and structure<sup>73</sup>. However, the conductivity is in general improved by a crystalline structure and so by a graphite-like structure in the carbon particle. In general, different groups can be recognised on the surface of a carbon particle, which may contain oxygen, hydrogen, nitrogen, sulphur or possibly halogens. These elements can be introduced during the various production steps of carbon fuel. Nevertheless, the functional groups that can most affect the physicochemical properties on the surface are the different complexes of carbon and oxygen, the oxygen functional group (hereafter 'OFG')<sup>72</sup>. Typical structures on a particle surface are shown in Fig. 9.

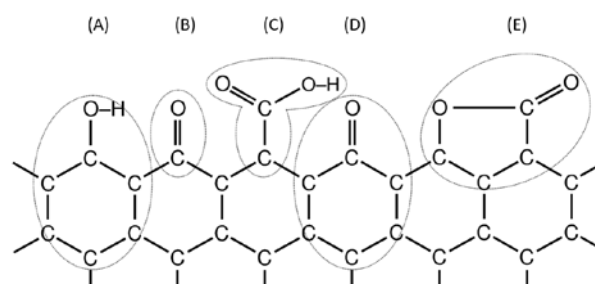


**Fig. 9.** OFG on a carbon particle: (a) phenol, (b) carbonyl, (c) carboxyl, (d) quinone, and (e) lactone.

As reported in the literature, simple aliphatic groups (C-H) increase the distance between polyaromatic regions from different particles<sup>74</sup>. This result in an increase in the contact resistance. Additionally, it is known that an increase in functional groups with oxygen and sulphur content on the surface decreases the conductivity<sup>75</sup>. Chemical composition of the fuel also has a notable effect on the lifetime of a fuel cell. As previously stated, it was observed that various mineral impurities in the carbon material lead to deterioration of DCFC performance<sup>57, 76</sup>. Additionally, Cherepy et al.<sup>60</sup> and Gong et al.<sup>77</sup> observed a degradation of cell performance caused by sulphur in the fuel.

Several references reported an enhancement of the performance of a DCFC by volatile matter<sup>67,70,78</sup>. Especially, carbon materials, formally hydrochars and biochars from refuse biomass, have a high content of volatile matter that can contribute to the cell performance.

## 5. Conclusion

Direct carbon fuel cell (DCFC) is a promising technology for the production of electricity using solid fuels. Its advantage is the production of electricity directly from the electrochemical reactions. It results in a much higher electrical efficiency (80%) for direct carbon fuel cells compared to coal combustion plants (up to 45%). DCFC can be divided into three types depending on the electrolyte used: solid oxide (ceramic material), molten carbonate ( $\text{Li}_2\text{CO}_3$ ,  $\text{Na}_2\text{CO}_3$ , and  $\text{K}_2\text{CO}_3$ ), and molten hydroxide ( $\text{LiOH}$ ,  $\text{NaOH}$ , and  $\text{KOH}$ ). Historically, in this type of fuel cell, the carbon material was used both as anode and fuel. However, due to technical problems such as the penetration of impurities from the carbonaceous anode to the electrolyte, a separate anode is currently used, and the carbon material is used as fuel. To increase the contact between the fuel and the anode, the anode compartment is operating in flow mode (e.g., fluidised bed). For this reason, the fuel should have a fine grain size. Direct carbon fuel cells operate at high temperatures (600–1000 °C), where corrosion of cell-forming materials is severe. Therefore, it is necessary to use fuel with low sulphur and ash content. It makes bio-based carbon materials an attractive feedstock for direct carbon fuel cells.

## Acknowledgements

This project has received funding from the European Union's Horizon 2020 research and innovation programme under the Marie Skłodowska-Curie grant agreement No 721991.

This work was partially financed by the ERANET-MED initiative (ERANETMED 2-72-251/MEDWASTE).

## References

- (1) Paraknowitsch, J. P.; Thomas, A.; Antonietti, M. Carbon Colloids Prepared by Hydrothermal Carbonization as Efficient Fuel for Indirect Carbon Fuel Cells. *Chem. Mater.* **2009**, *21* (7), 1170–1172.
- (2) Cao, D.; Sun, Y.; Wang, G. Direct Carbon Fuel Cell: Fundamentals and Recent Developments. *J. Power Sources* **2007**, *167* (2), 250–257.
- (3) WeiZi, C.; Qian, Z.; YongMin, X.; Jiang, L.; GuoHui, L.; Shuang, C.; MeiLin, L. A Direct Carbon Solid Oxide Fuel Cell Operated on a Plant Derived Biofuel with Natural Catalyst. *Appl. Energy* **2016**, *179*, 1232–1241.
- (4) Bergius, F. Die Anwendung Hoher Drucke Bei Chemischen Vorgängen Und Eine Nachbildung Des Entstehungsprozesses Der Steinkohle. *W. Knapp* **1913**.
- (5) Ruyter, P. Coalification Model \*. *Fuel* **1982**, *61* (12), 1182–1187.
- (6) Titirici, M.-M.; White, R. J.; Brun, N.; Budarin, V. L.; Su, D. S.; del Monte, F.; Clark, J. H.; MacLachlan, M. J. Sustainable Carbon Materials. *Chem. Soc. Rev.* **2015**, *44* (1), 250–290.
- (7) Kruse, A.; Funke, A.; Titirici, M.-M. Hydrothermal Conversion of Biomass to Fuels and Energetic Materials. *Curr. Opin. Chem. Biol.* **2013**, *17* (3), 515–521.
- (8) Funke, A.; Ziegler, F. Hydrothermal Carbonization of Biomass: A Summary and Discussion of Chemical Mechanisms for Process Engineering. *Biofuels, Bioprod. Biorefining* **2010**, *4* (2), 160–177.
- (9) Dinjus, E.; Kruse, A.; Tröger, N. Hydrothermal Carbonization - 1. Influence of Lignin in Lignocelluloses. *Chem. Eng. Technol.* **2011**, *34* (12), 2037–2043.
- (10) Titirici, M.-M.; White, R. J.; Falco, C.; Sevilla, M. Black Perspectives for a Green Future: Hydrothermal Carbons for Environment Protection and Energy Storage. *Energy Environ. Sci.* **2012**, *5* (5), 6796.
- (11) Sevilla, M.; Maciá-Agulló, J. A.; Fuertes, A. B. Hydrothermal Carbonization of Biomass as a Route for the Sequestration of CO<sub>2</sub>: Chemical and Structural Properties of the Carbonized Products. *Biomass Bioenergy* **2011**, *35* (7), 3152–3159.
- (12) Falco, C.; Sevilla, M.; White, R. J.; Rothe, R.; Titirici, M.-M. Renewable Nitrogen-Doped Hydrothermal Carbons Derived from Microalgae. *ChemSusChem* **2012**, *5* (9), 1834–1840.
- (13) Berge, N. D.; Ro, K. S.; Mao, J.; Flora, J. R. V.; Chappell, M. A.; Bae, S. Hydrothermal Carbonization of Municipal Waste Streams. *Environ. Sci. Technol.* **2011**, *45* (13), 5696–5703.
- (14) Liu, Z.; Quek, A.; Parshetti, G.; Jain, A.; Srinivasan, M. P.; Hoekman, S. K.; Balasubramanian, R. A Study of Nitrogen Conversion and Polycyclic Aromatic Hydrocarbon (PAH) Emissions during Hydrochar-Lignite Co-Pyrolysis. *Appl. Energy* **2013**, *108*, 74–81.
- (15) Parshetti, G. K.; Liu, Z.; Jain, A.; Srinivasan, M. P.; Balasubramanian, R. Hydrothermal Carbonization of Sewage Sludge for Energy Production with Coal. *Fuel* **2013**, *111*, 201–210.
- (16) Liu, Z.; Zhang, F. S.; Wu, J. Characterization and Application of Chars Produced from Pinewood Pyrolysis and Hydrothermal Treatment. *Fuel* **2010**, *89* (2), 510–514.
- (17) Kang, S.; Li, X.; Fan, J.; Chang, J. Characterization of Hydrochars Produced by Hydrothermal Carbonization of Lignin, Cellulose, d -Xylose, and Wood Meal. *Ind. Eng. Chem. Res.* **2012**, *51* (26), 9023–9031.
- (18) Sevilla, M.; Fuertes, A. B. The Production of Carbon Materials by Hydrothermal Carbonization of Cellulose. *Carbon* **2009**, *47* (9), 2281–2289.
- (19) Kruse, A.; Koch, F.; Stelzl, K.; Wüst, D.; Zeller, M. Fate of Nitrogen during Hydrothermal Carbonization. *Energy Fuels* **2016**, *30* (10), 8037–8042.

- (20) Kruse, A.; Kirchherr, M.; Gaag, S.; Zevaco, T. A. Hydrothermale Karbonisierung. 4. Thermische Eigenschaften Der Produkte. *Chemie Ing. Tech.* **2015**, *87* (12), 1707–1712.
- (21) Sevilla, M.; Fuertes, A. B. The Production of Carbon Materials by Hydrothermal Carbonization of Cellulose. *Carbon* **2009**, *47* (9), 2281–2289.
- (22) Chuntanapum, A.; Matsumura, Y. Formation of Tarry Material from 5-HMF in Subcritical and Supercritical Water. *Ind. Eng. Chem. Res.* **2009**, *48* (22), 9837–9846.
- (23) Brown, A. B.; McKeogh, B. J.; Tompsett, G. A.; Lewis, R.; Deskins, N. A.; Timko, M. T. Structural Analysis of Hydrothermal Char and Its Models by Density Functional Theory Simulation of Vibrational Spectroscopy. *Carbon* **2017**, *125*, 614–629.
- (24) Peterson, A. A.; Vogel, F.; Lachance, R. P.; Fröling, M.; Antal, M. J.; Tester, J. W. Thermochemical Biofuel Production in Hydrothermal Media: A Review of Sub- and Supercritical Water Technologies. *Energy Environ. Sci.* **2008**, pp 32–65.
- (25) Bobleter, O. Hydrothermal Degradation of Polymers Derived from Plants. *Progress in Polymer Science.* **1994**, pp 797–841.
- (26) Möller, M.; Nilges, P.; Harnisch, F.; Schröder, U. Subcritical Water as Reaction Environment: Fundamentals of Hydrothermal Biomass Transformation. *ChemSusChem* **2011**, *4* (5), 566–579.
- (27) Jung, D.; Zimmermann, M.; Kruse, A. Hydrothermal Carbonization of Fructose: Growth Mechanism and Kinetic Model. *ACS Sustain. Chem. Eng.* **2018**, *accsuschemeng.8b02118*.
- (28) Weingarten, R.; Conner, W. C.; Huber, G. W. Production of Levulinic Acid from Cellulose by Hydrothermal Decomposition Combined with Aqueous Phase Dehydration with a Solid Acid Catalyst. *Energy Environ. Sci.* **2012**, *5* (6), 7559–7574.
- (29) Körner, P.; Jung, D.; Kruse, A. The Effect of Different Brønsted Acids on the Hydrothermal Conversion of Fructose to HMF. *Green Chem.* **2018**, *20*, 2231–2241
- (30) Reza, M. T.; Rottler, E.; Herklotz, L.; Wirth, B. Hydrothermal Carbonization (HTC) of Wheat Straw: Influence of Feedwater PH Prepared by Acetic Acid and Potassium Hydroxide. *Bioresour. Technol.* **2015**, *182*, 336–344.
- (31) Libra, J. A.; Ro, K. S.; Kammann, C.; Funke, A.; Berge, N. D.; Neubauer, Y.; Titirici, M.-M.; Fühner, C.; Bens, O.; Kern, J.; et al. Hydrothermal Carbonization of Biomass Residuals: A Comparative Review of the Chemistry, Processes and Applications of Wet and Dry Pyrolysis. *Biofuels* **2011**, *2* (1), 71–106.
- (32) Sevilla, M.; Fuertes, A. B.; Mokaya, R. High Density Hydrogen Storage in Superactivated Carbons from Hydrothermally Carbonized Renewable Organic Materials. *Energy Environ. Sci.* **2011**, *4* (4), 1400.
- (33) Hu, B.; Yu, S. H.; Wang, K.; Liu, L.; Xu, X. W. Functional Carbonaceous Materials from Hydrothermal Carbonization of Biomass: An Effective Chemical Process. *Dalt. Trans.* **2008**, *40*, 5414–5423.
- (34) William W. Jacques. Method of Converting Potential Energy of Carbon into Electrical Energy. US patent 555511A, 1896.
- (35) Jiang, C.; Ma, J.; Corre, G.; Jain, S. L.; Irvine, J. T. S. Challenges in Developing Direct Carbon Fuel Cells. *Chem. Soc. Rev.* **2017**, *46* (10), 2889–2912.
- (36) Cooper, J. F. Direct Conversion of Coal and Coal-Derived Carbon in Fuel Cells, in: Second International Conference on Fuel Cell Science, Engineering and Technology, ASME, Rochester, NY, June 14-16. In *2nd International Conference on Fuel Cell Science, Engineering and Technology*; ASME, 2004; pp 375–385.
- (37) Lee, A. C.; Mitchell, R. E.; Gür, T. M. Thermodynamic Analysis of Gasification-Driven Direct Carbon Fuel Cells. *J. Power Sources* **2009**, *194* (2), 774–785.
- (38) Gür, T. M. Critical Review of Carbon Conversion in “Carbon Fuel Cells.” *Chem. Rev.* **2013**, *113*, 6179–6206.
- (39) Werhahn M.; Schneider O.; Stimming U. Direct Carbon Fuel Cell Global Energy Trends Motivation, (2012). <https://mediatum.ub.tum.de/doc/1110007/file.pdf> (accessed December 12, 2018).
- (40) Carrette, L.; Friedrich, K. A.; Stimming, U. Fuel Cells - Fundamentals and Applications. *Fuel Cells* **2001**, *1* (1), 5–39.
- (41) Atkins, P. W.; Paula, J. de. *Physical Chemistry*; John Wiley & Sons, 2006.
- (42) Kurzweil, P. *Brennstoffzellentechnik*; Springer, 2016.
- (43) Alexander, B. R.; Mitchell, R. E.; Gür, T. M. Oxy-Combustion of Solid Fuels in a Carbon Fuel Cell. *Proc. Combust. Inst.* **2013**, *34* (2), 3445–3452.
- (44) Hemmes, K.; Dijkema, G. P. J.; van der Kooi, H. J. From Chemical Processes to Electrochemical Processes: The Key to Minimal Entropy Production. *Russ. J. Electrochem.* **2004**, *40* (11), 1100–1104.
- (45) Ihsan Barin. *Thermochemical Data of Pure Substances*; 1997; Vol. 55.
- (46) Zecevic, S.; Patton, E. M.; Parhami, P. Carbon–air Fuel Cell without a Reforming Process. *Carbon N. Y.* **2004**, *42* (10), 1983–1993.
- (47) Guo, L.; Calo, J. M.; DiCocco, E.; Bain, E. J. Development of a Low Temperature, Molten Hydroxide Direct Carbon Fuel Cell. *Energy Fuels* **2013**, *27* (3), 1712–1719.
- (48) Vutetakis, D. G.; Skidmore, D. R.; Byker, H. J. Electrochemical Oxidation of Molten Carbonate-Coal Slurries. *J. Electrochem. Soc.* **1987**, *134* (12), 3027.
- (49) Wu, W.; Zhang, Y.; Ding, D.; He, T. A High-Performing Direct Carbon Fuel Cell with a 3D Architected Anode Operated Below 600 °C. *Adv. Mater.* **2018**, *30* (4), 1704745.
- (50) Jain, S. L.; Nabae, Y.; Lakeman, B. J.; Pointon, K. D.; Irvine, J. T. S. Solid State Electrochemistry of Direct Carbon/Air Fuel Cells. *Fuel Cells Bull.* **2008**, *11* (10), 10–13.
- (51) Nürnberger, S.; Buřar, R.; Desclaux, P.; Franke, B.; Rzepka, M.; Stimming, U. Direct Carbon Conversion in a SOFC-System with a Non-Porous Anode. *Energy Environ. Sci.* **2010**, *3* (1), 150–153.

- (52) Elleuch, A.; Boussetta, A.; Yu, J.; Halouani, K.; Li, Y. Experimental Investigation of Direct Carbon Fuel Cell Fueled by Almond Shell Biochar: Part I. Physico-Chemical Characterization of the Biochar Fuel and Cell Performance Examination. *Int. J. Hydrogen Energy* **2013**, *38* (36), 16590–16604.
- (53) Hemmes, K.; Cassir, M. A Theoretical Study of the Carbon/Carbonate/Hydroxide (Electro-) Chemical System in a Direct Carbon Fuel Cell. *J. Fuel Cell Sci. Technol.* **2011**, *8* (5), 051005.
- (54) Pesavento P. V. Carbon-air fuel cell, US6200697B1, 1999.  
<https://patents.google.com/patent/US6200697B1/en>
- (55) Eberz, A.; Franck, E. U. High Pressure Electrolyte Conductivity of the Homogeneous, Fluid Water-Sodium Hydroxide System to 400°C and 3000 Bar. *Berichte der Bunsengesellschaft für Phys. Chemie* **1995**, *99* (9), 1091–1103.
- (56) Héroid, C.; Héroid, A.; Lagrange, P. Ternary Graphite Intercalation Compounds Associating an Alkali Metal and an Electronegative Element or Radical. *Solid State Sci.* **2004**, *6* (1), 125–138.
- (57) Zecevic, S.; Patton, E. M.; Parhami, P. Direct Carbon Fuel Cell With Hydroxide Electrolyte: Cell Performance During Initial Stage of a Long Term Operation. In *3rd International Conference on Fuel Cell Science, Engineering and Technology*; ASME, 2005; Vol. 2005, pp 507–514.
- (58) Tanimoto, K.; Yanagida, M.; Kojima, T.; Tamiya, Y.; Matsumoto, H.; Miyazaki, Y. Long-Term Operation of Small-Sized Single Molten Carbonate Fuel Cells. *J. Power Sources* **1998**, *72* (1), 77–82.
- (59) Morita, H.; Kawase, M.; Mugikura, Y.; Asano, K. Degradation Mechanism of Molten Carbonate Fuel Cell Based on Long-Term Performance: Long-Term Operation by Using Bench-Scale Cell and Post-Test Analysis of the Cell. *J. Power Sources* **2010**, *195* (20), 6988–6996.
- (60) Cherepy, N. J.; Krueger, R.; Fiet, K. J.; Jankowski, A. F.; Cooper, J. F. Direct Conversion of Carbon Fuels in a Molten Carbonate Fuel Cell. *J. Electrochem. Soc.* **2005**, *152* (1), A80.
- (61) Li, X.; Zhu, Z. H.; Marco, R. De; Dicks, A.; Bradley, J.; Liu, S.; Lu, G. Q. Factors That Determine the Performance of Carbon Fuels in the Direct Carbon Fuel Cell. *Ind. Eng. Chem. Res.* **2008**, *47* (23), 9670–9677.
- (62) Cooper, J. F.; Selman, R. Electrochemical Oxidation of Carbon for Electric Power Generation: A Review. *ECS Trans.* **2009**, *19* (14), 15–25.
- (63) Lee, A. C.; Li, S.; Mitchell, R. E.; Gür, T. M. Conversion of Solid Carbonaceous Fuels in a Fluidized Bed Fuel Cell. *Electrochem. Solid State Lett.* **2008**, *11* (2), B20.
- (64) Ju, H.; Uhm, S.; Kim, J. W.; Song, R.-H.; Choi, H.; Lee, S.-H.; Lee, J. Enhanced Anode Interface for Electrochemical Oxidation of Solid Fuel in Direct Carbon Fuel Cells: The Role of Liquid Sn in Mixed State. *J. Power Sources* **2012**, *198*, 36–41.
- (65) Hund, F. Anomale Mischkristalle Im System  $ZrO_2 \cdot Y_2O_3$  Kristallbau Der Nernst-Stifte. *Zeitschrift für Elektrochemie und Angew. Phys. Chemie* **1951**, *55* (5), 363–366.
- (66) Li, C.; Shi, Y.; Cai, N. Mechanism for Carbon Direct Electrochemical Reactions in a Solid Oxide Electrolyte Direct Carbon Fuel Cell. *J. Power Sources* **2011**, *196* (2), 754–763.
- (67) Kaklidis, N.; Kyriakou, V.; Garagounis, I.; Arenillas, A.; Menéndez, J. A.; Marnellos, G. E.; Konsolakis, M. Effect of Carbon Type on the Performance of a Direct or Hybrid Carbon Solid Oxide Fuel Cell. *RSC Adv.* **2014**, *4* (36), 18792–18800.
- (68) Nabae, Y.; Pointon, K. D.; Irvine, J. T. S. Electrochemical Oxidation of Solid Carbon in Hybrid DCFC with Solid Oxide and Molten Carbonate Binary Electrolyte. *Energy Environ. Sci.* **2008**, *1* (1), 148–155.
- (69) White, S. H.; Twardoch, U. M. The Solubility and Electrochemistry of Alkali Metal Oxides in the Molten Eutectic Mixture of Lithium Carbonate-Sodium Carbonate-Potassium Carbonate. *J. Appl. Electrochem.* **1989**, *19* (6), 901–910.
- (70) Jang, H.; Ocon, J. D.; Lee, S.; Lee, J. K.; Lee, J. Direct Power Generation from Waste Coffee Grounds in a Biomass Fuel Cell. *J. Power Sources* **2015**, *296*, 433–439.
- (71) Ahn, S. Y.; Eom, S. Y.; Rhie, Y. H.; Sung, Y. M.; Moon, C. E.; Choi, G. M.; Kim, D. J. Utilization of Wood Biomass Char in a Direct Carbon Fuel Cell (DCFC) System. *Appl. Energy* **2013**, *105*, 207–216.
- (72) Kinoshita K. *Carbon: Electrochemical and physicochemical properties*, Wiley, 1988.
- (73) Donnet, J.-B.; Bansal, R. C.; Wang, M.-J. *Carbon Black: Science and Technology*; Dekker, 1993.
- (74) Pantea, D.; Darmstadt, H.; Kaliaguine, S.; Sümmechen, L.; Roy, C. Electrical Conductivity of Thermal Carbon Blacks: Influence of Surface Chemistry. *Carbon* **2001**, *39* (8), 1147–1158.
- (75) Verhelst, W. F.; Wolthuis, K. G.; Voet, A.; Ehrburger, P.; Donnet, J. B. The Role of Morphology and Structure of Carbon Blacks in the Electrical Conductance of Vulcanizates. *Rubber Chem. Technol.* **1977**, *50* (4), 735–746.
- (76) Cooper, J. F. Direct Conversion of Coal Derived Carbon in Fuel Cells BT - Recent Trends in Fuel Cell Science and Technology, In: S. Basu (Ed.), Springer New York, New York, NY, 2007, pp. 248–266.
- (77) Gong, M.; Liu, X.; Trembly, J.; Johnson, C. Sulfur-Tolerant Anode Materials for Solid Oxide Fuel Cell Application. *J. Power Sources* **2007**, *168* (2), 289–298.
- (78) Ahn, S. Y.; Eom, S. Y.; Rhie, Y. H.; Sung, Y. M.; Moon, C. E.; Choi, G. M.; Kim, D. J. Application of Refuse Fuels in a Direct Carbon Fuel Cell System. *Energy* **2013**, *51*, 447–456.
- (79) Kupiainen, L.; Ahola, J.; Tanskanen, J. Kinetics of Formic Acid-Catalyzed Cellulose Hydrolysis. *BioResources* **2014**, *9* (2), 2645–2658.
- (80) Penchini, D.; Cinti, G.; Discepoli, G.; Sisani, E.; Desideri, U. Characterization of a 100 W SOFC Stack Fed by Carbon Monoxide Rich Fuels. *Int. J. Hydrogen Energy* **2013**, *38* (1), 525–531.

## An overview of the methods used in the assessment of biochar carbon stability

R.M.D. Chaturika, Frederik Ronsse

Department of Green Chemistry and Technology, Ghent University, Coupure links 653, 9000 Gent, Belgium

### Abstract

Soil application of biochar has become popular worldwide due to its number of benefits as a soil amendment. High porosity, improving soil moisture retention, higher cation exchange capacity, liming effect, ability to bind organic pollutants and heavy metals, supplying habitats for microorganisms, high stability in soil due to high aromaticity, priming effect and carbon sequestration potential, reducing greenhouse gas emissions contribute to act as a potential soil amendment. However, all these mentioned beneficial outcomes depend on the quality of biochar. Biochar quality and the stability mainly depend on the feedstock type and biochar production conditions. The stability of biochar is fundamental to the knowledge of determining the residence time of biochar derived carbon within soil, further contributing to the mitigation of climate change and additional benefits to the environment. Biochar stability test methods are the key to understand the long term behaviour of biochar after its application to the soil. Those methods vary from simple to most sophisticated methods based on the simplicity, cost effectiveness and the technology involved during the analysis. For the better assessment of biochar stability, calibrating simple and cost effective methods from most sophisticated ones provides a great approach.

### 1. Importance of biochar as a soil amendment

*“Biochar is the porous, carbonaceous material produced by thermochemical treatment of organic materials in an oxygen-limited environment.”*<sup>1,2</sup> Pyrolysis of biomass has been used to produce biochar for several thousand years in history. During the charring process, biomass is subjected to several physicochemical breakdowns to produce a charred by-product. This solid by-product has diverse applications due to its special beneficial characteristics. Biochar plays an important role in the global carbon budget and carbon cycle due to its potential to act as a significant sink for atmospheric carbon dioxide<sup>3</sup>. In order to evaluate the influence of biochar on the global carbon cycle, a clear understanding about the stability of biochar is a necessity<sup>4</sup>. As a stable compound, biochar supplies several services to eco systems.

The main uses of biochar can be noted as soil improvers, a waste management strategy, as an energy source, gas absorbing advanced carbon material, microbial carriers in composting, and to help in rehabilitation of degraded unfertile soils and mitigating climate change. Biochar can enhance plant growth and increase crop yield by improving soil physical, chemical and biological properties due to its high porous nature and aromatic carbon compounds. Also, biochar acts on carbon sequestration in soil to mitigate the greenhouse gas emissions and it has the ability to retain pollutants and reduce pollution due to agrochemicals. Moreover, biochar has good nutrient retention capacity, therefore improves the soil fertility and decrease the demand for mineral fertilisers. Biochar inherently has alkaline pH, which facilitates the ameliorating of soil acidity. Due to high porosity of biochar, it will improve soil aeration and supply habitats for microbial growth. Biochar provides a unique opportunity to improve soil fertility and nutrient-use efficiency of locally available, inexpensive and renewable materials for a sustainable soil fertility management with the minimum use of expensive fertiliser additions.

Reduction of soil organic carbon is a major constraint that limits the productivity of agricultural lands. In order to increase the productivity of a land, the chemical, physical and biological resilience should increase. Biochar is identified as a feasible

approach for that. Application of biochar in to soil enhances water holding capacity. It facilitates the moisture retention in the soils in arid climates. High porosity improves aeration and moisture retention thus increase the plant shoot and root growth in soil. Also, biochar has high surface area which creates a better cation exchange capacity in nutrient low unfertile soils. Also, it helps to reduce the leaching losses of ions by binding with active sites. Indirectly, this phenomenon could help to reduce the eutrophication in surface waterbodies. As a carbon rich source, biochar contains a lot of aromatic compounds which are resistant to weathering process. Therefore, it lowers the mineralisation of soil organic matter and increases the soil organic carbon content.<sup>5,6</sup>

The use of manure and compost directly as fertilisers may create problems such as the scarcity of them in long-term use, serious ground water and stream nutrient pollution, containment of pathogens and heavy metals, and can increase the emission of greenhouse gases. But, the production and application as biochar could be a better way of disposing agricultural and industrial wastes, livestock manure, etc. with less greenhouse gas emission while reducing pollution and rehabilitating degraded land and bringing poor soils into production<sup>7</sup>. Previous studies reported that the addition of biochar to soils resulted, on average, in increased above ground productivity, crop yield, soil microbial biomass, rhizobia nodulation, plant K tissue concentration, soil phosphorus (P), soil potassium (K), total soil nitrogen (N), and total soil carbon (C) compared with the controlled conditions<sup>8-10</sup>. Soil pH also tended to increase, becoming less acidic, following the addition of biochar. Also, higher nutrient retention and nutrient availability were observed after charcoal addition to soil, related to higher cation exchange capacity, surface area and direct nutrient additions<sup>4</sup>. Soil water retention, saturated hydraulic conductivity and nutrient availability increased with the application of biochar<sup>11</sup>. Rather than applying easily mineralisable organic material into soil, application of biochar as a recalcitrant material provides above advantages (as shown in Fig. 1). The addition of straw to soil resulted in high CO<sub>2</sub> emissions, indicating lower soil carbon sequestration potential compared with the straw biochar amended soils. Furthermore, biochar amendment showed increasing effects on some of the

investigated soil parameters, such as CEC and soil pH. Soil respiration was lower in biochar amended soils than in residue-amended soils<sup>12,13</sup>. Biochar has been used to rehabilitate acidic and unfertile soils to ameliorate soil acidity and improve the nutrient retention capacity and soil physiochemical properties such as soil structure and soil aggregation. Also, biochar is used to remediate soils contaminated with poly aromatic hydrocarbons and heavy metals where its' special binding ability will reduce the bio availability of certain compounds.

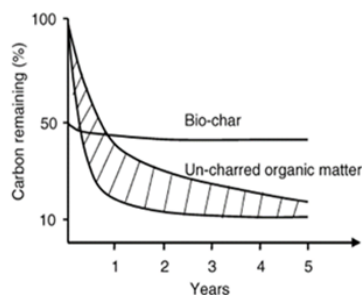


**Figure 1.** Decomposition of biochar and un-charred organic matter in soil.<sup>14</sup>

Highly aromatic nature of biochar facilitates reduction of the soil organic carbon mineralisation. Soil is the largest terrestrial carbon source and it releases a significant amount of carbon dioxide through explosion of soil organic matter by intensive agriculture related activities and excavation of peat lands. Application of biochar into soil as a carbon negative approach will reduce the emissions of greenhouse gases from the soil. Also, biochar is used to mitigate the emissions during composting and used as a scrubber to adsorb syngas. Due to higher number of promising benefits after applying biochar into the soil, application of biochar is identified as a globally recognised approach to improve soil fertility and rehabilitation of other soil degradation related issues and mitigating climate change.

## 2. Factors affecting the biochar stability in soil

The use of biochar varies with its characteristics and has a diverse range of applications. Stability of biochar is important in supplying the above mentioned advantages over long-term. The stability of biochar is fundamental to the knowledge of determining the residence time of biochar derived carbon within soil, further contributing to the mitigation of climate change and additional benefits to the environment<sup>15</sup>. After addition of biochar into soil, its stability mainly depends on its decomposition rate in soil. Biochar decomposition in soil and its effect on soil organic carbon mineralisation depends on various factors under different environmental conditions. Characteristics of biochar itself also effects on the stability in soil. Different studies conducted under various environmental conditions have resulted different Mean Residence Times (MRT) for the same biochar. There are several factors and processes which affect the biochar stability in soil such as properties of biochar, abiotic and biotic environmental factors, abiotic and biotic processes and indirect processes. Biochar and its properties can be significantly altered according to the

production method, and this has consequences towards how biochar behaves once added to soil.<sup>15,16</sup> MRT of biochar varies with factors and processes as summarised in Table 1.

**Table 1.** Mean Residence Time (MRT) of biochar reported in different studies.

Source	Estimated MRT (Years)
Rosa et al. (2018) <sup>17</sup>	Decadal
Hamer et al. (2004) <sup>18</sup>	Decadal
Fang et al. (2014) <sup>19</sup>	Decadal to Centennial (44 to 610 years)
Murray et al. (2015) <sup>20</sup>	Decadal to Centennial
Santos et al. (2012) <sup>21</sup>	centennial (390 to 600 years)
Peng et al. (2011) <sup>22</sup>	Centennial to millennial (244 to 1700 years)
Singh et al. (2012) <sup>23</sup>	Centennial to millennial ( 90 to 1600 years)
Fang et al. (2015) <sup>24</sup>	Centennial to millennial
Kuzyakov et al. (2009) <sup>25</sup>	Millennial (2000 years)
Liard et al. (2008) <sup>26</sup>	Millennial (2000 years)
Schmidt et al. (2002) <sup>27</sup>	Millennial (1160 – 5040 years)
Cheng et al. (2006) <sup>28</sup>	Millennial (1000 years)
Cheng et al. (2008) <sup>29</sup>	Millennial (1335 years)

### 2.1. Effects of feedstock type and pyrolysis conditions on biochar stability in soil

Properties of biochar play an important role when it is used as a soil amendment. They basically depend on the feedstock type and the pyrolysis conditions used for biochar production. Different substrates like agricultural wastes, manure, food wastes and urban solid wastes can be used as feedstock for biochar production. Depending on the chemical composition of feedstock, the chemical composition and the stability of the resulted biochar could be varying. Especially, the moisture content, ash content and inorganic matter content could be varying according to the feedstock material. Even for the same type of feedstock, the composition could be varying with the maturity of the plant or the particular component used for the biochar production (e.g., leaves, stems, etc.) and with the pre-process conditions<sup>30</sup>. This is mainly determined by the carbon content of the biochar, which could be divided into two pools: as recalcitrant (no-labile) pool and labile (easily accessible) pool. According to the recent review done by Wang et al., MRT of the labile and recalcitrant biochar C pools were estimated to be about 108 days and 556 years with pool sizes of 3% and 97%, respectively<sup>31</sup>. Also, depending on the ash content of the biochar, their MRT can vary<sup>20</sup>. On the other hand, the oxidation resistance ability of a biochar increases with the increase in aromatic C and endogenous mineral content<sup>32</sup>. Pyrolysis temperature heavily affects the stability of biochar and its

carbon sequestration potential in different soils<sup>33</sup>. The biochar–mineral interactions that affect the stability of biochar in soil vary with the biochar production temperature, since it has been proved that the wood biochar produced at high temperature is more stable than low temperature biochar in different types of soils and different incubation temperatures<sup>34</sup>. With the increase in temperature, main oxygen-containing functional groups decrease gradually while the degree of aromatisation increases. Due to these high aromatic compounds, biochar produced in higher pyrolysis temperatures showed higher stability. With the increasing pyrolysis temperature, the amount of oxidised carbon with respect to the total carbon of the biochar decreases. As a result of that, the H:C and O:C molar ratios will decrease.<sup>35</sup>

The yield of biochar decreased considerably with pyrolysis temperature and the yield of stable carbon showed only minor dependence on the pyrolysis temperature, despite the increase in concentration of the stable carbon in the biochar produced with increasing temperature. The non-stable fraction of biochar consists predominantly of semi-labile carbon with the labile carbon presenting only in a minor fraction. Despite its low yield, the labile fraction can play an important role in application of biochar, as it is important in soil processes<sup>36</sup>. Most of the inherent properties of the biochar are determined by the feedstock type and the pyrolysis conditions of biochar production. But, as a soil amendment, its' stability and other soil interactions depends on the soil environmental conditions.

## 2.2. Effect of abiotic and biotic environmental factors and processes on biochar stability in soil

With the growing interest of biochar as a soil amendment, the behaviour of biochar in different soil environments took a special attention in the biochar research community. Due to the slow decomposition rate in soil, biochar has been identified as having a carbon sequestration potential. There are numerous abiotic and biotic soil factors and processes that affect the stability of biochar in soil. Temperature of the soil environment is crucial for the microbial activity in soil. Also, chemically mediated oxidations could be accelerated through the increase in temperature. According to several studies conducted with elevated soil incubation temperatures (> 30 °C), MRT of biochar was decreased with higher incubation temperatures<sup>37,38</sup>. Moreover, high temperatures in many tropical and subtropical regions occur in the same months as the highest precipitations, providing ideal conditions for microbial degradation of pyrogenic carbon on the soil surface<sup>38</sup>. Global warming and tropical climates may lower the C sequestration potential of biochar, by reducing its capacity to decline the mineralisation of labile organic matter carbon content, while increasing the mineralisation of native soil organic carbon.<sup>39</sup>

Biochar decomposition in soil is mainly a biotic mediated process, despite that several abiotic processes can simultaneously occur. Due to the biotic oxidation and decomposition formation of oxygen-containing functional groups, loss of aryl carbon content in biochar can happen<sup>40</sup>. Since biochar has a high porosity, it can increase water holding capacity in soil and alter soil pH. It will create favourable conditions for inhabitant microbes of biochar. Also, the labile carbon content in biochar provides food for the microbes.

Labile carbon content of biochar is very low and due to high recalcitrant carbon content, this microbial-mediated carbon mineralisation get lower with the time<sup>41,42</sup>. However, this carbon assimilation in soil microorganisms is also important because it is another way of soil carbon sequestration potential of biochar<sup>25</sup>. The available substrates in soil determine the activity of the microbes present. Biochar has extremely low availability for microbial consumption<sup>43</sup>. So biochar will decompose mainly through co-metabolism and it has a very low significance as a carbon source for microorganisms. The assimilation of biochar carbon in microorganisms varied between 1.5% and 2.6% of total application.<sup>25</sup>

Abiotic factors determine the decomposition rate of the microbial decomposition. When a soil receives an input, bacteria are the first group to trap it and metabolise. Fungi, which can withstand low nutrient contents, get involved in the decomposition with the rest of poorly available substrates for bacteria<sup>44–46</sup>. In addition, the compounds released by microorganisms affect the biochar degradation. The plant rhizo depositions also facilitate microorganism growth (increase their growth) and those microorganisms and soil fauna facilitate to the overall process.<sup>47</sup>

Abiotic and biotic processes are also important in initial oxidation of fresh biochar. Due to these processes, rapid oxidation of biochar happens. This may facilitate further decomposition by microorganisms. Therefore, this aspect has a significant effect on biochar stability. As a result of the biochar decomposition, soil fertility will improve by increasing surface cation retention<sup>28,48</sup>. Scanning electronic microscopy (SEM) images of biochar particles aged with soil showed colonisation by microbes and widespread organic matter coatings. Thus, sorption of both microbially produced organic matter and soil organic matter are likely processes that enhance biochar aging<sup>49</sup>. Due to highly aromatic nature of the biochar, it is resistant to microbial degradation. However, it is added to the matrix, which is more susceptible to the microbial degradation. With the surface mineralisation, biochar carbon is exposed to the environment. Physical mechanisms such as abrasion, erosion due to rain splash and trampling will accelerate this process. After mineralisation of the labile carbon content in the biochar, the rest of the recalcitrant carbon content exists in the environment with different lifespans, which may vary from few decades to millennia.<sup>38</sup>

## 2.3. Effect of soil properties on biochar stability in soil

The stability of biochar in soils may not be solely attributable to its chemical characteristics, but also to its reduced accessibility when it is involved in organo-mineral associations. Biochar can be stabilised through chemical interactions with soil minerals and subsequent physical occlusions in organo-mineral fractions, thereby limiting its spatial accessibility to soil microorganisms and their enzymes.<sup>42</sup> Both the biochar-mineral interactions and the intrinsic chemical recalcitrance of biochar are important in determining the long-term C sequestration potential of biochar in soils<sup>19</sup>. Soils containing high minerals seem to favour long-term stability of biochar due to the enhanced oxidation resistance. Clayey soils, which are rich in minerals, such as kaolinite, Fe- and Al- oxides, could be a beneficial environment for biochar in terms of long-term

carbon sequestration<sup>50</sup>. The combined spectroscopy-microscopy approach revealed the accumulation of aromatic-C in discrete spots in the solid-phase of micro aggregates and its co-localisation with clay minerals in soils amended with biochar.<sup>13</sup> Enhanced oxidation resistance of biochar surface was likely due to the physical isolation from newly formed minerals, while organometallic complex formation was probably responsible for the increase in oxidation resistance of entire biochar particles. As a result, mineral-rich soils seemed to be a beneficial environment for biochar, since soil minerals could increase biochar stability, which displays an important environmental significance of biochar for long-term carbon sequestration<sup>50</sup>. Soil mineral attachment may occur directly on the biochar surface because of the formation of carboxylic and phenolic functional groups on the aged biochar surface by oxidation reactions. For biochar, adsorption of organic matter from soil facilitate the interactions between biochar and minerals in the soil. Calcium is believed to be important in this process.<sup>51</sup>

Moisture content of the soil has an important role in the degradation of biochar stability in soil. With the altered conditions of saturated and unsaturated moisture, it will increase biochar carbon mineralisation compared to the saturated conditions, probably due to the increased carboxylic and hydroxide functional groups while decreasing aliphatic groups. Carbon loss through this process strongly correlated with changes in O:C values of biochar indicating that oxidation of biochar was most likely the main mechanism to control its stability<sup>52</sup>. In contrast, an increase in greenhouse gas emissions (CH<sub>4</sub> and CO<sub>2</sub> efflux) was recorded in moist soils compared to the dry soils. Authors argued that this may be due to an additive effect, due to the decomposition of biochar or an interactive synergistic effect originating both from the decomposition of the biochar and priming effects stimulating the decomposition of the soil organic matter.<sup>53</sup>

### 3. Methods to determine biochar carbon stability

Biochar stability test methods are the key to understand the long term behaviour of biochar after its applications to the soil. Several methods have been developed to measure it. In most of the test methods, elemental composition, ash content, volatile matter content, organic and inorganic carbon content, carbon functional groups and aromatic moieties were assessed. Those test methods can be categorised into three groups based on the feasibility, knowledge, technology and cost effectiveness involved during the testing procedure<sup>15</sup>. According to the guidelines of the International Biochar Initiative, simple and reliable measures of the relative stability of carbon in biochar that are readily available at a low cost are categorised as alpha methods. Some of alpha methods are the hydrogen to organic carbon molar ratio (H:C<sub>org</sub>), oxygen to carbon molar ratio (O:C) and volatile matter content. Methods focused on directly quantify the biochar loss over a period of time are grouped as beta methods<sup>15</sup>. Laboratory and field-based incubations as well as field chronosequence measurements are examples of currently used Beta methods. A third category is the gamma methods, which measure the biomolecules regarding to the

biochar stability. Accordingly, Gamma methods can be used to calibrate the Alpha and Beta methods. The following paragraphs give the short description about major biochar stability testing methods/indicators used in different studies.

#### 3.1. Elemental ratios

Hydrogen to organic carbon molar ratio (H:C<sub>org</sub>) and oxygen to carbon molar ratio (O:C) are identified as the mostly used element basis biochar stability indicators. Especially, organic carbon content (C<sub>org</sub>) is used to assign the biochar material to a class that is dependent on the percentage of C<sub>org</sub> in the material. Carbon stability is indicated by the molar ratio of hydrogen to organic carbon. Lower values of this ratio are correlated with greater carbon stability<sup>54</sup>. Elemental composition of the biochar is assessed through elemental analysis. At present, the dry combustion method is used for the CHNS total elemental analysis. According to the literature, in most of the studies these elemental ratios reported a good correlation with pyrolysis conditions, since indicating a good prediction of biochar stability<sup>1</sup>. Especially, the O:C ratio depicted a very good correlation with biochar production temperature and the volatile matter content, biochar carbon loss and volatile matter/fixed-carbon ratio in the biochar and other elemental ratio like H:C<sub>org</sub><sup>1,55-57</sup> (see Fig. 2). In addition, O:C ratio showed a good correlation with the stable carbon content measured through the Edinburgh stability tool<sup>2</sup>. Lower O:C molar ratios correlated with longer predicted biochar half-life. O:C ratios are typically higher near the surface than at the interior of the black C particles<sup>58</sup>. Therefore, the O:C ratio could be used as an indicator of black C oxidation. Depending on the O:C ratio, biochar could be categorised into three stability classes, as reported in Table 2.

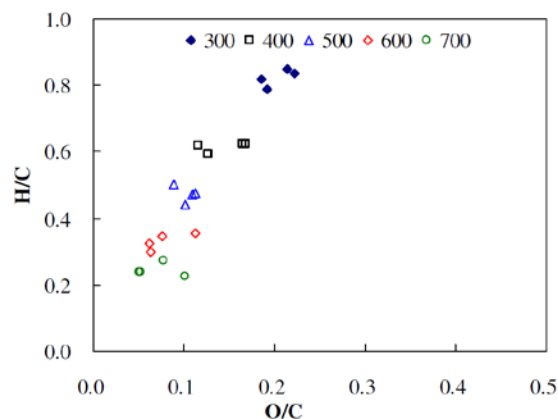


**Figure 2.** Van Krevelen plot for rice straw-derived biochar produced at different temperatures.<sup>57</sup>

**Table 2.** Predicted half-life based on the Biochar O:C ratio.<sup>1</sup>

O:C molar ratio	Predicted half life
< 0.2	> 1000 years
0.2–0.6	100–1000 years
> 0.6	over 100 years

As an element based ratio, hydrogen to organic carbon molar ratio ( $H:C_{org}$ ) also has an important role. It also has a very strong correlation with biochar production temperature and other elemental ratios like O:C ratio and proximate analysis results, such as volatile matter content/fixed carbon mass fraction ratio.  $H:C_{org}$  was selected as the preferred alpha method for being cost effective and simple measure to predict the biochar degradation in soil<sup>15</sup>. However, the O:C molar ratio showed a weak correlation ( $r = 0.73$ ) with biochar stability determined by Edinburgh stability tool<sup>58</sup>. As the upper limit of  $H:C_{org}$ , 0.7 is used to distinguish biochars from biomass that does not have the fused aromatic structure that is the source of C stability in biochar materials.<sup>54</sup>

Most often, C and H contents of the biochar are directly analysed in the lab and the O content is determined by difference. During the analysis of elemental composition, precautions should be taken to prevent any over or lower estimation of elements. By increasing intensity of oxidative treatment, it is possible to eliminate more carbon, resulting in an increased surface O:C and  $H:C_{org}$  ratios<sup>55</sup>. Since some biochar contain high carbon content, the sample amount needed to measure should be very small and that small sample weight should be measured with high accuracy.

Furthermore, as a measure of stability, organic carbon content of the biochar is mostly important than its total carbon content. Therefore, the pre-treatments to remove inorganic carbon content of the biochar are essential and the method to remove inorganic carbon in biochar should not do excessive removal of carbon in biochar. Biochar contains a highly aromatic carbon structure; the fully destruction or combustion of the aromatic structure cannot be assured in some cases. Also, relative to the higher carbon content, the relatively small peaks of other elements such as H, N and S should be carefully assessed to not to underestimate their quantity during total elemental analyses<sup>59</sup>. Therefore, using of a combination of volatile matter, and O:C or  $H:C_{org}$  ratios to classify the stability of biochar would be the best option.<sup>55</sup>

### 3.2. Chemical oxidation methods

Resistant to chemical oxidation is another measure to assess the biochar stability. Few studies reported the stability of biochar carbon content with different chemical oxidation methods such as hydrogen peroxide oxidation, potassium dichromate oxidation and potassium permanganate oxidation. Those methods provide very good idea on labile biochar fraction and the chemically resistant stable biochar fraction. Wet oxidation with potassium dichromate and potassium permanganate revealed the strong correlation with H:C atomic ratio, O:C atomic ratio and thermo-degradable fraction of biochar obtained through TG/DTG analyses<sup>60</sup>. Stable carbon content of the biochar, which is assessed after eliminating the less stable portion of biochar by oxidation with hydrogen peroxide ( $H_2O_2$ ), is used as an analogue for the accumulated effect of oxidation over extended periods of time in soil. Comparison of results from direct oxidation of biochar with stability indicators derived from proximate and ultimate analysis showed a strong correlation between the approaches across feedstock and production conditions (pyrolysis temperature and heating rate)<sup>2,58</sup>. Such modifications of alpha

methods improve the applicability of them as biochar stability measurements to depict the actual biochar stability. Chemical oxidation methods can supply low cost determinations on biochar stability while correlating good with higher and advanced biochar stability measures. Nonetheless, these methods should be validated with different types of biochar produced with different type of feedstock and biochar production conditions.

### 3.3. Fixed-carbon, volatile matter and ash contents of biochar

Fixed-carbon content, volatile matter content and ash content are the results of proximate analysis of biochar. As thermal decomposition methods, manual proximate analysis and thermogravimetric analysis decompose thermally labile component of the biochar, which is called as "volatile matter". This is done by heating the biochar sample under an inert atmosphere to avoid combustion, while the ash content is determined by heating in an oxidative atmosphere<sup>59</sup>. The most resistant part, which is neither ash nor volatile, is called as fixed-carbon content. As shown in Fig. 3, fixed-carbon content of the biochar showed a good correlation with the baseline attenuated total reflectance–Fourier transmission Infrared (ATR-FTIR) absorbance ( $4393\text{ cm}^{-1}$ ), which gives the quantitative benchmarks for estimating the degree of carbonisation of biochar.<sup>61</sup> In most of the studies, proximate analysis of biochar is used as a biochar characterisation method to predict biochar stability. However, practical drawbacks can lead to less accurate estimate of fixed-carbon by underestimation of ash content. Proximate analysis relies on thermal decomposition for calculation of products, which does not provide an analogue for the degradative processes that exist in soil.<sup>2</sup>

Greater pyrolysis temperature for low-ash biochars increased fixed-carbon content, but decreased it for biochars with more than 20% ash<sup>1,55</sup>.  $H:C_{org}$  and O:C molar ratios correlated best with the fixed-carbon content<sup>61</sup>, volatile matter/fixed-carbon mass fraction ratio. C and O mass fractions correlated best with mass fractions of volatile matter (VM), fixed carbon (FC), and ash; whereas H mass fraction correlated best with VM, FC and VM/FC<sup>56</sup>. Evaluation of volatile matter (VM) in biochar samples was proposed as the simplest method for the evaluation of biochar stability<sup>62</sup>. A volatile matter above 80% (w/w biochar ash-free mass) may indicate biochars with no carbon sequestration value. A volatile matter below 80% (w/w biochar ash-free mass) and an O:C ratio above 0.2 or  $H:C_{org}$  above 0.4 may indicate moderate sequestration ability, and a volatile matter below 80% (w/w biochar ash-free mass) and an O:C ratio below 0.2 or  $H:C_{org}$  below 0.4 may indicate high C sequestration potential<sup>1</sup>. For an accurate and reliable prediction of biochar stability, a combination of methods is a good approach<sup>55</sup>, since single parameter itself do not predict the biochar stability correctly.

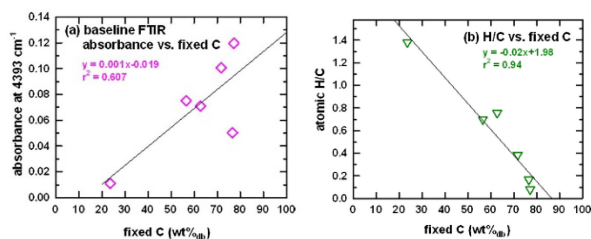


**Figure 3.** Linear regression for (a) baseline ATR-FTIR absorbance ( $4393\text{ cm}^{-1}$ ) and (b) atomic H:C ratio as a function of fixed-carbon content in biochar.<sup>61</sup>

### 3.4. Recalcitrance index

Temperature programmed oxidation (TPO) is used to calculate the recalcitrance index. Based on the thermograms (which were corrected for ash and water content) obtained through thermogravimetric or coupled TGA-DSC analysers, the mass loss resulting from oxidation of carbon is continuously monitored and used to calculate the recalcitrance index ( $R_{50}$ ) according to the following equation<sup>63</sup>:

$$R_{50} = T_{50 X} / T_{50 \text{ graphite}} \quad (1)$$

where  $T_{50 X}$  and  $T_{50 \text{ graphite}}$  are the temperatures corresponding to the 50% mass loss as a result of oxidation/volatilisation of biochar (X) and graphite, respectively. The resulting  $R_{50}$  value depends on the nature of the carbon stability of the sample. With the higher stability, the value for the  $T_{50}$  will increase. Depending on the value obtained for the recalcitrance index, biochar can be categorised into three different stability classes in terms of their carbon sequestration ability: class A biochar ( $R_{50} \leq 0.70$ ), Class B biochar ( $0.50 \leq R_{50} < 0.70$ ) and Class C biochar ( $R_{50} < 0.50$ ). Class A and Class C biochars would have carbon sequestration potential comparable to soot/graphite and uncharred plant biomass, respectively; whereas Class B biochars would have intermediate carbon sequestration potential<sup>58</sup>. As a result of the refinement of the recalcitrance index, “the gained stability” with washed biochar prior to analyse with TGA is also used for assessing the biochar stability. These values showed a strong correlation with the values of accelerated aging test.<sup>64,65</sup>

### 3.5. Laboratory incubation and field based methods and chronosequence to assess biochar stability in soil

Both laboratory incubation studies<sup>19,24,37,68–72</sup> and field application<sup>68,69,73</sup> of biochar are using in the context of assessing the temporal and spatial biochar decomposition patterns. Studies based on the field application of biochar depict the more realistic conditions compared to the laboratory incubation studies of soil and biochar. But field based methods constraint with different mineralisation pathways and losses. In addition, it will restrict the use and comparison of various types of biochar in field studies. Compared to the field studies, laboratory incubation studies do with the more controlled environmental conditions such as moisture and temperature etc. Also, constraint with the limited time durations and absence of additions of litter and manure, real fluctuations of moisture and temperature and other soil management practices related to the agriculture. But, laboratory incubations allow to do the comparison between numbers of biochar samples and provide overall outlook within short time period

though the resulted MRT of biochar is vary from the actual conditions<sup>74</sup>. Different models such as single exponential model, double exponential model and triple exponential models were used to extrapolate biochar carbon stability. Single and double exponential models can underestimate the stability of biochar carbon compared to the three pool model, since with the greater number of pools added the prediction ability will be greater<sup>15</sup>. Therefore, precautions should take before extrapolating the data from incubation studies or field studies. Percentage of carbon in biochar that can remain stable for more than 100 years predicted from MRT has a good correlation with the proximate results ( $H/C_{org}$ )<sup>15</sup>, as shown in Fig. 4.

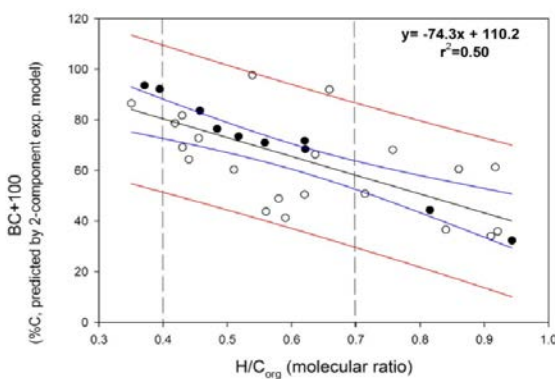


**Figure 4.** The correlation between  $H/C_{org}$  and biochar C remained after 100 years as predicted by a two component model.<sup>15</sup>

Both increase<sup>75,76</sup> and decrease<sup>5,6,77</sup> priming has been recorded after addition of biochar into the soil. Higher carbon released from biochar amended soils at the beginning of the incubation than the non-amended soils was observed with biochar produced at lower temperature from grass in lower organic matter content soils. However, opposite pattern was observed with hardwood-derived biochar produced at higher temperatures and in higher organic matter containing soils. Initial increase in carbon mineralisation after biochar addition was decreased in the later stages of the incubations observed<sup>5,24,25,31,47</sup>. Adsorption (sorption of native soil organic matter to the surface of the pyrogenic organic matter) and dilution were identified as the two major mechanisms for the negative priming observed after additions of the biochar into the soil. These mechanisms heavily contribute to the long term carbon storage in soils. Other than that, substrate switching and co-metabolism also affect to the negative priming effect but in very lower contribution<sup>71</sup>. For the better understanding of pyrogenic carbon decomposition in soil, the long-term field and laboratory incubation studies are important, since very few long-term field and laboratory incubation studies are reported in the literature.

Chronosequences, a set of sites that share many similar soil forming factors (climate, organisms, relief, and parent materials) but with soils of different ages<sup>78</sup>, can be used to determine the biochar carbon loss. According to the results reported from the measurements of biochar distribution from sites that vary in time interval since biochar was applied, several factors governing the stability of biochar in soil were identified. Oxidation, erosion and biochar particles transport (physical

transport) into the depth in the soil were identified as factors that accelerate the biochar decomposition. Also, adsorption of organic and inorganic materials was identified as a factor that protect biochar from mineralisation<sup>79–81</sup>. Especially, the biochar carbon in more stable organo mineral fraction and lower carbon mineralisation in biochar rich Anthrosols compared to the biochar poor adjacent soils were observed.<sup>4</sup>

### 3.6. Nuclear magnetic resonance (NMR) spectroscopy

NMR spectroscopy has been used in several studies to assess the degree of aromatic condensation of several compounds<sup>82</sup>. In the context of biochar, solid state NMR spectroscopy was used to identify the distribution of major biomolecules in biochar<sup>83,84</sup>. Aromatic condensation of biochar is measured using the NMR spectroscopy. The upfield shift in the peak position of a probe molecule (13C- benzene) which is sorbed into a biochar that contains aromatic structures capable of sustaining ring currents is used in this technique. That shift in the peak position ( $\Delta\delta$ ) can be expressed according to Eq. (2)<sup>85</sup>. More condensed aromatic structures,  $\Delta\delta$  becomes increasingly negative as the ring current increases in strength.

$$\Delta\delta = \delta_{\text{sorbed benzene}} - \delta_{\text{neat benzene}} \quad (2)$$

The aromaticity and the condensation derived from the NMR spectroscopic analysis showed a clear influence of production temperature and the type of feedstock. Degree of aromaticity of biochar increased with increasing pyrolysis temperature<sup>57</sup>. Higher amount of aromatic condensation was observed in biochar derived from woody materials compared to biochar from mineral-rich feedstocks produced at same pyrolysis temperature<sup>85</sup>. According to the 13C NMR spectroscopy results, aged biochar showed increased amounts of O-alkyl C and alkyl C at the expense of aromatic-C, revealing that aged biochars are less aromatic and more functionalised than fresh ones.<sup>17,86</sup> Therefore, 13C NMR spectra can be used as a marker to detect black carbon in soil<sup>48</sup>. The fraction of aromatic C in the biochar strongly increases with peak temperature, fixed-carbon yield, and decrease with increased H:C<sub>org</sub> and O:C ratios<sup>88</sup>. Also, 13 C NMR analyses can be used to assess the O-containing functional groups, including substituted aryl, carboxyl and carbonyl C, and losses of O-alkyl groups in aged biochar<sup>49</sup>. Furthermore, the aromaticity and aromatic condensation derived from NMR analysis have a good correlation with fixed-carbon content from proximate analysis and MRT of biochar, as can be observed in Figs. 5 and 6.

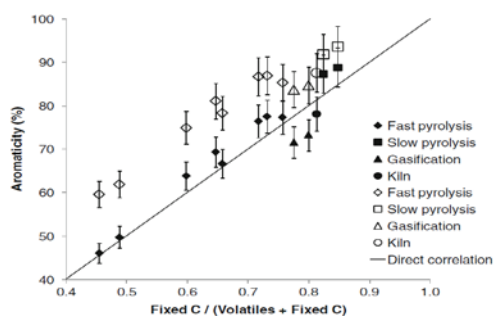


**Figure 5.** Biochar aromaticity from quantitative NMR analysis as a function of fixed-carbon fraction from proximate analysis.<sup>89</sup>

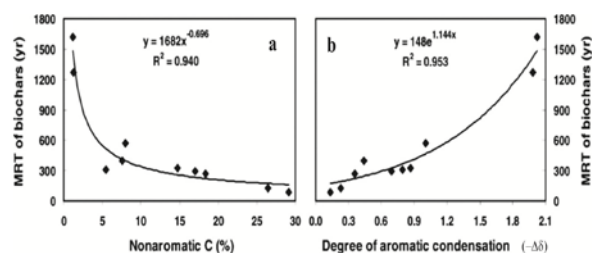


**Figure 6.** Relationships between mean residence time (MRT) of biochar carbon (using 5-year mineralisation data set) and nonaromatic C proportion (a) and degree of aromatic condensation (b) determined by 13C CP-NMR.<sup>23</sup>

### 3.7. Pyrolysis Gas Chromatography Mass Spectrometry (Py-GC-MS)

Pyrolysis gas chromatography is a chemical analysis method where the sample is heated, under an inert atmosphere, for decomposition to produce smaller molecules that can be separated by gas chromatography and detected using mass spectrometry.

The resulting pyrolysis products can be categorised into hundreds of groups based on their chemical composition. The sum of most released compounds can be used to assess the degree of charring/aromatic carbon content in biochar. This technique has been used in recent studies with different purposes, such as identifying the molecular composition of biochars to assess the biochar stability<sup>60,90,91</sup>, as well as identifying poly aromatic hydrocarbons in biochar<sup>92</sup>. The effect of feedstock type and biochar production conditions on biochar stability correlated well with the analytical pyrolysis results. Also, Py-GC-MS results correlated well with the results from thermogravimetric tests, 13C NMR spectroscopy results and biochar wet oxidation tests<sup>60</sup>. Therefore, analytical pyrolysis can be identified as a gamma method which provides a good idea about biomolecules present in biochar. Hence, it is a very good proxy to calibrate low cost alpha methods.

The molecular ratio toluene/naphthalene is governed by the extent of carbonisation and the presence of proteins in the original substrate. This was well correlated with the volatile matter content of biochar<sup>91</sup>. Pyrolysis products resulting from the analytical pyrolysis act as a pyrolysis fingerprint of a particular substance. Therefore, thermal stability index derived from these pyrolysis products could be used to assess the stability of biochar, since it is considered as a more reliable indicator than other pyrolytic proxies, such as benzene/toluene or naphthalene/C1-naphthalene ratios<sup>93</sup>. A decrease in the H:C<sub>org</sub> molar ratio was observed when the intensity and the variety of pyrolysis products in the resulted pyrolysis products decreased. In highly carbonised biochar (i.e., H:C<sub>org</sub> < 0.4), the released compounds were mainly highly aromatic. Their relative abundance (% charred) with respect to other pyrolysis products was linearly correlated with the H:C<sub>org</sub> ratio<sup>90</sup>, as shown in Fig. 7.

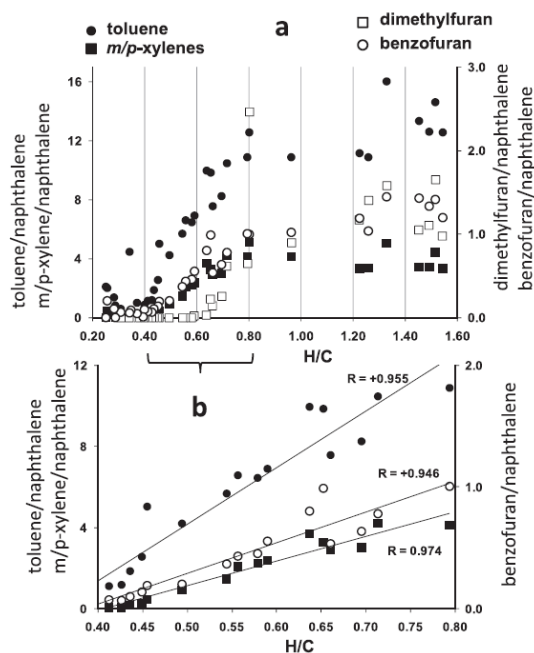


**Figure 7.** Py-GC-MS yield ratios of selected pyrolysis products with naphthalene in the whole (a) and in a selected  $H/C_{org}$  molar ratio interval (b).<sup>90</sup>

### 3.8. Benzene poly carboxylic acid (BPCA)

Condensed aromatic moieties were the most stable fraction compared to all other biochar compounds and the high portion of BPCA in biochar explains its very high stability and its contribution to long-term C sequestration in soil<sup>94</sup>. Therefore, BPCA can be used as a molecular marker to assess black carbon in soils and sediments. The analytical procedure to determine BPCA includes acid digestion, oxidation, sample clean-up, derivatisation, and gas chromatography<sup>95</sup>. The degree of polymerisation in individual monomers varies with their degree of carboxylation. This can be used to determine the stability of biochar via assessing the degree of aromatisation. Single-ring aromatic molecules with different degree of carboxylation (i.e., B3-, B4-, B5- and B6-CA) represent BPCA with three, four, five and six carboxylic groups. These BPCA monomers reflect the size of the original polycyclic structure. The proportion of BPCA normalised to total organic carbon content and the proportion of individual BPCA monomers to the total BPCA were used as indicators to depict the degree of aromatic condensation and the aromaticity of the black carbon.<sup>96</sup>

## 4. Future perspectives

Biochar application into soil as a soil amendment has become popular among globally due to its beneficial effects on soil fertility, remediation of contaminated soils and degraded lands and mitigating climate change. However, the use of biochar is still under experimental investigations. As a highly stable recalcitrant substance, biochar has a long-term persistence in soil. Therefore, before using it as a soil amendment, precautions should be taken to avoid the introduction of contaminants and harmful substances through biochar into soil. Accordingly, proper characterisation of biochar is a key to identify and predicting its behaviour in soil environment.

**Table 3.** Advantages and disadvantages of different methods focused on assessing biochar carbon stability.<sup>12,15,97</sup>

Method	Advantages	Disadvantages
Elemental ratios ( $H/C_{org}$ and O/C molar ratios)	Low cost, simple and reliable. High robustness and repeatability. Strongly correlated with the data from incubation studies, thermogravimetry and Biochar production conditions.	Qualitative indicator. Conservative.
Chemical oxidation method	Simple and low cost. Quantitative.	Hydrophobic nature of biochar can make disturbances. Need to take precautions while doing measuring.
Proximate analysis (Ash, Fixed-carbon and volatile matter contents)	Simple and low cost. Repeatability is high.	Conservative. Qualitative
Recalcitrance index	Simple and low cost. Higher accuracy.	Qualitative.
Field application of biochar	More realistic data on temporal and spatial pattern of biochar decomposition. Quantitative.	Constraint with different mineralisation pathways and losses. Difficult for using different types of biochar.
Laboratory incubation studies	Able to quantify biochar carbon mineralisation without any other losses. Quantitative.	Most of the studies constrained with the limited time duration and actual field environmental conditions.
NMR spectroscopy	Quantitative. It gives better idea about aromaticity and aromatic condensation. High accuracy.	Higher cost comparatively. Need of a good analytical knowledge. Large variation between different NMR equipment.
Pyrolysis Gas Chromatography Mass Spectrometry	High accuracy.	High cost. Not much reliable for highly aromatised biochar. Excessive charring can happen.
Benzene poly carboxylic Acid (BPCA)	Quantitative. High accuracy.	It needs several sample treatment procedures and precise analysis.

Biochar stability assessment methods play an important role in predicting biochar stability. Both advantages and disadvantages involved in those analysis methods are summarised in Table 3. Among the prevailing biochar stability indicators, laboratory soil incubation studies and field-based studies provide more realistic insight about biochar decomposition patterns and its effect on soil chemical, physical and biological properties. However, these methods are constrained by time and cost involved during the stability assessments. As a result, lab-based simple and low-cost proxies can be used for assessing biochar stability such as elemental ratios, proximate analysis, etc. These proxies have strong correlation with biochar mineralisation in soil.

### Acknowledgements

“This project has received funding from the European Union’s Horizon 2020 research and innovation programme under the Marie Skłodowska-Curie grant agreement No 721991”.

### References

- (1) Spokas, K. A. Review of the stability of biochar in soils: predictability of O:C molar ratios. *Carbon Manage.*, **2010**, *1*, 289–303.
- (2) Crombie, K.; Mašek, O.; Sohi, S. P.; Brownsort, P.; Cross, A. The effect of pyrolysis conditions on biochar stability as determined by three methods. *GCB Bioenergy*, **2013**, *5*, 122–131.
- (3) Woolf, D.; Lehmann, J. Modelling the long-term response to positive and negative priming of soil organic carbon by black carbon. *Biogeochemistry* **2012**, *111*, 83–95.
- (4) Liang, B.; Lehmann, J.; Solomon, D.; Sohi, S.; et al. Stability of biomass-derived black carbon in soils. *Geochim. Cosmochim. Acta*, **2008**, *72*, 6069–6078
- (5) Zimmerman, A. R.; Gao, B.; Ahn, M. Y. Positive and negative carbon mineralization priming effects among a variety of biochar-amended soils. *Soil Biol. Biochem.* **2011**, *43*, 1169–1179.
- (6) Whitman, T.; Enders, A.; Lehmann, J. Pyrogenic carbon additions to soil counteract positive priming of soil carbon mineralization by plants. *Soil Biol. Biochem.* **2014**, *73*, 33–41.
- (7) Barrow, C. J. Biochar: potential for countering land degradation and for improving agriculture. *Appl. Geography* **2012**, *34*, 21–28.
- (8) Mukherjee, S.; Weihermueller, L.; Tappe, W.; Vereecken, H.; Burauel, P. Microbial respiration of biochar-and digestate-based mixtures. *Biol. Fert. Soils* **2016**, *52*, 151–164.
- (9) Biederman, L. A.; Harpole, W. S. Biochar and its effects on plant productivity and nutrient cycling: a meta-analysis. *GCB Bioenergy* **2013**, *5*, 202–214.
- (10) Glaser, B.; Lehmann, J.; Zech, W. Ameliorating physical and chemical properties of highly weathered soils in the tropics with charcoal—a review. *Biol. Fert. Soils* **2002**, *35*, 219–230.
- (11) Jeffery, S.; Verheijen, F. G. A.; Van Der Velde, M.; Bastos, A. C. A quantitative review of the effects of biochar application to soils on crop productivity using meta-analysis. *Agric. Ecosyst. Environ.* **2011**, *144*, 175–187.
- (12) Hansen, V.; Müller-Stöver, D.; Munkholm, L. J.; Peltre, C.; et al. The effect of straw and wood gasification biochar on carbon sequestration, selected soil fertility indicators and functional groups in soil: an incubation study. *Geoderma* **2016**, *269*, 99–107.
- (13) Hernandez-Soriano M. C.; Kerré, B.; Kopittke, P. M.; Horemans, B.; Smolders, E. Biochar affects carbon composition and stability in soil: a combined spectroscopy-microscopy study. *Scientific Reports* **2016**, *6*, 25127.
- (14) Lehmann, J.; Gaunt, J.; Rondon, M. Bio-char sequestration in terrestrial ecosystems—a review. Mitigation and adaptation strategies for global change. *Mitig. Adapt. Strat. Glob. Chang.* **2006**, *11*, 403–427.
- (15) Budai, A.; Zimmerman, A.; Cowie, A. L.; Webber, J. B.; et al. Biochar Carbon Stability Test Method: An assessment of methods to determine biochar carbon stability. Technical report, International Biochar Initiative: 2013, pp. 1–10.
- (16) Ameloot, N.; Graber, E. R.; Verheijen, F. G.; De Neve, S. Interactions between biochar stability and soil organisms: review and research needs. *Eur. J. Soil Sci.* **2013**, *64*, 379–390.
- (17) De la Rosa, J. M.; Rosado, M.; Paneque, M.; Miller, A. Z.; Knicker, H. Effects of aging under field conditions on biochar structure and composition: Implications for biochar stability in soils. *Sci. Total Environ.* **2018**, *613–614*, 969–976.
- (18) Hamer, U.; Marschner, B.; Brodowski, S.; Amelung, W. Interactive priming of black carbon and glucose mineralisation. *Org. Geochem.* **2004**, *35*, 823–830.
- (19) Hilscher, A.; Knicker, H. Carbon and nitrogen degradation on molecular scale of grass-derived pyrogenic organic material during 28 months of incubation in soil. *Soil Biol. Biochem.* **2011**, *43*, 261–270.
- (20) Murray, J.; Keith, A.; Singh, B. The stability of low-and high-ash biochars in acidic soils of contrasting mineralogy. *Soil Biol. Biochem.* **2015**, *89*, 217–225.
- (21) Santos, F.; Torn, M. S.; Bird, J. A. Biological degradation of pyrogenic organic matter in temperate forest soils. *Soil Biol. Biochem.* **2012**, *51*, 115–214.
- (22) Peng, X. Y.; Ye, L. L.; Wang, C. H.; Zhou, H.; Sun, B. Temperature-and duration-dependent rice straw-derived biochar: Characteristics and its effects on soil properties of an Ultisol in southern China. *Soil Tillage Res.* **2011**, *112*, 159–166.
- (23) Singh, B. P.; Cowie, A. L.; Smernik, R. J. Biochar carbon stability in a clayey soil as a function of feedstock and pyrolysis temperature. *Environ. Sci. Technol.* **2012**, *46*, 11770–11778.
- (24) Fang, Y.; Singh, B.; Singh, B. P. Effect of temperature on biochar priming effects and its stability in soils. *Soil Biol. Biochem.* **2015**, *80*, 136–145.

- (25) Kuzyakov, Y.; Subbotina, I.; Chen, H.; Bogomolova, I.; Xu, X. Decomposition of <sup>14</sup>C labeled pyrogenic carbon and its incorporation into soil microbial biomass estimated during 4 years incubation. In: EGU General Assembly Conference Abstracts 2009, p. 7254.
- (26) Laird, D. A. The charcoal vision: a win-win-win scenario for simultaneously producing bioenergy, permanently sequestering carbon, while improving soil and water quality. *Agronomy J.* **2008**, *100*, 178–181.
- (27) Schmidt, M. W.; Skjemstad, J. O.; Jäger, C. Carbon isotope geochemistry and nanomorphology of soil black carbon: Black chernozemic soils in central Europe originate from ancient biomass burning. *Glob. Biogeochem. Cycles* **2002**, *16*, 70–71.
- (28) Cheng, C. H.; Lehmann, J.; Thies, J. E.; Burton, S. D.; Engelhard, M. H. Oxidation of black carbon by biotic and abiotic processes. *Org. Geochem.* **2006**, *37*, 1477–1488.
- (29) Cheng, C. H.; Lehmann, J.; Thies, J. E.; Burton, S. D. Stability of black carbon in soils across a climatic gradient. *J. Geophys. Res.* **2008**, *113*, G02027.
- (30) Vassilev, S. V.; Baxter, D.; Andersen, L. K.; Vassileva, C. G. An overview of the chemical composition of biomass. *Fuel* **2010**, *89*, 913–933.
- (31) Wang, J.; Xiong, Z.; Kuzyakov, Y. Biochar stability in soil: meta-analysis of decomposition and priming effects. *GCB Bioenergy* **2016**, *8*, 512–523.
- (32) Yang, Y.; Sun, K.; Han, L.; Jin, J.; et al. Effect of minerals on the stability of biochar. *Chemosphere* **2018**, *204*, 310–317.
- (33) Purakayastha, T. J.; Das, K. C.; Gaskin, J.; Harris, K.; et al. Effect of pyrolysis temperatures on stability and priming effects of C3 and C4 biochars applied to two different soils. *Soil Tillage Res.* **2016**, *155*, 107–115.
- (34) Fang, Y.; Singh, B.; Singh, B. P.; Krull, E. Biochar carbon stability in four contrasting soils. *Eur. J. Soil Sci.* **2014**, *65*, 60–71.
- (35) Chen, D.; Yu, X.; Song, C.; Pang, X.; et al. Effect of pyrolysis temperature on the chemical oxidation stability of bamboo biochar. *Bioresour. Technol.* **2016**, *218*, 1303–1306.
- (36) Mašek, O.; Brownsort, P.; Cross, A.; Sohi, S. Influence of production conditions on the yield and environmental stability of biochar. *Fuel* **2013**, *103*, 151–155.
- (37) Dempster, D. N.; Gleeson, D. B.; Solaiman, Z. I.; Jones, D. L.; Murphy, D. V. Decreased soil microbial biomass and nitrogen mineralisation with Eucalyptus biochar addition to a coarse textured soil. *Plant Soil* **2012**, *354*, 311–324.
- (38) Zimmermann, M.; Bird, M. I.; Wurster, C.; Saiz, G.; et al. Rapid degradation of pyrogenic carbon. *Glob. Chang. Biol.* **2012**, *18*, 3306–3316.
- (39) Fang, Y.; Singh, B. P.; Matta, P.; Cowie, A. L.; Van Zwieten, L. Temperature sensitivity and priming of organic matter with different stabilities in a Vertisol with aged biochar. *Soil Biol. Biochem.* **2017**, *115*, 346–356.
- (40) Hilscher, A.; Heister, K.; Siewert, C.; Knicker, H. Mineralisation and structural changes during the initial phase of microbial degradation of pyrogenic plant residues in soil. *Org. Geochem.* **2009**, *40*, 332–342.
- (41) Lehmann, J.; Kinyangi, J.; Solomon, D. Organic matter stabilization in soil microaggregates: implications from spatial heterogeneity of organic carbon contents and carbon forms. *Biogeochemistry* **2007**, *85*, 45–57.
- (42) Lehmann, J.; Rillig, M. C.; Thies, J.; Masiello, C. A.; et al. Biochar effects on soil biota—a review. *Soil Biol Biochem.* **2011**, *43*, 1812–1836.
- (43) Kemmitt, S. J.; Lanyon, C. V.; Waite, I. S.; Wen, Q.; et al. Mineralization of native soil organic matter is not regulated by the size, activity or composition of the soil microbial biomass—a new perspective. *Soil Biol. Biochem.* **2008**, *40*, 61–73.
- (44) Paterson, E.; Gebbing, T.; Abel, C.; Sim, A.; Telfer, G. Rhizodeposition shapes rhizosphere microbial community structure in organic soil. *New Phytologist.* **2007**, *173*, 600–610.
- (45) Blagodatskaya, E. V.; Blagodatsky, S. A.; Anderson, T. H.; Kuzyakov, Y. Priming effects in Chernozem induced by glucose and N in relation to microbial growth strategies. *Appl. Soil Ecology* **2007**, *37*, 95–105.
- (46) Otten, W.; Hall, D.; Harris, K.; Ritz, K.; Young, I. M.; Gilligan, C. A. Soil physics, fungal epidemiology and the spread of *Rhizoctonia solani*. *New Phytologist* **2001**, *151*, 459–468.
- (47) Kuzyakov, Y.; Friedel, J. K.; Stahr, K. Review of mechanisms and quantification of priming effects. *Soil Biol Biochem.* **2000**, *32*, 1485–1498.
- (48) Bird, M. I.; McBeath, A. V.; Ascough, P. L.; et al. Loss and gain of carbon during char degradation. *Soil Biol Biochem.* **2017**, *106*, 80–89.
- (49) Mukherjee, A.; Zimmerman, A. R.; Hamdan, R.; Cooper, W. T. Physicochemical changes in pyrogenic organic matter (biochar) after 15 months of field aging. *Solid Earth* **2014**, *5*, 693–704.
- (50) Yang, F.; Zhao, L.; Gao, B.; Xu, X.; Cao, X. The interfacial behavior between biochar and soil minerals and its effect on biochar stability. *Environ. Sci. Technol.* **2016**, *50*, 2264–2271.
- (51) Lin, Y.; Munroe, P.; Joseph, S.; Kimber, S.; Van Zwieten, L. Nanoscale organo-mineral reactions of biochars in ferrosol: an investigation using microscopy. *Plant Soil* **2012**, *357*, 369–380.
- (52) Nguyen, B. T.; Lehmann, J. Black carbon decomposition under varying water regimes. *Org. Geochem.* **2009**, *40*, 846–853.
- (53) Rittl, T. F.; Butterbach-Bahl, K.; Basile, C. M.; Pereira, L. A.; et al. Greenhouse gas emissions from soil amended with agricultural residue biochars: Effects of feedstock type, production temperature and soil moisture. *Biomass Bioenergy* **2018**, *117*, 1–9.
- (54) International Biochar Initiative. *Guidelines for specifications of biochars for use in soils*, 2012.

- (55) Enders, A.; Hanley, K.; Whitman, T.; Joseph, S.; Lehmann, J. Characterization of biochars to evaluate recalcitrance and agronomic performance. *Bioresour. Technol.* **2012**, *114*, 644–653.
- (56) Klasson, K. T. Biochar characterization and a method for estimating biochar quality from proximate analysis results. *Biomass Bioenergy* **2017**, *96*, 50–58.
- (57) Wu, W.; Yang, M.; Feng, Q.; McGrouther, K.; et al. Chemical characterization of rice straw-derived biochar for soil amendment. *Biomass Bioenergy* **2012**, *47*, 268–276.
- (58) Cross, A.; Sohi, S. P. A method for screening the relative long-term stability of biochar. *GCB Bioenergy* **2013**, *5*, 215–220.
- (59) Singh, B.; Camps-Arbestain, M.; Lehmann, J.; Eds. Biochar: a guide to analytical methods. Csiro Publishing, 2017.
- (60) Pereira R. C.; Kaal, J.; Camps-Arbestain, M.; Lorenzo, R. P.; et al. Contribution to characterisation of biochar to estimate the labile fraction of carbon. *Org. Geochem.* **2011**, *42*, 1331–1342.
- (61) Uchimiya, M.; Orlov, A.; Ramakrishnan, G.; Sistani, K. In situ and ex situ spectroscopic monitoring of biochar's surface functional groups. *J. Anal. Appl. Pyrolysis* **2013**, *102*, 53–59.
- (62) Zimmerman, A. R. Abiotic and microbial oxidation of laboratory-produced black carbon (biochar). *Environ. Sci. Technol.* **2010**, *44*, 1295–1301.
- (63) Harvey, O. R.; Kuo, L. J.; Zimmerman, A. R.; Louchouart, P.; et al. An index-based approach to assessing recalcitrance and soil carbon sequestration potential of engineered black carbons (biochars). *Environ. Sci. Technol.* **2012**, *46*, 1415–1421.
- (64) Gómez, N.; Rosas, J. G.; Singh, S.; Ross, A. B.; et al. Development of a gained stability index for describing biochar stability: Relation of high recalcitrance index (R50) with accelerated ageing tests. *J. Anal. Appl. Pyrolysis* **2016**, *120*, 37–44.
- (65) Carrier, M.; Loppinet-Serani, A.; Denux, D.; Lasnier, J. M.; et al. Thermogravimetric analysis as a new method to determine the lignocellulosic composition of biomass. *Biomass Bioenergy* **2011**, *35*, 298–307.
- (66) Keith, A.; Singh, B.; Dijkstra, F. A. Biochar reduces the rhizosphere priming effect on soil organic carbon. *Soil Biol. Biochem.* **2015**, *88*, 372–379.
- (67) Ventura, M.; Alberti, G.; Viger, M.; Jenkins, J. R.; et al. Biochar mineralization and priming effect on SOM decomposition in two European short rotation coppices. *GCB Bioenergy* **2015**, *7*, 1150–1160.
- (68) Weng, Z. H.; Van Zwieten, L.; Singh, B. P.; Kimber, S.; et al. Plant-biochar interactions drive the negative priming of soil organic carbon in an annual ryegrass field system. *Soil Biol. Biochem.* **2015**, *90*, 111–121.
- (69) Rasse, D. P.; Budai, A.; O'Toole, A.; Ma, X.; et al. Persistence in soil of Miscanthus biochar in laboratory and field conditions. *Plos One* **2017**, *12*, e0184383.
- (70) Cui, J.; Ge, T.; Kuzyakov, Y.; Nie, M.; et al. Interactions between biochar and litter priming: a three-source  $^{14}\text{C}$  and  $\delta^{13}\text{C}$  partitioning study. *Soil Biol. Biochem.* **2017**, *104*, 49–58.
- (71) DeCuiques, S.; Whitman, T.; Woolf, D.; Enders, A.; Lehmann, J. Priming mechanisms with additions of pyrogenic organic matter to soil. *Geochim. Cosmochim. Acta.* **2018**, *238*, 329–342.
- (72) Dharmakeerthi, R. S.; Hanley, K.; Whitman, T.; Woolf, D.; Lehmann, J. Organic carbon dynamics in soils with pyrogenic organic matter that received plant residue additions over seven years. *Soil Biol. Biochem.* **2015**, *88*, 268–274.
- (73) Munda, S.; Bhaduri, D.; Mohanty, S.; Chatterjee, D.; et al. Dynamics of soil organic carbon mineralization and C fractions in paddy soil on application of rice husk biochar. *Biomass Bioenergy* **2018**, *115*, 1–9.
- (74) Lehmann, J.; Joseph, S.; Eds. Biochar for environmental management: science, technology and implementation. Routledge, 2015.
- (75) Luo, Y.; Durenkamp, M.; De Nobili, M.; Lin, Q.; Brookes, P. C. Short term soil priming effects and the mineralisation of biochar following its incorporation to soils of different pH. *Soil Biol. Biochem.* **2011**, *43*, 2304–2314.
- (76) Wardle D. A.; Nilsson, M. C.; Zackrisson, O. Fire-derived charcoal causes loss of forest humus. *Science* **2008**, *320*, 629–629.
- (77) Whitman, T.; Zhu, Z.; Lehmann, J. Carbon mineralizability determines interactive effects on mineralization of pyrogenic organic matter and soil organic carbon. *Environ. Sci. Technol.* **2014**, *48*, 13727–13734.
- (78) Sauer, D. Pedological concepts to be considered in soil chronosequence studies. *Soil Res.* **2015**, *53*, 577–591.
- (79) Nguyen, B. T.; Lehmann, J.; Kinyangi, J.; Smernik, R.; et al. Long-term black carbon dynamics in cultivated soil. *Biogeochemistry* **2009**, *92*, 163–176.
- (80) Major, J.; Lehmann, J.; Rondon, M.; Goodale, C. Fate of soil-applied black carbon: downward migration, leaching and soil respiration. *Glob. Chang. Biol.* **2010**, *16*, 1366–1379.
- (81) Foereid, B.; Lehmann, J.; Major, J. Modeling black carbon degradation and movement in soil. *Plant Soil* **2011**, *345*, 223–236.
- (82) Duer, M. J.; Ed. *Solid state NMR spectroscopy: principles and applications*, John Wiley & Sons, 2008.
- (83) Krull, E. S.; Baldock, J. A.; Skjemstad, J. O.; Smernik, R. J. Characteristics of biochar: organo-chemical properties. In: *Biochar for environmental management: Science and technology*. Earthscan, 2009, p. 2053.
- (84) Smernik, R. J.  $^{13}\text{C}$  Analysis of biochars by  $^{13}\text{C}$  nuclear magnetic resonance spectroscopy. In: *Biochar: A Guide to Analytical Methods*. Csiro Publishing, 2017.

- (85) McBeath, A. V.; Smernik, R. J.; Krull, E. S.; Lehmann, J. The influence of feedstock and production temperature on biochar carbon chemistry: a solid-state <sup>13</sup>C NMR study. *Biomass Bioenergy* **2014**, *60*, 121–129.
- (86) Joseph, S. D.; Camps-Arbestain, M.; Lin, Y.; Munroe, P.; et al. An investigation into the reactions of biochar in soil. *Soil Res.* **2010**, *48*, 501–515.
- (87) De la Rosa, J. M.; Knicker, H.; López-Capel, E., Manning, D. A.; et al. Direct detection of black carbon in soils by Py-GC/MS, carbon-13 NMR spectroscopy and thermogravimetric techniques. *Soil Sci Soc Am. J.* **2008**, *72*, 258–267.
- (88) Manyà, J. J.; Laguarda, S.; Ortigosa M. A.; Manso, J. A. Biochar from slow pyrolysis of two-phase olive mill waste: effect of pressure and peak temperature on its potential stability. *Energy Fuels* **2014**, *28*, 3271–3280.
- (89) Brewer, C. E.; Unger, R.; Schmidt-Rohr, K.; Brown, R. C. Criteria to select biochars for field studies based on biochar chemical properties. *Bioenergy Res.* **2011**, *4*, 312–323.
- (90) Conti, R.; Rombolà, A. G.; Modelli, A.; Torri, C.; Fabbri, D. Evaluation of the thermal and environmental stability of switchgrass biochars by Py–GC–MS. *J. Anal. Appl. Pyrolysis* **2014**, *110*, 239–247.
- (91) Conti, R.; Fabbri, D.; Vassura, I.; Ferroni L. Comparison of chemical and physical indices of thermal stability of biochars from different biomass by analytical pyrolysis and thermogravimetry. *J. Anal. Appl. Pyrolysis* **2016**, *122*, 160–168.
- (92) Fabbri, D.; Rombolà, A. G.; Torri, C.; Spokas, K. A. Determination of polycyclic aromatic hydrocarbons in biochar and biochar amended soil. *J. Anal. Appl. Pyrolysis* **2013**, *103*, 60–67.
- (93) Suárez-Abelenda, M.; Kaal, J.; McBeath, A. V. Translating analytical pyrolysis fingerprints to Thermal Stability Indices (TSI) to improve biochar characterization by pyrolysis-GC-MS. *Biomass Bioenergy* **2017**, *98*, 306–320.
- (94) Rombolà, A. G.; Meredith, W.; Snape, C. E.; Baronti, S.; et al. Fate of soil organic carbon and polycyclic aromatic hydrocarbons in a vineyard soil treated with biochar. *Environ. Sci. Technol.* **2015**, *49*, 11037–11044.
- (95) Glaser, B.; Haumaier, L.; Guggenberger, G.; Zech, W. Black carbon in soils: the use of benzenecarboxylic acids as specific markers. *Org. Geochem.* **1998**, *29*, 811–819.
- (96) Camps-Arbestain, M.; Shen, Q.; Wang, T.; van Zwieten, L.; Novak, J. 10 Available nutrients in biochar. In: *Biochar: A Guide to Analytical Methods*. Csiro Publishing, 2017, p. 109.
- (97) Leng, L.; Huang, H.; Li, H.; Li, J.; Zhou, W. Biochar stability assessment methods: a review. *Sci. Total Environ.* **2019**, *647*, 210–222.

## Synergies in sequential biochar systems

Christian Wurzer, Saran Sohi, Ondrej Mašek

UK Biochar Research Institute, School of Geoscience, University of Edinburgh, Edinburgh EH9 3FF, UK

### Abstract

Biochar still lacks widespread and large-scale applications. Past concepts have failed to define systems that are economically attractive, new ways to deliver biochar's environmental benefits are needed. This chapter starts by evaluating the original idea of biochar as a simple soil amendment and the implications of depending on a price for carbon stabilisation. Developments of biochar systems are discussed with a special emphasis on the potential competition for pyrolysed biomass between biochar and activated carbon. The concept of a sequential use system is introduced. Based on the diffusion-of-innovation theory, the advantage of a centralised biochar system is highlighted and compared to alternative systems. A brief description of potential synergies in sequential biochar systems outlines opportunities for further research. Examples of applications relevant to these systems are briefly discussed.

### 1. Introduction

The continuing rise of atmospheric CO<sub>2</sub> concentrations poses the greatest environmental challenge in the 21<sup>st</sup> century. While considerable efforts are underway to cut CO<sub>2</sub> emissions, it is now acknowledged that even an immediate halt in emissions would not avoid continuing temperature rise within this century<sup>1</sup>. Relying on emission reductions alone will not be sufficient. Carbon negative technologies are geoengineering options that have potential to actively removing CO<sub>2</sub> from the atmosphere at globally relevant scale. These may become essential to limit global warming and stabilise atmospheric greenhouse gas emissions during societal decarbonisation<sup>2</sup>. The most prominent technologies range from bioenergy with carbon capture and storage to direct air capture as well as biochar. Each technology has its own limitations regarding their scalability and energy requirements. Biochar is one of the few technologies that offer additional benefits beside the reduction of atmospheric carbon.<sup>2</sup>

Despite these beneficial effects for a number of environmental management applications<sup>3</sup>, commercial production is still a niche activity in most parts of the world. Although biochar research has increased to over 1300 publications per year within a decade<sup>4</sup>, economic studies of biochar have focused on established use concepts rather than re-specifying more efficient meta-concepts for the technology itself<sup>5,6</sup>. Due to this limitation, only a few concepts for biochar systems exist today. To become "Green Carbon", economic as well as social and environmental sustainability must be incorporated.

In the first part of this chapter we review the established concepts for biochar use and the major obstacles that these present. The second part of the chapter defines a new concept that we describe as a sequential biochar system. This is explored by populating the concept with specific examples of how this alternative concept might be applied.

### 2. Biochar systems

#### 2.1. Pyrolysis-biochar-soil system

According to the original definition of biochar, the main intended use is in building soil fertility, inspired by the *terra preta* example.<sup>7</sup>

The first concept for a biochar system was based on a simple biomass-pyrolysis-soil scheme<sup>8</sup>. Waste or marginal biomass pyrolysed to produce biochar and applied to agricultural land could be used to improve crop yields. The condensable and gaseous by-products of the pyrolysis process, bio-oil and pyrolysis gas, would be burned to provide heat and/or electricity<sup>9</sup>. The concept was built on the premise of a win-win-win situation whereby waste streams could be utilised to improve soils and simultaneously sequester carbon into land.<sup>10</sup>

From an economic point of view, the concept rests on two main sources of return. These concern increased revenue from higher crop yield and a new revenue stream for carbon sequestration<sup>12</sup> (see Fig. 1).

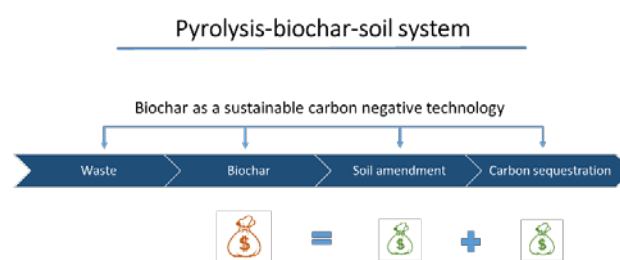


Figure 1. Original concept of a biochar system.

Early studies showed promising results with regards to crop yields as well as the long-term stability of the carbon within the soil<sup>13</sup>. However, the largest yield responses were observed in marginal soils with less impact on productive land. Field and pot experiments have also been based on experimental doses of 1–140 tonnes per hectare<sup>14</sup>. Due to the considerable cost of biochar production and high dosage<sup>15</sup>, the additional revenue of a higher crop yield of 13 % (grand mean)<sup>16</sup> is not sufficient to make biochar application attractive, especially on marginal land with an extensive agricultural system<sup>17</sup>. Although biochar is expected to show long-term benefits, a pay-back time of

decades makes market driven application of biochar currently unrealistic in agricultural systems.<sup>18</sup>

Shackley et al.<sup>8</sup> highlighted the impact of feedstock costs on the overall biochar price. While virgin biomass is becoming increasingly expensive due to increasing demand from bioenergy, non-virgin biomass potentially offers additional revenue to biochar systems through avoided costs for waste disposal (such as gate fees). However, non-virgin waste or marginal biomass are among the most challenging feedstocks for subsequent use due to their general heterogeneity, moisture content as well as potential contaminants and regulatory hurdles.<sup>19</sup>

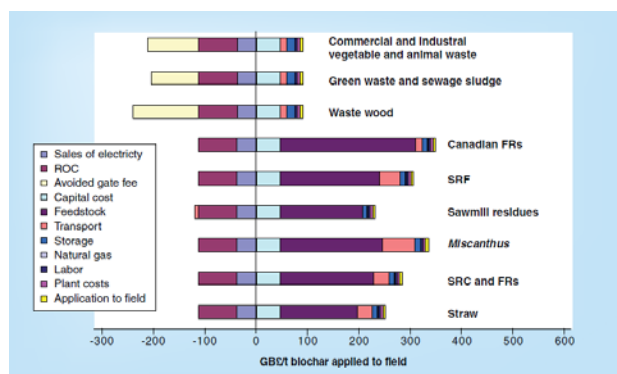


Figure 2. Breakdown of cost for biochar production at large scale.<sup>20</sup>

The current price of synthetic chemical fertiliser is between 270–380 € t<sup>-1</sup>.<sup>21</sup> A comparison with the feedstock price for biochar production (see Fig. 2) indicates that biochar has to be equally efficient as chemical fertilisers on a mass basis, which is highly unrealistic<sup>22,23</sup>. It is therefore clear that an accepted carbon accounting methodology for biochar systems and a higher carbon price is a necessary part of the concept to make biochar competitive in normal agricultural practice.<sup>12,24</sup>

In the largest (regional) scheme for emissions trading, the European Trading Scheme, the current price for carbon emissions sits at 20 € t<sup>-1</sup> CO<sub>2</sub>.<sup>25</sup> National schemes like the carbon price support in the United Kingdom exist, but the combined price in the United Kingdom does not exceed 38 € t<sup>-1</sup>CO<sub>2</sub>.<sup>26</sup> Even when assuming that pyrolysis would be acknowledged within such trading schemes, it would not be sufficient to drive carbon markets as large scale effects are expected to start around 200 € per ton CO<sub>2</sub>.<sup>21</sup> Due to these economic problems, only a handful of companies are commercially successful to date such as Sonnenerde in Austria or Soil Reef in the USA.

Research increasingly focusses on areas where biochar can have economic benefits besides a simple crop yield increase. These might be through improvements to the dynamics in soil water to mitigate drought stress and control erosion, or to interface or slowly release fertiliser to avoid groundwater contamination and increase fertiliser use efficiency<sup>27,28</sup>. Another way to address the high cost of biochar is to decrease the dose. Biochar usually has a low to negligible native nutrient content, but adding biochar to traditional fertilisers can increase the overall nutrient efficiency. This can be done either by doping biochar with

fertiliser or by doping fertilising compost with biochar<sup>17</sup>. Another way to minimise area dosage is targeting biochar towards plant roots in row crops, rather than simple broadcasting or blanket application.<sup>29</sup>

A profitable model for biomass pyrolysis that depends on direct soil amendment has yet to be demonstrated. Successful examples may emerge in limited circumstances such as converting marginal feedstock or where soil physical improvements are exceptional. General application will likely depend on a change in governmental policy with an increased focus on carbon abatement rather than simply emissions reduction.<sup>20</sup>

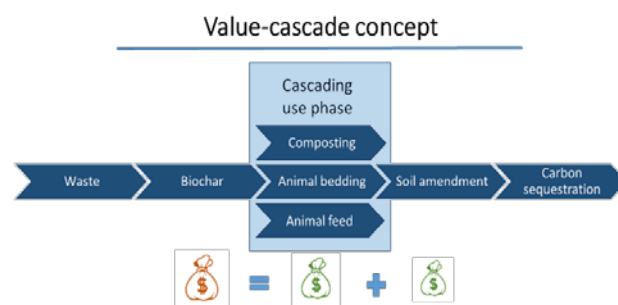


Figure 3: Value-cascade concept.

## 2.2. Value-cascade system

A concept put forward to add value using the multifunctional nature of biochar can be found in the value cascade system proposed by Schmidt<sup>30</sup>. It is based on the idea that the full value of a given biochar can only be extracted incrementally (i.e., through repeated contrasting use). The residual value diminishes through the value-cascade, as shown in Fig. 3.

The value in the cascade constitutes an economic unit obtained from the sum of uses, either in series or in parallel<sup>31</sup>. The original example placed biochar in a farm setting, involving use of biochar in applications such as silage management, as an additive to animal feed and bedding, for liquid manure management, or as an aid to composting<sup>32</sup>. The concept was captured in the phrase “use it nine times – pay for it only once”.<sup>32</sup>

The concept of integrating several properties of biochar for several applications within an economic unit assumes that one biochar can be defined to deliver a range of applications without interim diminution of relevant functionality<sup>33</sup>. Biochar is certainly a multifunctional material but it is unlikely that one biochar will be adequately effective in all these different applications. A simultaneous optimisation for multiple uses will be difficult to achieve, if not impossible. It is simpler to define a type of biochar that works well as a feed additive, but which might, for example, be less effective in aiding the composting process. The concept clearly has potential to increase the economic efficiency of the whole biochar life-cycle, but relying on initial functionality to deliver all cascaded uses likely fall short in maximising its sum potential.

The idea of cascading use can be seen as part of a “paradigm shift”<sup>17</sup> towards applications beyond those traditionally seen as within the domain of biochar<sup>31</sup>. Experimental studies have gradually aligned with this new paradigm. In one example, a filter to fertiliser scheme has been explored, where phosphorus-rich wastewater sludge is used to make biochar and then used to recover phosphorus from wastewater aqueous phase, with subsequent transfer of the phosphorus enriched biochar to land.<sup>34</sup>

### 2.3. Engineered biochar

Initial research concentrated on qualitative assessments of biochar properties for a wide variety of feedstock, with incremental understanding of biomass pyrolysis. This has translated into quantitative relationships between feedstock properties, pyrolysis parameters and biochar function<sup>35</sup>. The capacity to produce biochars with prescribed function by manipulation of production parameters and feedstock selection leads to the principle of engineered biochar<sup>35–37</sup>. While not a standalone concept for a biochar system, the potential to engineer biochar clearly changes the perception of biochar as a material. Biochar is seen less as a multi-functional material and increasingly as a platform structure with predictable and tuneable properties. With the possibility of manipulating or adding native function by methods such as surface doping, surface modification or pore structure tailoring, the range of potential biochar applications is considerably increased (see Fig.4).<sup>38</sup>

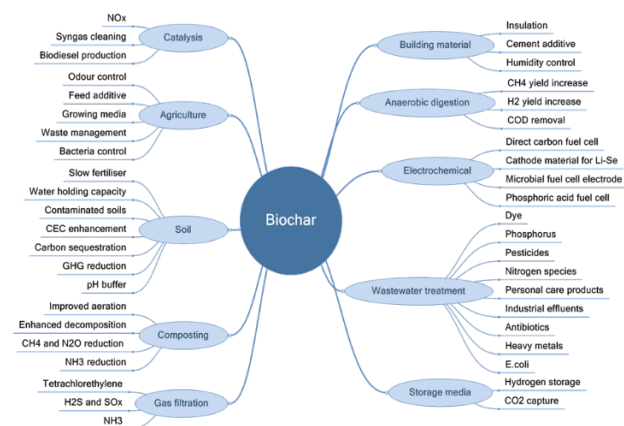


Figure 4. Overview of biochar applications.

Conception of biochar as a platform material is accompanied by a shift of focus towards the efficiency of engineered biochars for specific singular applications rather than life-cycle efficiency<sup>39</sup>. Reflecting this development are the use of environmentally problematic materials such as toxic chemicals<sup>40</sup>, nanomaterials<sup>39</sup> or the addition of rare elements<sup>38</sup>. Studies that assess the potential environmental concerns of engineered biochar in the manner put forward for traditional biochar are few<sup>19,41</sup>. In particular, the use of different nanomaterials will be difficult to assess and could impose long-term risks in relation to handling, soil application, or even incineration<sup>39,42</sup>. If these novel engineered biochars

unsuitable for soil applications should be called biochar is yet to be decided<sup>43,44</sup>. Definitions of biochar may or may not preclude engineered biochars unsuitable for soil applications; however, with regard to a sustainable biochar concept, the potential for long term carbon sequestration is likely to be lost without a final application into soil<sup>43</sup>. Much of the development to engineer biochar is focussed on the production of advanced materials based on a renewable carbon structure rather than the idea of biochar as a tool for carbon sequestration in soils<sup>38,40,45</sup> (see Fig. 5).

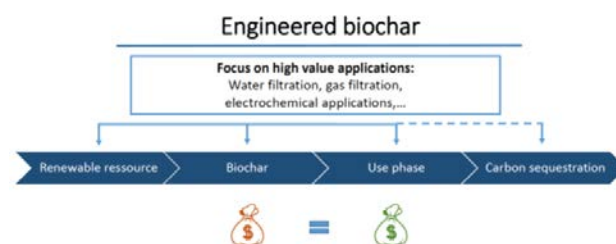


Figure 5. Concept of an engineered biochar system.

The concept of targeting biochar properties to specific higher-value applications in comparison to soil amendment is one step forward to obtain economically sustainable biochar systems. However, in most applications biochar will have to compete with other materials already in place. In wastewater or gas filtration, activated carbon has a long tradition of being a highly effective adsorbent and will be the benchmark to compete with.<sup>46–48</sup>

## 3. Biochar versus activated carbon

Activated carbon (AC) is a common adsorbent and catalyst in a wide variety of industrial processes<sup>49</sup>. Biochar and activated carbon are both classes of carbon materials with a wide variety of different properties. The materials are commonly distinguished despite no commonly accepted differentiation in functional terms<sup>44</sup>. Their main characteristics are essentially similar, namely a high carbon content, a recalcitrant carbon skeleton, a highly porous structure and surface activity. Biochar is by definition made from renewable biomass. Activated carbon in comparison can also be produced from fossil resources such as petroleum coke, coal or derived wastes such as used road tires<sup>50</sup>. The production of activated carbon also utilises similar pyrolysis techniques to biochar, albeit with some modifications. The main difference lies in an explicit activation step. Activated carbons are commonly differentiated according to (1) chemical activation or (2) physical activation (see chapter 8 for more details). Chemical activation utilises an activation agent such as ZnCl, H<sub>3</sub>PO<sub>4</sub> or KOH to partially degrade the feedstock prior to pyrolysis at medium to high temperatures. Subsequent washing of activated carbons results in considerably increased micro-porosity. Major drawbacks of this method are the need for a chemical activation agent as well as a post-pyrolysis washing step, resulting in considerable environmental impacts. A large consumption of acidic activation agents, a problematic wastewater production

and an additional post-production drying step are obstacles to a widespread use of this activation method.<sup>51,52</sup>

Physical activation is more common<sup>52</sup>. The feedstock is partially oxidised using an oxidising gas such as CO<sub>2</sub>, water steam or air, by applying higher temperatures than in chemical activation. A major disadvantage of physical activation is the higher loss of carbon associated with the high temperatures and the oxidising effect of the activation agents. This results in a yield of activated carbon from raw feedstock as low as 10%–15% of the original biomass mass.<sup>50</sup>

The high reactivity of oxygen typically limits use of air to post-activation at low to medium temperatures. Although high temperature activation is possible at low partial oxygen pressures.<sup>53</sup>

Biochar is generally produced using lower pyrolysis temperatures than activated carbon. Several studies of biochar draw on techniques from the vast accumulated literature on activated carbon to adapt production methods. The biochar literature therefore encompasses research in which biochars have been activated by similar methods to activated carbon, leading to materials often termed activated biochars<sup>54</sup>. In these examples, differentiation based on production is no longer useful. A distinction based solely on the feedstock is also not sufficient, since both materials can be produced from renewable resources. As biochar research expands to consider new applications such as wastewater filtration with almost no mention of post-sorption utilisation, the differentiation of biochar from activated carbon based on the targeted application also becomes increasingly indistinct and overlapping<sup>55</sup>. Hagemann et al.<sup>44</sup> proposed a characterisation based on feedstock and potential for use in carbon sequestration as more promising (see Fig.6).

Despite it being often produced from fossil material, its high energy demand and overall low carbon conversion efficiency and abatement potential, the exceptionally efficient performance of activated carbon in many industrial applications and the maturity of the production technology make it highly attractive for the removal of a variety of contaminants<sup>54</sup>. Filtration using activated carbon as an adsorbent is of increasing interest due to demands of more stringent environmental protection and expanding environmental pressure on surface and groundwaters worldwide.

Biochar as a low-cost and high-volume material for adsorption applications will most likely not be as effective as high-cost low-volume activated carbons. This means that other properties must be targeted in order for it to become directly competitive<sup>56</sup>. In general, adsorbent materials can be divided into those of high-removal capacity per mass and considerably higher production costs such as activated carbon, carbon nanotubes or resins and low-cost low capacity materials such as clay, sand or biochar. Beside the traditional characteristic of removal capacity, a comparison of low-cost and high-cost materials have to be based on a more comprehensive foundation<sup>5</sup>. The price of adsorbent per removed contaminant can be used for the comparison of different materials<sup>57</sup>. The economic assessment of adsorbent costs can extend to potential regeneration pathways and regeneration losses to provide a more realistic comparison of adsorbent costs. An important difference between low-cost and high-cost adsorbents is often neglected based on a knowledge gap in current biochar research. Literature seldom reports the properties of post-use biochar. Potential secondary applications are therefore usually neglected. The absence of a second phase use option for biochars can be seen in several comparative life-cycle assessments of biochar and AC, where different disposal or recycling routes have been omitted<sup>6,58</sup>. Only a few studies have emphasised the need to further examine the potential post-use value of sorbent materials so far.<sup>39,56</sup>

The potential to recycle biochar for further use could be a key advantage. Recycling spent biochars seems a logical route for a material originally conceived as a soil amendment<sup>39</sup>. Cleaning and recycling might not be possible for all kinds of adsorbed contaminants, but low-cost adsorbents could have an additional competitive advantage where suitable post-sorption options can be identified.<sup>56</sup>

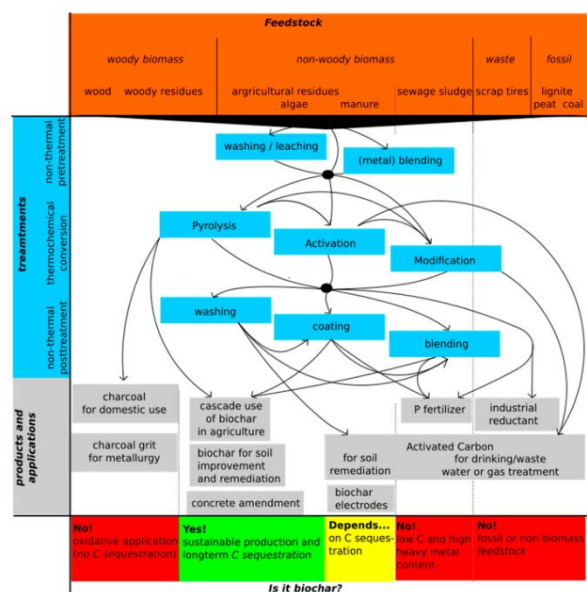


Figure 6. Overview on feedstock (orange), treatments for production (blue) and applications (grey) of pyrogenic carbonaceous materials.<sup>44</sup>

#### 4. The idea of sequential biochar systems

As outlined above, past concepts for biochar systems are not economically efficient and compromise the full environmental potential of biochar use. The original conception of biochar as one of few carbon negative technologies has become lost<sup>2</sup>. Alternative biochar systems synthesising the benefits of engineering biochar and utilising biochar as a carbon negative technology are needed. The proposed concept of a sequential biochar system balances the cost of biochar production with a

sequence of uses values, realising the potential to sequester carbon as a side-benefit. Focus can be placed on establishing recycling and reuse opportunities for biochar that increase its life-time and maximise environmental gain.

A sequential biochar system can be defined as a stepwise sequence of different applications. A recycling intervention between each step allows the properties of the material to be manipulated and optimised for the subsequent application. This essentially reverses the idea of engineering biochar for certain applications, each application phase requires tailoring of a certain specific characteristic. In contrast to the value-cascade, the limitation for biochar to be used multiple times within the same economic unit is abolished to deliver the most effective use of biochar's changed properties in recycled biochars.

The main advantage of this stepwise combination of post-use biochars with subsequent applications can be based on simple economic considerations. When post-use biochar can be valued as an input material into a subsequent application, initial feedstock, transport, and production costs can be distributed over different use phases and therefore reduced for each single application (see Fig. 7).

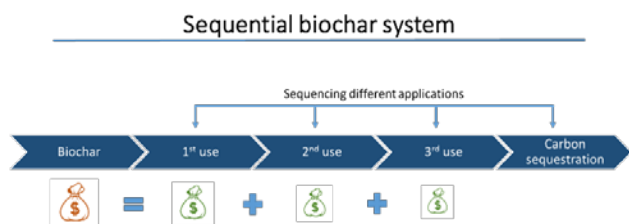


**Figure 7.** Concept of a sequential biochar system.

The benefit to the first customer in the sequential biochar system will be solely on the buyer's site. The ownership rights are transferred, and the first user can sell the biochar to the next user. This means that the price to the first user would still be the same as in a single use transaction, the seller covering the full cost of production to the first buyer. Feedstock, production and transport costs will be fully accounted for this first transaction. The only difference would lie in the potential for the first user to sell the biochar after its use.

To facilitate the potential benefits of cost-distribution over several use phases the ownership of the biochar within a sequential system would be kept constant. This means that a biochar producer in a sequential biochar system acts as a service provider, presenting biochar as a carrier of environmental services rather than a product (see Fig. 8). This means the producer may sell a function such as wastewater filtration to a user, but would remain the owner of the char and the responsibility for its recovery. After a first use, the biochar is recycled and provided to the next user in sale of an alternate service. Such systems are already established in other sectors such as car sharing, where a service rather than a car is sold, alongside a wide variety of industries leasing capital-intensive equipment.

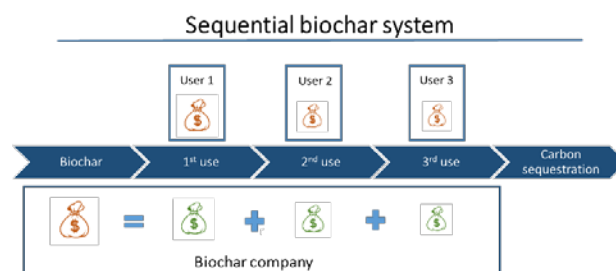


**Figure 8.** Ownership rights in a sequential biochar system.

The benefit to the biochar producer in this system is the lowering of price for the first user in expectation of additional revenue through reselling to subsequent users. Flexibility to changing market demands is another attractive advantage, as the price for biochar can be individually adjusted between each step in the sequence. This will ensure that not only the initial production costs will be shared by several users, but also the costs of recycling steps can be shared. The biochar producer has full information over the cost distribution of the whole sequence and this knowledge can be utilised to adjust prices individually and distribute costs to applications that are more competitive on the market.

The main driver for the biochar producer will be an optimised revenue from the whole sequence. Lowering the price for one application below its maximum profit can therefore still be economically attractive. As it is the case if a lower profit in one application ensures that mass flows of biochar can be adjusted between different applications and the additional subsequent revenues offset the lower profit of the previous step. The flexibility in individually adjusted prices for each step of the sequence can not only increase the resilience for demand changes, but additionally adjust mass flows within the system.

Users of sequential biochar system will benefit from purchasing a service rather than a product. This will lower transaction costs associated with waste disposal as well as the overall benefit of a reduced price in comparison to traditional systems.

From an environmental perspective, the use of biochar for multiple applications potentially lowers energy and material input through a focus on recycling of the material. The lower price will make biochar more competitive as a soil amendment, potentially abolishing the need for a carbon price. However, opportunity costs from incineration for energy generation would still be the competing price to match.<sup>59</sup>

#### 4.1. Biochar integration into existing markets

Activated carbon suppliers can provide an example for future sequential biochar operators, as some already operate partly as service companies selling not only the activated carbon but organising the transport, application equipment and regeneration of the material<sup>60</sup>. The activated carbon industry could play a key role for the organisation and the initial implementation of sequential biochar systems. The production technology of this industry can act as an analogue for biochar production<sup>59</sup>.

Synergies can be found in the similarities and overlapping applications of biochar and activated carbon as already outlined. AC companies may act as an entry point for the biochar concept into a variety of adsorption related markets. The existing production facilities, market knowledge and producer-user networks would lower initial costs for commercial trials of biochar in applications where activated carbon is less competitive due to its higher price. The market for activated carbon is growing at an expected annual growth rate of 13% until 2020<sup>61</sup>. However, it is subject to the availability of traditional biomass feedstock, such as coconut shells, which are already becoming scarce or it is subject to growing environmental concerns in the case of fossil coal or petroleum coke<sup>52,61</sup>. As a complementary material, biochar can act as a strategic investment to secure future applications, such as micropollutant removal from wastewaters as well as a general greening of the activated carbon industry.<sup>62</sup> The advantage of the incorporation of biochar into existing established markets can be explained by examining the problems of existing concepts, which often assume decentralised and small production as more efficient.<sup>63,64</sup>

#### 4.2. Diffusion of innovations theory

The success or failure of new technologies such as biochar depend on a process of uncertainty reduction among potential users, which if successful, lead to the adoption. The speed or rate of adoption can be estimated by five attributes<sup>65</sup>:

- **Relative Advantage** —the degree to which the innovation is better than the status quo. The higher relative advantage, the higher the rate of adaption. This attribute is not only understood in economic terms, such as profitability or initial costs, but also as social advantage. Green technologies such as biochar can have significant social benefits in the form of social status. Sustainability became a selling point for a variety of products and industries, not only in relation to customers and stakeholders but also to governments<sup>62</sup>. Governments tend to improve environmental protection over time, and industries move forward self-organising their own regulation in the face of new laws.<sup>66</sup> Another aspect of relative advantage is time-related. Short-term benefits are more influential than long-term. Considering biochar, the relative economic advantage due to high transaction costs and moderate yield increases is often minimal in the short term<sup>67</sup>. While soil application of biochar will eventually lead to a long-term increase in soil fertility, end-users will be focussed on short-term benefits such as crop yield or lower fertiliser requirements as compared with the additional cost of biochar.<sup>63</sup>
- **Compatibility** can be understood as the consistency of the innovation with current values and beliefs. If an innovation is diverting from an existing system, it is less likely to be adapted. In relation to biochar for soil application, the change of chemical fertilisation to a slow and complex fertiliser such as biochar can

be considered a gradual break with an existing system. In contrast, biochar in wastewater filtration to substitute AC is more compatible due to the similarities between the two materials. Compatibility also relates to the organisational structure of the innovation user<sup>65</sup>. If biochar production is based on small-scale on-farm production, for example, the technology will less likely be acknowledged by companies producing chemical fertilisers as it does not fit to the centralised nature of their business.

- **Complexity** of the innovation. Complex innovations are less likely to be adopted. Biochar may provide an example of how complexity can inhibit adaption. While the concept of amending soil with biochar is simple, biochar as a heterogenous class of materials can be more difficult to understand. Matching of biochar with a specific soil type and crop species requires sufficient expert knowledge to avoid negative results.<sup>68</sup>
- **Trialability** defines the degree to which adopters can test the innovation. If an innovation is trialable, it is more likely to be adapted. Biochar is a relatively easy material to trial if the material is available in small quantities from qualitative producers.
- **Observability** of the idea to other potential users. The more visible an innovation is to current non-users, the higher the rate of their adoption. Although the influence of biochar application can be visible within a crop season, additional benefits such as a higher drought resilience of the soil or increased soil carbon stocks are unlikely to be seen in a short trial.

#### 4.3. Rate of biochar adoption

According to these innovation attributes, the adoption rate of biochar in developed countries can be assessed. Biochar for soil amendment lacks relative economic advantage in the short term in competition with chemical fertilisers based on the generally lower crop responses to biochar<sup>23</sup>. Due to the absence of widespread large-scale production, current users must invest considerable time and know-how in the production of specific biochar, adding further costs to the technology<sup>69</sup>. Self-production of biochar might correlate with a production-oriented role of farmers, but it is often only partially compatible with current agricultural practices due to a further addition of workload to the farmers<sup>70</sup>. High complexity in matching soil properties, crop species and biochars requires expert knowledge and can impose entry barriers for agricultural adopters. Therefore, adoption of biochar is still concentrated on entrepreneurs with a higher risk affinity rather than the average agricultural farm and overall adoption rate remains small.<sup>63,64,70</sup>

For other applications of biochar, especially in the context of a sequential biochar system, there is still a relative advantage in terms of social status, but also an additional short-term economic advantage, as wastewater filtration costs are almost directly measurable. Furthermore, biochar will be highly compatible to current systems operating with activated carbon as these materials are

almost similar and already used in industry. In contrast to agricultural farms, the end users of wastewater treatment plants or industrial plants are used to complexity. It seems promising for sequential biochar systems to use the similarity with activated carbon as an entry point to existing markets and users of this industry.

Therefore, the choice of applications is of importance to increase not only the speed of adaption of the biochar technology, but also to enable additional synergies of a sequential biochar system.

## 5. Synergies in sequential biochar systems

The concept of sequencing different applications implies that the output material from one application will be the input material of the subsequent application with minimum treatment in-between. Therefore, one of the determining processes of the efficiency of the system will be the necessary recycling of the spent biochar between two applications. As the recycling process, the transport and handling of spent biochar are additional costs for the sequence, it is crucial to find a combination of applications, which make recycling superior to disposal or incineration (see Fig. 9).

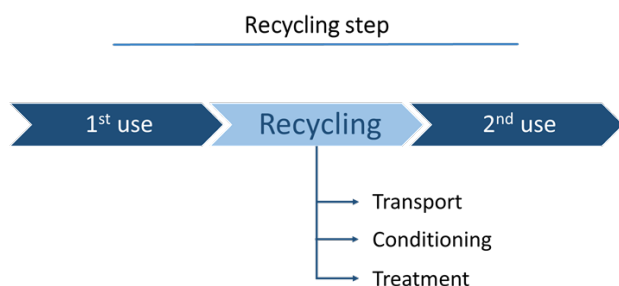


Figure 9. Recycling step between different applications.

Two types of a recycling step could be differentiated in sequential biochar systems:

- **“Contaminant to nutrient”** —where a contaminant adsorbed or loaded on biochar in one application constitutes a valuable nutrient in the subsequent application. Examples of this context-specified contaminant/nutrient scenario are various filter-to-fertiliser sequences. Prominent contaminants in this context include phosphorus, nitrogen and sulphur species, which may pose environmental concerns in aquatic environments. On the other side, in an agricultural setting these species are essential plant nutrients. For recycling based on a “contaminant to nutrient” type, almost no relevant treatment must be conducted. The recycling step could consist only of drying or other necessary conditioning treatments as well as delivery to the next user. Due to these low treatment requirements and the added nutritional value for subsequent applications, this type of recycling step represents the best-case scenario for a synergistic combination of applications.

- **“Contaminant to constituent”** —if a contaminant has to be decomposed due to environmental concerns, (e.g., pharmaceuticals) or has to be desorbed like in the case of heavy metals. In contrast to a “contaminant to nutrient” type of recycling, decomposing or desorbing a contaminant from the adsorbent will require more elaborate treatment technologies similar to regeneration methods currently applied in activated carbon regeneration.

### 5.1. Regeneration methods for activated carbon

Two general indicators for analysing the efficiency of these methods are : (1) desorption and extraction efficiency —the amount of contaminant recovered as a proportion of that initially adsorbed; and (2) regeneration efficiency —the adsorption capacity of the regenerated adsorbent relative to its original capacity<sup>71</sup>. Regeneration efficiency is the more commonly used indicator as the general aim is to prolong the lifetime of the adsorbent within the same application. In the case of decontaminating within a sequential system, a modified desorption efficiency will be of interest. This would describe the removal (either by desorption or decomposition) of the contaminant to the level required for a safe application of the decontaminated product in a subsequent use step.

		Type of Regeneration Mechanism				
		Extraction:	pH changes	Reaction/ Degradation	Thermal desorption	Vacuum
Type of Regeneration Agent	Hot gases			THERMAL REGENERATION		
	Physical waves			THERMAL REGENERATION		
	Electrical currents			THERMAL REGENERATION		
	Chemical Reagents	CHEMICAL REGENERATION				
	Supercritical Fluids	CHEMICAL REGENERATION				
	Microorganisms			MICROBIOLOGICAL REGENERATION		
					VACUUM REGENERATION	

Figure 10. General classification of regeneration methods of adsorbent carbonaceous materials.<sup>71</sup>

According to one scheme<sup>71</sup>, regeneration methods for AC can be classified according to four main approaches: thermal, chemical, microbiological and vacuum (see Fig.10). Only thermal and chemical regeneration reflect current industrial practice and are discussed in more detail. **Thermal regeneration** is the dominant technique to desorb or decontaminate the adsorbent. In general, thermal regeneration applies enough thermal energy to the adsorbent, either by inert gas, steam or an electrical current to desorb or decompose the contaminant. If a contaminant desorbs or decomposes depends on the adsorbate and its interaction with the adsorbent. Liu et al.<sup>72</sup> classified organic compounds into three classes: type 1: vaporisation; type 2: decomposition and type 3: char formation. Classification depends on their reaction to thermal energy input in regeneration as well as their binding energy with the adsorbent. As regeneration efficiency is the most important indicator in activated

carbon regeneration, the dominant techniques are gasification methods utilising a hot gas stream of H<sub>2</sub>O or CO<sub>2</sub> to desorb the contaminants and gasify charred residues. Typical temperatures are above 800 °C, the temperature range to enable mild oxidation of the adsorbent. A drawback of this techniques is the partial oxidation of the adsorbent leading to relevant mass loss of 5%–15% during regeneration as well as a gradual degradation of the adsorption capacity<sup>49</sup>. While still being the only large-scale regeneration method for activated carbon, regeneration of spent activated carbon is expensive<sup>73</sup>. Costs are seldom reported in literature, but a model calculation in Switzerland for the upgrade of a public wastewater treatment using a granular activated carbon filter reported €1300 t<sup>-1</sup> for fresh granular activated carbon and €900 t<sup>-1</sup> for regenerated carbon.<sup>74</sup>

**Chemical regeneration** has been developed in response to the high energy demands of traditional thermal regeneration methods<sup>75</sup>. The main aim is to lower the energy requirements as well as the mass loss of the adsorbent during regeneration. A conceptual problem of chemical regeneration is the production of a considerable solvent waste stream. When looking at the whole life cycle of water pollutant removal using chemical regeneration, the pollutant is transferred from a low concentration stream into a higher concentrated liquid solvent stream. In some cases, the solvent itself can be regarded a pollutant adding additional treatment costs<sup>49</sup>.

Promising methods include sub- and supercritical extraction using water or CO<sub>2</sub> as solvents. At elevated pressure and temperature, CO<sub>2</sub> and H<sub>2</sub>O change their solvent properties. Water near or above its critical point ( $P_c = 221$  bar,  $T_c = 374$  °C) has a drastically decreased dielectric constant and an increased dissociation constant<sup>75</sup>. At these elevated conditions, water solubility of organic compounds is elevated, making this extraction methods highly effective. Additionally to a high extraction efficiency, regeneration efficiency sometimes even exceeds 100% by opening up additional adsorption sites<sup>49</sup>. While most studies exposed the adsorbent to a constant stream of water, a few studies highlighted the possibility to use a hydrothermal batch process instead<sup>76,77</sup>. Using a closed system can substantially reduce the amount of polluted solvent in the regeneration process, making the regeneration environmentally favourable. Similar to current hydrothermal carbonisation techniques, the reactor is heated to mild temperatures between 180 and 240 °C and autogenic pressure<sup>76</sup>. In contrast to stream-based extraction methods, the process is targeted at decomposing the pollutant rather than extraction. However, this also means that the closed system does not allow to remove the dissolved contaminant from the system during the treatment. As the system eventually has to cool down, re-adsorption can occur if the pollutant is not decomposed. Another problematic implication of this technique can be the production and adsorption of stable intermediate decomposition products, which might be even less favourable than the original pollutant<sup>78</sup>. An adaption of this method can be found in the wet-oxidation

method, which adds an oxidising agent into the hydrothermal treatment<sup>79</sup>. Wet oxidation is already conducted in industrial applications to completely destroy organic matter in polluted wastewaters<sup>80</sup>. This process is rather aimed at decomposing organic carbon instead of adsorbent regeneration, making it a promising technique for the decontamination of biochar in a sequential system. However, the production of intermediate products is not precluded by wet-oxidation methods and problematic intermediates can be formed<sup>75,80</sup>, making additional research necessary.

The regeneration methods mentioned so far focus on organic contaminants. Only a few studies have focused on inorganic pollutants such as heavy metals<sup>81</sup>. Desorption of heavy metals from adsorbents such as activated carbon is conducted by using alkalis, acids or chelating agents<sup>82</sup>. Another alternative technique includes the use of ultrasound to desorb metals or decompose organic matter from activated carbon.<sup>49</sup>

**Regeneration versus recycling.** Although much research has been done in the field of carbon regeneration, the nature of activated carbon as an expensive material and the aim to reuse the material limits regeneration research to a focus on adsorption capacity. However, within the concept of sequential biochar systems, decontamination of the spent adsorbent is more important than conserving its adsorptive properties. While biochar research is still in its infancy and many important research questions are still unanswered, the integration of biochar's recycling potential and post-sorption utilisation into research designs can open opportunities for novel treatment methods. While current regeneration methods might be sufficient to decontaminate biochar, it can be hypothesised that pure decontamination techniques can increase the efficiency of the process and open a new research field focussed on low-cost adsorbents.

Additionally, several applications for biochar itself can act as decontamination methods with anaerobic digestion and composting being the most prominent ones. Both applications can destroy pathogens and decompose a variety of different contaminants through elevated temperatures, acidic conditions as well as a high microbiological activity<sup>83,84</sup>. However, the non-separability of post-use biochar from neither digestate nor compost will determine that these applications will only be relevant as the last application before the use as a soil amendment.

## 6. Suitable applications for sequential biochar systems

Not every potential application of biochar is suitable for regeneration or decontamination. The characteristic of separability of post-use biochar is an additional characteristic that must be fulfilled by an application to be suitable within a sequential biochar system. Separability can be defined as the ability to obtain biochar particles contaminated or non-contaminated with homogenous properties. This means that any application which mixes biochar with other solids or non-water liquids is most likely

not promising as a first sequence. This includes applications such as the use in anaerobic digestion, as a litter additive in agriculture, as a building material or any soil or composting application.

While a variety of different applications fulfil the criteria of separability, ranging from the use of biochar as a catalyst in biodiesel production to its use as an electrode, not all these applications are at a stage of development where a realistic assessment of biochars post-application properties can be conducted. However, two examples of promising applications for a sequential biochar system are described briefly. While both resembling existing applications currently utilising activated carbon, they are also based on the before mentioned principles of “contaminant to nutrient” and “contaminant to constituent”.

### 6.1. Adsorption of hydrogen sulphide

Hydrogen sulphide is a common contaminant of biogas from different sources such as anaerobic biogas plant or landfills. It is an acidic and corrosive gas, toxic to humans. The removal of hydrogen sulphide prior to combustion is a necessary step to prevent engine damage. It is well known that H<sub>2</sub>S can be removed by carbon surfaces, with activated carbon currently used as a commercially available material suitable for H<sub>2</sub>S removal due to its high carbonaceous surface area and porosity.<sup>85</sup>

Biochar has gained increasing interest in substituting the use of activated carbon. While not fully understood yet, it is postulated that although having a lower surface area, the alkaline nature of biochar and a high mineral matter content are determining the adsorption performance of biochar<sup>85,86</sup>, beside a general influence of moisture content. Therefore, mineral-rich biochar seems to be a promising and sustainable biochar additive for enhanced H<sub>2</sub>S removal<sup>87</sup>. H<sub>2</sub>S adsorbs on biochar in the form of elemental sulphur within pores or SO<sup>4-</sup> on the surface of biochar. While regeneration seems to be possible, spent S-enriched biochar could potentially be further used as sulphur is an essential plant nutrient and sulphur contents of soils are gradually declining due to decreasing S-depositions from atmosphere through emissions as well as insufficient fertilisation.<sup>88</sup>

### 6.2. Pollutants of emerging concern in wastewater

Emerging micropollutants such as pharmaceuticals and personal care products are of increasing concern in wastewaters and their treatment<sup>89</sup>. The release of pharmaceuticals such as human and veterinary antibiotics or hormone active substances can not only lead to unpredictable changes in ecosystems, but also to an increase in antibiotic resistance genes, a potential threat to human health<sup>90</sup>. Current wastewater treatment plants are generally not equipped to remove these pollutants<sup>91</sup>. Additional treatment techniques must be added to remove or decompose these contaminants. Although the problem of emerging pollutants is known, Switzerland is the only European country with existing legislation for the removal of micropollutants in wastewater treatment plants

indicating the high costs of current removal techniques<sup>92-94</sup>.

While a variety of different techniques are currently being researched, adsorption is seen as one of the most promising techniques due to its technical simplicity and high removal efficiency<sup>94</sup>. Additionally, no metabolites are formed during this wastewater treatment. The use of biochar for the adsorption of antibiotics and pollutants of emerging concern are increasingly studied and showed promising results. In this context, biochar is often highlighted as a low-cost adsorbent. Although no studies exist on decontamination of the spent adsorbent to be used in subsequent applications, regeneration studies on activated carbon show promising removal rates for these organic contaminants. The use and subsequent recycling of biochar could potentially enable a wider application of tertiary wastewater treatment to areas currently not targeting micropollutants due to its low-cost nature. However, research still has to prove that full decontamination of micropollutants on biochar is possible.

## 7. Conclusion

Based on the analysis of past biochar concepts, we introduced the idea of a sequential biochar system to synthesise the recent advancements of biochar research with its carbon sequestration potential. We showed that the perception of biochar solely as a material is a rather narrow perspective on its multiple characteristics. In contrast, the view of biochar as a carrier for environmental services enables a more flexible conceptualisation of biochar systems.

The economic focus of our concept is based on distributing initial production costs over several users, and associated risks over several applications. We showed that continuous ownership rights for biochar within a sequence are a necessity for this cost and risk distribution. While the activated carbon industry can act as an analogue and promising entry point to large-scale application of biochar, a sequential biochar system will ultimately have to develop a distinct organisational form based on the different cost structure of biochar being a low-cost material. At present, research is often focused on simultaneously boosting the efficiency as well as the costs of biochar into the range of activated carbons. However, we think that the nature of biochar as a high volume and low-cost material is a prerequisite to retain a globally relevant carbon sequestration potential.

We highlighted the need to find synergies between value-adding and cost-adding steps as essential to enable efficient sequential biochar systems. At present, potential sequences can only be hypothesised due to the lack of practical knowledge with most biochar applications. However, our analysis suggests that recycling of used biochars will be a key advantage for economic competitiveness. As literature generally neglected the utilisation of a second use phase so far, recycling treatments for biochar seem a promising area for further research.

## Acknowledgements

“This project has received funding from the European Union’s Horizon 2020 research and innovation programme under the Marie Skłodowska-Curie grant agreement No 721991”.

## References

- (1) Frölicher, T. L.; Winton, M.; Sarmiento, J. L. Continued Global Warming after CO<sub>2</sub> Emissions Stoppage. *Nat. Clim. Chang.* **2014**, *4* (1), 40–44.
- (2) Smith, P. Soil Carbon Sequestration and Biochar as Negative Emission Technologies. *Glob. Chang. Biol.* **2016**, *22* (3), 1315–1324.
- (3) Verheijen, F. G. A.; Montanarella, L.; Bastos, A. C. Sustainability, Certification, and Regulation of Biochar. *Pesqui. Agropecu. Bras.* **2012**, *47* (5), 649–653.
- (4) Rosales, E.; Meijide, J.; Pazos, M.; Sanromán, M. A. Challenges and Recent Advances in Biochar as Low-Cost Biosorbent: From Batch Assays to Continuous-Flow Systems. *Bioresour. Technol.* **2017**, *246*, 176–192.
- (5) Alhashimi, H. A.; Aktas, C. B. Life Cycle Environmental and Economic Performance of Biochar Compared with Activated Carbon: A Meta-Analysis. *Resour. Conserv. Recycl.* **2017**, *118*, 13–26.
- (6) Thompson, K. A.; Shimabuku, K. K.; Kearns, J. P.; Knappe, D. R. U.; Summers, R. S.; Cook, S. M. Environmental Comparison of Biochar and Activated Carbon for Tertiary Wastewater Treatment. *Environ. Sci. Technol.* **2016**, *50* (20), 11253–11262.
- (7) Glaser, B.; Haumaier, L.; Guggenberger, G.; Zech, W. The “Terra Preta” Phenomenon: A Model for Sustainable Agriculture in the Humid Tropics. *Naturwissenschaften* **2001**, *88* (1), 37–41.
- (8) Shackley, S.; Hammond, J.; Gaunt, J.; Ibarrola, R. The Feasibility and Costs of Biochar Deployment in the UK. *Carbon Manage.* **2011**, *2* (3), 335–356.
- (9) Crombie, K.; Mašek, O. Pyrolysis Biochar Systems, Balance between Bioenergy and Carbon Sequestration. *GCB Bioenergy* **2015**, *7* (2), 349–361.
- (10) Laird, D. A. The Charcoal Vision: A Win–Win–Win Scenario for Simultaneously Producing Bioenergy, Permanently Sequestering Carbon, While Improving Soil and Water Quality. *Agronomy J.* **2008**, *100* (1), 178–181.
- (11) Verheijen, F.; Jeffery, S.; Bastos, A. C.; Van Der Velde, M.; Diapas, I. Biochar Application to Soils: A Critical Scientific Review of Effects on Soil Properties, Processes and Functions. *JRC Scientific and Technical Reports* **2010**, EUR 24099, 151.
- (12) Galinato, S. P.; Yoder, J. K.; Granatstein, D. The Economic Value of Biochar in Crop Production and Carbon Sequestration. *Energy Policy* **2011**, *39* (10), 6344–6350.
- (13) Lehmann, J.; Gaunt, J.; Rondon, M. Bio-Char Sequestration in Terrestrial Ecosystems - A Review. *Mitig. Adapt. Strateg. Glob. Chang.* **2006**, *11* (2), 403–427.
- (14) Jeffery, S.; Verheijen, F. G. A.; van der Velde, M.; Bastos, A. C. A Quantitative Review of the Effects of Biochar Application to Soils on Crop Productivity Using Meta-Analysis. *Agric. Ecosyst. Environ.* **2011**, *144* (1), 175–187.
- (15) Co, T.; Preta, T.; Preta, T.; The, C.; Preta, T.; Technique, C. *Ithaka J.* **2012**, *289*, 286–289.
- (16) Jeffery, S.; Abalos, D.; Prodana, M.; Bastos, A. C.; Van Groenigen, J. W.; Hungate, B. A.; Verheijen, F. Biochar Boosts Tropical but Not Temperate Crop Yields. *Environ. Res. Lett.* **2017**, *12* (5).
- (17) Joseph, S.; Graber, E. R.; Chia, C.; Munroe, P.; Donne, S.; Thomas, T.; Nielsen, S.; Marjo, C.; Rutledge, H.; Pan, G. X.; et al. Shifting Paradigms: Development of High-Efficiency Biochar Fertilizers Based on Nano-Structures and Soluble Components. *Carbon Manage.* **2013**, *4* (3), 323–343.
- (18) Vochozka, M.; Maroušková, A.; Váchal, J.; Straková, J. Biochar Pricing Hampers Biochar Farming. *Clean Technol. Environ. Policy* **2016**, *18* (4), 1225–1231.
- (19) Buss, W.; Graham, M. C.; Shepherd, J. G.; Mašek, O. Risks and Benefits of Marginal Biomass-Derived Biochars for Plant Growth. *Sci. Total Environ.* **2016**, *569–570*, 496–506.
- (20) Shackley, S.; Hammond, J.; Gaunt, J.; Ibarrola, R. The Feasibility and Costs of Biochar Deployment in the UK. *Carbon Manage.* **2011**, *2* (3), 335–356.
- (21) Shackley, S. The Economic Viability and Prospects for Biochar in Europe - Shifting Paradigms in Uncertain Times. In *Biochar in European Soils and Agriculture: Science and Practice*; Shackley, S., Ed.; Routledge: London; New York, 2016; p 301.
- (22) Crombie, K.; Mašek, O.; Cross, A.; Sohi, S. Biochar - Synergies and Trade-Offs between Soil Enhancing Properties and C Sequestration Potential. *GCB Bioenergy* **2015**, *7* (5), 1161–1175.
- (23) Chan, K. Y.; Van Zwieten, L.; Meszaros, I.; Downie, A.; Joseph, S. Agronomic Values of Greenwaste Biochar as a Soil Amendment. *Soil Res.* **2007**, *45* (8), 629–634.
- (24) Roberts, K. G.; Gloy, B. A.; Joseph, S.; Scott, N. R.; Lehmann, J. Life Cycle Assessment of Biochar Systems: Estimating the Energetic, Economic, and Climate Change Potential. *Environ. Sci. Technol.* **2010**, *44* (2), 827–833.
- (25) Finanzen.net. CO<sub>2</sub> European Emission Allowances <http://www.finanzen.net/rohstoffe/co2-emissionsrechte/historisch> (accessed Aug 25, 2018).
- (26) Hirst, D. Carbon Price Floor (CPF) and the Price Support Mechanism. *Brief. Pap. House Commons* **2018**, No. 05927.
- (27) Liang, C.; Zhu, X.; Fu, S.; Méndez, A.; Gascó, G.; Paz-Ferreiro, J. Biochar Alters the Resistance and Resilience to Drought in a Tropical Soil. *Environ. Res. Lett.* **2014**, *9* (6), 064013.

- (28) Ding, Y.; Liu, Y.; Liu, S.; Li, Z.; Tan, X.; Huang, X.; Zeng, G.; Zhou, L.; Zheng, B. Biochar to Improve Soil Fertility. A Review. *Agron. Sustain. Dev.* **2016**, *36* (2).
- (29) Schmidt, H.P.; Pandit, H.; Cornelisson, G.; Kammann, C. Organic Biochar Based Fertilization. *Geophysical Research Abstracts* **2017**, *19*, 5683.
- (30) Schmidt, H.P.; Wilson, K. The 55 Uses of Biochar. *biochar J.* **2014**, 1–8.
- (31) Shackley, S. Shifting Chars? Aligning Climate Change, Carbon Abatement, Agriculture, Land Use and Food Safety and Security Policies. *Carbon Manage.* **2014**, *5* (2), 119–121.
- (32) Schmidt, H.P. Novel uses of biochar. **2013**, Proc., USBI North American Biochar Symp., Center for Agriculture, Univ. of Massachusetts, Amherst, MA.
- (33) Simon Shackley, Abbie Clare, Stephen Joseph, Bruce A McCarl, H.-P. S. Economic Evaluation of Biochar Systems: Current Evidence and Challenges. In *Biochar for Environmental Management—Science and Technology (2nd Ed)* Earthscan, London; Lehmann, J., Joseph, S., Eds.; Routledge, **2015**; pp 813–852.
- (34) Shepherd, J. G.; Sohi, S. P.; Heal, K. V. Optimising the Recovery and Re-Use of Phosphorus from Wastewater Effluent for Sustainable Fertiliser Development. *Water Res.* **2016**, *94*, 155–165.
- (35) Morales, V. L.; Pérez-Reche, F. J.; Hapca, S. M.; Hanley, K. L.; Lehmann, J.; Zhang, W. Reverse Engineering of Biochar. *Bioresour. Technol.* **2015**, *183*, 163–174.
- (36) Rajapaksha, A. U.; Chen, S. S.; Tsang, D. C. W.; Zhang, M.; Vithanage, M.; Mandal, S.; Gao, B.; Bolan, N. S.; Ok, Y. S. Engineered/Designer Biochar for Contaminant Removal/Immobilization from Soil and Water: Potential and Implication of Biochar Modification. *Chemosphere* **2016**, *148*, 276–291.
- (37) Dieguez-Alonso, A.; Funke, A.; Anca-Couce, A.; Rombolà, A.; Ojeda, G.; Bachmann, J.; Behrendt, F. Towards Biochar and Hydrochar Engineering—Influence of Process Conditions on Surface Physical and Chemical Properties, Thermal Stability, Nutrient Availability, Toxicity and Wettability. *Energies* **2018**, *11* (3), 496.
- (38) Liu, W. J.; Jiang, H.; Yu, H. Q. Development of Biochar-Based Functional Materials: Toward a Sustainable Platform Carbon Material. *Chem. Rev.* **2015**, *115* (22), 12251–12285.
- (39) Harikishore Kumar Reddy, D.; Vijayaraghavan, K.; Kim, J. A.; Yun, Y. S. Valorisation of Post-Sorption Materials: Opportunities, Strategies, and Challenges. *Adv. Colloid Interface Sci.* **2017**, *242*, 35–58.
- (40) Xiong, X.; Yu, I. K. M.; Cao, L.; Tsang, D. C. W.; Zhang, S.; Ok, Y. S. A Review of Biochar-Based Catalysts for Chemical Synthesis, Biofuel Production, and Pollution Control. *Bioresour. Technol.* **2017**, *246*, 254–270.
- (41) Mumme, J.; Getz, J.; Prasad, M.; Lüder, U.; Kern, J.; Mašek, O.; Buss, W. Toxicity Screening of Biochar-Mineral Composites Using Germination Tests. *Chemosphere* **2018**, *207*, 91–100.
- (42) Wang, B.; Gao, B.; Fang, J. Recent Advances in Engineered Biochar Productions and Applications. *Crit. Rev. Environ. Sci. Technol.* **2017**, *47* (22), 2158–2207.
- (43) European Biochar Foundation (EBC). Guidelines for a Sustainable Production of Biochar. *Eur. Biochar Found.* **2016**, No. August, 1–22.
- (44) Hagemann, N.; Spokas, K.; Schmidt, H. P.; Kägi, R.; Böhler, M. A.; Bucheli, T. D. Activated Carbon, Biochar and Charcoal: Linkages and Synergies across Pyrogenic Carbon's ABCs. *Water (Switzerland)* **2018**, *10* (2), 1–19.
- (45) Gao, Z.; Zhang, Y.; Song, N.; Li, X. Biomass-Derived Renewable Carbon Materials for Electrochemical Energy Storage. *Mater. Res. Lett.* **2017**, *5* (2), 69–88.
- (46) Huggins, T. M.; Haeger, A.; Biffinger, J. C.; Ren, Z. J. Granular Biochar Compared with Activated Carbon for Wastewater Treatment and Resource Recovery. *Water Res.* **2016**, *94*, 225–232.
- (47) Christina Berger. Biochar and Activated Carbon Filters for Grey Water Treatment - Comparidson of Organiv Matter and Nutrient Removal. *Swedish Univ. Agric. Sci.* **2012**, 1–36.
- (48) Ahmed, M. B.; Zhou, J. L.; Ngo, H. H.; Guo, W. Insight into Biochar Properties and Its Cost Analysis. *Biomass Bioenergy* **2016**, *84*, 76–86.
- (49) Zanella, O.; Tessaro, I. C.; Féris, L. A. Desorption- and Decomposition-Based Techniques for the Regeneration of Activated Carbon. *Chem. Eng. Technol.* **2014**, *37* (9), 1447–1459.
- (50) Stavropoulos, G. G.; Zabaniotou, A. A. Minimizing Activated Carbons Production Cost. *Fuel Process. Technol.* **2009**, *90* (7–8), 952–957.
- (51) Hjailla, K.; Baccar, R.; Sarrà, M.; Gasol, C. M.; Blánquez, P. Environmental Impact Associated with Activated Carbon Preparation from Olive-Waste Cake via Life Cycle Assessment. *J. Environ. Manage.* **2013**, *130*, 242–247.
- (52) Correa, C.; Kruse, A. Biobased Functional Carbon Materials: Production, Characterization, and Applications—A Review. *Materials (Basel)*. **2018**, *11* (9), 1568.
- (53) Plaza, M. G.; González, A. S.; Pis, J. J.; Rubiera, F.; Pevida, C. Production of Microporous Biochars by Single-Step Oxidation: Effect of Activation Conditions on CO<sub>2</sub> Capture. *Appl. Energy* **2014**, *114*, 551–562.
- (54) Ahmad, M.; Rajapaksha, A. U.; Lim, J. E.; Zhang, M.; Bolan, N.; Mohan, D.; Vithanage, M.; Lee, S. S.; Ok, Y. S. Biochar as a Sorbent for Contaminant Management in Soil and Water: A Review. *Chemosphere* **2014**, *99*, 19–23.
- (55) Cha, J. S.; Park, S. H.; Jung, S. C.; Ryu, C.; Jeon, J. K.; Shin, M. C.; Park, Y. K. Production and Utilization of Biochar: A Review. *J. Ind. Eng. Chem.* **2016**, *40*, 1–15.

- (56) De Gisi, S.; Lofrano, G.; Grassi, M.; Notarnicola, M. Characteristics and Adsorption Capacities of Low-Cost Sorbents for Wastewater Treatment: A Review. *Sustain. Mater. Technol.* **2016**, *9*, 10–40.
- (57) Ahmed, M. B.; Zhou, J. L.; Ngo, H. H.; Guo, W. Adsorptive Removal of Antibiotics from Water and Wastewater: Progress and Challenges. *Sci. Total Environ.* **2015**, *532*, 112–126.
- (58) Moreira, M. T.; Noya, I.; Feijoo, G. The Prospective Use of Biochar as Adsorption Matrix - A Review from a Lifecycle Perspective. *Bioresour. Technol.* **2017**, *246*, 135–141.
- (59) Shackley, S.; Clare, A.; Joseph, S.; A McCarl, B.; Schmidt, H.-P. *Economic Evaluation of Biochar Systems: Current Evidence and Challenges*; 2015.
- (60) Jacobi Carbon Group. Services. <https://www.jacobi.net/services> (accessed Aug 21, 2018).
- (61) Radiant Insights. Global activated carbon market. <https://www.radiantinsights.com/press-release/global-activated-carbon-market> (accessed August 25, 2018).
- (62) Tariq, A.; Badir, Y. F.; Tariq, W.; Bhutta, U. S. Drivers and Consequences of Green Product and Process Innovation: A Systematic Review, Conceptual Framework, and Future Outlook. *Technol. Soc.* **2017**, *51*, 8–23.
- (63) Bach, M.; Wilske, B.; Breuer, L. Current Economic Obstacles to Biochar Use in Agriculture and Climate Change Mitigation. *Carbon Manage.* **2016**, *7* (3–4), 183–190.
- (64) Ahmed, S.; Hammond, J.; Ibarrola, R.; Shackley, S.; Haszeldine, S. The Potential Role of Biochar in Combating Climate Change in Scotland: An Analysis of Feedstocks, Life Cycle Assessment and Spatial Dimensions. *J. Environ. Plan. Manag.* **2012**, *55* (4), 487–505.
- (65) Rogers, E. *Diffusion of Innovations*, Fifth edit.; Free Press: New York, 2003.
- (66) Gunningham, N. Environment Law, Regulation and Governance: Shifting Architectures. *J. Environ. Law* **2009**, *21* (2), 179–212.
- (67) Vochozka, M.; Maroušková, A.; Váchal, J.; Straková, J. The Economic Impact of Biochar Use in Central Europe. *Energy Sources, Part A Recover. Util. Environ. Eff.* **2016**, *38* (16), 2390–2396.
- (68) Borchard, N.; Siemens, J.; Ladd, B.; Möller, A.; Amelung, W. Application of Biochars to Sandy and Silty Soil Failed to Increase Maize Yield under Common Agricultural Practice. *Soil Tillage Res.* **2014**, *144*, 184–194.
- (69) Salo, E. Current state and future perspectives of biochar applications in Finland. M.Sc. Thesis, Jyväskylä University School of Business and Economics, Jyväskylä, Finland, **2018**.
- (70) Otte, P. P.; Vik, J. Biochar Systems: Developing a Socio-Technical System Framework for Biochar Production in Norway. *Technol. Soc.* **2017**, *51*, 34–45.
- (71) Salvador, F.; Martin-Sanchez, N.; Sanchez-Hernandez, R.; Sanchez-Montero, M. J.; Izquierdo, C. Regeneration of Carbonaceous Adsorbents. Part I: Thermal Regeneration. *Microporous Mesoporous Mater.* **2015**, *202* (C), 259–276.
- (72) Liu, P. K. T.; Feltch, S. M.; Wagner, N. J. Thermal Desorption Behavior of Aliphatic and Aromatic Hydrocarbons Loaded on Activated Carbon. *Ind. Eng. Chem. Res.* **1987**, *26* (8), 1540–1545.
- (73) Santadkha, T.; Skolpap, W. Economic Comparative Evaluation of Combination of Activated Carbon Generation and Spent Activated Carbon Regeneration Plants. *J. Eng. Sci. Technol.* **2017**, *12* (12), 3329–3343.
- (74) Wermter, P.; Herbst, H.; Türk, J. Ertüchtigung von Kläranlagen, Investitionen & Kosten in NRW, BW & CH. Presented at Maßnahmenprogramm WRRLL **2015**, Bezirksregierung Münster, 10.10.2013. Flussgebietsmanagement, <https://www.fiw.rwth-aachen.de/neo/index.php?id=192> (accessed August 25, 2018).
- (75) Salvador, F.; Martin-Sanchez, N.; Sanchez-Hernandez, R.; Sanchez-Montero, M. J.; Izquierdo, C. Regeneration of Carbonaceous Adsorbents. Part II: Chemical, Microbiological and Vacuum Regeneration. *Microporous Mesoporous Mater.* **2015**, *202*, 277–296.
- (76) Sühnhholz, S.; Kopinke, F. D.; Weiner, B. Hydrothermal Treatment for Regeneration of Activated Carbon Loaded with Organic Micropollutants. *Sci. Total Environ.* **2018**, *644*, 854–861.
- (77) Weiner, B.; Sühnhholz, S.; Kopinke, F. D. Hydrothermal Conversion of Triclosan-The Role of Activated Carbon as Sorbent and Reactant. *Environ. Sci. Technol.* **2017**, *51* (3), 1649–1653.
- (78) Weiner, B.; Baskyr, I.; Poerschmann, J.; Kopinke, F. D. Potential of the Hydrothermal Carbonization Process for the Degradation of Organic Pollutants. *Chemosphere* **2013**, *92* (6), 674–680.
- (79) Ledesma, B.; Román, S.; Sabio, E.; Álvarez-Murillo, A. Improvement of Spent Activated Carbon Regeneration by Wet Oxidation Processes. *J. Supercrit. Fluids* **2015**, *104*, 1–10.
- (80) Riedel, G.; Koehler, R.; Poerschmann, J.; Kopinke, F. D.; Weiner, B. Combination of Hydrothermal Carbonization and Wet Oxidation of Various Biomasses. *Chem. Eng. J.* **2015**, *279*, 715–724.
- (81) Da'Na, E.; Awad, A. Regeneration of Spent Activated Carbon Obtained from Home Filtration System and Applying It for Heavy Metals Adsorption. *J. Environ. Chem. Eng.* **2017**, *5* (4), 3091–3099.
- (82) Lata, S.; Singh, P. K.; Samadder, S. R. Regeneration of Adsorbents and Recovery of Heavy Metals: A Review. *Int. J. Environ. Sci. Technol.* **2015**, *12* (4), 1461–1478.

- (83) Godlewska, P.; Schmidt, H. P.; Ok, Y. S.; Oleszczuk, P. Biochar for Composting Improvement and Contaminants Reduction. A Review. *Bioresour. Technol.* **2017**, *246*, 193-202.
- (84) Youngquist, C. P.; Mitchell, S. M.; Cogger, C. G. Fate of Antibiotics and Antibiotic Resistance during Digestion and Composting: A Review. *J. Environ. Qual.* **2016**, *45* (2), 537.
- (85) Xu, X.; Cao, X.; Zhao, L.; Sun, T. Comparison of Sewage Sludge- and Pig Manure-Derived Biochars for Hydrogen Sulfide Removal. *Chemosphere* **2014**, *111*, 296–303.
- (86) Bamdad, H.; Hawboldt, K.; MacQuarrie, S. A Review on Common Adsorbents for Acid Gases Removal: Focus on Biochar. *Renew. Sustain. Energy Rev.* **2016**, *91*(2), 1705-1720.
- (87) Xu, X.; Zhao, Y.; Sima, J.; Zhao, L.; Mašek, O.; Cao, X. Indispensable Role of Biochar-Inherent Mineral Constituents in Its Environmental Applications: A Review. *Bioresour. Technol.* **2017**, *241*, 887–899.
- (88) Webb, J.; Jephcote, C.; Fraser, A.; Wiltshire, J.; Aston, S.; Rose, R.; Vincent, K.; Roth, B. Do UK Crops and Grassland Require Greater Inputs of Sulphur Fertilizer in Response to Recent and Forecast Reductions in Sulphur Emissions and Deposition? *Soil Use Manag.* **2016**, *32* (1), 3–16.
- (89) Bo, L.; Shengen, Z.; Chang, C.-C.; Zhanfeng, D.; Hongxiang, L. Emerging Pollutants - Part II: Treatment. *Water Environ. Res.* **2015**, *87* (10), 1873–1900.
- (90) Dulio, V.; van Bavel, B.; Brorström-Lundén, E.; Harmsen, J.; Hollender, J.; Schlabach, M.; Slobodnik, J.; Thomas, K.; Koschorreck, J. Emerging Pollutants in the EU: 10 Years of NORMAN in Support of Environmental Policies and Regulations. *Environ. Sci. Eur.* **2018**, *30* (1), No. 5.
- (91) Méndez, E.; González-Fuentes, M. A.; Rebollar-Perez, G.; Méndez-Albores, A.; Torres, E. Emerging Pollutant Treatments in Wastewater: Cases of Antibiotics and Hormones. *J. Environ. Sci. Heal. Part A* **2016**, *52* (3), 1–19.
- (92) Müller, S. Micropollutants in municipal waste water - the Swiss strategy; Reference: N222-2504; Federal Office for the Environment: Bern, Switzerland, 2015.
- (93) Abegglen, C.; Siegrist, H. Mikroverunreinigungen aus kommunalem Abwasser - Verfahren zur weitergehenden Elimination aus Kläranlagen; Bundesamt für Umwelt: Bern, Switzerland, 2012: 210.
- (94) Eggen, R. I. L.; Hollender, J.; Joss, A.; Scha, M. Reducing the Discharge of Micropollutants in the Aquatic Environment: The Benefits of Upgrading Wastewater Treatment Plants. *Environ. Sci. Technol.* **2014**, *48*, 7683–7689.





